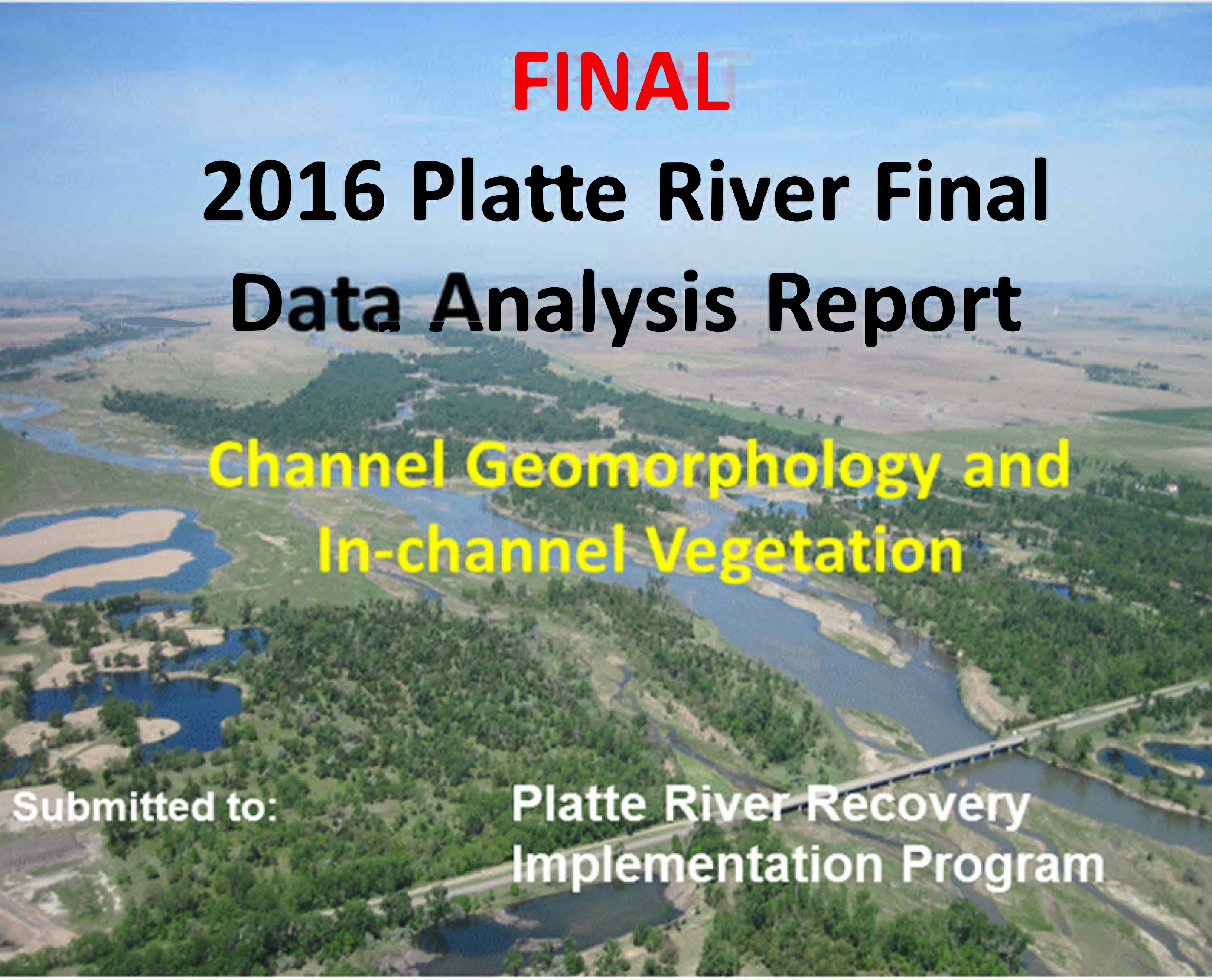

FINAL

2016 Platte River Final Data Analysis Report

Channel Geomorphology and In-channel Vegetation

Submitted to: Platte River Recovery Implementation Program

TETRA TECH

Submitted by: 3801 Automation Way, Suite 100
Fort Collins, CO 80525

July 24, 2017

Page intentionally left blank

Channel Geomorphology and In-Channel Vegetation

2016 Data Analysis Report for Eight Year Monitoring Program

PLATTE RIVER RECOVERY IMPLEMENTATION PROGRAM
Office of the Executive Director
4111 4th Avenue, Suite 6
Kearney, Nebraska 68845

July 24, 2017

Page intentionally left blank

TABLE OF CONTENTS

1 INTRODUCTION 1
1.1 Background 1
1.2 Scope of the Monitoring Program 1
1.2.1 Area of Interest 1
1.2.2 Anchor Points 3
1.2.3 Pure and Rotating Panel Points 3
1.2.4 Channel Geomorphology Monitoring 3
1.2.5 In-channel Vegetation Monitoring 4
1.2.6 Airborne Mapping of Topography (LiDAR) 4
1.3 Hypotheses and Performance Metrics 5
1.4 Big Questions and Broad Hypotheses 5
1.5 Priority Hypotheses 6
1.6 Performance Metrics 8
2 METHODS 9
2.1 Field Data Collection 9
2.1.1 Landowner Contact 11
2.1.2 Topographic Ground Survey Methods 11
2.1.3 Survey Control 11
2.1.4 Geomorphic Transects 11
2.1.5 Unobstructed Channel Width 13
2.1.6 Vegetation Survey Methods 14
2.1.7 Sediment Sampling Methods 17
2.2 Data Analysis Methods 19
2.2.1 Spatial and Temporal Scales 19
2.2.2 Performance Metrics 20
2.2.3 Trend Analysis 29
3 RESULTS 33
3.1 Hydrologic Metrics 33
3.1.1 Annual Peak Flow Event Discharge and Duration (DAP 5.1.1) 33
3.1.2 Germination Season Discharge (DAP 5.1.2) 37

3.1.3 Spring and Fall Whooping Crane Migration Season Discharge (DAP 5.1.3) 37
3.2 Hydraulic Metrics 41
3.2.1 Stage-discharge Relationships (DAP 5.2.1) 41
3.3 Geomorphic Metrics 41
3.3.1 Braiding Index (DAP 5.3.1) 41
3.3.2 Total Channel Width (DAP 5.3.2) 46
3.3.3 Wetted Channel Width (DAP 5.3.3) 50
3.3.4 Mean Channel Depth (DAP 5.3.4) 54
3.3.5 Maximum Channel Depth (DAP 5.3.5) 54
3.3.6 Channel Width-to-Depth Ratio (DAP 5.3.6) 62
3.3.7 Channel Cross-sectional Area (DAP 5.3.6) 67
3.4 Vegetation Metrics 75
3.4.1 Green Line Elevation (GLE) (DAP 5.4.1) 75
3.4.2 Total Unvegetated Channel Width (DAP 5.4.2) 81
3.4.3 Frequency of Occurrence by Species (DAP 5.4.3) 85
3.4.4 Percent Cover by Species (DAP 5.4.4) 91
3.4.5 Comparison of Vegetation Trends at Rotating and Pure Panels Points 97
3.4.6 Areal Cover by Species (DAP 5.4.5) 103
3.4.7 Frequency of Communities 108
3.4.8 Bare Ground 110
3.4.9 Mean Elevation by Species (DAP 5.4.6) 112
3.4.10 Mean Vegetation Height (DAP 5.4.7) 116
3.5 Sediment Metrics 117
3.5.1 Bed-load versus Discharge Rating Curves (DAP 5.5.1) 117
3.5.2 Suspended Sediment Load versus Discharge Rating Curves (DAP 5.5.2) 127
3.5.3 Bed-material Grain-size Distribution and Distribution Parameters (DAP 5.5.3) 134
3.5.4 Bar Material Grain-size Distribution (DAP 5.5.4) 137
3.5.5 Bank Material Grain Size Distribution (DAP 5.5.5) 137
3.6 Whooping Crane Performance Metrics 139
3.6.1 Unobstructed Channel Width (DAP 5.6.1) 139
3.6.2 Channel Width Less Than Eight Inches Deep or Sand (DAP 5.6.2) 143

4 Hypothesis Testing and Trend Analysis 155
4.1 Flow #1 155
4.1.1 Sediment Balance Based on Transect Surveys 155
4.1.2 Sediment Balance Based on Sediment Load Rating Curves 163
4.1.3 Uncertainty in Sediment Balance Estimate 171
4.2 Flow #3 200
4.2.1. Height of Green Line above 1,200 cfs Water Surface 200
4.2.2. Green Line Elevation versus Stage at Annual Peak Discharge 200
4.2.3. Green Line Elevation versus Stage at Germination Season Discharge 204
4.2.4. Total Unvegetated Channel Width 204
4.2.5. Total Unvegetated Channel Width versus Stage at Annual Peak Discharge 207
4.2.6. Total Unvegetated Channel Width versus Stage at Mean Germination Season Discharge 207
4.2.7. Total Unvegetated Channel Width versus Green Line Elevation 207
4.3 Flow #5 211
4.4 Mechanical #2 237
5 SUMMARY AND CONCLUSIONS 2
6 REFERENCES 2

LIST OF FIGURES

Figure 1.1. Location map showing the project reach for the Channel Geomorphology and In-channel Vegetation Monitoring. Bed-load and suspended-sediment sampling bridge sites are shown as red circles. 2
Figure 1.2. Clockwise from top left, illustrations of Priority Hypothesis Flow #1, Flow #3, and Flow #5. 7
Figure 1.3. Illustration of Priority Hypothesis Sediment #1 (left) and Mechanical #2 (right). 8
Figure 2.1. Mean daily flow hydrographs at Overton and Grand Island and the periods over which the annual monitoring was conducted. 10
Figure 2.2. Anchor Point 29 (RM 226.5) showing the typical layout of the geomorphology and vegetation monitoring transects. Detailed geomorphology data are collected and analyzed at Transects 1, 4 and 7. Prior to 2013, vegetation monitoring was conducted at all seven transects. Beginning in 2013, vegetation monitoring at Transects 2 and 6 was discontinued. 12
Figure 2.3. Pipe dredge used to collect bed-material samples. 18

Figure 3.1. Maximum mean daily discharge (Q_P) between January 1 of and the end of monitoring surveys for each year, 2009-2016. 35

Figure 3.2. Duration of flows exceeding 5,000 cfs between January 1 and the dates of the monitoring surveys (DUR_{5000}) for each year, 2009-2016. (Note that flows did not exceed 5,000 cfs anywhere in the reach during 2009, 2012 and 2013.) 36

Figure 3.3. Average mean daily discharge during the germination season (Q_{GER}; June 1 – July 15) from 2009 through 2016. 38

Figure 3.4. Average mean daily discharge during the spring whooping crane migration season (Q_{WC_Spring}; March 21 – April 29) during 2009 through 2016. 39

Figure 3.5. Average mean daily discharge during the fall whooping crane migration season (Q_{WC_Fall}; October 9 – November 10) during 2009 through 2016. 40

Figure 3.6a. Average braiding index by anchor point. Rotating APs are shown by individual symbols only; pure panel APs connected with lines. 43

Figure 3.6b. Average braiding index for the overall study reach, based on the pure panel AP data. Whiskers represent ±1 standard error on mean value. Also shown is the peak discharge at Kearney. 44

Figure 3.6c. Average braiding index by geomorphic reach, based on the pure panel AP data. Also shown are Fotherby (2008) braiding indices. Whiskers represent ±1 standard error on mean value. 45

Figure 3.7a. Average total channel width at pure panel APs. Rotating APs are shown by individual symbols only; pure panel APs connected with lines. 47

Figure 3.7b. Average total channel width for the overall study reach, based on the pure panel AP data from 2009 through 2015, omitting the J-2 return channel. Whiskers represent ±1 standard error on mean value. 48

Figure 3.7c. Average total channel width by reach, based on the pure panel AP data from 2009 through 2015. Whiskers represent ±1 standard error on mean value. Also shown are valley confinement widths from Fotherby (2008) (Right-hand scale). Values near Fotherby (2008) data points are ratio of Fotherby's valley confinement width to average total channel width from this study. 49

Figure 3.8a. Average wetted width at 1,200 cfs at pure panel APs. Rotating APs are shown by individual symbols only; pure panel APs connected with lines. 52

Figure 3.8b. Average wetted width at 1,200 cfs for the overall study reach, based on the pure panel AP data. Whiskers represent ±1 standard error on mean value. 53

Figure 3.8c. Average wetted width at 1,200 cfs by geomorphic reach, based on the pure panel AP. Whiskers represent ±1 standard error on mean value. 54

Figure 3.9a. Mean channel (i.e., hydraulic) depth at 1,200 cfs at pure panel APs. Rotating APs are shown by individual symbols only; pure panel APs connected with lines. 55

Figure 3.9b. Average mean channel (i.e., hydraulic) depth at 1,200 cfs for the overall study reach, based on the pure panel AP data. Whiskers represent ±1 standard error on mean value. 56

Figure 3.9c. Average mean channel (i.e., hydraulic) depth at 1,200 cfs by geomorphic reach, based on the pure panel AP data. Whiskers represent ±1 standard error on mean value. 57

Figure 3.9d. Surveyed cross-section profiles at AP15, transect four in 2011 and 2012. Note the removal of instream bars and the aggradation of the thalweg, which resulted in a wider, shallower channel. 58

Figure 3.10a. Average maximum channel depth at 1,200 cfs at pure panel APs. Rotating APs are shown by individual symbols only; pure panel APs connected with lines. 59

Figure 3.10b. Average maximum channel depth at 1,200 cfs for the overall study reach, based on the pure panel AP data. Whiskers represent ±1 standard error on mean value. 60

Figure 3.10c. Average maximum channel depth at 1,200 cfs by geomorphic reach, based on the pure panel AP data. Whiskers represent ±1 standard error on mean value. 61

Figure 3.11a. Average width-to-depth (maximum depth) ratio at 1,200 cfs at pure panel APs. Rotating APs are shown by individual symbols only; pure panel APs connected with lines. 63

Figure 3.11b. Average width-to-depth (maximum depth) ratio at 1,200 cfs for the overall study reach, based on the pure panel AP data. Whiskers represent ±1 standard error on mean value. 64

Figure 3.11c. Average width-to-depth (maximum depth) ratio at 1,200 cfs by geomorphic reach, based on the pure panel AP data from 2009 through 2015. Whiskers represent ±1 standard error on mean value. Also shown are the width-to-depth ratios from Fotherby (2008). Note: Fotherby (2008) did not report W/D for Reach 1. 65

Figure 3.11d. Average width-to-mean depth ratio at 1,200 cfs by geomorphic reach, based on the pure panel AP data from the 2009 to 2015 data. Also shown are the width-to-depth ratios from Fotherby (2008). Note: Fotherby (2008) does not report W/D for reach 1. 66

Figure 3.12a-1. Year-to-year change in average cross-sectional area at pure panel APs from 2009 through 2015. [Aggradation (+), Degradation (-)]. 68

Figure 3.12a-2. Change in average cross-sectional area at all APs over four-year periods between rotating AP surveys. Line connecting AP33 on the 2009 to 2010 series is dashed to show effect of mechanical bar removal. [Aggradation (+), Degradation (-)]. 69

Figure 3.12b. Year-to-year aggradation/degradation volumes in the overall study reach from 2009 through 2015. Quantity for 2009 to 2010 does not include changes at AP33 associated with mechanical removal of a large mid-channel bar. 70

Figure 3.12c. Year-to-year aggradation/degradation volumes by geomorphic reach from 2009 through 2016. Quantity for Reach 3 during 2009 to 2010 does not include changes at AP33 associated with mechanical removal of a large mid-channel bar. 71

Figure 3.12d. Year-to-year change in mean bed elevation from 2009 through 2016, by geomorphic reach. [Aggradation (+), Degradation (-)]. 72

Figure 3.13a. Aerial photographs showing the locations of the surveyed cross sections at AP33: (a) July 2009 (Disharge~310 cfs), (b) October 2010 (Discharge~720 cfs). 73

Figure 3.13b. Surveyed cross section profiles at AP33 (a) Downstream (XS7), (b) Upstream (XS1). 74

Figure 3.14a. Difference between average green line elevation at pure panel APs between the indicated year and the initial green line elevation surveyed in 2009. (AP13 at different location in 2009; changes referenced to 2010.) 78

Figure 3.14b. Reach-wide average difference in green line elevation at pure panel APs between a given survey year and the 2009 greenline elevation. 79

Figure 3.14c. Average difference in greenline elevation by geomorphic subreach between the initial survey in 2009 and the indicated year. 80

Figure 3.15. Average difference between greenline elevation and the water-surface elevation associated with the maximum preceding discharge (Q_P) at the pure panel APs. 80

Figure 3.16a. Average unvegetated channel width at Pure Panel APs from 2009 through 2015. Rotating APs are shown by individual symbols only; pure panel APs connected with lines. 82

Figure 3.16b. Reach-wide average unvegetated channel width at pure panel APs. Also shown is the mean germination season discharge and the Program's minimum and target width thresholds. 83

Figure 3.16c. Average unvegetated channel width by geomorphic reach. 84

Figure 3.17. Frequency of occurrence of the top-25 most commonly observed species in 2016, and species of interest not among the 25 most commonly observed, 2009-2016. Results are organized by decreasing frequency according to the 2016 data. 86

Figure 3.18. Frequency of occurrence for the four species of primary interest for the 2009 through 2016 vegetation surveys. Also shown is each species' annual rank by frequency amongst all species. 87

Figure 3.19. Mean frequency of occurrence of purple loosestrife (*Lythrum salicaria*) by geomorphic reach, 2009-2016. 88

Figure 3.20. Mean frequency of occurrence of common reed (*Phragmites australis*) by geomorphic reach, 2009-2016. 89

Figure 3.21. Mean frequency of occurrence of eastern cottonwood (*Populus deltoides*) by geomorphic reach, 2009-2016. 90

Figure 3.22. Mean frequency occurrence of willow (*Salix sp.*) by geomorphic reach, 2009-2016. 91

Figure 3.23. Percent cover of the top-25 most commonly observed species in 2016 and species of interest not among 25 most commonly observed, 2009-2016. Results are organized by decreasing frequency according to the 2016 data. 92

Figure 3.24. Percent cover of the species of primary interest from 2009 through 2016. 94

Figure 3.25. Mean percentage of ground cover for purple loosestrife (*Lythrum salicaria*), 2009 through 2016, by geomorphic reach. 95

Figure 3.26. Mean percentage of ground cover for common reed (*Phragmites australis*), 2009 through 2016, by geomorphic reach. 95

Figure 3.27. Mean percentage of ground cover for Eastern cottonwood (*Populus deltoides*), 2009 through 2016, by geomorphic reach. 96

Figure 3.28. Mean percentage of ground cover for willow (*Salix sp.*), 2009 through 2016, by geomorphic reach. 96

Figure 3.29. Comparison of frequency of occurrence of the four species of primary interest between the pure panel APs and the rotating panel APs....................................... 98

Figure 3.30. Comparison of percent cover of the four species of primary interest between the pure panel APs and the rotating panel APs.. 99

Figure 3.31. Change in frequency of occurrence for the four species of primary interest from the year of a rotating panel group's initial survey to the year of its resurvey............... 100

Figure 3.32. Change in percent cover for the four species of primary interest from the year of a rotating panel group's initial survey to the year of its resurvey............................. 102

Figure 3.33. Total surveyed area and area with measurable vegetation for each survey year, based on Daubenmire cover-class data.. 103

Figure 3.34. Areal cover of the top-25 most commonly observed species in 2016 and species of interest not among 25 most commonly observed, 2009-2016. Results are organized by decreasing frequency according to the 2016 findings..................................... 104

Figure 3.35. Areal cover of the four species of primary interest, 2009-2016............................ 105

Figure 3.36. Areal cover of purple loosestrife (*Lythrum salicaria)*, 2009-2016 by geomorphic reach. 106

Figure 3.37. Areal cover of common reed (*Phragmites australis)*, 2009-2016 by geomorphic reach. 106

Figure 3.38. Areal cover of Eastern cottonwood (*Populus deltoides)*, 2009-2016 by geomorphic reach.. 107

Figure 3.39. Areal cover of willow (*Salix sp.)*, 2009-2016 by geomorphic reach....................... 107

Figure 3.40. Frequency of specific community types observed during field surveys between 2012 and 2016.. 109

Figure 3.41. Frequency of vegetated community types observed during field surveys between 2012 and 2016, normalized by removing water and sandbar/mudflat types. 110

Figure 3.42. Average cover percentage of bare ground in all quadrats, survey years 2012-2016. 111

Figure 3.43. Frequency of occurrence of water and of quadrats with greater than 75% bare ground, survey years 2012-2016.. 112

Figure 3.44a. Mean elevation of the top 25 most commonly observed species and additional species of interest not among the 25 most common, organized by decreasing frequency in 2016. Standard error bars (±1) are included.. 114

Figure 3.44b. Mean elevation above the local 1,200 cfs water surface of the top 25 most commonly observed species in 2015 and additional species of interest not among the 25 most common, organized by decreasing frequency in 2015. Standard error bars (±1) are included. 115

Figure 3.44c. Mean height above the 1,200 cfs water surface of the four vegetation species of interest from 2010 through 2016. Also shown is the mean germination season discharge. 116

Figure 3.45. Bed-load transport rates measured at the Darr Bridge between 2009 and 2016. Also shown is the best-fit power-function through the data, the upper and lower 95-percent confidence bands on the best-fit line, and the MVUE bias-corrected line. 118

Figure 3.46. Bed-load transport rates measured at the Overton Bridge between 2009 and 2016. Also shown is the best-fit power-function through the data, the upper and lower 95-percent confidence bands on the best-fit line, and the MVUE bias- corrected line...... 119

Figure 3.47. Bed-load transport rates measured at the Kearney Bridge between 2009 and 2016. Also shown is the best-fit power-function through the data, the upper and lower 95-percent confidence bands on the best-fit line, and the MVUE bias- corrected line...... 120

Figure 3.48. Bed-load transport rates measured at the Shelton Bridge between 2009 and 2016. Also shown is the best-fit power-function through the data, the upper and lower 95-percent confidence bands on the best-fit line, and the MVUE bias- corrected line...... 121

Figure 3.49. Bed-load transport rates measured at the Grand Island Bridge between 2009 and 2016. Also shown is the best-fit power-function through the data, the upper and lower 95-percent confidence bands on the best-fit line, and the MVUE bias- corrected line. 122

Figure 3.50. Power-function, best-fit curves for the measured bed- and suspended-sediment-transport rates at the five measurement sites. 123

Figure 3.51. Average percentage of sand and gravel in the bed-load samples from the five primary measurement sites and the samples collected at Elm Creek and Wood River. Embedded values represent number of samples at each site; whiskers represent ±1 standard error about the mean. 124

Figure 3.52a. Median (D_{50}) particle size of bed-load samples with discharge for the five measurement sites (2009-2016). 125

Figure 3.52b. Variation in D84 particle size of bed-load samples with discharge at the five measurement sites (2009-2016). 126

Figure 3.53. Variation in D_{84} particle size of bed-load samples with discharge at the five measurement sites (2009-2016).Average percentage of silt/clay and sand in the suspended sediment samples from the five primary measurement sites. Embedded values represent number of samples at each site; whiskers represent ±1 standard error about the mean. 128

Figure 3.54. Suspended sand transport rates measured at the Darr Bridge between 2009 and 2016. Also shown is the best-fit power-function through the data, the upper and lower 95-percent confidence bands on the best-fit line, and the MVUE bias- corrected line. 129

Figure 3.55. Suspended sand transport rates measured at the Overton Bridge between 2009 and 2016. Also shown is the best-fit power-function through the data, the upper and lower 95-percent confidence bands on the best-fit line, and the MVUE bias-corrected line. 130

Figure 3.56. Suspended sand transport rates measured at the Kearney Bridge between 2009 and 2016. Also shown is the best-fit power-function through the data, the upper and lower 95-percent confidence bands on the best-fit line, and the MVUE bias-corrected line. 131

Figure 3.57. Suspended sand transport rates measured at the Shelton Bridge between 2009 and 2016. Also shown is the best-fit power-function through the data, the upper and lower

95-percent confidence bands on the best-fit line, and the MVUE bias-corrected line. 132
Figure 3.58. Suspended sand transport rates measured at the Grand Island Bridge between 2009 and 2016. Also shown is the best-fit power-function through the data, the upper and lower 95-percent confidence bands on the best-fit line, and the MVUE bias-corrected line. 133
Figure 3.59. Average median (D_{50}) size of bed-material samples collected at the APs during 2009 through 2016 monitoring surveys. Also shown are the D_{50} sizes of the samples collected by Reclamation in 1989. 135
Figure 3.60. Reach averaged median (D_{50}) particle size of samples collected for this monitoring program in 2009 through 2016, and by Reclamation in 1989. Whiskers represent reach-averaged D_{16} and D_{84}. 136
Figure 3.61. Reach-averaged median (D_{50}) size of bar-material samples collected during 2009 through 2016 monitoring surveys. Also shown are the average values for the 8-year monitoring period. 138
Figure 3.62a. Average unobstructed channel width at pure panel APs. Rotating APs are shown by individual symbols only; pure panel APs connected with lines. 140
Figure 3.62b. Average unobstructed channel width for the overall study reach, based on the pure panel AP data. Whiskers represent ±1 standard error on mean value. 141
Figure 3.62c. Average unobstructed channel width by reach, based on the pure panel AP data. Whiskers represent ±1 standard error on mean value. Note that the 2009 and 2010 values for Reach 2 include both AP35B and AP37B, while 2011-2013 include only AP35B. Average values for AP35B in 2009 and 2010 were 540 and 420 ft, respectively. 142
Figure 3.63a. Width of channel less than 8 inches deep (including exposed sandbars) at 2,400 cfs. Dashed black line is total channel width between bank stations.. 144
Figure 3.63b. Overall reach-averaged width less than 8 inches deep (including exposed sandbars) at 2,400 cfs. Whiskers represent ±1 standard error. Note: AP37B excluded from the average because data are available only for 2009 through 2010 145
Figure 3.63c. Average width less than 8 inches deep (including exposed sandbars) at 2,400 cfs by geomorphic reach. Whiskers represent ±1 standard error. Note: AP37B excluded. 146
Figure 3.64a. Width of channel less than 8 inches deep (including exposed sandbars) at spring migration season discharge. Dashed black line is total channel width between bank stations. 148
Figure 3.64b. Overall reach-averaged width less than 8 inches deep (including exposed sandbars) at the spring migration season discharge. Whiskers represent ±1 standard error. Note: AP37B excluded. 149
Figure 3.64c. Average width less than 8 inches deep (including exposed sandbars) at the spring migration season discharge by geomorphic reach. Whiskers represent ±1 standard error. Note: AP37B excluded. 150
Figure 3.65a. Width of channel less than 8 inches deep (including exposed sandbars) during fall migration season discharge. Dashed black line is total channel width between bank stations. 151

Figure 3.65b. Overall reach-averaged width less than 8 inches deep (including exposed sandbars) at the fall migration season. Whiskers represent ±1 standard error. Note: AP37B excluded. 152

Figure 3.65c. Average width less than 8 inches deep (including exposed sandbars) at the fall migration season discharge by geomorphic reach. Whiskers represent ±1 standard error. Note: AP37B excluded.......... 153

Figure 3.66. Typical relationship between discharge and (a) width of the channel and (b) percentage of total active channel width with depth less than 8 inches, based on the three primary monitoring cross sections at AP17 and AP29. 154

Figure 4.1. Vicinity map of the pilot sediment augmentation area showing the location of the Dyer Outfall and the five monitoring cross sections. 157

Figure 4.2a. Mean bed elevations at the Overton, based on USGS field measurement data collected during WY1987 through WY2016. 159

Figure 4.2b. Mean bed elevations at the Overton, based on USGS field measurement data collected during WY2010 through WY2016 (same data as Figure 4.2a). 159

Figure 4.3. Mean bed elevations at the Cottonwood Ranch Mid-Channel gage, based on USGS field measurement data collected during WY2002 through WY2016. 161

Figure 4.4. Mean bed elevations at the Kearney gage, based on USGS field measurement data collected during WY1982 through WY2016. 162

Figure 4.5. Mean bed elevations at the Grand Island gage, based on USGS field measurement data collected during WY1982 through WY2016. 164

Figure 4.6a. Best-estimate of annual bed load passing the Darr, Overton, Kearney, Shelton and Grand Island measurement points during Survey Years (SY) 2010 through SY2016, based on integration of the bias-corrected bed-load rating curves over the survey year mean daily hydrograph. Whiskers are upper and lower 95-percent confidence limits from Monte Carlo simulation described in the next section. 165

Figure 4.6b. Best-estimate of annual suspended sand load passing the Darr, Overton, Kearney, Shelton and Grand Island measurement points during Survey Years (SY) 2010 through SY2016, based on integration of the bias-corrected suspended sand rating curves over the survey year mean daily hydrograph. Whiskers are upper and lower 95-percent confidence limits from Monte Carlo simulation described in the next section. 166

Figure 4.6c. Best-estimate of annual total sand/gravel load passing the Darr, Overton, Kearney, Shelton and Grand Island measurement points during SY2010 through SY2016, based on addition of the best estimates of bed-load and suspended sand load. Whiskers are upper and lower 95-percent confidence limits from Monte Carlo simulation described in the next section; bar labels are percent bed load. 167

Figure 4.7. Best-estimate of the annual sand transport balance between the five measurement locations from SY2010 through SY2014. Also shown are the 5-year averages from the rating curves and from the survey-based estimates. (Note figure is plotted at same scale as Figure 4.8, below, to facilitate direct comparison.) 168

Figure 4.8. Estimated annual aggradation/degradation quantities from the pure panel AP survey data in the reaches encompassed by the five sediment-transport measurement sites.

Also shown are the average annual aggradation/degradation quantities from both the surveys and the rating curves. ... 170

Figure 4.9. (a) Suspended sand rating curves at Overton. Light grey lines are sample curves from the Monte Carlo simulation; (b) Distribution of estimated sediment loads at the mean (log) discharge of the measured data set from Monte Carlo simulation; (c) Distribution of the exponents on the Overton suspended sand-load rating curve from the Monte Carlo simulation. ... 173

Figure 4.10. Distribution of estimated annual suspended sand loads at Overton based on the 1,000 Monte Carlo trials for each of the five years covered by the monitoring surveys... 176

Figure 4.11. Area used to test agreement between cross section-based volume estimates and estimates based on the complete LiDAR surface (~RM245.5, south channel at Jeffreys Island approximately midway between AP36 and AP37). ... 180

Figure 4.12. Average change in cross sectional area at Rotating APs plotted against the corresponding change at the next upstream Pure Panel AP over the 4 years between AP surveys. Data labels are APs from which the data were taken (odd numbers = Pure Panel; even numbers = Rotating). ... 181

Figure 4.13. Average change in cross sectional area over indicated 4-year periods by geomorphic reach at pure panel APs and all available APs. Where no are shown, rotating panel points surveyed during the indicated period within the reach. ... 182

Figure 4.14. Average change in cross sectional area over indicated 4-year periods by gage reach at pure panel APs and all available APs. ... 183

Figure 4.15a. Best-estimate of aggradation/degradation volumes based on the survey data (bars) and mean and upper and lower 95-percent confidence limits on the volumes predicted by the sediment rating curves (symbols) for SY2010. ... 184

Figure 4.15b. Best-estimate of aggradation/degradation volumes based on the survey data (bars) and mean and upper and lower 95-percent confidence limits on the volumes predicted by the sediment rating curves (symbols) for 2011. ... 185

Figure 4.15c. Best-estimate of aggradation/degradation volumes based on the survey data (bars) and mean and upper and lower 95-percent confidence limits on the volumes predicted by the sediment rating curves (symbols) for 2012. ... 186

Figure 4.15d. Best-estimate of aggradation/degradation volumes based on the survey data (bars) and mean and upper and lower 95-percent confidence limits on the volumes predicted by the sediment rating curves (symbols) for 2013. ... 187

Figure 4.15e. Best-estimate of aggradation/degradation volumes based on the survey data (bars) and mean and upper and lower 95-percent confidence limits on the volumes predicted by the sediment rating curves (symbols) for 2014. ... 188

Figure 4.15f. Best-estimate of aggradation/degradation volumes based on the survey data (bars) and mean and upper and lower 95-percent confidence limits on the volumes predicted by the sediment rating curves (symbols) for 2015. ... 189

Figure 4.15g. Best-estimate of aggradation/degradation volumes based on the survey data (bars) and mean and upper and lower 95-percent confidence limits on the volumes predicted by the sediment rating curves (symbols) for 2016. ... 190

Figure 4.16. Annual total runoff volume at the USGS Overton gage between WY1943 and WY2016. Also shown are the mean flows for the 48-year record used for the DOI et al. (2006) model, the Tetra Tech (2010) model and the 6-year monitoring period. 191

Figure 4.17. Estimated average annual total sand load passing the Overton, Kearney, and Grand Island gages during individual years from WY1984 through WY2016, based on integration of the respective rating curves over the USGS published mean daily flows. Also shown are the upper and lower 95-percent confidence limits from the Monte Carlo simulations. 194

Figure 4.18. Average annual total sand load passing the Overton, Kearney, and Grand Island gages based on integration of the respective rating curves over the USGS published mean daily flows for the period from WY1984 through WY2016. Also shown are the median values and 5th and 95th percentiles from the Monte Carlo simulations...... 195

Figure 4.19a Estimated annual sand transport balance between Overton, Kearney and Grand Island from WY1984 through WY2016, based on integration of rating curves produced by the Monte Carlo simulation. 196

Figure 4.19b. Estimated annual sand transport balance between Overton, Kearney and Grand Island from WY1984 through WY2016. Same as Figure 4.16a with 95% confidence limits from Monte Carlo simulations. 197

Figure 4.20. Mean and median annual sand transport balance between Overton, Kearney and Grand Island from WY1984 through WY2016. Also shown are the 5th and 95th percentile results from the Monte Carlo simulations. 198

Figure 4.21a. Relationship between estimated mean sand balance and total flow volume in the Overton to Kearney and Kearney to Grand Island reaches. 198

Figure 4.21b. Relationship between annual total flow volume and probability of degradation in the Overton to Kearney and Kearney to Grand Island reaches. 199

Figure 4.21c. Relationship between annual peak streamflow and probability of degradation in the Overton to Kearney and Kearney to Grand Island reaches. 199

Figure 4.22. Relationship between annual peak streamflow and probability of degradation in the Overton to Kearney and Kearney to Grand Island reaches.Reach-wide average height of the GLE points above the 1,200 cfs water surface at the pure panel APs. 201

Figure 4.23. Average height of the GLE above the 1,200 cfs water surface at the pure panel APs. Also shown is the 1.5 ft performance benchmark. 202

Figure 4.24. Yearly change in GLE versus year-to-year difference in stage at maximum mean daily flow preceding each survey at the pure panel APs (Kendall's τ = 0.45, p=<0.0001). 203

Figure 4.25. Yearly change in GLE versus year-to-year difference in stage at mean germination season discharge preceding each survey at the pure panel APs (Kendall's τ = 0.61, p=<0.0001). 205

Figure 4.26. Yearly change in GLE versus year-to-year difference in stage at maximum germination season discharge preceding each survey at the pure panel APs (Kendall's τ = 0.53, p=<0.0001). 206

Figure 4.27. Yearly difference in total unvegetated channel width versus year-to-year difference in stage at maximum mean daily flow preceding each survey at the pure panel APs (Kendall's τ = 0.33, p=<0.0001)....... 208

Figure 4.28. Yearly change in total unvegetated channel width versus year-to-year difference in stage at mean discharge during the germination season at the pure panel APs (Kendall's τ = 0.37, p=<0.0001)....... 209

Figure 4.29. Yearly change in total unvegetated channel width versus year-to-year difference in GLE at the primary geomorphic transects of pure panel APs (Kendall's τ = 0.43, p=<0.0001). 210

Figure 4.30. Average frequency of occurrence and percent cover for common reed (*Phragmites australis*) on a reach averaged basis observed during each of the six monitoring surveys. 212

Figure 4.31. Average percent cover of common reed (*Phragmites australis*) at the pure panel anchor points during the six monitoring periods. 213

Figure 4.32. Total runoff volume at Overton during four periods of the water year and the maximum mean daily discharge during the entire water year and between April 1 and August 1 (~time of monitoring surveys) from WY1990 through WY2016. Long-term average volume based on gage data from WY1941 through WY2016. 215

Figure 4.33. Cumulative distribution of inundation depths at the maximum discharge during the growing season for quadrats containing common reed during each of the five monitoring surveys. 216

Figure 4.34. Depths and velocities from the Elm Creek 2-D model at a discharge of approximately 3.200 cfs: (a) Elm Creek Bridge to Kearney Diversion Structure, (b) downstream from Kearney Diversion Structure. 219

Figure 4.35. Incremental probability of plant removal for 1- and 2-year-old Cottonwood (1- and 2-year CW), common reed (PHRAG) and reed canary grass (RCG) based on results from Pollen-Bankhead et al. (2011). 220

Figure 4.36. Typical lateral erosion and undercutting of the edge of a sand bar with common reed in the Elm Creek Complex. 221

Figure 4.37. Total precipitation during the period from April through July in each of the seven monitoring years at five weather stations along the project reach. [Global Historical Climatology Network (GHCN) station numbers used as the data source follow the names]. 222

Figure 4.38. Growing degree days (GDD) above a baseline temperature of 50°F and average temperature at the GHCN Grand Island Station (GCHND Sta USW00014935) during the period from April through July during the monitoring period. 223

Figure 4.39. Percentage of individual vegetation sampling quadrats sprayed at each of the pure panel APs prior to each sampling period. Spraying typically occurs in early-fall; thus, the spraying indicated for each year occurred during fall of the previous year. 226

Figure 4.40. Percentage of all sampled quadrats sprayed at pure panel anchor points and number of pure panel APs receiving at least some spraying during the preceding fall of the indicated year. First number in each label is number of quadrats sprayed; second number is total number of sampled quadrats. 227

Figure 4.41. Change in percent cover of common reed versus percent of quadrats sprayed at pure panel APs with more than 3.5 percent average cover of common reed during the 2009 survey. 234

Figure 4.42a. Change in percent cover of common reed versus growing degree days at pure panel APs with more than 3.5 percent average cover of common reed during the 2009 survey. 235

Figure 4.42b-e. Clockwise from top left, change in percent cover of common reed versus average inundation depth, duration of inundation, total precipitation during the growing season measured at Grand Island, and the 90 percent exceedance discharge during the growing season. 236

Figure 4.43. Clockwise from top left, change in percent cover of common reed versus average inundation depth, duration of inundation, total precipitation during the growing season measured at Grand Island, and the 90 percent exceedance discharge during the growing season.Percent flow consolidation (i.e., percent of flow in the main flow path) at 8,000 cfs. 239

Figure 4.44. Total unvegetated channel width versus braiding index (Kendall's t = 0.22, p<0.001). 240

Figure 4.45. Total unvegetated channel width versus percent flow consolidation at 8,000 cfs (Kendall's t = 0.26, p<0.001). 241

Figure 4.46. Braiding index versus percent flow consolidation at 8,000 cfs (Kendall's t = 0.23, p<0.001). 242

Figure 4.47. Mean unvegetated channel width at sites with greater than and less than 85-percent flow consolidation: (a) All APs, (b) Excluding AP9, AP21, and AP33. 243

Figure 4.48. Mean braiding index at sites with greater than and less than 85-percent flow consolidation: (a) All APs, (b) Excluding AP9, AP21, and AP33. 243

Figure 5.1. Annual peak discharges at the USGS Overton, Kearney, and Grand Island gages (note that Kearney record started in 1982). Also shown by the black mark is the approximate WY2013 peak discharges prior to the September flood at the three locations. 3

Figure 5.2. Flood-frequency curves for the annual peak flows from WY1942 through WY2013 at the USGS Overton, Kearney (WY1982-WY2013, only), and Grand Island gages. ... 4

Figure 5.3. Annual aggradation/degradation rate by geomorphic reach over the 8-year monitoring period, based on the cross section surveys at the pure panel APs. 6

LIST OF TABLES

Table 1.1. Anchor Point Locations. 3

Table 1.2. PRRIP Big Questions relevant to the Geomorphology and Vegetation Monitoring Program (from PRRIP, 2012a). 5

Table 1.3. Performance Metrics Relevant to the Priority Hypotheses. 8

Table 2.1. Summary of Annual Survey Dates and Discharges 9

Table 2.2 Species Grouped as Genera. 15

Table 2.3. Summary of bed-load sediment discharge measurements taken since the start of the monitoring program in 2009. Also shown are the correlation coefficients (R2) for best-fit, power-function regression lines through each of the data sets. 19

Table 2.4. Summary of suspended sand-load measurements taken since the start of the monitoring program in 2009. Also shown are the correlation coefficients (R2) for best-fit power-function regression curves through each of the data sets. 19

Table 2.5. Geomorphic Reaches from Fotherby (2008). 21

Table 2.6. Performance metrics defined in the Channel Geomorphology and In-channel Vegetation Data Analysis Plan. 22

Table 2.7. Species considered in the analyses—the 25 most frequently observed species in 2015, and species of interest observed at lower frequencies. 28

Table 2.8. Summary of Trend Analysis Specified in the Data Analysis Plan. 31

Table 3.1. Summary of Vegetation Survey Sites (2009-2015). 75

Table 3.2. Average green line elevations at pure panel APs observed during the six monitoring surveys. 76

Table 3.3. Summary Statistics for Trends in Median Grain Size with Distance Along the Monitoring Reach (□=0.10). 134

Table 4.1. Summary of Bed and Suspended Sand Load Regression Equations and Associated Statistics. 172

Table 4.2. Probability of degradation when rating curve indicates degradation, or aggradation when mean indicates aggradation. 177

Table 4.3. Gage reaches in which the survey-based aggradation/degradation estimate is within the 90% (2-tailed) confidence bands on the rating curve-based estimate. 178

Table 4.4. Anchor points at which at least some aerial spraying occurred during the indicated year. 225

Table 4.5. Summary of PRRIP mechanical and other direct treatments at the APs for 2008 through 2015 other than aerial spraying. 228

Table 4.6. Correlation (Spearman) and p-values for percent cover of common reed versus possible influencing variables. 230

Table 4.7. Correlation (Spearman) and p-values for year-to-year change in percent cover of common reed versus possible influencing variables. 232

Table 4.8. Correlation matrix for percent flow consolidation, average braiding index and average unvegetated channel width at all of the pure panel APs, and all pure panel APs, except AP9, AP21 and AP33. 238

Table 5.1. Comparison of predicted direction aggradation/ degradation trends between rating curves and AP surveys. 9

LIST OF APPENDICES

Appendix A.1: Mean Daily Flow-duration Curves for Germination Season
Appendix A.2: Mean Daily Flow-duration Curves for Spring Whooping Crane
Appendix A.3: Mean Daily Flow-duration Curves for Fall Whooping Crane
Appendix B.1: Summary of Geomorphic and Selected Vegetation Metrics - 2009
Appendix B.2: Summary of Geomorphic and Selected Vegetation Metrics - 2010
Appendix B.3: Summary of Geomorphic and Selected Vegetation Metrics - 2011
Appendix B.4: Summary of Geomorphic and Selected Vegetation Metrics - 2012
Appendix B.5: Summary of Geomorphic and Selected Vegetation Metrics - 2013
Appendix B.6: Summary of Geomorphic and Selected Vegetation Metrics - 2014
Appendix B.7: Summary of Geomorphic and Selected Vegetation Metrics – 2015
Appendix B.8: Summary of Geomorphic and Selected Vegetation Metrics – 2016
Appendix C: Vegetation Data

LIST OF ACRONYMS AND ABBREVIATIONS

AMP	Adaptive Management Plan
AP	Anchor Point
cfs	cubic ft per second
DAP	Data Analysis Plan
DOI	Department of the Interior
EA	Environmental Account
FAC	Facultative
FACU	Facultative Upland
FACW	Facultative Wetland
ft	foot/feet
FSM	Flow, Sediment, and Mechanical
GDD	Growing Degree Days
GHCN	Global Historical Climate Network
GIS	Geodata Interoperability Specification
GLE	Greenline Elevation
GPS	Global Positioning System
HEC	Hydrologic Engineering Center
KDC	Kearney Diversion Channel
LiDAR	Light Detection and Ranging
MVUE	Maintenance of Variance Unbiased Estimator
NAD83	North American Datum of 1983
NAVD88	North American Vertical Datum of 1988
NDNR	Nebraska Department of Natural Resources
NWIS	National Water Information System
OBL	Obligate Wetland
PRRIP	Platte River Recovery Implementation Program
RCG	reed canary grass
RM	River Mile
RP	Rotating Panel
SEDVEG	Bureau of Reclamation model of sedimentation and vegetation processes

SDHF	Short-duration High Flow
SMDF	Short-duration Medium Flow
SY	survey year
tpd	tons per day
tpy	tons per year
USACE	U.S. Army Corps of Engineers
USFWS	U.S. Fish and Wildlife Service
USGS	U.S. Geological Survey
VSZ	Vegetation Survey Zone
WY	Water Year

Page Intentionally Left Blank

1 INTRODUCTION

1.1 Background

The Platte River Recovery Implementation Program (Program, aka PRRIP) was initiated on January 1 2007, between Nebraska, Wyoming, Colorado, and the Department of the Interior to address endangered species concerns in the central and lower Platte River. Four “target” species are of primary concern to the Program: the whooping crane, piping plover, interior least tern, and pallid sturgeon. The intent of the Program is to rehabilitate habitat in the Platte River for the three bird species by restoring a braided channel morphology with sand bars free of vegetation, increased channel widths, and unobstructed views, while avoiding impacts to pallid sturgeon habitat.

Because of the uncertainty in how the river will respond to management actions, the Program has developed several *Big Questions* and priority hypotheses related to the linkage between channel geomorphology, in-channel vegetation, and habitat for the target species (PRRIP, 2006). To help answer these questions and test the hypotheses, a Channel Geomorphology and Vegetation Monitoring Program was carried out to collect and analyze a suite of data over a multi-year time-frame with the following specific objectives:

- Document trends in channel geomorphology parameters throughout the Central Platte River during the 13-year First Increment (2007-2019) of the Program. Parameters of specific interest include cross sectional shape, width, planform, aggradation/degradation trends, bed-material grain sizes, and sediment loads.
- Provide system-wide status in areal coverage and elevation range of in-channel seedlings and invasive vegetation to assist in implementing the Program’s Adaptive Management Plan (AMP) (PRRIP, 2012b) and use of water in the Environmental Account (EA), evaluate the extent of existing native and non-native invasive species infestations, and serve as a mechanism for identification of new invasive species populations before infestations become widespread.

A previous contractor team consisting of Ayres Associates and Olsson Associates implemented the Program’s monitoring protocol (PRRIP, 2010) during the first three years of the monitoring program, with the first year of the data collection occurring in 2009 (Ayres and Olsson, 2010, 2011 and 2012). The Program has also developed a draft Data Analysis Plan (PRRIP, 2012a).

Tetra Tech continued to carry out the program from 2012 through 2016, including implementation of the Data Analysis Plan that was not included in the earlier contract. Results from the 2012 through 2015 data collection and interim analysis results for the data collected through 2015 were previously presented in the 2012 through 2015 annual reports (Tetra Tech, 2013, 2014, 2015, and 2016). This report summarizes the data and results from implementation of the entire eight (8) year monitoring program.

1.2 Scope of the Monitoring Program

1.2.1 Area of Interest

The specific area of interest for the monitoring program includes the channels within approximately 0.5 miles on either side of the centerline of the Platte River, beginning at the junction of U.S. Highway 283 and Interstate 80 near Lexington, Nebraska, and extending 100 miles eastward to Chapman, Nebraska (**Figure 1.1**). Certain areas within this portion of the central Platte River have been prioritized for monitoring based on key priority hypotheses, ecological need, and Program actions undertaken during the First Increment.

Figure 1.1. Location map showing the project reach for the Channel Geomorphology and In-channel Vegetation Monitoring. Bed-load and suspended-sediment sampling bridge sites are shown as red circles.

1.2.2 Anchor Points

A systematic sample of locations along the river have been identified to serve as "anchors" for the data collection. These locations, referred to as anchor points (APs), are spaced at approximately 4,000-meter (2.5-mile) intervals along the centerline of the river, and each point has been labeled with a U.S. Army Corps of Engineers (USACE) River Mile (RM) (**Table 1.1**). The specific locations of some of the APs were selected to accommodate previously established cross sections within the historical database and to accommodate some land access issues; thus, the actual spacing varies by up to 800 meters (0.5 miles) from the typical, 4,000-meter spacing. The basic geomorphic sampling unit consists of three transects spaced at approximately 150-meter intervals. The transects extend laterally across the historic flood plain and incorporate the current main channel, as well as all primary split-flow channels. Although the north channel (Reach 1) and south channel (Reach 2) of Jeffreys Island share the same AP number, these two channels are treated as separate reaches because the flows in the north channel are derived from the upstream river, while the flows in the south channel are mostly derived from flow releases from the J-2 Return.

1.2.3 Pure and Rotating Panel Points

The APs were divided into two subsets, referred to as “pure panel” subset and a “rotating panel” subset. A panel is made up of a group of sampling sites that are always visited at the same time. Data collection is conducted at the pure panel sites (odd numbered sites in Table 1.1) every year, and the rotating panel sites have been divided into four groups that are visited once every four years on a rotating basis. As a result, 25 sample sites are surveyed each year (20 pure panels and 5 rotating panels). As of the end of the 2016 field season, the pure panel points have been sampled eight times, and all of the rotating panel points have been surveyed twice. Per the Monitoring Protocol, the secondary channels at the Pure Panel points were initially surveyed in 2009 and re-surveyed in 2013.

1.2.4 Channel Geomorphology Monitoring

The geomorphology portion of this monitoring program is designed to document trends in channel morphology at specific sites or groups of sites and along the entire study reach. The monitoring is focused on measuring and tracking changes in river planform, cross-sectional geometry (including bed elevation and channel width), longitudinal bed profile, streamflow, sediment loads, and bed, bar and bank material grain-size distributions. The monitoring data are collected through a combination of aerial photographs, airborne terrestrial LiDAR, topographic ground surveys, bed material sampling, ground photography, and sediment-transport measurements at the active gaging stations within the reach.

Table 1.1. Anchor Point Locations.

Anchor Point No.	River Miles and Channel Designation	Pure (P) or Rotating (R) Panel	Location
40	254.4	R1	Lexington
39	250.8	P	Lexington Bridge (Hwy 283)
38	249	R2	
37	246.5 N, S	P	J2 Return – Jeffreys Island
36	244.0 N, S	R3	
35	241.5 N, S	P	
34	239.1	R4	D/S Overton Bridge (Rd 444)
33	236.4	P	Cottonwood Ranch transects
32	234.1 M, N, S	R1	
31	231.5	P	U/S Elm Creek Bridge
30	228.6	R2	D/S Kearney Diversion
29	226.4	P	
28	224.3	R3	Odessa Rd. Bridge

Anchor Point No.	River Miles and Channel Designation	Pure (P) or Rotating (R) Panel	Location
27	221.9	P	
26	219	R4	
25	216.5	P	
24	214	R1	D/S Kearney Bridge (Hwy 44)
23	211.5 M, N1, N2	P	
22	208.4 M, N1	R2	U/S 32 Rd. Bridge (Hwy 10)
21	206.7 M, N1	P	
20	204.0 M, N1	R3	
19	201.1 M, N1	P	D/S Lowell Rd Bridge
18	199.5	R4	
17	196.4	P	U/S Shelton Rd. Bridge
16	193.8	R1	
15	190.7	P	
14	189.3	R2	
13	186.7 M, N1	P	D/S Hwy 11 Bridge
12	184.0 M, N1	R3	
11	181.8 M, N1	P	D/S S Alda Rd. Bridge
10	179.0 M, N1, N2, N3	R4	
9	176.5 M, N1, N2, N3	P	U/S SR 34/281 Bridge
8	174 M, N1, N2, N3	R1	Grand Island
7	171.5 M, N1, N2, N3	P	D/S I-80 Bridge
6	169.1 M, N1	R2	
5	166.9	P	D/S SR 34/Hwy 2 Bridge
4	164	R3	
3	161.8	P	Phillips
2	158.7	R4	
1	156.6	P	D/S Bader Park Rd. Bridge

1.2.5 In-channel Vegetation Monitoring

The vegetation monitoring portion is designed to document the areal extent of species of interest within the Vegetation Survey Zone[1] (VSZ) between the historic high banks. The vegetation surveys were conducted in conjunction with the field component of the geomorphology monitoring (and at the same locations) so that the vegetation data points can be readily included in the topographic surveys.

Current vegetation species of interest include six woody species: narrow-leaf willow (*Salix exigua*), peach-leaf willow (*S. amygdaloides*), eastern cottonwood (*Populus deltoides*), false indigo (*Amorpha fruticosa*), saltcedar (*Tamarix ramosissima*), and Russian olive (*Elaeagnus angustifolia*), as well as several herbaceous species, including purple loosestrife (*Lythrum salicaria*), common reed (*Phragmites australis*), rice cut grass (*Leersia oryzoides*), and river bulrush (*Bolboschoenus fluviatilis*). In addition, reed canary grass (*Phalaris arundinacea*) was also included because it is a vigorous competitor, is present in high densities in some areas, and has a tendency to form dense rootmats and monocropic stands. Although the analysis focuses on these species of interest, it is important to note that all plant species encountered at each sample point were documented in the field notes.

1.2.6 Airborne Mapping of Topography (LiDAR)

Because of the characteristics of the vegetation on the historic overbanks and islands within the corridor between historic banks, ground surveys outside the active channel and mechanically modified areas would be very laborious and costly. As a result, contour base mapping has been

[1] Defined in the Monitoring Protocol as the area within the belt transect at each AP that includes the active channel but generally excludes areas of permanent woody vegetation taller than 4 meters in height or other areas that are clearly beyond the effect of high water flows.

developed from airborne terrestrial LiDAR data. Originally, airborne terrestrial LiDAR flights for mapping were to be flown at the beginning (baseline conditions) and end of the First Increment. Recognizing the high value of the LiDAR data, the Program changed these requirements and LiDAR data are now collected during the fall of each year in conjunction with Color Infrared (CIR) photography. The Program has used these data to develop topographic surfaces with ±6-inch vertical accuracy, sufficient for 1 ft contour interval mapping of the area between the historic outer banks (approximately 1 mile in width).

1.3 Hypotheses and Performance Metrics

The AMP (PRRIP, 2006) for the 13-year, First Increment of the Program focuses on several critical scientific and technical uncertainties about the target species, physical processes, and the response of the target species to management actions. These uncertainties are captured in statements of broad hypotheses in the AMP and, as a means of better linking science learning to Program decision-making, those uncertainties comprise a set of "Big Questions" that provide a template for linking specific hypotheses and performance measures to management objectives and overall Program goals.

1.4 Big Questions and Broad Hypotheses

The monitoring program is focused on four Big Questions that specifically relate to river morphology and in-channel vegetation (**Table 1.2**), and these Big Questions are related to the following suite of system-scale hypotheses:

Table 1.2. PRRIP Big Questions relevant to the Geomorphology and Vegetation Monitoring Program (from PRRIP, 2012a).

PRRIP Big Questions = What we don't know but want to learn	Broad Hypothesis	Priority Hypotheses
Implementation – Program Management Actions and Habitat		
1. Will implementation of (SDHF) produce suitable tern and plover riverine nesting habitat on an annual or near-annual basis?	*PP-1a. Flows of 5,000 to 8,000 cubic feet per second (cfs) magnitude in the habitat reach for a duration of three days at Overton on an annual or near-annual basis will build sandbars to an elevation suitable for least tern and piping plover habitat.*	Flow #1
2. Will implementation of SDHF produce and/or maintain suitable whooping crane riverine roosting habitat on an annual or near-annual basis?	*PP-1b. Flows of 5,000 to 8,000 cfs magnitude in the habitat reach for a duration of three days at Overton on an annual or near-annual basis will increase the average width of the vegetation-free channel.*	Flow #3, Flow #5
3. Is sediment augmentation necessary for the creation and/or maintenance of suitable riverine tern, plover, and whooping crane habitat?	*PP-2. Between Lexington and Chapman, eliminating the sediment imbalance of approximately 400,000 tons annually in eroding reaches will reduce net erosion of the river bed, increase the sustainability of a braided river, contribute to channel widening, shift the river over time to a relatively stable condition, and reduce the potential for degradation in the north channel of Jeffrey Island resulting from headcuts.*	Sediment #1
4. Are mechanical channel alterations (channel widening and flow consolidation) necessary for the creation and/or maintenance of suitable riverine tern, plover, and whooping crane habitat?	*PP-3. Designed mechanical alterations of the channel at select locations can accelerate changes towards braided channel conditions and desired river habitat.*	Mechanical #2

S-1: A combination of flow management, sediment management, and land management (i.e., Clear/Level/Pulse) will/will not generate detectable changes in the channel morphology of the Platte River on Program lands, and/or habitats for whooping crane, least tern, piping plover, pallid sturgeon, and other species of concern.

S-2: A combination of non-managed flows, sediment management, and land management (i.e., Clear/Level/Mechanical Maintenance) will/will not generate detectable changes in the channel morphology of the Platte River, and/or habitats for whooping crane, least tern, piping plover, pallid sturgeon, and other species of concern.

S-4: Program management actions will/will not be of sufficient scale and magnitude to cause detectable system wide changes in channel morphology and/or habitats for the target species.

PP-1: Flows of varying magnitude, duration, frequency and rate of change affect the morphology and habitat quality of the river, including:

- Flows of 5,000 cfs to 8,000 cfs in the habitat reach for a duration of three days at Overton on an annual or near-annual basis will build sand bars to an elevation suitable for least tern and piping plover habitat;
- Flows of 5,000 cfs to 8,000 cfs in the habitat reach for a duration of three days at Overton on an annual or near-annual basis will increase the average width of the vegetation free channel;
- Variations in flows of lesser magnitude will positively or negatively affect the sand bar habitat benefits for least terns and piping plovers.

PP-2: Eliminating the sediment imbalance of approximately 400,000 tons annually in eroding reaches between Lexington and Chapman will:

- reduce net erosion of the river bed,
- increase the sustainability of a braided river,
- contribute to channel widening,
- shift the river over time to a relatively stable condition, and
- reduce the potential for degradation in the North Channel of Jeffrey Island.

1.5 Priority Hypotheses

The AMP (PRRIP, 2006) formalizes several detailed hypotheses that specifically address uncertainty in the underlying physical process relationships related to potential flow, sediment, and mechanical (FSM) actions. The Tier 1 physical process priority hypotheses related to potential FSM actions include (**Figure 1.2**):

Flow #1: Increasing the variation between river stage at peak (indexed by the $Q_{1.5}$ @ Overton) and average flows (1,200 cfs index flow), by increasing the stage of the $Q_{1.5}$ through Program flows, will increase the height of sandbars between Overton and Chapman by 30 to 50 percent from existing conditions, assuming balanced sediment budget.

Flow #3: Increasing $Q_{1.5}$[2] with Program flows will increase local boundary shear stress and frequency of inundation at the existing green line (elevation at which riparian vegetation can establish). These changes will increase riparian plant mortality along the margins of the channel, raising the elevation of the green line, providing more exposed sandbar area and a wider, unvegetated main channel.

Flow #5: Increasing the magnitude and duration of the $Q_{1.5}$ will increase riparian plant mortality along the margins of the river. There will be different relations for different species. This will in turn lead to increasing channel width.

[2] $Q_{1.5}$ is the variable designation for the 1.5-year recurrence interval peak flow.

Sediment #1: Average sediment augmentation near Overton of 185,000 tons/year under the existing flow regime and 225,000 tons/year under the GC proposed flow regime achieves a sediment balance to Kearney (**Figure 1.3**).

Mechanical #2: Increasing the $Q_{1.5}$ in the main channel by consolidating 85 percent of the flow, and aided by Program flows and a sediment balance, will exceed stream power thresholds that will convert the main channel from meandering morphology in anastomosed reaches to braided morphology with an average braiding index greater than 3 (Figure 1.3).

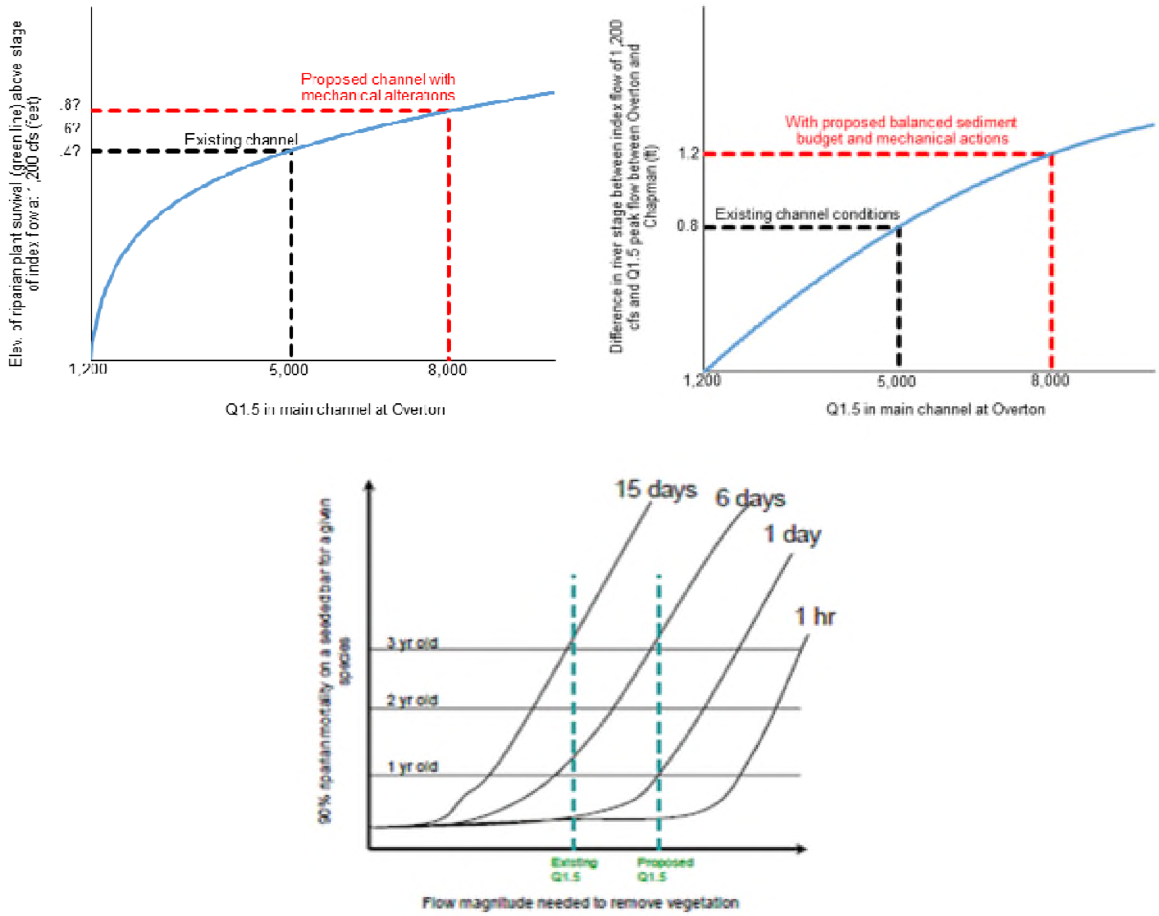

Figure 1.2. Clockwise from top left, illustrations of Priority Hypothesis Flow #1, Flow #3, and Flow #5.

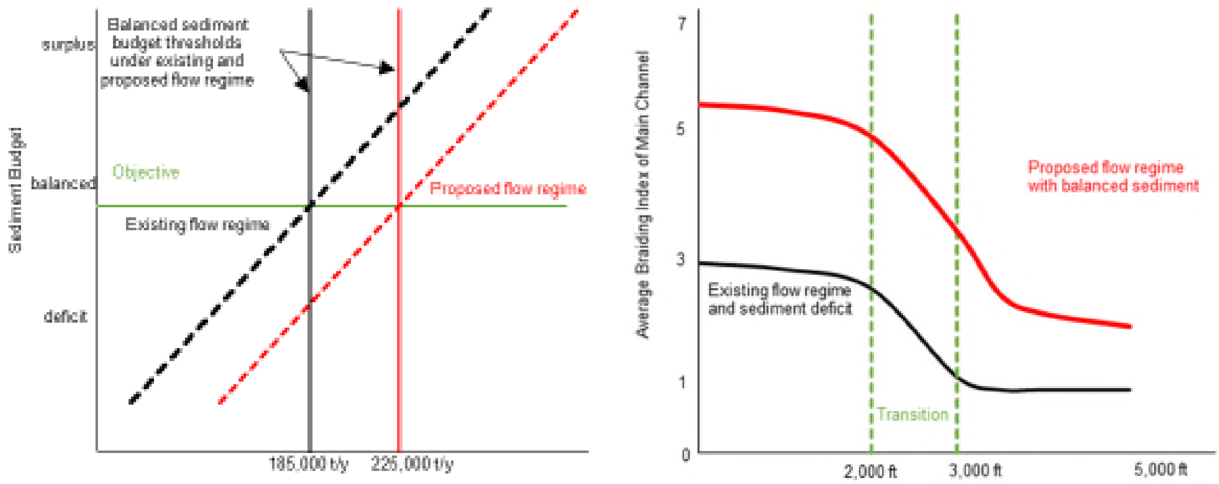

Figure 1.3. Illustration of Priority Hypothesis Sediment #1 (left) and Mechanical #2 (right).

1.6 Performance Metrics

The Program has identified a suite of performance metrics that are quantified using the data from the monitoring program in conjunction with the available data from the various USGS stream gages and results from the Program's system-wide 1-D hydraulic model. Data and results from other Program activities, including the Elm Creek and Shoemaker Island FSM Experiments, the Pilot-scale Sediment Augmentation Project, and the Cottonwood Ranch Flow Consolidation project will also be considered, where appropriate, to supplement the data collected specifically for this monitoring program. Most of these performance metrics are directly associated with the above-described priority hypotheses (**Table 1.3**), while others are related to secondary purposes, including invasive species monitoring.

Table 1.3. Performance Metrics Relevant to the Priority Hypotheses.

Hypothesis	Performance Metric(s)
Flow #1	• Stage-discharge relation
Flow #3	• Green line elevation • Vegetation percent cover • Unvegetated channel width • Channel stage-width relationship
Flow #5	• Vegetation species-specific elevation data • Vegetation species-specific areal coverage data • Stage-discharge relation • Green-line elevation
Sediment #1	• Sediment load • Bed and bar material grain-size distribution • Bank material grain-size distribution • Channel volume • Braiding index • Longitudinal profile
Mechanical #2	• Braiding index

2 METHODS

The Program's Monitoring Protocol (PRRIP, 2010) and draft Data Analysis Protocol (PRRIP, 2012a) describe the methods that are to be used to collect and analyze the data from this program. A summary of the key elements of those protocols that have been implemented for this report are described in the following paragraphs.

2.1 Field Data Collection

As discussed in Chapter 1, the field data fit into three general categories:

- Geomorphic data that describe the physical characteristics of the river, including dimension, planform, pattern, and boundary sediments.
- Vegetation data that describe the distribution, frequency, density and other relevant characteristics of the in-channel vegetation.
- Sediment-transport data to quantify the relationship between discharge and sediment-transport rates along the reach.

In accordance with the monitoring protocol, the geomorphology and vegetation data were collected annually during July and August (**Table 2.1, Figure 2.1**). Although the monitoring protocol envisioned that the data would be collected at low flows (ideally between 250 cfs and 500 cfs), flows were substantially above the target range in at least parts of the reach during 4 of the 8 years because of unanticipated hydrologic conditions.

Table 2.1. Summary of Annual Survey Dates and Discharges

Year	Survey Dates		Discharge during Survey Periods (cfs)	
	Start	End	Minimum	Maximum
2009	14-Jul	22-Aug	0	920
2010	20-Jul	25-Aug	510	2,470
2011	19-Jul	27-Aug	1,050	6,630
2012	10-Jul	12-Aug	0	330
2013	9-Jul	12-Aug	0	740
2014	8-Jul	8-Aug	0	990
2015	21-Jul	22-Aug	570	2,370
2016	12-Jul	13-Aug	220	1,780

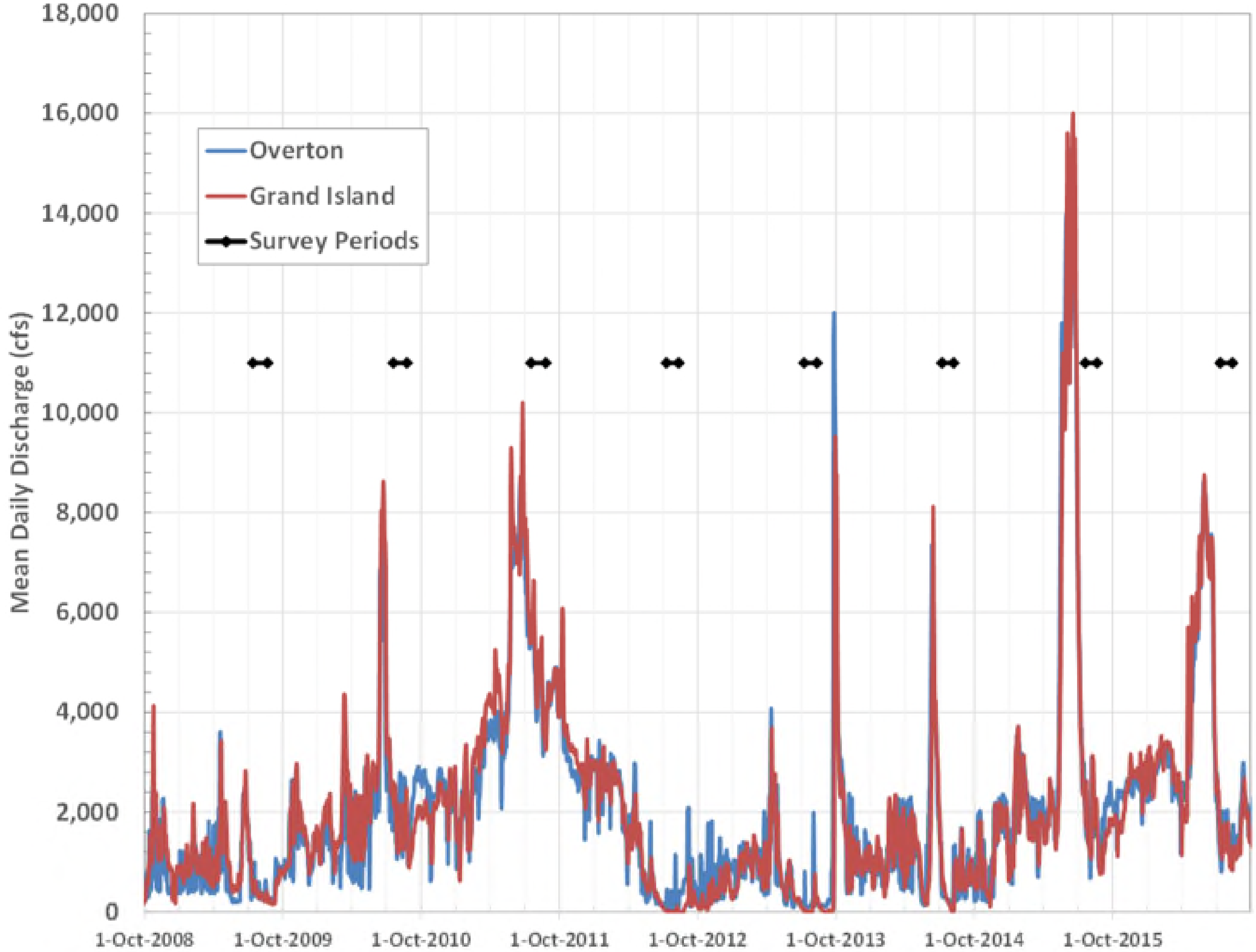

Figure 2.1. Mean daily flow hydrographs at Overton and Grand Island and the periods over which the annual monitoring was conducted.

2.1.1 Landowner Contact

A protocol for obtaining landowner permission was established by the Program and the previous contractor before conducting the field survey work in Year 1 (2009). Program staff made the initial contacts with the landowners and obtained written permission allowing access to their properties. Program staff also created a geodatabase that included landowner contact information for each AP. This database was updated during each of the subsequent years of the program. The signed permission forms and the updated geodatabase were provided to Tetra Tech prior to the start of the 2012 field work. A binder containing copies of the landowner permission forms was kept with the field crews in case questions or disputes arose while in the field. As landowner-program relationships are of paramount importance, the affected landowners were contacted by telephone before the start of each field effort to maintain communication, notify landowners in advance of the intent to work near their property, and coordinate river access.

In addition, significant coordination was conducted between the field crews and Program staff during the fieldwork to ensure that property access protocols were followed, obtain updates on new landowner requirements, and report problems with landowners or access. In this regard, it should be noted that Pure Panel AP37B was not surveyed between 2012 and 2015 because permission to access the property has been revoked by the property owner due to a dispute that arose during the 2011 field season. Additionally, Pure Panel AP25 was not surveyed in 2013 or 2014 because the landowner on the south side of the river at this location revoked permission for access. Monitoring at AP25 re-commenced in 2015 after the land on the south side of the river was purchased by the Program.

2.1.2 Topographic Ground Survey Methods

Ground surveys were conducted to obtain elevation profiles within the active channel at each of the 20 pure panel and five rotating panel points during each survey year. The surveys also included the horizontal and vertical location of all vegetation sample quadrats, and the location and elevation of all bed and bar material samples.

2.1.3 Survey Control

The horizontal coordinates of topographic survey points were referenced to the North American Datum of 1983 (NAD) and the elevations were referenced to the North American Vertical Datum of 1988 (NAVD88). The original primary control for the project was established by Ayres Associates at approximately 12-mile intervals along the reach based on static GPS observations over an approximately 4-hour period at each point. Secondary control was subsequently established between the primary control points using RTK GPS. A more detailed description of the procedure for setting the primary and secondary control points can be found in Ayres and Olsson (2010, 2011 and 2012).

2.1.4 Geomorphic Transects

Detailed topographic surveys of the geomorphology transects (**Figure 2.2**, Transects 1, 4 and 7) included only the portion of the cross sections where the ground had been inundated since the previous survey, and also included areas where the ground has been disturbed by discing, mowing, or grading, where natural processes have created significant topographic changes (i.e., channels and islands where sediment could have been deposited or eroded), and locations where new dikes or other river training structures have been placed or removed by landowners. The transect surveys included the channels, banks, and small islands within the accretion zone, but not the upland portions of the cross section beyond the potential bank erosion/deposition zone. As will be described below, data for these portions of the cross sections were obtained from the Program's LiDAR data.

Figure 2.2. Anchor Point 29 (RM 226.5) showing the typical layout of the geomorphology and vegetation monitoring transects. Detailed geomorphology data are collected and analyzed at Transects 1, 4 and 7. Prior to 2013, vegetation monitoring was conducted at all seven transects. Beginning in 2013, vegetation monitoring at Transects 2 and 6 was discontinued.

The transects were surveyed using a Leica survey-grade Global Positioning System (GPS) per the requirements defined in the monitoring protocol. When each of the surveyed APs was originally established, transects were oriented perpendicular to the principal flow direction and extended through all channels at the AP. In some instances, where a single transect alignment would not remain perpendicular to the primary flow direction across all active channels; the transects were divided into an appropriate number of segments bounded by internal nodes that were also monumented in the field with a marker pin. The end-points of each cross section were monumented on both historic outer banks with a permanent metal marker (pin) set above the flood elevation and far enough from the active channel to avoid all but the most severe erosion effects.

The location of cross-section and transect marker pins, their monumentation, and the extent of the survey beyond the pins depended on accessibility and private property requirements and restrictions. The marker pins consist of approximately 18-inch long, 1/2-inch (#4) rebar, driven flush with the ground surface, and topped with an aluminum cap that is stamped with the AP and transect identification. The geographic coordinates and elevation of each marker pin were established with vertical and horizontal accuracies of 0.1 ft or less using standard survey techniques. In cases where previously established marker pins were lost, damaged, or displaced, a new marker pin was set at a suitable location prior to conducting the surveys.

In performing the surveys, a code was recorded in the GPS datalogger to identify the feature represented by each point to facilitate reduction and interpretation of the data. Typical features included:

- Top and toe of bank,
- Bed or ground elevation,
- Left and right edge of water of all channels,
- Water surface at exposed bars and islands,
- Edge of canopy of permanent woody vegetation >1.5 meters tall,
- Edge of vegetation (green line[3]), and
- Other significant geomorphic features.

To ensure that the ground profile across each transect was adequately described, GPS readings were also taken at all significant breaks in slope. Where no obvious breaks in slope were present, GPS survey points were recorded at a maximum spacing of 15 meters (50 ft).

2.1.5 Unobstructed Channel Width

During the first four years of data collection, a key purpose of collecting the vegetation height data (described in the following section) was to facilitate analysis of the unobstructed channel width that is related to maximum sight distance for whooping cranes. In using these data to compute the sight distance metric, it became apparent that a direct measurement of the maximum distance between visual obstructions on each transect would simplify the analysis, improve the accuracy and reduce the uncertainty of the result. For this reason, the data collection protocol was changed in 2013 to direct measurement. This was accomplished at each of the surveyed transects, as follows:

1. When a substantial opening in vegetation that was greater than 1.5 m (4.9 ft) high occurred along the transect (e.g., bare sand and open water areas, grassy islands, etc.), the location of the edge

[3] Green line is defined in the Monitoring Protocol as the edge of vegetation on a sand bar or adjacent to the wetted channel, defined by at least 25 percent cover of vegetation.

of water at 2,400 cfs on one side of the opening was determined using the RTK GPS, based on the modeled water-surface elevation for the transect.

2. A Simmons LRF 600 laser rangefinder, with magnification set at 4x and reported accuracy of ±3 ft, was held at approximately 4.9 ft (1.5 m) above the ground and the distance to the next obstruction along the transect at that same height was measured and recorded.

When more than one opening occurred along the transect, a measurement was typically taken at each opening, and the largest of the measurements was used as the unobstructed channel width.

2.1.6 Vegetation Survey Methods

Vegetation sampling is conducted along belt transect that are centered on each AP. The total width of each belt transect is approximately 300 meters (1,000-ft), extending for approximately 150 meters (500-ft) upstream and downstream of the AP. During the first four years of data collection, the overall belt transect consisted of seven, roughly parallel, transects spaced approximately 50 meters (165-ft) apart. The upstream, downstream and middle vegetation transects correspond to the three primary geomorphology transects (Figure 2.2). Subsampling and statistical analyses of the large volume of data collected during the first four field seasons showed no significant difference ($p>0.05$ for all analysis) between vegetation data collected at all seven transects versus only five transects when Transects 2 and 6 are removed. Sampling two fewer transects per AP substantially increases the efficiency of the field component of this work, while retaining full comparability to vegetation data collected in prior years. As a result, the Monitoring Protocol was modified in 2013 to eliminate Transects 2 and 6.

The start and end points of the vegetation survey zone (VSZ) along each transect were determined in the field by assessing local vegetation characteristics and topography. Areas identified as out of the active channel were not surveyed. These areas included any portion of the transect dominated by mature woody vegetation having greater than 25 percent tree canopy cover and/or areas that were located topographically above the active channel and dominated by upland vegetation. The first quadrat on each linear transect was sampled at the start of each VSZ. All subsequent quadrats along each linear transect were sampled at regular 15-meter intervals until the end of the VSZ was reached. Occasionally, more than one VSZ was identified on a single linear transect. In these cases, the start and end points of each VSZ were determined as described above. Areas along a transect identified as not within the VSZ were typically upland vegetated islands. Areas within the VSZ that were submerged in water were sampled at standard increments and coded as “water” under community type.

The Daubenmire (1959) canopy cover method was used to collect vegetation data within each quadrat using a 1 square-meter quadrat frame that was placed on the ground at the sample point. All plant species within the quadrat frame and present at greater than trace densities (i.e., >~2% of the quadrat area) were identified, and their cover was documented using Daubenmire cover classes. Plant species were identified primarily using *The Flora of Nebraska* (Kaul et al., 2011), although other field guides [e.g., *Weeds of the Great Plains* (Stubbendieck et al., 2003; *Grasses of Colorado* (Shaw, 2008)] were also referenced where necessary. Plant taxonomy was based primarily on Kaul et al. (2011), but was standardized using the PLANTS Database (USDA-NRCS, 2014) and the National Wetland Plant List (Lichvar et al., 2014).

Evaluation of the sampling methodology has shown that, in many cases, analyzing data composed of individual species can obscure trends and patterns, leading to ineffective hypothesis testing. Additionally, during the earlier years of the monitoring program, data were collected largely to the genus level. To control for these two factors during analysis, related species within a genera have been grouped together because they share similar ecological niches (**Table 2.2**), as determined by their natural history and wetland indicator status (Lichvar et al.,2014). Although the discussion that follows refers frequently to “species”, some vegetation may be referred to at the genus level. The term “species” was retained for consistency with prior years, and is used loosely in this report. Species grouped under shared genera for analysis are as follows:

Table 2.2 Species Grouped as Genera.

Genus	Common Name
Ambrosia sp.	Ragweed species
Ammania sp.	Redstem
Artemisia sp.	Artemisia species
Bidens sp.	Beggarticks species
Chamaesyce sp.	Sandmat
Cyperus sp.	Flatsedge
Echinochloa sp.	Barnyard grass species
Eleocharis sp.	Spikerush
Euphorbia sp.	Euphorbia species
Hackelia sp	Hackelia species
Helianthus sp.	Sunflower
Heterotheca sp.	Heterotheca species
Mentha sp.	Mint species
Polygonum sp.	Polygonum species
Potentilla sp.	Cinquefoil
Rorippa sp.	Yellowcress
Salix sp.	Willow
Schoenoplectus sp.	Bullrush
Solidago sp.	Goldenrod
Typha sp.	Cat-tail
Vernonia sp.	Ironweed

In previous annual reports, five species of primary interest: purple loosestrife (*Lythrum salicaria*), common reed, eastern cottonwood, willow (*Salix* sp.), and cattail (*Typha* sp.), were analyzed in greater detail than other species because of their importance to the overall objectives of the monitoring program. Because cattail has been encountered relatively infrequently, its importance to the Program is less than originally believed. This species continues to be documented but is not analyzed in detail under the data analysis protocol.

Additional data collected at each quadrat included height of herbaceous and woody species, and vegetation community type. All quadrats with quantifiable vegetation cover (those with standing, live vegetation) were photographed and archived. Specific data collected at each quadrat included the following:

- **Spatial data:** Horizontal coordinates and elevation of each quadrat, recorded at the center point with an RTK GPS on the same coordinate system used for the geomorphic data.
- **Plant species:** All plant species present within a quadrat frame at densities greater than approximately 2 percent of the total quadrat area. Vegetation that was dead, standing, and identifiable was recorded as a plant species from 2009 through 2013 if it retained the same structural characteristics as analogous living vegetation. Beginning in 2014, dead, standing

vegetation was recorded as *Percent Dead Organic Matter* to more readily describe vegetation changes due to maintenance activities.

- **Percent cover by species[4]:** Percent cover was recorded in the following *Daubenmire Cover* classes.
    - Cover class 1: 2-5%
    - Cover class 2: 6-25%
    - Cover class 3: 26-50%
    - Cover class 4: 51-75%
    - Cover class 5: 76-95%
    - Cover class 6: 96-100%

- **Areal cover (acres) by species:** Areal cover was quantified by multiplying the percent cover by total area sampled for each plant species.
- **Herbaceous vegetation height:** Herbaceous vegetation height was recorded based on visual estimate of the actual maximum height of herbaceous vegetation in each quadrat. From 2009 through 2012, vegetation height was collected categorically using mean height classes, or directly as a mean height. Beginning 2013, actual maximum height values were recorded to improve data resolution for hypothesis testing. Maximum height data are generally suitable for comparison with data from prior years.
- **Woody vegetation height:** Woody vegetation height was recorded using the same procedures described above for herbaceous vegetation height.
- **Percent dead organic matter**: This parameter represents the percentage of each quadrat covered by dead organic matter, whether standing or downed. During the 2012 and 2013 surveys, *Dead Organic Matter* was quantified only as downed organic matter (e.g., thatch, downed woody debris, etc.). (This parameter was not recorded during the 2009 through 2011 surveys.) Identifiable standing dead vegetation were quantified as living specimens under the *Plant Species* category. Beginning in 2014, dead standing vegetation was instead recorded as *Percent Dead Organic Matter* to more adequately describe vegetation changes due to maintenance activities, particularly spraying of common reed.
- **Percent bare ground**: Beginning in 2012, the percent of each quadrat that is bare, exposed ground with no organic matter, living or dead was recorded as *bare ground*.
- **Vegetation community:** The predominant vegetation community type within the quadrat. Community types were based on *Terrestrial Ecological Systems and Natural Communities of Nebraska* (Rolfsmeier and Steinauer, 2010), although several that were quantified in the field were not officially recognized by this resource (due to the predominance of non-native species). Community types and/or habitat types identified during the 2012 and 2013 vegetation surveys were categorized by the following:
    - Eastern cottonwood – (peachleaf willow)/coyote willow woodland (Rolfsmeier and Steinauer, 2010),
    - Riparian dogwood – false indigo shrubland (Rolfsmeier and Steinauer, 2010),
    - Sandbar willow shrubland (Rolfsmeier and Steinauer, 2010),
    - Sandbar/mudflat (Rolfsmeier and Steinauer, 2010),
    - Russian olive sandbar,

[4] A measure of the degree to which above ground portions of plants cover the ground surface area. The potential presence of more than one vegetation layer in a quadrat allows total cover to exceed 100 percent in some cases, due to foliage overlap.

- o Perennial sandbar (Rolfsmeier and Steinauer, 2010),
- o Freshwater marsh (Rolfsmeier and Steinauer, 2010),
- o Fallow agricultural land,
- o Ruderal upland,
- o Water,
- o Upland community.

All vegetation data were collected using either a Trimble Geo XT or XH datalogger. A data dictionary was developed specifically for this work and uploaded into the datalogger using Trimble GPS Pathfinder Office (version 5.30) software. During field sampling, each quadrat was uniquely identified by capturing the associated AP number, transect number, and quadrat number.

Each AP was surveyed using two teams of two biologists. In general, each survey team was responsible for 2 to 3 transects at each AP, allowing the survey for each AP to be completed in one day, concurrent with the geomorphic surveys.

2.1.7 Sediment Sampling Methods

2.1.7.1 Bed and Bar Material

Up to 10 bulk bed-material samples and at least one composite bar-material sample were collected at each AP in accordance with the Monitoring Protocol. Typically, each transect was subdivided into three segments, and a representative bed-material sample was collected from each segment, insuring that one sample was taken from near the thalweg and the other two taken from the lowest elevation surface in other two segments. Beginning in 2012, the samples were analyzed in Tetra Tech's Fort Collins soils laboratory to determine the particle size gradations. Samples collected by the previous contractor in 2009, 2010 and 2011 were analyzed in a similar manner at a local soils laboratory. The samples were collected using a sampler constructed from a 4-inch diameter by 12-inch long PVC pipe, beveled at one end and covered with a 200-micron mesh at the other end (**Figure 2.3**). In collecting the samples, the sampler was pushed 4 to 6 inches deep at an angle into the bed of the channel at the sampling location. The resulting sample sizes ranged from about 350 g to 3,500 g, and averaged about 800 g to 1,000 g. Since the samples were often collected from below the water, the sampler was oriented with the opening facing upstream so that the water could drain from the sampler with minimal sorting and loss of the sample material. All bed samples collected from the main and secondary channels were transferred to individual sample bags that were labeled with the sampled AP, transect ID, sample number, and date, and the sample locations were determined using an RTK GPS roving unit.

Bar material samples were generally collected at the head of a high bar in the area with the coarsest material. Samples were taken at three different locations on the bar within relatively close proximity to each other to insure that the overall sample site was on the same geomorphic feature. The bar samples were collected with a shovel after noting and removing any armor or coarse lag material. This method results in an accurate estimation of the distribution of bed material mobilized and transported through the reach at flows in the range of the channel-forming discharge. An approximately equal volume of materials was collected at each of the three locations, and the material was placed in one or more sample bags that were labeled with the sampled AP, transect ID, sample number, and the date the sample was taken. The total weights of the bar samples ranged from about 250 to 1,200 g, and averaged about 800 g. A single, georeferenced survey point was taken at the approximate center of the area encompassed by the three sites using one of the RTK GPS roving units.

Figure 2.3. Pipe dredge used to collect bed-material samples.

2.1.7.2 Bed-load and Depth-Integrated Suspended Sediment Sampling

The Monitoring Protocol calls for bed-load and depth-integrated suspended-sediment sampling at the following five bridge locations during pre-defined flow ranges:

- Lexington (SH-L24A/Rd 755),
- Overton (SH-L24B/Rd 444),
- Kearney (SH-44/S. 2nd Ave.),
- Shelton (SH-L10D/Shelton Road), and
- Near Grand Island (US-34/Schimmer Drive).

The target flow ranges and corresponding number of samples was as follows:

- 1,000 to 3,000 cfs – 3 samples,
- 3,000 to 5,000 cfs – 2 samples,
- >5,000 cfs – at least 1 sample, if such flows occur.

In addition, the sampling protocol called for a single depth-integrated suspended sediment sample at each location during the bed-load sampling in the greater than 5,000 cfs flow increment. Beginning in 2012, suspended sediment samples were generally collected in conjunction with the bed load sampling at all flows. In addition, it was not always possible to follow the specific protocol due to flow conditions and access to some of the bridges that were under repair during sampling period. As of the end of the 2016 field season, a total of 85 bed load samples and 92 suspended sediment samples had been collected (**Tables 2.3 and 2.4**).

Table 2.3. Summary of bed-load sediment discharge measurements taken since the start of the monitoring program in 2009. Also shown are the correlation coefficients (R^2) for best-fit, power-function regression lines through each of the data sets.

Sample Location	Discharge Range (cfs)			Total Samples	R^2
	1,000-3,000	3,000-5,000	>5,000		
Darr	10	2	5	17	0.62
Overton	8	8	5	21	0.29
Elm Creek	0	0	1	1	N/A
Kearney	3	5	4	12	0.47
Shelton	8	7	5	21	0.33
Wood River	1	0	1	2	N/A
Grand Island	3	4	4	11	0.58
Total Samples	**33**	**26**	**26**	**85**	

Table 2.4. Summary of suspended sand-load measurements taken since the start of the monitoring program in 2009. Also shown are the correlation coefficients (R^2) for best-fit power-function regression curves through each of the data sets.

Sample Location	Discharge Range (cfs)			Total Samples	R^2
	1,000-3,000	3,000-5,000	>5,000		
Darr/Lexington	13	1	5	**19**	0.68
Overton	10	7	6	**23**	0.69
Elm Creek	0	0	1	**1**	N/A
Kearney	5	2	5	**12**	0.77
Gibbon	0	0	1	**1**	N/A
Shelton	10	5	6	**21**	0.68
Wood River	1	0	1	**2**	N/A
Grand Island	5	3	5	**13**	0.77
Total Samples	**44**	**18**	**30**	**92**	

2.2 Data Analysis Methods

The basic data collected during the field program were evaluated in accordance with the draft Data Analysis Plan (PRRIP, 2012a).

2.2.1 Spatial and Temporal Scales

The Data Analysis Plan specifies that the data are to be evaluated at a range of spatial and temporal scales. The relevant *spatial* scales include the following:

- Transect—analyses to be summarized (i.e., mean and standard deviation) by transect. The draft Data Analysis Plan specifies that vegetation data are to be collected at seven transects that are spaced approximately 165-ft apart, and the geomorphic data are to be collected at three of these transects. This protocol was followed in 2009, 2010 and 2011. During 2012, geomorphic data were collected at all seven transects. As described elsewhere in this document, statistical analysis indicates that the information obtained from only five transects is essentially the same as that obtained from seven transects; thus, geomorphic and vegetation data were collected at five transects at each AP from 2013 through 2016.

- AP—analyses to be summarized (mean and standard deviation) by anchor point, with one summary for anchor point transects on the main channel, and a second summary for all side channel transects that occur at the anchor point. AS noted above, there are 40 anchor points spaced approximately 2.5 miles apart from Lexington to Chapman.
- Complex—analyses to be summarized for each of the following Platte River Recovery Implementation Program complexes: Plum Creek (AP35, AP36, AP37), Cottonwood Ranch (AP32, AP33), Elm Creek (AP29, AP30), Fort Kearney (AP22, AP23), and Shoemaker Island (AP12). Average and standard deviation will be reported for complex anchor points, and separately for non-complex anchor points.
- Bridge segment—analyses to be summarized (mean and standard deviation) by bridge segment: Lexington to Overton, Overton to Elm Creek, Elm Creek to Odessa, Odessa to Kearney, Kearney to Newark, Newark to Shelton, Shelton to Wood River, Wood River to Grand Island, and Grand Island to Chapman. The main channel will be summarized separately from the side channels.
- Geomorphic reach—reach-averaged results (mean and standard deviation) to be summarized by reach, based on reaches with consistent planform, as characterized in Fotherby (2008) (**Table 2.5**).
- System—analyses to be summarized (mean and standard deviation) for the overall study reach from Lexington to Chapman (i.e., all anchor points). The main channel will be summarized separately from the side channels.

The relevant *temporal* scales include the following:

- Annual—Main channel transect data at the 20 pure-panel anchor points that are monitored annually were reduced and analyzed each year.
- Four-year (rotating panel and side channels)—Data for side channels at the pure-panel APs were initially collected in 2009 and 2013. The data from the rotating panel points were reduced and summarized as part of the annual report for the year in which they were collected, and a final summary is presented in this report.
- First Increment—All data collected for this Program were to be analyzed after the 2019 monitoring season to assess the change in each of the metrics over the course of the First Increment. With the Program's decision to end the current data collection protocol with the 2016 season, this report provides a final summary of 8 annual data sets (2009-2016).

2.2.2 Performance Metrics

A suite of 38 individual performance metrics that can be quantified from the field data from this program and other available data sources were identified for use in evaluating trends in channel morphology and in-channel vegetation for purposes of answering the Big Questions and testing the priority hypotheses (**Table 2.6**). As shown in the table, these metrics fall into six general categories: Hydrologic, Hydraulic, Geomorphic, Vegetation, Sediment, and Whooping Crane. A brief description of the data and methods that were used to quantify each of the metrics is provided in the following sections. Specific definitions and criteria are spelled out in more detail in the draft Data Analysis Protocol (PRRIP, 2012a).

Table 2.5. Geomorphic Reaches from Fotherby (2008).

Reach	Description	River Miles	Main Channel AP	Side Channel AP
1	Lexington Bridge to Overton Bridge (including north channel of Jeffrey Island)	239.5-254.5	38 to 40; 37a, 36b, 35a	None
2	South channel of Jeffrey Island from J2 Return to Overton Bridge	239.5-247	37a, 36b, 35b	37b, 36a, 35b
3	Overton Bridge to Elm Creek Bridge	231-239.5	31, 32a, 33a, 34	32b-c, 33b-c
4	Elm Creek Bridge to Odessa Bridge	224-231	28-30	None
5	Odessa Bridge to Minden	208-231	22a, 22b, 23a, 24-27	23bS, 23bN
6	Minden to Gibbon Bridge	202-207	20a, 21a	20b, 21bS, 21bN
7	Gibbon Bridge to Wood River	187.5-202	14-18, 19a	19b
8	Wood River to Grand Island	173-187.5	8a, 9a, 10a, 11a, 12a, 13a	8b-c, 9bS, 9bN, 9c, 10b-c, 11b, 12b, 13b
9	Grand Island to Chapman	156.5-173	1-5, 6b, 7a	6a, 7bS, 7bN, 7c

Table 2.6. Performance metrics defined in the Channel Geomorphology and In-channel Vegetation Data Analysis Plan.

Variable/ Relationship	Monitoring Plan Section	Definition	Type	Reporting Scale	
				Temporal	Spatial
Hydrologic Performance Measures					
Q_P	5.1.1	Annual instantaneous peak discharge (1/1-7/31)	Value	Annual	By Gage
DUR_{5000}	5.1.1	Duration of Q>5,000 cfs	Value	Annual	By Gage
FDC_{Ger}	5.1.2	Flow duration curve for germination season (6/1-7/15)	Curve	Annual	By Gage
Q_{Ger}	5.1.2	Germination season discharge (Q_{Mean} 6/1-7/15)	Value	Annual	By Gage
Q_{WC_Spring}	5.1.3	Spring Whooping Crane migration discharge (Q_{mean} 3/21-4/29)	Mean Value	Annual	By Gage
Q_{WC_Fall}	5.1.3	Fall Whooping Crane migration discharge (Q_{mean} 10/9-11/10)	Mean Value	Annual	By Gage
FDC_{WC_Spring}	5.1.4	Spring Whooping Crane migration flow duration curve (3/21-4/29)	Curve	Annual	By Gage
FDC_{WC_Fall}	5.1.4	Fall Whooping Crane migration flow duration (10/9-11/10)	Curve	Annual	By Gage
Hydraulic Performance Measures					
Stg-Q	5.2.1	Stage-discharge rating curves for 500 cfs <= Q <= 8,000 cfs	Curve	Annual	AP Transect
Geomorphic Performance Measures					
BI	5.3.1	Braiding index	Value	By Survey[1]	Anchor Point and Subreach
W_T	5.3.2	Total channel width @ 1,200 cfs	Value	By Survey[1]	Transect and Anchor Point
$W_{T\text{-}Wetted}$	5.3.3	Wetted Channel Width (Total channel width (W_T)-Total width above 1,200 cfs WSEL)	Value	By Survey[1]	Transect and Anchor Point

Variable/ Relationship	Monitoring Plan Section	Definition	Type	Reporting Scale	
				Temporal	Spatial
D_H	5.3.4	Average channel depth (Cross sectional area @ 1,200 cfs / $W_{T\text{-Wetted}}$)	Value	By Survey[1]	Transect and Anchor Point
D_{Max}	5.3.5	Maximum channel depth (WSEL @ 1,200 cfs – Thalweg Elevation)	Value	By Survey[1]	Transect and Anchor Point
W/D	5.3.6	Wetted channel width ($W_{T\text{-Wetted}}$)/Maximum Channel Depth	Value	By Survey[1]	Transect and Anchor Point
ΔA_i	5.3.7	Change in cross sectional area @ 1,200 cfs from previous survey	Value	By Survey[1]	Transect and Anchor Point
ΔA_t	5.3.7	Change in cross sectional area @ 1,200 cfs from 2009 survey	Value	By Survey[1]	Transect and Anchor Point
LProf	5.3.8	Plot of longitudinal thalweg profile by ACOE River Mile (2009 and 2019, only)	Curve	2009, 2019	Reach
Vegetation Performance Measures					
GLE	5.4.1	Green line elevation (edge of 25% cover)	Value	By Survey[1]	Transect and Anchor Point
W_{Unveg}	5.4.2	Cumulative distance between pairs of GLE points within main channel, by transect	Value	By Survey[1]	Transect and Anchor Point
$f_{species}$	5.4.3	Frequency of occurrence for each species of interest and/or 25 most common species in current year	Value	By Survey[1]	Transect and Anchor Point
%Cover	5.4.4	Percent cover for each species of interest and/or 25 most common species in current year	Value	By Survey[1]	Transect and Anchor Point
$AC_{Species}$	5.4.5	Aerial cover occupied by each species of interest and/or 25 most common species in current year (Surface Area of AP X %Cover)	Value	By Survey[1]	Anchor Point

Variable/ Relationship	Monitoring Plan Section	Definition	Type	Reporting Scale	
				Temporal	Spatial
$\bar{E}_{Species}$	5.4.6	Mean elevation by species of interest and/or 25 most common species in current year	Value	By Survey[1]	Transect and Anchor Point
$H_{species}$	5.4.7	Mean vegetation height (not species specific)	Value	By Survey[1]	Transect and Anchor Point
Sediment Performance Measures					
Q_{s_bed}-Q	5.5.1	Bed-load versus discharge rating curve	Scatter Plot and Fitted Curve	Cumulative by sampling event	Five specified locations
Q_{s_susp}-Q	5.5.2	Suspended-sediment load versus discharge rating curve	Scatter Plot and Fitted Curve	Cumulative by sampling event	Five specified locations
GSD_{bed}	5.5.3	Bed material grain-size distribution curve of percent finer by weight	Curve	By Survey[1]	Transect and Anchor Point
GSD_{bar}	5.5.4	Bar material grain-size distribution curve of percent finer by weight	Curve	By Survey[1]	Transect and Anchor Point
GSD_{bank}	5.5.5	Bank material grain-size distribution curve of percent finer by weight	Curve	By Survey[1]	Transect and Anchor Point
$D_{50\_bed, bar, bank}$	5.5.3-.5	Median size of bed, bar and bank distributions	Value	By Survey[1]	Transect and Anchor Point
$D_{16\_bed, bar, bank}$	5.5.3-.5	16th percentile size of bed, bar and bank distributions	Value	By Survey[1]	Transect and Anchor Point
$D_{84\_bed, bar, bank}$	5.5.3-.5	84th percentile size of bed, bar and bank distributions	Value	By Survey[1]	Transect and Anchor Point

Variable/ Relationship	Monitoring Plan Section	Definition	Type	Reporting Scale	
				Temporal	Spatial
$G_{bed,\ bar,\ bank}$	5.5.3-.5	Gradation coefficient for bed, bar and bank material samples ($G_i=D_{84}/D_{50}+D_{50}/D_{16}$)	Value	By Survey[1]	Transect and Anchor Point
Whooping Crane Performance Metrics					
W_{c_unobs}	5.6.1	Maximum distance in main channel between obstructions higher than 4.9 ft above 2,400 cfs WSEL	Value	By Survey[1]	Transect and Anchor Point
$W_{c\_unobs\_S}$	5.6.1	Maximum distance in main channel between obstructions higher than 4.9 ft above Q_{WC_Spring}	Value	By Survey[1]	Transect and Anchor Point
$W_{c\_unobs\_F}$	5.6.1	Maximum distance in main channel between obstructions higher than 4.9 ft above Q_{WC_Fall}	Value	By Survey[1]	Transect and Anchor Point
$W_{D<8\_in}$	5.6.2	Maximum width in main channel with flow <8" deep, including exposed sandbars	Value	By Survey[1]	Transect and Anchor Point

[1]Annual for Pure Panel Points/every 4 years for rotating points

2.2.2.1 Hydrologic Performance Metrics

Data for eight hydrologic (or flow-related) performance metrics were derived primarily from the following gages that are maintained and operated by the U.S. Geological Survey (USGS) or the Nebraska Department of Natural Resources (NDNR):

- Platte River at Lexington (NDNR 228400)[5],
- Platte River near Overton (USGS 06768000),
- Spring Creek near Overton (USGS 06768020),
- Buffalo Creek near Overton (USGS 06769000),
- Elm Creek near Elm Creek (USGS 06769525),
- Platte River near Kearney (USGS 06770200),
- Platte River near Shelton (NDNR 229300), and
- Platte River near Grand Island (USGS 06770500).

In the 2012 annual report, the Platte River near Odessa gage (NDNR 6770000) was also used; however, further evaluation of the data from that gage shows inconsistencies that make the data suspect for purposes of this study, particularly at high flows. For this reason, data from the Odessa gage are not used in the analysis.

Data for the USGS gages were obtained from the National Water Information System (NWIS) website (http://waterdata.usgs.gov/nwis), and data for the NDNR gages were obtained from the NDNR real time gage index website (http://data.dnr.nebraska.gov/RealTime/Gage/Index). The specific values of the seven hydrologic performance metrics were computed by estimating a mean daily flow record for each AP using distance-weighted interpolation between each of the mainstem gages, adjusting for gaged tributary inflows and ungaged losses or gains between the mainstem gages. The ungaged rate of gain or loss in each segment of the reach was estimated by taking the difference between the corresponding mean daily flows at the mainstem gages, subtracting the reported tributary inflows or adding the reported diversions (at the Kearney Canal Diversion), as appropriate, and dividing the remainder by the length of the segment.

The following specific clarifications to the DAP were employed in computing the hydrologic performance metrics:

- The annual peak flow event discharge (DAP 5.1.1; Q_P) was defined as the maximum mean daily discharge between January 1 and the date of the respective surveys during each year. The maximum mean daily flow is being used because instantaneous peak flow data are not available at all locations, and from a riverine process perspective, the mean daily discharge is a more meaningful value because it occurs for a sufficient duration to do work within the channel.
- DAP 5.1.2 defines the germination season discharge exceedance as *the frequency of flows within the April 1 to July 31 germination season*. Because a key use of this metric is to assess the effects of flow on cottonwood germination and persistence, the time-frame was modified to June 1 through July 15 to more closely correspond to the timing of cottonwood seed dispersal and germination. Although the duration of discharges is important, a specific, representative discharge during the germination season is also necessary to facilitate the trend analyses. As a

[5] In some cases, data from the Cozad gage (NDNR 6466500 for 1992 and later; USGS Gage No. 06766498 prior to 1992).

result, the representative germination season discharge (Q_{GER}) was defined as the mean discharge during the period.

2.2.2.2 Hydraulic Performance Metrics

The hydraulic performance metrics consist of stage versus discharge relationships at the transects that make-up each of the APs. These relationships were developed by making multiple-profile runs with the 1-D hydraulic model that uses the available channel geometry that is most applicable to each annual data set. The original model was based primarily on the 2009 LiDAR data and the transect survey data from the initial 2009 survey for this monitoring program, supplemented with other available survey data that had been collected in specific locations for other purposes. Certain of the geomorphic performance metrics from the 2012 and 2013 data appeared to be unreasonable, suggesting that the channel geometry had changed sufficiently since 2009 so that the relationships were no longer valid. As a result, the model was updated using the 2012 LiDAR and survey data, and the updated model was used to quantify the hydraulic performance metrics for the 2012 through 2016 data sets.

2.2.2.3 Geomorphic Performance Metrics

The geomorphic performance metrics include nine specific measures of channel geometry and form. Eight of the nine metrics were quantified for the original three years of data collected by the previous contractor and the 2012 through 2016 data collected by Tetra Tech. Data for the 9th metric (longitudinal thalweg profile) were only collected in 2009 as part of the initial surveys.

In quantifying the metrics, one relatively minor deviation from the draft Data Analysis Plan was employed. Total channel width is defined in the DAP as total channel width at 1,200 cfs, including non-wetted areas (e.g., exposed sand bars, and vegetated islands), but excluding ineffective flow areas. After evaluating the data in more detail for the 2012 data set, Tetra Tech recommended that the ineffective flow areas should be included in the width calculations, and Program staff agreed to the change (Jason Farnsworth, personal communication, March 2013).

2.2.2.4 Vegetation Performance Metrics

The vegetation performance metrics are quantified directly from the field data. Although over 170 individual species have been identified during the field surveys, the analysis considered only the 25 most frequently observed during the each sampling year, based on data collected in the main channel at the Pure Panel APs, and at APs 35b and 37b in Reach 2, due to their relationship with the J-2 Return (**Table 2.7**). In cases where species of interest (see Section 1.2.5 for species list) were not among the 25 most frequently observed species, they were also included to maintain consistency with analyses from prior years. Data for all documented species have been retained in the master dataset and are available for additional analysis.

Hypotheses testing and trend analyses were restricted to a select subset of four of the species of interest: purple loosestrife, common reed, eastern cottonwood, and willow (*Salix exigua* and *S. amygdaloides* combined). These taxa were chosen because of their rapid growth rate, colonization of bars and wide distribution in the Platte River system. Other taxa were excluded from the analysis to streamline the statistical calculations that support hypothesis testing and trend analysis.

Table 2.7. Species considered in the analyses—the 25 most frequently observed species in 2015, and species of interest observed at lower frequencies.

Scientific Name	Common Name	Wetland Indicator Status[1]	Native (Y/N)[2]
Cyperus sp.	Flatsedge	NA	Yes
Xanthium strumarium	Rough cockleburr	FAC	Yes
Bidens sp.	Beggarticks species	NA	Yes
Eragrostis sp.	Lovegrass	NA	Yes
Phalaris arundinacea	Reed canary grass	FACU	Yes
Polygonum sp.	Polygonum species	NA	Both
Leptochloa fusca	Sprangletop	FACW	Yes
Ambrosia sp.	Ragweed species	FACU	Yes
Populus deltoides	Eastern cottonwood	FAC	Yes
Amaranthus retroflexus	Redroot amaranth	FACU	Yes
Echinochloa sp.	Barnyard grass species	NA	Both
Phragmites australis	Common reed	FACW	Yes
Spartina pectinata	Freshwater cord grass	FACW	Yes
Panicum sp.	Panic grass	NA	Yes
Carex sp.	Sedge	NA	Yes
Lythrum salicaria	Purple loosestrife	OBL	No
Rumex sp.	Dock species	NA	Both
Bolboschoenus fluviatilis	River bulrush	OBL	Yes
Salix sp.	Willow	NA	Yes
Mollugo verticillata	Green carpetweed	FAC	Yes
Amorpha fruticosa	False indigo-bush	FACW	Yes
Eclipta prostrata	False daisy	FACW	Yes
Phyla lanceolata	Fogfruit	FACW	Yes
Verbena hastata	Blue Vervain	FACW	Yes
Elaeagnus angustifolia	Russian olive	FACU	No
Leersia oryzoides	Rice cut grass	OBL	Yes
Setaria viridis	Green bristlegrass	NL	No

[1] *Source: North American Digital Flora: National Wetland Plant List (Lichvar and Kartesz 2012); Midwest Region; National Wetland Plants List (Lichvar et al., 2014)*
[2] *Source: PLANTS Database (USDA-NRCS, 2014)*
[3] *Program species of special interest*

Evaluation of the vegetation performance metrics provides at least three essential insights that facilitate understanding of the ecology of the study area and guide management actions, as follows:

1. Describes baseline conditions,
2. Provides a basis for tracking ecosystem changes through time, and
3. Provides a benchmark to measure response to experimental management actions.

Vegetation performance metrics for each survey year were partially examined in the various annual reports (Ayres and Olsson, 2010, 2011, 2012; Tetra Tech 2013, 2014, 2015, 2016).

2.2.2.5 Sediment Performance Metrics

The sediment performance metrics fall into two general categories:

- Sediment-transport rates
- Bed-, bar- and bank-material particle-size gradations

The sediment-transport data from the 2009, 2010 and 2011 data collection efforts were reduced and plotted in the form of sediment discharge rating curves to support a variety of sediment-transport analyses, including the modeling that was conducted for the Sediment Augmentation Feasibility Study (Tetra Tech, 2010) and the Elm Creek FSM Experiment (Tetra Tech, 2012). These rating curves were updated after each subsequent sampling year with the new measurements. Performance metrics related to bed and bar material were quantified after each field season. Bank material samples were only collected during the first year of the monitoring program.

2.2.2.6 Whooping Crane Performance Metrics

The whooping crane performance metrics are intended to quantify the available sight distances and associated channel widths within the channel corridor. These metrics are based on a combination of direct measurements of unobstructed widths (2013 and later data), vegetation height data (2009 through 2012) and hydraulic model results. The hydraulic model results were used to quantify the widths of the channel that consist of either bare sand or flow depths of less than 8 inches at a discharge of 2,400 cfs and at the whooping crane migration season discharges[6]. As discussed in the 2012 annual report (Tetra Tech, 2013), there are at least two significant challenges in quantifying these metrics with the 2009-2012 data:

1. Vegetation heights were not collected in a consistent manner across years; thus, interpretation of the data is confounded by differences in the data sets,
2. The data were collected in broad categories of vegetation heights which introduces significant uncertainty into the actual height of the vegetation.

2.2.3 Trend Analysis

For the 2012 annual report, a broad range of statistical comparisons were made across the 2009 through 2012 data sets to identify trends in the geomorphic, vegetation and sediment variables (**6**). This resulted in a large number of analyses that are difficult to interpret in the context of Program priorities. Beginning with the 2013 annual report, the Program directed that the trend analysis be restricted to the following priority hypotheses to provide a more focused analysis:

1. <u>Flow 1</u> –A detailed analysis of changes in bed sediment volume within the main channel was conducted for each of the 8 years of available data, and the results were evaluated in the context of the sediment balance along the overall study reach. In presenting the analysis, the variability in sediment loads (and the resulting sediment balance) and the implications of this variability to conclusions about the aggradation/degradation status of each portion reach, including the magnitude of any identified sediment transport imbalance, were evaluated
2. <u>Flow 3</u> –The correlation between flow, green line elevation (GLE) and unvegetated width was evaluated. As specified in the Data Analysis Plan (**Table 2.8**), the edges of unvegetated segments along each transect were identified by the GLE points. The total unvegetated width was then defined as the cumulative length of all unvegetated segments between GLE points within the main channel at each transect. To remove the effects of river slope in the correlations, the difference between the GLE and the local 1,200 cfs water surface was used rather than the

[6] Average, mean daily discharge during the period from March 21 through April 29 for the spring migration season and October 9 through November 11 for the fall migration season.

actual elevation. The following specific correlations were evaluated using the metrics defined in this manner:

a. GLE versus annual peak discharge (Q_p, Monitoring Plan Section 5.1.1), defined as the maximum mean daily discharge between January 1 and the date of the survey in each year.

b. GLE versus germination season discharge (Q_{Ger}, Monitoring Plan Section 5.1.2), defined as the representative mean daily discharge between June 1 and July 15 (the primary season for establishment of cottonwood seedlings). For this analysis, both the mean and median discharge during the period were evaluated to assess which one provides the best correlation.

c. Total unvegetated width (W_{unveg}) versus annual peak discharge (Q_{Ger}).

d. Total unvegetated width (W_{unveg}) versus germination season discharge (Q_{Ger}).

e. GLE versus total unvegetated width (W_{unveg}).

3. Flow 5 –The influence of spraying versus peak flows on phragmites distribution and frequency were evaluated using vegetation plot data in conjunction with Geodata Interoperability Specification (GIS)-formatted records of annual spraying.

4. Mechanical 2 –The correlation between total unvegetated width (W_{unveg}), braiding index (BI) and percent consolidation at bankfull discharge was evaluated.

Table 2.8. Summary of Trend Analysis Specified in the Data Analysis Plan.

Analysis Plan Section	Specified Analysis	Performance Metrics		Spatial Analysis Scale	
		Variable	Analysis Plan Section	Geomorphic Reach	System
6.1	**Analyses for Broad Hypotheses S-1, S-2, and S-4**				
6.1.1.1	Braiding Index Trend Analysis	BI	5.3.1	X	X
6.1.1.2	Aggradation/Degradation Trend Analysis	DA	5.3.7	X	X
6.1.1.3	Total Channel Width Trend Analysis	W_T	5.3.2	X	X
6.1.1.4	Wetted Channel Width Trend Analysis	$W_{T\text{-}Wetted}$	5.3.3	X	X
6.1.1.5	Unvegetated Channel Width Trend Analysis	W_{Unveg}	5.4.2	X	X
6.1.1.6	Width-to-Depth Ratio Trend Analysis	W/D	5.3.6	X	X
6.2	**Analyses for Broad Hypothesis PP-1**				
6.2.1	Relationship between Annual Peak Flow and Unvegetated Channel Width	W_{Unveg}, Q_P	5.4.2, 5.1.1	X	X
6.2.2	Relationship between Germination Season Discharge and Unvegetated Channel Width	W_{Unveg}, Q_{PGer}	5.4.2, 5.1.2	X	X
6.3	**Analyses for Broad Hypothesis PP-2**				
6.3.1	Relationship between Sediment Augmentation and Channel Volume Change	DAi, V_{SedAug}	5.3.7*	N/A	N/A
6.3.2	Relationship between Sediment Augmentation and Braiding Index	BI, V_{SedAug}	5.3.7*	N/A	N/A
6.3.3	Relationship between Sediment Augmentation and Total Channel Width	W_T, V_{SedAug}	5.3.7*	N/A	N/A
6.3.4	Relationship between Sediment Augmentation and Width-to-Depth Ratio	W/D, V_{SedAug}	5.3.7*	N/A	N/A
6.4	**Analyses for Priority Hypothesis Flow 3**				
6.4.1	Relationship between Annual Peak Flow and GLE	GLE, Q_P	5.4.1, 5.1.1	X	X
6.4.2	Relationship between GLE and 1,200 cfs WSEL	GLE, $WSEL_{1200}$	5.4.1, 5.2.1	X	X
6.4.3	Relationship between GLE and Unvegetated Channel Width	GLE, W_{Unveg}	5.4.1, 5.4.2	X	X
6.5	**Analyses for Priority Hypothesis Flow 5**				
6.5.1	Relationship between annual peak flow and mean vegetation elevation by species	$\bar{E}_{species}$, Q_P	5.4.6, 5.1.1	X	X
6.5.2	Relationship between germination season discharge and mean vegetation elevation by species	$\bar{E}_{species}$, Q_{PGer}	5.4.6, 5.1.2	X	X
6.6	**Analyses for Priority Hypothesis Sediment 1**				
6.6.1	Relationship between Sediment Augmentation and trends in bed and bar grain size distribution	D_i, V_{SedAug}	5.5.3, 5.5.5*	N/A	N/A
6.7	**Analyses for Priority Hypothesis WC-X**				
6.7.1	Analysis of Wetted Widths across a Range of Discharges	$W_{T\text{-}Wetted}$	5.6.2	X	X
6.7.2	Analysis of Portion of Channel with flow depth <8in. at a range of discharges	$W_{D<8\_in}$	5.6.2	X	X
6.8	**Analyses for Vegetative Species of Interest**				
6.8.1	Frequency of Occurrence Trend Analysis	$f_{species}$	5.4.3	X	X
6.8.2	Percent Cover Trend Analysis	% Cover	5.4.4	X	X
6.8.3	Aerial Coverage Trend Analysis	$AC_{Species}$	5.4.5	X	X

* Sediment augmentation volume developed from sediment augmentation monitoring records.

Page Intentionally Left Blank

3 RESULTS

The performance metrics for the 2009 through 2016 data were quantified using the procedures described in Chapter 2. As noted, the specific definition of some of the metrics have been changed from the original definitions to better represent the intent of the analysis. Associated adjustments to the values were made for all years of data. The hydrologic, geomorphic and selected vegetation metrics are summarized in **Appendices A through C**, respectively**.**

3.1 Hydrologic Metrics

To facilitate quantification of the suite of hydrologic performance measures, a record of mean daily flows from October 1, 2008 through the date of the last 2016 monitoring survey was compiled for all of the USGS and NDNR mainstem and tributary gages within the reach (Figure 1.1). These flow records were then used to estimate an equivalent record for each of the APs by distance-weighted interpolation between the measured mainstem flows, taking into account measured tributary inflows and diversions, as described in Chapter 2. Flow-duration curves at the mainstem gages for each the flow-duration related metrics are provided in Appendix A.

3.1.1 Annual Peak Flow Event Discharge and Duration (DAP 5.1.1)

The maximum mean daily flows between January 1 and the surveys (Q_P) during 2009, 2012 and 2013 were in the range of 1,500 to 2,000 cfs upstream from Overton and the confluence of the north and south channels at Jeffreys Island, and 3,000 to 4,000 cfs downstream from Overton (**Figure** 3.1). The flows were much higher in 2010, 2011, 2014, and 2016 generally ranging from 7,000 to 8,500 cfs in 2010 and 2016, from 7,200 cfs to over 10,000 cfs in 2011, and from 6,000 to 8,000 cfs in 2014. Flows in 2015 were the highest since program inception, with flows exceeding 15,000 cfs at all APs downstream from Overton. During the five high-flow years, the maximum mean daily discharge tended to increase in the downstream direction. Maximum mean daily flows from the J-2 Return into the south channel at Jeffreys Island (Geomorphic Reach 2) were in the range of 1,800 cfs to 2,000 cfs during all eight years.

The maximum mean daily discharge did not exceed 5,000 cfs (DUR_{5000}) at any location in the reach during the runoff season prior to each of the 2009, 2012, and 2013 surveys. In 2010, flow exceeded 5,000 cfs for six days upstream from Overton and for 15 to 17 days downstream from Overton (**Figure 3.2**). During the sustained high-flow period in 2011, the discharge exceeded 5,000 cfs for about 50 days upstream from Overton, and between 65 and 70 days downstream from Overton. At Overton, flows were above 5,000 cfs from May 24 until July 27. During 2014, the maximum mean daily discharge exceeded 5,000 cfs for at least 4 days throughout the entire reach, with a maximum duration of eight days (at 14 APs). In 2015, flow at every AP exceeded 5,000 cfs for between 47 days and 54 days. The 2015 flood, while greater in magnitude, was shorter in duration than the 2011 high flows. In 2016, discharge exceeded 5,000 cfs for at least 50 days at every AP downstream from Overton. The USGS gage at Grand Island recorded mean daily discharge above 5,000 cfs every day from April 27 to June 24.

To place the flows during the 8-year monitoring period into the context of the longer-term flow regime, the annual runoff at the USGS Overton gage for the available 75-year record from 1942 to 2016 were ranked and subdivided into wet, normal, or dry years based on their ranking within the top, middle and lower third of the data set. The total annual runoff in 2009 and 2013 fell in the lower third 586,000-acre-ft and 607,000 ac-ft, respectively, and were classified as “dry” years. Five years (2010-2012[7], and 2015-2016) fell in the upper third, ranging from about 1.25M acre ft (2012) to 2.29M

[7] The classification of 2012 as “wet” may seem contradictory to the other hydrologic analyses in this section. However, while the 2012 summer flows were particularly dry (the total runoff between April and September

acre-ft (2015) of total runoff, and were classified as “wet” years. Three of the “wet” years were among the top 10 wettest years on record: 2011 (4th), 2015 (6th), and 2016 (8th). Water Year 2014 was classified as “normal”, with total runoff of 978,000 acre ft.

Based on these rankings, the 8-year monitoring program was conducted during a relatively wet cycle. The average annual runoff during the period of 12M ac-ft ranked in the top 20 percent of 8-year running averages for the period of record. Periods with higher 8-year running average runoff include 1974[8] through 1977 and 1984 through 1991. It is also interesting to note that 2009 ended the 8-year period with the lowest average runoff during the period of record.

2012 ranked 52nd of 75 water years), the winter flows between October 2011 and March 2012 were the seventh wettest on record.

[8] Listed by the last year of the average (e.g., 1974 is the average of 1969 through 1974).

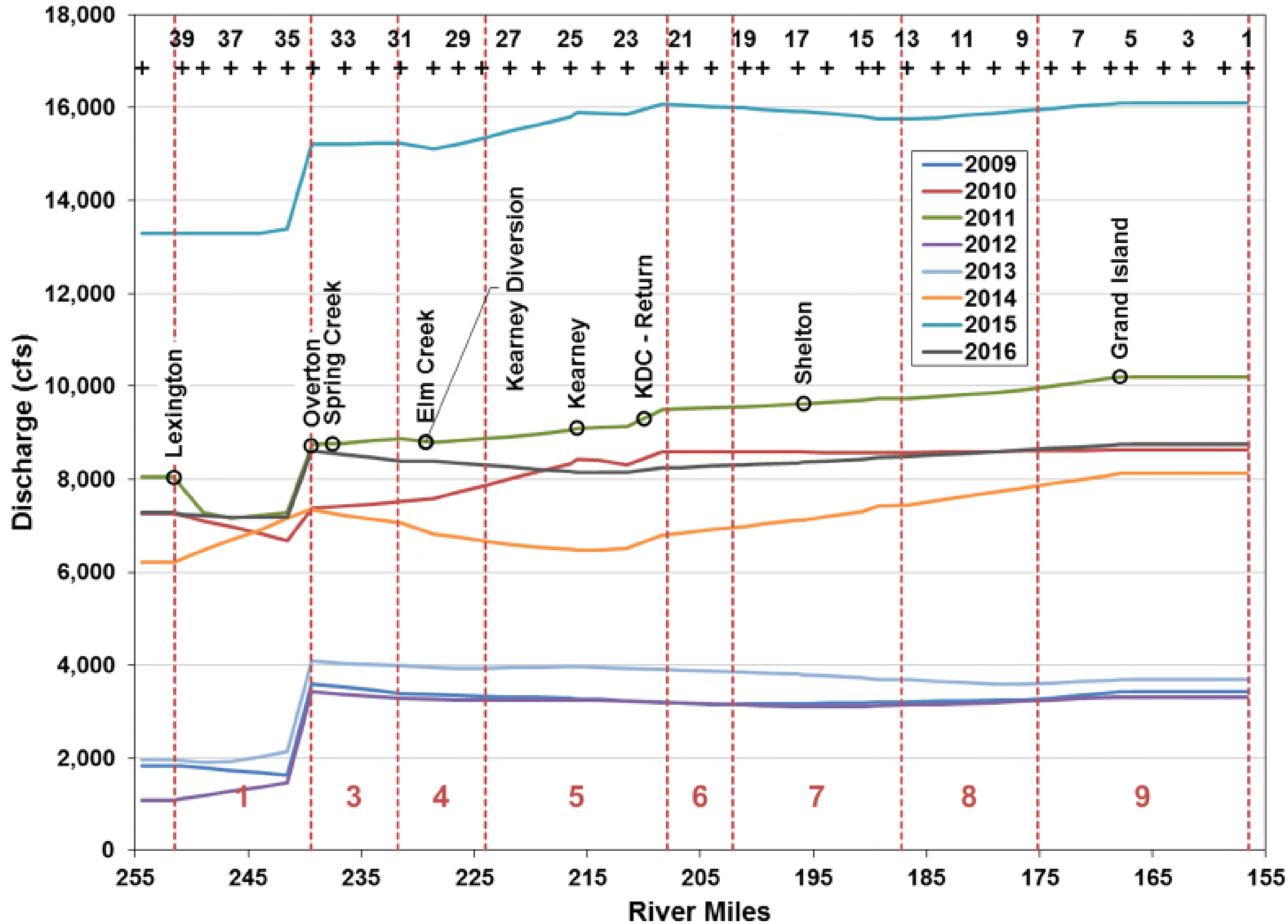

Figure 3.1. Maximum mean daily discharge (Q_P) between January 1 of and the end of monitoring surveys for each year, 2009-2016.

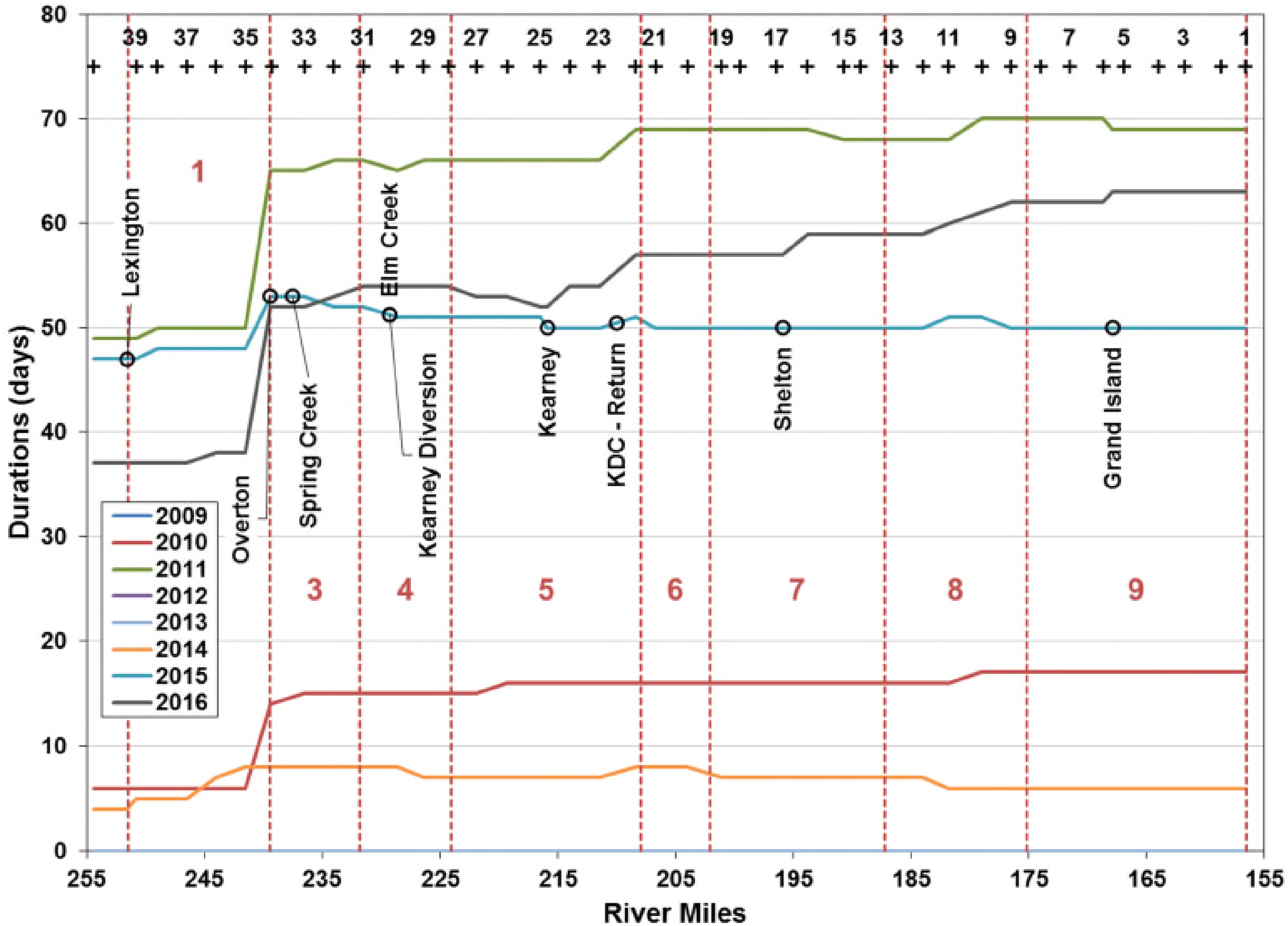

Figure 3.2. Duration of flows exceeding 5,000 cfs between January 1 and the dates of the monitoring surveys (DUR_{5000}) for each year, 2009-2016. (Note that flows did not exceed 5,000 cfs anywhere in the reach during 2009, 2012 and 2013.)

3.1.2 Germination Season Discharge (DAP 5.1.2)

Consistent with the annual runoff volumes, the mean discharge during the germination season (Q_{GER}, defined as June 1 through July 15 for purposes of this study) was relatively low during 2009, 2012 and 2013 (generally less than 1,000 cfs throughout the reach), intermediate during 2010, 2014 and 2016 (~2,500 cfs to 5,000 cfs downstream from Overton) and relatively high in 2011 and 2015 (~7,000 cfs to 7,500 cfs and ~10,000 cfs downstream from Overton, respectively) (**Figure 3.3**).

3.1.3 Spring and Fall Whooping Crane Migration Season Discharge (DAP 5.1.3)

Discharge at the APs during the spring whooping crane migration season (Q_{WC_Spring}, defined as March 31 through April 29 for purposes of this study) were similar, in the range from 1,200 cfs to about 1,800 cfs downstream from Overton, for all years except 2011 and 2016. (**Figure 3.4**). From Jeffreys Island to the upstream end of the monitoring reach, flows ranged between 240 and 680 cfs for all years except 2011, when the flows were about 2,000 cfs. During 2016, the flow downstream from Overton ranged from about 2,500 cfs to 3,000 cfs, and in 2011, flows ranged from about 3,600 cfs to 4,400 cfs.

Fall whooping crane migration season discharges (Q_{WC_Fall}, defined as the average mean daily discharge between October 9 and November 10) can be divided into three general groups (low flows in 2012 and 2014, high flows in 2011, and intermediate in all other years (**Figure 3.5**). During all five years, average flow was between 1,500 and 2,500 cfs between Overton and Shelton, and between 1,500 and 2,000 cfs downstream from Shelton. Upstream from Overton, flows were generally less than 500 cfs for all 5 years. The driest fall for the monitoring program occurred in 2012, with average flows below 500 cfs for the entire reach. The fall flows were slightly higher in 2014, with average flows at or below 850 cfs for the entire reach. Consistent with the other discharge metrics, the fall whooping crane migration season discharge was much higher throughout the reach in 2011, ranging from 1,200 cfs to nearly 1,500 cfs upstream from Overton, and from about 3,200 to 3,700 cfs downstream from Overton, with a general trend of increasing discharge in the downstream direction.

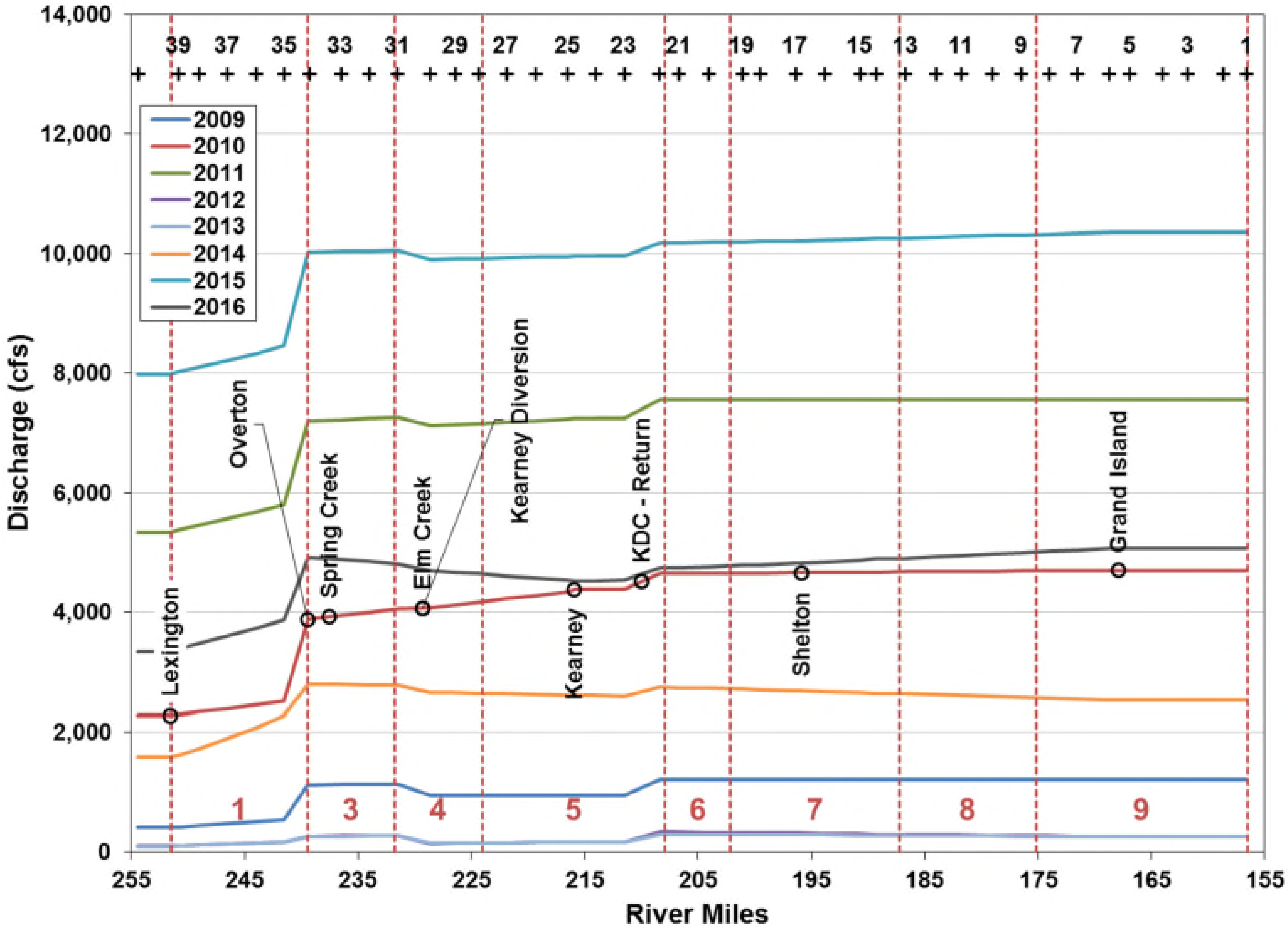

Figure 3.3. Average mean daily discharge during the germination season (Q_{GER}; June 1 – July 15) from 2009 through 2016.

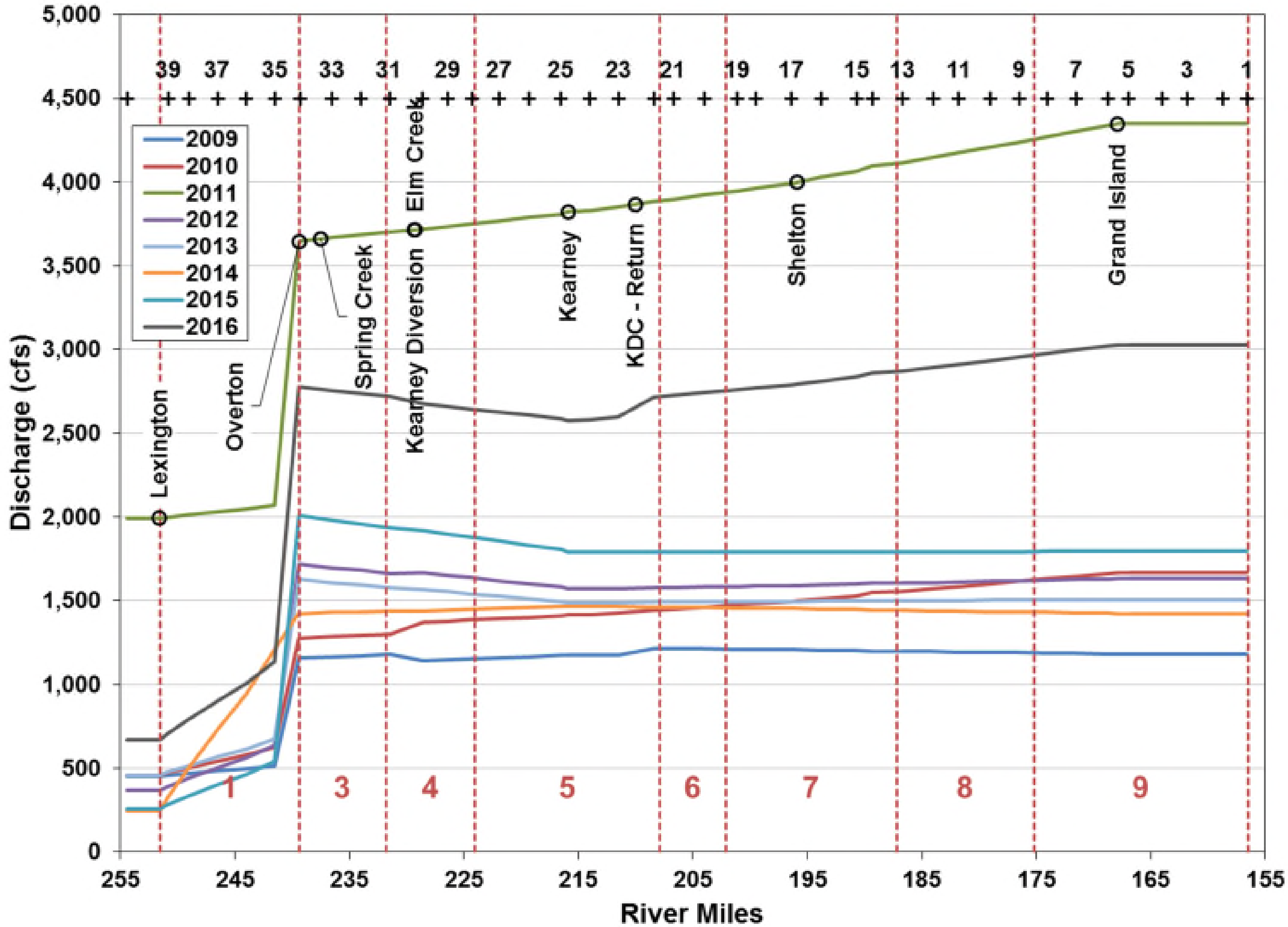

Figure 3.4. Average mean daily discharge during the spring whooping crane migration season (Q_{WC_Spring}; March 21 – April 29) during 2009 through 2016.

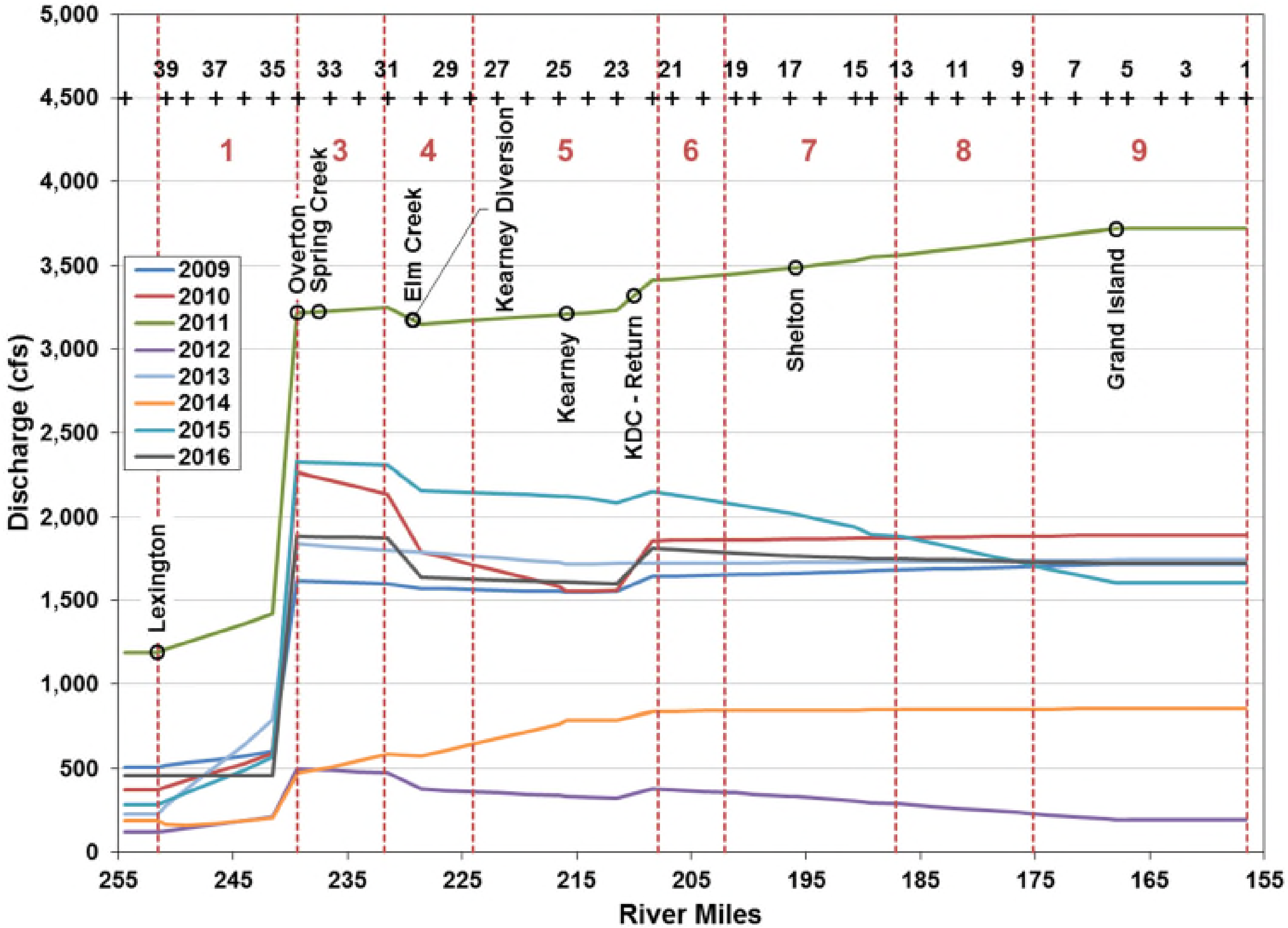

Figure 3.5. Average mean daily discharge during the fall whooping crane migration season (Q_{WC_Fall}; October 9 – November 10) during 2009 through 2016.

3.2 Hydraulic Metrics

3.2.1 Stage-discharge Relationships (DAP 5.2.1)

As noted above, the PRRIP 1-D hydraulic model that was based primarily on the 2009 topography was used in analyzing the 2009 through 2011 monitoring data, and the model constructed with the 2012 LiDAR and survey data was used for the 2012 through 2015 data. Specific rating curves for each AP can be obtained from the applicable HEC-RAS model output files.

3.3 Geomorphic Metrics

A suite of six geomorphic metrics are defined in the DAP to describe various aspects of the channel planform and cross sectional geometry (Table 2.3):

- Braiding Index (DAP 5.3.1) – Average number of wetted channels crossed by each transect at a given AP at the 1,200 cfs reference flow,
- Total Channel Width (DAP 5.3.2) – Total width, including non-wetted areas (e.g., exposed sand bars) at the 1,200 cfs reference flow,
- Wetted Channel Width (DAP 5.3.3) – Cumulative width of individual wetted channels at the 1,200 cfs reference flow,
- Mean Channel Depth (DAP 5.3.4) – Average water depth (hydraulic depth) at the 1,200 cfs reference flow,
- Maximum Channel Depth (DAP 5.3.5) – Maximum depth (i.e., depth at thalweg) at the 1,200 cfs reference flow, and
- Channel Width-to-Depth Ratio (DAP 5.3.6) – Ratio of wetted channel width to maximum channel depth at the 1,200 cfs reference flow.

The values of these metrics for both the Pure Panel and Rotating APs are provided in Appendix B; however, the discussion below focuses on the Pure Panel AP results because inclusion of the Rotating APs in the average and statistical evaluation confounds the ability to compare year-to-year trends. The average values at the rotating panel points are shown in the initial plot for each metric for reference. Average values for the various scales being considered in the analysis were developed from the individual transect results.

3.3.1 Braiding Index (DAP 5.3.1)

Based on the initial, 2009 survey data, the average braiding index at the Pure Panel APs ranged from about 1.3 (AP37) to 7.3 (AP1) (**Figure 3.6a**). The overall range was similar in subsequent years, with maximum values exceeding 8 at AP1 and AP17 in 2010, at AP19 in 2013, at AP21 in 2014 and 2015, and at AP27 in 2016. Relatively large changes occurred at several of the APs over the period of the surveys, particularly AP1, AP15, AP17, AP21, AP27 and AP35. At AP1, the transects at the upstream and downstream limits of the site had several small channels that were inundated by only a small amount at the estimated 1,200 cfs water surface in 2009, 2010 2011 and 2014, and these channels either disappeared or the slight year-to-year change in water-surface elevation inundated the bars that separated several of these channels in 2012 and 2013, and again in 2015. Similar year-to-year variability occurred at AP15, AP17 and AP21, although activities at the Rowe Sanctuary likely also affected AP21. Based on these results, it appears that the braiding index is very sensitive to small changes in water-surface elevation, especially when it is referenced to the 1,200 cfs water surface that barely inundates many of the low-elevation, in-channel bars.

The reach-wide average braiding index showed some variation throughout the survey period, varying from about 4.1 in 2012 to 5.2 in 2016 (**Figure 3.6b**)[9]. None of the year-to-year differences are statistically significant at the 5% level based on the nonparametric Kruskal-Wallis test. Geomorphic Reach 6 (Minden to Gibbon) consistently had the highest braiding index, followed by Reach 4 (Elm Creek to Odessa) and Reach 7 (Gibbon to Wood River) (**Figure 3.6c**). Reach 9 (Grand Island to Chapman) also had relatively high-braiding indices. The braiding index for Reach 6 is derived from only AP21. Rotating AP20 had a braiding index of 4.7 when surveyed in 2011, and had a braiding index of 10 when re-surveyed in 2015. AP22 was surveyed in 2010 and 2014, and had braiding indices of 6.0 and 4.0, respectively, suggesting that AP21 may not be representative of the remainder of Reach 6. AP20 and AP21 are both located on the Rowe Sanctuary and are subjected to more intensive channel maintenance practices, which may have contributed to the increase in braiding index during the monitoring period at these two locations. Reaches 1, 2 and 8 (Lexington to Overton, south channel at Jeffreys Island, and Wood River to Grand Island, respectively) consistently had the lowest braiding index. The braiding index in Reach 8 increased from about 3 during the first 4 years of the program to over 4 in 2014, decreased back to about 3 in 2015 and then increased to about 3.5 in 2016.

Fotherby (2008) states that "*a reach of river was …labeled as having a fully braided river pattern if the main channel had a braiding index of 3 or more throughout the reach.*" In her analysis, however, she categorized reaches with main channel braiding index (defined as the average number of channels) less than 2.5 as wandering or meandering, 2.5 to 3.5 as braided and greater than 3.5 as anastomosed (See Fotherby, 2008, Section 4.1). The currently defined PRRIP subreaches were classified by Fotherby (2008) (Table 2.2) as follows[10]:

- Reach 1 – Wandering,
- Reach 2 – Meandering,
- Reach 3 (*Reach 3A*) – Anastomosed with some braiding,
- Reach 4 (*Reach 3B*) – Braided,
- Reach 5 – Anastomosed with some braiding (*Reach 3C*); anastomosed (*Reach 3D*),
- Reach 6 (*Reach 4A*) – Braided,
- Reach 7 (*Reach 4B*) – Anastomosed with some braiding,
- Reach 8 – Anastomosed with some braiding (*Reach 4C*); braided (*Reach 4D*),
- Reach 9 (*Reach 5*) – Alternating braided and anastomosed.

---

[9]Because APs 25 and 37 were not surveyed in all years, it was assumed that the values of the geomorphic variables during the non-surveyed years remained the same as the last surveyed year for purposes of developing the geomorphic and overall reach averages to avoid bias resulting from simply eliminating these values.
[10]Fotherby (2008) reach designations in *italics*, where different from current definition.

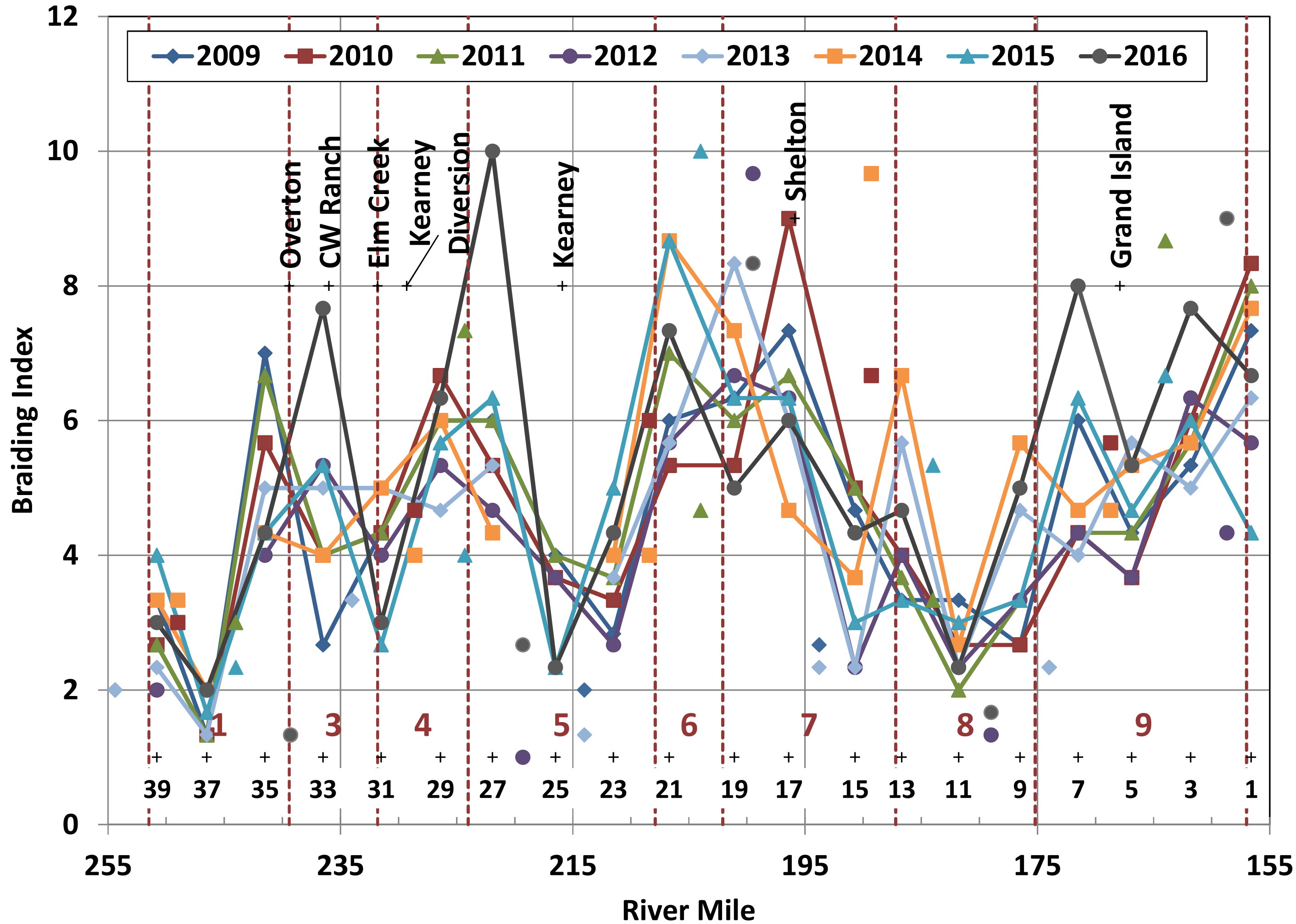

Figure 3.6a. Average braiding index by anchor point. Rotating APs are shown by individual symbols only; pure panel APs connected with lines.

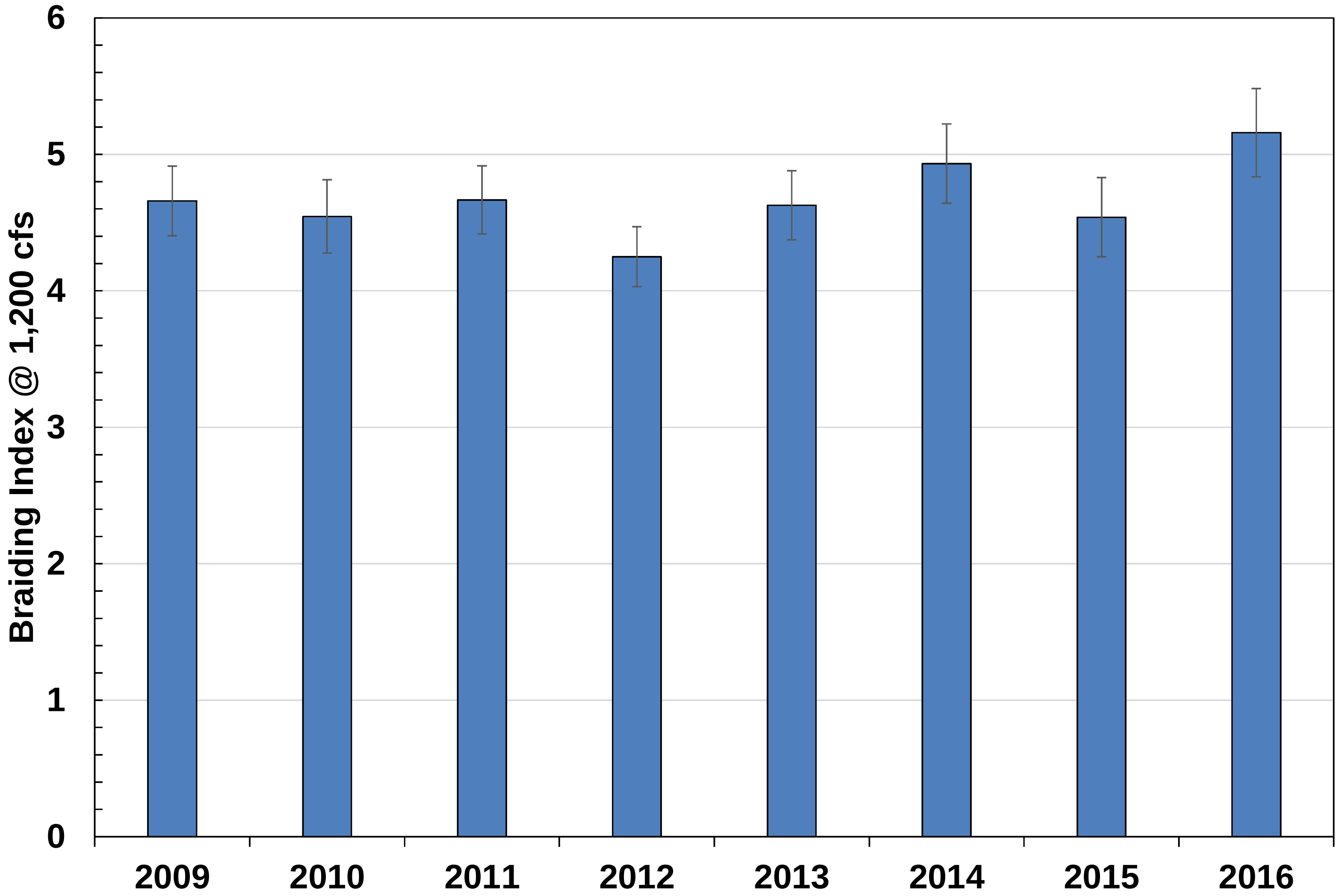

Figure 3.6b. Average braiding index for the overall study reach, based on the pure panel AP data. Whiskers represent ±1 standard error on mean value. Also shown is the peak discharge at Kearney.

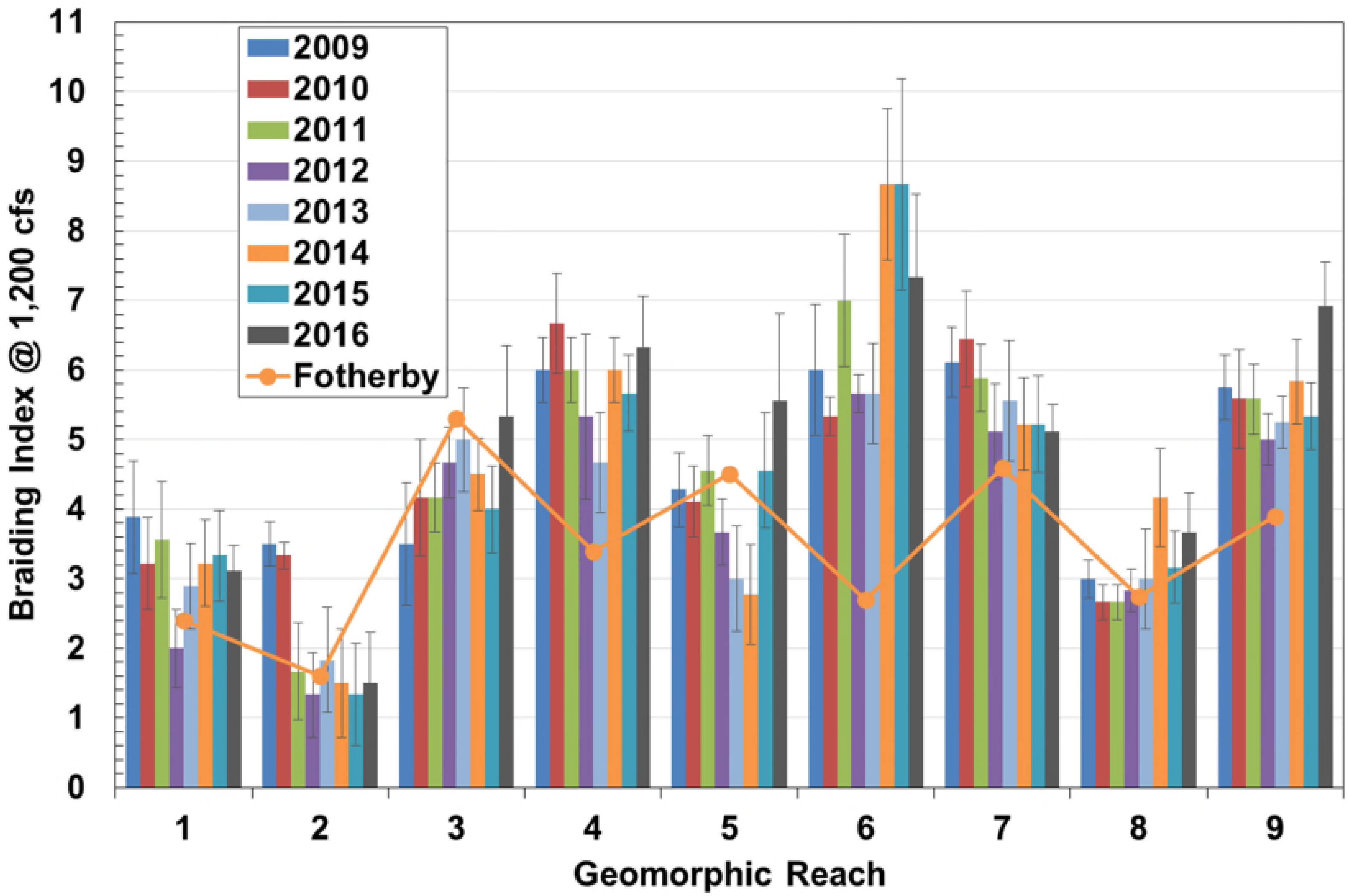

Figure 3.6c. Average braiding index by geomorphic reach, based on the pure panel AP data. Also shown are Fotherby (2008) braiding indices. Whiskers represent ±1 standard error on mean value.

Fotherby's (2008) braiding indices were developed by counting the number of individual channels evident in the 1998 color-infrared (CIR) photography that was taken when the discharge along the reach varied from about 450 cfs at Overton to 1,030 cfs at Grand Island (Friesen et al., 2000). The braiding indices for Reaches 1 and 2 developed for this study (reference discharge of 1,200 cfs) are considerably higher than those from Fotherby (2008) [The braiding index averaged about 3.2 in Reaches 1 and 2 over the eight-year monitoring period versus 2.4 and 1.6 from Fotherby (2008), respectively. Note that the low value of the braiding index in Reach 2 in 2011 through 2016 is based only on AP35 because access to AP37 was denied by the landowner.] Fotherby's (2008) braiding index for Reach 5 of 4.5 is most similar to result from this study of 4.4. Fotherby's (2008) braiding indices for the remaining reaches were lower than those obtained for this study for all reaches except Reach 3, with Reach 6 having the greatest difference [average of 6.8 over the eight surveys for this study versus 2.7 from Fotherby (2008)]. Differences in methodology likely account for most of the differences, and activities associated with Program and partner activities that include channel grading, discing and herbicide spraying to eliminate noxious weeds (primarily phragmites), and tree and riparian vegetation clearing to promote channel widening also contribute the differences. As noted above, this is especially true for Reach 6, where the value for this study is based on conditions at AP21 at the Rowe Sanctuary where the channel was modified extensively during the monitoring period to improve habitat.

Based on Fotherby's (2008) classification system and the average values for this study, none of the reaches would be classified as meandering or wandering, Reaches 1, 2 and 8 would be in the braided category, and the remainder would be in the anastomosed category. Although some portions of the reach are certainly anastomosed, as evidenced by the presence of one or more relatively persistent, secondary channels, all of the pure panel APs, with the possible exception of APs 35, 37 and 39, exhibit at least some degree of braiding.

3.3.2 Total Channel Width (DAP 5.3.2)

The total channel width at 1,200 cfs generally increases in the downstream direction for all data sets, with the widths ranging from slightly more than 200 ft at AP37 (north channel at Jeffreys Island) to about 1,800 ft at AP1 (**Figure 3.7a**). This metric changed very little at most APs over the 7-year monitoring period. Along with AP 37, the APs with the narrowest channel include AP23, AP25, AP31, AP 37 and AP39. The widest, in addition to AP1, include AP17, AP21, AP27, AP29, AP33, and AP35. In spite of the general downstream-increasing trend, the total channel width tends to alternate between wide and narrow segments along the overall reach. The very large width at AP1 is somewhat deceptive because this part of the reach is highly anastomosed, with roughly one-third of the width occupied by large islands covered with mature woody vegetation. Similar conditions occur at AP17 near Shelton, and AP27 between Kearney and the KDS, although the proportion of total width occupied by vegetated islands is less than at AP1. The wide channels at AP21 and AP33 most likely result from restoration activities at the Rowe Sanctuary and Cottonwood Ranch, respectively.

The average total channel width for the overall reach has remained relatively consistent at between 800 ft and 850 ft throughout the 8-year monitoring period (**Figure 3.7b**). There is, however, considerable variability among the geomorphic reaches, with Reaches 1 and 2, at the upstream end of the monitoring reach, having the narrowest average widths (500 ft to 550 ft), and Subreach 6 (Minden to Gibbon) the widest at about 1,260 ft) (**Figure 3.7c**).

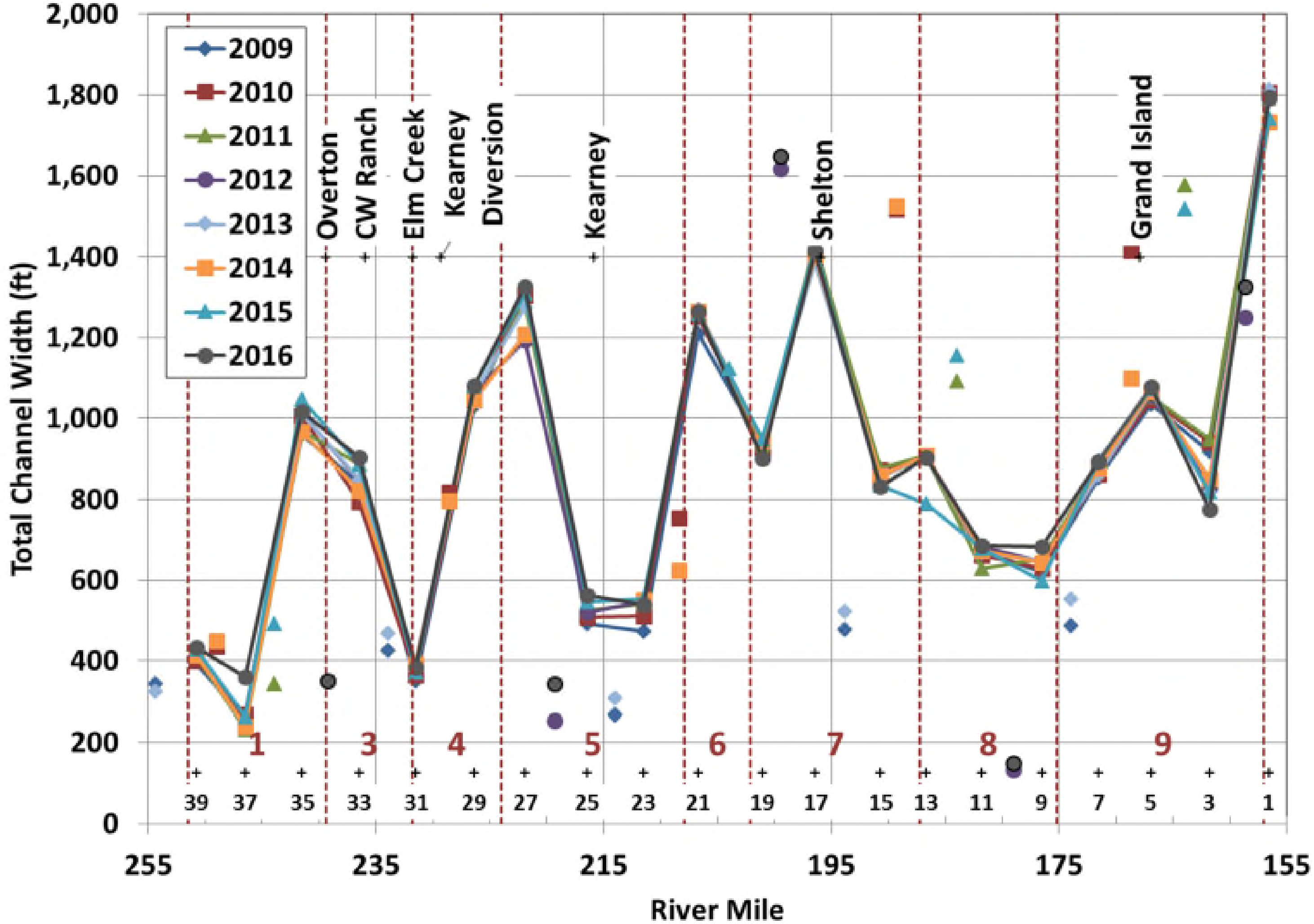

Figure 3.7a. Average total channel width at pure panel APs. Rotating APs are shown by individual symbols only; pure panel APs connected with lines.

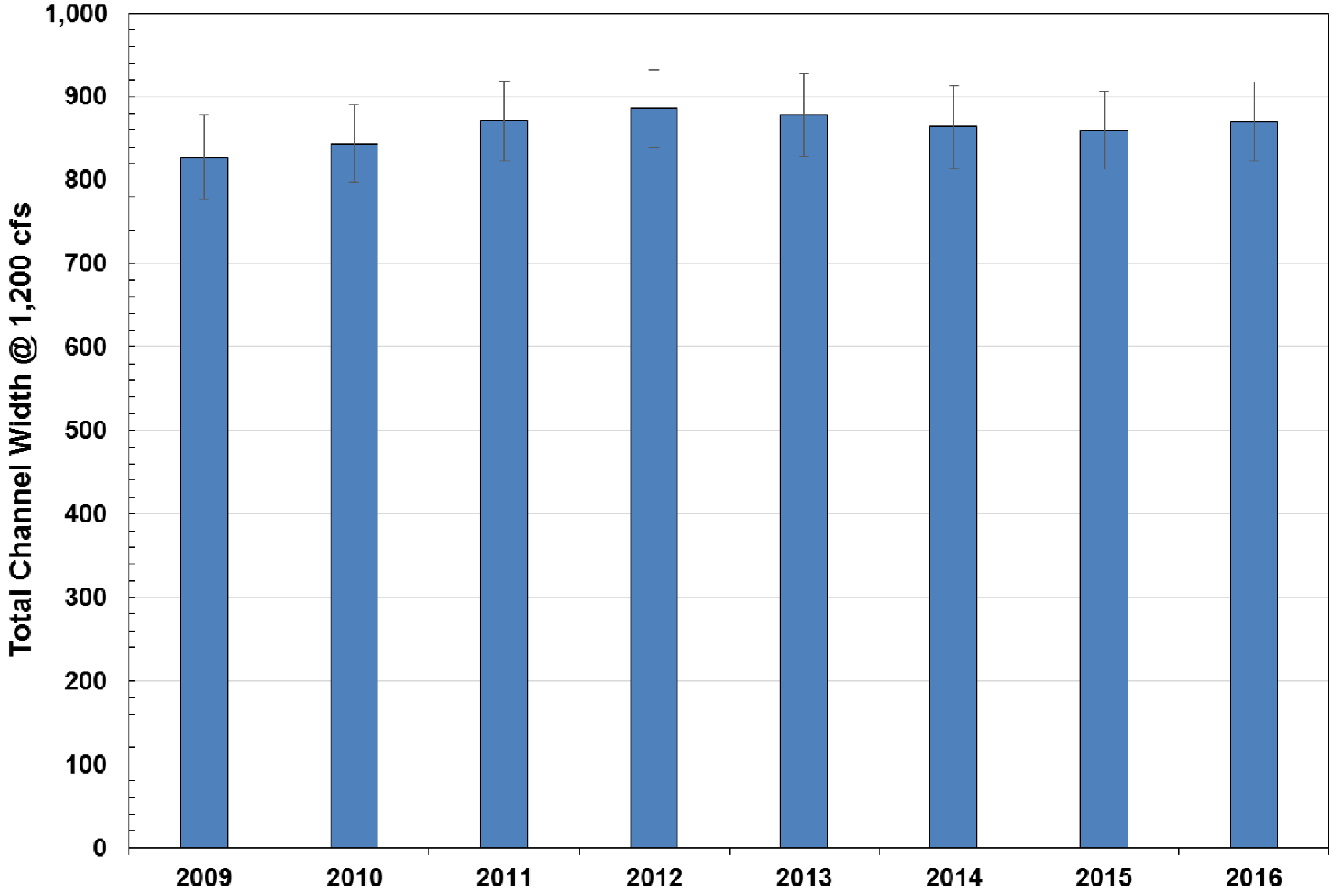

Figure 3.7b. Average total channel width for the overall study reach, based on the pure panel AP data from 2009 through 2015, omitting the J-2 return channel. Whiskers represent ±1 standard error on mean value.

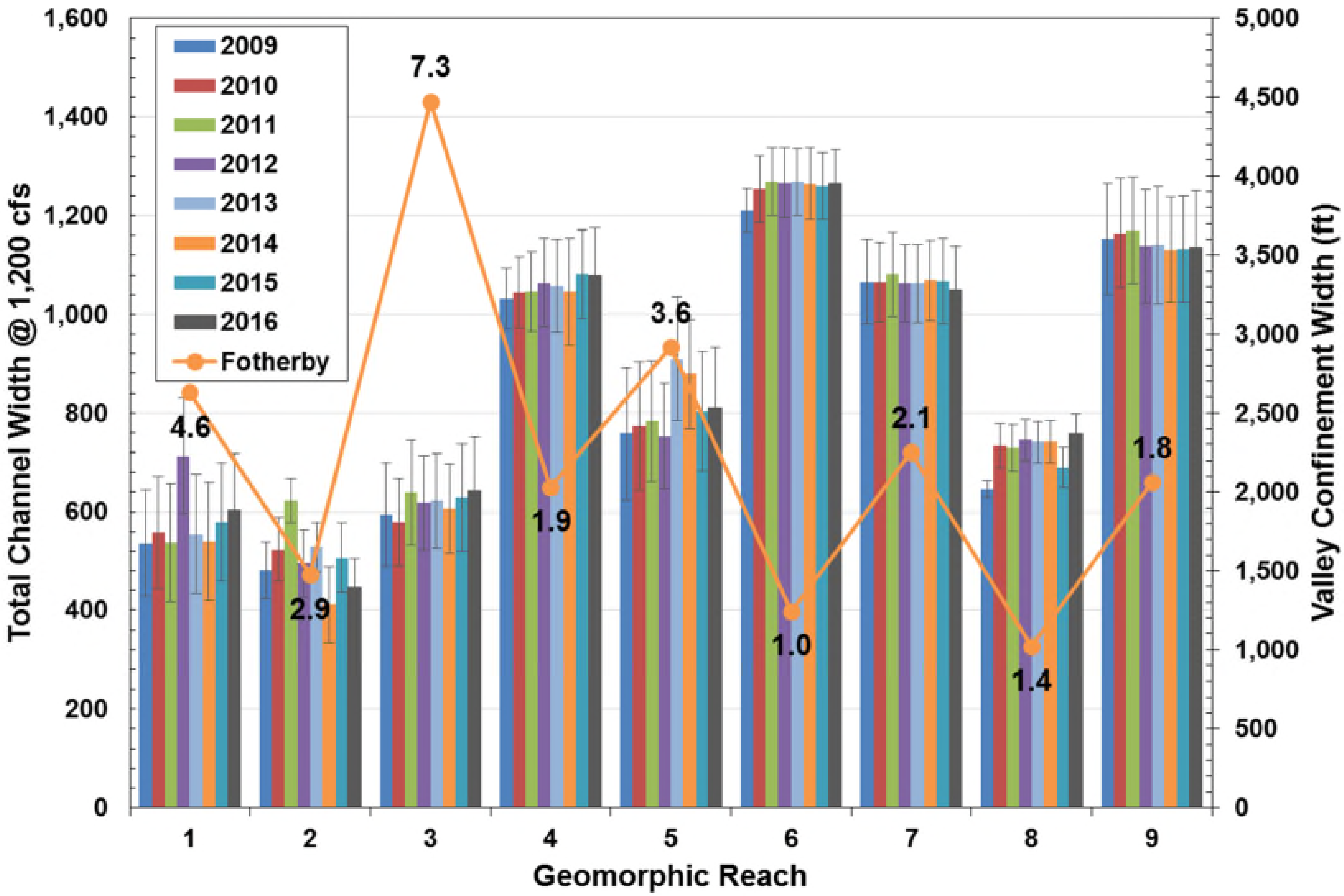

Figure 3.7c. Average total channel width by reach, based on the pure panel AP data from 2009 through 2015. Whiskers represent ±1 standard error on mean value. Also shown are valley confinement widths from Fotherby (2008) (**Right-hand scale).** Values near Fotherby (2008) data points are ratio of Fotherby's valley confinement width to average total channel width from this study.

Fotherby (2008) concluded that valley confinement associated with both the natural geology of the reach and human influences is the primary driver of channel form in essentially the entire monitoring reach downstream from Overton, while sediment size and transport capacity are the primary drivers upstream from Overton. With the exception of Reach 6, where Fotherby's (2008) valley confinement width is about the same as the total channel width and Reach 8, where it is about 40 percent larger, the confinement widths through the reach are significantly larger than the total channel width (Figure 3.7c). The margin between the valley confinement feature and the total channel width in Reaches 6 and 8 may be sufficiently small to have a direct influence on the channel pattern, however, this is probably not the case in other portions of the reach. It is particularly interesting to note that AP21 (Reach 6), where Fotherby's (2008) valley confinement width is essentially the same as the total channel width, is one of the most braided of all of the Pure Panel APs.

3.3.3 Wetted Channel Width (DAP 5.3.3)

The wetted channel width at 1,200 cfs ranged from about 200 ft (AP37, 2011 and 2014) to over 1,000 ft (AP21, 2013) (**Figure 3.8a**). Similar to total channel width, wetted width generally increases in the downstream direction, although AP33 at Cottonwood Ranch and AP29 downstream from the Kearney Diversion are also relatively wide compared to the adjacent APs. The wetted widths at AP7, AP23, AP31, and AP37 are narrower than the typical widths in other parts of the reach (generally in the 200- to 300-ft range). Unlike total channel width, the wetted width changed substantially at many of the APs over the 7-year monitoring period as the channels and macro-scale bedforms and bars changed shape.

The reach-wide average wetted width increased by a modest (but not statistically significant) amount from about 450 in 2009 to about 530 ft in 2012, and then declined back to about 450 ft in 2014 (**Figure 3.8b**). In 2015, the reach-averaged width increased to about 500 ft, and it increased again to about 540 ft in 2016. Similar to the total width, there is considerable variability among the geomorphic reaches, with Reaches 1 and 2 being the narrowest at 325 ft to 330 ft, averaged across all years, and Subreach 6 (Minden to Gibbon) the widest [690 ft (2009) to 1,000 ft (2013)] (**Figure 3.8c**). The year-to-year variability in wetted width is generally greater in most reaches than the variability in total width, again due to changes in shape of the macro-scale bedforms and bars.

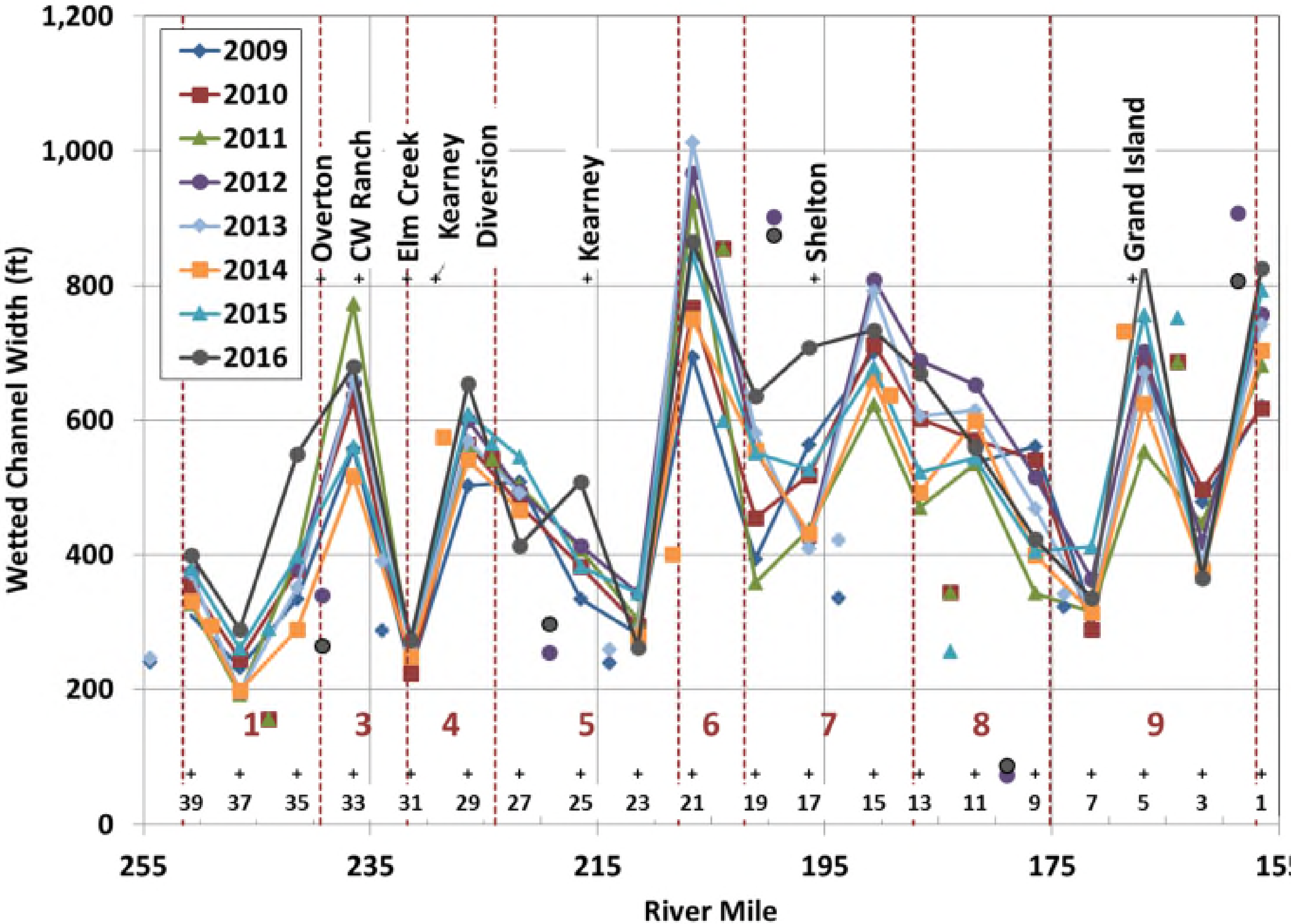

Figure 3.8a. Average wetted width at 1,200 cfs at pure panel APs. Rotating APs are shown by individual symbols only; pure panel APs connected with lines.

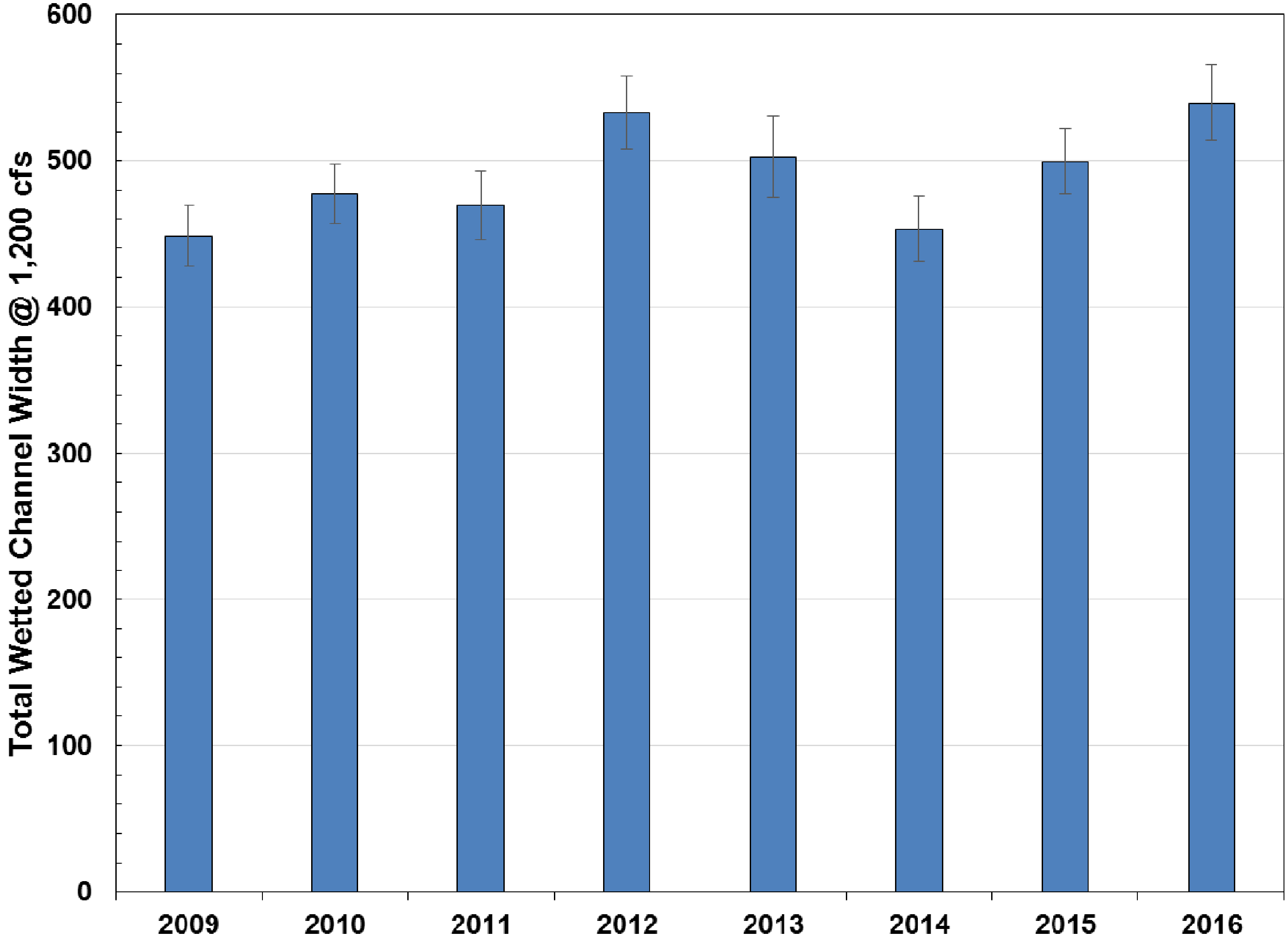

Figure 3.8b. Average wetted width at 1,200 cfs for the overall study reach, based on the pure panel AP data. Whiskers represent ±1 standard error on mean value.

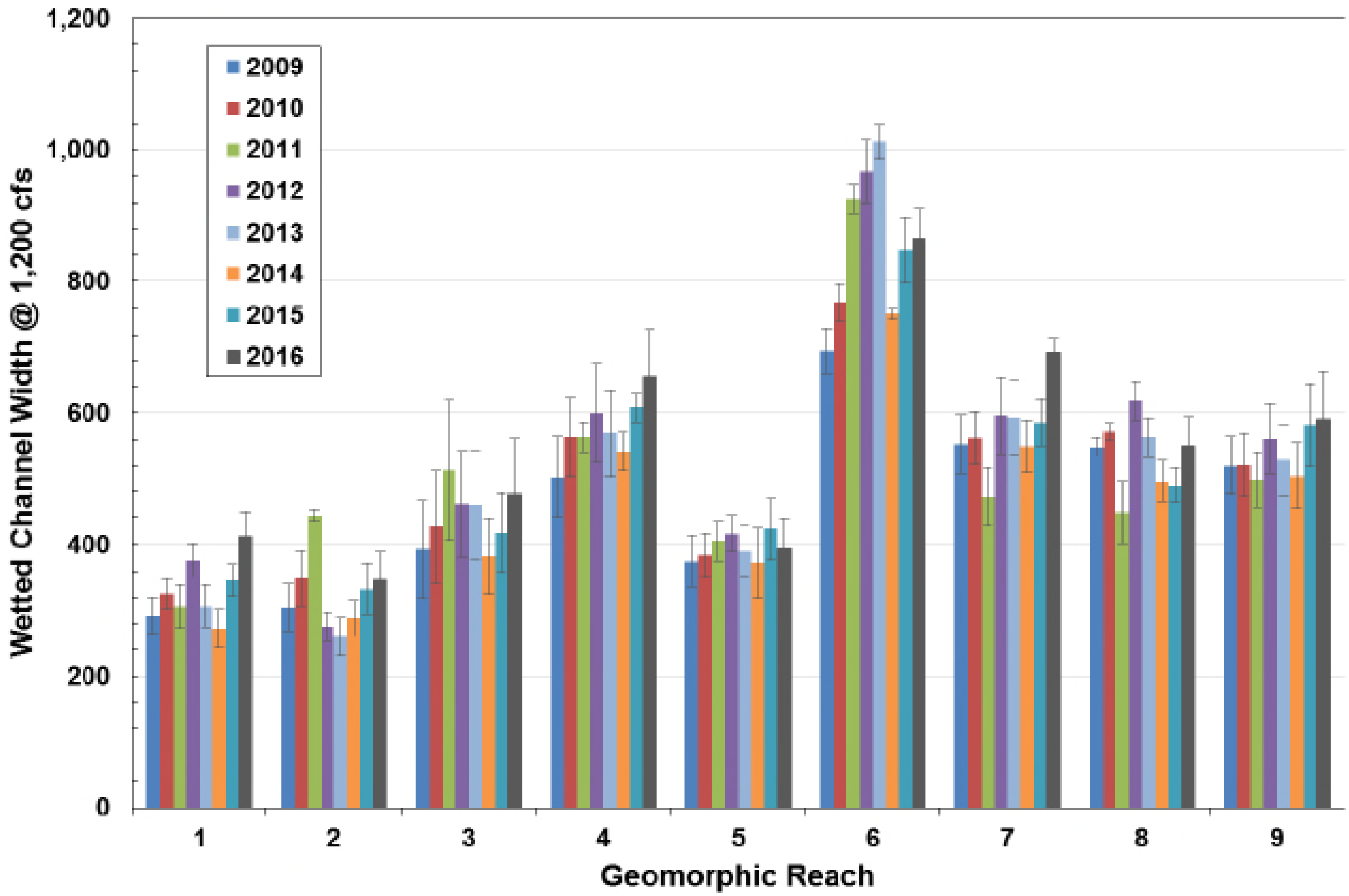

Figure 3.8c. Average wetted width at 1,200 cfs by geomorphic reach, based on the pure panel AP. Whiskers represent ±1 standard error on mean value.

3.3.4 Mean Channel Depth (DAP 5.3.4)

In 2009, mean channel depth along the mainstem (i.e., not considering the south channel at Jeffreys Island) at 1,200 cfs ranged from about 0.7 ft (AP9) to 2.0 ft (AP37A), with a general trend of decreasing depth in the downstream direction (**Figure 3.9a**). Mean channel depth at AP37B, in the south channel, was approximately 2.3 ft. Mean channel depths in subsequent years followed a similar pattern, but varying by up to 1 ft from year to year.

The mean channel depth over the entire study reach averaged about 1.3 ft in 2009, increasing to nearly 1.5 ft in 2011, and then decreasing back to about 1 ft and 1.1 ft in 2012 and 2013, respectively (**Figure 3.9b**). The 2014 and 2015 data show a progressive rebound to about 1.3 ft, and the value declined by to about 1.1 in 2016. The differences between 2009, 2010 2011 and 2015 are not statically significant (based on the Kruskal-Wallis test, α=0.05), nor are the differences between 2012, 2013 and 2016 (p=0.202). The differences between these two groups of years are, however, statistically significant (p<0.0001). The differences between 2014 and all of the other years are not statistically significant.

Geomorphic Reach 2 (south channel at Jeffreys Island) consistently had the largest mean depth through the eight-year monitoring period, followed by Reaches 1 and 3 (**Figure 3.9c**). Reaches 6 and 8 typically exhibit the smallest mean depth. These depths tend to be inversely proportional to the wetted channel width.

Some of the differences in depth between years are attributable to changes in the stage-discharge rating curve at the individual transects. There appears to have been a systematic shift in channel geometry as a result of the 2011 high flows that reduce the topographic variability of the channel, widening the wetted channel and decreasing the mean depth (see Section 3.3.3). As a result, the mean depth downstream from Overton (Reaches 3 to 9) was significantly less in 2012 than in 2011. A typical example occurred at AP15, Transect 4, where the wetted width increased from about 500-ft to over 780-ft due to general flattening of the bed across the river (**Figure 3.9d**).

3.3.5 Maximum Channel Depth (DAP 5.3.5)

The relative magnitudes and trends in the maximum channel depth (i.e., the thalweg depth) at 1,200 cfs are very similar to those for the mean channel depth, but as expected, the individual magnitudes are 2.5 to 3 times greater (**Figure 3.10a**). Maximum channel depth tends to decrease in the downstream direction, although trends are somewhat obscured by scatter in the data. Such scatter is to be expected because thalweg depth is more strongly influenced by local controls and scour processes than mean channel depth that provides a better analytical point for reach-scale processes.

The reach-wide average maximum depth increased from about 3.0 ft in 2009 to about 3.8 ft in 2011, and then declined back to about 2.2 ft in 2012 and 2.4 ft in 2013. The 2014 average maximum depth increases back to approximately 3.2 ft, and the 2015 data show a further increase to 3.4 ft (**Figure 3.10b**). In 2016, this parameter decreased back to about 2.9 ft. Consistent with the mean channel depth, the average maximum depth in the geomorphic subreaches generally declines in the downstream direction, with the highest values occurring in Reaches 1 and 2 and the lowest values occurring in Reaches 6 (AP21), 8 and 9 (**Figure 3.10c**). Similar to trends observed with mean channel depth, there is a noticeable decrease in maximum channel depth between the 2011 and 2012 datasets, most likely due to processes similar to the illustration of Figure 3.9d. The progressive increase in maximum depth from 2013 to 2015 may have been caused by bed scour during the floods in Fall 2013 and Spring 2015.

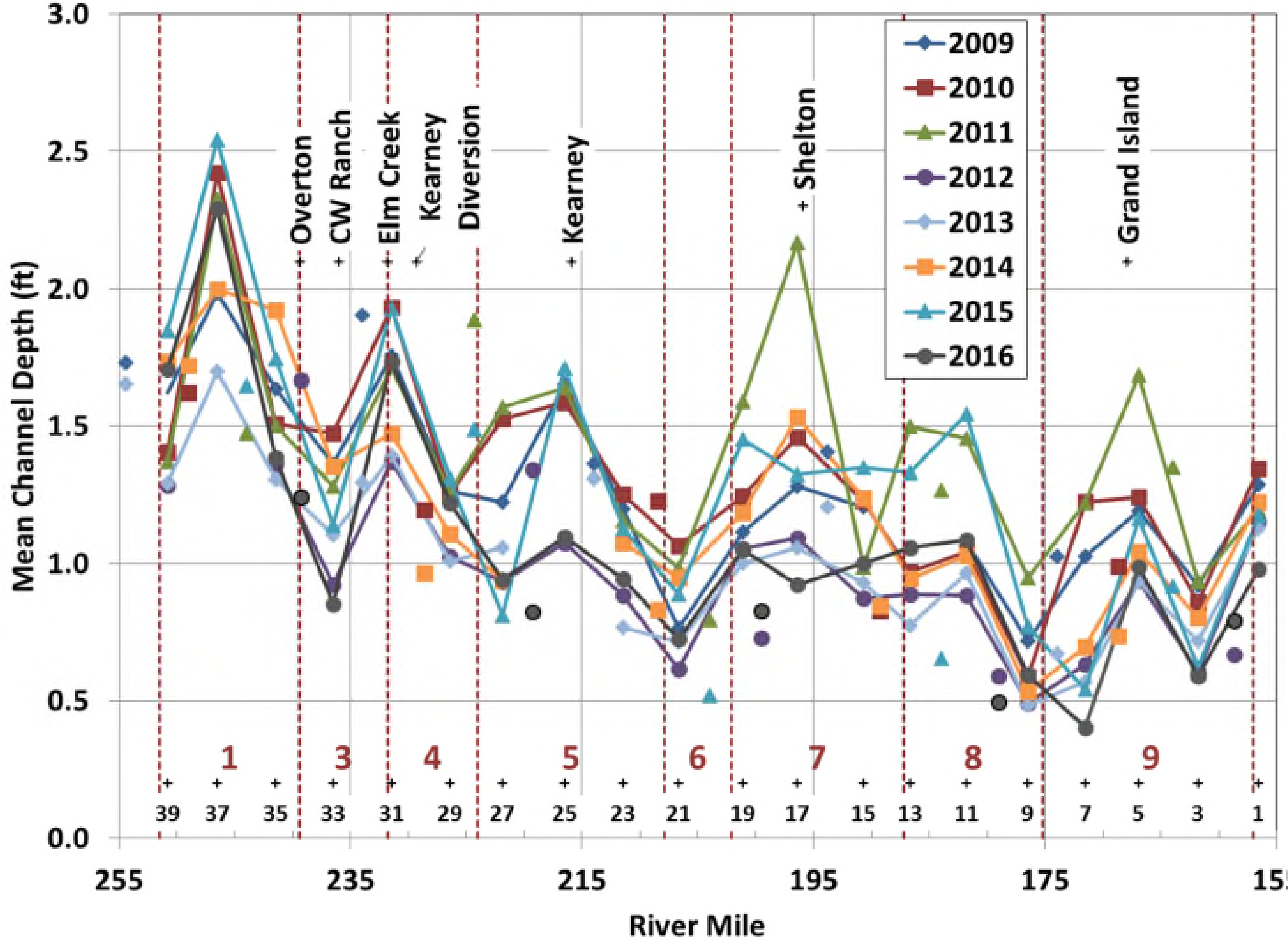

Figure 3.9a. Mean channel (i.e., hydraulic) depth at 1,200 cfs at pure panel APs. Rotating APs are shown by individual symbols only; pure panel APs connected with lines.

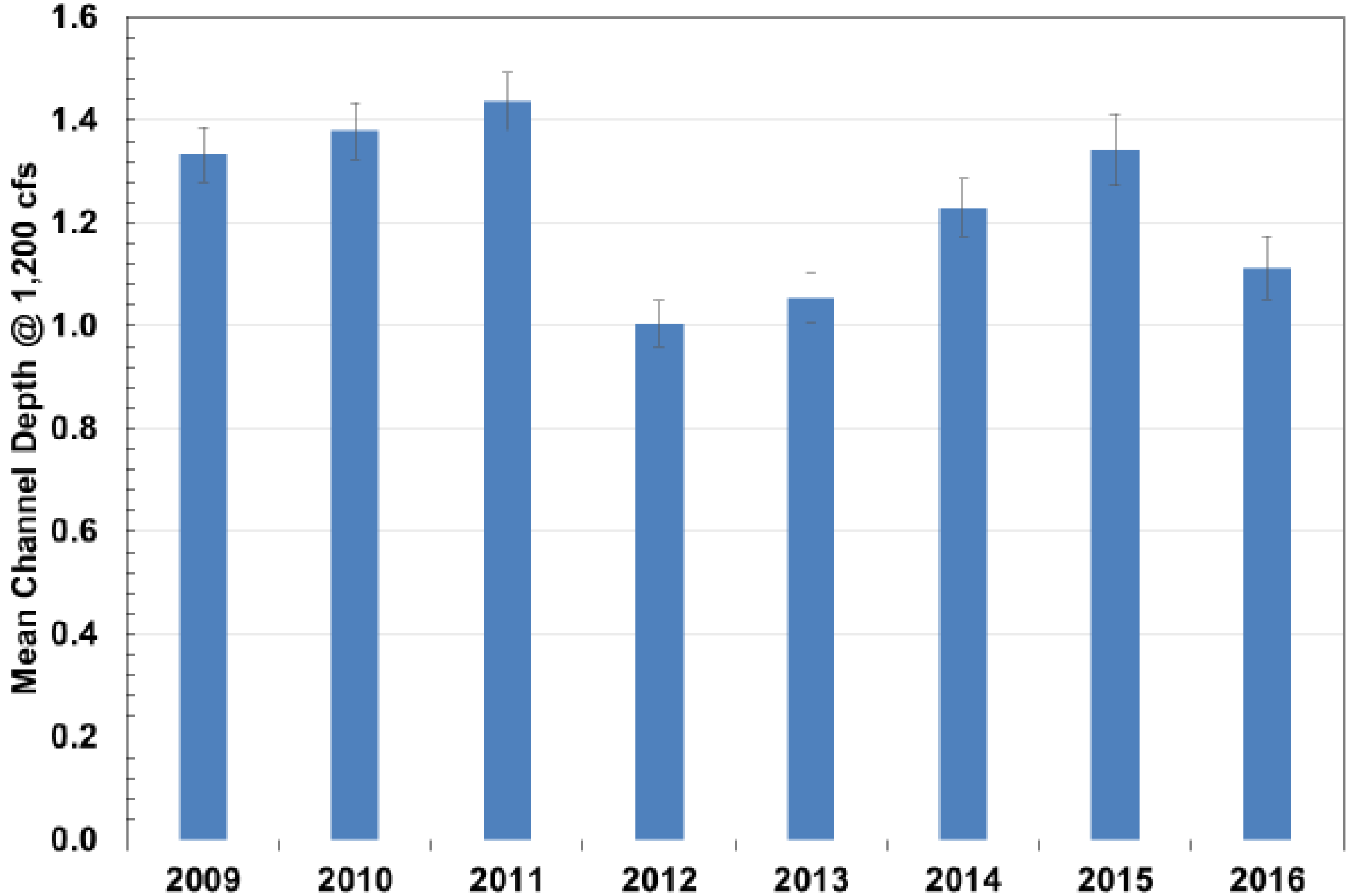

Figure 3.9b. Average mean channel (i.e., hydraulic) depth at 1,200 cfs for the overall study reach, based on the pure panel AP data. Whiskers represent ±1 standard error on mean value.

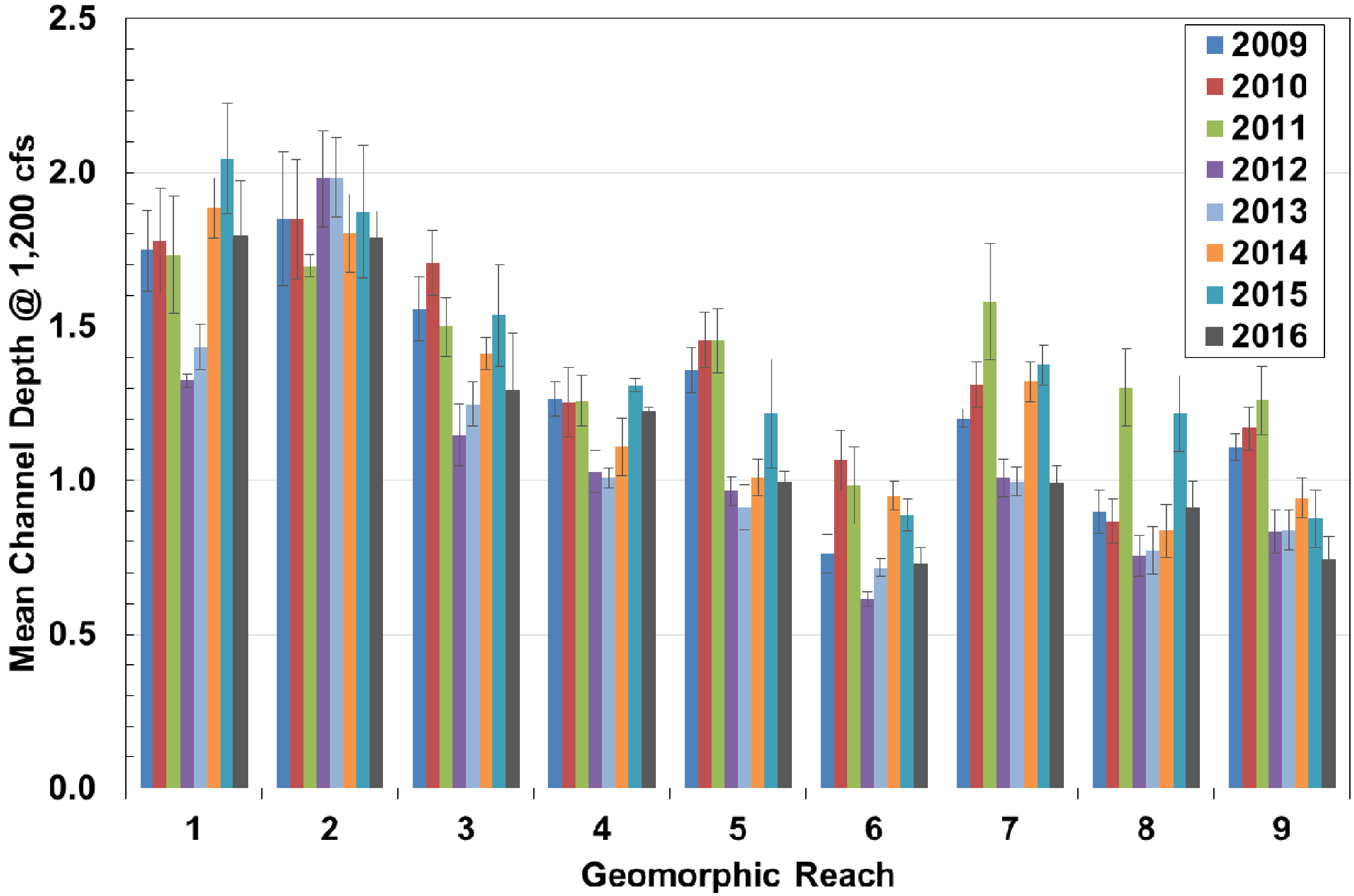

Figure 3.9c. Average mean channel (i.e., hydraulic) depth at 1,200 cfs by geomorphic reach, based on the pure panel AP data. Whiskers represent ±1 standard error on mean value.

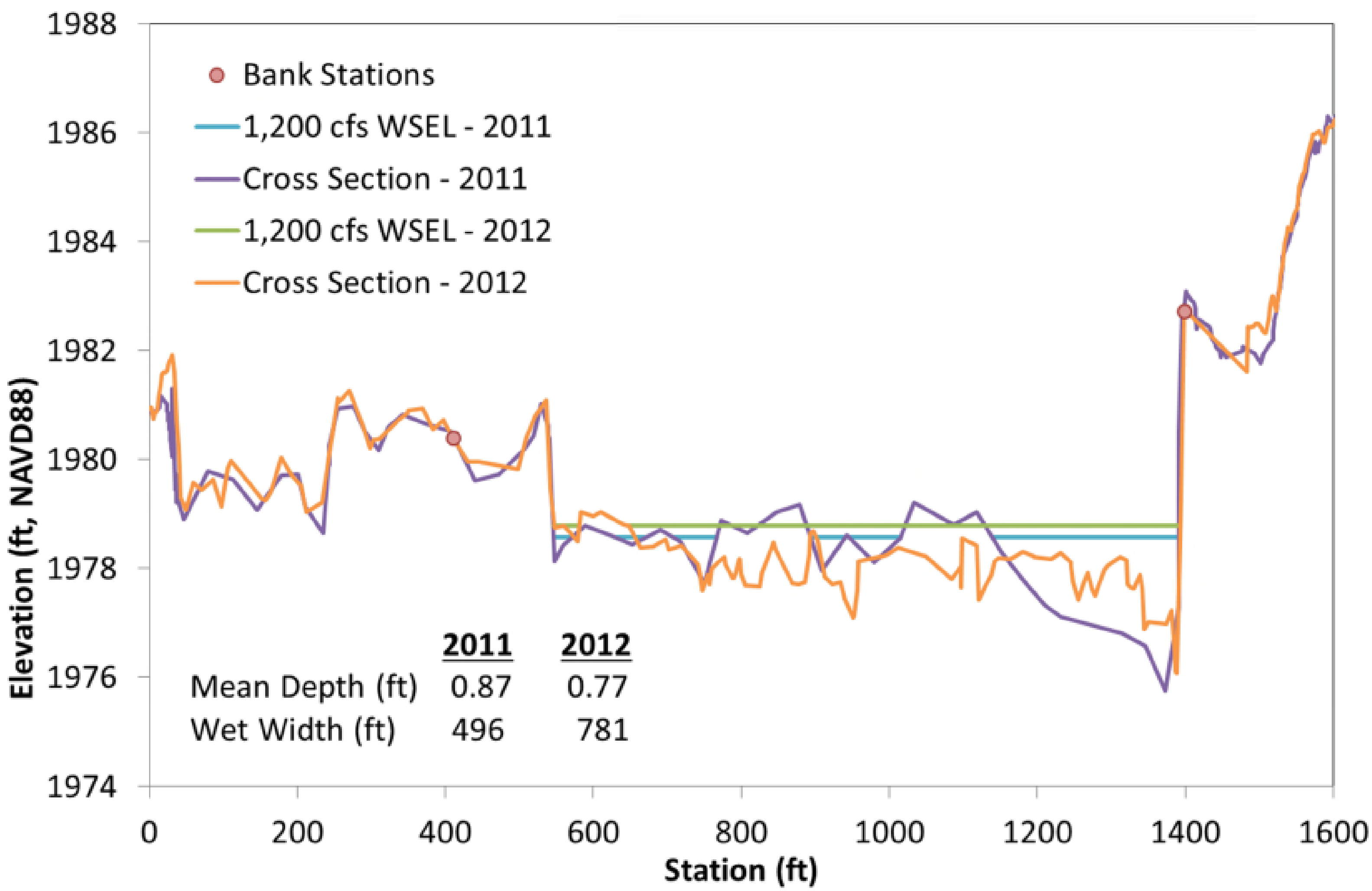

Figure 3.9d. Surveyed cross-section profiles at AP15, transect four in 2011 and 2012. Note the removal of instream bars and the aggradation of the thalweg, which resulted in a wider, shallower channel.

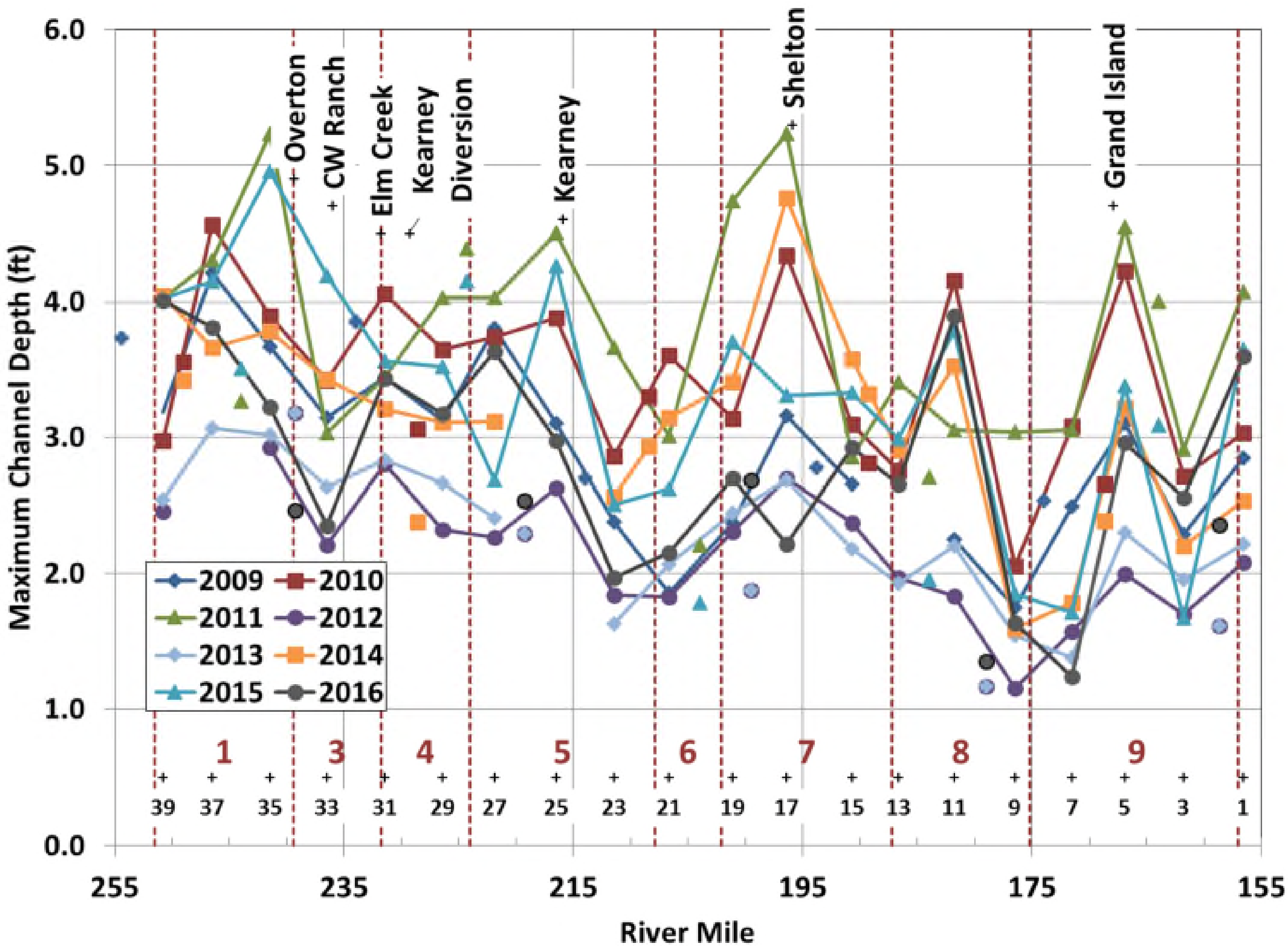

Figure 3.10a. Average maximum channel depth at 1,200 cfs at pure panel APs. Rotating APs are shown by individual symbols only; pure panel APs connected with lines.

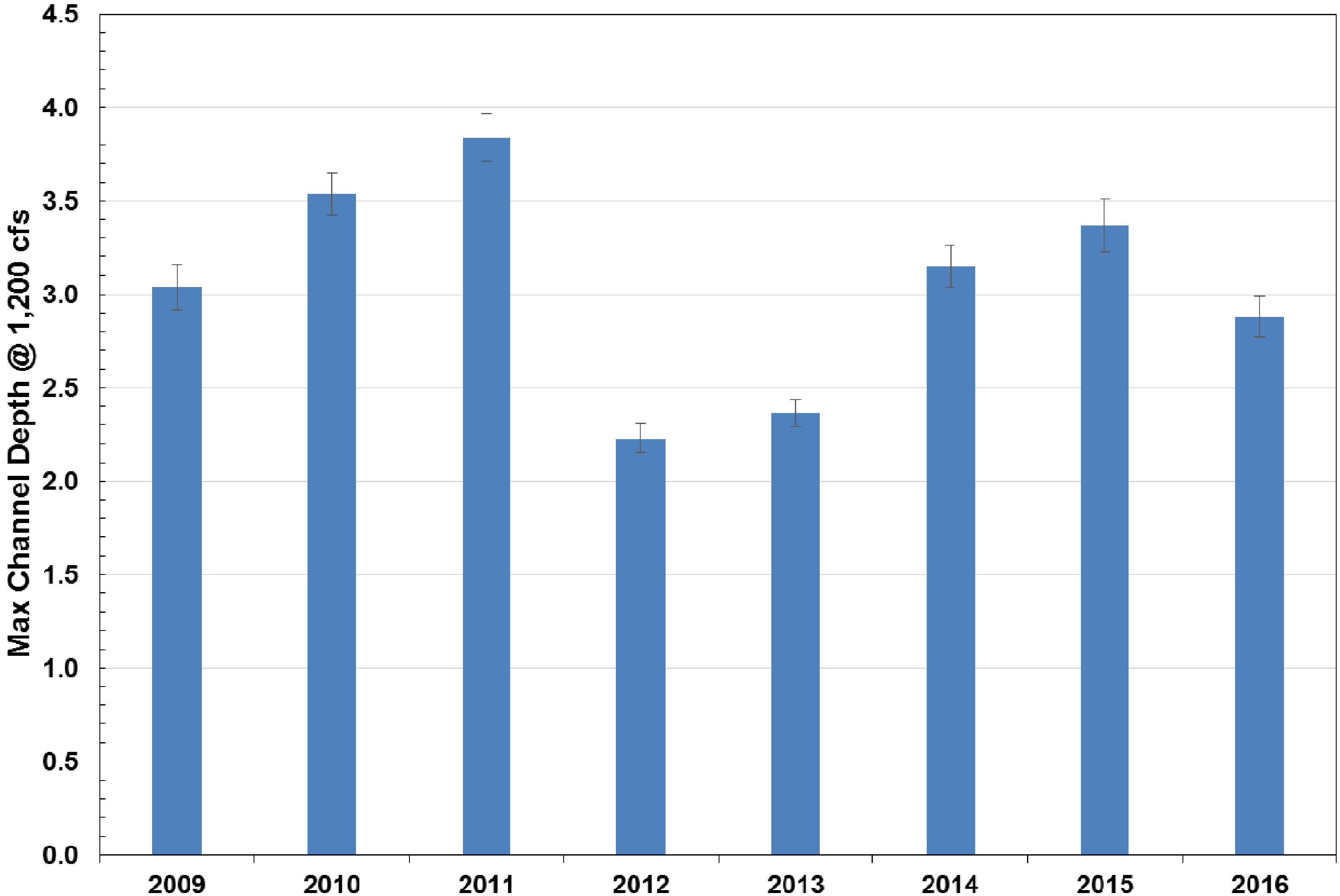

Figure 3.10b. Average maximum channel depth at 1,200 cfs for the overall study reach, based on the pure panel AP data. Whiskers represent ±1 standard error on mean value.

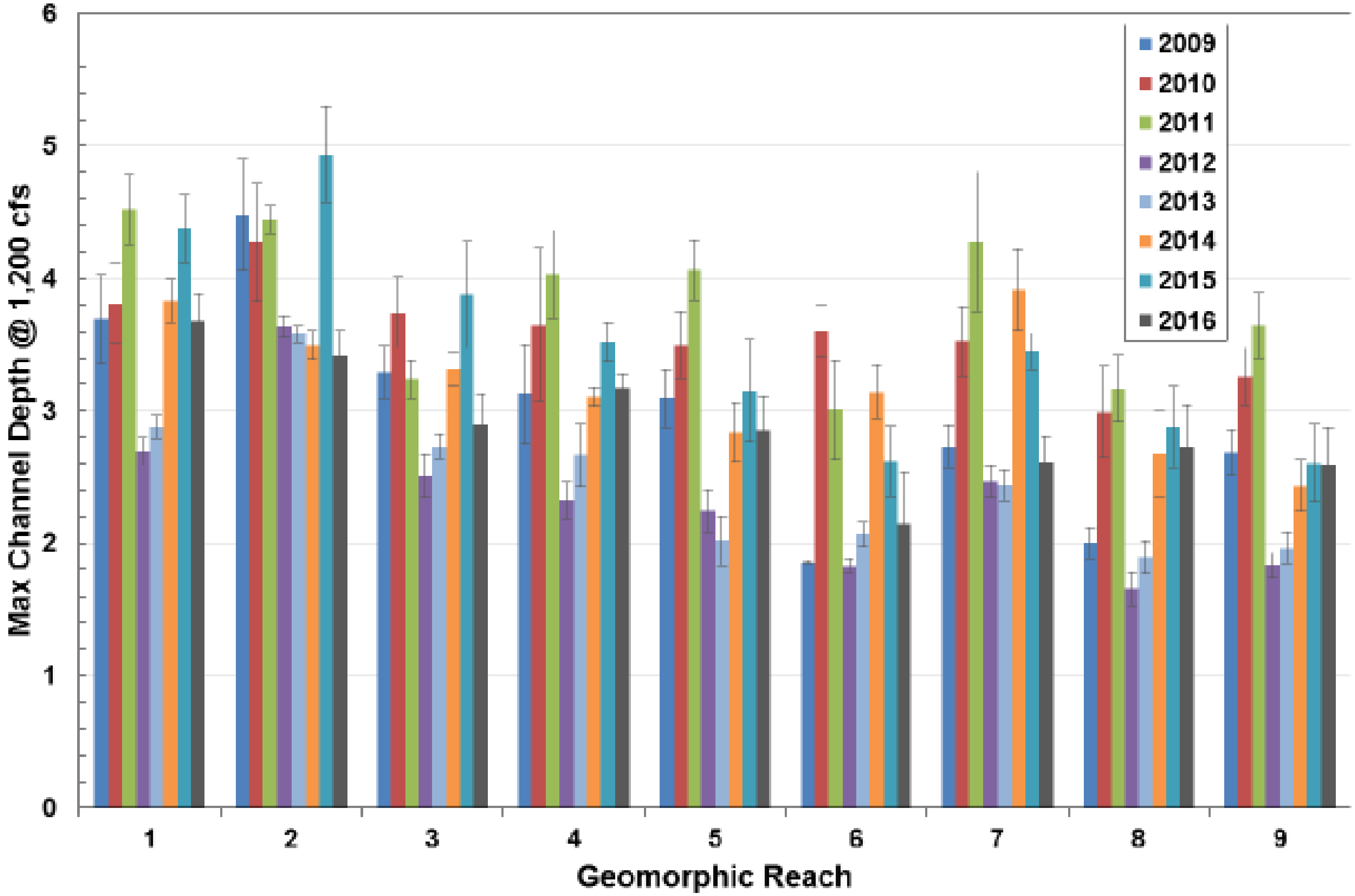

Figure 3.10c. Average maximum channel depth at 1,200 cfs by geomorphic reach, based on the pure panel AP data. Whiskers represent ±1 standard error on mean value.

3.3.6 Channel Width-to-Depth Ratio (DAP 5.3.6)

The average width-to-depth[11] ratio at 1,200 cfs at the pure panel APs ranges from about 50 (AP37A, 2011) to over 500 (AP21, 2012), with a general trend of increasing values in the downstream direction (**Figure 3.11a**). In 2011 and 2012, AP21 had the highest width-to-depth ratios observed in the entire monitoring reach. Several APs in the downstream part of the reach (AP1, 5, 9, 11, 13 and 15) also had relatively high width-to-depth ratios in 2012. Most of the APs experienced a substantial decline in width-to-depth ratios from 2013 to 2014. Data collected in 2015 and 2016 are generally consistent with data collected in previous years.

For the overall reach, the average width-to-depth ratio declined from about 170 in 2009 to 130 in 2011 (**Figure 3.11b**). Between the 2011 and 2012 surveys, the ratio increased to about 260, and it then declined back to about 160 by 2014, after which it increased progressively in 2015 and 2016 to about 170 and 210, respectively. This trend is consistent with the trends in channel width and depth discussed above, in which the topographic variability across many of the cross sections tended to decrease as the individual braid channels filled in and the sand bars flattened during the 2011 high flows (see Figure 3.9d). The average width-to-depth ratios for the geomorphic reaches follow the same general trend as the individual AP averages, with Reach 2 having the smallest values and Reach 6 (again, as represented by AP21) having the largest values (**Figure 3.11c**). The ratios for the three downstream reaches (Reaches 7, 8 and 9) are generally larger than Reaches 3, 4 and 5.

Fotherby (2008) computed width-to-depth ratios using results from the hydraulic model discussed by Murphy et al. (2006) at a discharge of 2,000 cfs. Her calculations differ from those specified in the DAP, and reported above, in that she used the mean depth rather than the maximum (thalweg) depth and she used a higher discharge, both of which tend to make the ratios larger. The width-to-depth ratios obtained from the data from this monitoring program using the mean depth (and a discharge of 1,200 cfs) are, however, reasonably consistent with Fotherby's (2008) values, except in Reach 6, where the current data indicate much larger ratios (**Figure 3.11d**). Again, this difference is most likely due to mechanical activities in the channel at the Rowe Sanctuary.

[11] Maximum channel depth was used to quantify this metric, per the DAP.

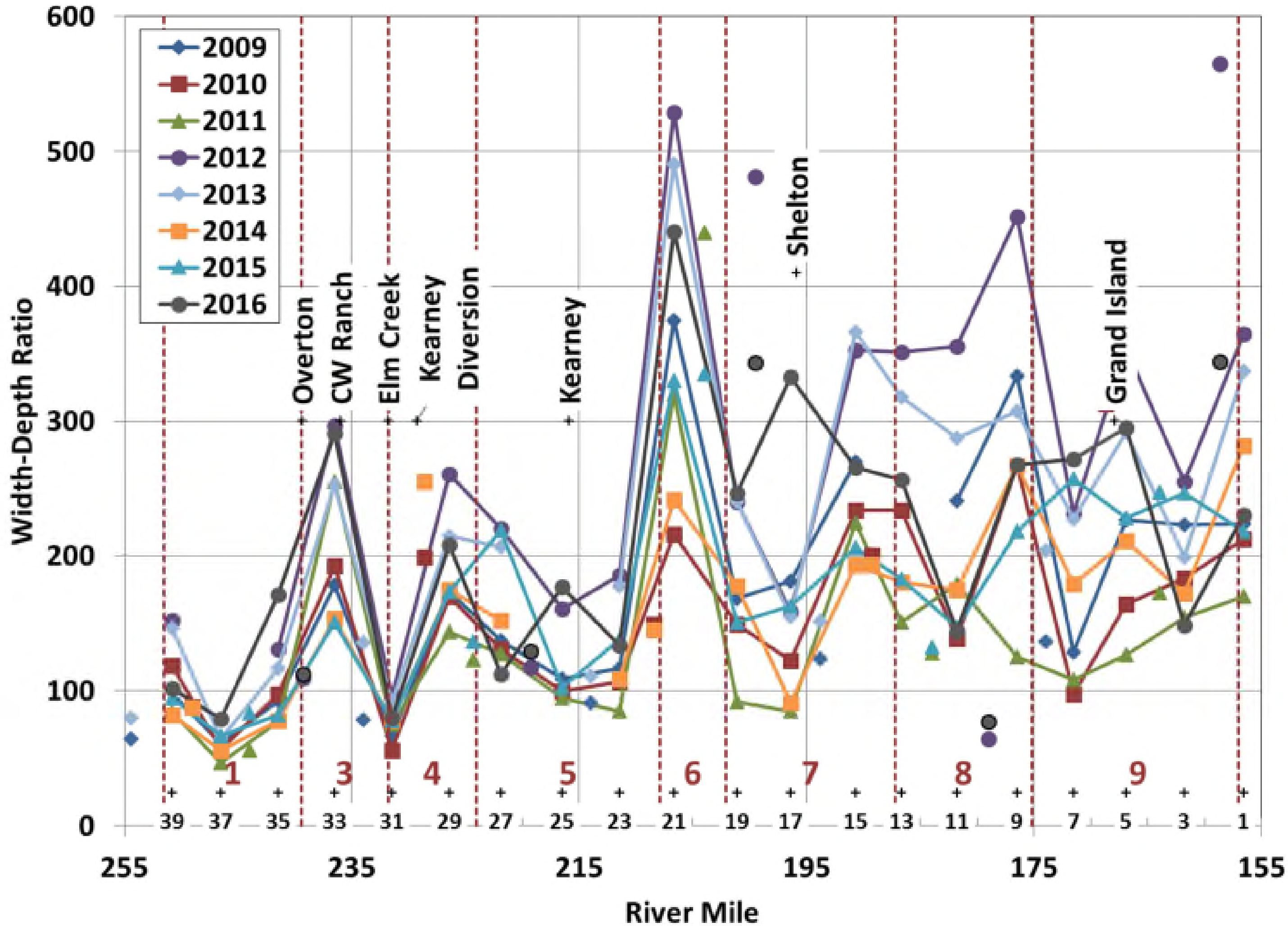

Figure 3.11a. Average width-to-depth (maximum depth) ratio at 1,200 cfs at pure panel APs. Rotating APs are shown by individual symbols only; pure panel APs connected with lines.

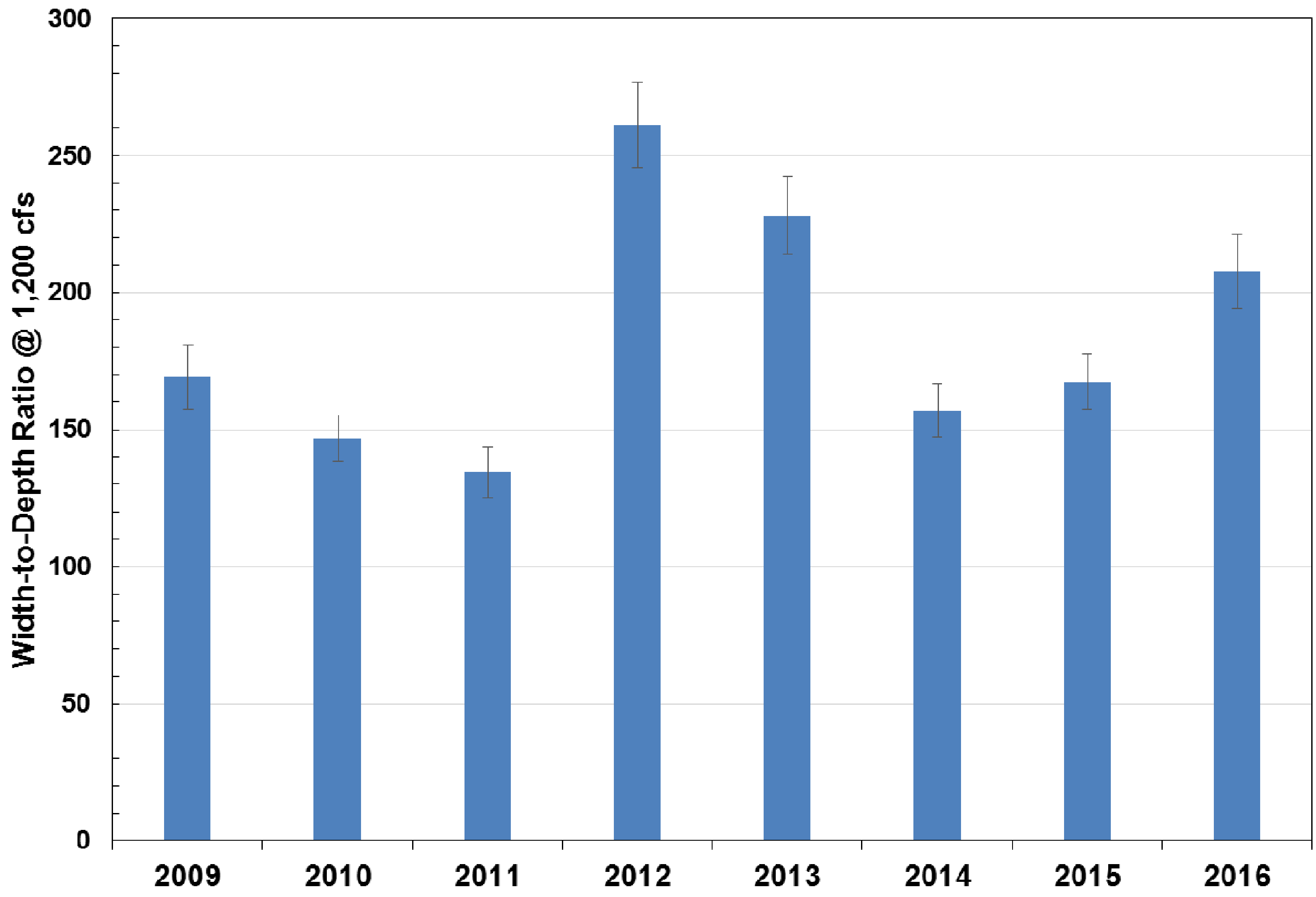

Figure 3.11b. Average width-to-depth (maximum depth) ratio at 1,200 cfs for the overall study reach, based on the pure panel AP data. Whiskers represent ±1 standard error on mean value.

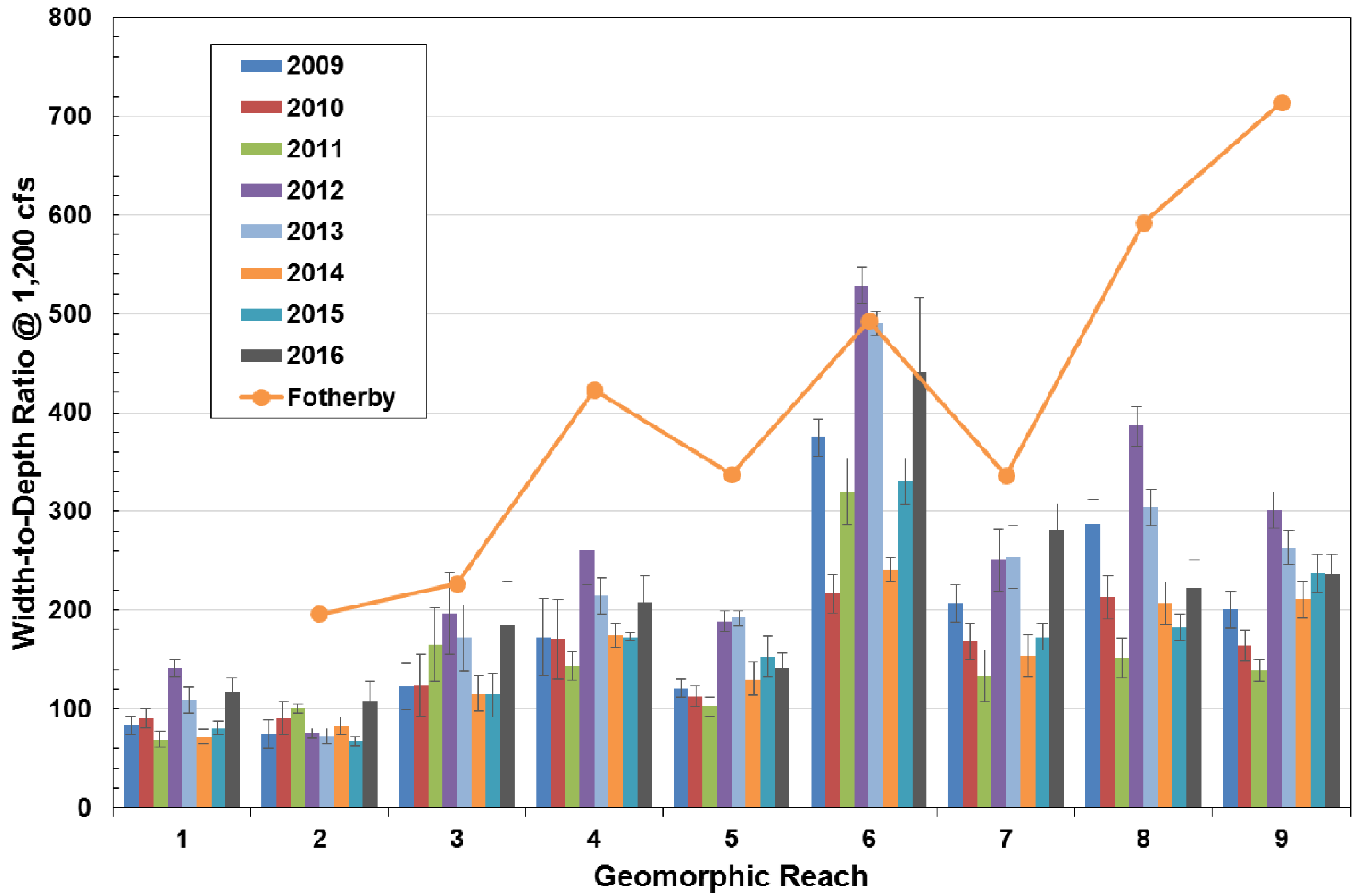

Figure 3.11c. Average width-to-depth (maximum depth) ratio at 1,200 cfs by geomorphic reach, based on the pure panel AP data from 2009 through 2015. Whiskers represent ±1 standard error on mean value. Also shown are the width-to-depth ratios from Fotherby (2008). *Note: Fotherby (2008) did not report W/D for Reach 1.*

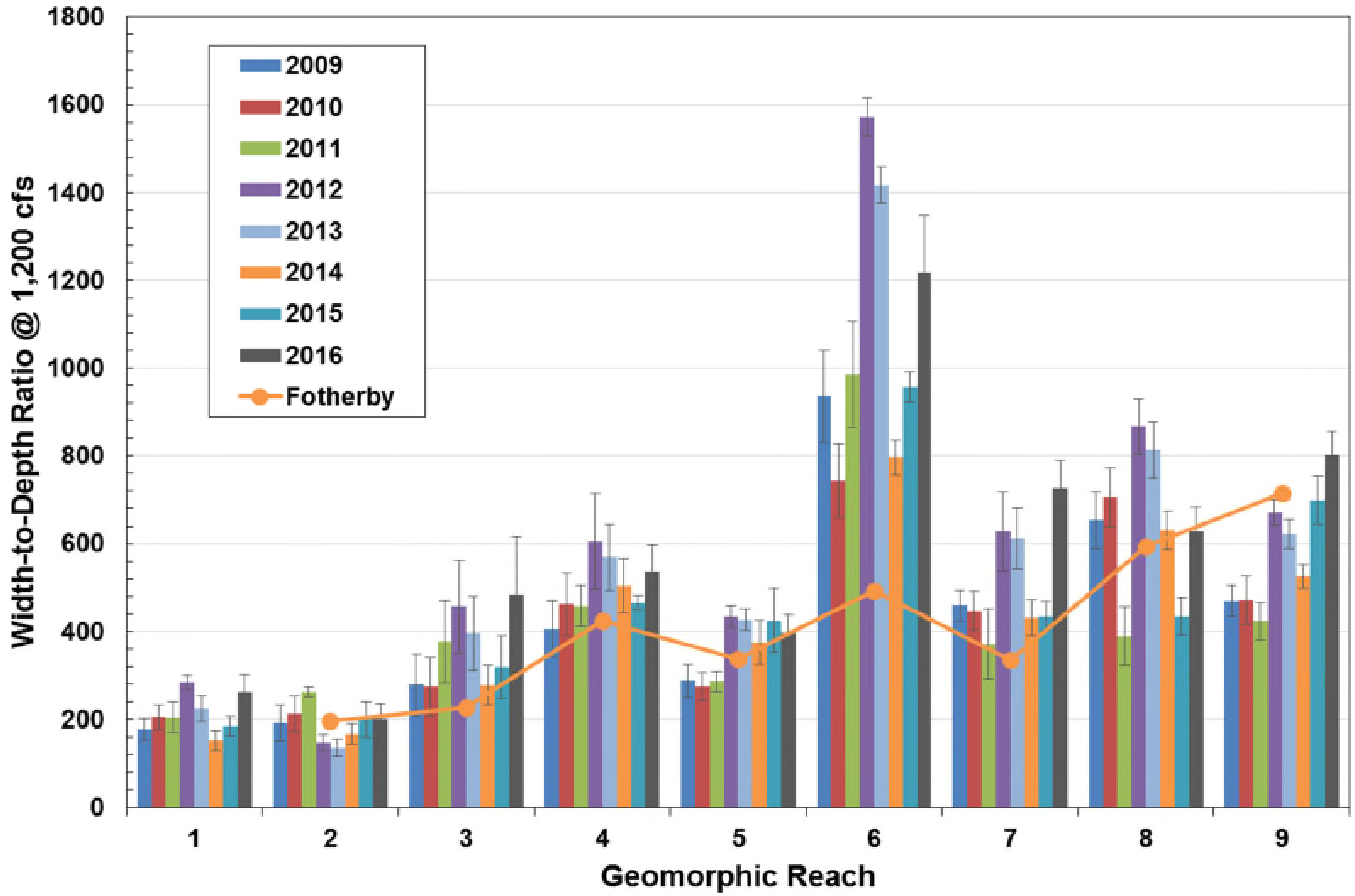

Figure 3.11d. Average width-to-**mean** depth ratio at 1,200 cfs by geomorphic reach, based on the pure panel AP data from the 2009 to 2015 data. Also shown are the width-to-depth ratios from Fotherby (2008). *Note: Fotherby (2008) does not report W/D for reach 1.*

3.3.7 Channel Cross-sectional Area (DAP 5.3.6)

The cross-sectional area data at the individual APs indicates considerable variability in the aggradation/degradation response from year-to-year (**Figure 3.12a-1**[12]**)** In general, with the exception of 2011 to 2012, the APs in the upstream approximately half of the reach (i.e., upstream from the Rowe Sanctuary) were mostly degradational throughout of the monitoring period, while the downstream half of the reach was neutral to slightly aggradational. Most of the reach was strongly aggradational in response to the sustained high flows that occurred between the 2011 and 2012 surveys. The changes that occurred over the 4-year periods between surveys at the rotating APs are generally consistent with those at the adjacent pure panel APs over the equivalent time periods (**Figure 3.12a-2**).

The overall aggradation/degradation quantities for the monitoring reach over the 8-year monitoring period were estimated based on the assumption that the changes at the pure panel APs are representative of the changes in the intervening reaches of the river. The 2009 to 2010 changes at AP33 were excluded from the analysis because this calculation is intended to provide information about the overall sediment-transport balance in the reach, and the changes at AP33 result from mechanical grading rather than differences in sediment-transport rates (**Figures 3.13a and b**). Not considering the changes at AP33, the overall study reach degraded by about 2.0M tons between 2009 and 2010, and degradation also occurred between 2010 and 2011 (~1.2M tons), 2013 and 2014 (0.6M tons) and between 2014 and 2015 (~4.5M tons) (**Figure 3.12b**). The overall reach aggraded substantially between the 2011 and 2012 surveys (~5.6M tons), and it also aggraded between 2012 and 2013 (~1.9M tons). The overall reach was only slightly aggradation between the 2015 and 2016 surveys (~0.1M tons). Over the 8-year monitoring period, the overall reach was slightly degradational (~0.7M tons total, or about 90,600 tons per year, on average).

All of the geomorphic reaches, as defined by Fotherby (2008) (Table 2.2), upstream from Minden (Reaches 1 through 5) were net degradational over the period and the four reaches downstream from Minden (Reaches 6 through 9) were aggradational (**Figure 3.12c**). About 740,000-tons of material was evacuated from Reach 1 (essentially the north channel at Jeffreys Island) over the period or an average annual rate of 106,000 tons. The south channel at Jeffreys Island lost about 98,000-tons of material during the period, or about 14,000-tons per year. Reach 3 (Overton to Elm Creek; essentially the Cottonwood Ranch Reach) degraded by about 340,000 tons or about 49,000-tons per year, and Reach 4 (Elm Creek to Odessa) degraded by about 468,000 tons (~67,000 tons per year). Reach 5 (Odessa to Minden) experienced the greatest volume of degradation, totaling about 1.54M tons over the 8-year period, or about 220,000 tons per year. Aggradation in the downstream four reaches ranged from about 352,000 tons (Reach 6 – Minden to Gibbon) to about 1.08M tons (Reach 8 – Wood River to Gibbon), or 50,000 to 155,000 tons per year on an average annual basis. The average aggradation/ degradation depths over the 8-year monitoring period associated with the above quantities range from 0.5 ft of degradation in Geomorphic Reach 5 to about 0.2 ft of aggradation in Reach 9 (**Figure 3.12d**).

[12]Note that the indicated degradation at AP33 between the 2009 and 2010 surveys resulted from mechanical removal of a large, vegetated mid-channel bar; the loss of sediment volume does not reflect a general sediment imbalance in the reach. The most upstream cross section at AP33 also widened by about 135 feet during the period between 2009 and 2011, due primarily to deflection of the flow around the graded material and into the banks. The material from the bar was graded directly into the channel where most, if not all, was entrained and carried downstream.

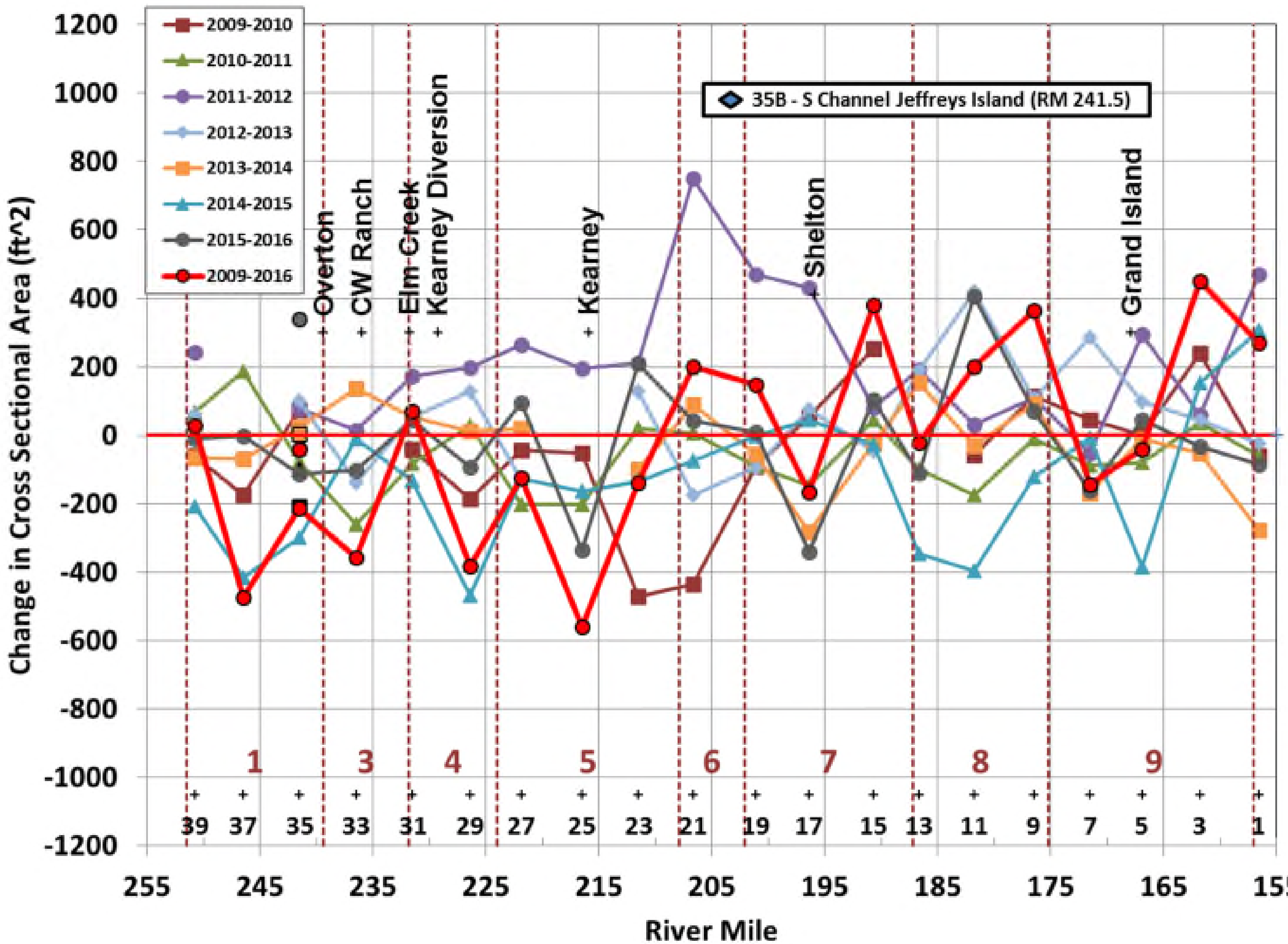

Figure 3.12a-1. Year-to-year change in average cross-sectional area at pure panel APs from 2009 through 2015. [Aggradation (+), Degradation (-)].

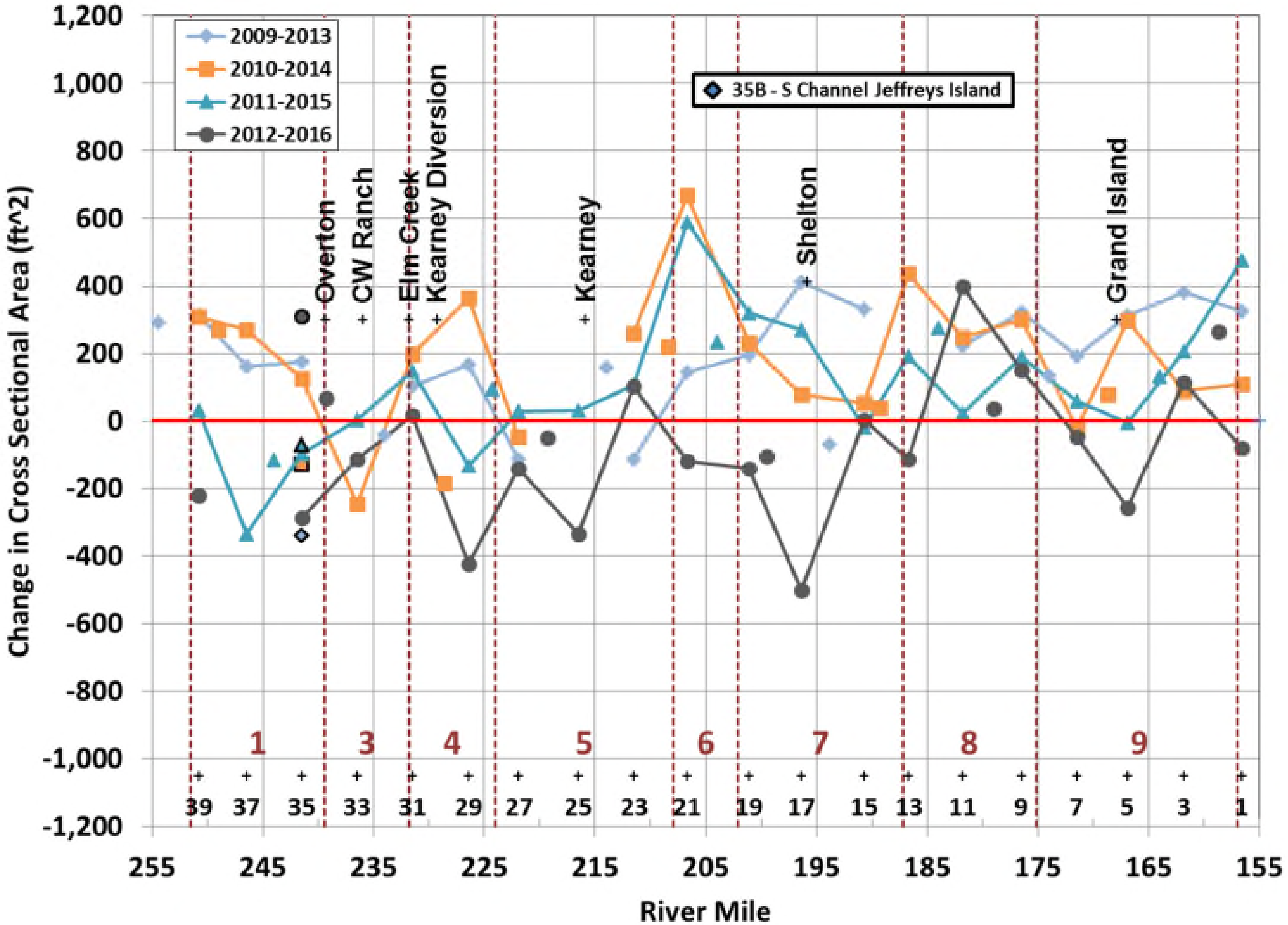

Figure 3.12a-2. Change in average cross-sectional area at all APs over four-year periods between rotating AP surveys. Line connecting AP33 on the 2009 to 2010 series is dashed to show effect of mechanical bar removal. [Aggradation (+), Degradation (-)].

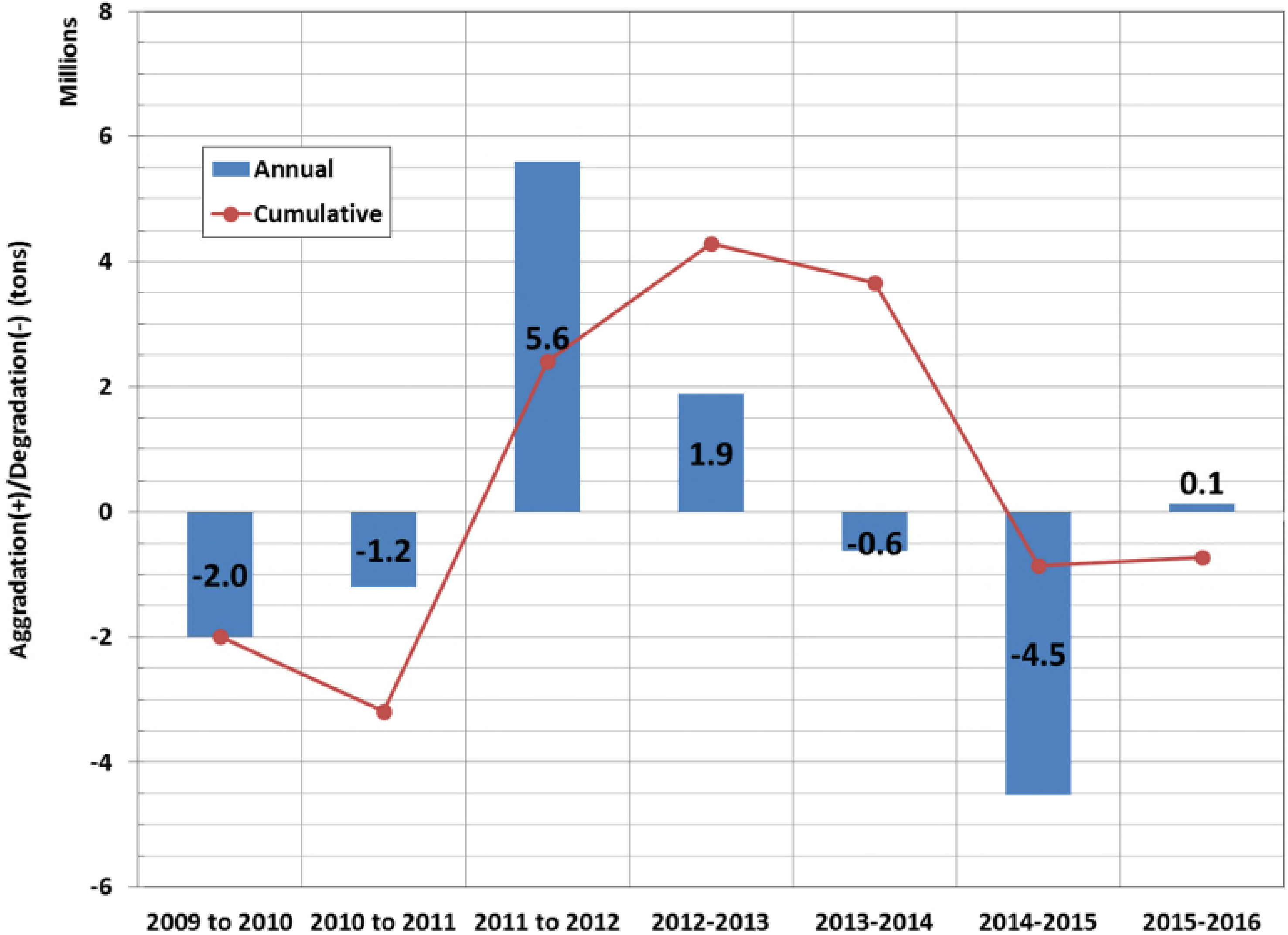

Figure 3.12b. Year-to-year aggradation/degradation volumes in the overall study reach from 2009 through 2015. Quantity for 2009 to 2010 does not include changes at AP33 associated with mechanical removal of a large mid-channel bar.

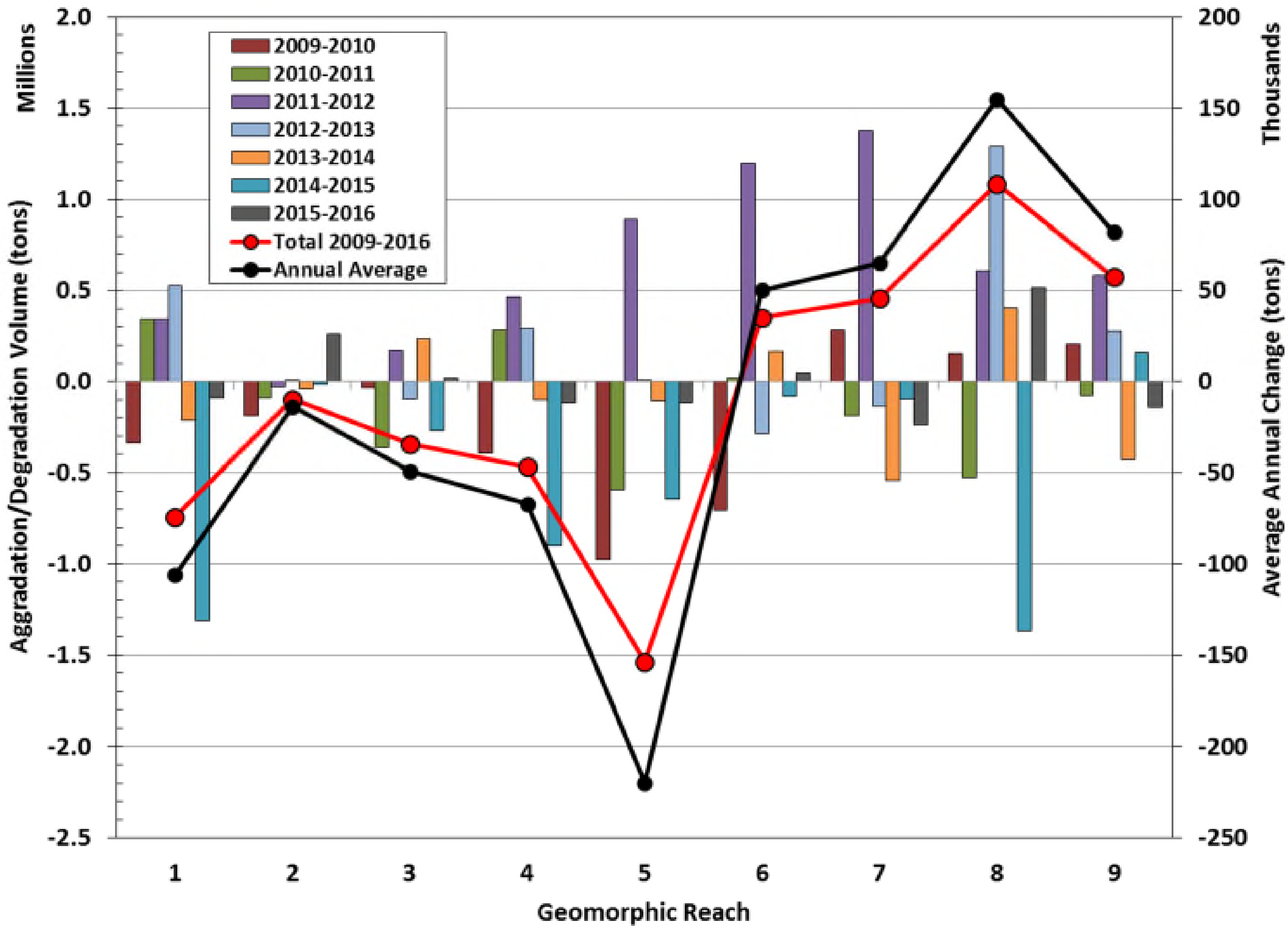

Figure 3.12c. Year-to-year aggradation/degradation volumes by geomorphic reach from 2009 through 2016. Quantity for Reach 3 during 2009 to 2010 does not include changes at AP33 associated with mechanical removal of a large mid-channel bar.

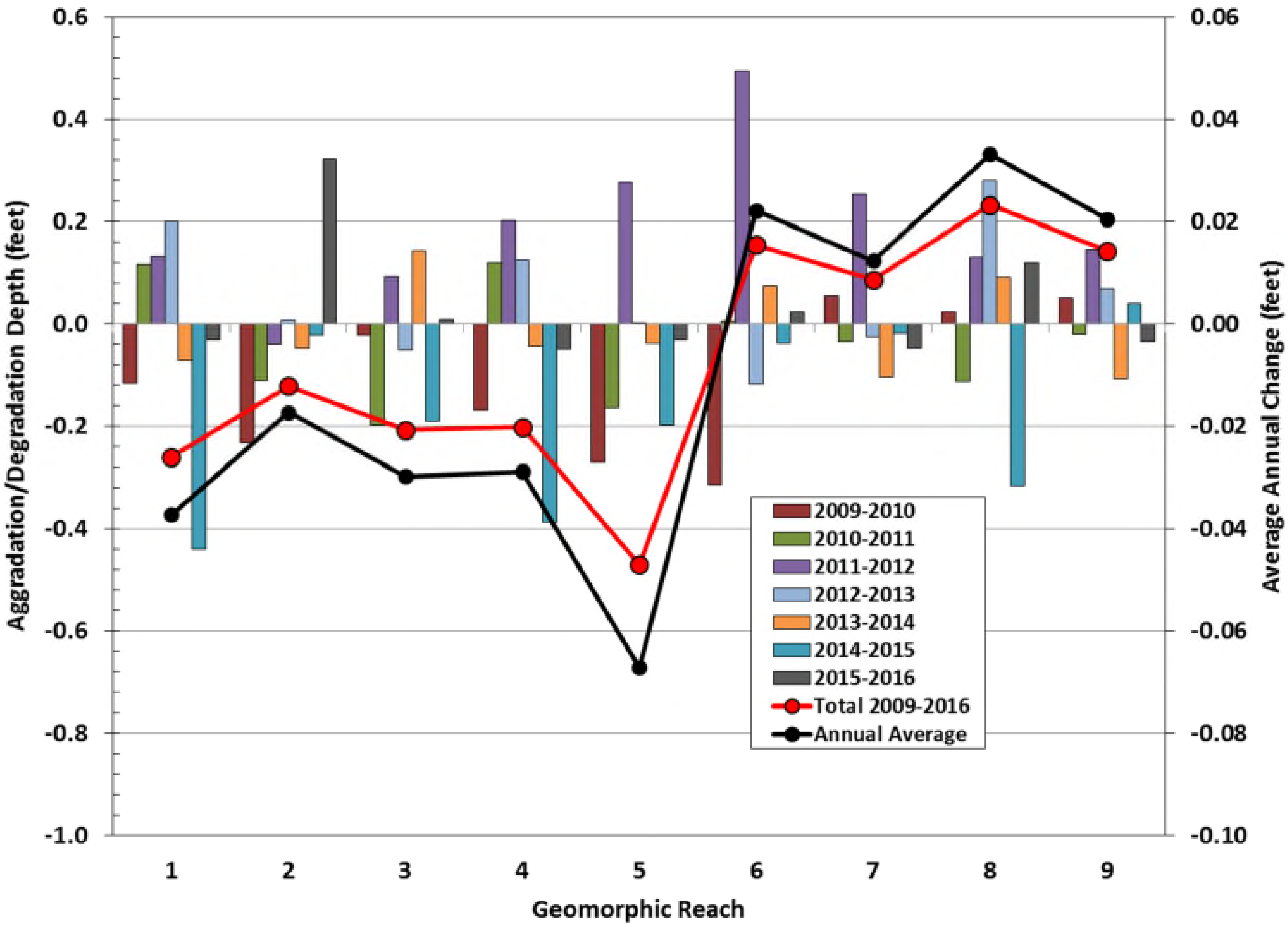

Figure 3.12d. Year-to-year change in mean bed elevation from 2009 through 2016, by geomorphic reach. [Aggradation (+), Degradation (-)].

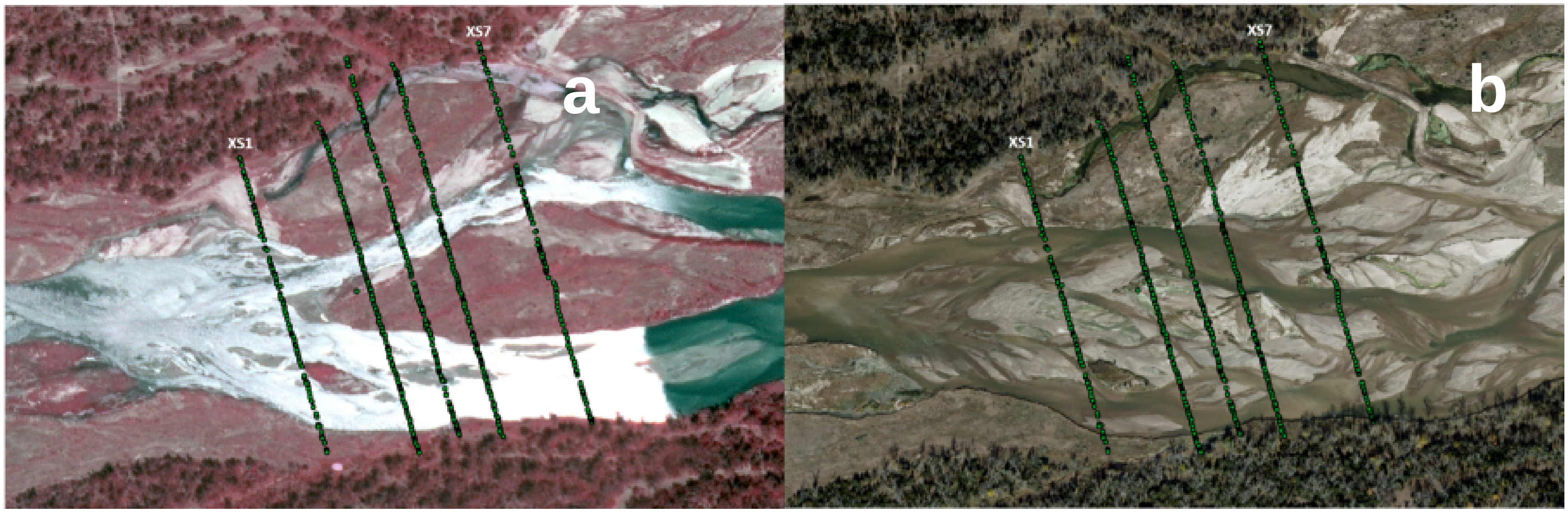

Figure 3.13a. Aerial photographs showing the locations of the surveyed cross sections at AP33: (a) July 2009 (Disharge~310 cfs), (b) October 2010 (Discharge~720 cfs).

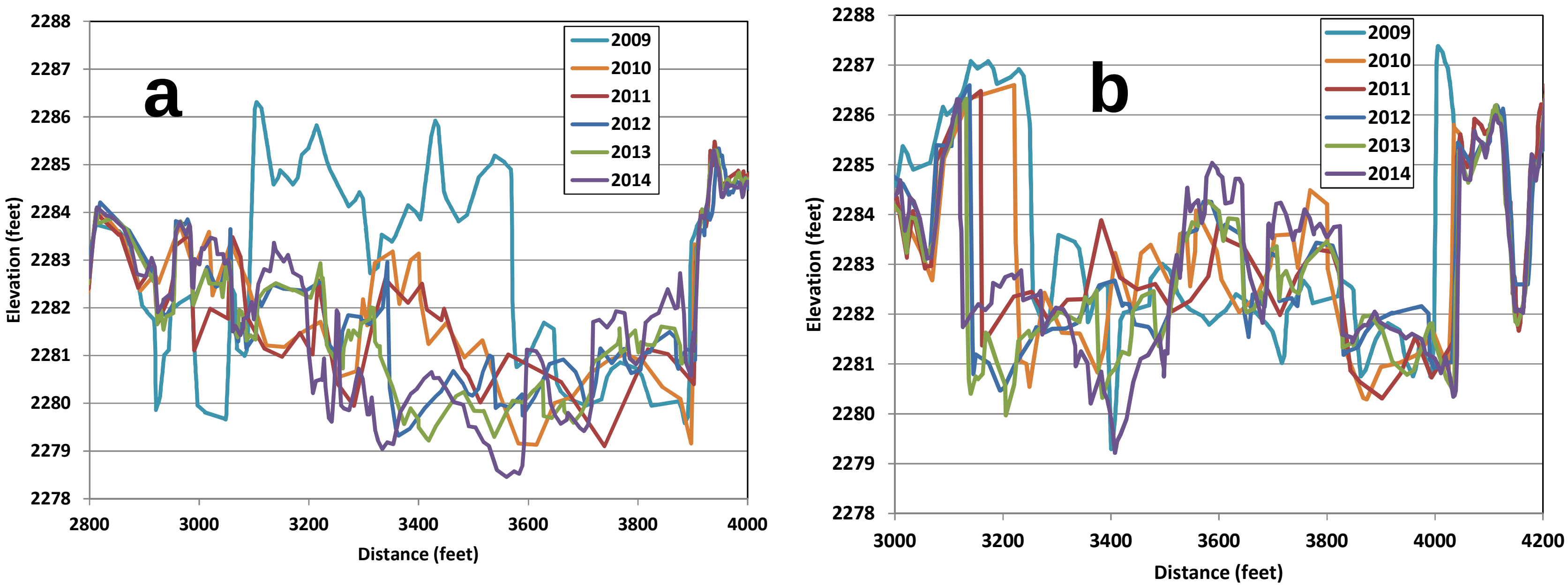

Figure 3.13b. Surveyed cross section profiles at AP33 (a) Downstream (XS7), (b) Upstream (XS1).

3.4 Vegetation Metrics

The vegetation monitoring surveys have produced large datasets (**Table 3.1**) that provide the basis for a broad range of analyses. In 2009, a total of 4,285 quadrats were sampled along 308 individual transects at 27[13] APs (from 41 independent survey sites including primary and secondary channels at most APs); with 2,817 quadrats and 154 transects from pure panel APs. Only species of inquiry for that year were quantified; totaling 26 individual species. In 2010, 5,224 quadrats (approximately 1,000 more than in 2009) were sampled at 26 APs and 29 independent sites, along 210 transects. Unlike in 2009, all specimens encountered in quadrats were documented, totaling 125 separate species – this protocol was followed in subsequent years. In 2011, 5,694 quadrats (4,310 at pure panel APs) and 102 separate species were documented. The 2012 survey totaled 4,134 quadrats (3,085 at pure panel APs) and 125 species at 25 APs and 27 total survey sites. In 2013, secondary channels were surveyed for the second time (2009 being the first), and the monitoring protocol was modified to surveying only 5 transects per AP. That year, a total of 3,304 quadrats were sampled at 41 independent sites. Of the 179 species identified, 64 were encountered no more than twice. In 2014, a total of 2,973 quadrats were sampled at 28 independent sites. Comparatively large portions of the channel were inundated during the 2015 field surveys, and only 1,902 quadrats were surveyed. Less species were encountered in 2015 because of either the flood flows or the lumping of some species under shared genera.

Table 3.1. Summary of Vegetation Survey Sites (2009-2016).

Year	Anchor Points	Sites	No. of Transects		No. of Quadrats		No. of Individual Species
			Pure Panel	Total	Pure Panel	Total	
2009†	27	41	154	308	2,817	4,285	26
2010	26	29	154	210	3,936	5,224	125
2011	27	29	147	189	4,310	5,694	102
2012	25	27	140	189	3,085	4,134	125
2013†‡	25	41	105	220	2,189	3,304	179
2014‡	24	28	120	140	2,259	2,973	149
2015‡	25	29	105	125	2,366	2,984	135
2016‡	25	29	105	145	2,341	3,099	147

† Includes Secondary channels surveyed once every four years
‡ Only 5 transects sampled at each AP

3.4.1 Green Line Elevation (GLE) (DAP 5.4.1)

The green line elevations (GLEs) during the monitoring surveys varied by up to 5 ft over the 8-year monitoring period of data, with the highest elevations recorded during 2011, 2015 and 2016 when long-duration, high flows were present in the reach, and the lowest elevations occurring during the very low-flow conditions in 2013 (**Table 3.2**; **Figure 3.14a**). GLEs were also very low in the relatively dry 2009. Differences in GLE from the initial survey in 2009 ranged from 0.2 ft below (2013) to 1.8 ft above (2011 and 2016) (**Figure 3.14b**). As expected from the detailed data, the year-to-year

[13] APs 35A, 36B and 37A are in the north channel at Jeffreys Island and 35B, 36A and 37B are in the south channel. All 6 of these sites are considered to be primary APs for purposes of the analysis because the flows are derived from different sources (upstream main channel for the former; J-2 Return for the latter) and because they represent different geomorphic reaches.

variation in the averages for the geomorphic reaches was consistent with those at the individual anchor points (**Figure 3.14c**).

During all years except 2012 and 2013, the GLEs were consistently in the range of 1 to 2 ft below the water surface associated with the maximum preceding discharge (Q_p; DAP 5.1.1) (**Figure 3.15**). During the low-flow years in 2012 and 2013, the GLE tended to be above the preceding maximum water-surface elevation. In 2015, the GLE was generally further below the maximum water surface than in any other year, with the difference exceeding 2 ft at most APs, and exceeding 3 ft at AP 19, 37, and 39.

Table 3.2. Average green line elevations at pure panel APs observed during the six monitoring surveys.

Anchor Point	River Mile	Green line Elevation (ft)							
		2009	2010	2011	2012	2013	2014	2015	2016
39	250.8	2372.6	2374.5	2375.1	2373.6	2373.5	2373.9	2375.6	2375.0
37	246.5	2347.5	2348.5	2349.2	†	2347.2	2347.9	2349.2	2349.3
35	241.5	2315.1	2316.6	2317.7	2315.5	2314.4	2315.9	2317.6	2318.4
33	236.5	2281.8	2282.8	2283.2	2282.4	2281.1	2282.5	2283.4	2283.4
31	231.5	2249.5	2250.6	2251.4	2249.6	2249.3	2250.1	2251.2	2250.6
29	226.4	2215.2	2216.2	2217.1	2215.9	2214.8	2216.2	2217.2	2217.3
27	221.9	2184.3	2185.8	2186.5	2184.5	2184.1	2185.5	2187.1	2186.9
25	216.5	2148.4	2149.7	2150.3	2148.3	†	†	2150.2	2150.2
23	211.5	2114.0	2115.0	2115.9	2114.1	2114.2	2115.4	2115.5	2115.6
21	206.7	2083.7	2085.6	2084.2	2083.9	2083.6	2084.3	2084.7	2084.9
19	201.1	2047.3	2048.2	2048.9	2047.5	2047.3	2048.6	2048.7	2048.9
17	196.4	2016.0	2017.1	2018.2	2016.1	2015.8	2017.2	2017.6	2018.3
15	190.7	1978.1	1979.2	1980.2	1978.1	1978.2	1979.5	1979.6	1981.1
13	186.7	†	1953.8	1954.5	1952.4	1952.7	1953.73	1953.9	1954.9
11	181.8	1921.8	1922.8	1923.3	1921.6	1921.9	1922.1	1922.7	1923.6
9	176.5	1888.9	1889.7	1890.0	1889.5	1888.6	1889.6	1890.9	1889.9
7	171.5	1856.6	1857.5	1858.3	1856.6	1855.8	1856.9	1857.9	1857.9
5	166.9	1828.3	1829.0	1829.8	1827.9	1827.8	1828.6	1829.5	1829.6
3	161.8	1792.1	1793.1	1793.6	1792.0	1791.1	1792.6	1793.6	1793.9
1	156.6	1762.0	1762.7	1763.5	1761.7	1761.3	1762.4	1764.0	1763.7

†No data collected at this AP for the indicated year.

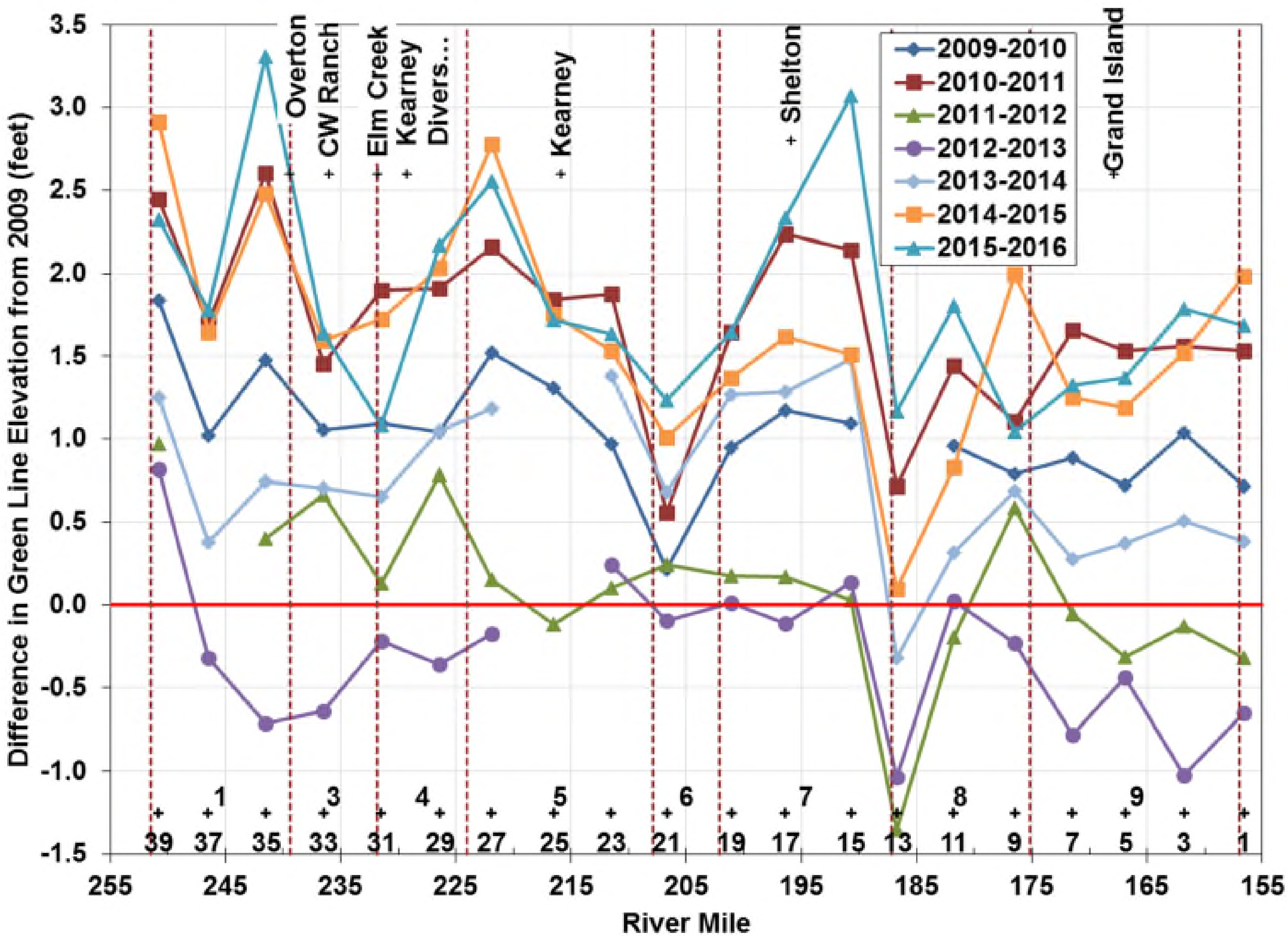

Figure 3.14a. Difference between average green line elevation at pure panel APs between the indicated year and the initial green line elevation surveyed in 2009. (AP13 at different location in 2009; changes referenced to 2010.)

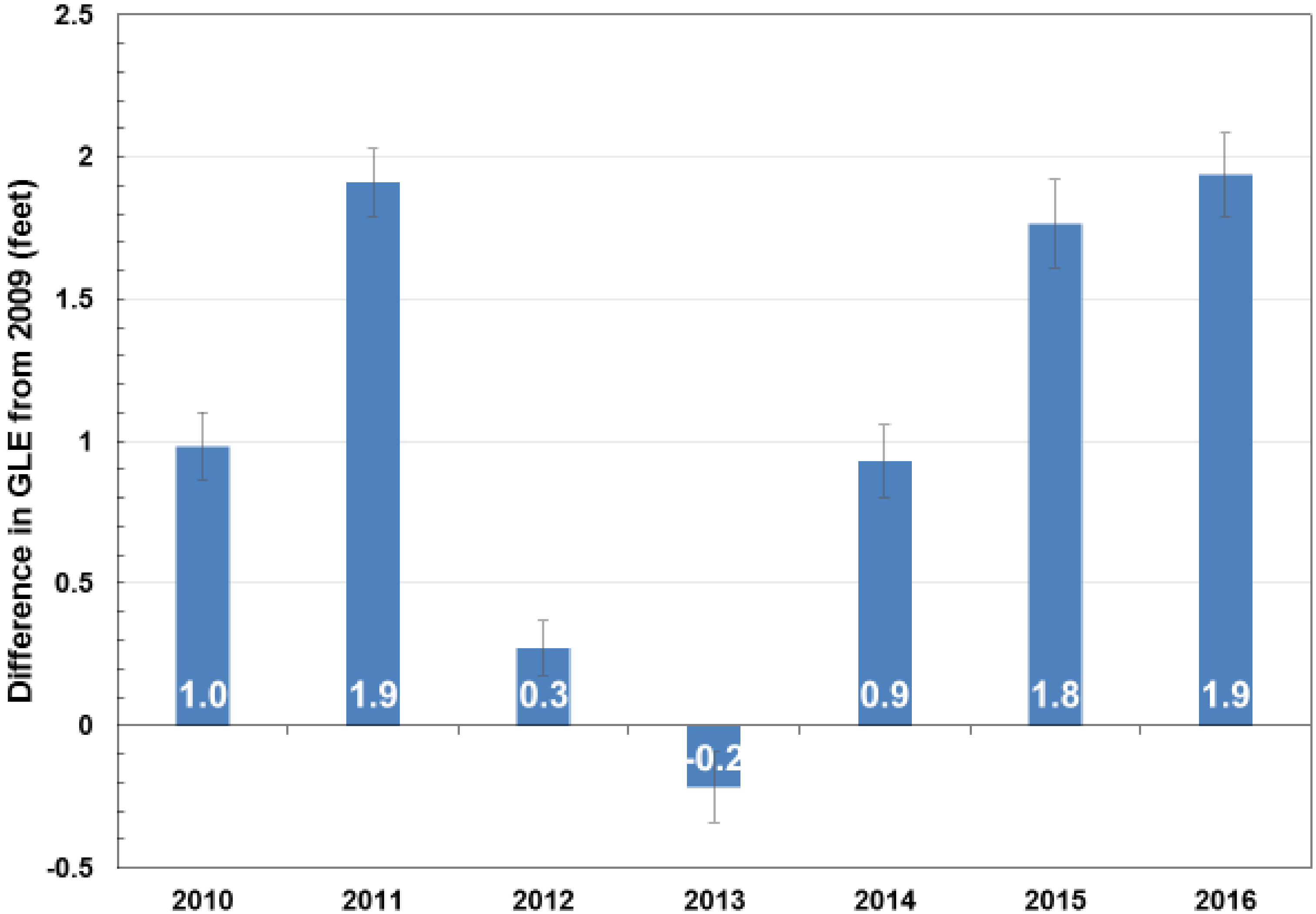

Figure 3.14b. Reach-wide average difference in green line elevation at pure panel APs between a given survey year and the 2009 greenline elevation.

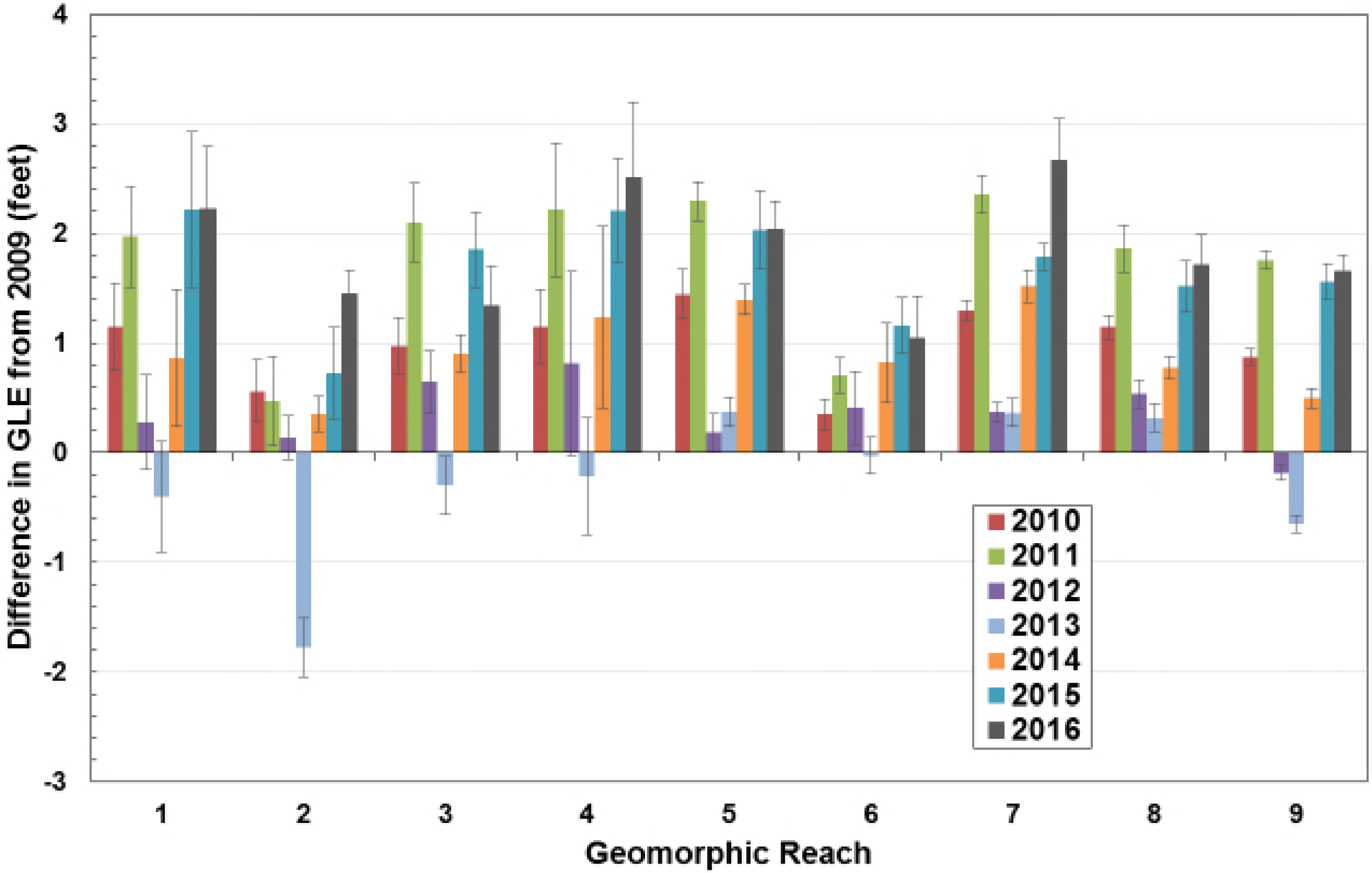

Figure 3.14c. Average difference in greenline elevation by geomorphic subreach between the initial survey in 2009 and the indicated year.

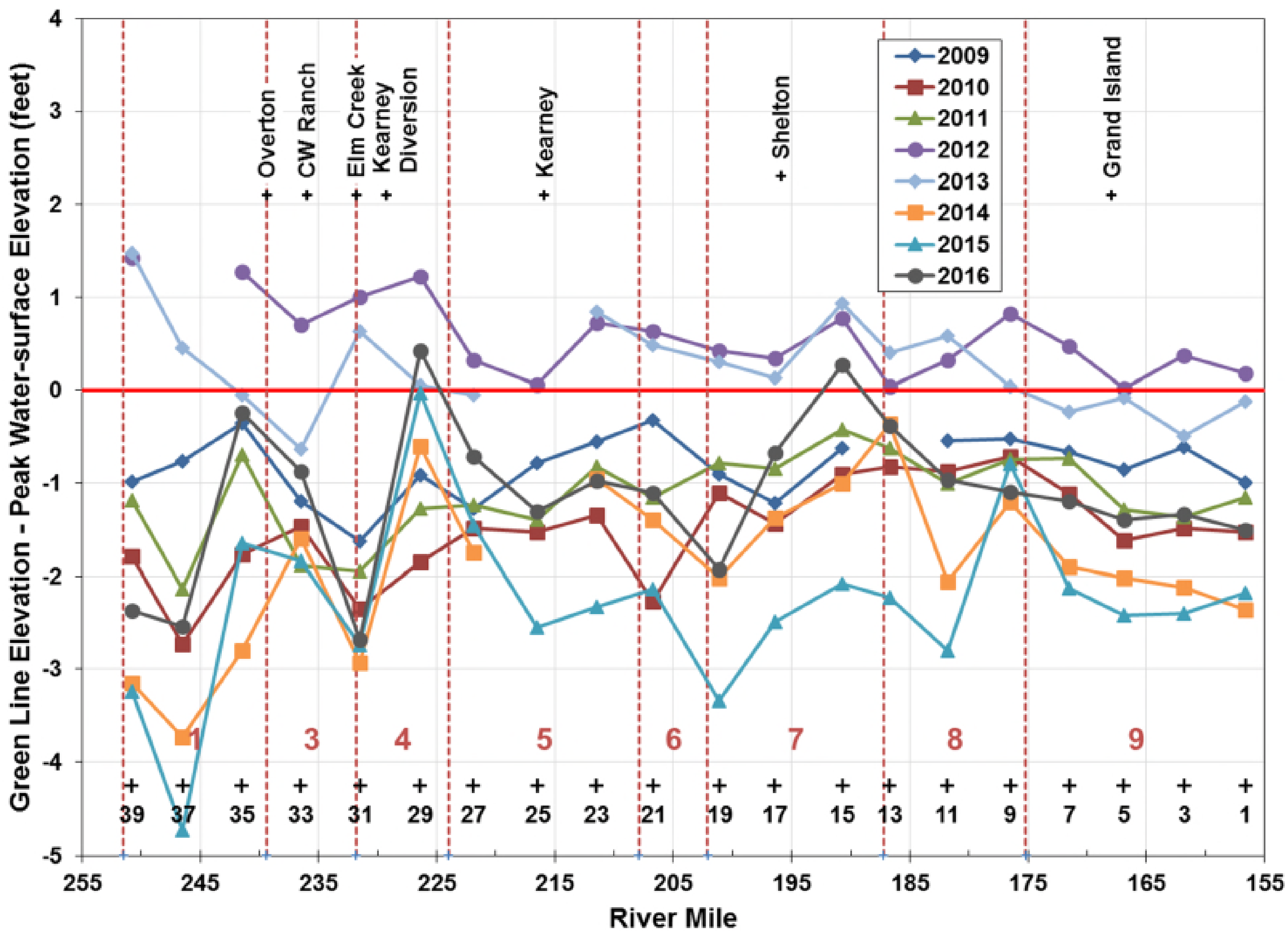

Figure 3.15. Average difference between greenline elevation and the water-surface elevation associated with the maximum preceding discharge (Q_P) at the pure panel APs.

3.4.2 Total Unvegetated Channel Width (DAP 5.4.2)

The Program has established a benchmark to maintain a target unvegetated channel width of 1,125 ft with a minimum width of at least 750 ft. The draft DAP defines unvegetated channel width (W_{Unveg}) as the *maximum width between vegetation within the channel and/or the channel banks*, and specifies that it is to be quantified by calculating *the distance between each pair of GLE points that bound the unvegetated channel segment*. After evaluating the first four years of data, it was determined that the total unvegetated width (sum of all unvegetated lengths across each transect) would better represent the original intent of this metric. The widths were determined by overlaying the surveyed GLE points over the applicable aerial photography and physically measuring the unvegetated distance between pairs of points using GIS software. This resulted in a shapefile and summary table with georeferenced points that define the ends of each unvegetated segment and the associated widths. For a variety of reasons, a suitable GLE point was not measured on one side of the unvegetated zone in every location. These reasons included the presence of rock or other bank protection or a raw vertical bank where vegetation could not establish at an elevation comparable to the other GLE points at the site. In these cases, the aerial photography, adjacent survey data, and in some cases, ground photographs were used to identify an appropriate location for the missing GLE points. The measurements for the 2009, 2010 and 2011 data were initially made by Program staff, and Tetra Tech staff made the measurements for the 2012 through 2016 data. Tetra Tech also checked the 2009, 2010, and 2011 measurements to ensure consistency with the approach used for the later data.

The resulting measurements indicate that the unvegetated width varied considerably throughout the reach and from year-to-year. The narrowest unvegetated widths typically occurred at AP7, AP23, AP31 and AP35 through AP39, and the widest occurred at AP1, AP15, AP17, AP21 (Rowe Sanctuary), AP25, AP29 and AP33 (Cottonwood Ranch) (**Figure 3.16a**). The reach-wide average unvegetated width for the Pure Panel APs increased from about 470 ft in 2009 to 725 ft in 2011, and then declined back to about 340 ft by the 2013 survey that was conducted after two successive very low germination season discharges (**Figure 3.16b**). The germination season flows were higher during the next three years, and the unvegetated widths increased to about 610 in 2014, 840 ft in 2015 and 850 ft in 2016. The only years in which the reach-wide average exceeded the minimum width threshold occurred in 2015 and 2016. Geomorphic Reach 6 had the widest average width during all six years, followed by Reaches 4 and 7 (**Figure 3.16c**). The average unvegetated width exceeded the Program's minimum width threshold in Reaches 4, 5, 6, 7, and 9 during one or more of the eight monitoring years, and the target threshold was actually exceed in Reach 6 in both 2015 and 2016.

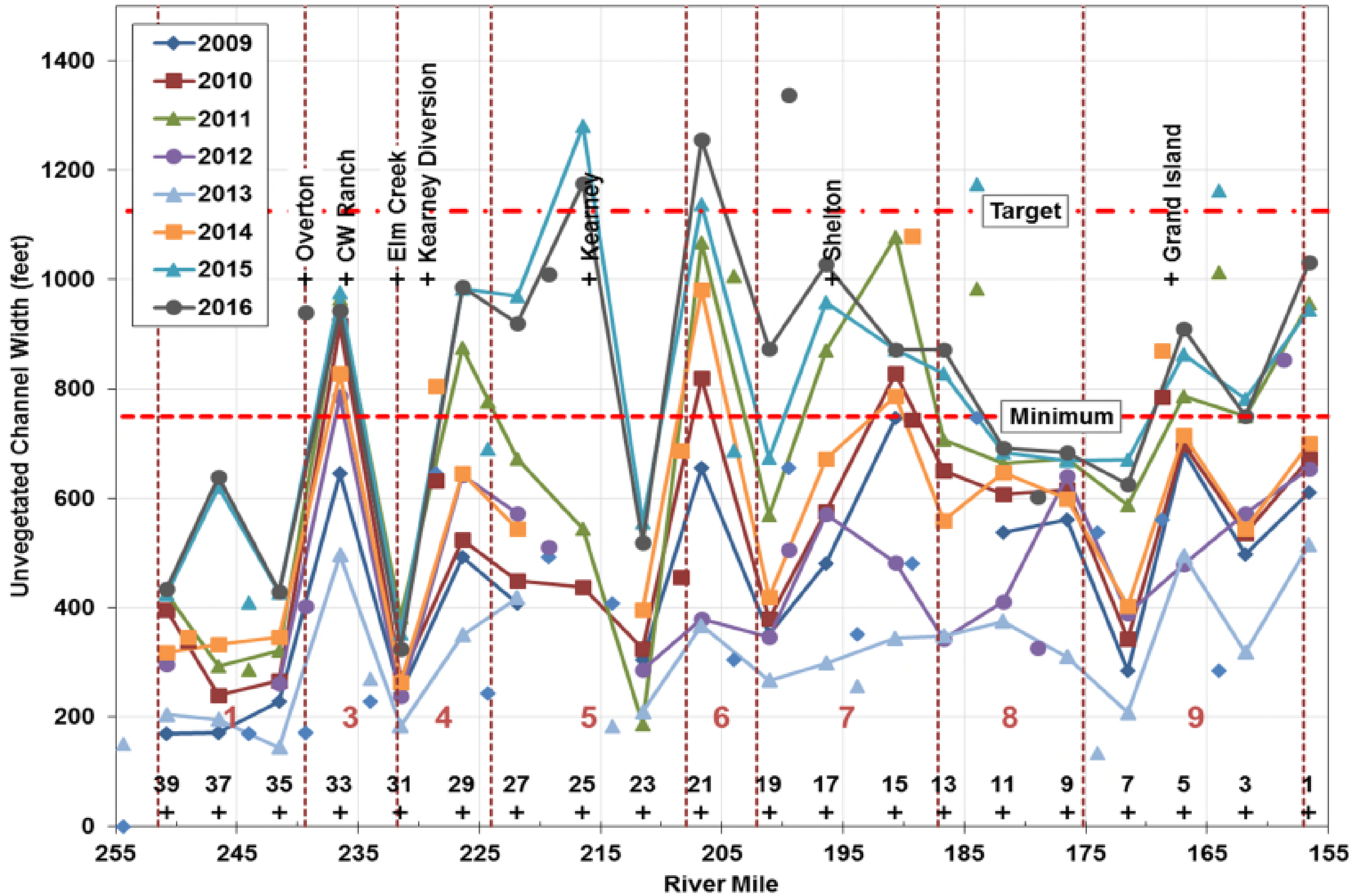

Figure 3.16a. Average unvegetated channel width at Pure Panel APs from 2009 through 2015. Rotating APs are shown by individual symbols only; pure panel APs connected with lines.

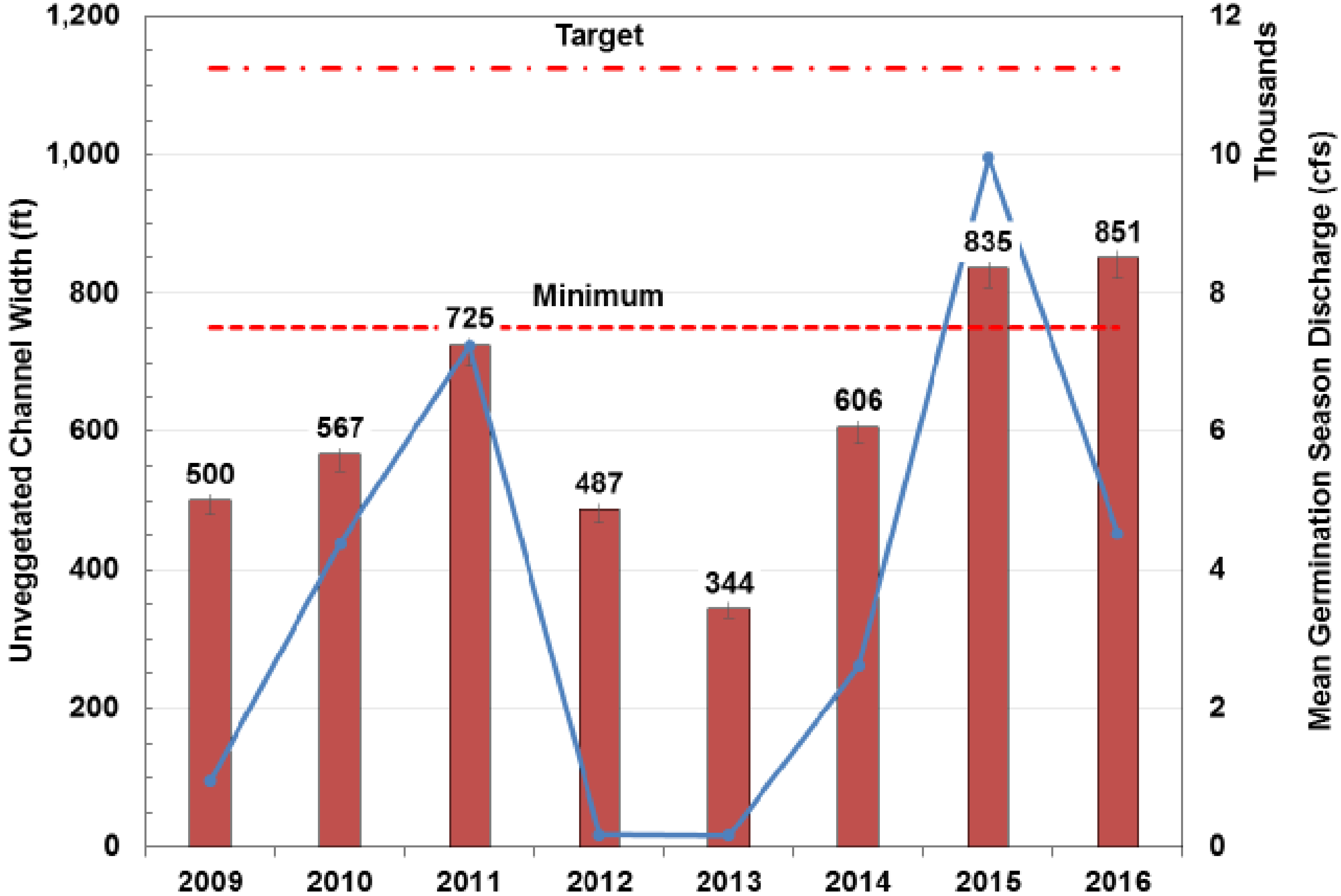

Figure 3.16b. Reach-wide average unvegetated channel width at pure panel APs. Also shown is the mean germination season discharge and the Program's minimum and target width thresholds.

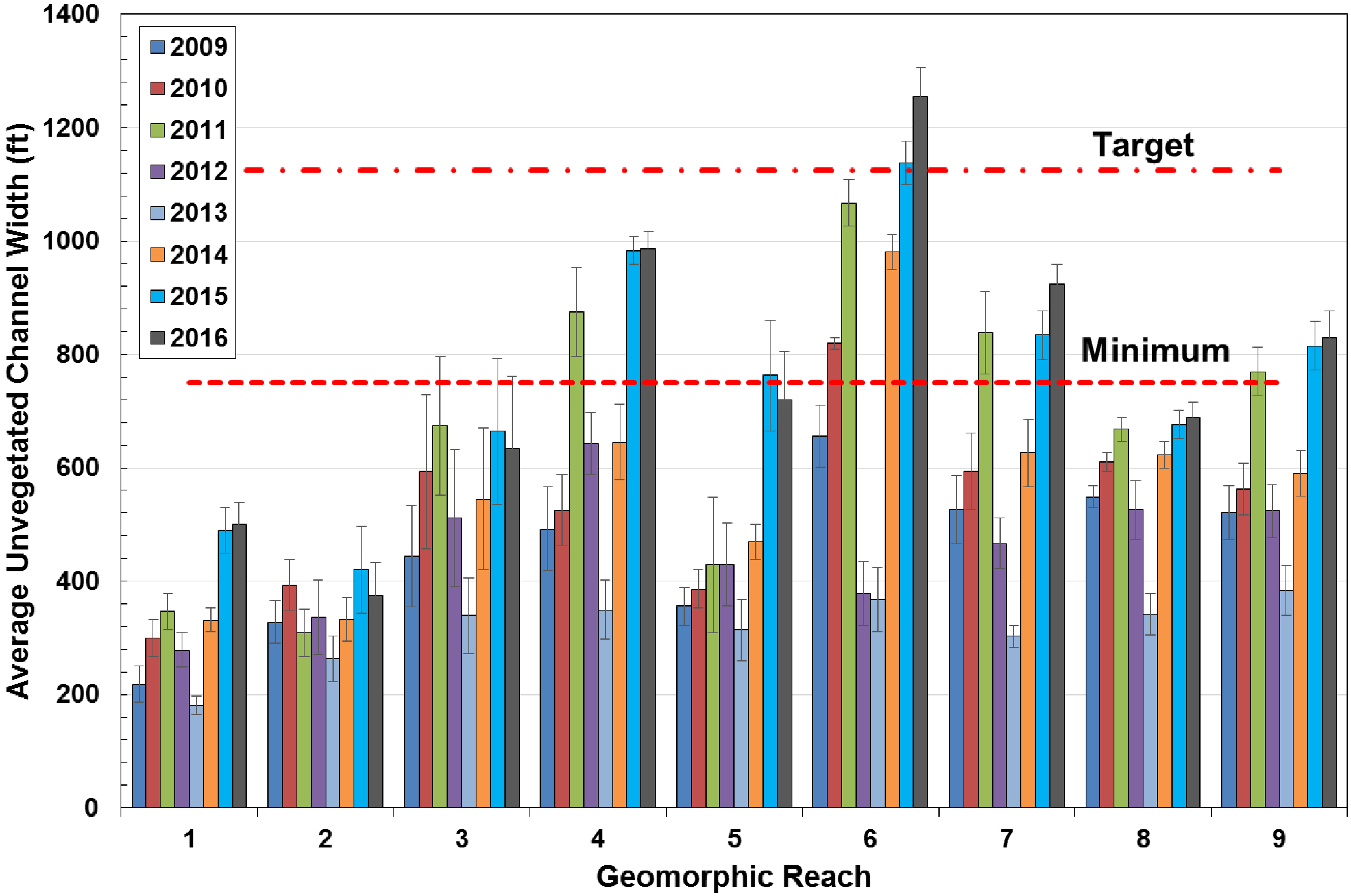

Figure 3.16c. Average unvegetated channel width by geomorphic reach.

3.4.3 Frequency of Occurrence by Species (DAP 5.4.3)

Based on the frequency of occurrence analysis, ragweed (*Ambrosia* sp.) was the most common taxa encountered in the reach during the initial survey in 2009 (20 percent of all quadrats), followed by rough cocklebur (*Xanthium strumarium*, 15 percent), purple loosestrife (14 percent), common reed (14 percent), and reed canary grass (*Phalaris arundinacea*, 11 percent) (**Figure 3.17**). The moderately high-flow years of 2010 and 2011 resulted in an increase in the frequency of some hydrophytic species. The most frequently occurring species in 2010 was flatsedge (*Cyperus* sp.) (26 percent), common reed (13 percent), beggar's tick (*Bidens* sp.) (11 percent), rice cut grass (*Leersia oryzoides*) (11 percent), and reed canary grass (10 percent). Flatsedge again was the most frequently observed species in 2011 (11 percent) followed by reed canary grass (8 percent), common reed (6 percent), purple loosestrife (4 percent), and beggar's tick (4 percent).

During the post-flood, but dry 2012 survey year, the most common species were hydrophytic or pioneering, including flatsedge (43 percent), sprangletop (*Leptochloa fusca*) (14 percent), Eastern cottonwood (14 percent, almost exclusively seedlings), ragweed (14 percent), and barnyard grass (*Echinochloa* sp.) (11 percent). In 2013, when flows were also low, annual ragweed (29 percent) returned as the most frequent species and flatsedge (28 percent) was nearly as common. These were followed by sprangletop (18 percent), rough cocklebur (14 percent), and reed canary grass (12 percent). The 2014 survey year mostly maintained the same pattern as 2013, with ragweed being the most common taxa (24 percent), followed by reed canary grass (13 percent), rough cocklebur (12 percent), flatsedge (11 percent), and dock (10 percent). Interestingly, sprangletop was much less common with a frequency of 3 percent in 2014.

Ragweed was much less common (8 percent) following the high spring flows in 2015. Flatsedge was the most frequently observed (23 percent), followed by cocklebur (14 percent), beggar's tick (11 percent) and reed canary grass (*Phalaris pectinacea*, 10 percent). In 2016, reed canary grass had the highest frequency at 13 percent, followed by flatsedge and ragweed at 12.4 and 12.3 percent, respectively. Cocklebur and cottonwood followed with 9 and 7 percent.

In total, fourteen species have been ranked in the top five most common species observed in any one year. Of those, ten maintained their top five ranking for more than one year, while four only were among the five most frequently-occurring only once (rice cutgrass, smartweed, lovegrass, and dock). Flatsedge, reed canary grass, ragweed, and cockleburs are consistently very common (in the top five in at least five out of eight survey years). Eastern cottonwood is the only woody species that has been relatively common, in the top five in 2012 and 2016. All fourteen taxa are pioneering and/or invasives, and with the exception of ragweed, have wetland indicator classifications of Facultative (FAC) or wetter, meaning they generally occur more than 50% of the time in wetlands. These characteristics strongly suggest that these species respond favorably to disturbance in a wet habitat, and often are the first to colonize an area after a disturbance. Other, more long-term ecological factors are responsible for determining whether these pioneering species would continue to persist across years. The cycle of high flows and vegetation disturbance followed by low flows has appeared to drive the vegetation frequencies within the survey area.

Ragweed and cottonwood were among the five most commonly-occurring species in 2016. The high flows of 2015 created suitable substrate for cottonwood regeneration, and some of the cottonwoods may have survived from 2015. Moderate flows during the 2016 growing season potentially minimized seedlings of many annuals and other pioneering species, such as flatsedge, and may have benefitted existing wetland plants such as reed canary grass and cottonwood that can withstand some inundation and grew rapidly with good water table conditions.

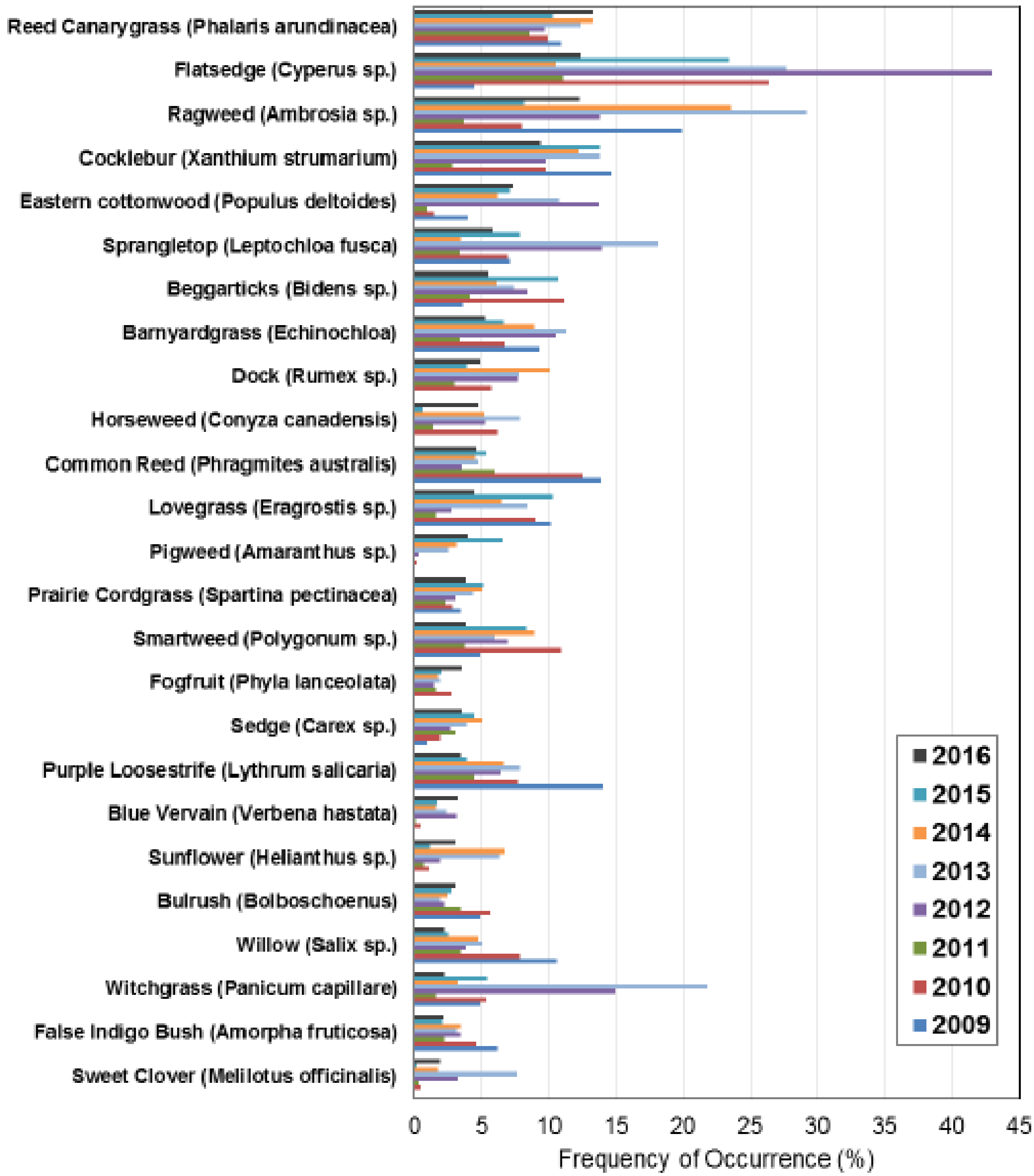

Figure 3.17. Frequency of occurrence of the top-25 most commonly observed species in 2016, and species of interest not among the 25 most commonly observed, 2009-2016. Results are organized by decreasing frequency according to the 2016 data.

Frequencies of the four species of primary interest ranged widely between years (**Figure 3.18**). The frequency of all four species declined substantially from 2009 to 2011, increased from 2011 to 2013 and then most declined again over the ensuing 3 years. Eastern cottonwood experienced the largest increase from only about 1 percent in 2011 to nearly 14 percent in 2012, and it has remained above 6 percent since 2012. The frequency of all four species was about the same in 2015 and 2016. Willow declined from about 11 percent in 2009 to 2 percent to 2.5 percent in 2015 and 2016, common reed declined from about 14 percent in 2009 to 4 percent to 5 percent in 2015 and 2016, and purple loosestrife declined from about 14 percent in 2009 to 3 percent to 4 percent in 2015 and 2016. The decline in common reed was most likely due to spraying and other active maintenance programs intended to reduce its coverage. Field observations in 2012 regularly noted high densities of Eastern cottonwood seedlings lining the water's edge on bare sandbars or shorelines, indicating that the high frequency was due to recruitment on the large area of sandbars exposed during dry conditions. Conditions in 2015 were somewhat analogous to those of 2012, with the high flows and subsequent increase in new bare habitat potentially driving the small increase in frequency that year. However, because the flows were high and persisted later in 2015, recruitment was not as wide-spread as many areas of bare sand were still under water at the time of seed dispersal. Flows in the spring of 2016 were elevated, but the moderately high flows continuing in June most likely minimized substantial recruitment of first-year seedlings.

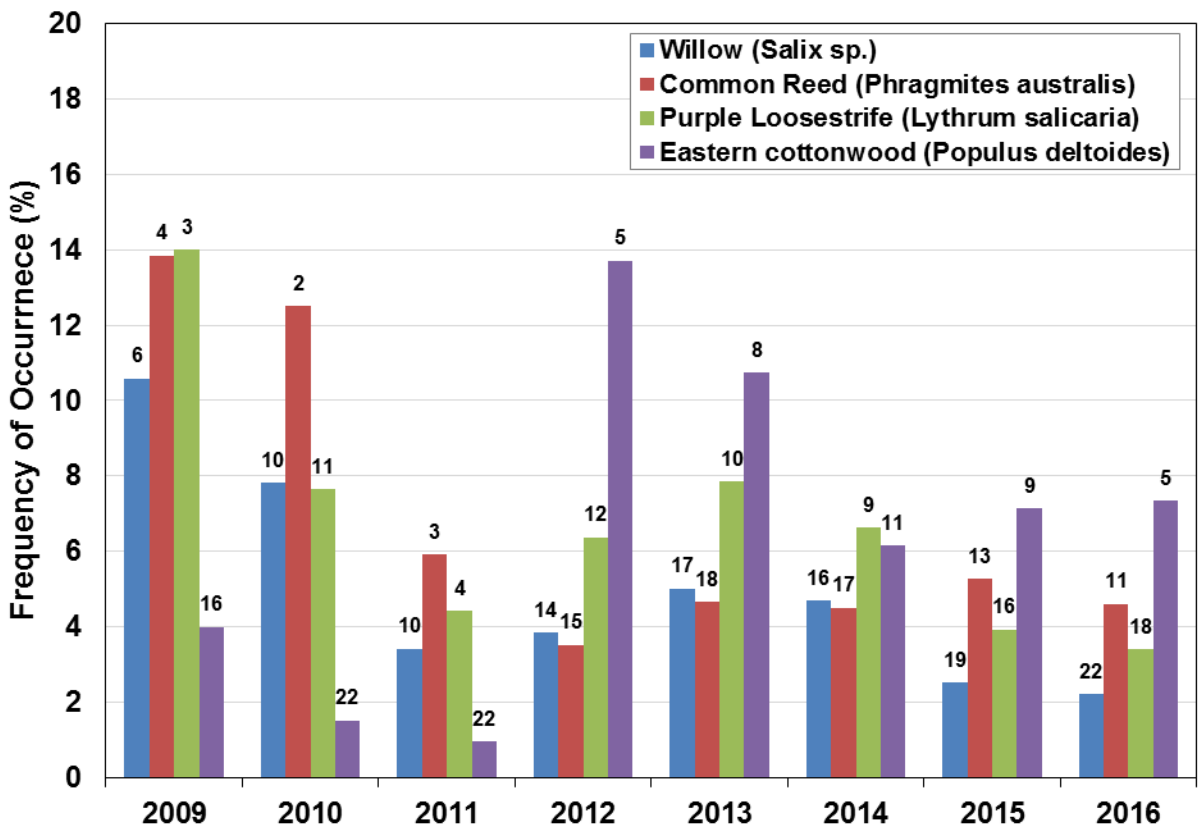

Figure 3.18. Frequency of occurrence for the four species of primary interest for the 2009 through 2016 vegetation surveys. Also shown is each species' annual rank by frequency amongst all species.

The distribution of the species of primary interest along the study reach was assessed based on the average frequency of occurrence within each of the nine geomorphic reaches. In general, purple loosestrife (*Lythrum salicaria*) has consistently been most prevalent in the downstream half of the study reach (Geomorphic Reaches 6 through 9), although in 2009, it was also present in relatively high frequencies (~7 percent) in Reach 1 (**Figure 3.19**). There have only been two observations of purple loosestrife in the south channel of Jeffrey's Island since 2009, both of which occurred in 2010. In general, the frequency of purple loosestrife has been in decline in all reaches since 2009. In 2016, in reaches where purple loosestrife is most abundant (Geomorphic Reaches 6-9), frequency generally increased. Frequency decreased considerably in Reaches 7 and 5.

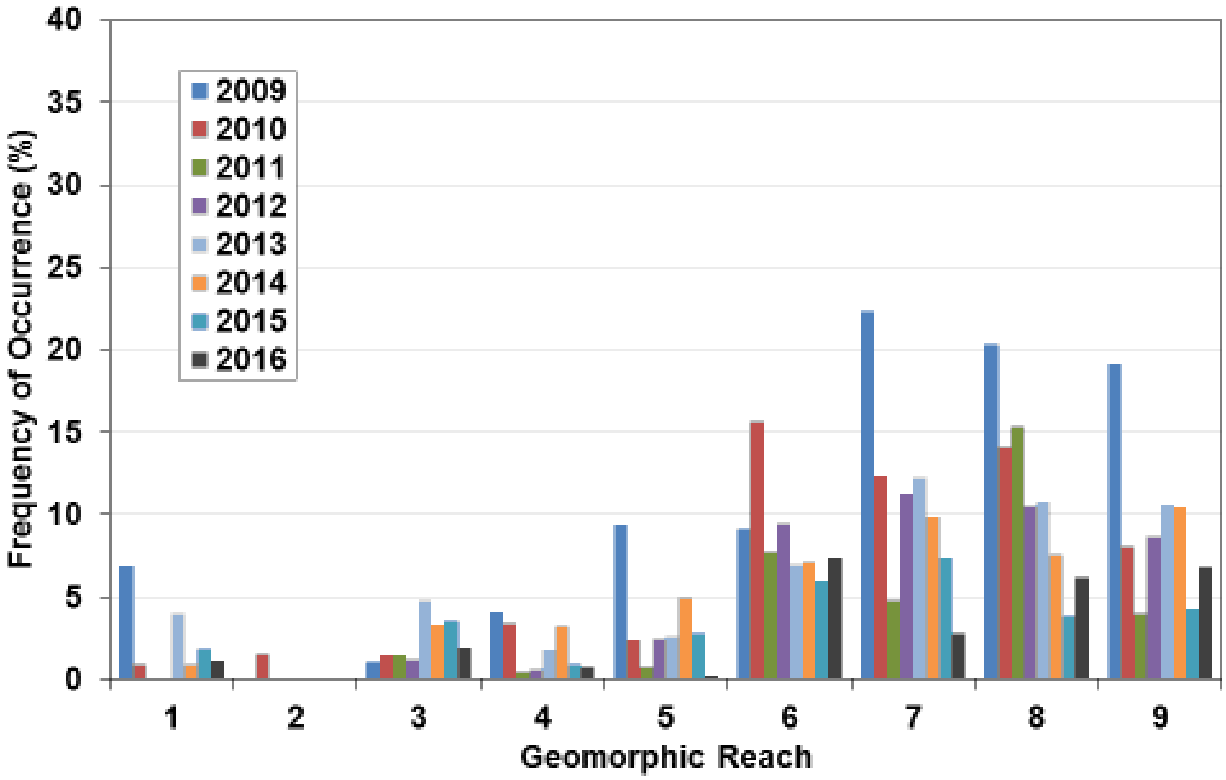

Figure 3.19. Mean frequency of occurrence of purple loosestrife (*Lythrum salicaria*) by geomorphic reach, 2009-2016.

In 2009, common reed (*Phragmites australis*) was most prevalent in the middle and downstream portion of the monitoring reach (Reaches 4, 5, 7 and 9) (**Figure 3.20**). A relatively large amount of common reed (>10 percent) was also present in Reach 1 at the upstream end of the study reach. The frequency remained relatively high in Reaches 5, 7 and 9 in 2010, followed by a substantial decrease in 2011. Overall, prevalence of common reed has drastically decreased since 2009; most likely in response to spraying and other management activities. Observations in 2016 included many rhizomes of common reed spreading onto bare sandbars. It is likely that common reed would rapidly recolonize in the absence of active management.

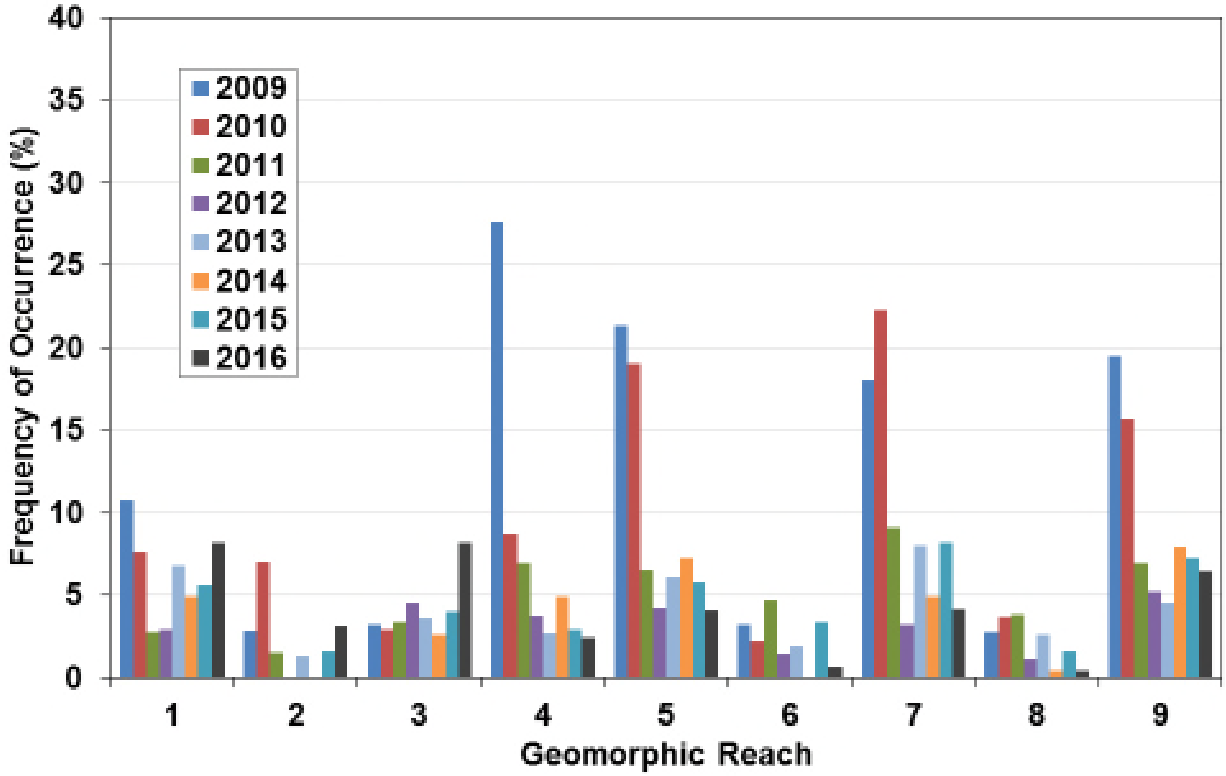

Figure 3.20. Mean frequency of occurrence of common reed (*Phragmites australis*) by geomorphic reach, 2009-2016.

Eastern cottonwood (*Populus deltoides*) was present at relatively low frequencies throughout the entire study reach in 2009, with slightly higher frequency in the downstream part of the monitoring reach (6 percent and 7 percent in Reaches 8 and 9, respectively) (**Figure 3.21**). Except for Reaches 2 and 3, where it increased from trace amounts to 4 percent to 5 percent, the frequency of cottonwood generally declined throughout the survey area in 2010. A general decline also occurred in most reaches in 2011. Every reach, except Reach 2, experienced a substantial increase in frequency. Cottonwood was observed in 21 percent of quadrats in Reach 1, and at frequencies over 10 percent in Reaches 3, 4, 5, 7, 8, and 9. In 2013, the frequency of cottonwoods was relatively unchanged in all reaches except Reach 3, where it decreased to about 7 percent. A continued decline in cottonwood frequency was observed in 2014. This trend reversed in 2015 and cottonwood frequency was maintained into 2016. Cottonwood frequency stayed the same in Reaches 1 and 8; increased in Reaches 3, 4, and 9; and declined in Reaches 2, 5, 6, and 7. Overall, cottonwood was present at frequencies from 4.6 to 10.7 percent in 2016.

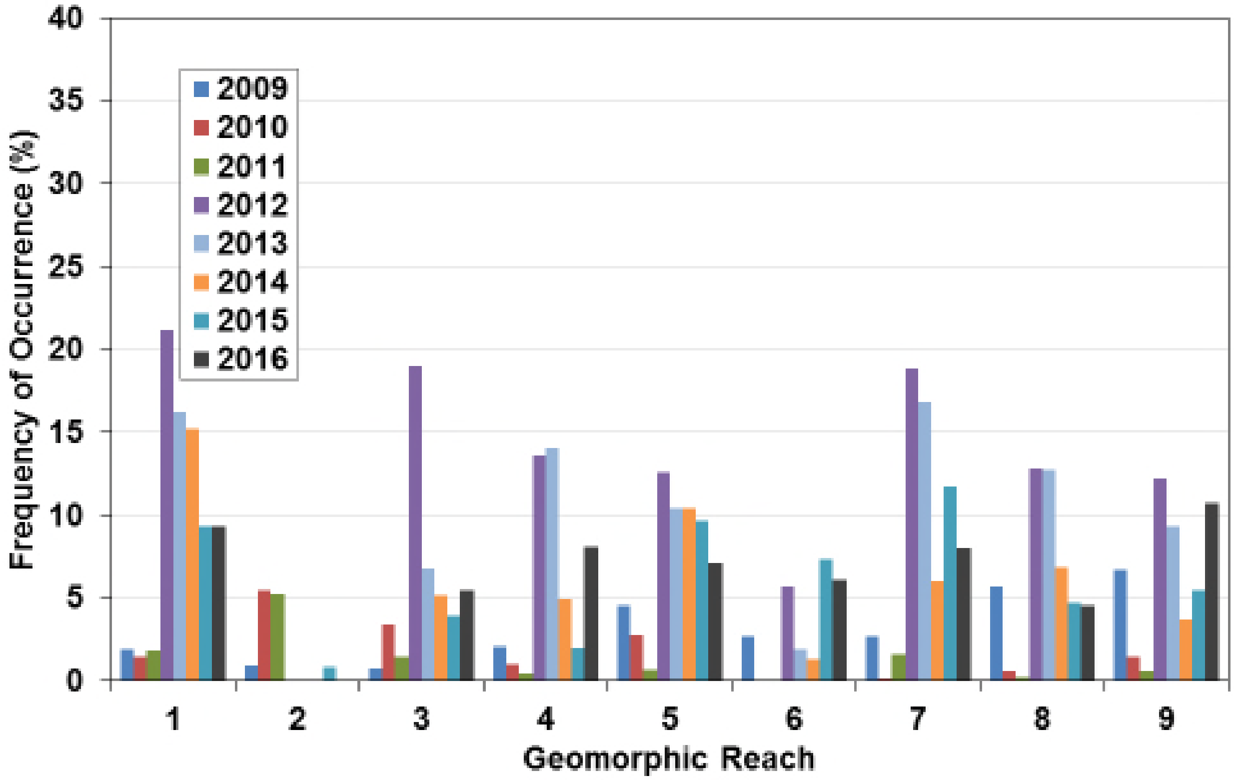

Figure 3.21. Mean frequency of occurrence of eastern cottonwood (*Populus deltoides*) by geomorphic reach, 2009-2016.

Willow (*salix sp.*) was present throughout the study reach in 2009, with the highest frequency occurring in Reach 4 (38 percent), followed by Reach 5 (17 percent), and Reach 2 (16 percent) (**Figure 3.22.**). Other reaches where willow was present at frequencies greater than 5 percent include Reaches 1, 7, 8, and 9. In 2010, willow increased in frequency in Reach 2 to about 27 percent, and increased to 9 percent in Reach 8, while frequency in all other reaches declined. The decline in Reach 4 was the greatest year-to-year change for any species of interest in any subreach, declining from 38 percent to 7 percent. In 2011, willow was not observed in any quadrats in Reaches 1 or 6, and appeared in less than 1 percent of quads in Reach 9. All other reaches showed declines from 2010 to 2011. Willow frequency increased in about half the reaches in 2012. Interestingly, it was observed most frequently (7 percent) in Reach 6, which had no specimens observed the previous year. Further increases were observed in all reaches except Reach 9 during the 2013 field season. In general, willow frequency was stable or declining in all reaches in 2014 and 2015. By the 2016 field season, the frequency of willow had slightly decreased overall, with specific declines in Reaches 4, 5, 7, and 8; and despite increases in Reach 1, 2, 3, 6, and 9.

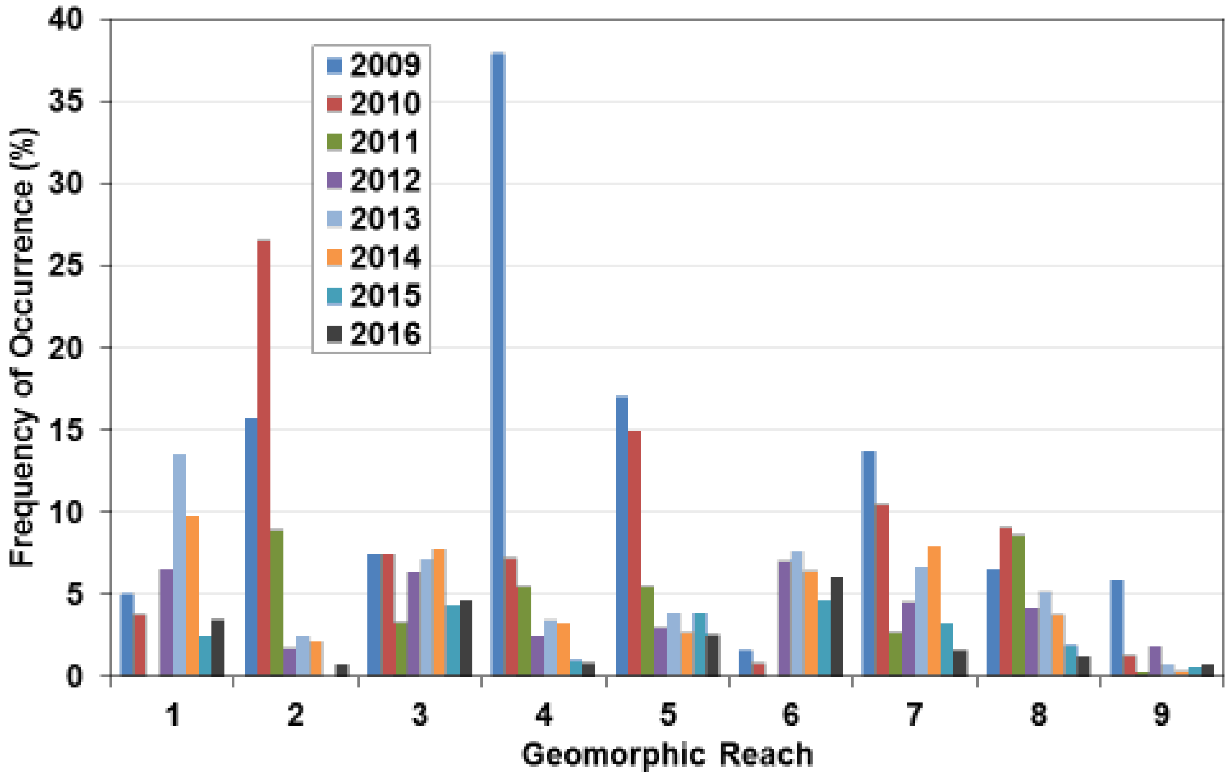

Figure 3.22. Mean frequency occurrence of willow (*Salix sp.*) by geomorphic reach, 2009-2016.

3.4.4 Percent Cover by Species (DAP 5.4.4)

In 2009, the percent cover for the 25 most prevalent species, plus the two additional species of interest, discussed in the previous section ranged from effectively 0 to 6.2 percent across all sampled main channel quadrats at the pure panel APs (**Figure 3.23**). The ranges were similar in subsequent years (up to 6 percent in 2010, 4.8 percent in 2011, 3.7 percent in 2012, 6.3 percent in 2013, 7.3 percent in 2014, 7.2 percent in 2015, and 7.5 in 2016). These data indicate that no single species accounted for more than about 8-percent cover of the survey area during any year. Reed canary grass covered about 7.5 percent of the quadrat area in 2016, the highest percentage of any single species during the 8-year monitoring period. Flatsedge covered about 7.3 percent of the area in 2015, and ragweed covered 7.3 percent in 2014. Reed canary grass also covered 6.2 percent of the area in 2014. The only other species that covered more than 6 percent of the survey area was common reed in 2009 (6.2 percent).

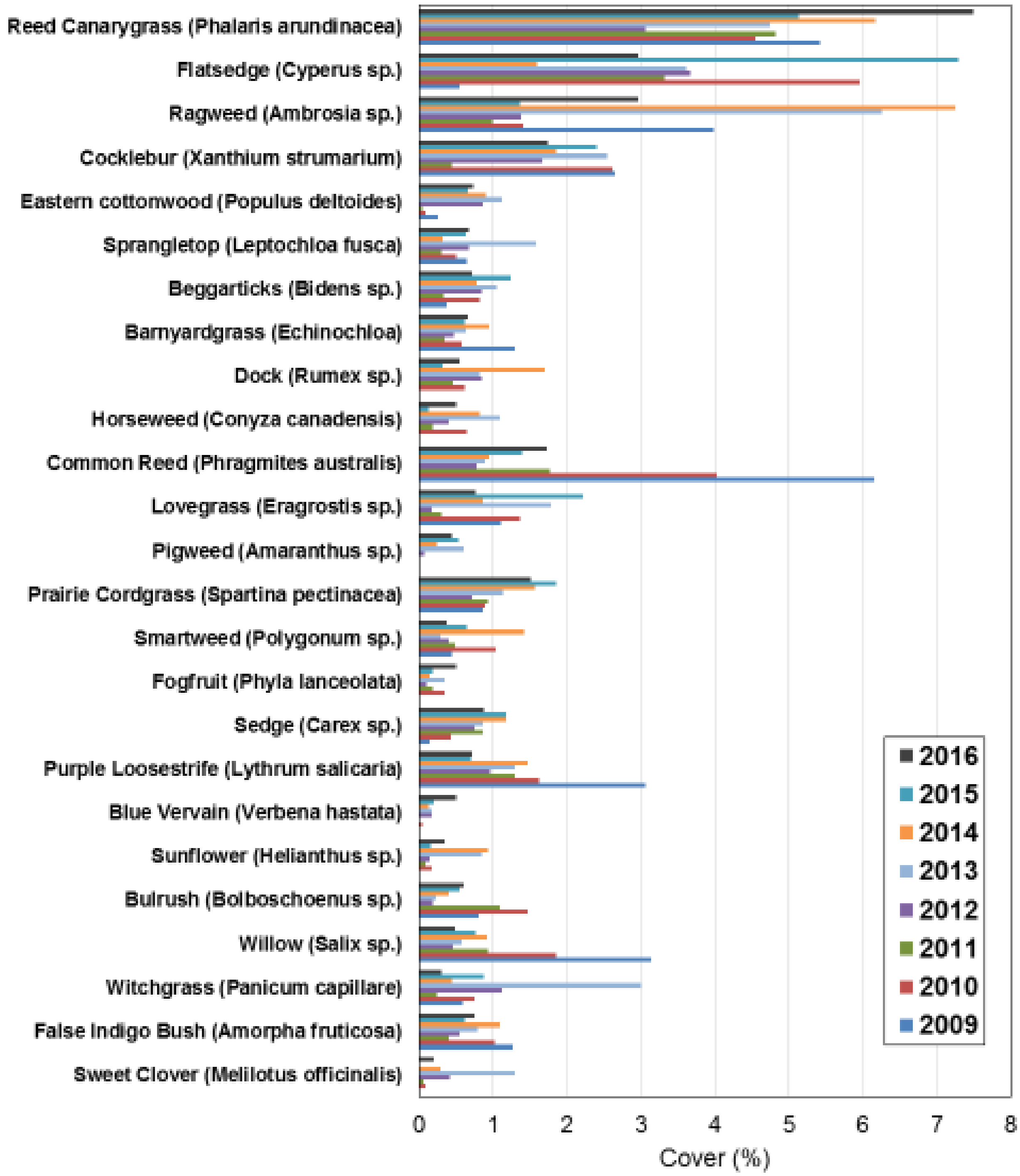

Figure 3.23. Percent cover of the top-25 most commonly observed species in 2016 and species of interest not among 25 most commonly observed, 2009-2016. Results are organized by decreasing frequency according to the 2016 data.

In assessing these results, it is important to understand that cover was sampled as a percentage category based on the area of each sample quadrat, and each species (or genera) was quantified separately. As a result, some areas can be counted more than once where overlap among species occurs. For example, if a quadrat is full of only live plants and only two species are present and occupy different strata, their total cover could be greater than 100 percent if the areas occupied by each overlap. This correctly reflects the ecological process in place along the Platte River by capturing the regular occurrences of neighboring plants with intermingled canopies.

Common reed was the species with the greatest percent cover in 2009 (6.2 percent), followed by reed canary grass (5.4 percent), ragweed (4 percent), willow (3.1 percent), and purple loosestrife (3 percent). The percent cover of common reed declined substantially after 2009, but remained in the top three in 2010 and 2011 (4 percent and 1.7 percent, respectively), then continued to decline to relatively low levels in 2012, 2013, and 2014 (1 percent or less in all three years). In 2015, it increased slightly to 1.4 percent, and increased slightly again in 2016 to 1.7 percent.

In 2010, four species had percent cover exceeding 3 percent: flatsedge (6 percent), reed canary grass (4.5 percent), common reed, and rice cutgrass (3.1 percent). From 2012 on, rice cutgrass never exceeded 0.5 percent ground cover.

Reed canary grass remained in the top two in every year, and had the highest cover of any species in 2011 (4.8 percent) and 2016 (7.5 percent). Reed canary grass covered only about 3.3 percent in 2012, and only flatsedge was more abundant (3.6 percent). Interestingly, in 2012, total vegetative cover was higher, but cover for all individual species was depressed. The high flows in 2011 followed by the prolonged atypically low flows in 2012 caused high recruitment of pioneering annuals within the channel margins, leading to higher overall cover but with no single species being particularly dominant.

In 2013 the species with the highest percent cover were ragweed (6.3 percent), reed canary grass (4.7 percent), flatsedge (3.6 percent), and witchgrass (*Panicum* capillare, 3 percent). In 2014, ragweed (7.5 percent) and reed canary grass (6.2 percent) were by far the most dominant species. No other species had ground cover exceeding 2 percent. The most dominant species by percent cover in 2015 were once again flatsedge (7.4 percent) and reed canary grass (5.5 percent). Other species with relatively high ground cover percentages in 2015 were cocklebur (2.4 percent), tufted love grass (2.2 percent), and prairie cord grass (1.8 percent). In general, species with the highest percent cover also had high frequencies of occurrence, although some high frequency species had lesser cover due to being smaller plants, such as eastern cottonwood seedlings.

In 2016, reed canary grass had the highest percent cover (7.5 percent), with ragweed and flatsedge both at 3 percent. Although lower in frequency than flatsedge, reed canary grass tended to be more dominant than flatsedge in any given quadrat, as flatsedge is commonly encountered as seedlings.

In general, the year-to-year patterns for percent cover of the four species of special interest are similar to those noted in frequency of occurrence. Willow, purple loosestrife and common reed generally showed significant decline in percent cover from 2009 to 2012, and then moderately increased through 2014 (**Figure 3.24**). Willow declined by about half from 2014 to 2016, while common reed continued to increase. Purple loosestrife also declined in 2015 and 2016. Eastern cottonwood showed an initial decline during the first three years (albiet from a very low level in 2009), and then increased substantially in 2012 and continued to increase in 2013. After peaking in 2013, the percent cover of eastern cottonwood declined in 2014 and 2015, with a slight increase in 2016. Although the trend is the same as that for frequency of occurrence, the scale of change is substantially smaller, particularly for 2012, suggesting that although this species was observed in many quadrats, its total area of cover was small because it occurred primarily as seedlings.

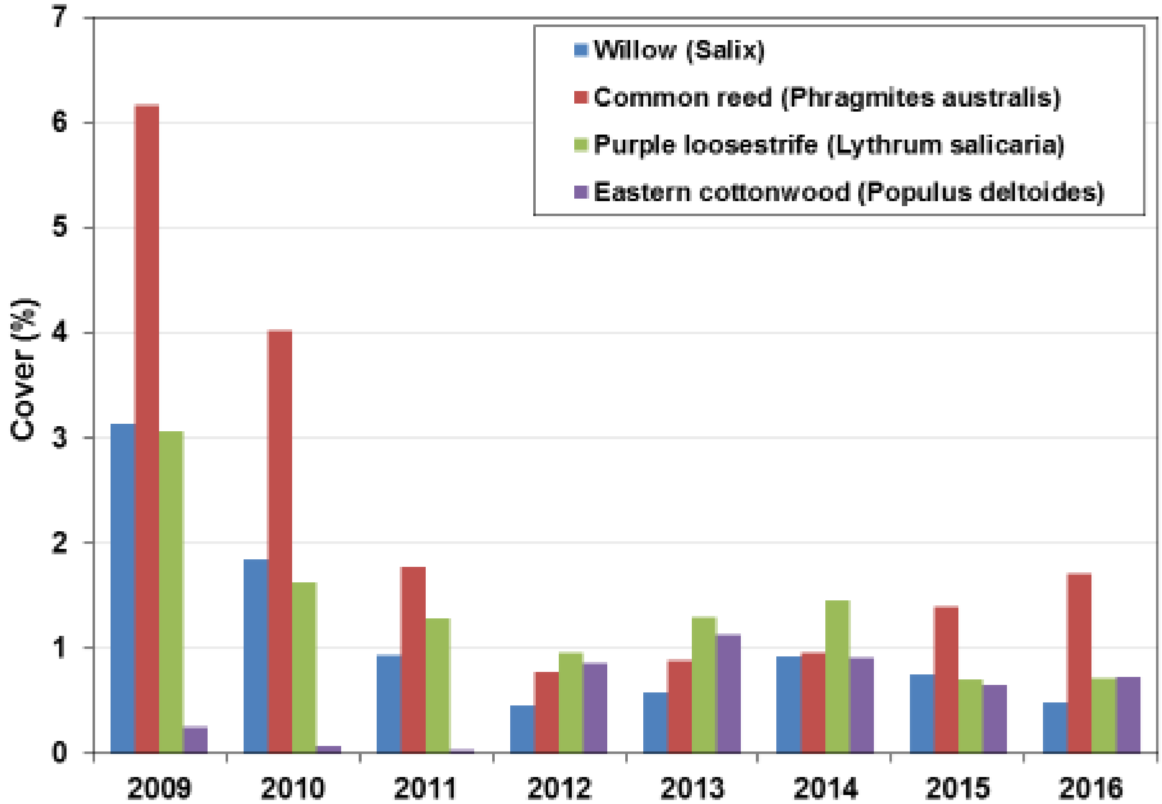

Figure 3.24. Percent cover of the species of primary interest from 2009 through 2016.

The spatial patterns of percent cover for the four species of primary interest were similar to those identified for frequency of occurrence. Purple loosestrife cover a greater amount of area in Reaches 6 through 9 than in upstream reaches, but the percent cover has been greatly reduced in those reaches since 2009 (**Figure 3.25**). Common reed was also common in the Reaches 4, 5, 7 and 9 in 2009, but has been substantially reduced throughout the entire program reach through active maintenance that includes herbicide spraying and disking (**Figure 3.26**). Common reed experienced an increase in percent in 2016 in Reaches 1, 3, and 9. Eastern cottonwood had low percent cover during the first three survey years, followed by a significant colonization event in 2012 (**Figure 3.27**). Percent cover of cottonwood remained relatively about the same 2013 and 2014 as in 2012, and it increased in several reaches in 2015. Only Reaches 4 and 9 experienced an increase in 2016. The percent cover of willow was generally highest in 2009 throughout the reach; the value in Reach 4 of over 12 percent was the highest of any reach during the 8-year monitoring period (**Figure 3.28**). The percent cover of willow did not exceed 3 percent in any reach after 2011. Slight increases in cover of willow occurred in Reaches 5, 6, and 9 in 2015, but only Reach 9 increased slightly in 2016.

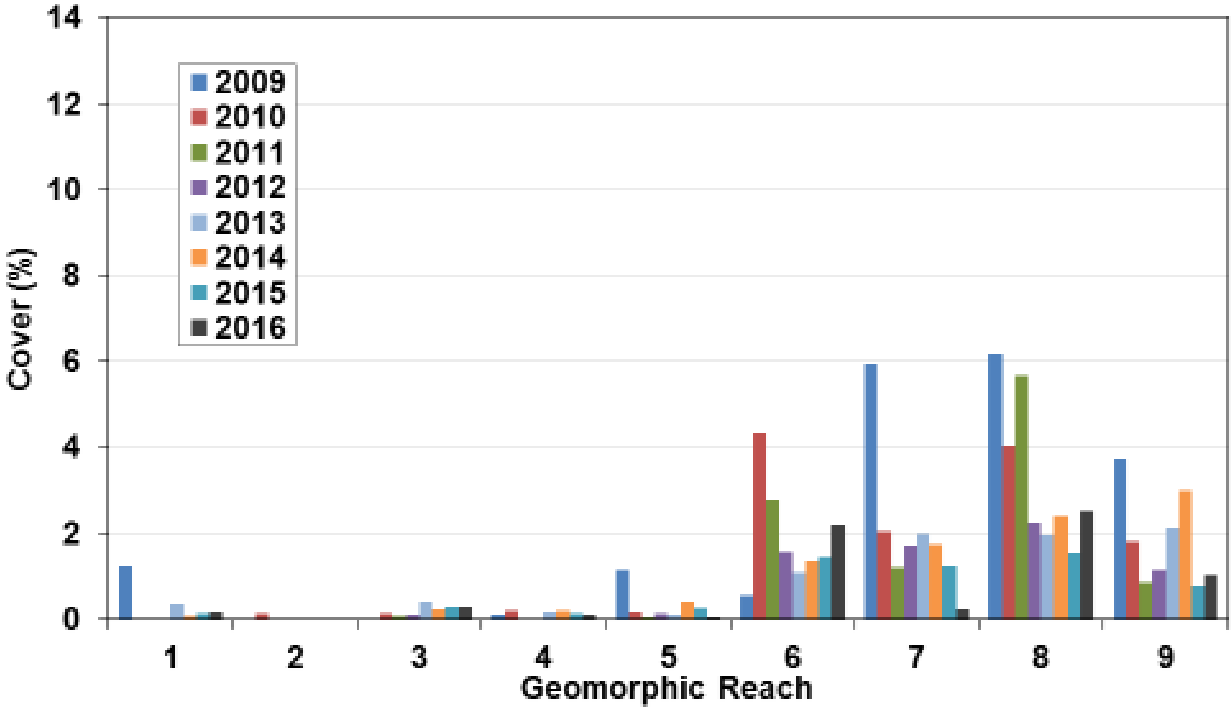

Figure 3.25. Mean percentage of ground cover for purple loosestrife (*Lythrum salicaria*), 2009 through 2016, by geomorphic reach.

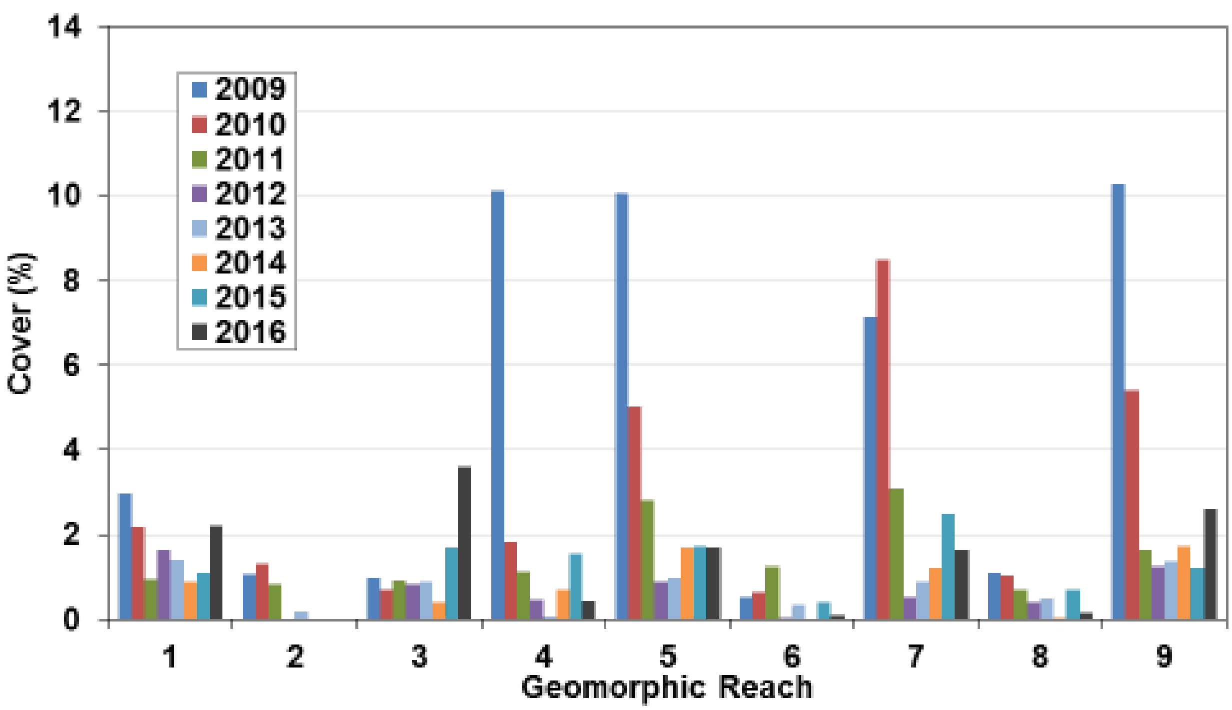

Figure 3.26. Mean percentage of ground cover for common reed (*Phragmites australis*), 2009 through 2016, by geomorphic reach.

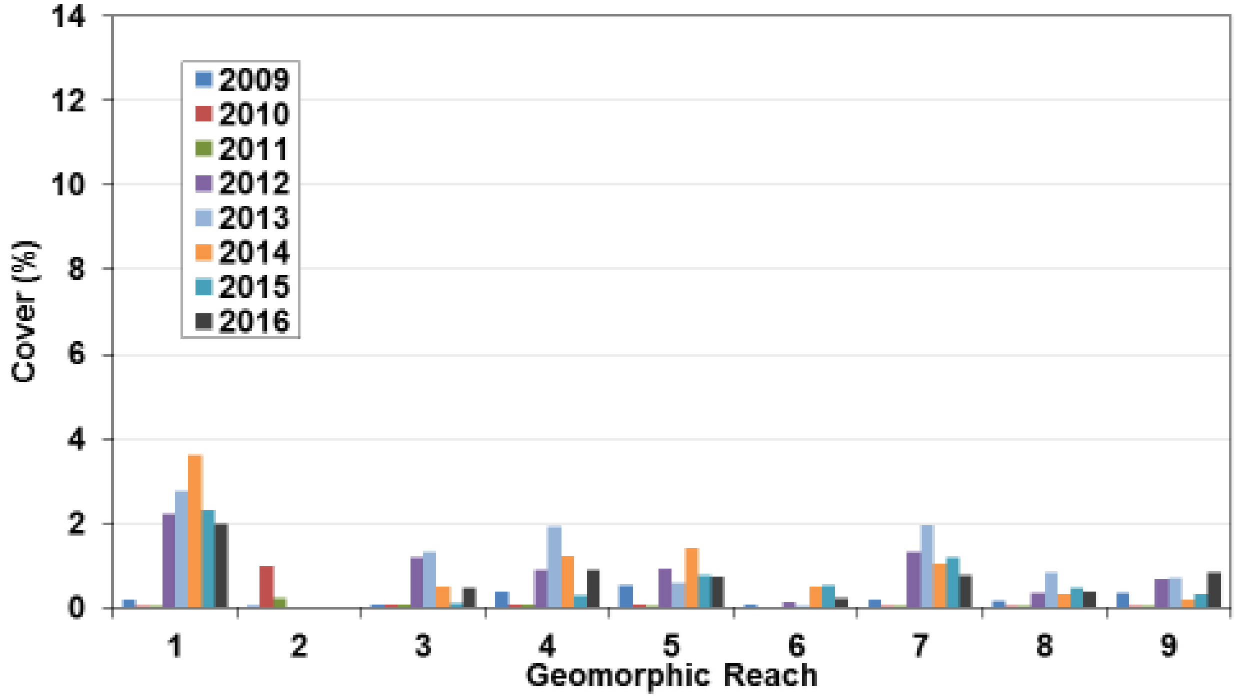

Figure 3.27. Mean percentage of ground cover for Eastern cottonwood (*Populus deltoides*), 2009 through 2016, by geomorphic reach.

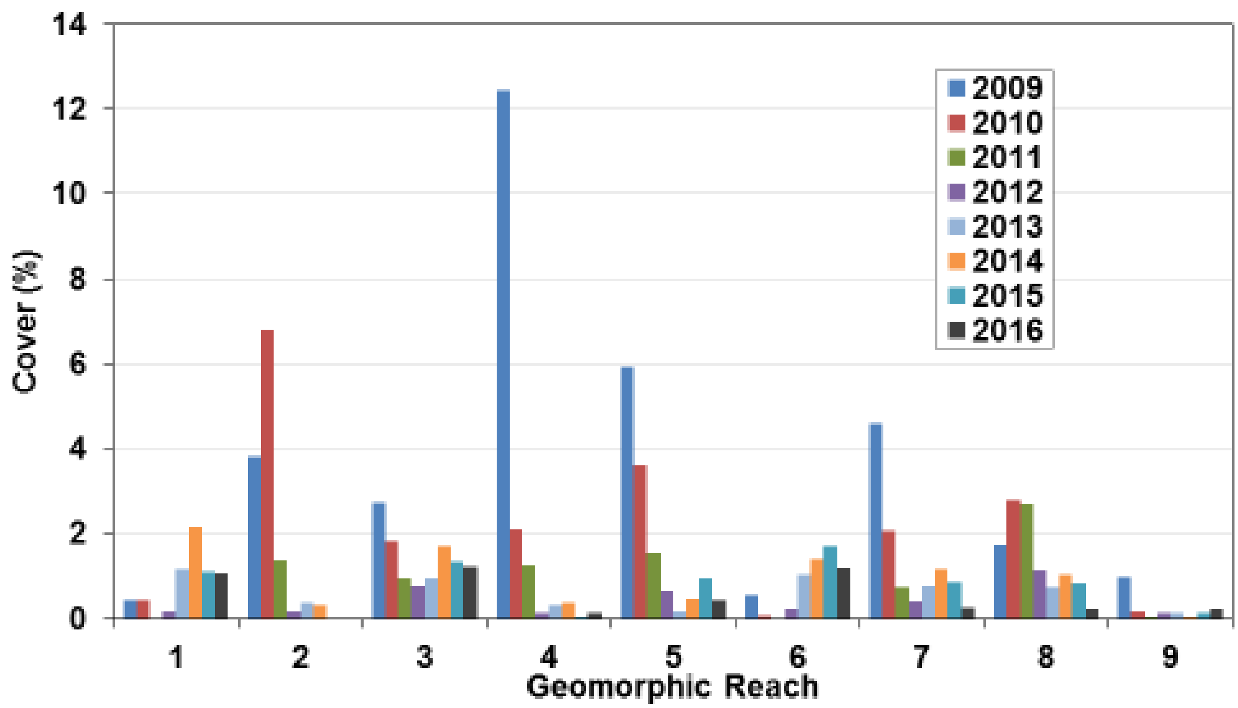

Figure 3.28. Mean percentage of ground cover for willow (*Salix sp.*), 2009 through 2016, by geomorphic reach.

3.4.5 Comparison of Vegetation Trends at Rotating and Pure Panels Points

Until the 2016 survey data were available, data collected at the rotating panels had not been incorporated into the analyses because not every rotating panel had been surveyed more than once. With the 2016 data, a meaningful comparison was possible between the trends indicated by the pure panel surveys and the rotating panel surveys. Frequency of occurrence (**Figure 3.29**) and percent cover (**Figure 3.30**) data were compared for the four species of primary interest.

In general, the frequency of occurrence of each species was similar between the rotating and pure panels in every year. For instance, in 2009, common reed was observed in 13.8 percent of pure panel quadrats, and in 13.6 percent of rotating panel quadrats. The difference in frequency of a single species of interest between the pure panel and rotating panel data was only more than 5 percent twice in the eight survey years, and both instances were in 2009. During that year, willow was observed in about 20 percent of rotating panel quadrats but only 10.6 percent of pure panel quadrats, and purple loosestrife was observed in 20.8 percent of rotating panel quadrats but only 14 percent of pure panel quadrats.

The change in frequency of occurrence between the two years in which each the rotating point was surveyed was compared with the change between the corresponding years at the pure panel points. In every single instance, the direction of the change was the same for both the rotating and pure panel point data, and in most cases, the magnitude of the change was similar (**Figure 3.31**).

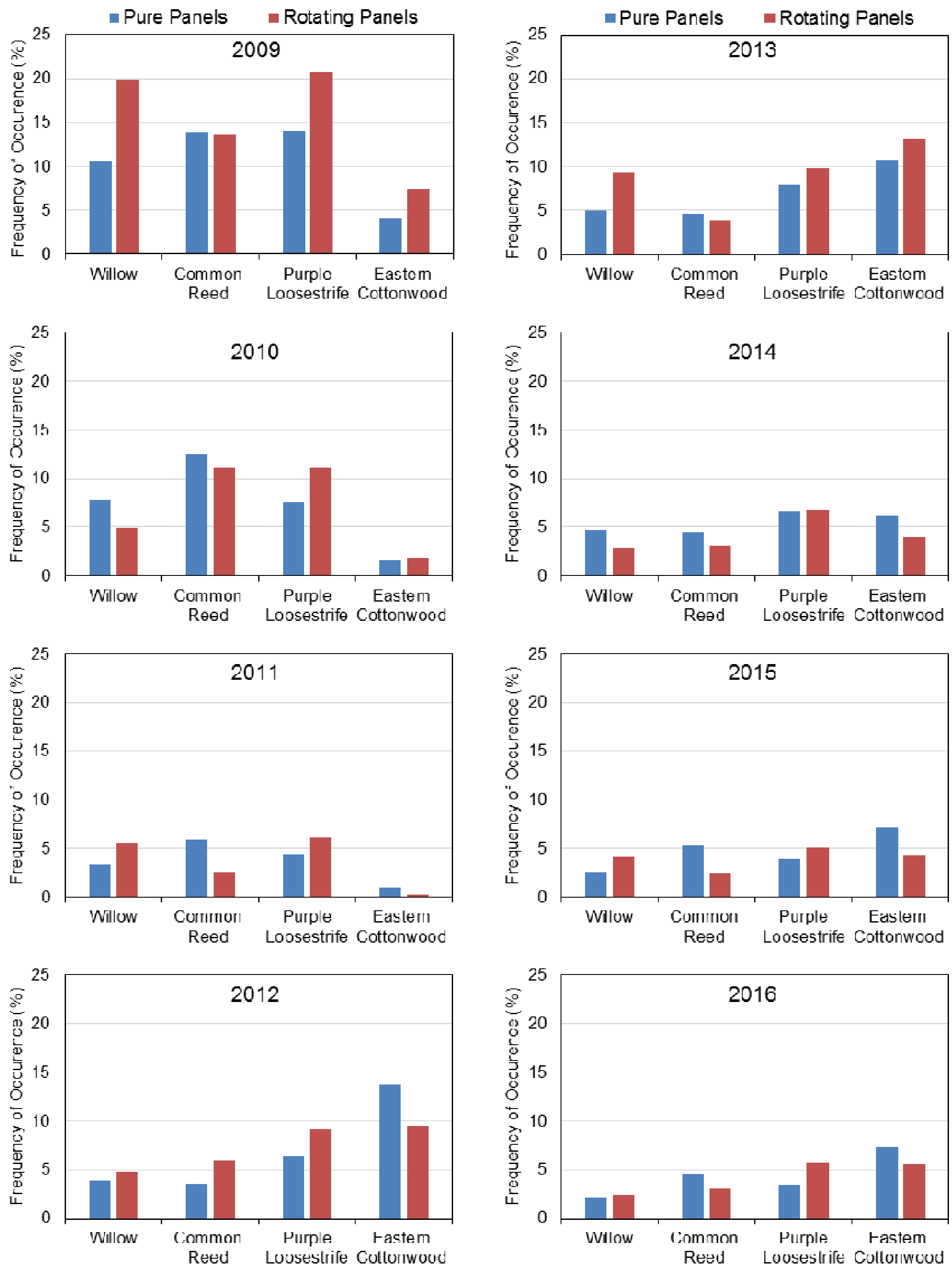

Figure 3.29. Comparison of frequency of occurrence of the four species of primary interest between the pure panel APs and the rotating panel APs.

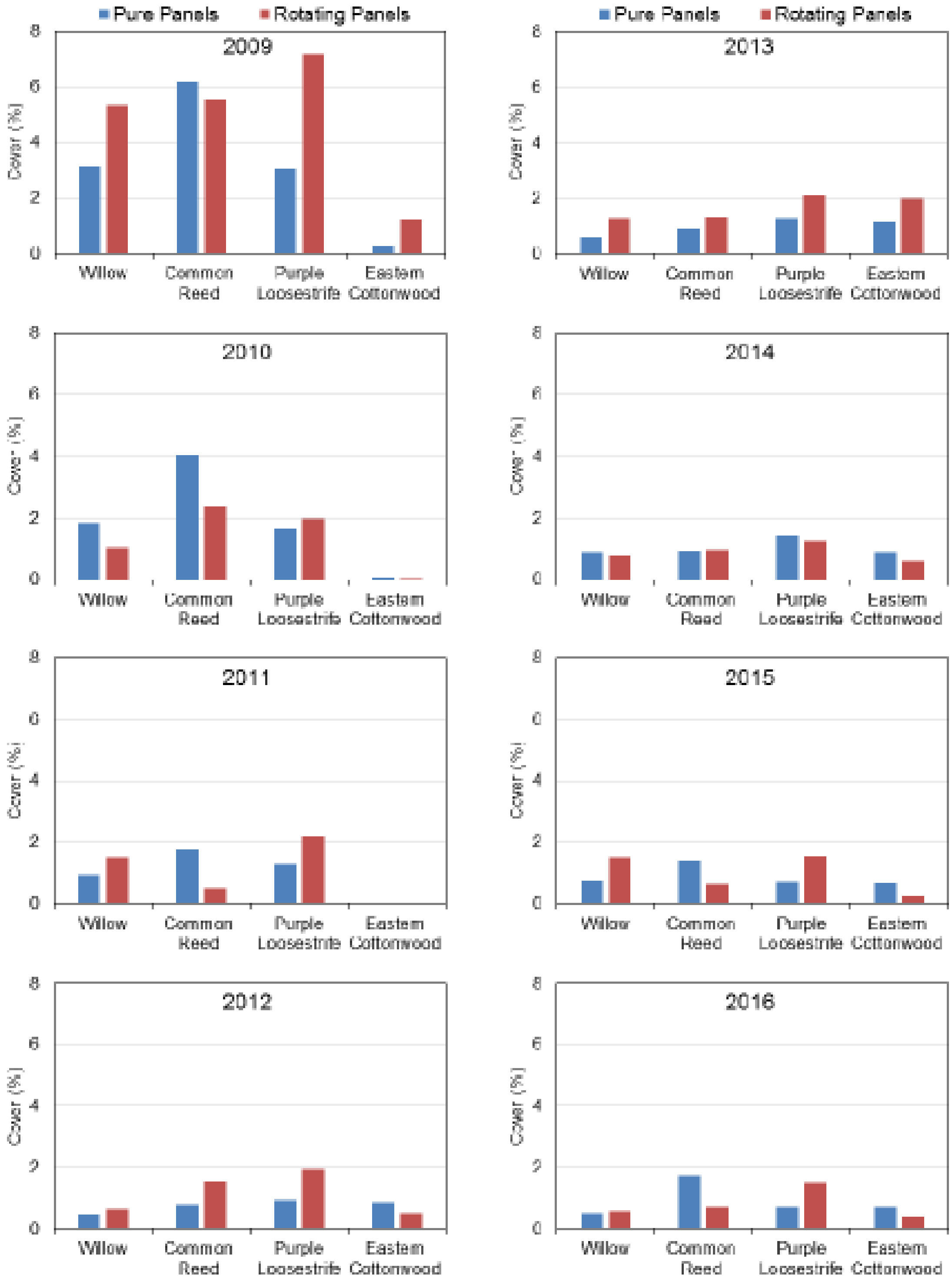

Figure 3.30. Comparison of percent cover of the four species of primary interest between the pure panel APs and the rotating panel APs.

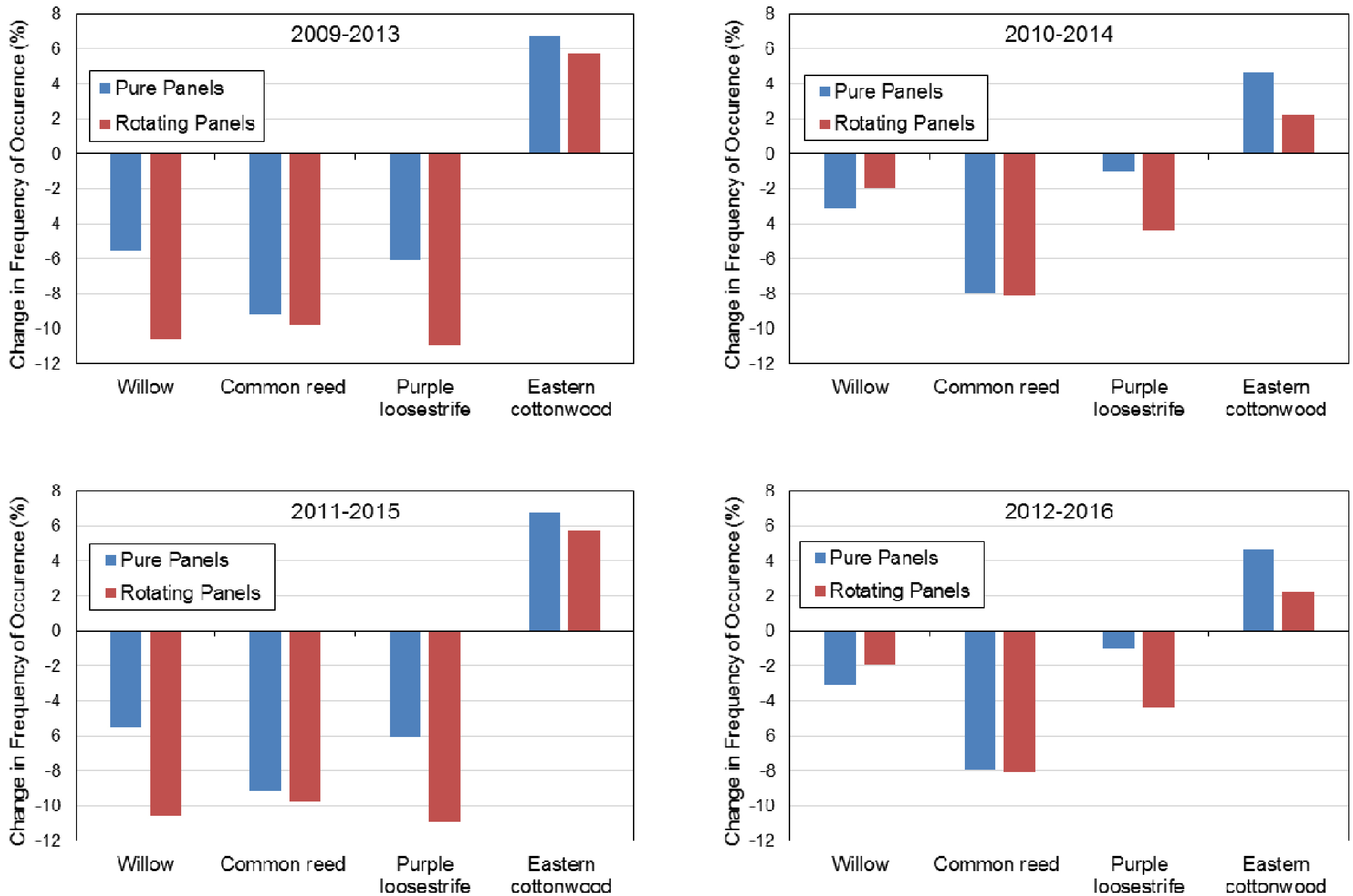

Figure 3.31. Change in frequency of occurrence for the four species of primary interest from the year of a rotating panel group's initial survey to the year of its resurvey.

A similar comparison was made with the change in percent cover. In every case where the change exceeded 1 percent, the direction of change was the same for both the pure and rotating panel points, and with a few exceptions, the magnitude was also similar (**Figure 3.32**). In general, vegetation data collected at the rotating panels agrees with data collected at the pure panels and supports conclusions drawn from the pure panel data.

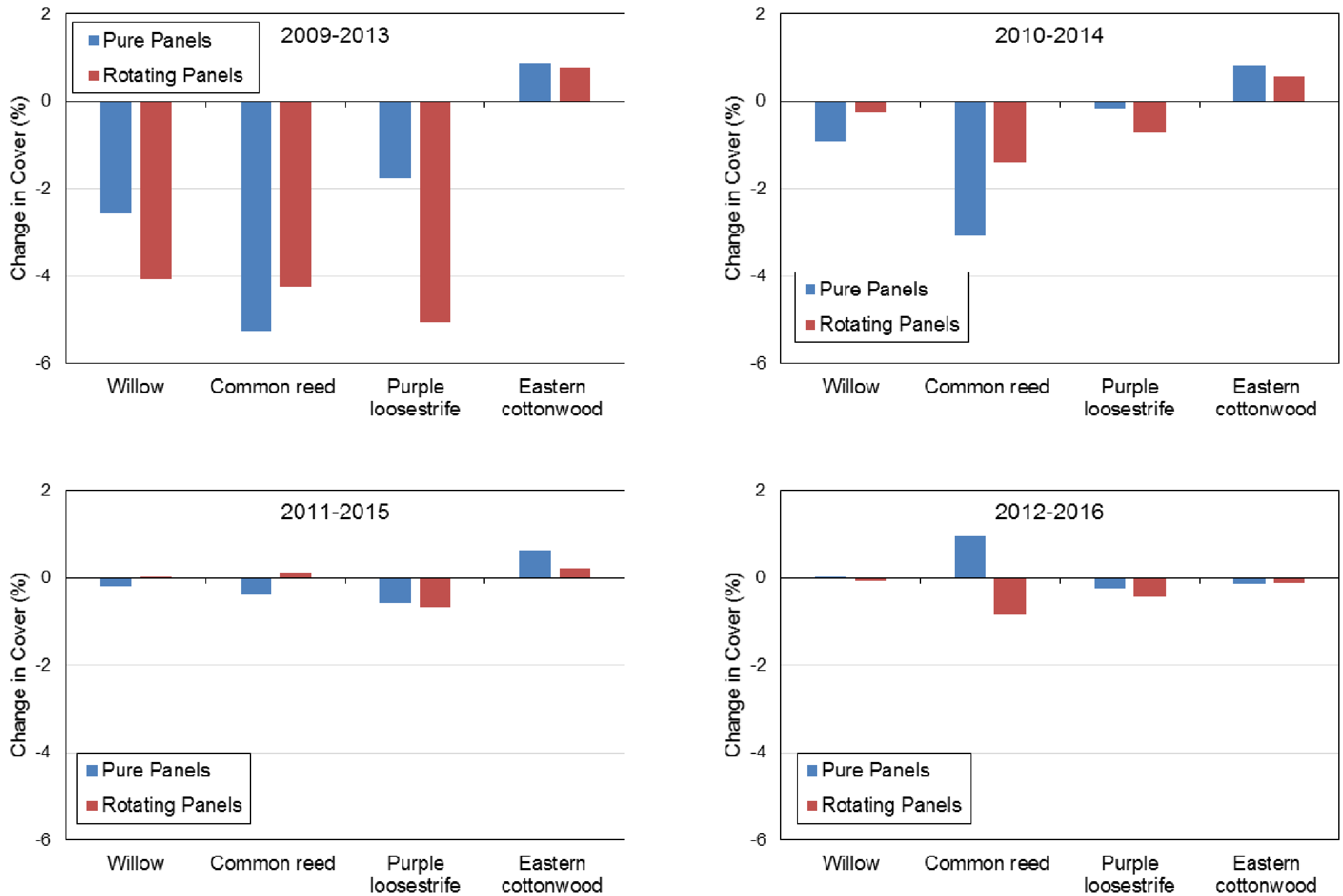

Figure 3.32. Change in percent cover for the four species of primary interest from the year of a rotating panel group's initial survey to the year of its resurvey.

3.4.6 Areal Cover by Species (DAP 5.4.5)

Aerial cover of each species was determined by multiplying the average percent cover by the total sampled area. The total area within the sampled transects varied by year from 475 acres (2015) about 590 acres (2010) (**Figure 3.33**). A substantial portion of the sampled area was classified as "no vegetation". These areas consisted of either bare ground, open water, or were covered in dead organic matter (including algal mat). The area classified with measurable vegetation ranged from about 29 percent in 2011, when flows during the survey period were relatively high, to about 73 percent during 2013 when flows low persisted throughout the sampling period. In general, the area of measurable vegetation within the overall belt transects decreased with increasing flow.

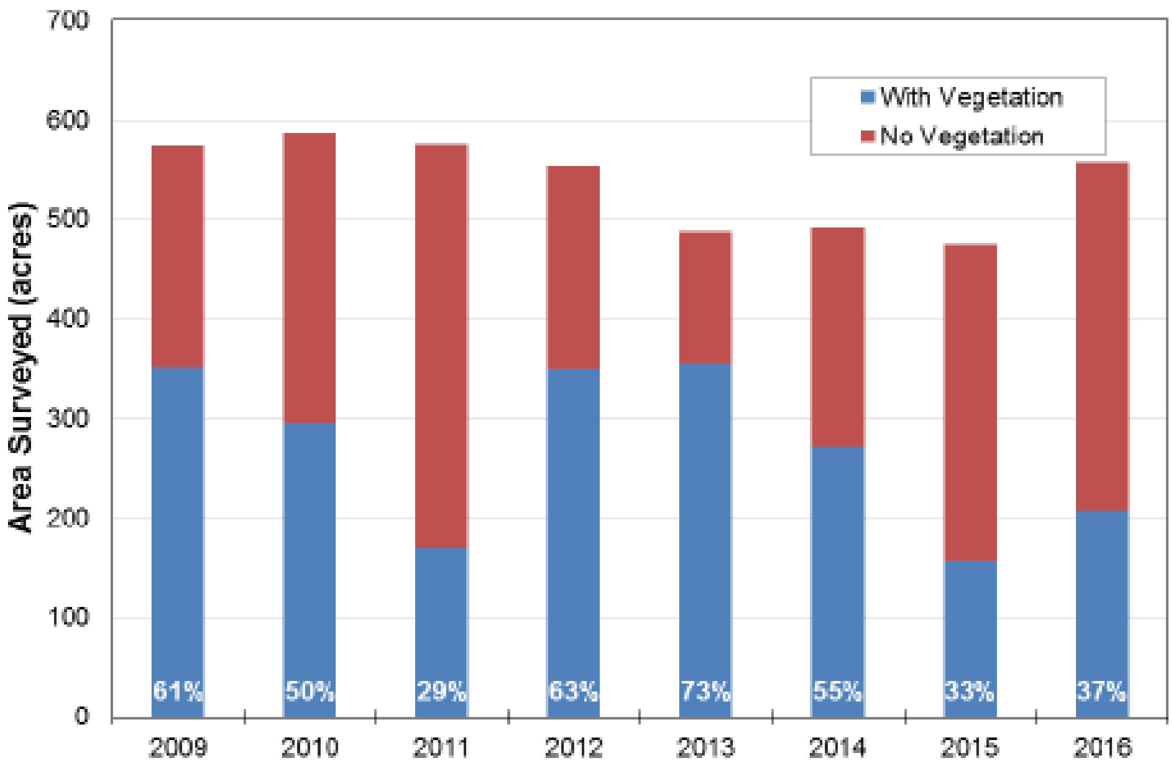

Figure 3.33. Total surveyed area and area with measurable vegetation for each survey year, based on Daubenmire cover-class data.

Areal cover may provide a more effective perspective for evaluating and understanding the size of each species distribution in each reach and throughout the entire survey area. Because areal cover is the mathematical product of the percent cover and the sample area, with a few exceptions, all trends and patterns identified for percent cover also apply to areal cover (**Figure 3.34**). Similar to percent cover, areal cover by reach for each species of interest provides an approximate representation of their distribution within the survey area, generally indicating the location of larger patches of the species. For example, areal cover of purple loosestrife in 2009 was highest in Reaches 7, 8, and 9, indicating large and/or numerous patches of that species at those locations. Those infestations appear to have substantially decreased in size in subsequent years, but are still currently the largest patches within the survey area.

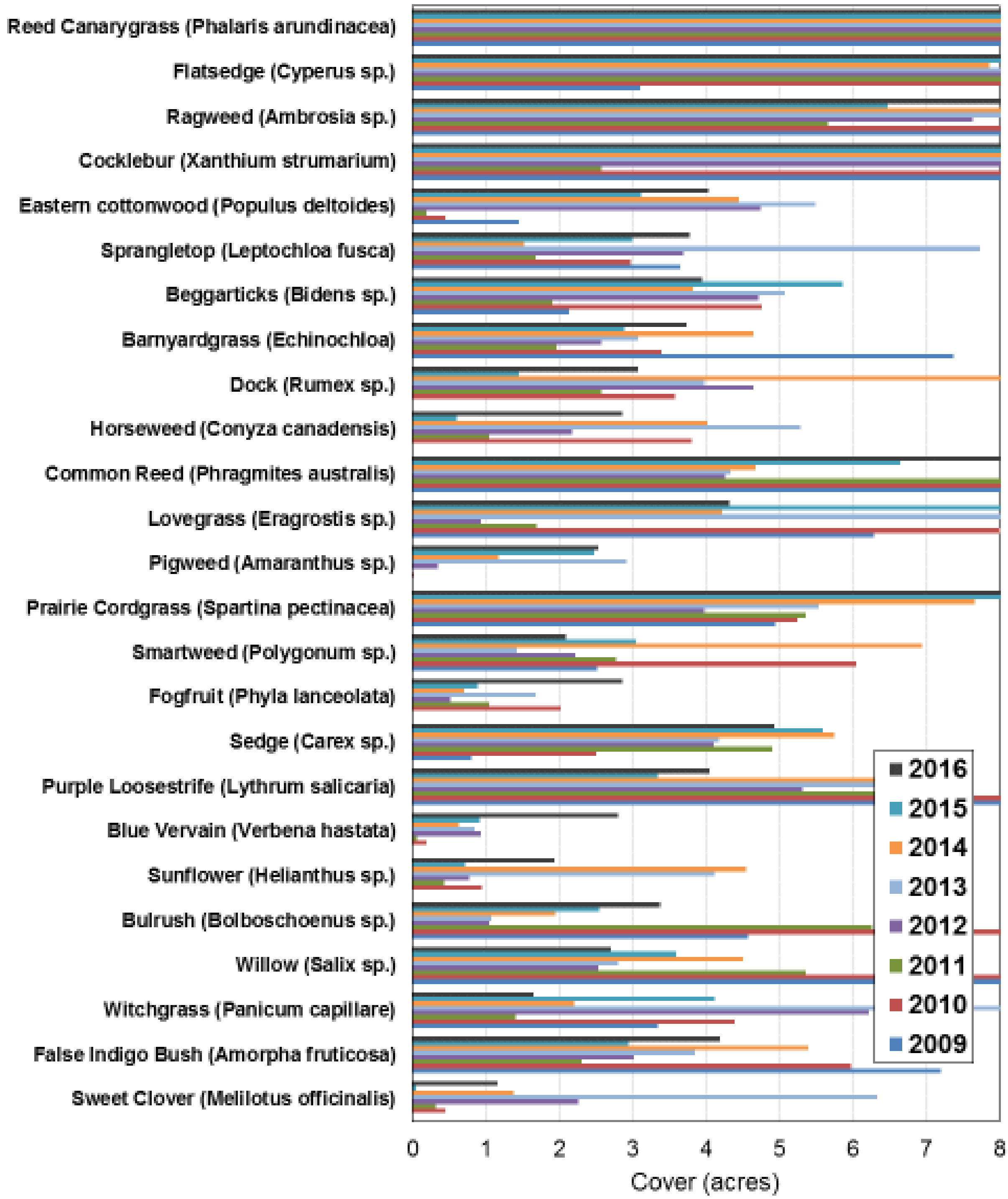

Figure 3.34. Areal cover of the top-25 most commonly observed species in 2016 and species of interest not among 25 most commonly observed, 2009-2016. Results are organized by decreasing frequency according to the 2016 findings.

The aerial cover of willow declined progressively from about 18 acres in 2009 to only about 2.5 acres in 2012, increased back to about 4.5 acres in 2014, and decreased again to about 2.7 acres in 2016 (**Figure 3.35**). Aerial cover of common reed also progressively declined from about 35 acres in 2009 to 4 acres in 2012, and then progressively increased back to about 10 acres by 2016. Purple loosestrife declined from about 18 acres in 2009 to about 5 acres in 2012, increased back to about 7.2 acres by 2014 and then declined back to 3.5 acres to 4 acres in 2015 and 2016. Areal cover of Eastern cottonwood was relatively small in 2009 at about 1.4 acres, and it remained well below 0.5 acres in 2010 and 2011, before increasing back to about 5 acres in 2012, and it has remained in the range of 3 acres to 5 acres since 2012.

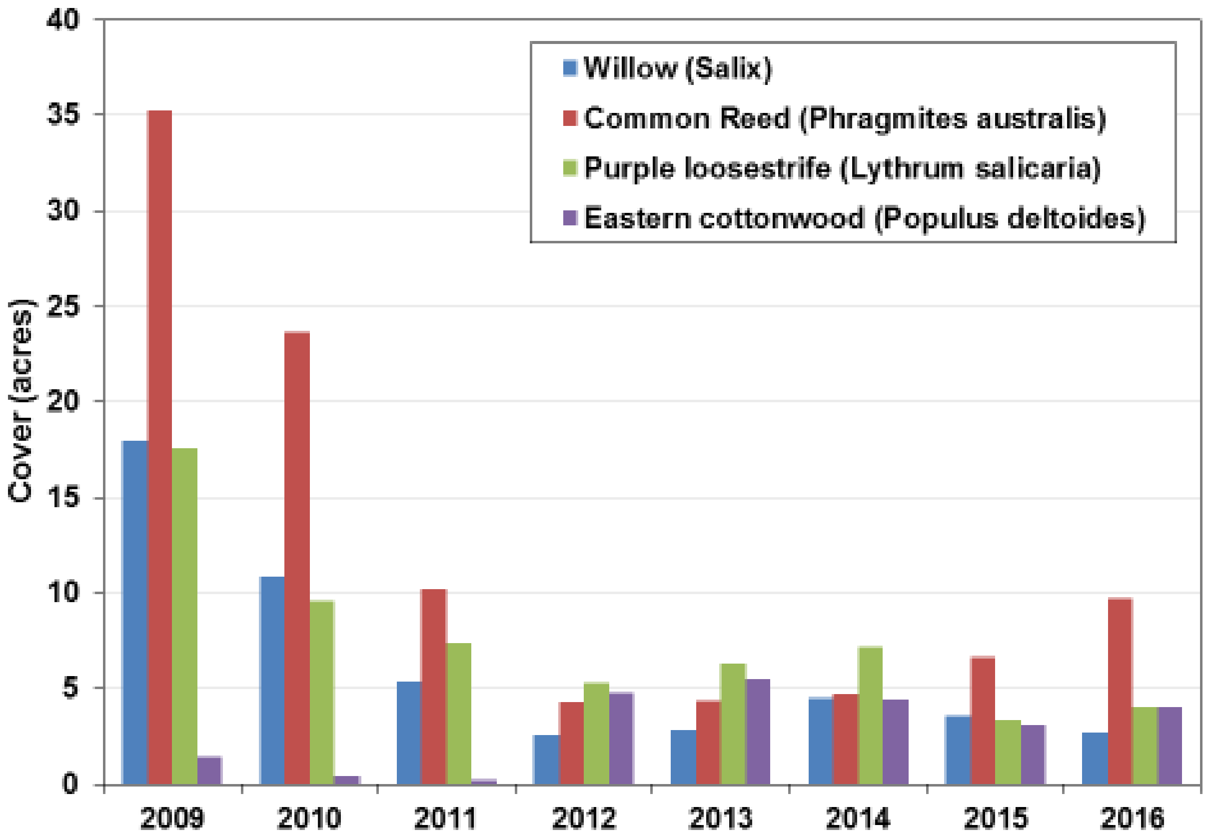

Figure 3.35. Areal cover of the four species of primary interest, 2009-2016.

As with percent cover, the spatial patterns of areal cover of the four species of primary interest are very similar to the frequency of occurrence. Throughout all 8 monitoring years, purple loosestrife was mostly located in Reaches 7, 8, and 9 at the downstream end of the study reach (**Figure 3.36**). Common reed has been relatively evenly distributed throughout the study reach, with the largest areal cover occurring in Reach 9 (**Figure 3.37**). Substantial aerial cover of common reed also occurred in Reaches 5 and 7 in 2009 and 2010. Eastern cottonwood occurred throughout the study reach in relatively small amount, with the greatest areal cover occurring in Reaches 1, 5, 7, and 9 (**Figure 3.38**). Willow, while somewhat greater than Eastern cottonwood, also occurred throughout the study reach in relatively small quantities, with the greatest cover occurring in Reaches 3, 5, 7, and 8 (**Figure 3.39**).

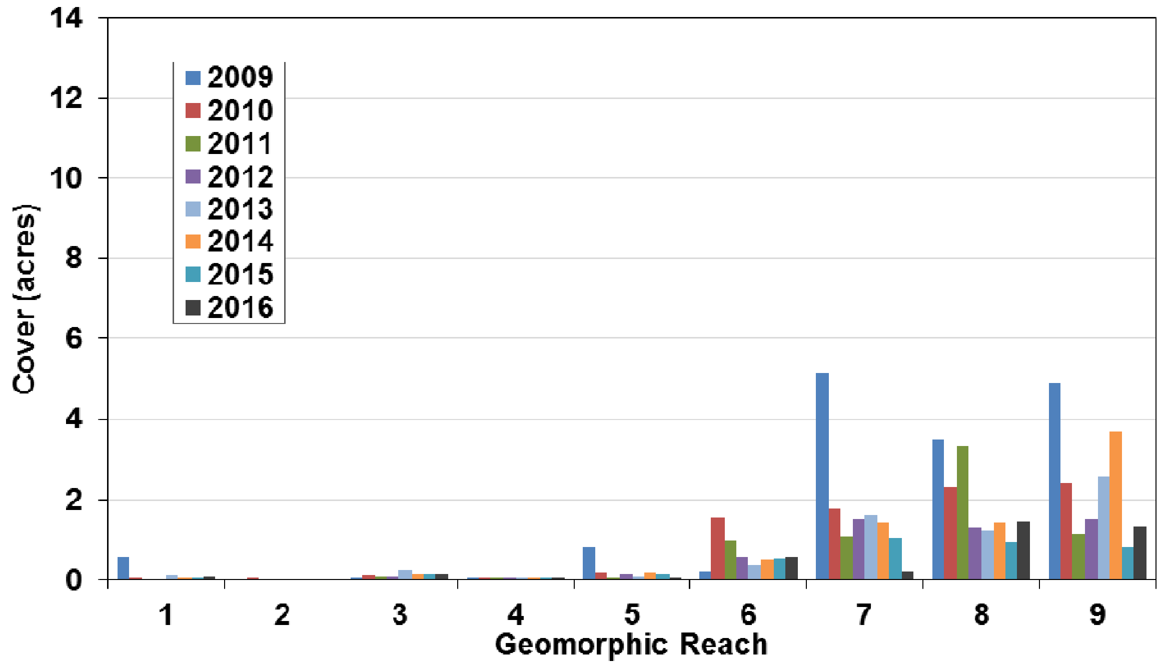

Figure 3.36. Areal cover of purple loosestrife (*Lythrum salicaria)*, 2009-2016 by geomorphic reach.

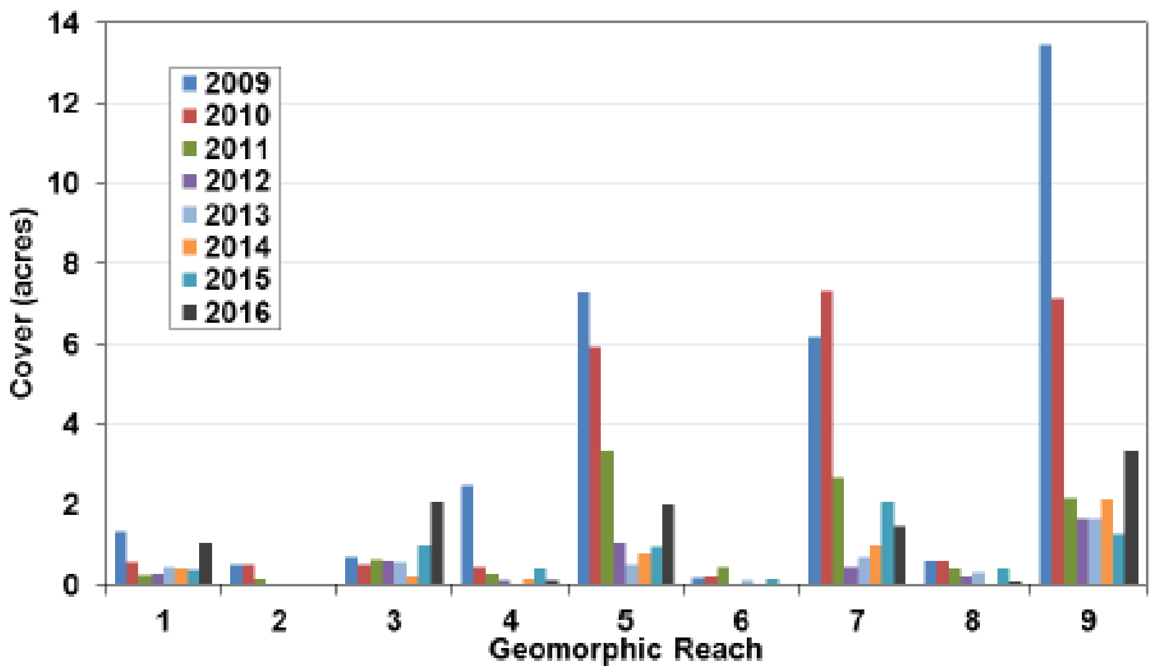

Figure 3.37. Areal cover of common reed (*Phragmites australis)*, 2009-2016 by geomorphic reach.

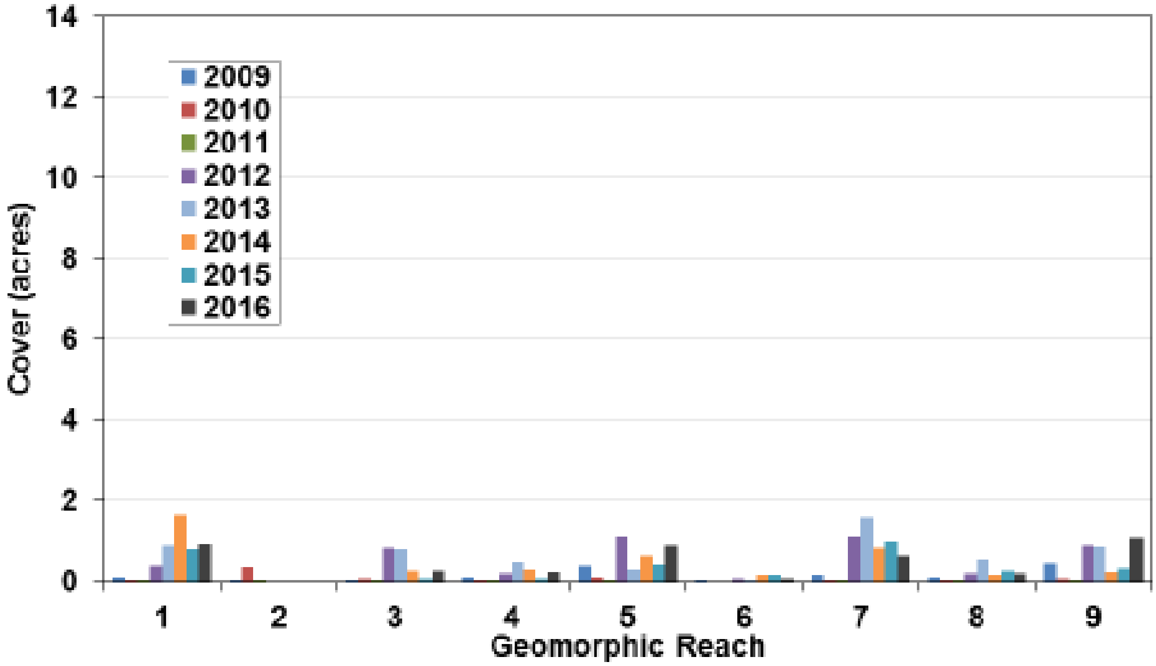

Figure 3.38. Areal cover of Eastern cottonwood (*Populus deltoides)*, 2009-2016 by geomorphic reach.

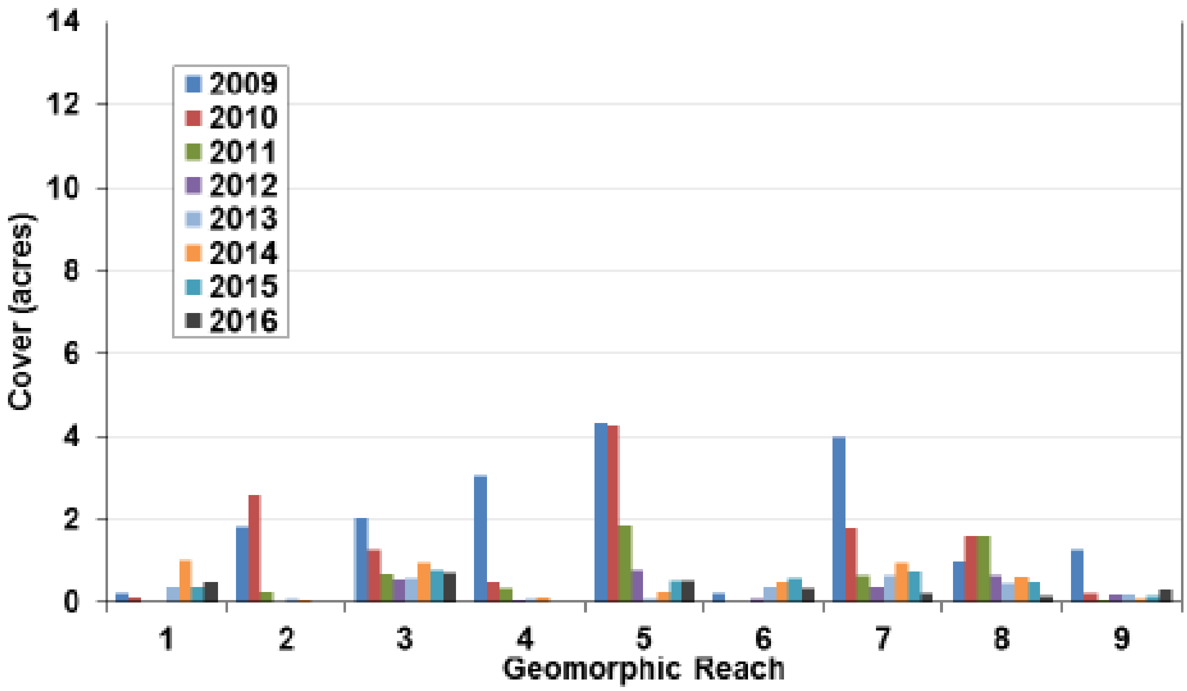

Figure 3.39. Areal cover of willow (*Salix sp.)*, 2009-2016 by geomorphic reach.

During 2011, the survey area was inundated with a long-duration, high-flow event, which reduced the amount of vegetation and increased the extent of bare ground. In 2012, the vegetated area doubled (Figure 3.32), suggesting that newly established bare ground became available for plant establishment and quickly colonized during the subsequent, dry spring and summer months. The frequency of occurrence of both Eastern cottonwood and willow increased much more in 2012 and 2013 than their cover values, indicating the establishment of new stands of young plants. Subsequent decreases in frequency and cover indicate the seedlings have gradually diminished through time. The high-flow event in the fall of 2013 likely influenced vegetation in a similar fashion, however, both cottonwood and willow occurrences declined from the previous year. That year, seedling establishment on newly disturbed bare ground was likely constrained by the relatively wet 2014 growing season, in which flows may have continued to inundate and/or disturb areas where germination had occurred. As documented in other parts of the Missouri River basin and the Western U.S., in general, large recruitment events of riparian, seed-dispersed species such as Eastern cottonwood require a disturbance event prior to the growing season, followed by low enough flows during the growing season to allow establishment (Auble, et al, 1998; Scott, et al, 1997; Shafroth, et al, 1995). Like most riparian seedlings, those of Eastern cottonwood require ample soil moisture to prevent desiccation, but cannot be submerged for extended periods. The dominance of only two cottonwood age classes in the survey area (seedlings/saplings and mature individuals), suggests an ongoing biological cycle of punctuated colonization and survival followed by years without colonization.

3.4.7 Frequency of Communities

As noted above, the vegetation data at each AP for the 2012 through 2016 data included the community classification code in accordance with the system outlined in Steinauer and Rolfsmeier (2003). Fifteen (15) total community types were encountered during the monitoring period, eight (8) of which were present in sufficient quantities to warrant analysis. Throughout the sampling years, community type has been a difficult category to consistently document, and this resulted in inconsistencies in the 2009 through 2011 data that prevent meaningful analysis. Going forward, Tetra Tech believes that this variable could potentially be more accurately documented from aerial photo interpretation. Based on the 2012 through 2016 data that were collected using a consistent protocol, the dominant overall community type in the monitoring reach, including the no-vegetation zones, was sandbar/mudflat for which the frequency ranged between 51 percent (2012) and about 60 percent in 2013 (**Figure 3.40**). This community type provides both nesting and foraging opportunities for avian species. Prior to the occurrence of human alterations to the river and floodplain, this habitat was common and widely distributed along the Platte River.

Perennial Sandbar is the second most commonly sampled community, ranging from about 5 percent (2014) to 13.5 percent (2016). This community type is dominated by perennial species including woody shrubs and small trees, and is generally located at elevations between the active stream channel and areas dominated by large trees. In general, the perennial sandbar community does not provide usable habitat for the avian species of concern to this Program because the least terns and piping plovers nest on bare sandbars and the taller vegetation tends to block sight lines for the whooping crane. Other community types encountered during the surveys in relatively low quantities include riparian dogwood-false indigo shrubland (2.3 percent to 9.7 percent), sandbar willow shrubland (0.9 percent to 3.3 percent), Eastern cottonwood-willow woodlands (0.4 percent to 5.4 percent), and freshwater marsh (0.4 percent to 3.4 percent).

Unsurprisingly, the combined frequency of water and sandbar/mudflat communities has remained largely unchanged since collection of community types began at 68 percent to 78 percent, reflecting the relatively modest changes in the margins of the active channel. The composition of the remaining 20 percent to 30 percent of community types has, however, been highly variable. For example, perennial sandbar made up only about 23 percent of the vegetated communities in

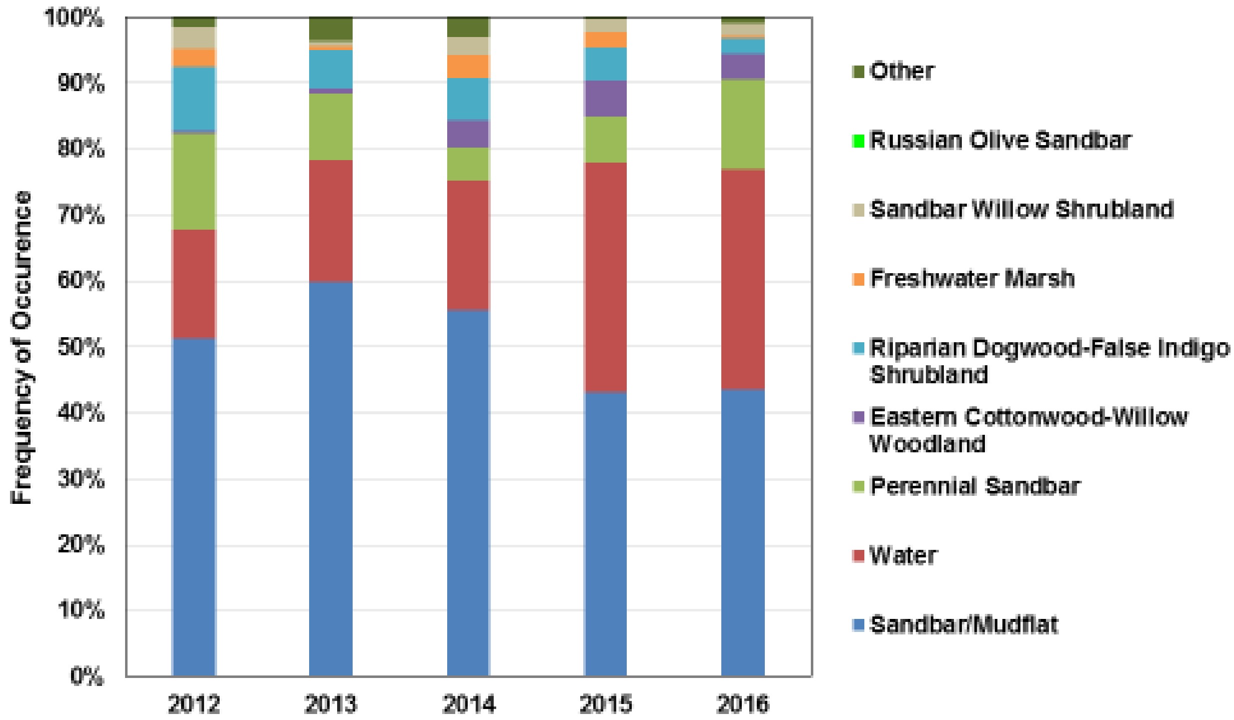

Figure 3.40. Frequency of specific community types observed during field surveys between 2012 and 2016.

2014, but this increased to over 60 percent by 2016 (**Figure 3.41**). Eastern cottonwood-willow woodland made up less than 1.5 percent of the communities in 2012, and this increased to about 25 percent in 2015, before declining by a relatively modest amount to about 18 percent in 2016. Riparian dogwood--false indigo shrubland ranged decreased from about 32 percent of the vegetated communities in 2012 and 2013 to about 10 percent in 2016.

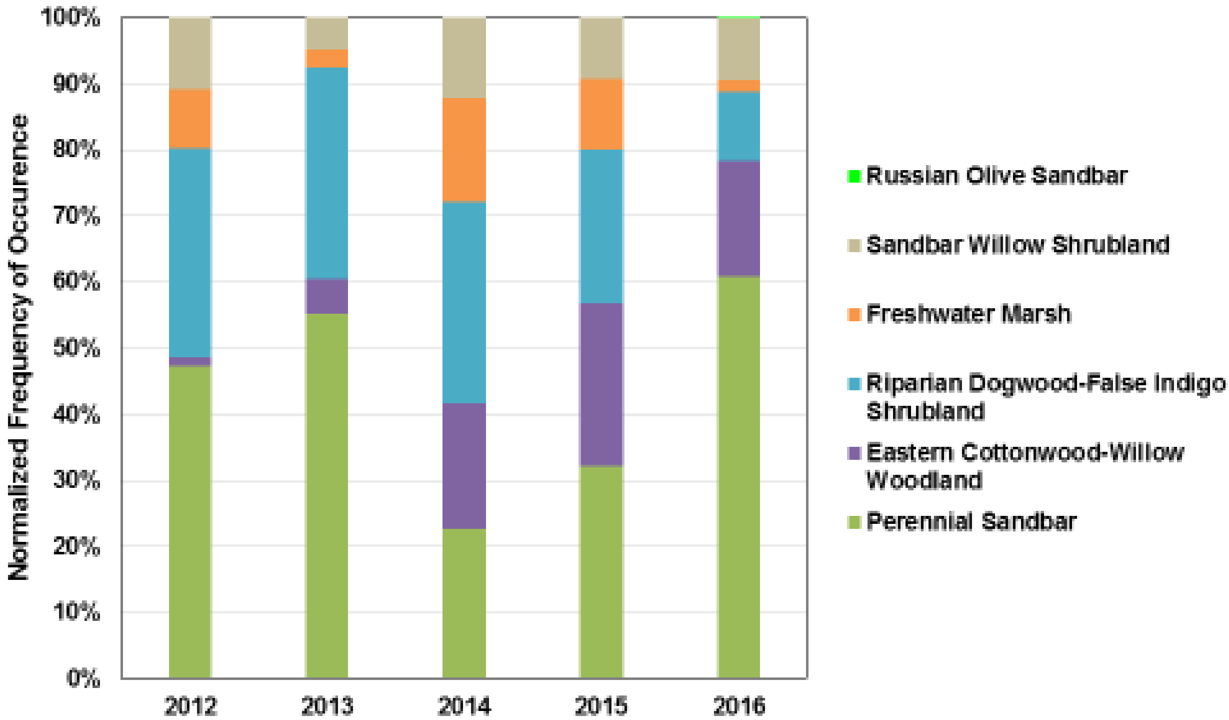

Figure 3.41. Frequency of vegetated community types observed during field surveys between 2012 and 2016, normalized by removing water and sandbar/mudflat types.

3.4.8 Bare Ground

Field crews began recording the percentage of bare ground in each quadrat beginning with the 2012 vegetation survey. The data ranged from about 26 percent of the area in 2012 to a maximum of 36 percent in 2014, and it remained in the 32 percent to 35 percent range in 2015 and 2016 (**Figure 3.42**). The relatively small area of bare ground in 2012 was likely due to the sustained low flows allowing for greater vegetation encroachment into the channel.

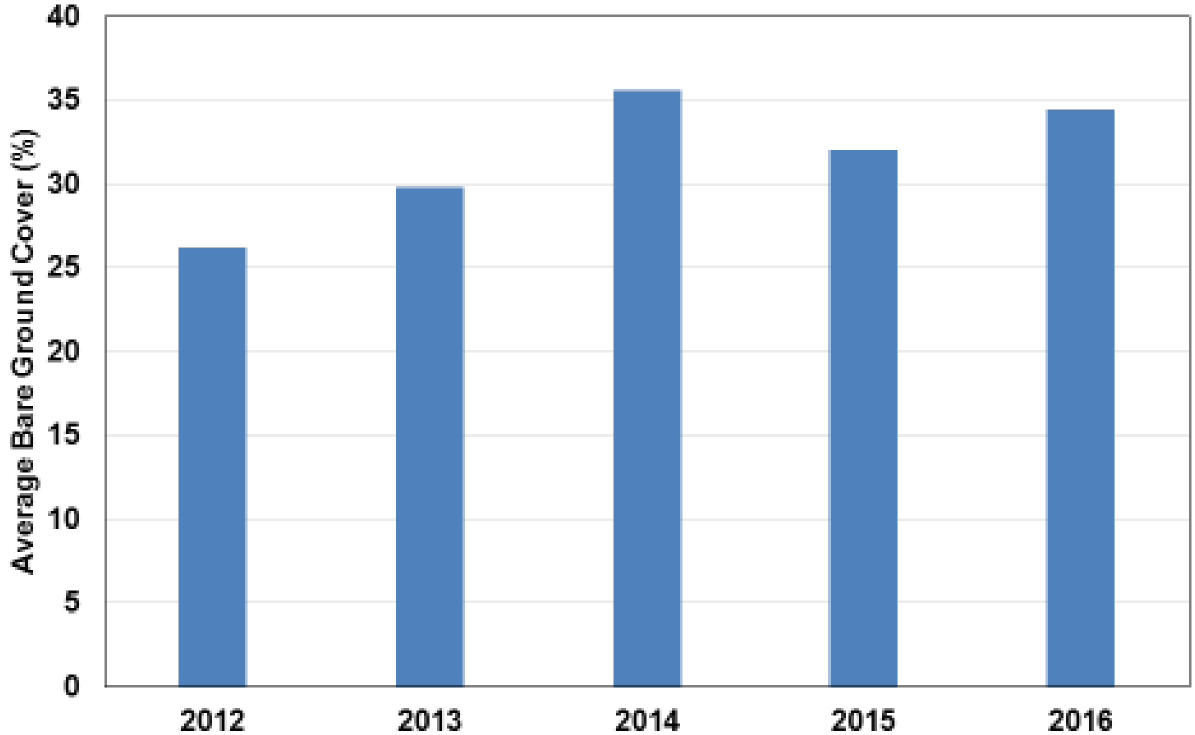

Figure 3.42. Average cover percentage of bare ground in all quadrats, survey years 2012-2016.

As an indicator of habitability for avian species of interest, the frequency of occurrence for quadrats with at least 75 percent bare ground or water were also considered, as 25 percent is the threshold for identification of the greenline (**Figure 3.43**). The 2016 vegetation survey had the greatest frequency of bare ground quadrats (31.2 percent), while 2013 had the lowest frequency (18.7 percent). Quadrats which were covered by water were relatively infrequent during the 2012 survey (12.5 percent), but were almost three times as frequent in 2015 and 2016 (34.8 and 33.4 percent, respectively).

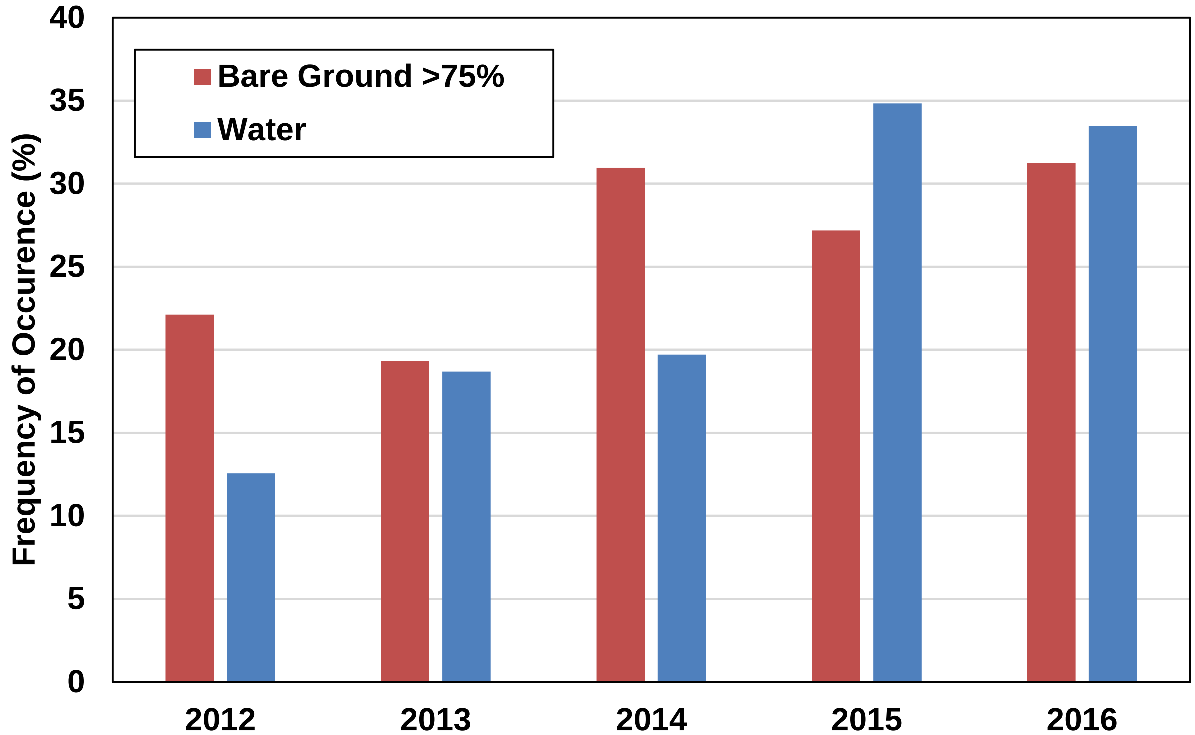

Figure 3.43. Frequency of occurrence of water and of quadrats with greater than 75% bare ground, survey years 2012-2016.

3.4.9 Mean Elevation by Species (DAP 5.4.6)

Mean elevation of each of the species of primary interest and other commonly occurring species were evaluated by averaging the elevations of all quadrats in which each species was observed, and also by evaluating the average elevation relative to the local 1,200 cfs water surface. The average elevation of each species is controlled by both the elevation profile of the river, and the local effects of flows and other factors. The differences in elevation between the APs is generally greater than the elevation range within each individual AP; thus, the raw averages are indicative of the most common locations of the species along the reach, while the elevation relative to the local 1,200 cfs water-surface is indicative of the effects of flow and other local factors.

The data indicate that Russian olive (*Elaeagnus angustifolia*) generally grows at the highest elevations among the sampled species; however, it was infrequently encountered and only occurred in a few reaches. Of the 25 most-commonly occurring species, ragweed (*Ambrosia*) prairie cordgrass (*Spartina pectinacea*), false indigo bush (*Amorpha fruticosa*), and common reed (*Phragmites australis*) were typically found at the highest elevations, while sedge (*Carex*), reed canarygrass (*Phalaris arundinacea*), horseweed (*Conyza canadensis*), and Eastern cottonwood (*Populus deltoides*) were found at the lowest elevations (**Figure 3.44a**). As noted above, these rankings are driven largely by the most common locations of the species along the monitoring reach. Based on the elevation above the 1,200 cfs water-surface, which is a better reflection of the location at which the species are found within the channel at any particular location, prairie cordgrass (*Spartina pectinacea*), horseweed (*Conyza canadensis*), sunflower (*Helianthus sp.*), and sedge (*Carex*) were typically found in the highest areas, while bulrush (*Bolboschoenus*), flatsedge (*Cyperus*), fogfruit (*Phyla lanceolata*), purple loosestrife (*Lythrum salicaria*) and smartweed (*Polygonum*) were found in the lowest areas. Prairie cordgrass (*Spartina pectinacea*) is classified at Facultative Wetland (FACW), indicating that it usually occurs in wetlands, but may occur in non-wetlands (**Figure 3.44b**). Horseweed (*Conyza canadensis*) and sedge (*Carex*) are classified as Facultative (FAC), indicating that these species occur about equally in wetlands and non-wetlands, and sunflower (*Helianthus sp*.) is classified as Facultative Upland (FACU); thus, typically occurs in non-wetlands, but may occur in wetlands. Of the species found at relatively low elevations in the channel, bulrush (*Bolboschoenus*), flatsedge (*Cyperus*), and purple loosestrife (*Lythrum salicaria*) are classified as Obligate (OBL), meaning they almost always occur in wetlands, and (*Phyla lanceolate*) and smartweed (*Polygonum*) fogfruit are classified as Facultative Wetland (FACW) when encountered in the Great Plains Region where the Platte River is located.

The four species of primary interest tended to be located at among the lowest elevations of the sampled species relative to the 1,200 cfs water-surface, and thus, are likely have more influence on the greenline elevation and sandbar habitats (**Figure 3.44c**). AS anticipated, the typical elevation of these species tended to be lower during years with low flows during the germination season and higher during years with higher flows.

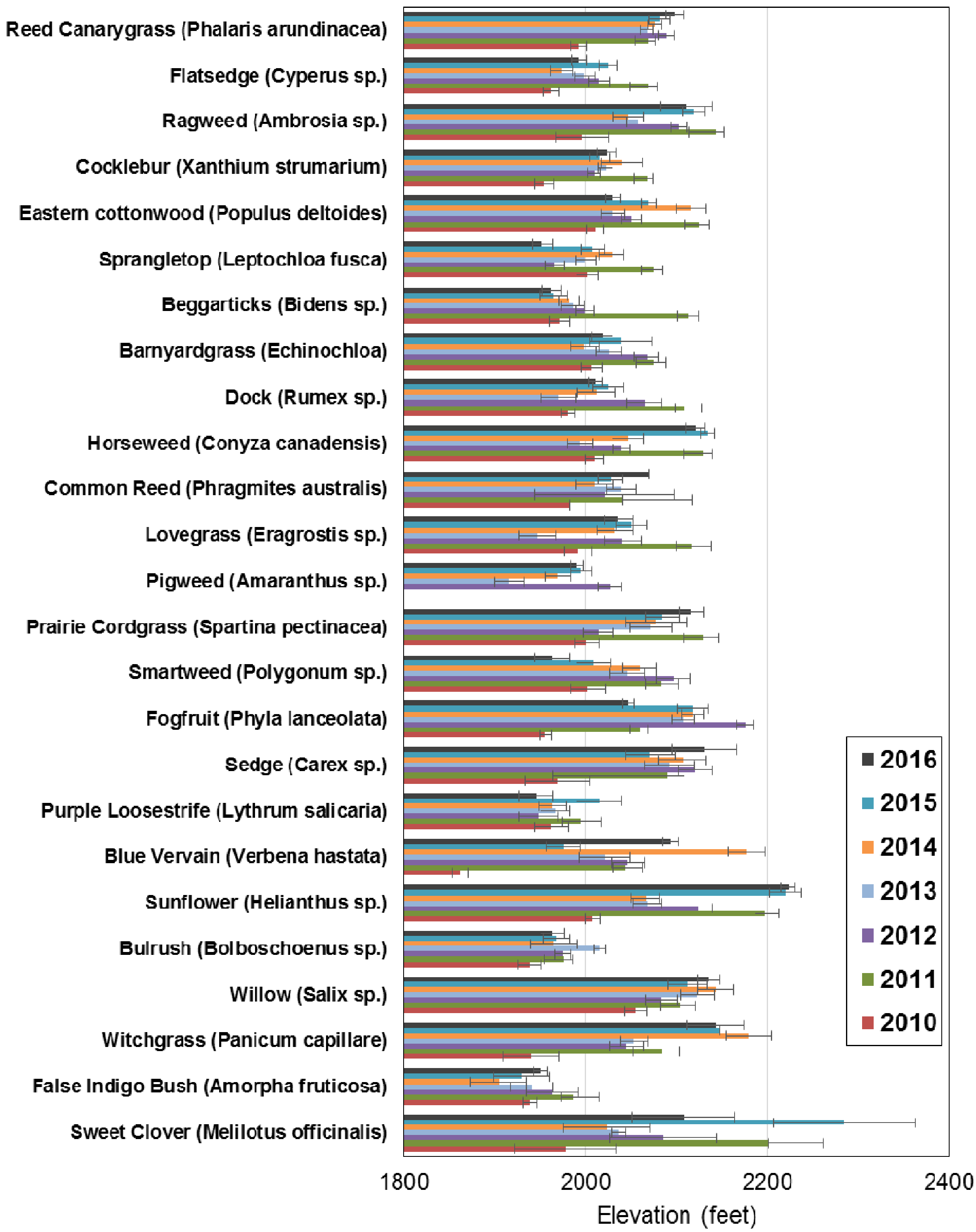

Figure 3.44a. Mean elevation of the top 25 most commonly observed species and additional species of interest not among the 25 most common, organized by decreasing frequency in 2016. Standard error bars (±1) are included.

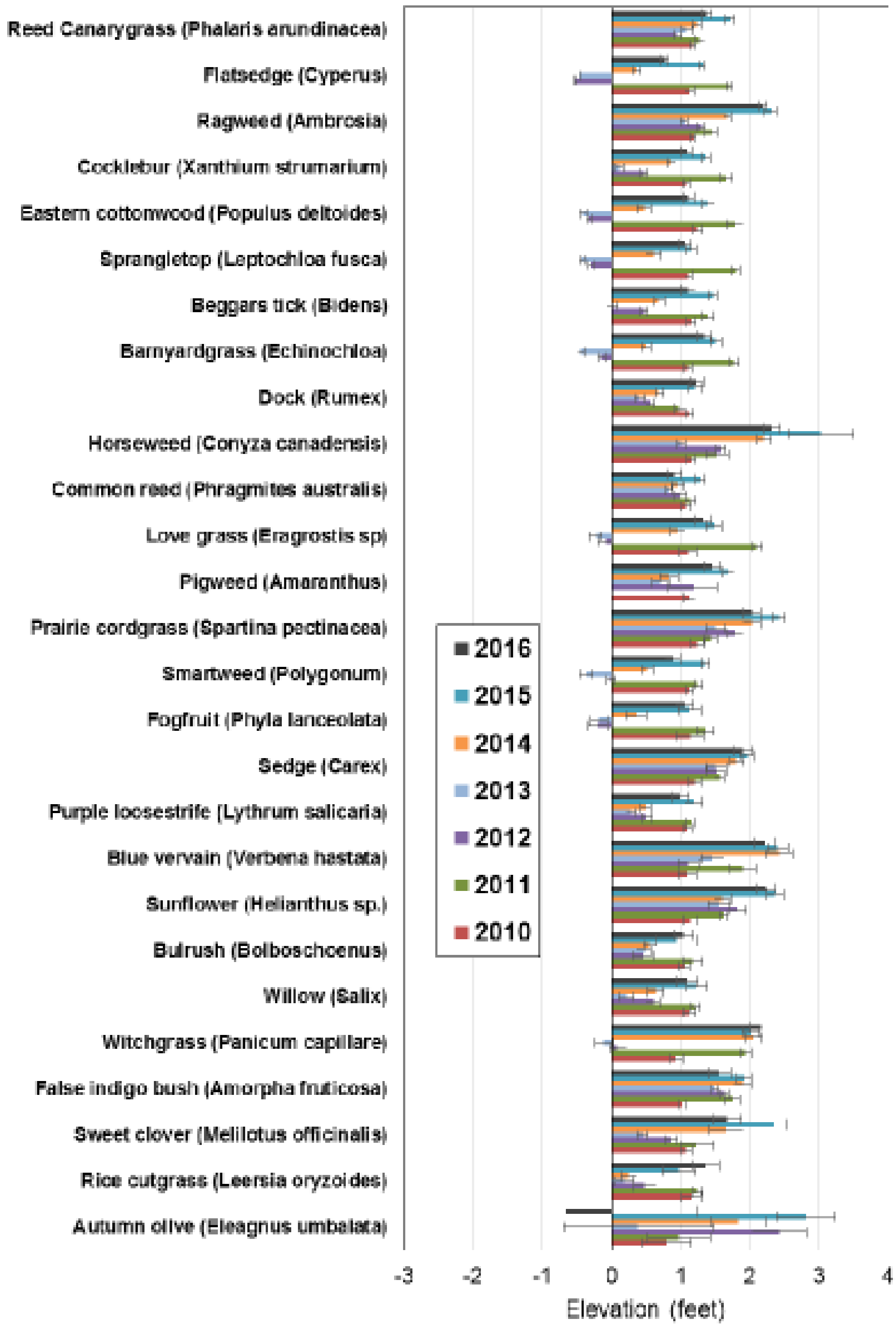

Figure 3.44b. Mean elevation above the local 1,200 cfs water surface of the top 25 most commonly observed species in 2015 and additional species of interest not among the 25 most common, organized by decreasing frequency in 2015. Standard error bars (±1) are included.

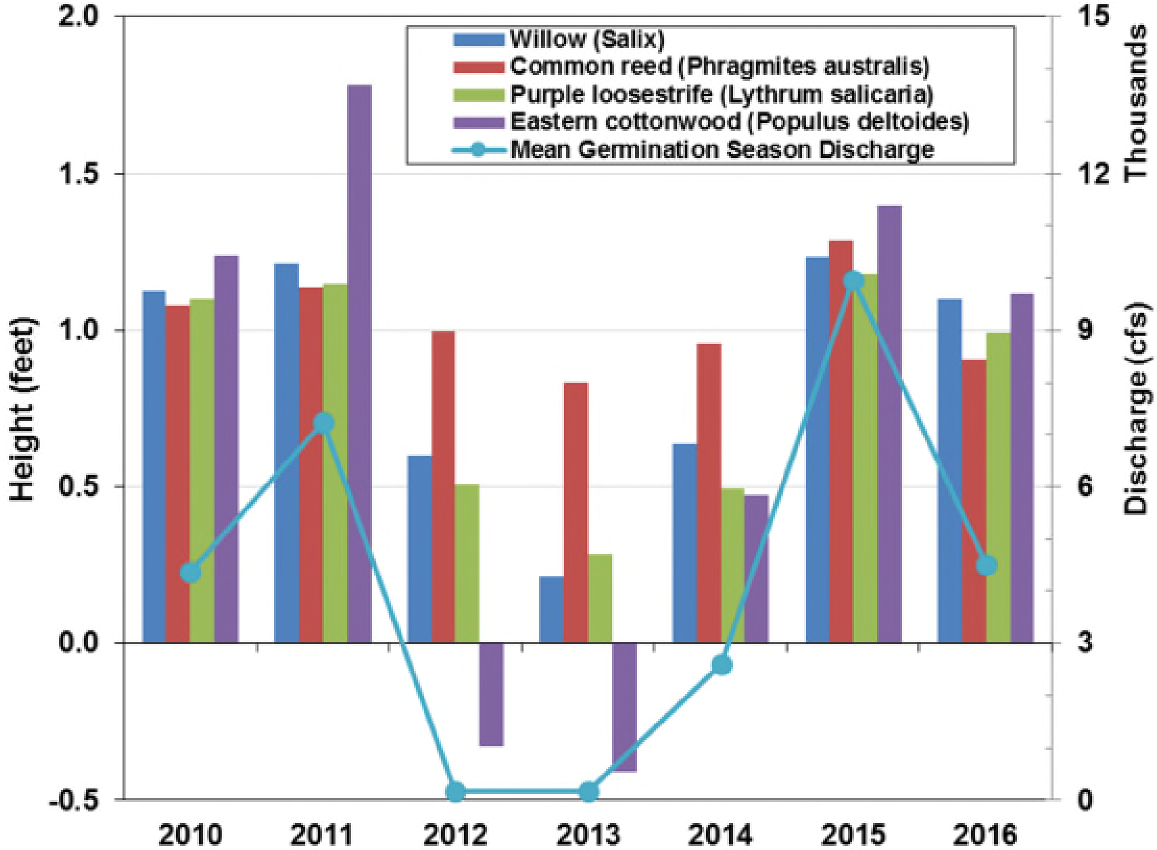

Figure 3.44c. Mean height above the 1,200 cfs water surface of the four vegetation species of interest from 2010 through 2016. Also shown is the mean germination season discharge.

3.4.10 Mean Vegetation Height (DAP 5.4.7)

Mean vegetation height was included among the original metrics to facilitate calculating estimates of unobstructed sight distance for whooping crane habitat. As described above, methods for sampling vegetation height has varied since the program's inception. In 2009, 2010, and 2012, the data were collected categorically as a mean value, whereas in 2011, data were collected as a combination of actual mean heights and categorical mean heights. In 2013 and 2014 the method was modified to document actual maximum heights only. Regardless of sample year, all heights were collected as average values across all woody or herbaceous species in each quadrat, and were not collected directly for each species. As noted elsewhere in this report, unobstructed sight distances were measured directly in the field using a laser rangefinder beginning in 2013. Consequently, the value of this metric for estimating unobstructed sight distance has been substantially reduced for years after 2012. Mean vegetation height data was, however, collected throughout the 8-year monitoring period to maintain consistency and allow for comparisons between all years of the study, if such analysis becomes necessary. A more complete discussion and analysis of Unobstructed Channel Width is presented in Section 3.6.1, below.

3.5 Sediment Metrics

3.5.1 Bed-load versus Discharge Rating Curves (DAP 5.5.1)

As discussed in Chapter 2, a total of 85 bed-load sediment samples were collected over the 8-year monitoring program at the five designated bridge sites: Darr (State Hwy L-24A), Overton (State Hwy 24B), Kearney (State Hwy 44), Shelton (State Hwy 10D), and Grand Island (US-34) (Table 2.4). In addition, one bed-load sample was collected at the Elm Creek Bridge (US-183) during the September 2013 flood, and two additional samples were collected at the Wood River Bridge (State Hwy 40D) in May 2015. Flows during the sampling were as low as 700 cfs, and ranged up to nearly 12,000 cfs during the September 2013 flood. At the end of the 2016 field season, 17 samples had been collected at Darr, 21 samples each had been collected at Overton and Shelton, 12 samples had been collected at Kearney, and 11 samples had been collected at Grand Island.

Typical of sediment-transport data, the sampled loads have exhibited high variability but show sufficiently strong trends to allow development of reasonable bed-load transport rating curves, although the confidence bands on these curves tend to be quite wide due to the small number of samples (**Figures 3.45** through **3.49**). To facilitate the sediment transport analysis, power-function rating curves were developed using least-squares, linear regression on the logarithms of the measured bed loads and corresponding discharges, a well-accepted procedure in sediment-transport analysis (Runkel, et al, 2004; Shen and Julien, 1993). Correlation coefficients (R^2) for the best-fit relationships range from 0.29 (Overton) to 0.69 (Darr). The curves indicate that the bed-load transport rates at the four downstream gages are reasonably consistent through the applicable portion of the reach, and the rates at Darr, at the upstream end of the reach, tend to be higher for equivalent discharges than at the other sites (**Figure 3.50**).

The individual samples contained 57- to 91-percent sand and 9- to 43-percent gravel, with the Grand Island samples being the finest (average of about 84-percent sand and 16-percent gravel) and the Overton samples being the coarsest (average of about 70-percent sand and 30-percent gravel) (**Figure 3.51**). Most of the coarser fraction of the samples was in the very fine to fine gravel size range (i.e., 2 to 8 mm), with a few containing small amounts of medium gravel (8 to 16 mm). The data at Darr and Overton show statistically-significant increases in the median (D_{50}) and D_{84} sizes with increasing discharge (**Figures 3.52a and 3.52b**). No trend in these two parameters with discharge is evident at the other sites.

As will be discussed in a later section of this report, the rating curves were developed to provide a means of estimating the quantity of sediment carried past each of the measurement locations over specific periods of time. Because the regressions are performed in logarithmic space, simply transforming the results back to linear space provides an unbiased estimate of the median value of the loads, but not the mean value that is most important to the analysis (Hirsch et al., 1993; Ferguson 1986; Thomas 1985; Walling 1977). Several methods for correcting for this bias have been proposed in the literature, including the *smearing estimate* (Duan, 1983) and the Maintenance of Variance Unbiased Estimator (*MVUE*) method (Cohn and Gilroy, 1991). The *smearing* estimate results in a constant percentage adjustment to all of the estimated loads, regardless of the distribution of the underlying data, while the *MVUE* method provides an adjustment for each load based on the statistical distribution of the data. USGS (1992) recommends the MVUE method, and this method was therefore selected for use in this study. The rating curves that reflect the MVUE adjustments are shown by the blue lines in Figures 3.45 through 3.51.

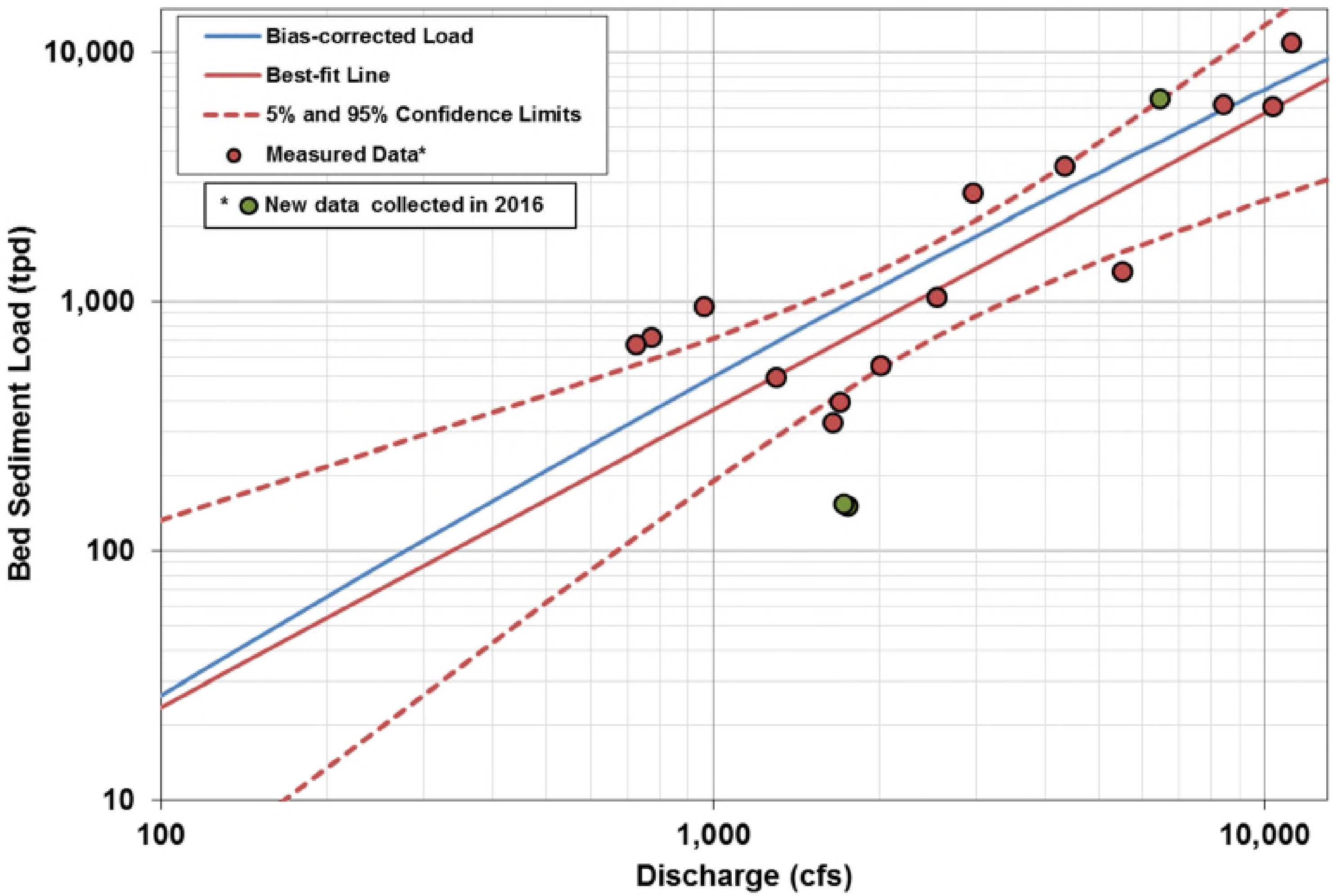

Figure 3.45. Bed-load transport rates measured at the Darr Bridge between 2009 and 2016. Also shown is the best-fit power-function through the data, the upper and lower 95-percent confidence bands on the best-fit line, and the *MVUE* bias-corrected line.

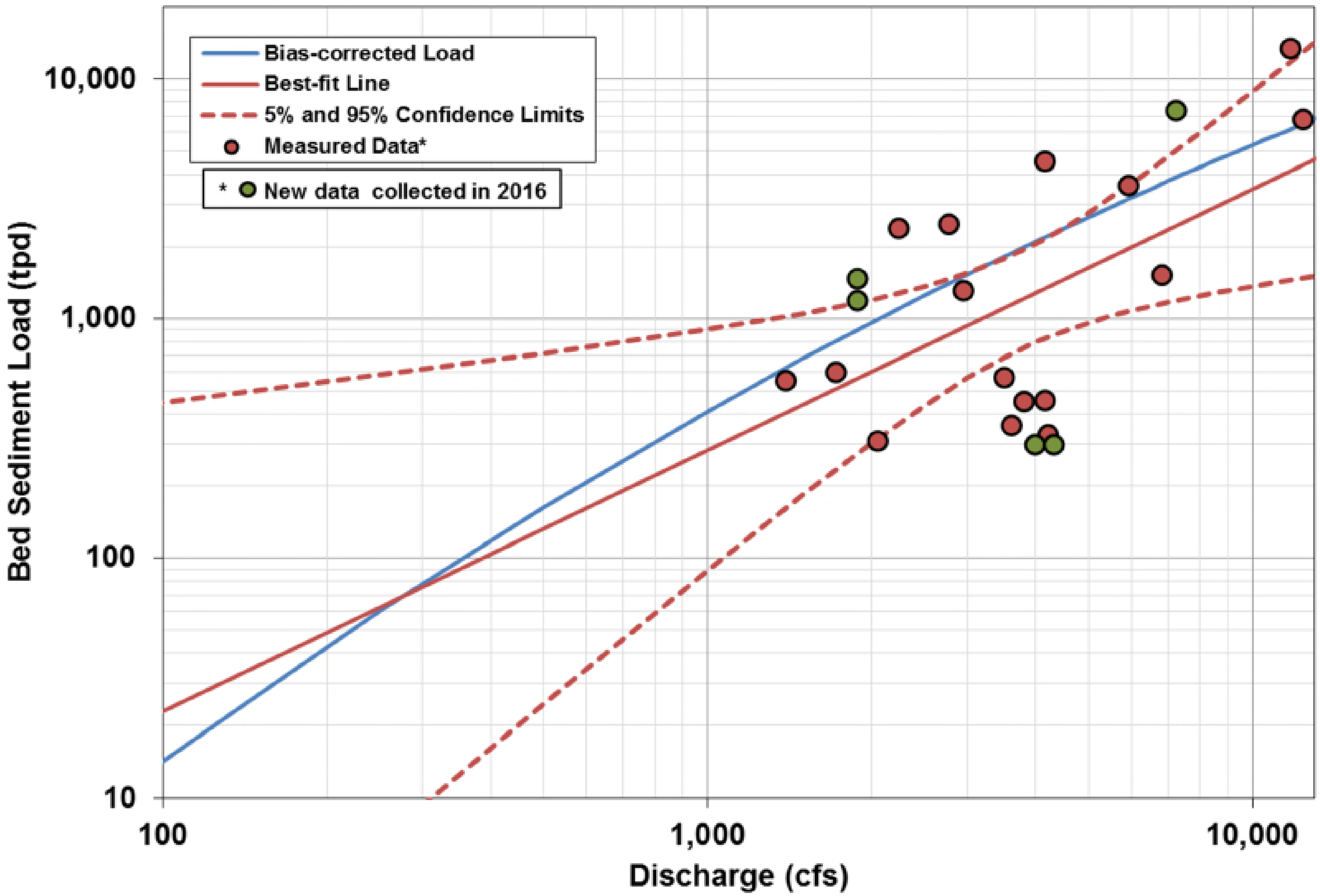

Figure 3.46. Bed-load transport rates measured at the Overton Bridge between 2009 and 2016. Also shown is the best-fit power-function through the data, the upper and lower 95-percent confidence bands on the best-fit line, and the MVUE bias- corrected line.

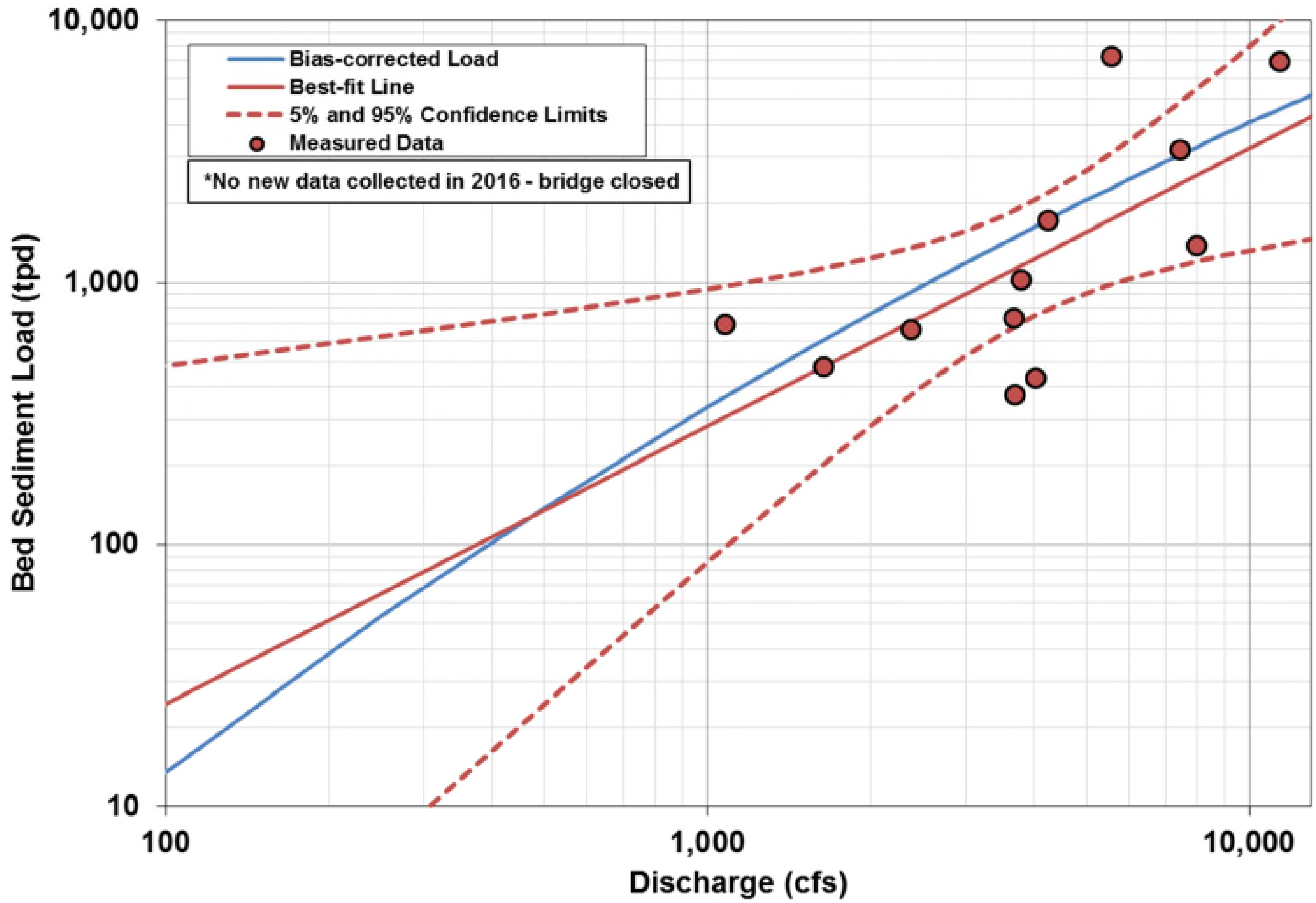

Figure 3.47. Bed-load transport rates measured at the Kearney Bridge between 2009 and 2016. Also shown is the best-fit power-function through the data, the upper and lower 95-percent confidence bands on the best-fit line, and the MVUE bias-corrected line.

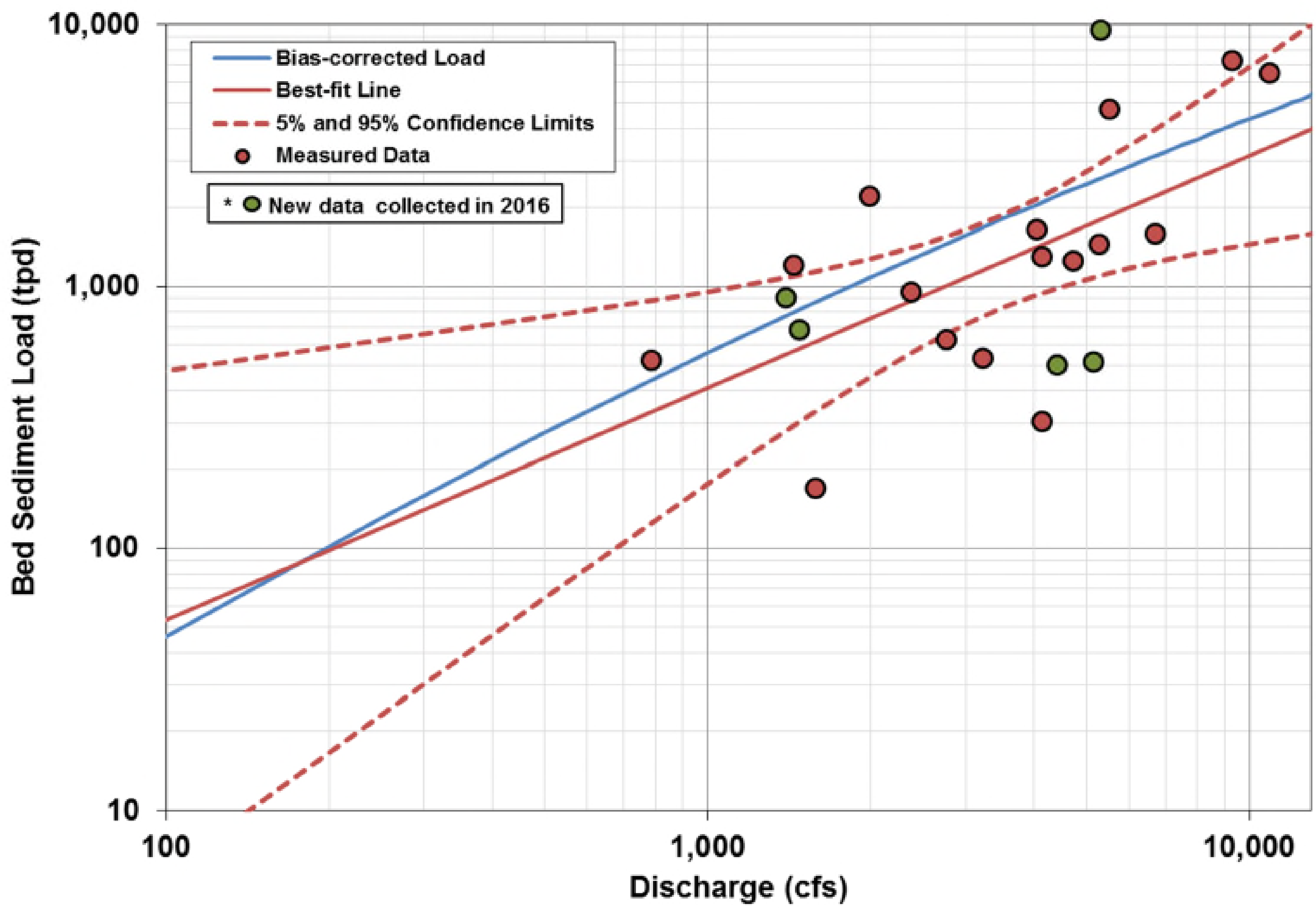

Figure 3.48. Bed-load transport rates measured at the Shelton Bridge between 2009 and 2016. Also shown is the best-fit power-function through the data, the upper and lower 95-percent confidence bands on the best-fit line, and the MVUE bias- corrected line.

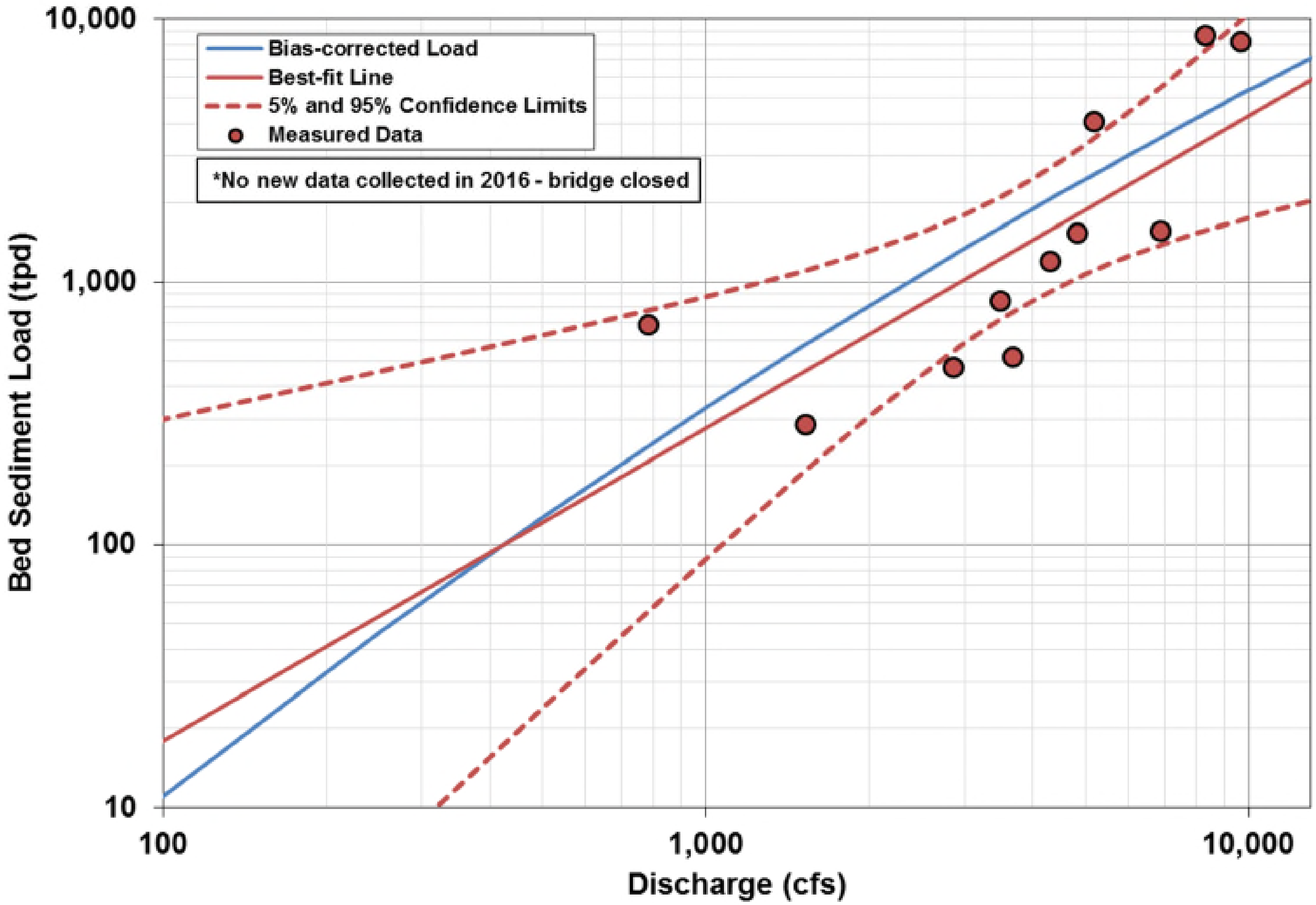

Figure 3.49. Bed-load transport rates measured at the Grand Island Bridge between 2009 and 2016. Also shown is the best-fit power-function through the data, the upper and lower 95-percent confidence bands on the best-fit line, and the MVUE bias-corrected line.

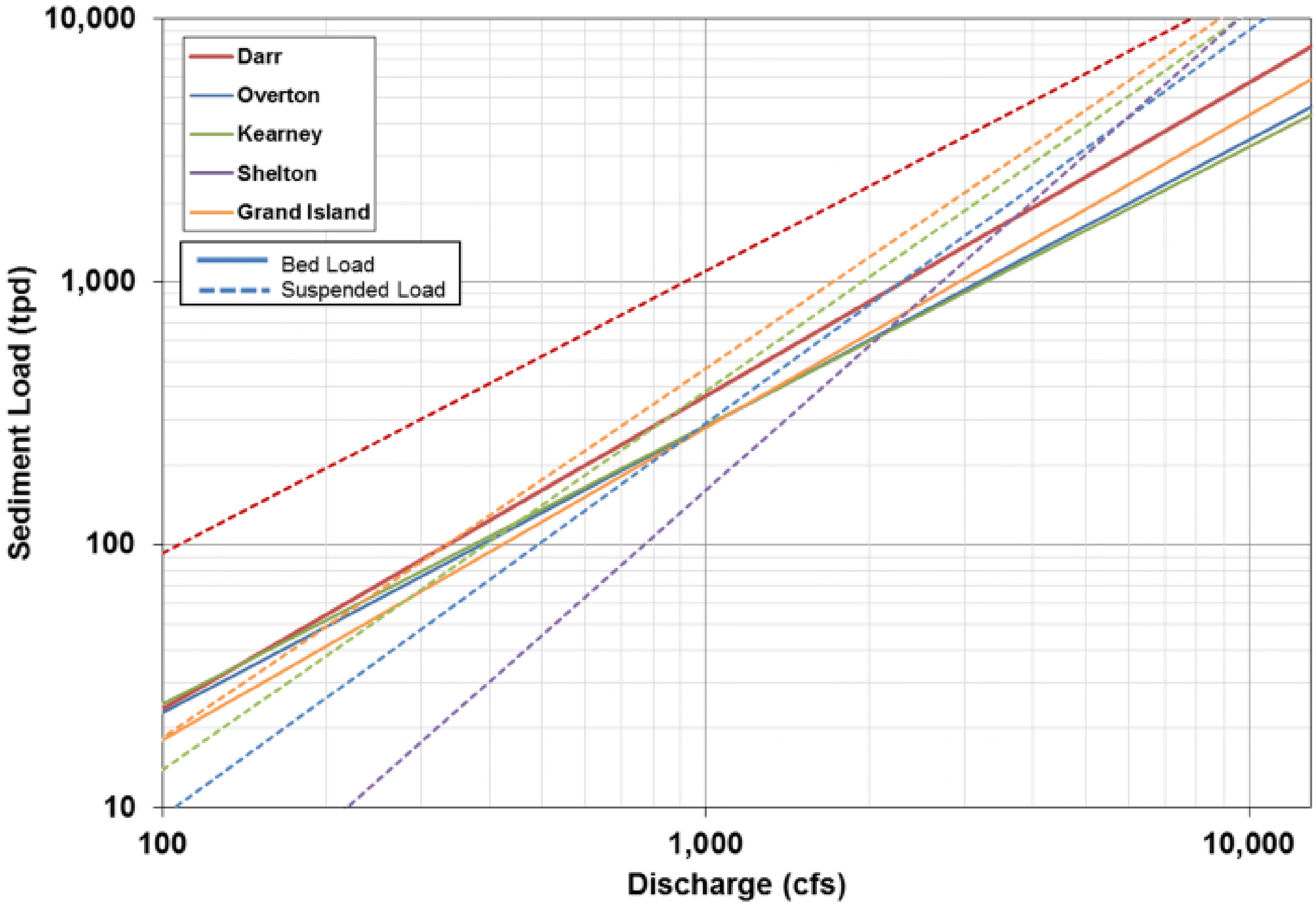

Figure 3.50. Power-function, best-fit curves for the measured bed- and suspended-sediment-transport rates at the five measurement sites.

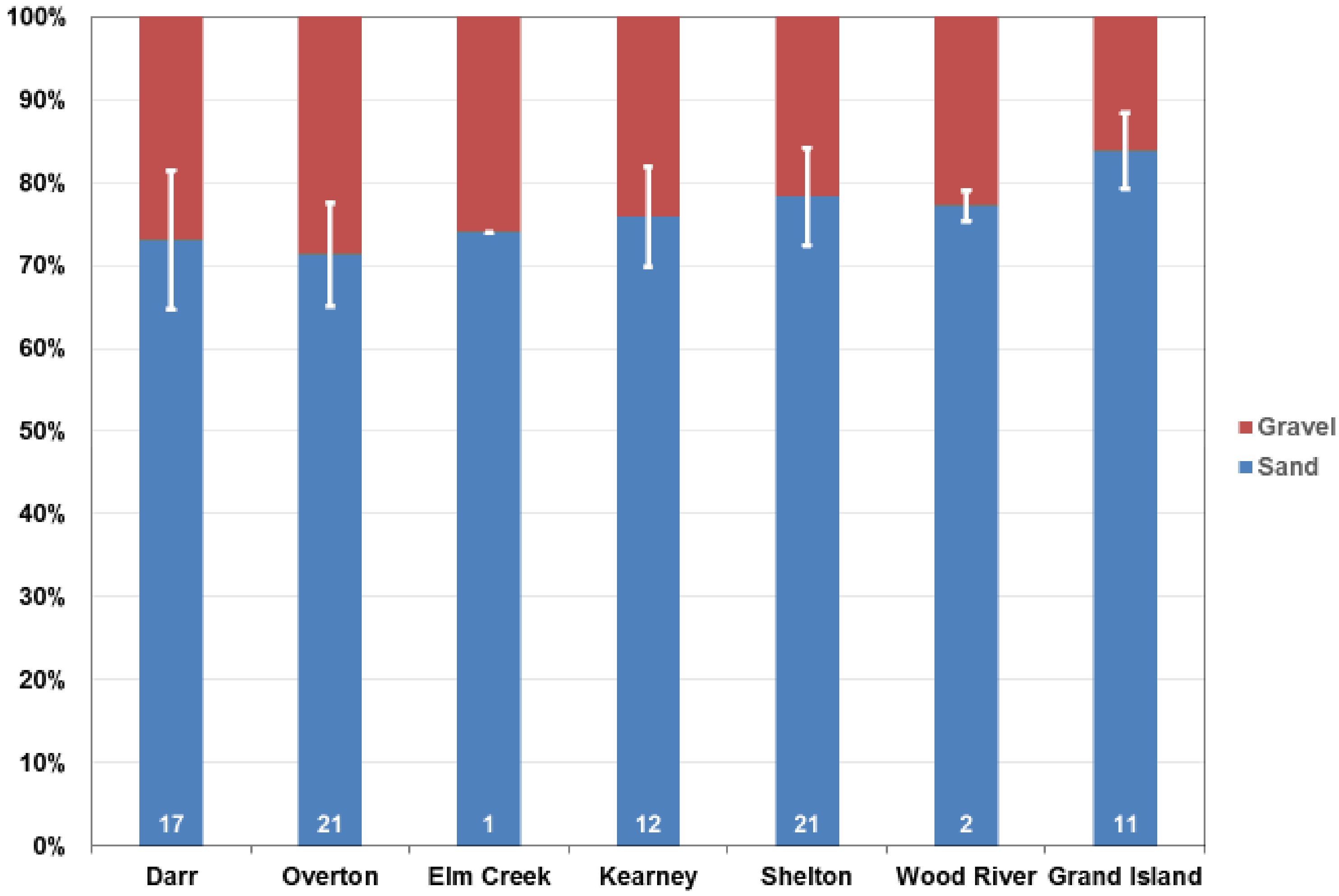

Figure 3.51. Average percentage of sand and gravel in the bed-load samples from the five primary measurement sites and the samples collected at Elm Creek and Wood River. Embedded values represent number of samples at each site; whiskers represent ±1 standard error about the mean.

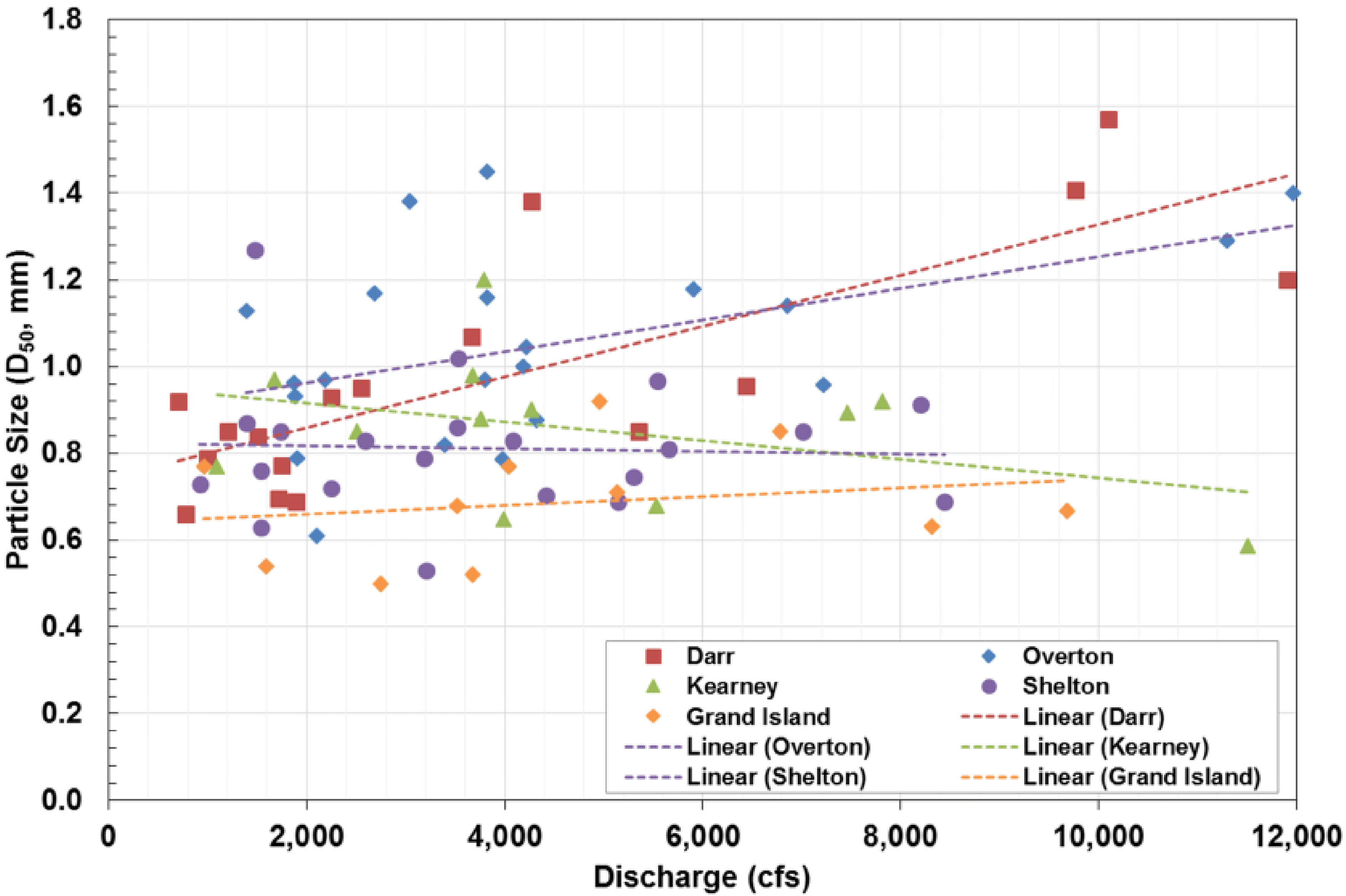

Figure 3.52a. Median (D_{50}) particle size of bed-load samples with discharge for the five measurement sites (2009-2016).

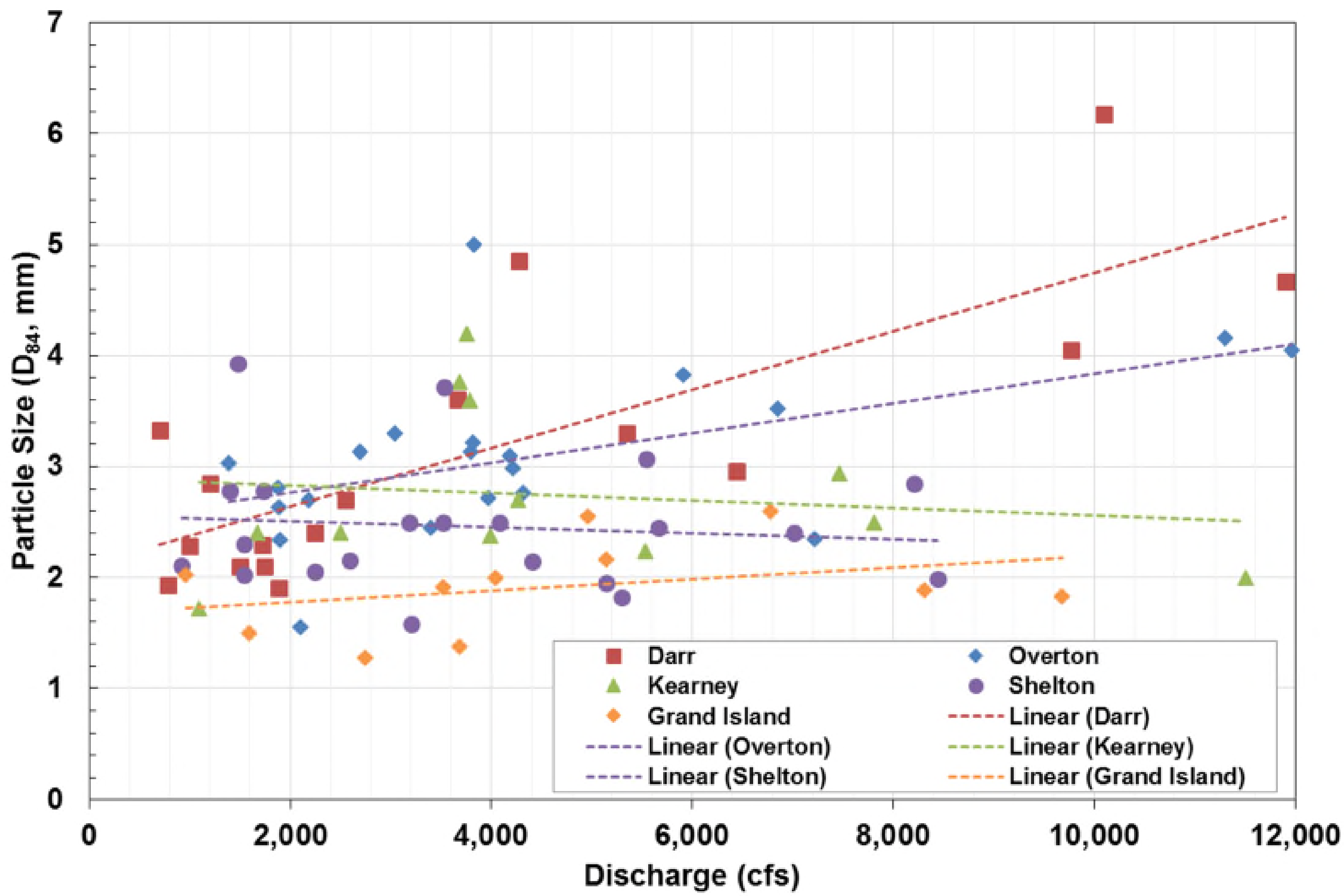

Figure 3.52b. Variation in D_{84} particle size of bed-load samples with discharge at the five measurement sites (2009-2016).

3.5.2 Suspended Sediment Load versus Discharge Rating Curves (DAP 5.5.2)

A total of 92 suspended sediment samples were collected at the five designated bridge sites at flows as low as 700 cfs and as high as 12,160 cfs (Table 3.2). An additional sample was also collected at the Elm Creek Bridge during the September 2013 flood, and single samples were collected at Lexington (US-283) in 2009 and at Gibbon (State Hwy 10C) in 2011. Two samples were also collected at the Wood River Bridge in 2015. For purposes of the analysis, the Lexington sample was included in the Darr data set. The total suspended sediment concentrations (i.e., silt/clay and sand) in the complete sample set ranged from about 125 ppm to 1,700 ppm.

The amount of silt and clay in the suspended sediment samples at the individual bridge sites ranged from about 31 and 49 percent. A substantial amount of the sand in these samples is less than 1 mm (i.e., fine, medium and coarse sand), with relatively minor amounts of very coarse sand (1 – 2 mm).The Grand Island samples contained the most sand (~70 percent), and the Shelton samples typically had the least sand (~50 percent) (**Figure 3.53**). There is essentially no correlation between the median size of the material in these samples and discharge.

To facilitate analysis of the sediment-transport balance that will be described in Section 4.1, the sand fraction of the samples was separated from the silt/clay fraction and suspended sand load rating curves were developed from the resulting sand-load data sets (**Figures 3.54** through **3.58**). Correlation coefficients (R^2) for the rating curves range from 0.68 (Darr) to 0.77 (Grand Island and Kearney). For purposes of estimating annual sediment loads, bias-correct lines were also developed using the MVUE method described previously. The curves indicate that the suspended sand loads vary considerably through the reach, with Darr being 3 to 5 times higher for a given discharge than at the other sites at flows in the range of 500 cfs, decreasing to 2 to 3 times higher in the range of 5,000 cfs (Figure 3.50).

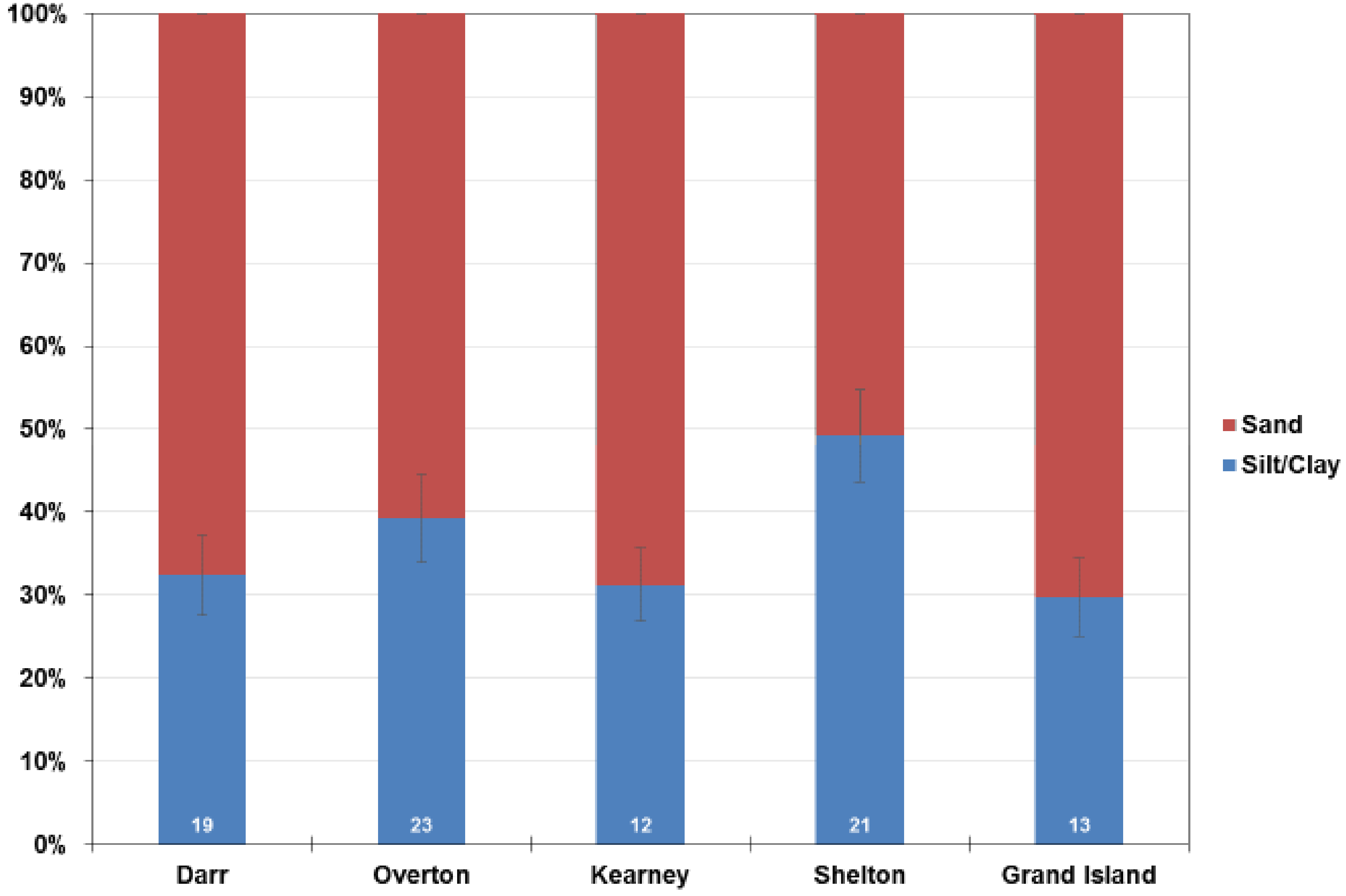

Figure 3.53. Variation in D_{84} particle size of bed-load samples with discharge at the five measurement sites (2009-2016).Average percentage of silt/clay and sand in the suspended sediment samples from the five primary measurement sites. Embedded values represent number of samples at each site; whiskers represent ±1 standard error about the mean.

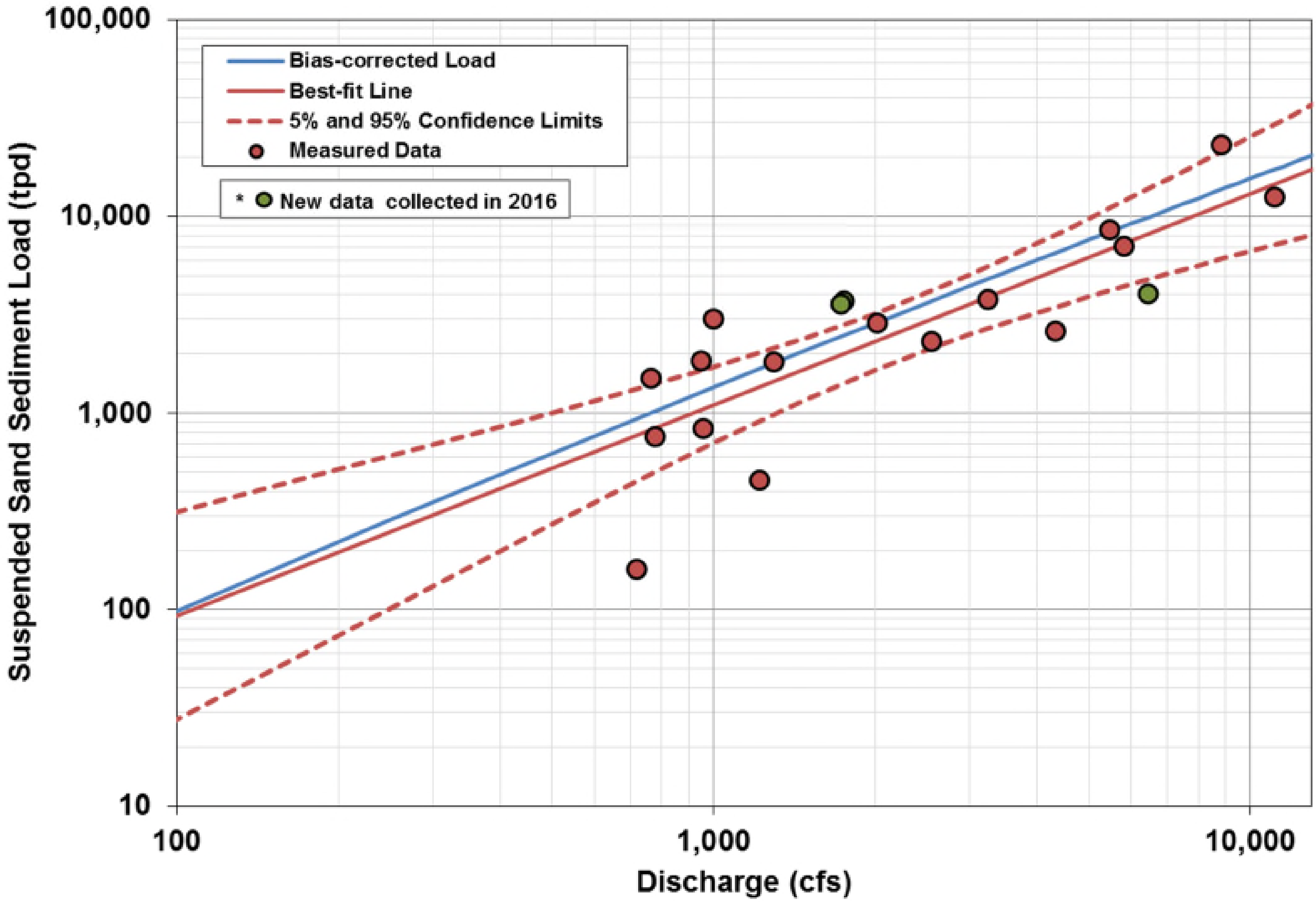

Figure 3.54. Suspended sand transport rates measured at the Darr Bridge between 2009 and 2016. Also shown is the best-fit power-function through the data, the upper and lower 95-percent confidence bands on the best-fit line, and the MVUE bias-corrected line.

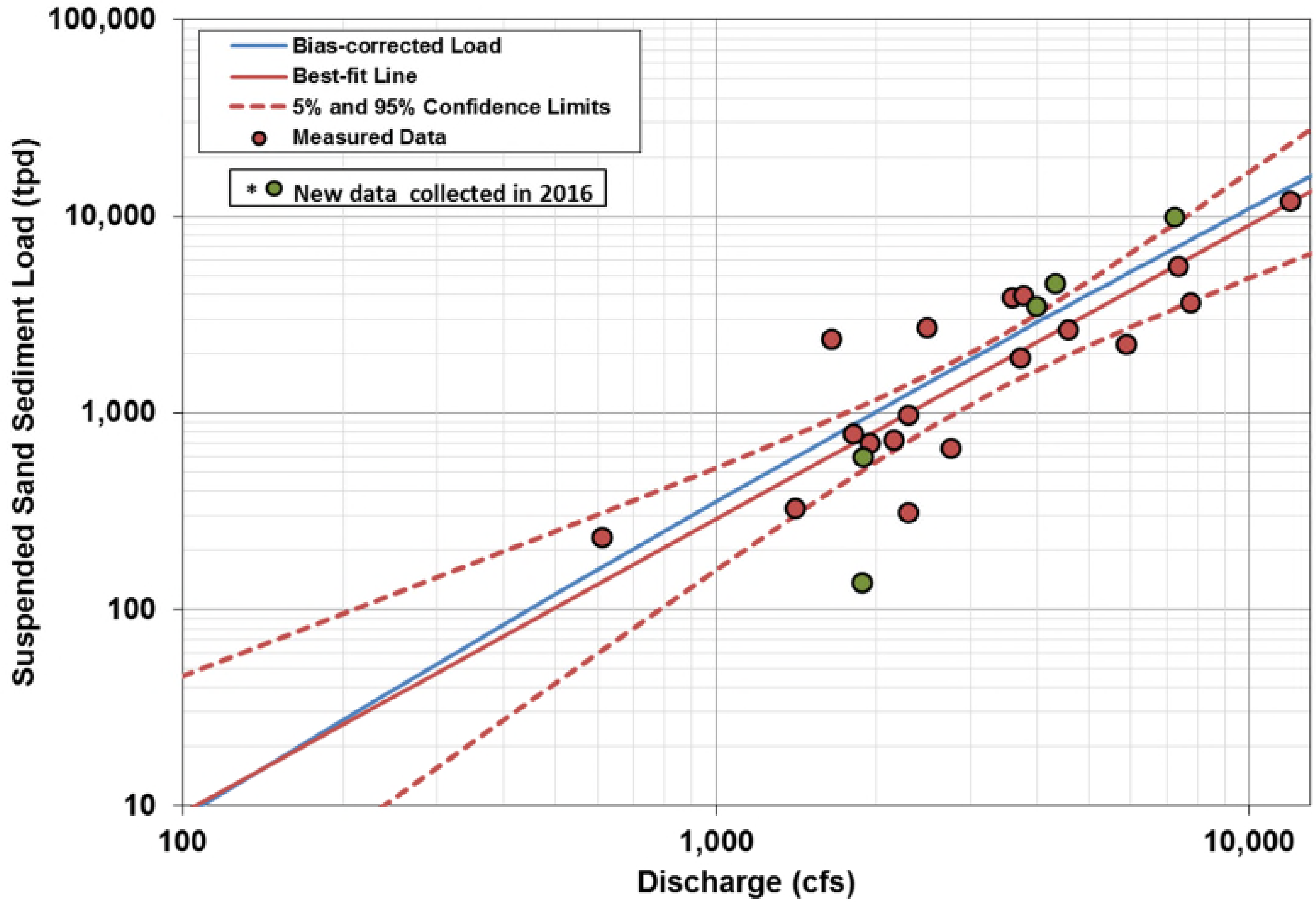

Figure 3.55. Suspended sand transport rates measured at the Overton Bridge between 2009 and 2016. Also shown is the best-fit power-function through the data, the upper and lower 95-percent confidence bands on the best-fit line, and the MVUE bias-corrected line.

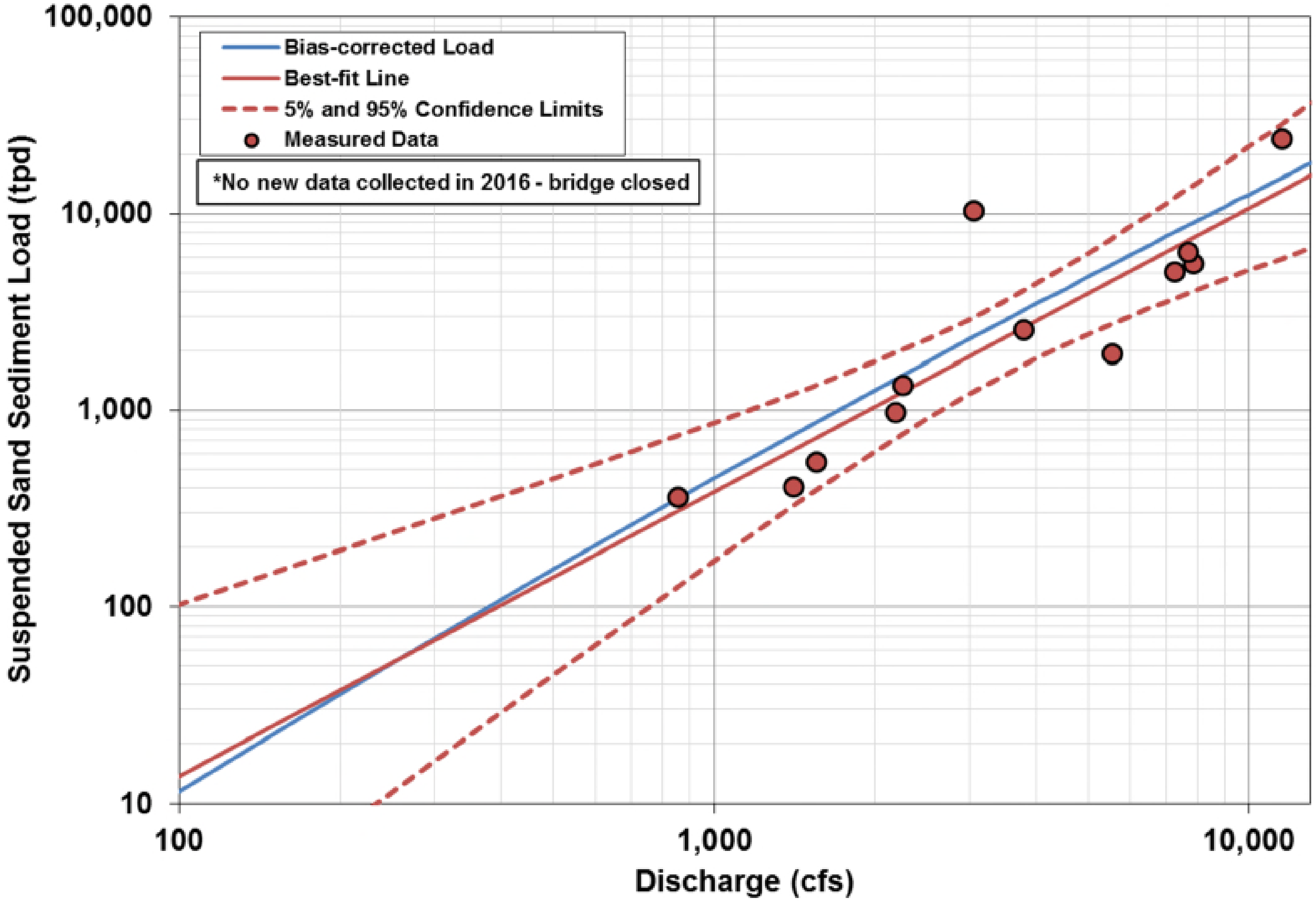

Figure 3.56. Suspended sand transport rates measured at the Kearney Bridge between 2009 and 2016. Also shown is the best-fit power-function through the data, the upper and lower 95-percent confidence bands on the best-fit line, and the MVUE bias-corrected line.

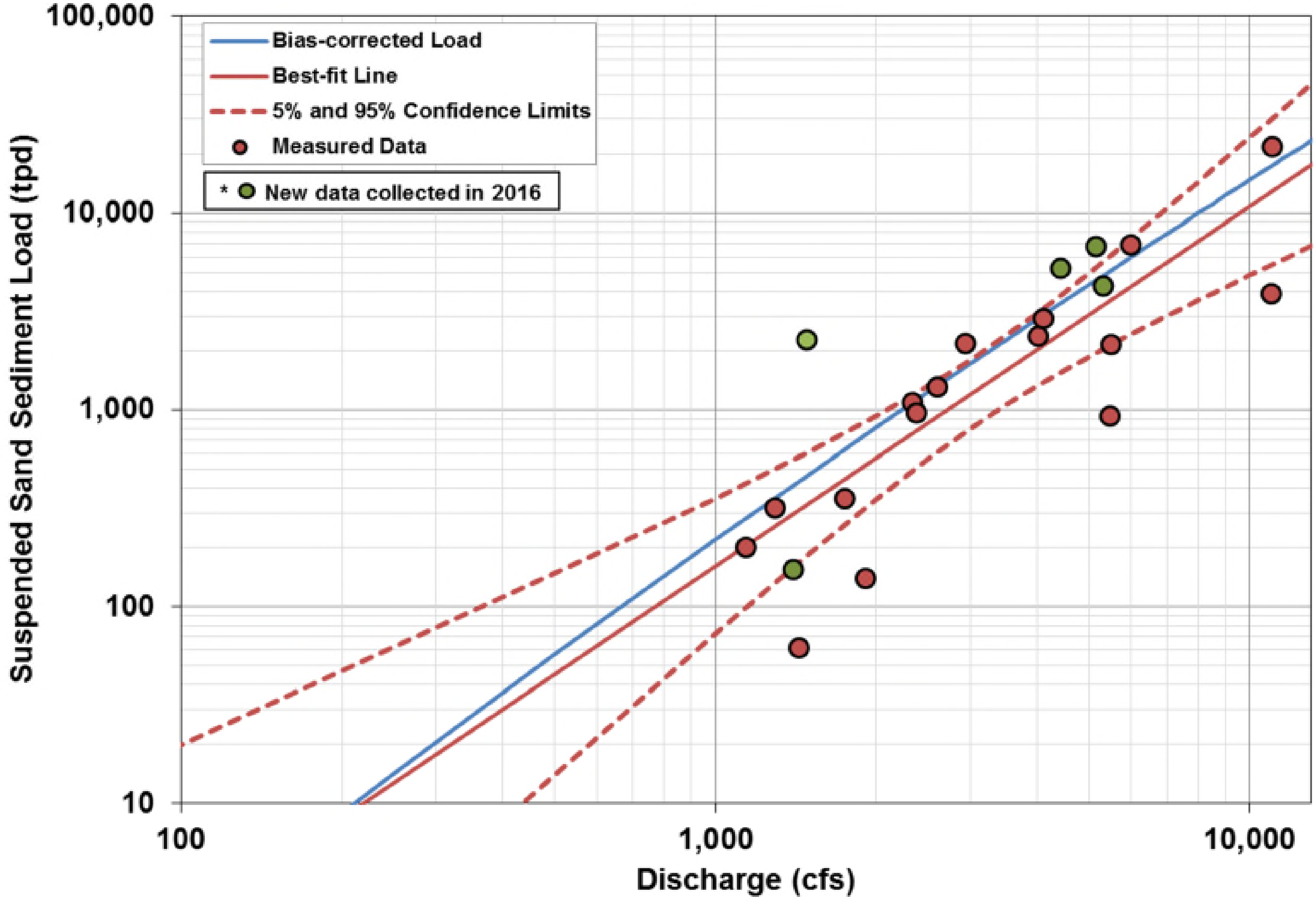

Figure 3.57. Suspended sand transport rates measured at the Shelton Bridge between 2009 and 2016. Also shown is the best-fit power-function through the data, the upper and lower 95-percent confidence bands on the best-fit line, and the MVUE bias-corrected line.

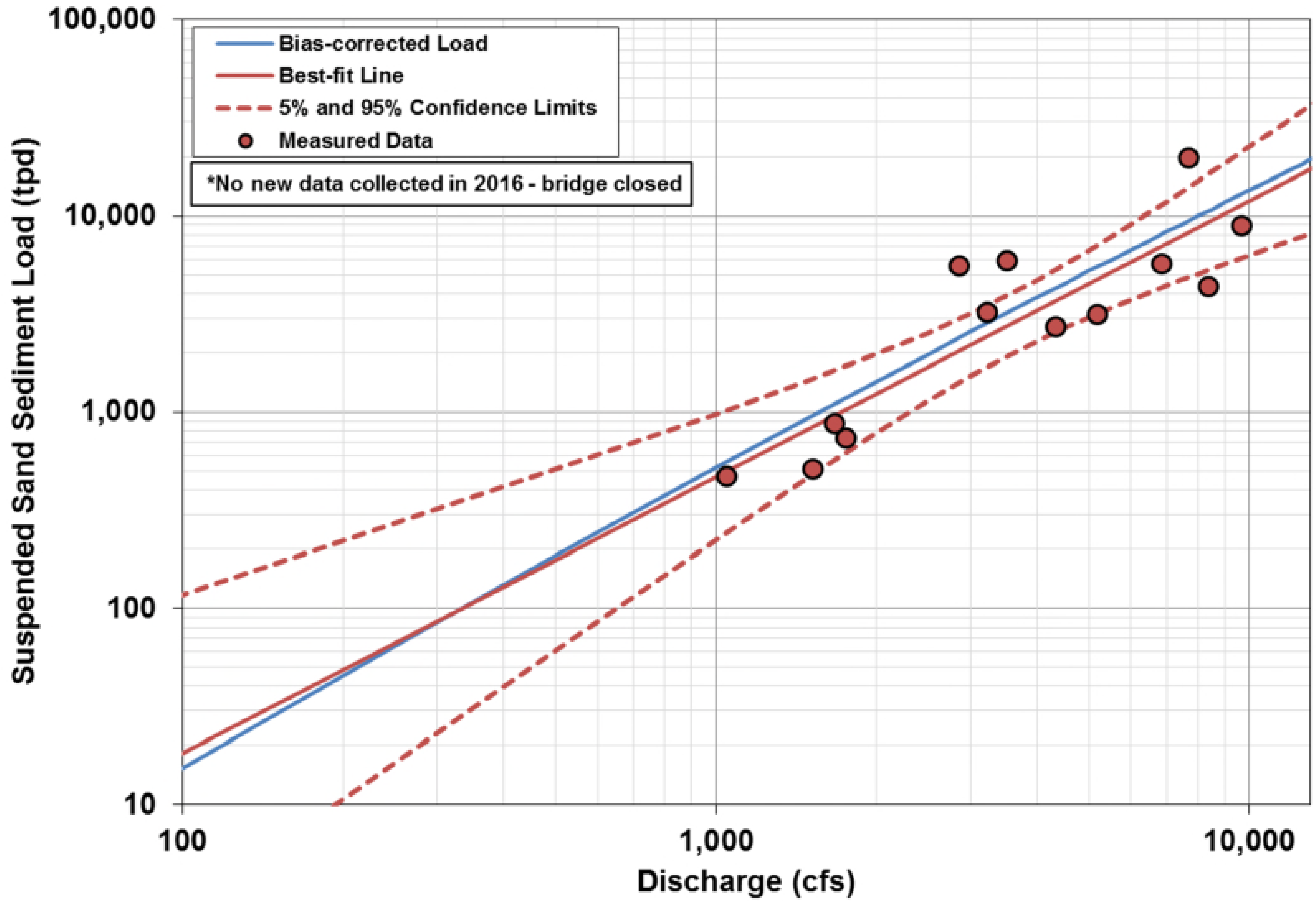

Figure 3.58. Suspended sand transport rates measured at the Grand Island Bridge between 2009 and 2016. Also shown is the best-fit power-function through the data, the upper and lower 95-percent confidence bands on the best-fit line, and the MVUE bias-corrected line.

3.5.3 Bed-material Grain-size Distribution and Distribution Parameters (DAP 5.5.3)

The total number of bed material samples collected during 8-year monitoring period ranged from 230 (2012) to 270 (2015). These sample sets included 9 to 10 samples at each of the surveyed APs and a single sample at each of the five bridges at which bed-load measurements were made (except for 2012, when no sample was collected at the Darr Bridge, and 2015 and 2016, when no samples were collected at the Kearney and Grand Island bridges). For purposes of evaluating trends in the typical bed material sizes along the reach, the samples at each of the APs were averaged to provide a representative bed-material gradation. The resulting median (D_{50}) bed-material size generally consisted of very coarse sand (1 to 2 mm) in the upstream part of the reach, decreasing to coarse sand (0.5 to 1 mm) in the downstream part of the reach (**Figure 3.59**). The trend of decreasing median size with distance along the reach is statistically significant in all years except 2014 (**Table 3.3**). The 2014 trend is not significant because the composited samples at AP29 and AP39, at the upstream end of the reach, were unusually fine and the samples at AP6, AP7, and AP 10, at the downstream end of the reach, were unusually coarse compared to the other years. With the exception of AP19, the 2015 samples were among the finest of all years. A sample set collected by the Bureau of Reclamation in 1989 showed a similar, statistically-significant trend, although the median grain size was typically finer that those collected as part of this monitoring program.

The reach-averaged median (D_{50}) of the bed material declined from about 1.2 mm in 2009 to about 0.7 mm in 2012, and then increased progressively back to 1 mm by 2016 (**Figure 3.60)**. The 1989 Reclamation sample had median size of about 0.7 mm, similar to the 2012 value. Based on the non-parametric Kruskal-Wallis test, the difference between the 2012 average and all of the other years except 2013 was statistically significant at the 90-percent confidence level, and the difference between 2009 and 2013 was also statistically significant. The differences between all other pairs of years were not statistically significant.

Table 3.3. Summary Statistics for Trends in Median Grain Size with Distance along the Monitoring Reach (α=0.10).

Year	Slope (D_{50} versus River Mile)			**p-value**
	Best-estimate	Lower Limit	Upper Limit	
2009	1.08E-02	7.19E-03	1.44E-02	**0.000**
2010	4.63E-03	2.32E-03	6.93E-03	**0.002**
2011	5.61E-03	2.45E-03	8.77E-03	**0.005**
2012	1.80E-03	7.72E-05	3.52E-03	**0.086**
2013	2.65E-03	1.15E-03	4.14E-03	**0.005**
2014	1.42E-04	-3.30E-03	3.59E-03	0.944
2015	2.87E-03	3.42E-04	5.41E-03	**0.064**
2016				
BOR 1989	3.07E-03	7.53E-04	5.40E-03	**0.033**

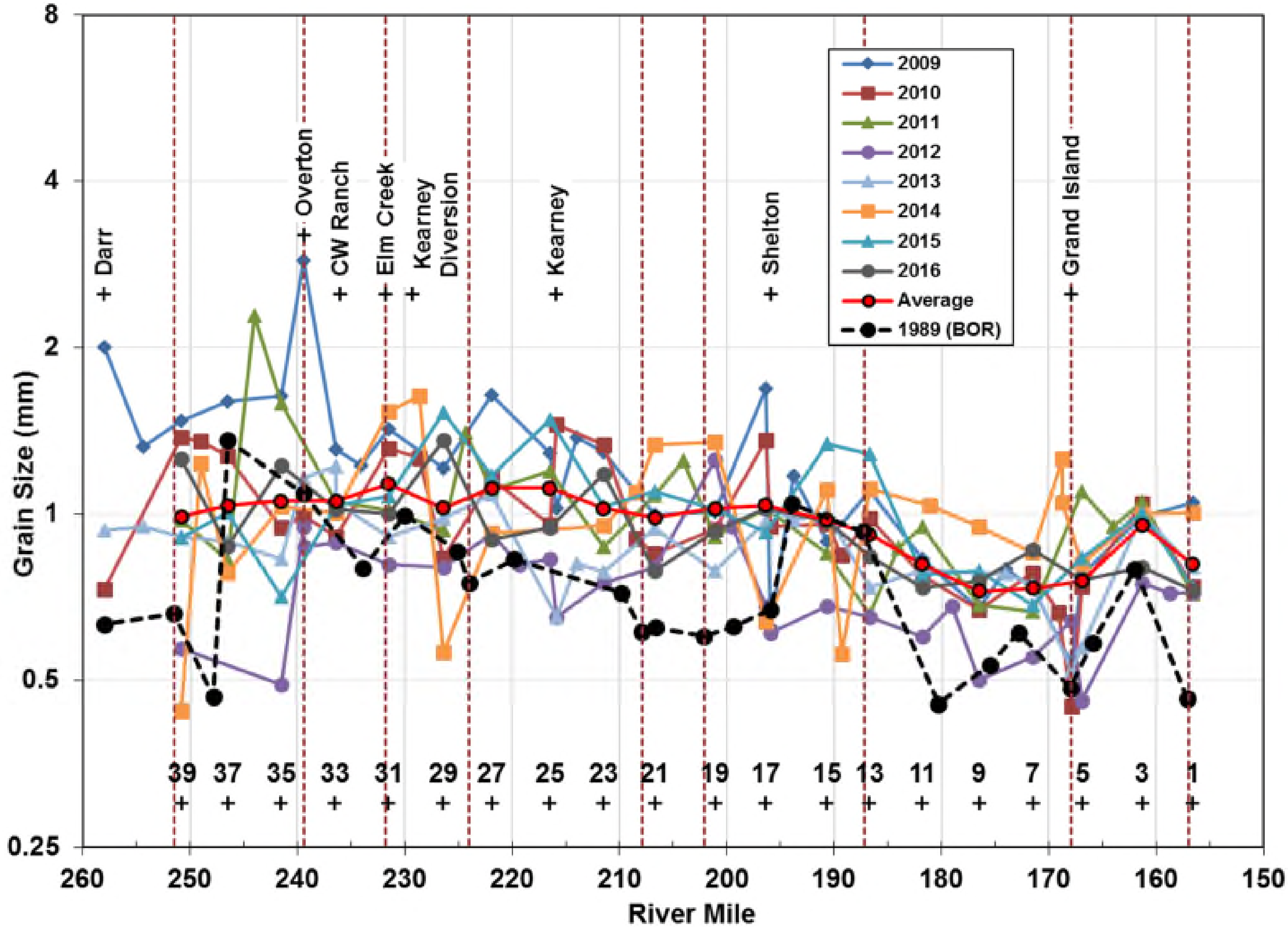

Figure 3.59. Average median (D_{50}) size of bed-material samples collected at the APs during 2009 through 2016 monitoring surveys. Also shown are the D_{50} sizes of the samples collected by Reclamation in 1989.

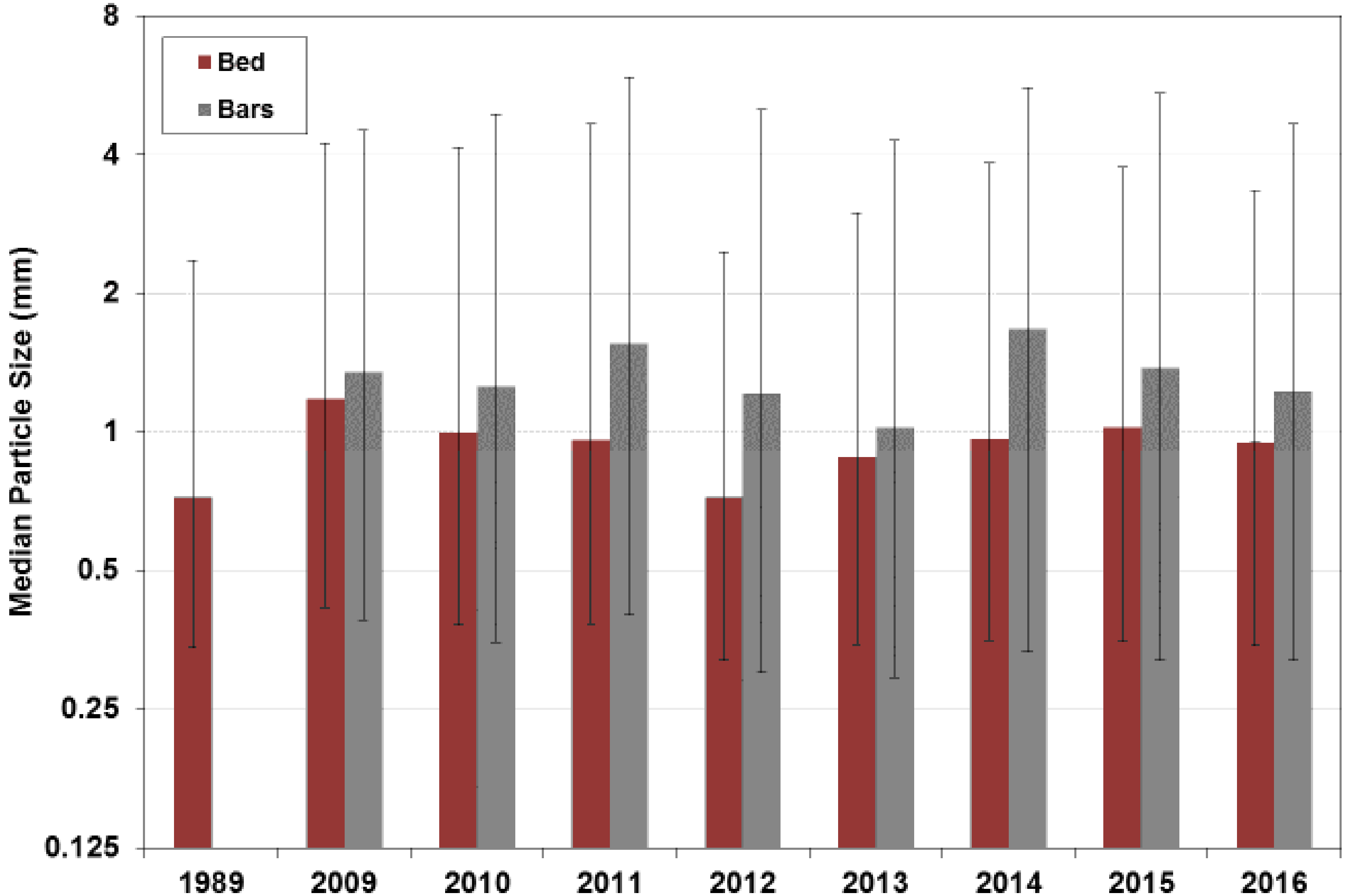

Figure 3.60. Reach averaged median (D_{50}) particle size of samples collected for this monitoring program in 2009 through 2016, and by Reclamation in 1989. Whiskers represent reach-averaged D_{16} and D_{84}.

3.5.4 Bar Material Grain-size Distribution (DAP 5.5.4)

The gradations of the bar material samples were generally coarser and more highly variable than the bed material samples, with the median (D_{50}) size ranging from medium sand (0.25-0.5 mm) to fine gravel (4 to 8 mm) (**Figure 3.61**). Visual inspection of the plot suggests a general fining trend in the downstream direction, similar to the bed material; however, the trend is not statistically significant due to the large variability along the reach. The reach-averaged D_{50} varied from about 1.0 mm in 2013 to 1.7 mm in 2014, with no apparent temporal trend.

3.5.5 Bank Material Grain Size Distribution (DAP 5.5.5)

Bank material samples are specified in the scope of work to be collected during the first and last year of the first increment. Therefore, no bank-material samples have been taken since 2009. Results from the 2009 samples are summarized in Ayres and Olsson (2010).

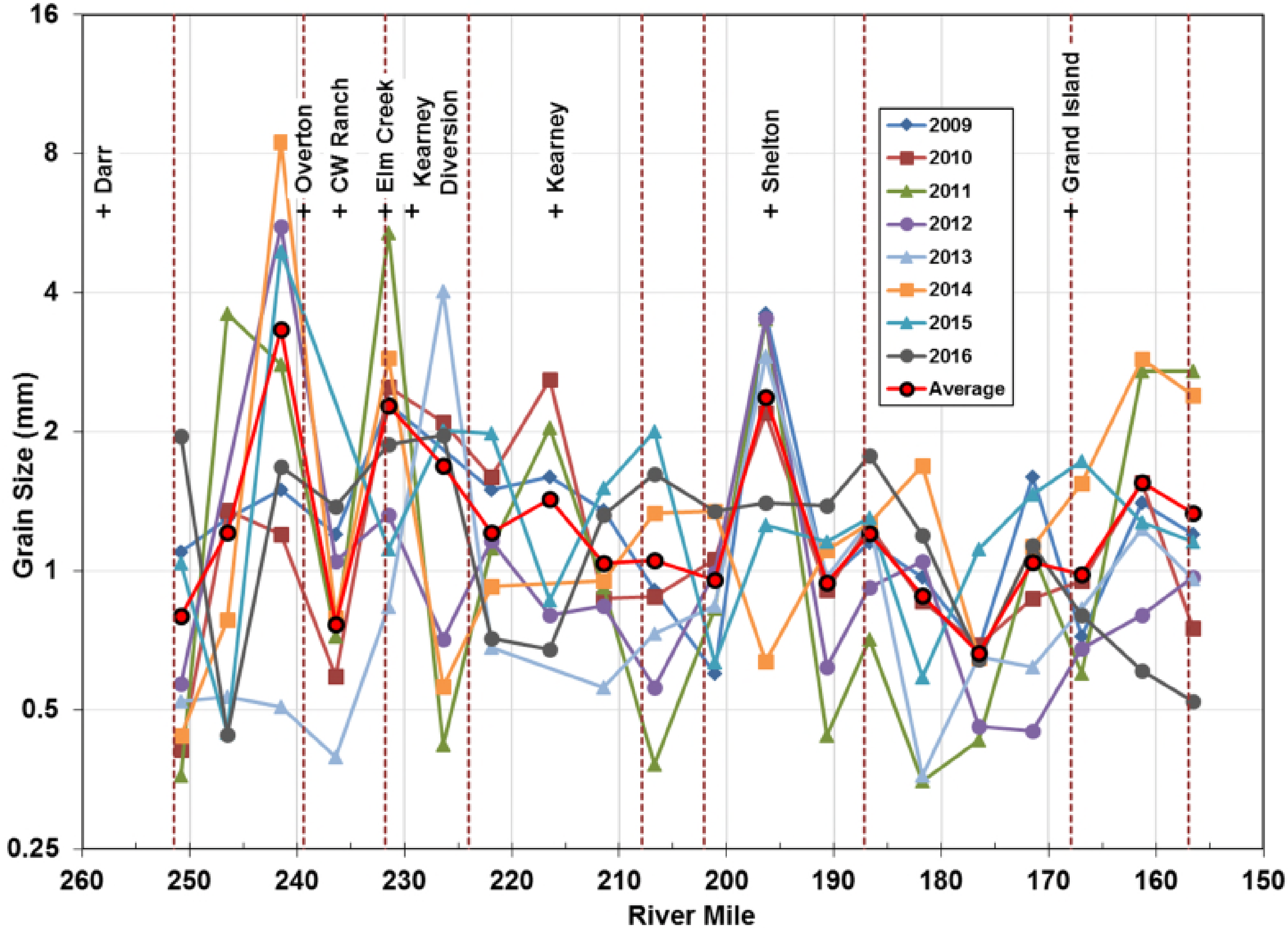

Figure 3.61. Reach-averaged median (D_{50}) size of bar-material samples collected during 2009 through 2016 monitoring surveys. Also shown are the average values for the 8-year monitoring period.

3.6 Whooping Crane Performance Metrics

3.6.1 Unobstructed Channel Width (DAP 5.6.1)

Unobstructed channel widths were determined based on the assumption that eye-height of the typical migrating whooping cranes is about 1.5 m (4.9 ft), and thus, vegetation taller than 1.5 m will obscure their sight lines. During the 2009 through 2012 surveys, vegetation heights were recorded in the field data in the following height classes:

- **Woody species:**
  - W1: 0-59 inches (<1.5 meters)
  - W2: 60-120 inches (1.5-3 meters)
- **Herbaceous species:**
  - H1: 0-12 inches (<0.3 meters)
  - H2: 13-59 inches (0.3 to 1.5 meters)
  - H3: 60-84 inches (1.5-2.1 meters)

For purposes of estimating unobstructed channel widths, the vegetation height for each quadrat was assumed to be the mid-point of the height class of the highest woody or herbaceous species that occurred in the quadrat. The elevation of the top of the vegetation was then estimated by adding the estimated height to the surveyed elevation in the center of the quadrat. The unobstructed width at each transect was then determined to be the longest distance between quadrats with top-of-vegetation elevation more than 4.9 ft above the reference elevation. Per the DAP, these distances were determined for three different reference elevations: (1) the water-surface elevation at 2,400 cfs, (2) the water-surface elevation corresponding to the median discharge during the spring migration season, and (3) the water-surface elevation for the median discharge during the fall migration season. As discussed in the methods section (Section 2.5.2.6), because of the uncertainty introduced by the height-class data, the data collection procedure was modified in 2013 to directly measure the unobstructed channel width using a laser range finder.

Excluding the south channel at Jeffreys Island, the average unobstructed channel widths at the pure panel APs ranged from about 210 ft (AP7, 2013) to about 1,350 ft (AP33, 2009 and 2010) (**Figure 3.62a**). With the exception of AP33 that is relatively wide compared to the adjacent APs, visual inspection of the data indicates that unobstructed widths are generally greater in the downstream approximately half of the reach than in the upstream portion of the reach. Because of the variability in the data, however, this trend is not statistically significant. AP33 typically had among the greatest widths, ranging from about 745 ft in 2014 to about 1,350 ft in both 2009 and 2010. AP21 was also relatively wide compared to the other APs, with widths ranging from 730 ft (2016) to 1,300 ft (2011).

The reach-wide average unobstructed channel widths were relatively consistent, but increasing, during the first 3 years of the monitoring surveys, ranging from about 650 ft in 2009 to 730 ft in 2011 (**Figure 3.62b**). The 2012 data indicate a slight narrowing to 700-ft. Based on the direct measurements, the average unobstructed width increased from about 520-ft in 2013 to 620-ft in 2015, and then declined slightly to about 580-ft in 2016. Since climatic and hydrologic conditions during 2012 and 2013 were similar, the sharp decline in average width between these two years may result more from differences in measurement technique than actual, on-the-ground changes. The data indicate that Geomorphic Reach 6 (represented by AP21 at the Rose Sanctuary) typically had the largest unobstructed width during all seven surveys, and Reaches 1 and 2 (north and south channels at Jeffreys Island) and Reach 5 (Odessa to Minden) had the narrowed unobstructed widths (**Figure 3.62c**). Reach 3 (Overton to Elm Creek, including Cottonwood Ranch) also typically had among largest unobstructed widths).

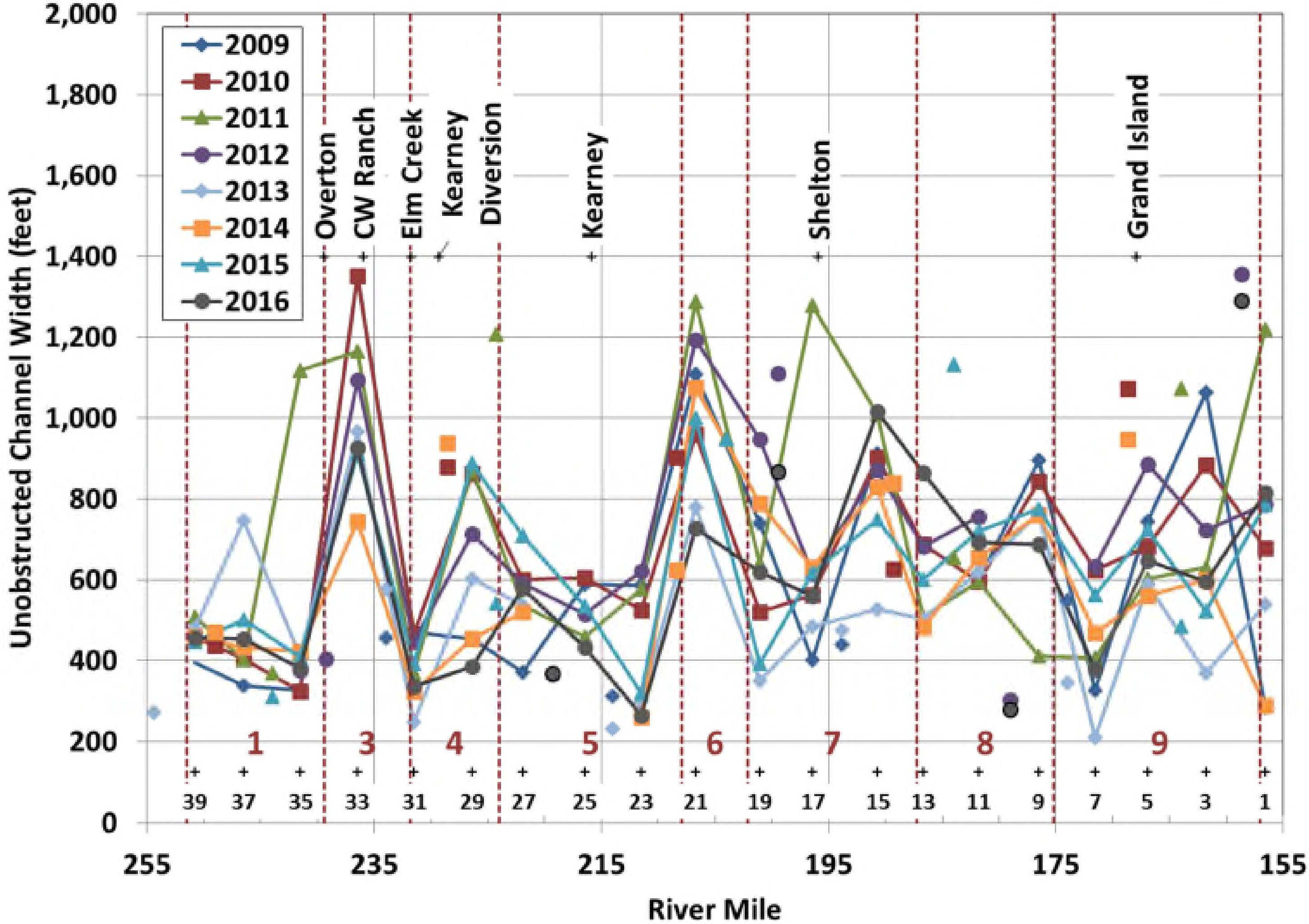

Figure 3.62a. Average unobstructed channel width at pure panel APs. Rotating APs are shown by individual symbols only; pure panel APs connected with lines.

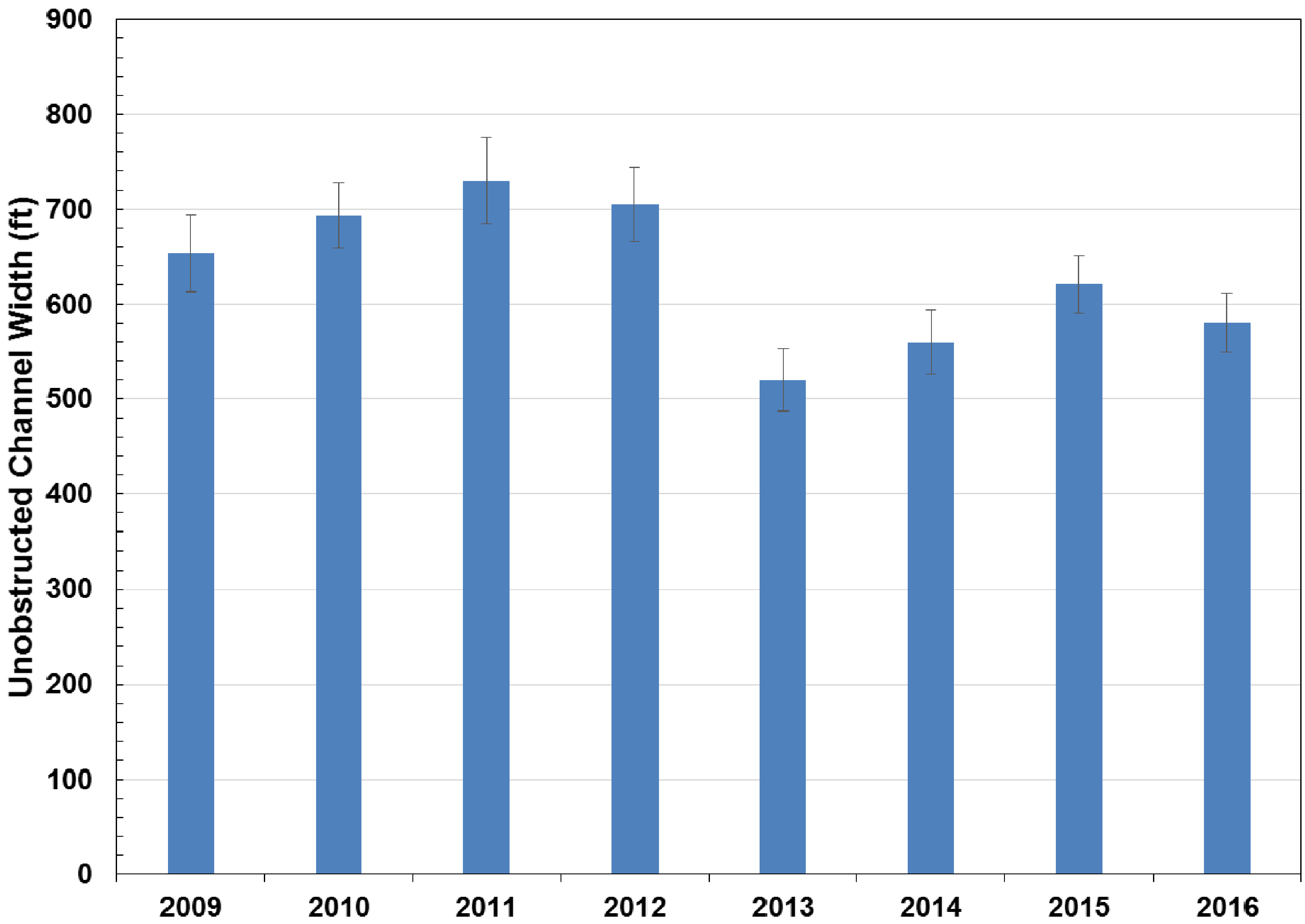

Figure 3.62b. Average unobstructed channel width for the overall study reach, based on the pure panel AP data. Whiskers represent ±1 standard error on mean value.

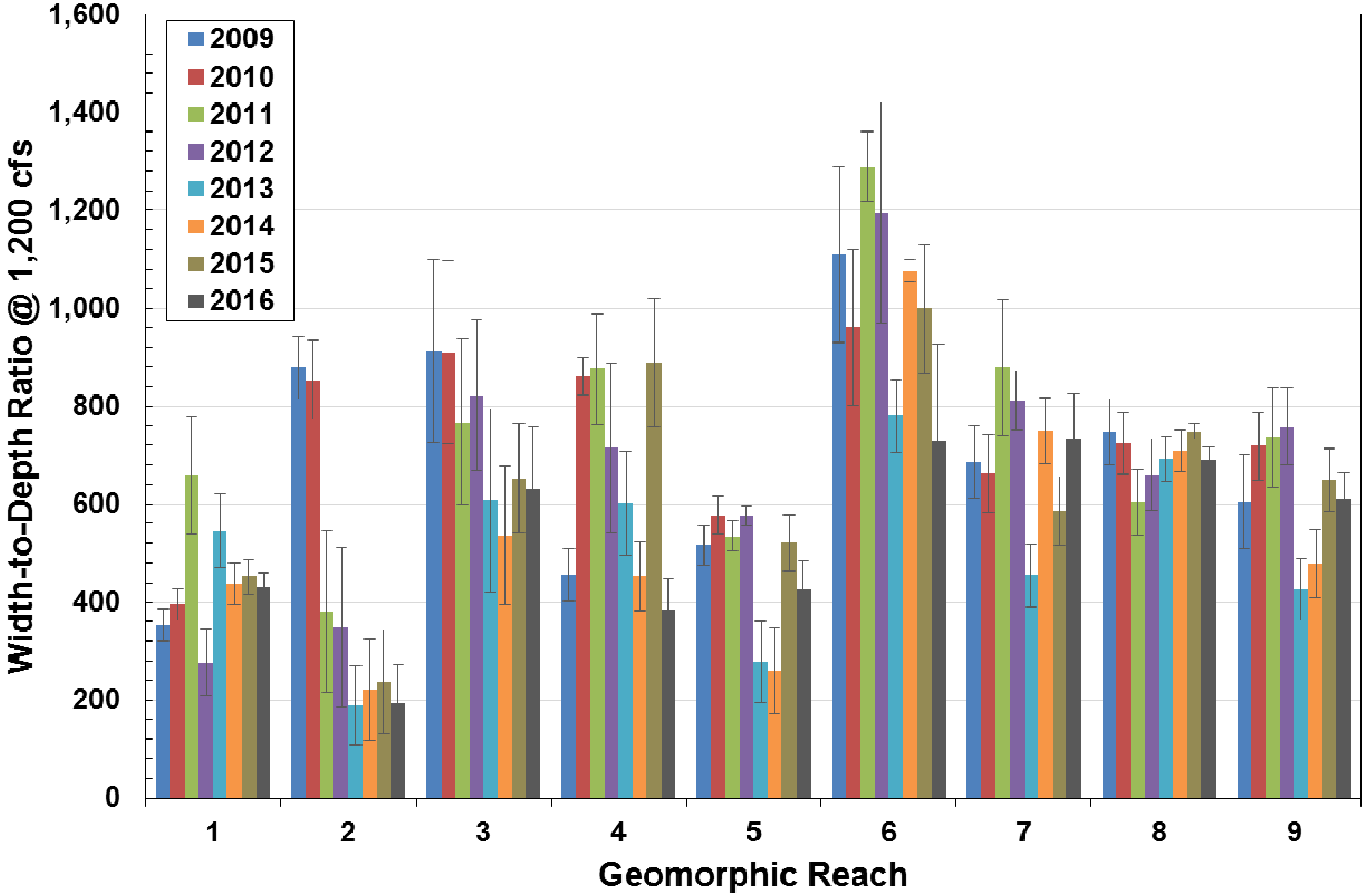

Figure 3.62c. Average unobstructed channel width by reach, based on the pure panel AP data. Whiskers represent ±1 standard error on mean value. Note that the 2009 and 2010 values for Reach 2 include both AP35B and AP37B, while 2011-2013 include only AP35B. Average values for AP35B in 2009 and 2010 were 540 and 420 ft, respectively.

3.6.2 Channel Width Less Than Eight Inches Deep or Sand (DAP 5.6.2)

The channel width inundated to a depth of 8 inches or less, including both vegetated and unvegetated, exposed sand bars[14], was evaluated for three different target discharges: (1) 2,400 cfs (2) the median discharge during the spring whooping crane migration season and (3) the median discharge during the fall whooping crane migration season. As discussed in Section 3.1, the spring discharge in the portion of the reach downstream from Overton ranged from a low of about 1,200 cfs (2009) to 3,600 cfs to 4,400 cfs (2011) (Figure 3.4). The fall discharge downstream from Overton varied from less than 500 cfs (2012) to 3,200 cfs to 3,700 cfs (2011) (Figure 3.5).

Based on the data at each AP, the widths less than 8 inches deep at 2,400 cfs were less than 200-ft at AP31, AP37A (north channel at Jeffreys Island) and AP39 during the entire 8-year monitoring period, and they ranged from 200- to 300-ft during all years at AP11 and AP25 (**Figure 3.63a**). Other pure panel APs with relatively small widths less than 8 inches deep include AP9, AP13, AP15, AP23 and AP33. Pure panel APs with relatively large widths less than 8 inches deep at 2,400 cfs (i.e., typically greater than 600 ft) include AP1, AP7, AP17, and AP27. AP1 had the largest width, generally in the range of 1,200 ft.

The reach-wide average width less than 8 inches deep at 2,400 cfs was relatively consistent throughout the monitoring period, averaging about 520-ft over the entire period and ranging from about 475-ft (2016) to about 560-ft (2014) (**Figure 3.63b**). Because of the relatively high variability in the basic data, none of these differences are statistically significant at the 90-percent confidence level based on the Kruskall-Wallace test. Geomorphic Reaches 1, 3 and 8 generally had the smallest width for this parameter (7-year average of 320-ft, 240-ft and 310-ft, respectively) (**Figure 3.63c**). Reach 6 (~690-ft), Reach 7 (~610-ft) and Reach 9 (~780-ft) typically had the widest average width for this parameter.

[14]The draft DAP indicates that this is the maximum **contiguous** width. Based on discussions with Jason Farnsworth, PRRIP, it was determined that this metric should be the total width with less than 8 inches of depth within the active channel in order to meet the intent of the metric. The widths from this analysis represent the total width of all areas within the active channel with less than 8 inches of depth, including vegetated and unvegetated sand bars.

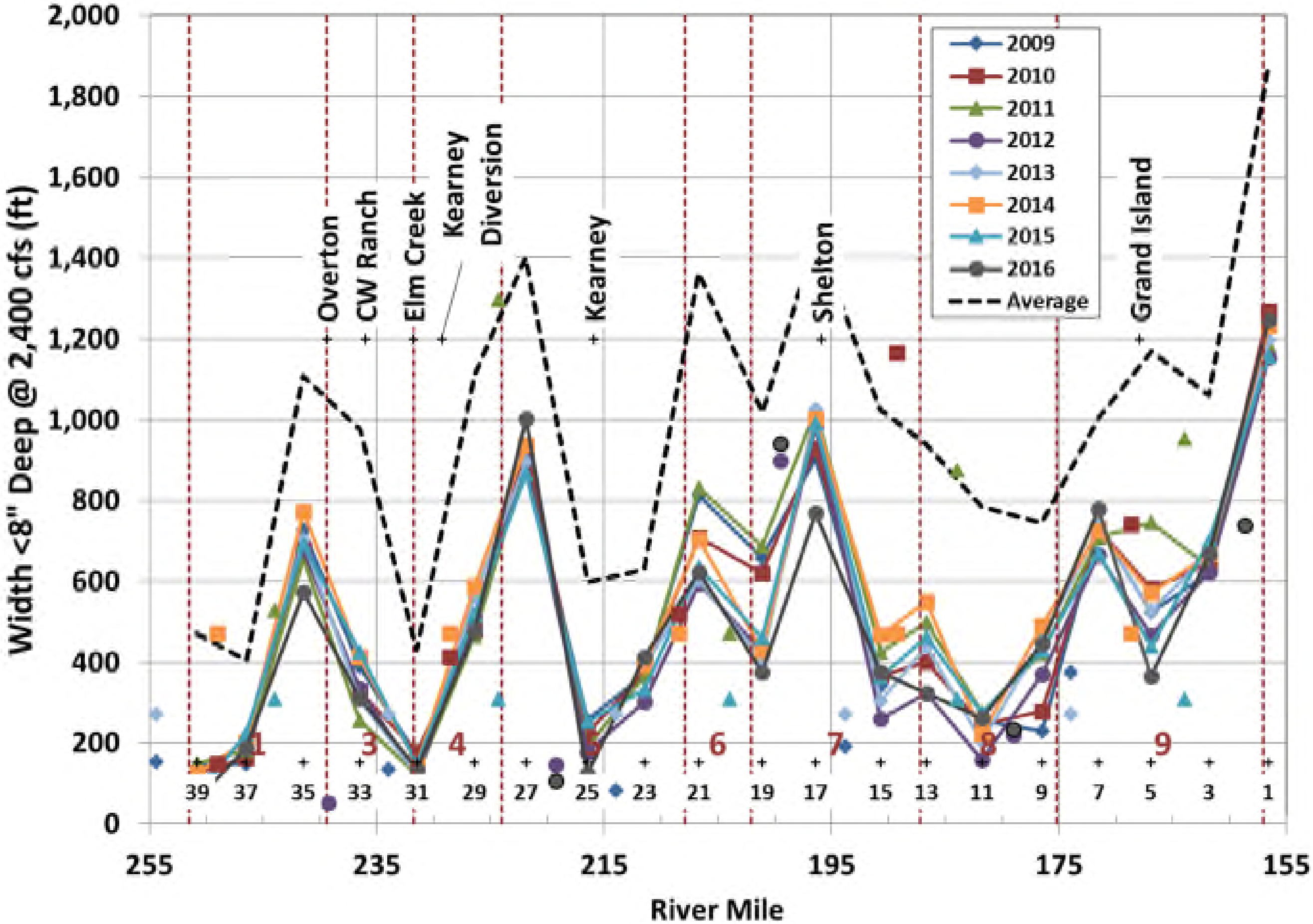

Figure 3.63a. Width of channel less than 8 inches deep (including exposed sandbars) at 2,400 cfs. Dashed black line is total channel width between bank stations.

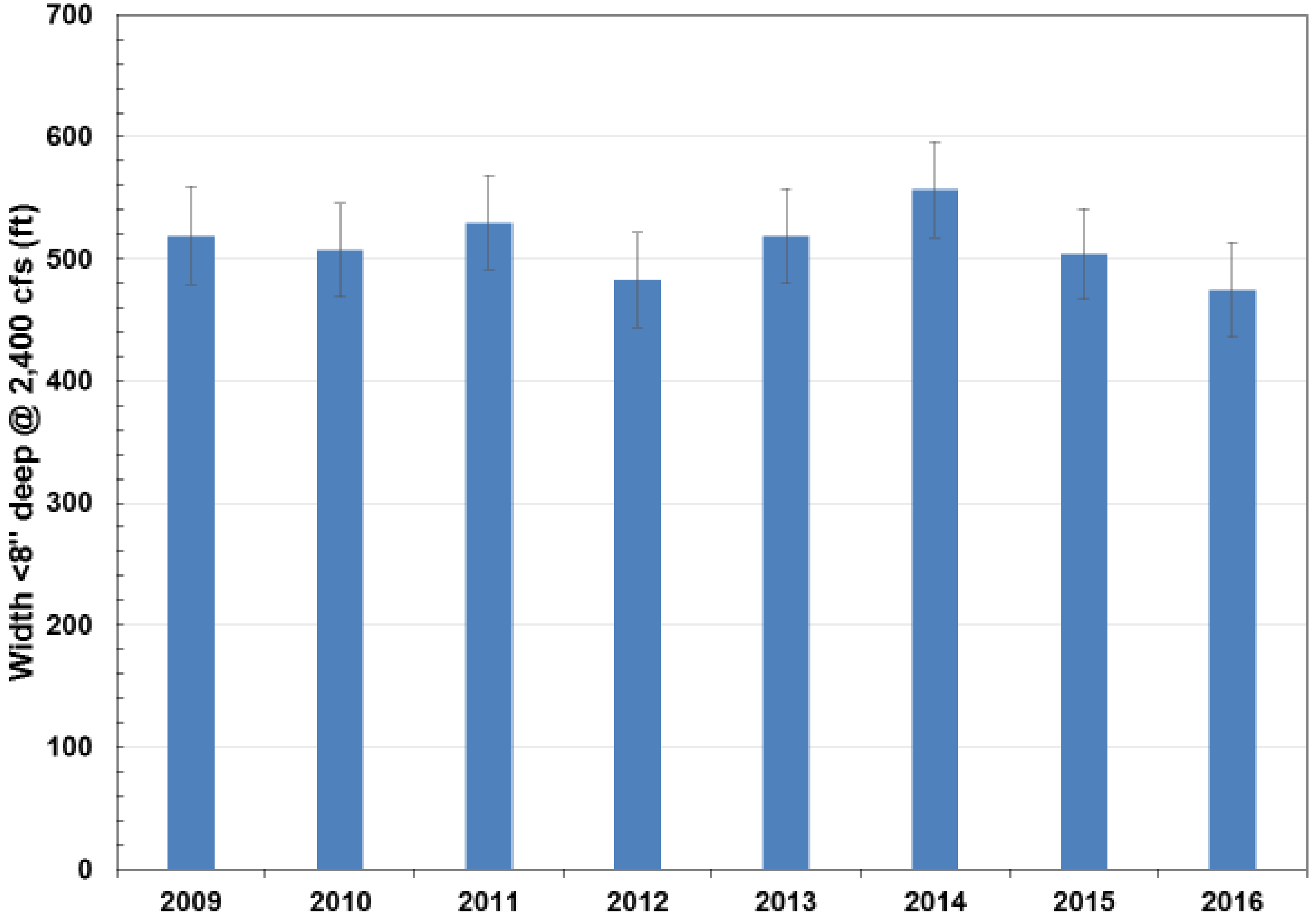

Figure 3.63b. Overall reach-averaged width less than 8 inches deep (including exposed sandbars) at 2,400 cfs. Whiskers represent ±1 standard error. *Note: AP37B excluded from the average because data are available only for 2009 through 2010.*

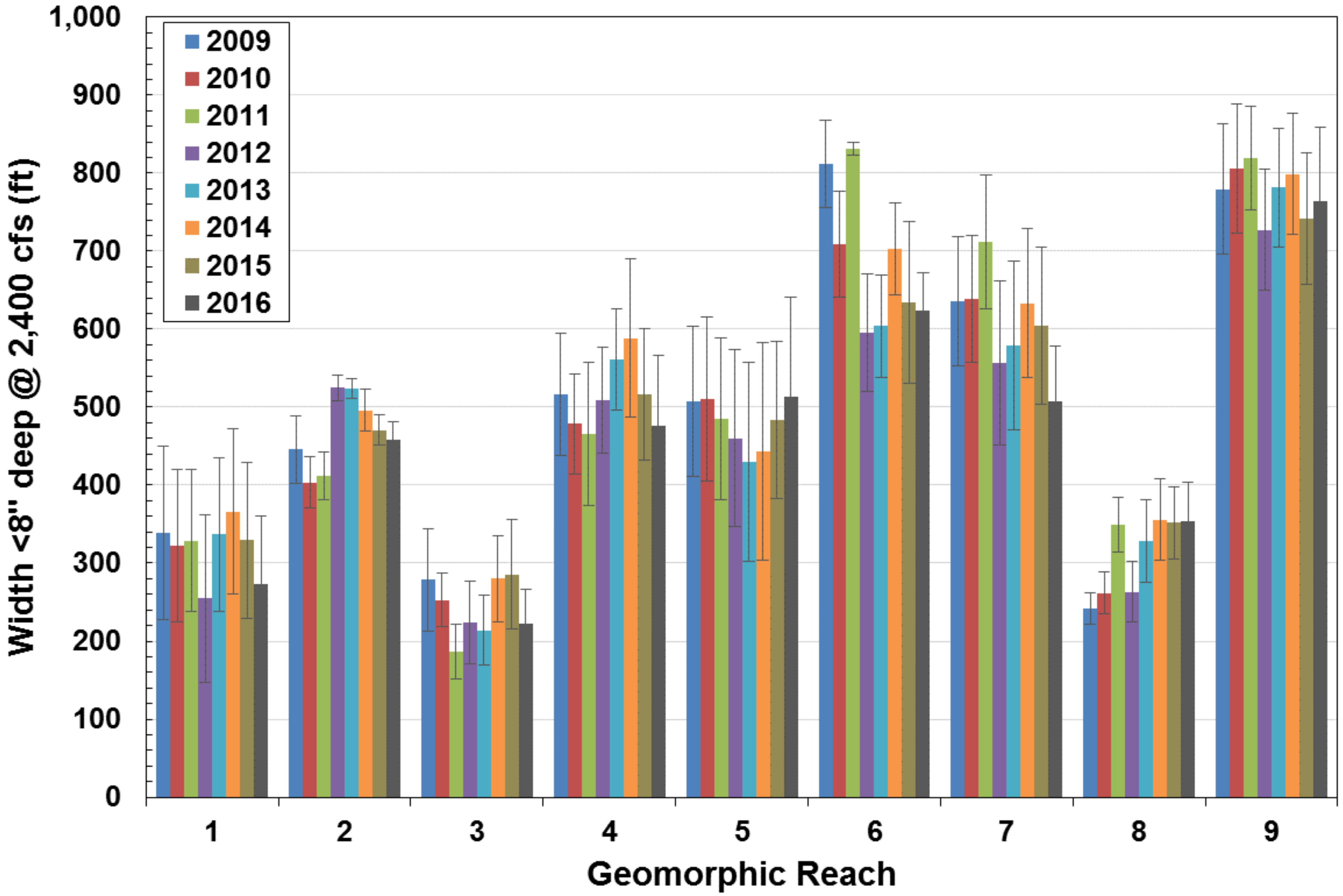

Figure 3.63c. Average width less than 8 inches deep (including exposed sandbars) at 2,400 cfs by geomorphic reach. Whiskers represent ±1 standard error. *Note: AP37B excluded.*

The spatial distribution of widths with depth less than 8 inches for the spring and fall whooping crane migration season discharges are similar to the patterns for 2,400 cfs; however, the year-to-year differences are greater because of the differences in the target discharge (**Figures 3.64a** and **3.65a**). The data also indicate that nearly the entire channel was inundated to a depth less than 8-inches during both fall migration period in 2012.

The reach-wide average for the spring whooping crane migration season discharge was about 710-ft in 2009, the maximum during the 8-year monitoring period (**Figure 3.64b**). High flows in 2011 caused the metric to decrease to about 420-ft. The fall discharge showed a similar pattern, decreasing from about 640-ft in 2009 to about 470-ft in 2011 (**Figure 3.65b**). The only year in which the metric was significantly different between the spring and fall periods was 2012 (940-ft versus 620-ft, respectively), most likely due to the tendency for reduced topographic complexity in the channel after the 2011 sustained high-flow period, as discussed above, and the very low flows during the fall of 2012. During the last two years of the monitoring period, the widths for this metric were in the range of 570-ft to 600-ft during both the spring and fall periods.

The spatial pattern of average width among the geomorphic reaches for the spring and fall discharges is essentially the same as the width at 2,400 cfs, and the year-to-year variability follows the same temporal pattern as the reach-wide averages (**Figures 3.64c** and **3.65c**).

As expected, the monitoring data indicate that both the actual width and the portion of the active channel with flow depth less than 8 inches tend to decrease with increasing discharge (**Figure 3.66**). The average widths at 2,400 cfs at the pure panel APs represent 15 to 75 percent of the bank-to-bank channel width, with an overall average of about 50 percent for all seven years. The average widths at the pure panel APs using the spring migration season discharge represent 15 percent to over 90 percent of the bank-to-bank width, with the reach-wide average ranging from 41 percent (2011) to 74 percent (2009). For the fall migration season discharge, the average widths at the APs represent about 20 percent (2011) to essentially 100 percent of the bank-to-bank channel width (2012), with the reach-wide average ranging from 47 percent (2011) to 94 percent (2012). The 2012 and 2014 values are very high because of the relatively low migration season discharge.

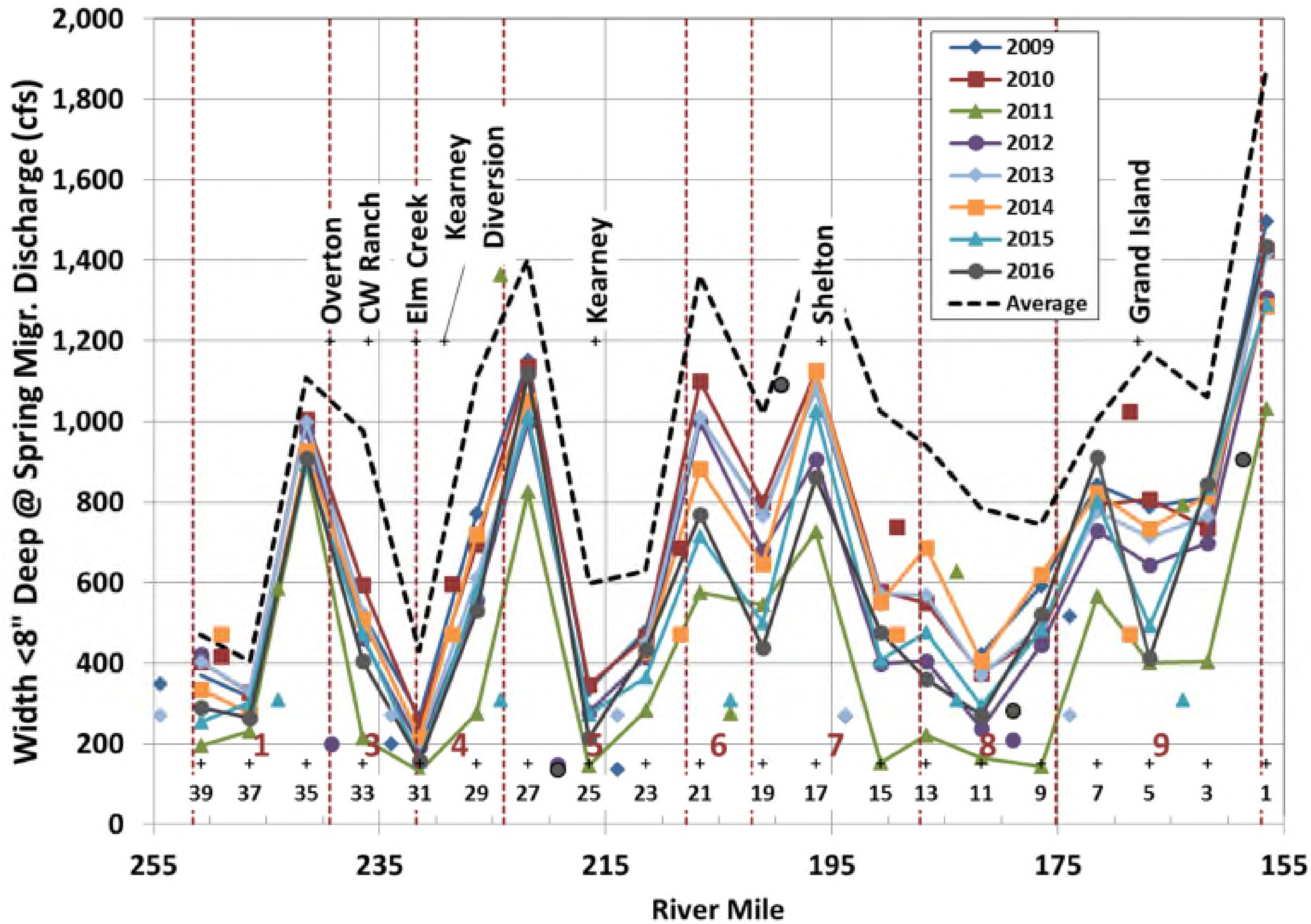

Figure 3.64a. Width of channel less than 8 inches deep (including exposed sandbars) at spring migration season discharge. Dashed black line is total channel width between bank stations.

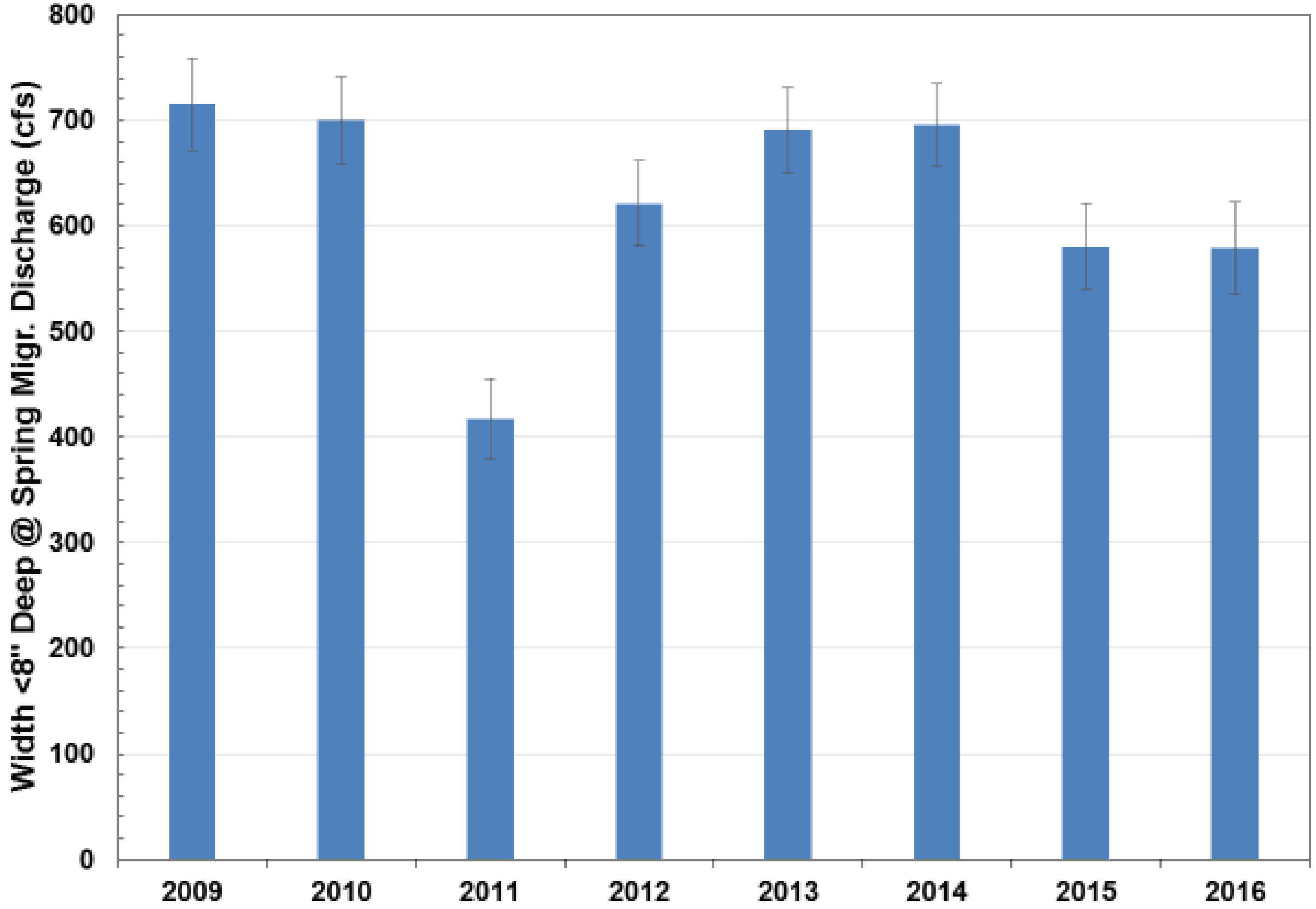

Figure 3.64b. Overall reach-averaged width less than 8 inches deep (including exposed sandbars) at the spring migration season discharge. Whiskers represent ±1 standard error. *Note: AP37B excluded.*

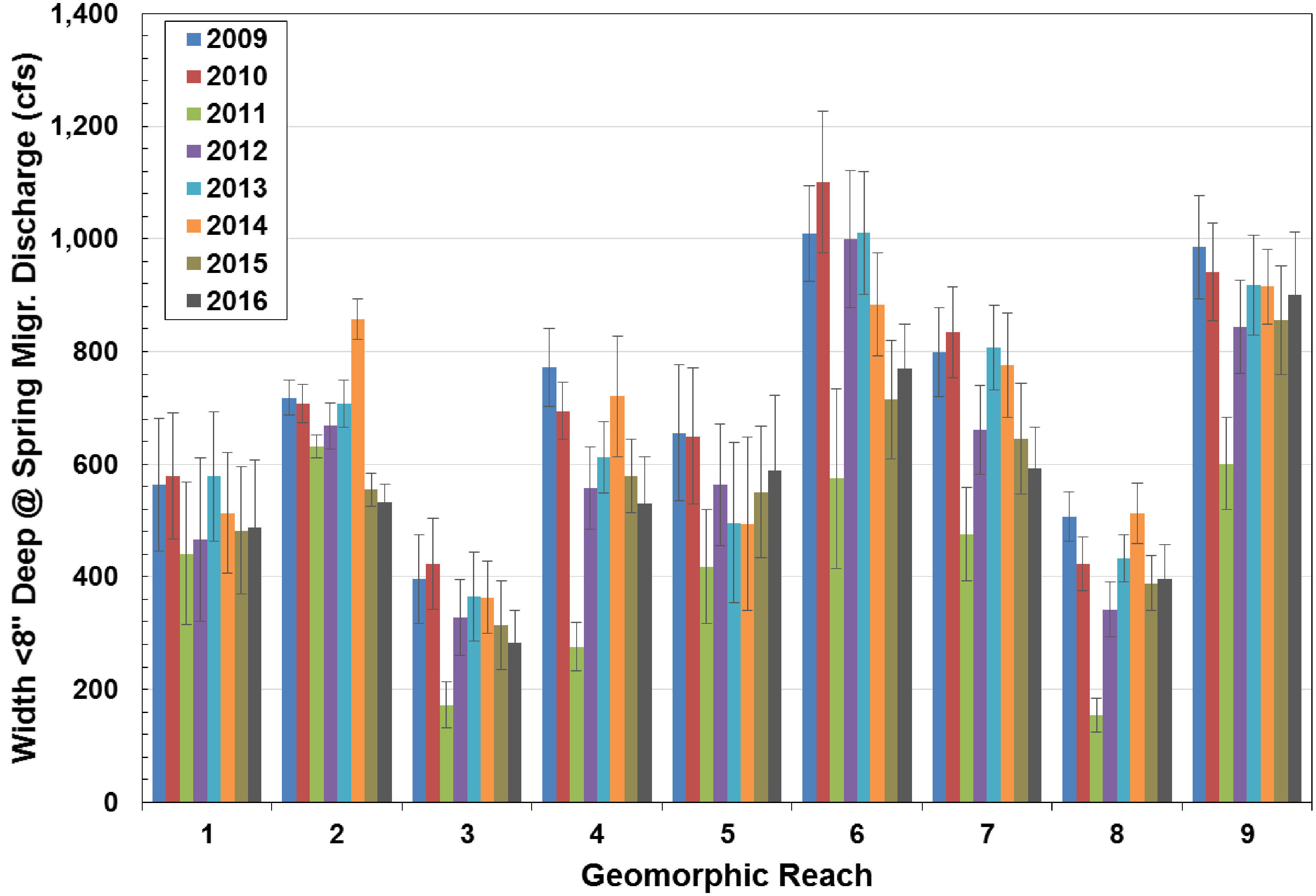

Figure 3.64c. Average width less than 8 inches deep (including exposed sandbars) at the spring migration season discharge by geomorphic reach. Whiskers represent ±1 standard error. *Note: AP37B excluded.*

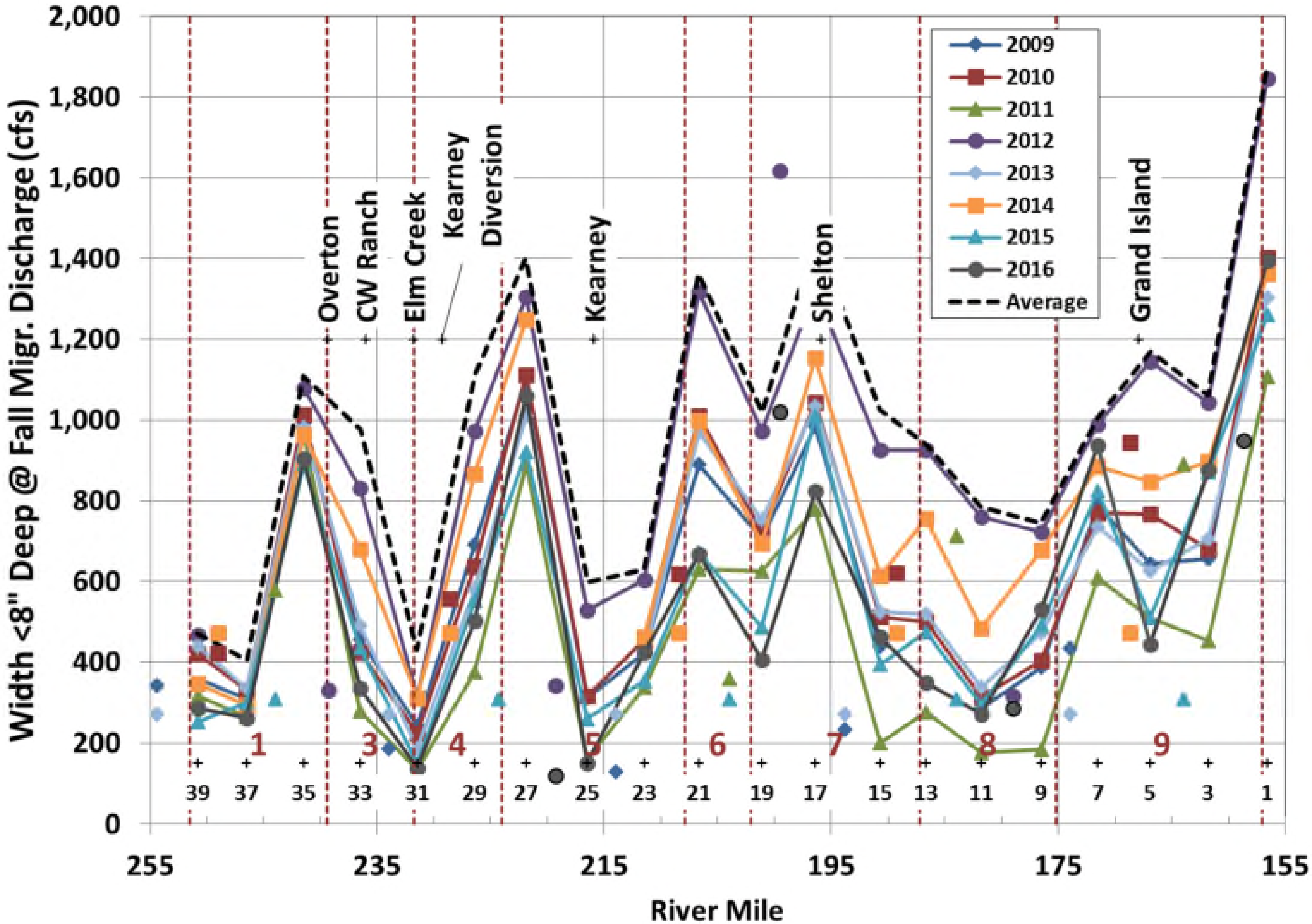

Figure 3.65a. Width of channel less than 8 inches deep (including exposed sandbars) during fall migration season discharge. Dashed black line is total channel width between bank stations.

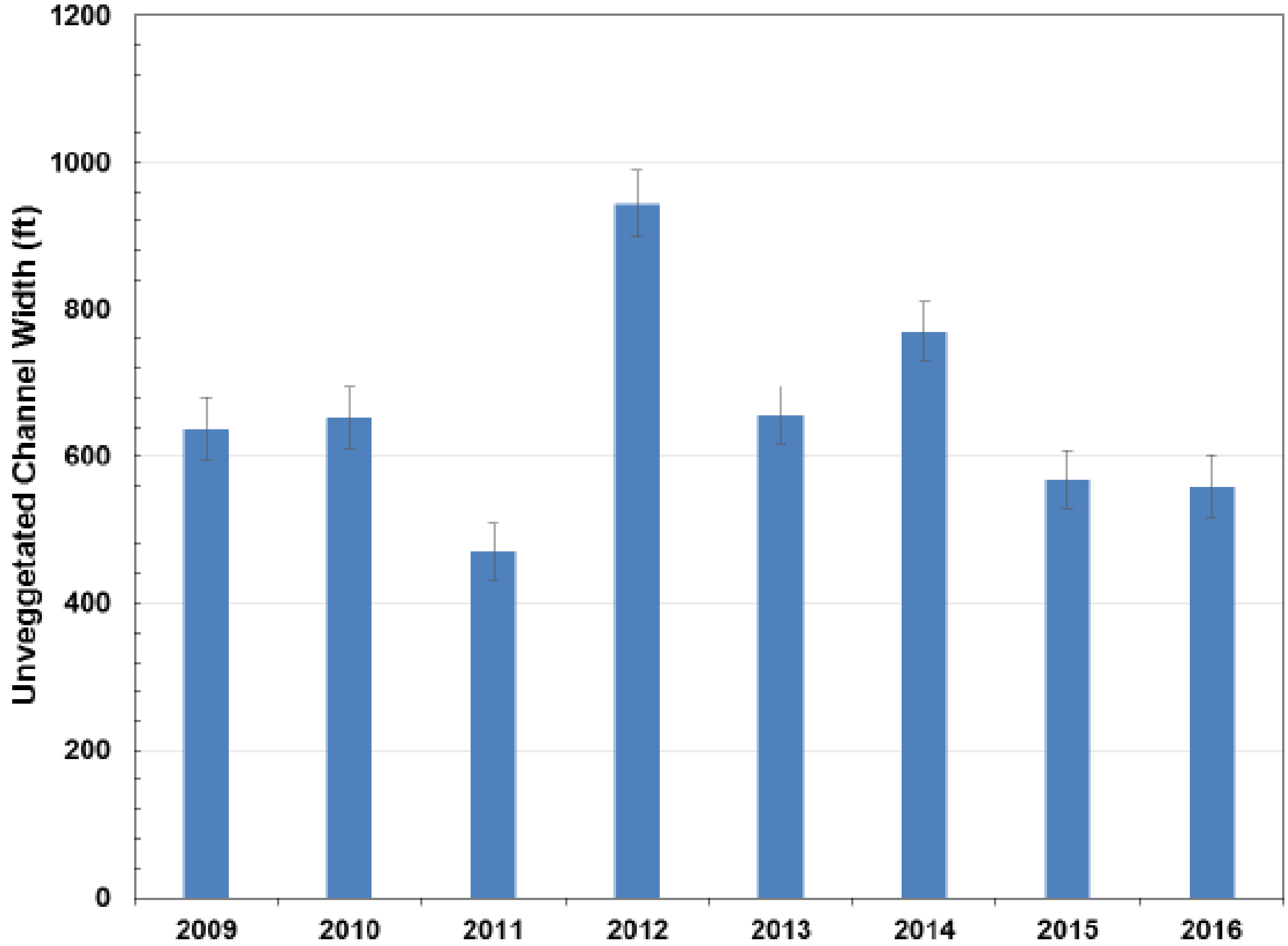

Figure 3.65b. Overall reach-averaged width less than 8 inches deep (including exposed sandbars) at the fall migration season. Whiskers represent ±1 standard error. *Note: AP37B excluded.*

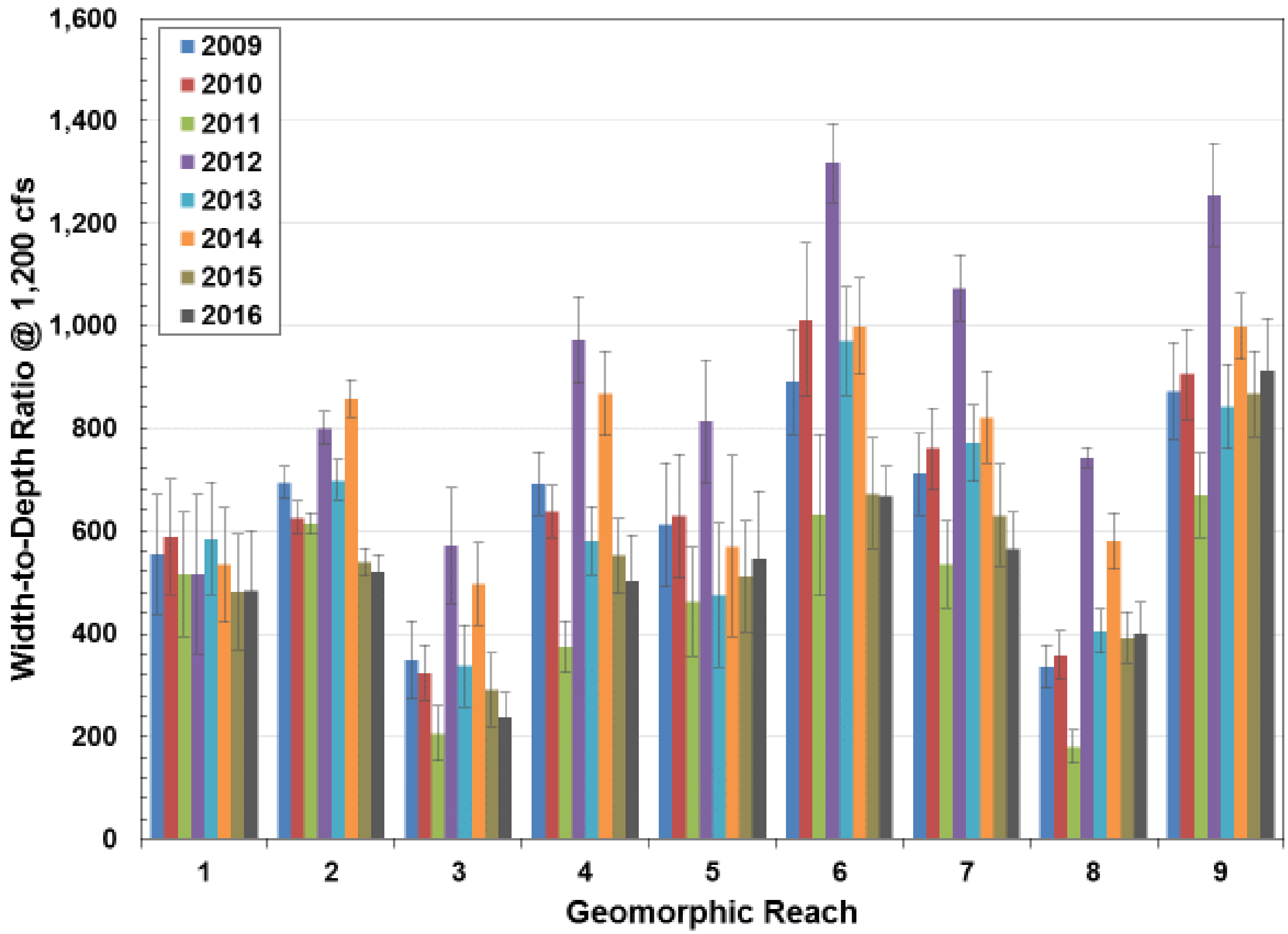

Figure 3.65c. Average width less than 8 inches deep (including exposed sandbars) at the fall migration season discharge by geomorphic reach. Whiskers represent ±1 standard error. *Note: AP37B excluded.*

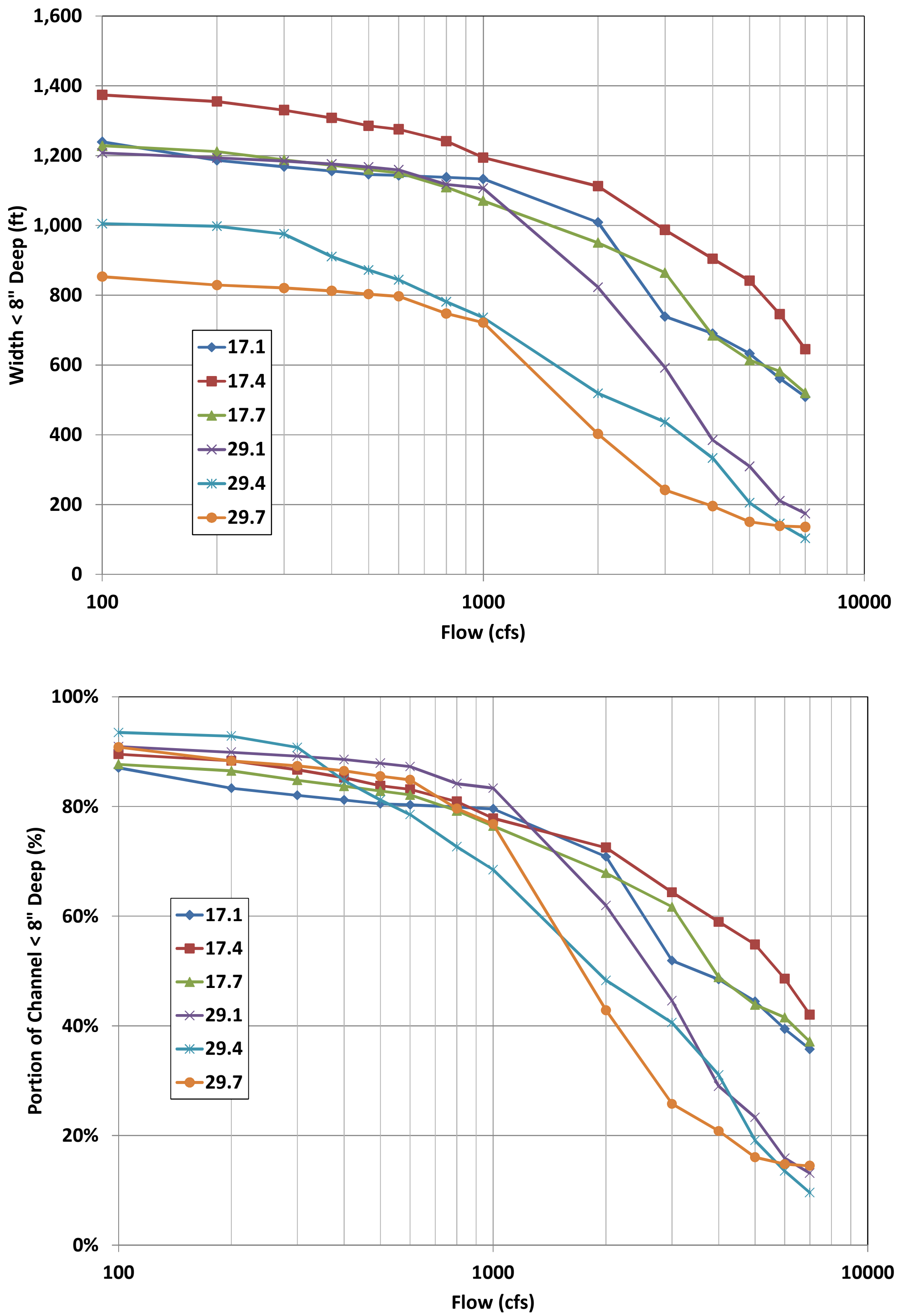

Figure 3.66. Typical relationship between discharge and (a) width of the channel and (b) percentage of total active channel width with depth less than 8 inches, based on the three primary monitoring cross sections at AP17 and AP29.

4 HYPOTHESIS TESTING AND TREND ANALYSIS

A large number of analyses could potentially be performed on the data presented in the previous chapters to identify trends in the geomorphic, vegetation and sediment variables (Table 2.5). To provide a focused analysis that is directed at key priorities, the Program directed that the analysis for this report be restricted to specific aspects of the following four hypotheses:

1. Flow #1
2. Flow #3
3. Flow #5
4. Mechanical #2

4.1 Flow #1

> *Increasing the variation* between *river stage at peak (indexed by the $Q_{1.5}$ @ Overton) and average flows (1,200 cfs index flow), by increasing the stage of the $Q_{1.5}$ through Program flows, will increase the height of sandbars between Overton and Chapman by 30 to 50 percent from existing conditions, assuming balanced sediment budget.*

Evaluation of the validity of this hypothesis hinges on an understanding of the relative sediment balance along the reach. Two primary sources of data are available to assess the sediment balance: (1) year-to-year changes in bed sediment volume, based on repeat surveys of the three geomorphic transects at the pure panel APs (Section 3.3.7), and the resulting changes over the 5-year period encompassed by the surveys at the rotating panel APs, and (2) comparison of the annual sediment loads passing each of the five measurement sites, obtained by integrating the sediment load rating curves over the applicable flow records (Sections 3.5.1 and 3.5.2).

4.1.1 Sediment Balance Based on Transect Surveys

As discussed in Section 3.3.7, extrapolation of the volume changes from the transect surveys at the pure panel APs over the intervening, unsurveyed reaches indicates that the overall reach between Lexington and Chapman degraded by about 2.0M tons during Survey Year (SY)[15] 2010, about 1.2M tons during SY2011, and then aggraded by about 5.6M tons during SY2012 and an additional 1.9M tons during SY2013 (Figure 3.12b). During SY2014, the reach degraded by about 0.6M tons, followed by an additional 4.5M tons of degradation occurred during SY2015. The data also showed a very small amount of net aggradation in SY2016 of about 100,000 tons. This resulted in net bed sediment loss of about 720,000 tons from the overall monitoring reach over the 8-year monitoring period.

Geomorphic Reach 1 (Lexington to Overton Bridge, including the north channel at Jeffreys Island) degraded by about 740,000 tons over the 8-year monitoring period, or an average of about 106,000 tons per year, with annual changes ranging from 1.31M tons of degradation (SY2015) to 528,000 tons of aggradation (SY2013) (Figure 3.12c). Based on the repeat surveys at AP35B, Reach 2 (south channel at Jeffreys Island, where essentially all of the flow is derived from the J-2 Return) degraded by about 97,000 tons over the period, or an average of about 14,000 tons per year. Two pure panel APs (AP35B and AP37B) are located in Reach 2. Because permission to access AP37B was revoked by the landowner prior to the 2011 surveys, the aggradation/ degradation quantities are based only on the repeat surveys at AP35B to insure consistency in the estimates across all years. (The 2009

---

[15]The transect surveys and other detailed field data during all years were generally collected between mid-July and late-August. To simplify the discussion and to facilitate comparison of the aggradation/degradation trends based on the surveys with those based on the sediment load rating curves, Survey Years are defined as the period between August 1 of the previous year and July 31 of the current year [e.g., Survey Year (SY) 2010 refers to the period from August 1, 2009 through July 31, 2010).

and 2010 data indicate that AP37B degraded by about 16,000 tons during the first year of the monitoring program, while AP35B degraded by only about 10,000 tons; thus, the estimates based on only AP35B may be on the low side for this reach). AP35B is located about 2 miles upstream from the Overton Bridge and about 1 mile upstream from the outfall at the Dyer Property where 82,000 tons of sand was pumped and mechanically graded into the river between September 2012 and June 2013 as part of the Program's Pilot Sediment Augmentation Project (The Flatwater Group et al., 2014). A monitoring cross section on the return channel about 1,200 ft upstream from the Dyer outfall (XS-1, **Figure 4.1**) showed little net change between the pre- and post-augmentation surveys in August 2012 and August 2013; thus, the augmentation does not appear to have affected aggradation/degradation patterns in the majority of Reach 2 upstream from the outfall. Surveys at the other Pilot Study monitoring sections indicate that about 26,000 tons of sediment accumulated between the outfall and XS-5 between August 2012 and August 2013. Since the pumped sediment was mechanically graded into the river, it is assumed that the remaining 56,000 tons of augmented sediment were transported downstream past the pilot-augmentation monitoring area.

Based on the surveys at AP31, Reach 3 (Overton Bridge to Elm Creek Bridge) degraded by about 344,000 tons over the 8-year monitoring period, or an average of about 49,000 tons per year[16]. Annual changes in this reach ranged from 364,000 tons of degradation (SY2010) to 171,000 tons of aggradation (SY2012). Other mechanical grading activities added about 200,000 tons of sediment into the main river channel during the monitoring period [50,000 tons each in SY2010 and SY2011, and 100,000 tons during SY2013 (Jason Farnsworth, personal communication, 2014; The Flatwater Group et al., 2014)]. About 130,000 tons of sediment were also graded into the channel during the 5-year period prior to the start of this monitoring program.

[16] AP33 was excluded from the SY2010 calculation because a large mid-channel bar was mechanically graded into the channel in Fall 2009; thus, the changes at that location do not reflect trends in the overall sediment-transport balance in the reach.

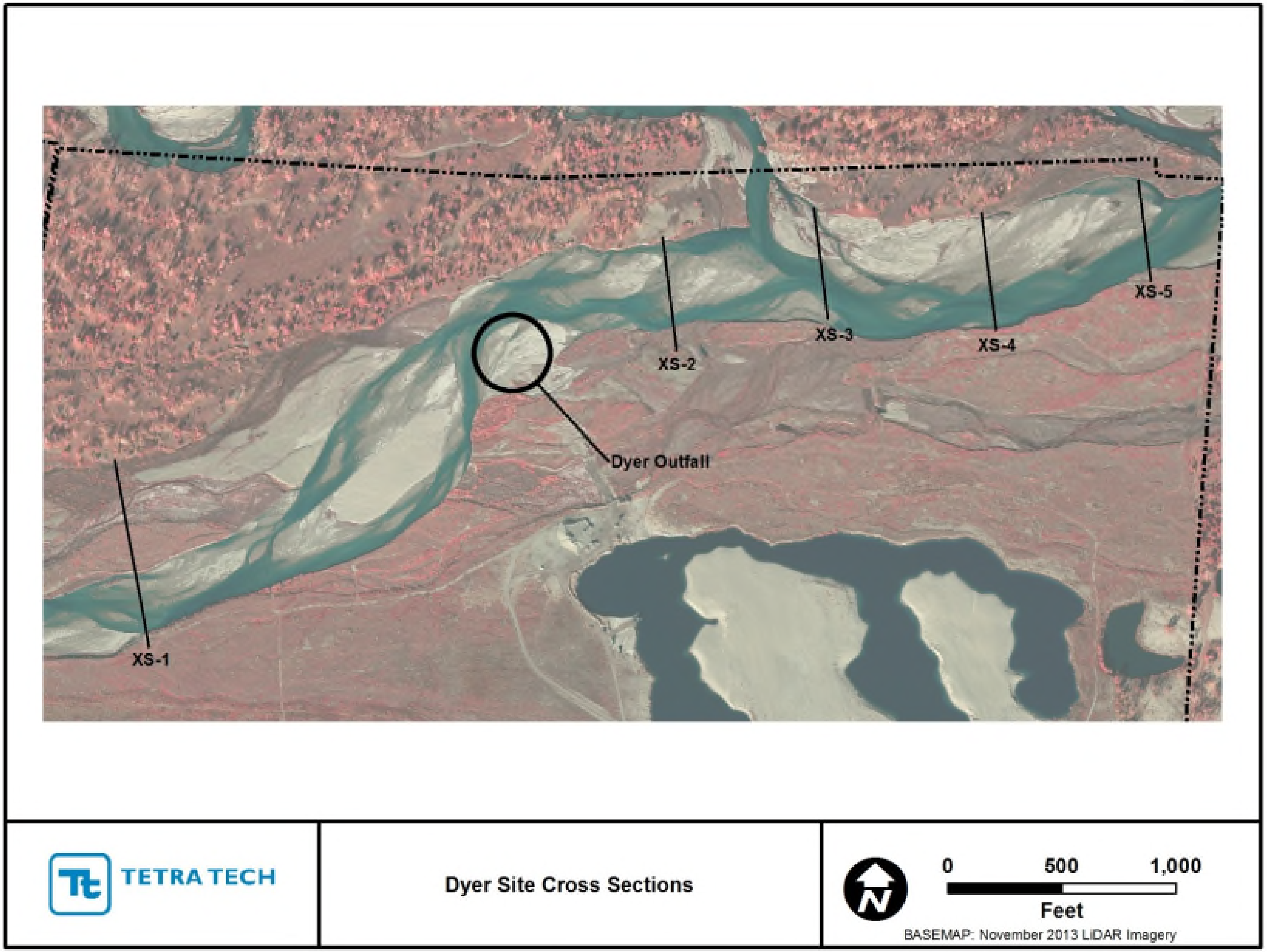

Figure 4.1. Vicinity map of the pilot sediment augmentation area showing the location of the Dyer Outfall and the five monitoring cross sections.

Long-term measurements by the USGS at the Overton gage that is located at the boundary between Reaches 1, 2 and 3 indicate that the channel steadily degraded by a total of about 3.5 ft between 1987 and 2010, and has been aggrading since early 2011 (**Figures 4.2a** and **4.2b**). Comparison of the data collected at rotating panel point AP34 (immediately downstream from the Overton Bridge) for this monitoring program in July 2012 with surveys conducted at the same transects for the Pilot Sediment Augmentation Study in December 2012 showed a modest degradational tendency. Similar measurements at the USGS Cottonwood Ranch Mid-Channel Gage, which is located about 3 miles upstream from the Elm Creek Bridge, indicate that this location degraded by about 1 ft between WY2001 and WY2007, aggraded by about 1.5 ft between WY2007 and early-WY2012, and has remained relatively stable since 2012 (**Figure 4.3**). These trends are qualitatively similar to the trends indicated by the anchor point surveys, in which Reach 3 degraded between SY2009 and SY2011, aggraded in SY2012 and SY2014, degradation in SY2013 and SY2015, and showed little net change in SY2016 (Figure 3.12c).

Based on the surveys at AP29, Reach 4 (Elm Creek to Odessa) degraded by about 390,000 tons during SY2010 surveys, and then aggraded in 2011, 2012 and 2013 (280,000, 470,000 and 29,000 tons, respectively). In 2014, this reach degraded by about 100,000 tons, and this was followed by nearly 900,000 tons of degradation in SY2015 and an addition 110,000 tons of degradation in SY2016. Over the 8-year monitoring period, Reach 4 experienced net degradation of about 470,000 tons, or about 67,000 tons per year. AP29 is located about midway between the Kearney Canal Diversion Structure (KDS) and the Odessa Bridge. Repeat surveys at 13 cross sections between the KDS and AP29 for the Elm Creek Adaptive Management Experiment indicate that this part of the reach aggraded by about 3,300 tons between April 2011 and August 2013, a rate considerably lower than is indicated by the monitoring data at AP29 (Tetra Tech, 2014). The Elm Creek data also indicate that the portion of the reach between the Elm Creek Bridge and the KDS degraded by about 57,000 tons during the 27-month period encompassed by the surveys, with about 22,000 tons of degradation between April 2011 and August 2011, about 9,000 tons of aggradation between August 2011 and August 2012, and the remaining 43,000 tons of degradation between August 2012 and August 2013. The downstream portion of the Elm Creek Reach degraded by about 17,000 tons between August 2011 and August 2012, and then aggraded back by about the same amount between August 2012 and August 2013. The modest amount of aggradation in the downstream portion of the reach occurred during summer, 2011. These results suggest that basing the aggradation/ degradation trends for Reach 4 solely on the surveys at AP29 may not accurately represent the amount of change that is actually occurring in the overall reach.

Reach 5 (Odessa to Minden), which includes pure panel AP23, AP25 and AP27, degraded by about 970,000 tons between the 2009 and 2010 surveys and an additional 590,000 tons during SY2011. The reach then aggraded by about 890,000 tons during SY2012, with very little change (~3,000 tons of aggradation) during SY2013. During the last 3 years of the monitoring program, the reach degraded by about 110,000 tons, 640,000 tons and 120,000 tons, respectively, resulting in net degradation of about 1.53M tons over the 8-year monitoring period, or about 220,000 tons per year. USGS gage measurement data indicate that the cross section at the Kearney gage, which is located in the middle of the reach, aggraded by 0.5 to 0.75 ft between 1982 and 1986, remained relatively stable until 2002, and degraded by about one ft between 2002 and 2005 (**Figure 4.4**). Based on the low-flow measurements, the mean bed elevation appears to have been relatively stable to slightly degradational since 2005, with a stronger degradational tendency in WY2015 and WY2016. There is, however, significant scatter in the data; thus, this conclusion should be considered with caution.

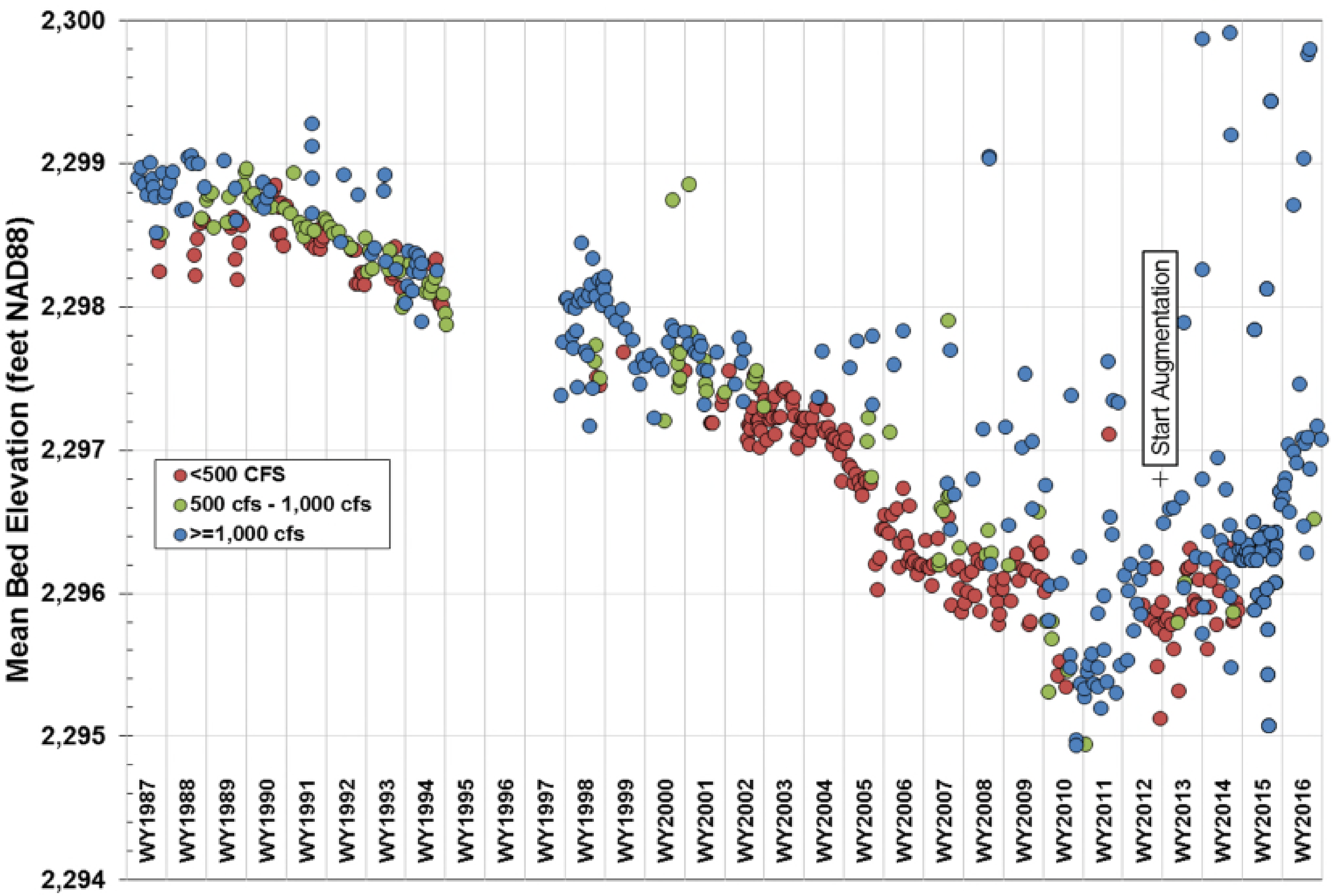

Figure 4.2a. Mean bed elevations at the Overton, based on USGS field measurement data collected during WY1987 through WY2016.

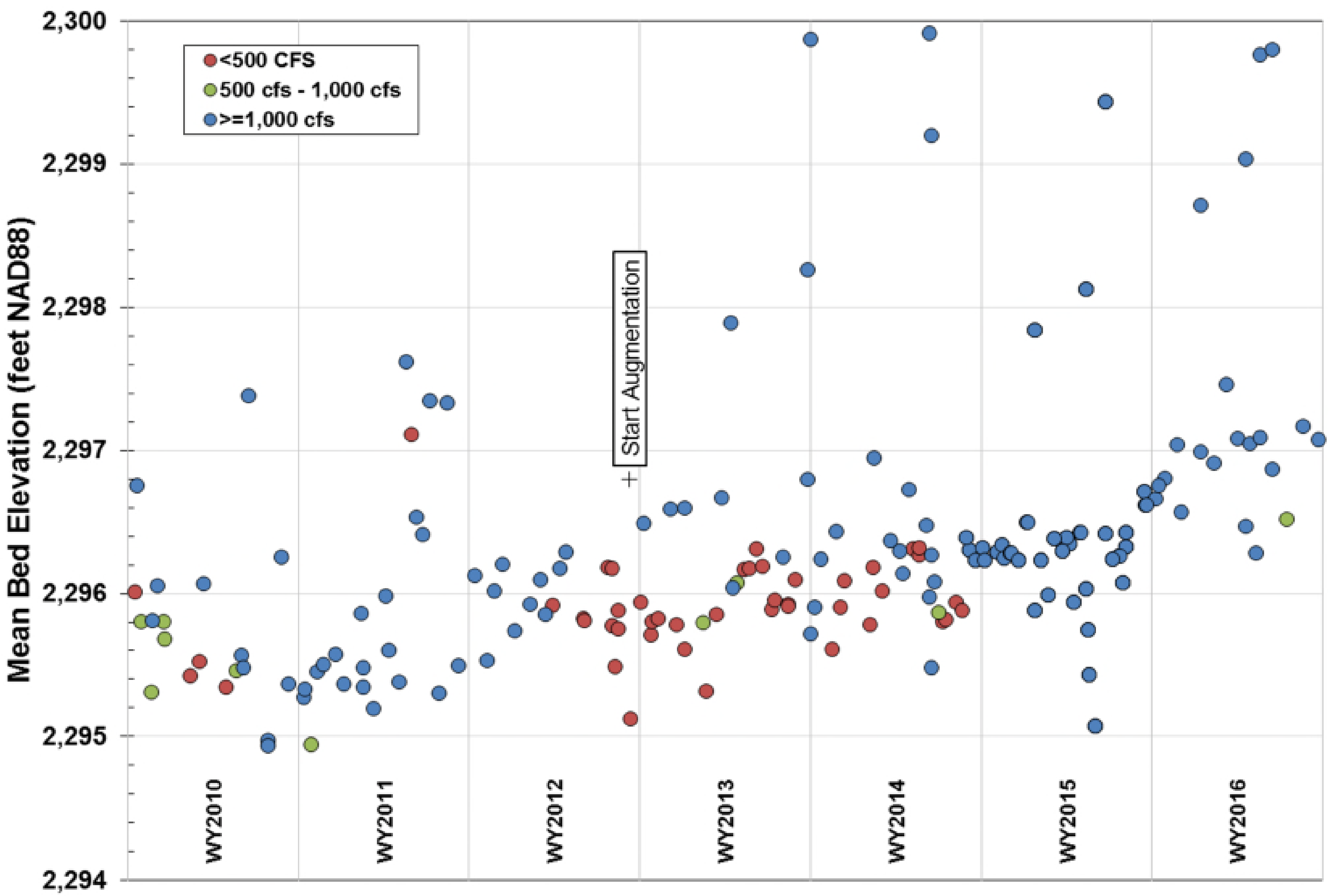

Figure 4.2b. Mean bed elevations at the Overton, based on USGS field measurement data collected during WY2010 through WY2016 (same data as Figure 4.2a).

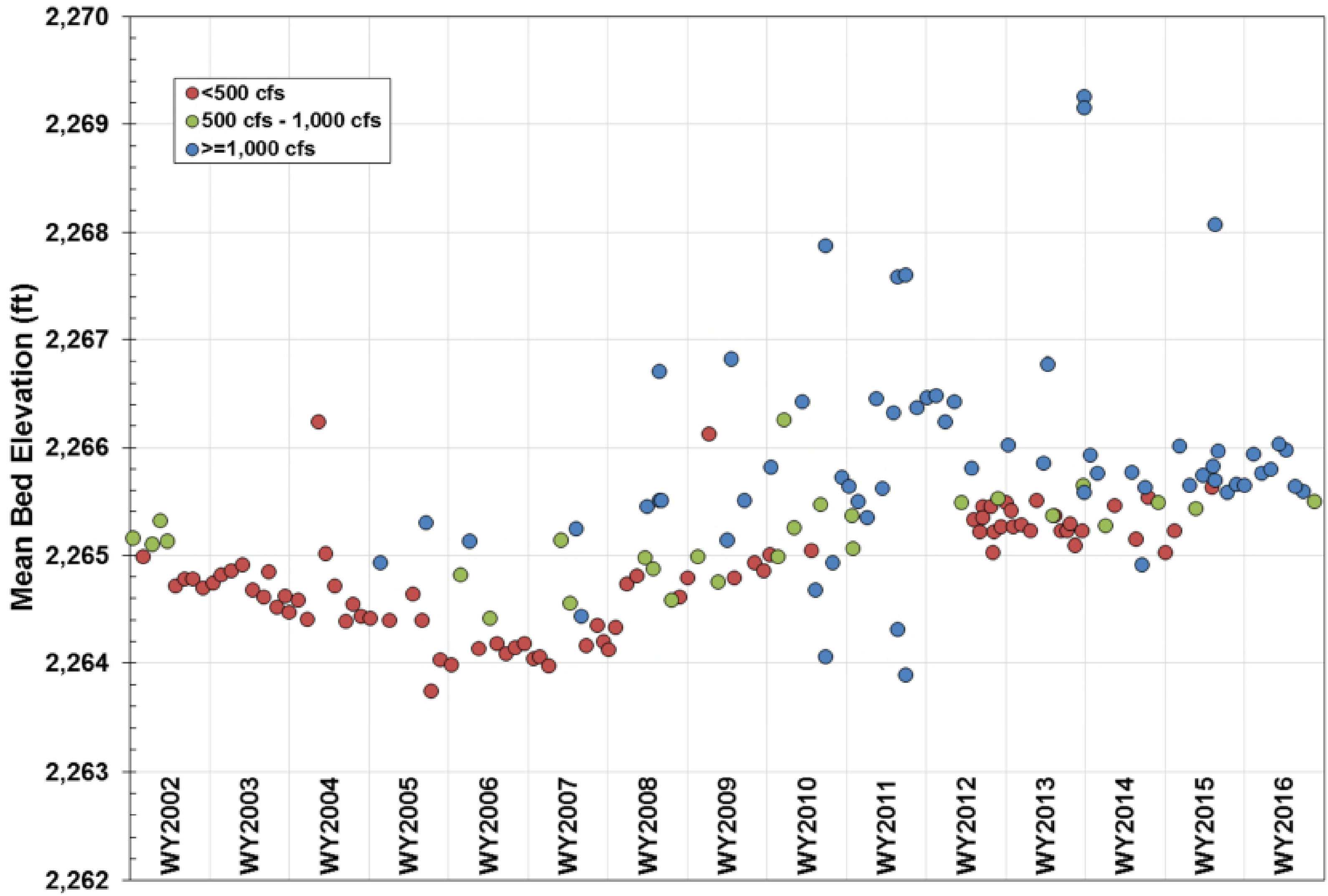

Figure 4.3. Mean bed elevations at the Cottonwood Ranch Mid-Channel gage, based on USGS field measurement data collected during WY2002 through WY2016.

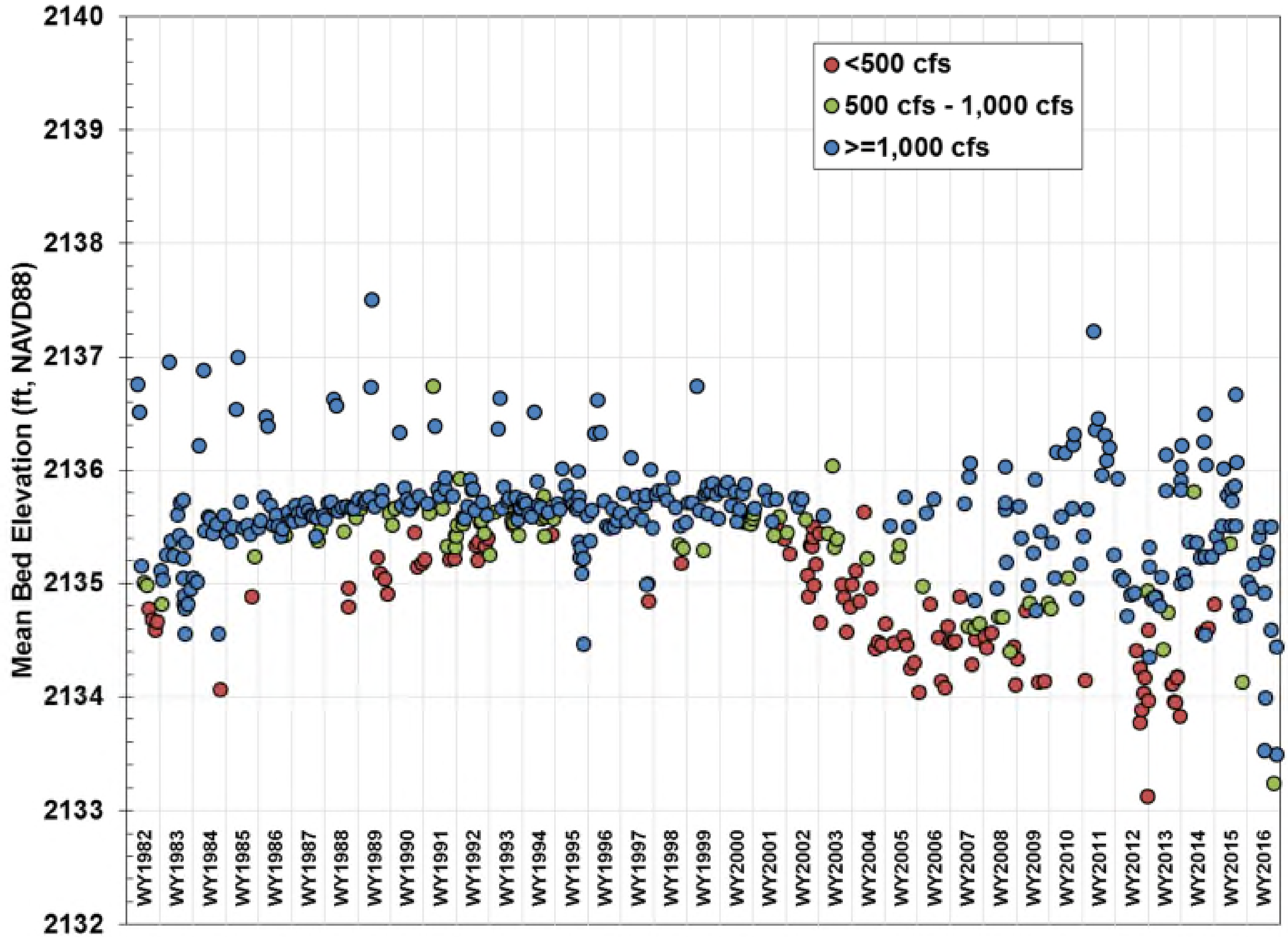

Figure 4.4. Mean bed elevations at the Kearney gage, based on USGS field measurement data collected during WY1982 through WY2016.

Based on the surveys at AP21, near the Rowe Sanctuary, Reach 6 aggraded by 350,000 tons over the 8-year monitoring period, or an average of about 50,000 tons/year. Similar to the other reaches, the year-to-year changes varied significantly from 710,000 tons of degradation (SY2010) to 1.2M tons of aggradation (SY2012).

All three of the downstream reaches experienced net aggradation over the 8-year monitoring period, by amounts ranging from 460,000 tons, or about 65,000 tons per year in Reach 7 to 1.08M tons, or about 155,000 tons per year in Reach 8. The combined net aggradation in Reaches 7, 8 and 9 over the 8-year period totaled about 2.1M tons, or about 300,000 tons per year, on average. USGS measurement data indicate that the cross section at the Grand Island gage, which is located at the boundary between Reaches 8 and 9, may have degraded by about 0.5 ft between the early-1980s and 2006, but has not shown a systematic aggradation/degradation trend since that time (**Figure 4.5**).

4.1.2 Sediment Balance Based on Sediment Load Rating Curves

The sediment balance during the 8-year monitoring period was estimated from the sand load rating curves discussed in Sections 3.5.1 and 3.5.2 by integrating the MVUE bias-corrected curves over the respective mean daily flow records and comparing the resulting loads between stations. The integrations were performed using flow data for the survey years that extend from August 1 of the previous year to July 31 of the current year to facilitate comparison of the sediment balance based on the rating curves with the aggradation/degradation estimates from the transect surveys.

Because the rating curves for the bed and suspended loads were developed separately using data points that do not necessarily represent the same time and discharge, the total load cannot be calculated by simply adding corresponding data points. In addition, the scatter in the data and resulting confidence bands on the two sets of curves are quite different; thus, quantification of the uncertainty associated with each part of the load, as discussed in the next section, requires separate treatment of the data sets. As a result, the bed- and suspended sand-load curves were integrated separately, and the resulting volumes were combined to estimate the total load of sand and coarser material. These volumes represent the “best-estimate” of the bed, suspended sand, and total sand/gravel load at each site (**Figures 4.6a through 4.6c**). The results indicate that the total sand load generally increased in the downstream direction during all survey years except during the very low flows of 2013[17], when the load at Overton with slightly larger than at the downstream gages.

Based on these results, the total sand load passing Overton exceeded the load passing Darr by a total of about 1.47M tons over the 8-year monitoring period, or about 210,000 tons per year (tpy), on average (**Figure 4.7**). Considering the 82,000 tons of sediment that was pumped and graded into the south channel at Jeffreys Island about one mile upstream from the Overton Bridge between September 2012 and June 2013 for the Pilot Sediment Augmentation Project and assuming that the sediment input from J-2 Return flows is negligible, this indicates that the segment of the study reach between the Darr Bridge and Overton (including the south channel at Jeffreys Island) degraded by about 1.39M tons over the 8-year period, or an average of about 174,000 tpy. About half of the total deficit occurred during SY2012 and SY2016 (~330,000 tons and 390,000 tons, respectively).

[17] A short-duration medium flow (SDMF) release with peak discharge of 4,090 cfs and discharge exceeding 3,800 cfs for about 54 hours at the Overton gage, was, however, made in early April 2013.

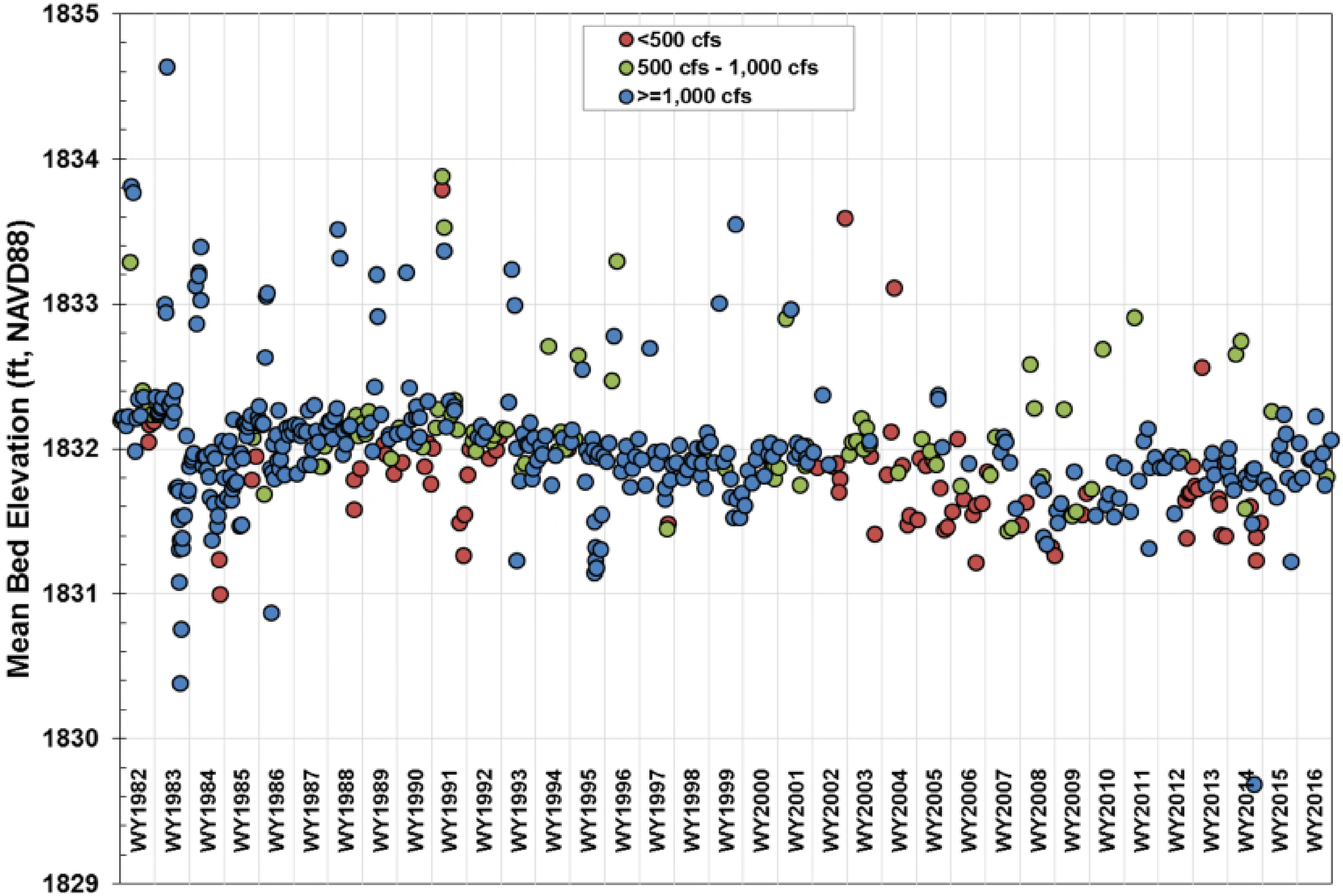

Figure 4.5. Mean bed elevations at the Grand Island gage, based on USGS field measurement data collected during WY1982 through WY2016.

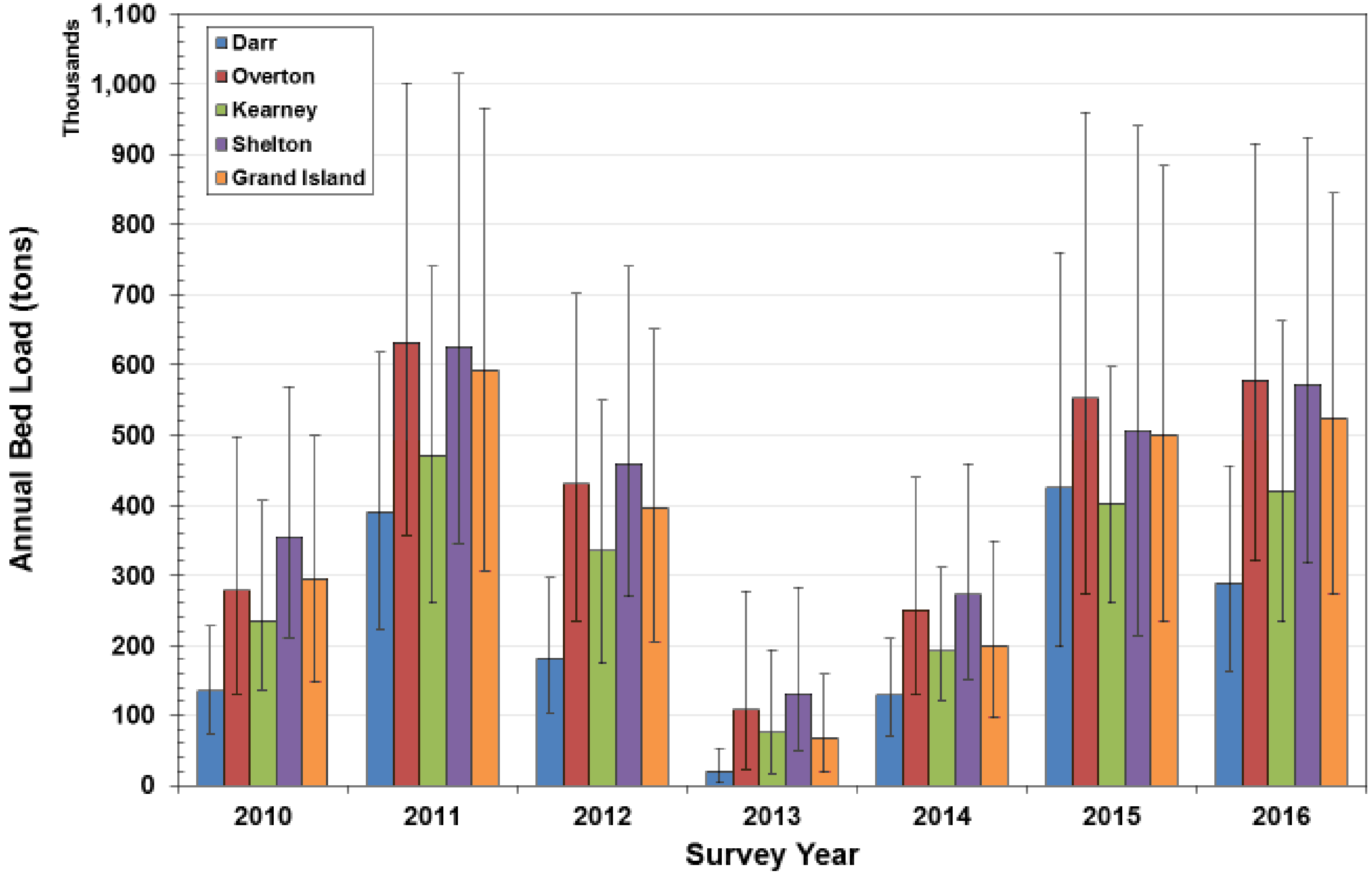

Figure 4.6a. Best-estimate of annual bed load passing the Darr, Overton, Kearney, Shelton and Grand Island measurement points during Survey Years (SY) 2010 through SY2016, based on integration of the bias-corrected bed-load rating curves over the survey year mean daily hydrograph. Whiskers are upper and lower 95-percent confidence limits from Monte Carlo simulation described in the next section.

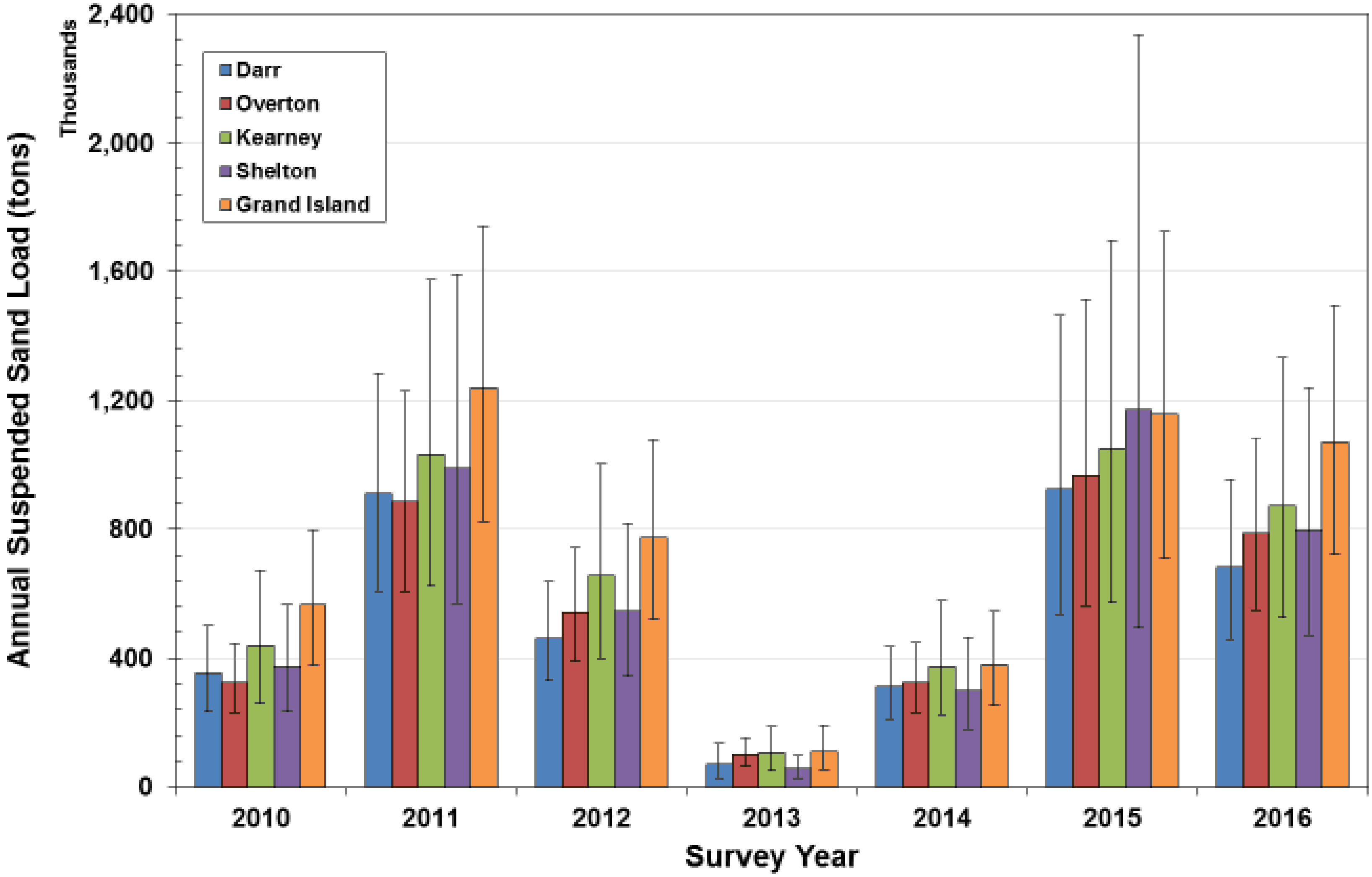

Figure 4.6b. Best-estimate of annual suspended sand load passing the Darr, Overton, Kearney, Shelton and Grand Island measurement points during Survey Years (SY) 2010 through SY2016, based on integration of the bias-corrected suspended sand rating curves over the survey year mean daily hydrograph. Whiskers are upper and lower 95-percent confidence limits from Monte Carlo simulation described in the next section.

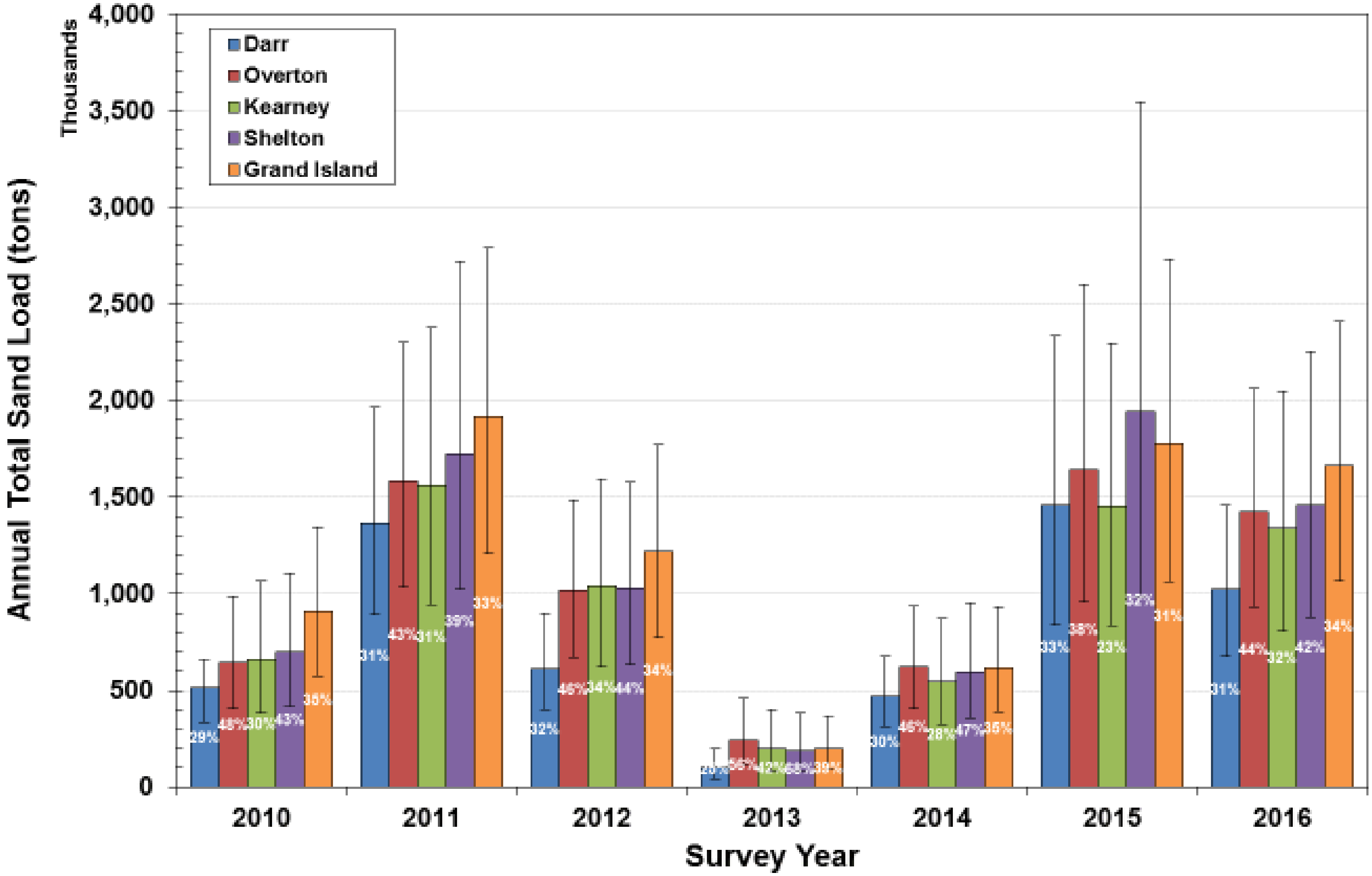

Figure 4.6c. Best-estimate of annual total sand/gravel load passing the Darr, Overton, Kearney, Shelton and Grand Island measurement points during SY2010 through SY2016, based on addition of the best estimates of bed-load and suspended sand load. Whiskers are upper and lower 95-percent confidence limits from Monte Carlo simulation described in the next section; bar labels are percent bed load.

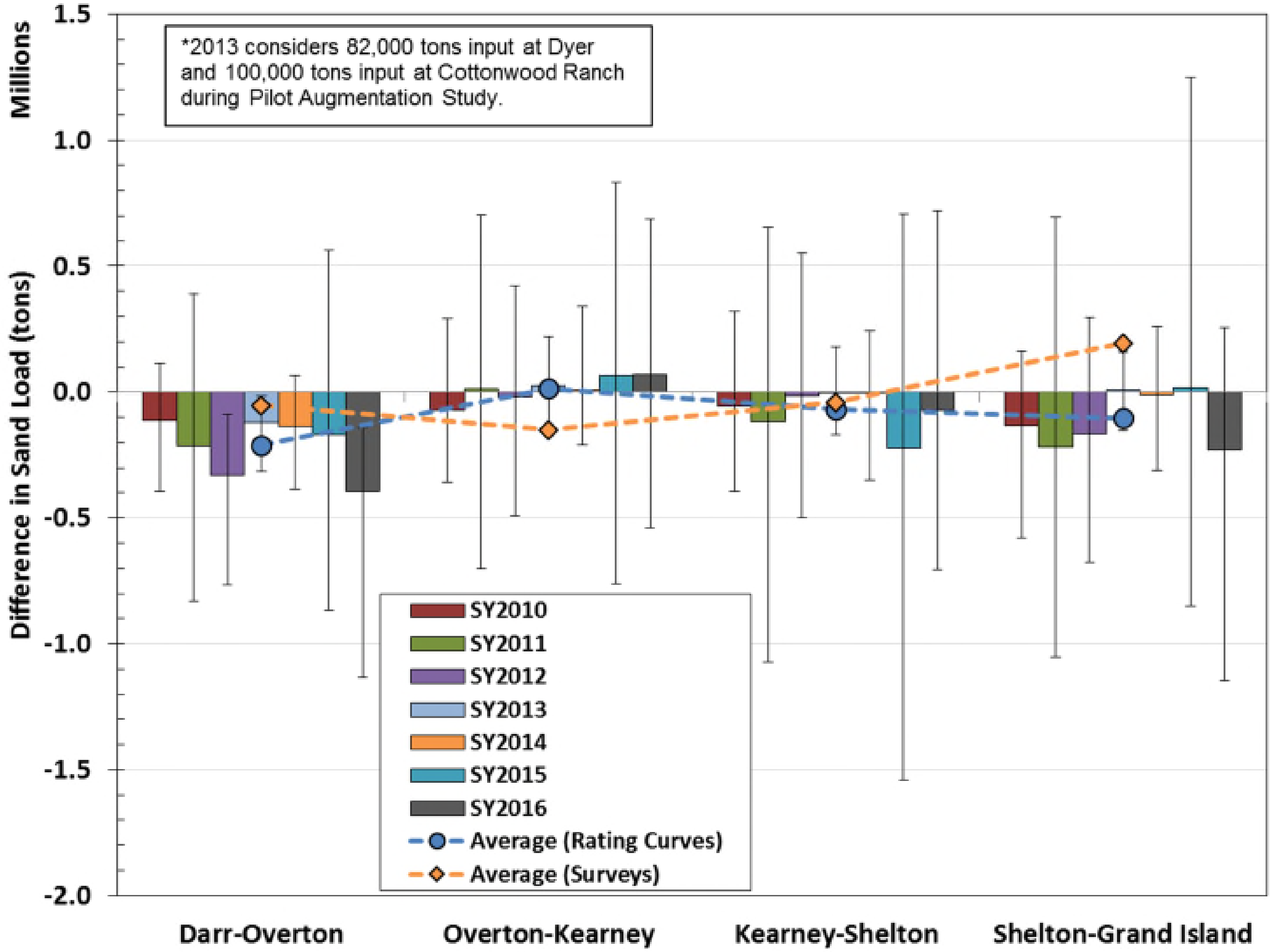

Figure 4.7. Best-estimate of the annual sand transport balance between the five measurement locations from SY2010 through SY2014. Also shown are the 5-year averages from the rating curves and from the survey-based estimates (Note figure is plotted at same scale as Figure 4.8, below, to facilitate direct comparison.)

The bias-corrected rating curves also indicate that the total sand load passing Overton exceeded the load at Kearney by about 96,000 tons over the 8-year period, or an average rate of about 14,000 tpy. As noted above, approximately 50,000 tons of sediment were graded into the river at Cottonwood Ranch, just downstream from AP31 during SY 2010 and SY2011, and 100,000 tons of sediment were graded into the channel at this location between September 2012 and April 2013 as part of the Pilot Sediment Augmentation project. Assuming none of the graded material would have been available for transport in the river in the absence of the grading, this additional input indicates that the reach between Overton and Kearney aggraded by about 250,000 tons over the 8-year period. The total sand load passing Shelton exceeded the load passing Kearney by about 480,000 tons, and the load passing Grand Island exceeded the load passing Shelton by about 725,000 tons over the 8-year period, or average degradation rates of about 69,000 tpy and 104,000 tpy, respectively.

Some of the apparent sediment deficit in the overall reach indicated by these results may be attributed to unquantified tributary input, although it is unlikely that tributary input is sufficient to substantively change the overall result. Reclamation (DOI, 2006) estimated that the total tributary input between Overton and Wood River (~8 river miles downstream from Shelton) was about 105,000 tpy over the 48-year period from 1947 through 1990, or 11 to 18 percent of the estimated loads in the river. It is not clear from the Reclamation (DOI, 2006) report whether these loads include silts and clays, as well as the sand load, but the context in which it was presented implies that it does not include the silts and clays. The incremental contributing drainage area between Overton and Grand Island is only about 1,320 mi^2, about 2.5 percent of the approximately 52,000 mi^2 total drainage area. Based on the relatively small incremental drainage area and the conditions at the mouths of the significant tributaries that include Plum Creek (south bank tributary to south channel at Jeffreys Island), Spring Creek (north bank tributary just downstream from Overton Bridge), Buffalo and Elm Creek (north bank tributary just upstream from the KDS), and North Dry Creek [south bank tributary just upstream from Kearney (Highway 44) Bridge], sand loading from the tributaries to the Platte River mainstem is likely much smaller than the Reclamation (DOI, 2006) estimate and negligible compared to the typical loads in the river. As a result, including the tributary sand/gravel inputs in the sediment balance would most likely have an insignificant impact on the overall results.

Both the bias-correct rating curves and the monitoring surveys indicated that the Darr to Overton reach was net degradational over the 8-year monitoring period, but the magnitude of changes is considerably larger from the rating curve analysis (~210,000 tpy versus 53,000 tpy, on average) (Figures 4.7 and **4.8**). The rating curves indicate a slight aggradation tendency (~13,000 tpy) in the Overton to Kearney reach over the 8-year monitoring period compared to about 150,000 tpy of degradation from the monitoring surveys. Both data sets indicate a degradational tendency of similar average magnitude over the 8-year period in the Kearney to Shelton reach (~69,00 tpy from the rating curves, ~41,000 tpy from the surveys). The discrepancy between the data sets is pronounced in the Shelton to Grand Island reach, with about 104,000 tpy of degradation from the rating curves and about 194,000 tpy of aggradation from the surveys.

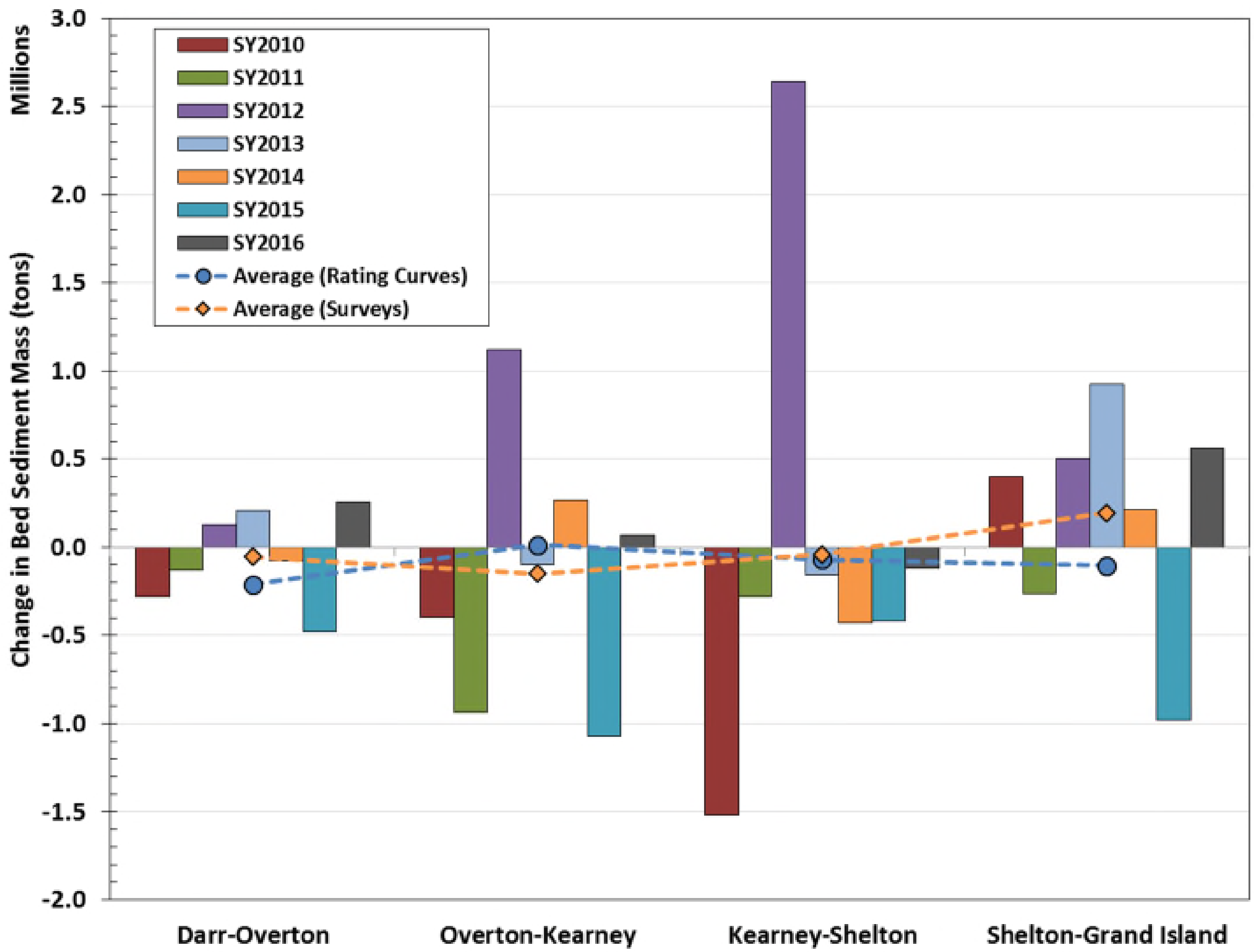

Figure 4.8. Estimated annual aggradation/degradation quantities from the pure panel AP survey data in the reaches encompassed by the five sediment-transport measurement sites. Also shown are the average annual aggradation/degradation quantities from both the surveys and the rating curves.

4.1.3 Uncertainty in Sediment Balance Estimate

There is considerable uncertainty in the sediment balance estimates for both of the above data sets. The survey-based estimates rely on data at only three transects that are spaced about 500 ft apart in each approximately 5-mile length of the river. Each transect represents the cross-section profile along only a single line across the river; thus, uncertainty is introduced into the result because the surveyed lines may not accurately reflect the changes that occur in the intervening approximately 500 ft of the river. In addition, the cumulative length encompassed by the three cross sections at each AP represents only about 4 percent of the total length that is being characterized by the AP, and there is uncertainty as to how well the aggradation/ degradation response at the AP represents the response in the longer, unsurveyed portions of the reach. Uncertainty in the elevations of the individual survey points also contributes to uncertainty, although this appears to be a minor factor compared to the other sources of uncertainty. The rating curve-based sediment balance is also subject to relatively large uncertainty because of the small number of samples and inherently high variability in the data used to develop the rating curves. These sources of uncertainty were quantified, to the extent possible with the available data to help understand the implications to the Program's ability to draw valid conclusions about whether each portion of the reach is aggrading, degrading or in dynamic equilibrium.

The uncertainty in the rating curve-based estimates was quantified by performing Monte Carlo simulations of the annual loads based on the uncertainty bands on each rating curve. The simulations were performed by generating 1,000 estimates of the annual loads for each site assuming that the variability in the logarithm of the individual, estimated loads at the mean of the logarithms of the discharges in each data set follows a normal distribution with mean equal to the load estimated from the rating curve and upper and lower 95-percent confidence limits equal to the corresponding confidence limits on the regression equation at the mean discharge (**Table 4.1**). It was also assumed that the slope of the regression line varies about the best-estimate slope based on a normal distribution parameterized by the standard error of the slope term from the regression analysis. The difference in annual sediment load between the sites was then calculated for each of the 1,000 sets of annual loads, and the resulting data set was used to assess the variability in the estimated aggradation/degradation volumes.

The above assumptions are illustrated using the suspended sand curves at the Overton site in **Figure 4.9**. The best-estimate sediment load at the back-transformed log mean discharge of the data set (3,068 cfs) is 1,541 tons per day (tpd), and the upper and lower 95-percent confidence limits on the regression line at this discharge are 1,137 and 2,088 tpd, respectively (green vertical line in Figure 4.9a). The resulting standard deviation of the predicted sediment loads in the log domain at this discharge is 0.08. The distribution of the predicted sediment loads at the mean from the Monte Carlo simulation ranged from about 1,105 to 3,448 tpd (Figure 4.9b). The best-estimate of the exponent on the rating curve is 1.494, and the standard deviation of this estimate is 0.221. The resulting exponents from the Monte Carlo simulation ranged from 0.786 to 2.255 (Figure 4.9c).

Table 4.1. Summary of Bed and Suspended Sand Load Regression Equations and Associated Statistics.

Measurement Site	Mean Discharge[1]	α^2	β^2		Average Bias-Correction Factor[3]	Best-estimate Sand Load at log Mean Discharge (tons)[4]			
			Mean	Standard Error		Mean	Lower 95% Confidence Limit	Upper 95% Confidence Limit	Standard Deviation (log)
Bed Load									
Darr	2,626	0.099	1.190	0.240	1.21	1,164	751	1,805	0.116
Overton	3,692	0.152	1.090	0.387	1.42	1,174	725	1,901	0.127
Kearney	3,940	0.189	1.059	0.356	1.09	1,212	719	2,045	0.138
Shelton	3,692	0.152	1.090	0.387	1.42	1,174	725	1,901	0.127
Grand Island	3,836	0.076	1.188	0.334	1.13	1,375	799	2,368	0.143
Suspended Sand Load									
Darr	2,178	0.663	1.073	0.181	1.16	2,530	1,813	3,532	0.088
Overton	3,068	0.010	1.494	0.221	1.21	1,541	1,137	2,088	0.080
Kearney	3,466	0.018	1.441	0.246	1.12	2,300	1,496	3,536	0.114
Shelton	3,138	0.001	1.826	0.287	1.34	1,301	868	1,949	0.107
Grand Island	3,556	0.028	1.405	0.232	1.07	2,780	1,946	3,970	0.094

[1] Discharge based on mean of logarithms of measured data set

[2] Coefficient and exponent of power function rating curve (Sediment Load=α*Discharge$^{\beta}$)

[3] Average bias-correction factor for mean daily discharges in the four-year data set

[4] Best-estimate sediment load, confidence limits and standard deviation (log domain) of regression confidence bands at mean discharge of measured data set

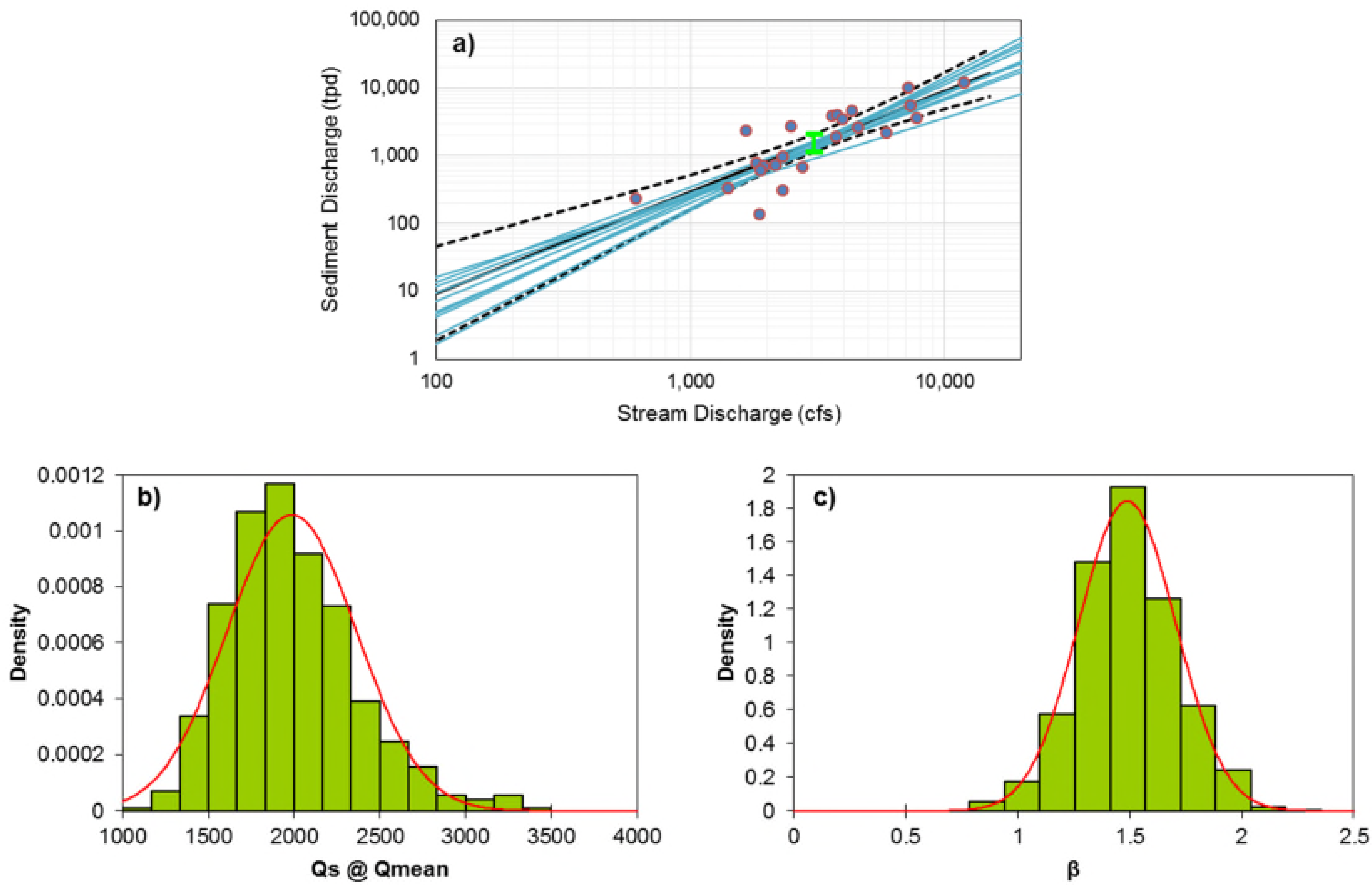

Figure 4.9. (a) Suspended sand rating curves at Overton. Light grey lines are sample curves from the Monte Carlo simulation; (b) Distribution of estimated sediment loads at the mean (log) discharge of the measured data set from Monte Carlo simulation; (c) Distribution of the exponents on the Overton suspended sand-load rating curve from the Monte Carlo simulation.

The coefficient (α) on the rating curve for each of the 1,000 estimates was back-calculated using the predicted sediment load (log) at the mean discharge and the exponent (β) for each step in the simulation. The annual suspended sediment loads at this site from the Monte Carlo simulations had central tendency very close to the best-estimate values for each year that was presented in the previous section, but ranged from 191,000 to 616,000 tons in SY2010, 470,000 to 1.82M tons in 2011, 306,000 to 992,000 tons in 2012, 46,000 to 258,000 tons in 2013, 182,000 to 650,000 tons in 2014, 441,000 to 2.51M tons in 2015, and 426,000 to 1.58M tons in 2014 (**Figure 4.10**).

The statistical distribution of total sediment loads at each site was estimated by performing independent Monte Carlo simulations for the bed and suspended sand loads, and adding the corresponding bed and suspended loads for each step in the simulation. The resulting distribution of total sand transport balances, computed from the difference between the upstream inflow and downstream outflow in each segment of the reach for each step in the simulation (Figure 4.7), suggest the following with respect to the statistical significance (α=.05, two-tailed) of the aggradation/ degradation trends:

1. Based on the median value of the sediment balance, the reaches from Darr to Overton, Kearney to Shelton, and Shelton to Grand Island were degradational, and the reach between Overton and Kearney was slightly aggradational.
2. Darr to Overton:
    a. The degradational trend is statistically significant during SY2012, SY2013, and SY2016.
    b. The probability that the reach was degradational during the other years ranged from 65 percent (SY2015) to 92 percent (SY2016) (**Table 4.2**).
    c. Considering all years, there is 81 percent probability that the reach was actually degradational.
3. Overton to Kearney:
    a. The differences in sand load at the bounding gages are small relative to the uncertainty bounds, and none of the annual trends is statistically significant.
    b. The highest probability that the reach was either aggradational or degradational in a given year was 68 percent (aggradation in SY2013 and SY2014).).
    c. Considering all years, there is 52 percent probability that the reach was actually aggradational.
4. Kearney to Shelton:
    a. The degradational trends indicated by the rating curves were not statistically significant in any of the survey years.
    b. The probability that the reach was degradational in any given year ranged from 43 percent (SY2013) to 74 percent (SY2015).).
    c. Considering all years, there is 57 percent probability that the reach was actually degradational.
5. Shelton to Grand Island:
    a. The differences in sand load at the bounding gages are small relative to the uncertainty bounds, and none of the annual trends is statistically significant.
    b. The probability that the reach was degradational ranged from 56 percent (SY2014) to 82 percent (SY2010).

c. The probability that the reach was aggradational was 42 percent in SY2013 and 56 percent in SY2015.
d. Considering all years, there is an 82 percent probability that the reach was actually degradational.

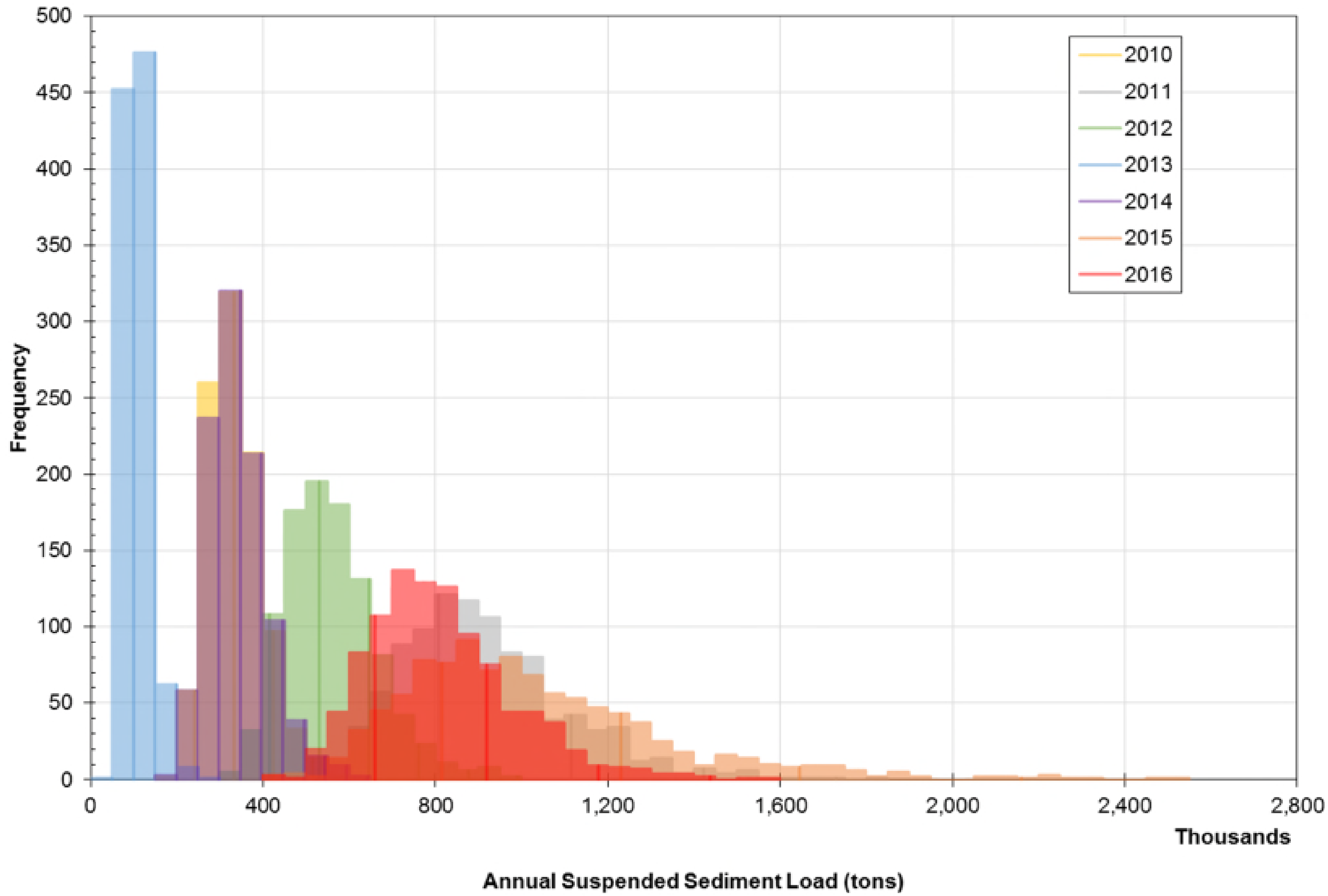

Figure 4.10. Distribution of estimated annual suspended sand loads at Overton based on the 1,000 Monte Carlo trials for each of the five years covered by the monitoring surveys.

Table 4.2. Probability of degradation when rating curve indicates degradation, or aggradation when mean indicates aggradation.

Survey Year	Darr-Overton (%)	Overton-Kearney (%)	Kearney-Shelton (%)	Shelton-Grand Island (%)
SY2010	81	52	57	82
SY2011	74	54	61	65
SY2012	**98**	50	48	73
SY2013	**97**	68	43	42
SY2014	87	68	61	56
SY2015	65	65	74	56
SY2016	92	61	60	69
2010-2016	**81**	**52**	**57**	**82**

Unfortunately, it is not possible to quantify the uncertainty in the survey-based estimates in the same manner as the rating curve-based estimates. Uncertainty associated with the elevations of individual survey points is quite small. Monte Carlo simulation for the 2013 annual report (Tetra Tech, 2013) using the reported error statistics from the GPS data logger showed that the potential error in the surveyed elevations at the individual points at the middle primary transect of AP29 would result in only about ±0.13 percent variability in year-to-year change in cross-sectional area. The amount of uncertainty associated with how well the transects represent the area changes within each AP, as well as the overall, approximately 5-mile reach represented by the AP, cannot be quantified with the available data. A simple test using the 2012 and 2013 LiDAR surfaces for a bar in the south channel at Jeffreys Island that was regularly inundated by J-2 Return hydropower releases but was dry during both LiDAR surveys showed that the volume change estimated from three transects in the middle of the bar was within about 2 percent of the volume change estimated by overlaying the two LiDAR surfaces (**Figure 4.11**). The excellent agreement for this test is due to the relatively uniform distribution of aggradation/degradation zones through the sample area. Attempts to perform a similar test on a larger reach of the river channel were not successful because of the confounding effects of the water surface at the time of the surveys and the fact that a significant part of the bed elevation changes occur in the inundated part of the channel. Further systematic testing of this issue may ultimately show that use of high-resolution LiDAR data, collected at low flows may provide improved estimates of the aggradation/ degradation status of the reach than the transect surveys. This is particularly true if tests using green LiDAR that can penetrate relatively clear, shallow water are successful.

With completion of the 2016 field season, each of the rotating APs was surveyed twice during the 8-year monitoring period. Survey data from the rotating APs were used to assess how a higher spatial-resolution dataset would affect the aggradation/degradation estimates in the geomorphic and larger-scale, gage-to-gage reaches by comparing the measured changes over the 4-year periods between rotating AP surveys using all of the surveyed points within each reach with the changes based only on the pure panel APs. The correlation coefficient between the area change at the rotating APs and the next upstream pure panel AP is 0.16, a relatively low value that suggests significant variability in the aggradation/degradation along the reach (**Figure 4.12**). (The correlation coefficient between the rotating APs and the next downstream pure panel AP is only 0.08.) In 10 of the 20 cases where direct comparison could be made, inclusion of the rotating AP data changes the 4-year aggradation/degradation estimate for the geomorphic reaches by more than 20 percent, and in 6 of the cases, the estimate changes by more than 50 percent (**Figure 4.13**). With a few exceptions (e.g., Reach 7 from 2009-2013, Reach 4 from 2010 to 2014, Reach 6 from 2011 to 2015), the large percentage changes occurred when the average change over the periods was relatively small. Despite the relatively large difference in result using all APs, the direction of change indicated by the data was the same in every case, although inclusion of the rotating AP data essentially eliminated the sediment deficit or excess in 5 of the 20 cases. Based on the sum of the average changes in cross sectional area for the paired data points, the amount of aggradation in aggrading reaches would have decreased by 20 percent to 25 percent, and the amount of degradation in degrading reaches would have decreased by about 40 percent to 45 percent if all APs had been surveyed in all years. When the data are combined by gage reach, the differences are much smaller, primarily because the variability from site to site is averaged out with the larger datasets (**Figure 4.14**).

The yearly aggradation/degradation volumes estimated from the pure panel AP survey data are within the 90-percent (two-tailed) confidence bands on the corresponding rating-curve based estimates in 13 of the 28 cases, and these cases are distributed with no apparent pattern among the reaches and survey years (**Table 4.3, Figures 4.15a-g**). The least number of years occurred in the Overton to Kerney reach, where the survey based estimates were within the confidence bands on the rating curve-based estimate in 2014 and 2016, followed by Shelton to Grand Island (2011, 2014 and 2015).

Table 4.3. Gage reaches in which the survey-based aggradation/degradation estimate is within the 90% (2-tailed) confidence bands on the rating curve-based estimate.

Survey Year	Darr-Overton	Overton-Kearney	Kearney-Shelton	Shelton-Grand Island
2010	X			
2011	X		X	X
2012				
2013			X	
2014	X	X		X
2015	X		X	X
2016		X	X	

Using the SEDVEG Gen3 Model with a 48-year flow record (1947-1990) that was adjusted to represent current operations of the system, Reclamation estimated that the reach between the Overton and Elm Creek Bridges has a net sediment deficit of about 185,000 tons/year under the existing flow regime (DOI Reclamation and USFWS, 2006). They also estimated that the reach between Elm Creek and Chapman had net sediment excess of about 62,000 tons/year, with most of the excess occurring downstream from Chapman. HEC-6T modeling by Tetra Tech (2010) using observed hydrology for the 12.5-year period from October 1989 through April 2002 estimated that the annual sediment deficit between Overton and Elm Creek was about 150,000 tons. Although the results were not presented in terms of volumes, HEC-6T modeling of the overall monitoring reach by Tetra Tech (see HDR and Tetra Tech, 2011) was consistent with the Tetra Tech (2010) findings in the Overton to Elm Creek Reach and showed that the reach between Kearney and Shelton was slightly aggradational, the reach between Shelton and Grand Island was degradational, and the remainder of the reach was approximately in balance, with localized zones of both aggradation and degradation. Flows during the monitoring period have been much higher than the typical flows in the records used for both the DOI et al. (2006) and Tetra Tech (2010) modeling (**Figure 4.16**).

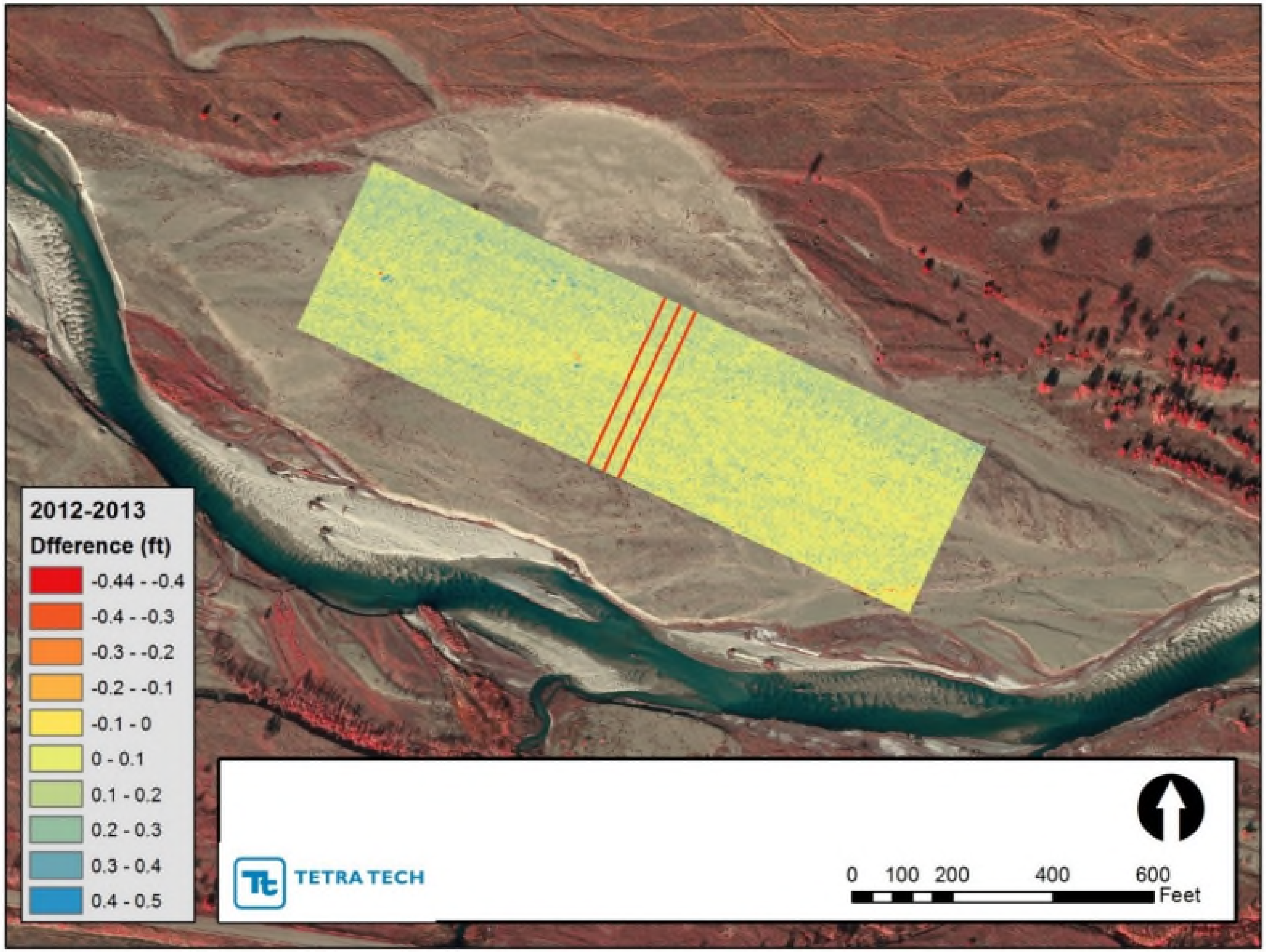

Figure 4.11. Area used to test agreement between cross section-based volume estimates and estimates based on the complete LiDAR surface (~RM245.5, south channel at Jeffreys Island approximately midway between AP36 and AP37).

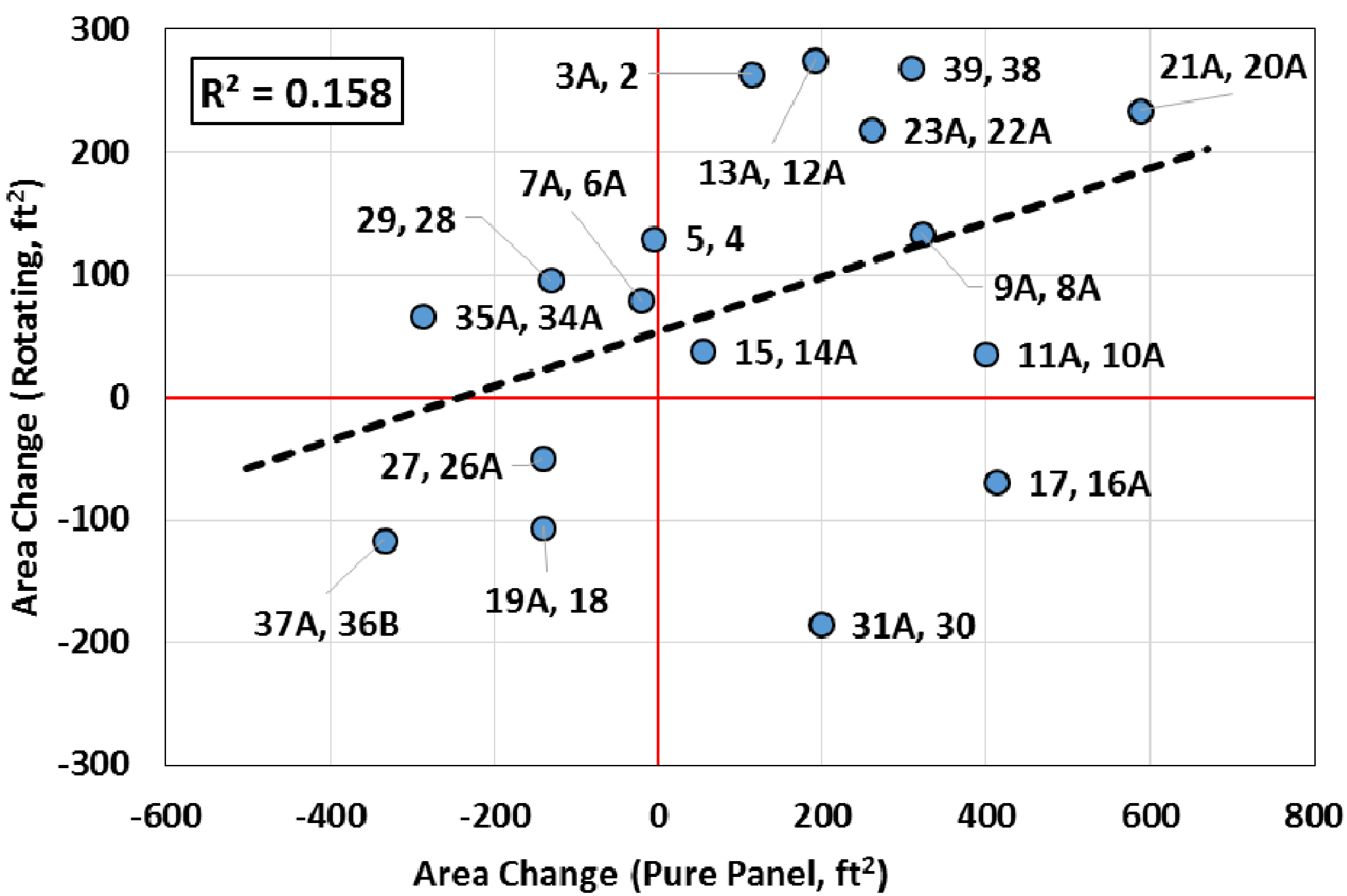

Figure 4.12. Average change in cross sectional area at Rotating APs plotted against the corresponding change at the next upstream Pure Panel AP over the 4 years between AP surveys. Data labels are APs from which the data were taken (odd numbers = Pure Panel; even numbers = Rotating).

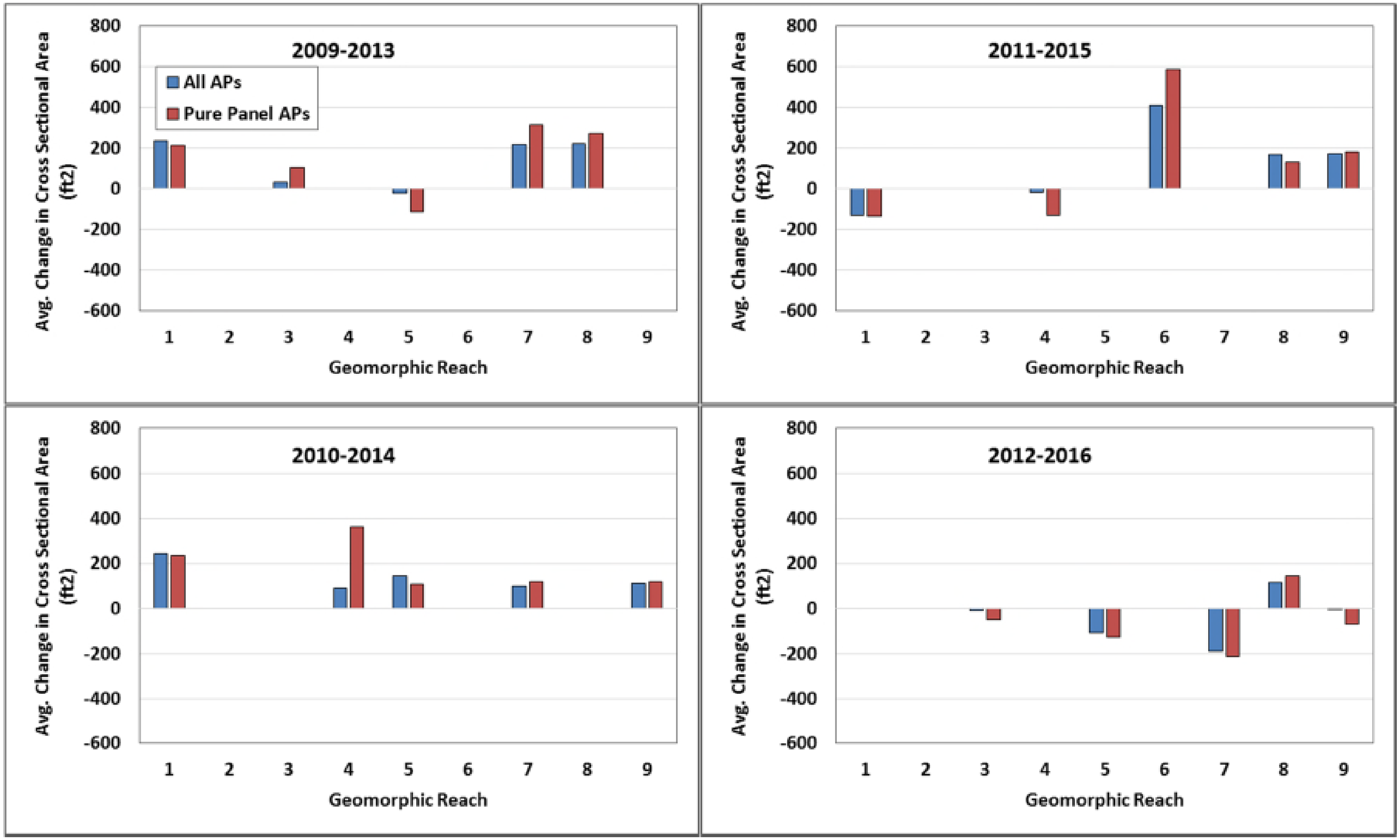

Figure 4.13. Average change in cross sectional area over indicated 4-year periods by geomorphic reach at pure panel APs and all available APs. Where no are shown, rotating panel points surveyed during the indicated period within the reach.

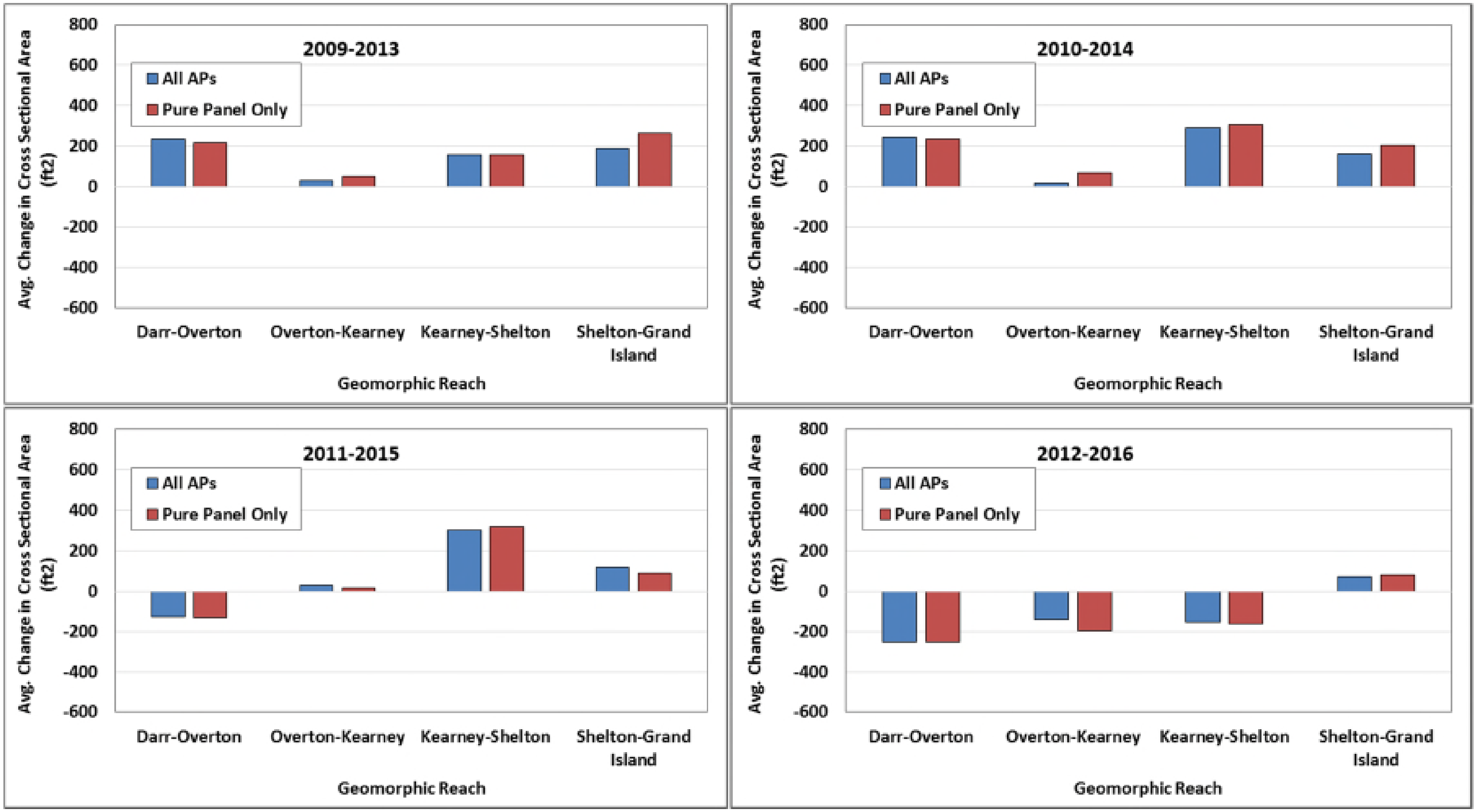

Figure 4.14. Average change in cross sectional area over indicated 4-year periods by gage reach at pure panel APs and all available APs.

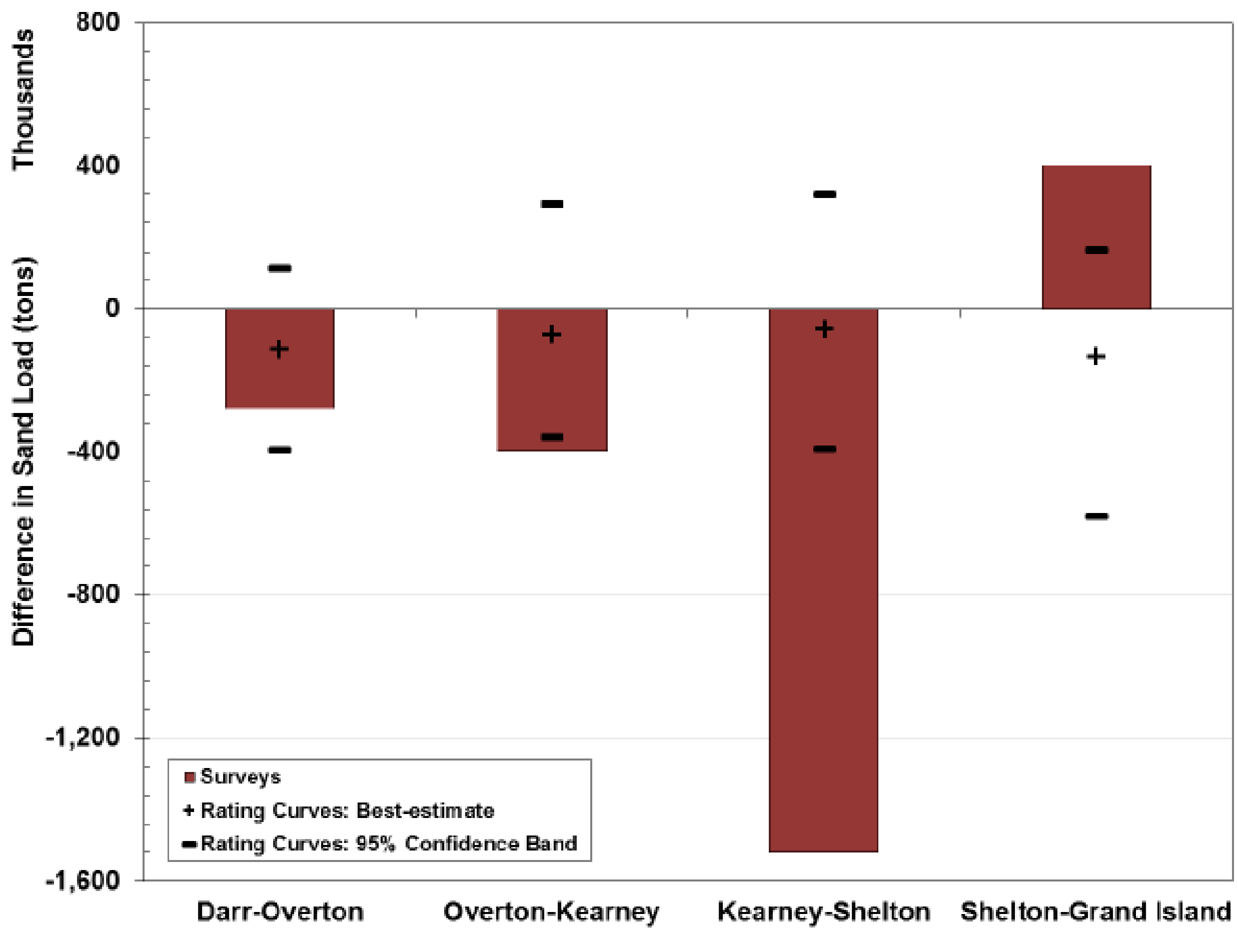

Figure 4.15a. Best-estimate of aggradation/degradation volumes based on the survey data (bars) and mean and upper and lower 95-percent confidence limits on the volumes predicted by the sediment rating curves (symbols) for SY2010.

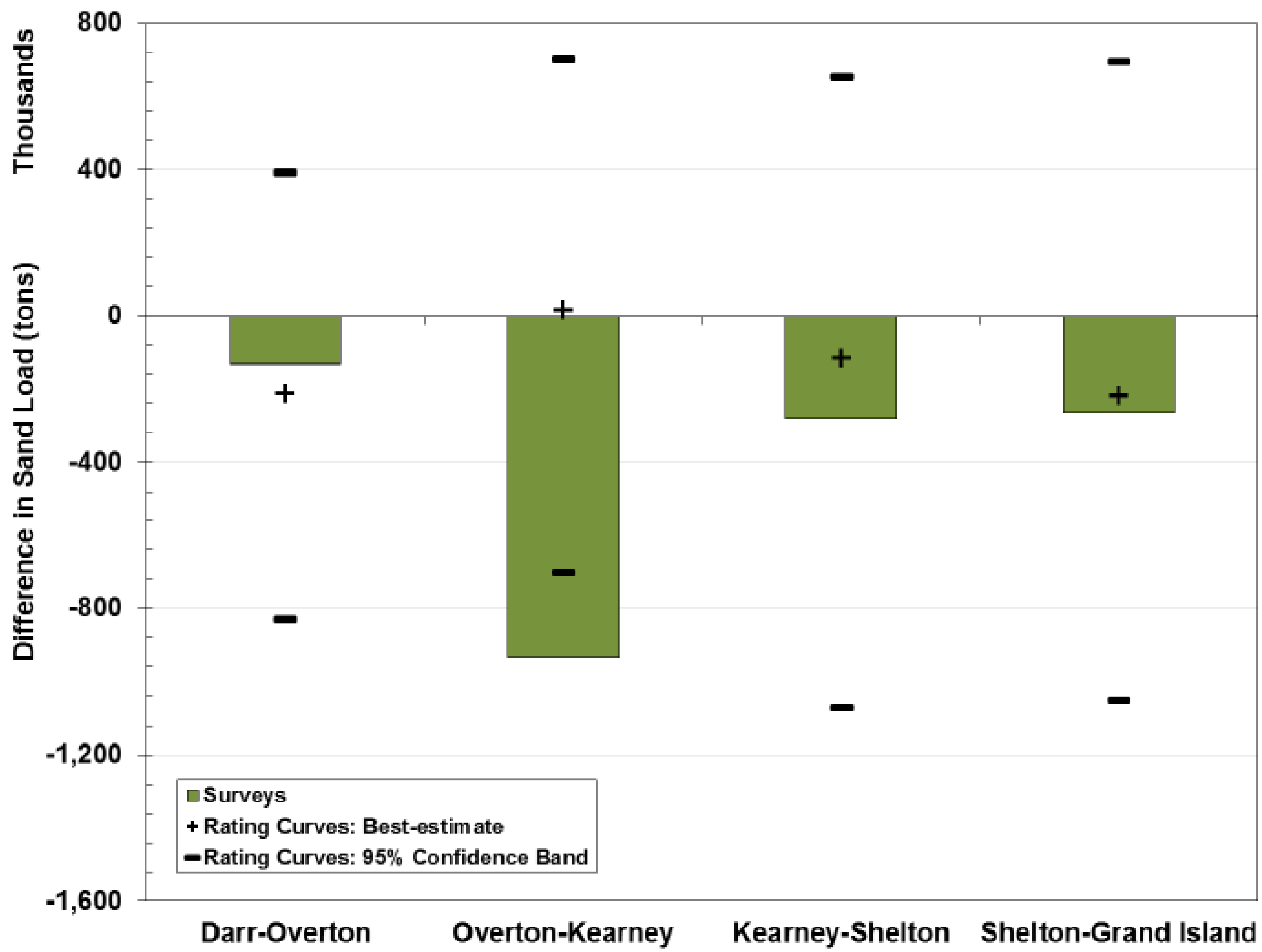

Figure 4.15b. Best-estimate of aggradation/degradation volumes based on the survey data (bars) and mean and upper and lower 95-percent confidence limits on the volumes predicted by the sediment rating curves (symbols) for 2011.

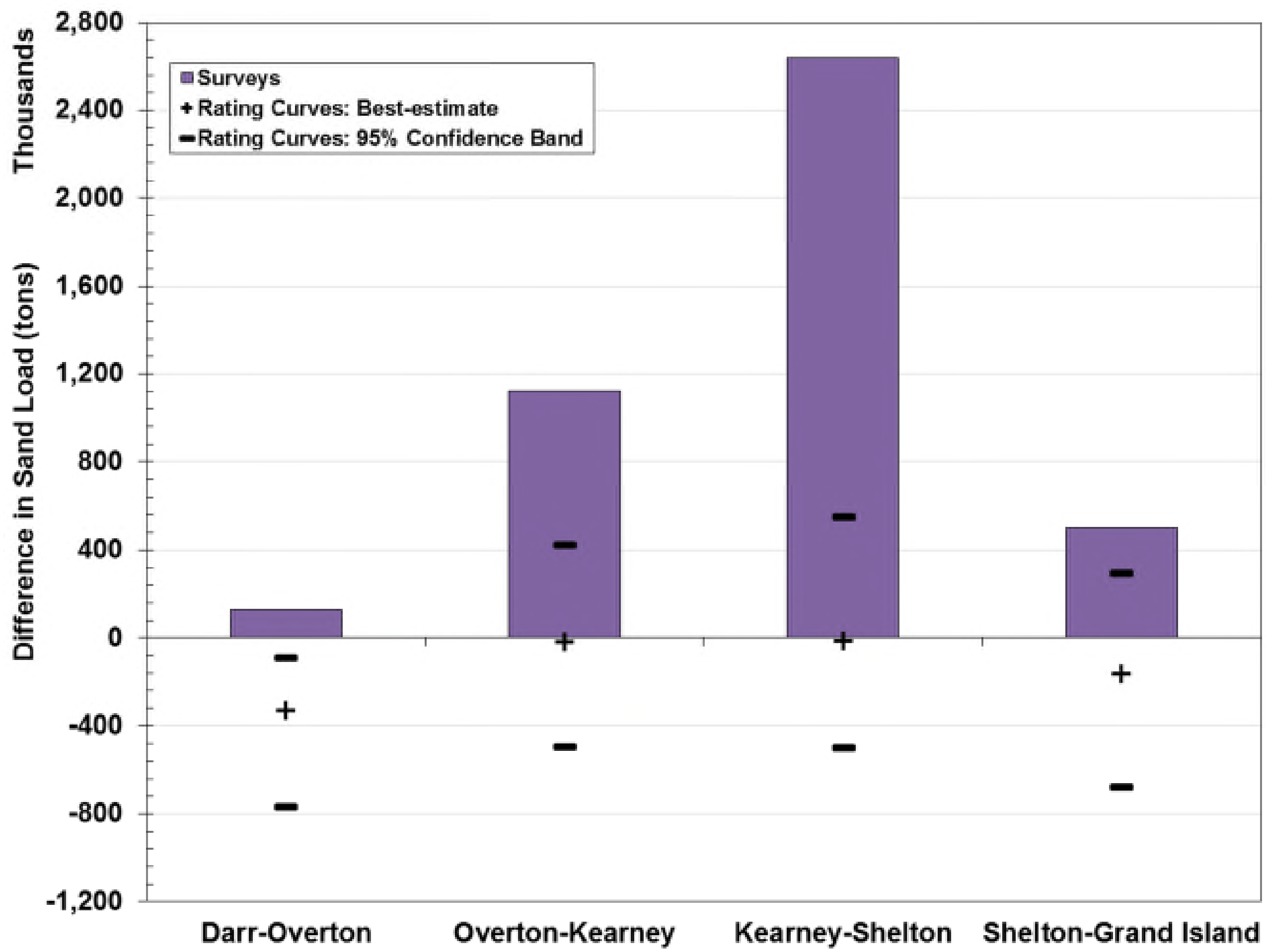

Figure 4.15c. Best-estimate of aggradation/degradation volumes based on the survey data (bars) and mean and upper and lower 95-percent confidence limits on the volumes predicted by the sediment rating curves (symbols) for 2012.

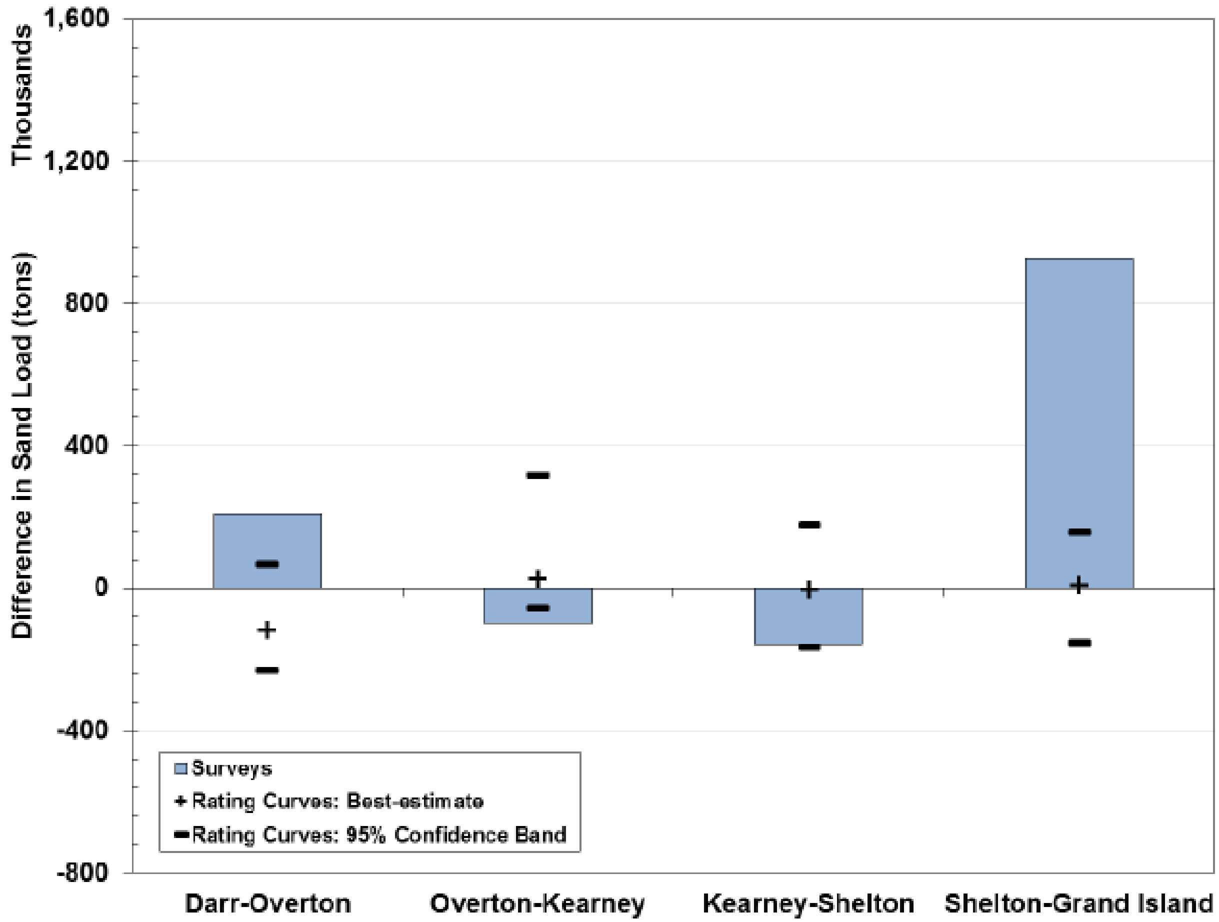

Figure 4.15d. Best-estimate of aggradation/degradation volumes based on the survey data (bars) and mean and upper and lower 95-percent confidence limits on the volumes predicted by the sediment rating curves (symbols) for 2013.

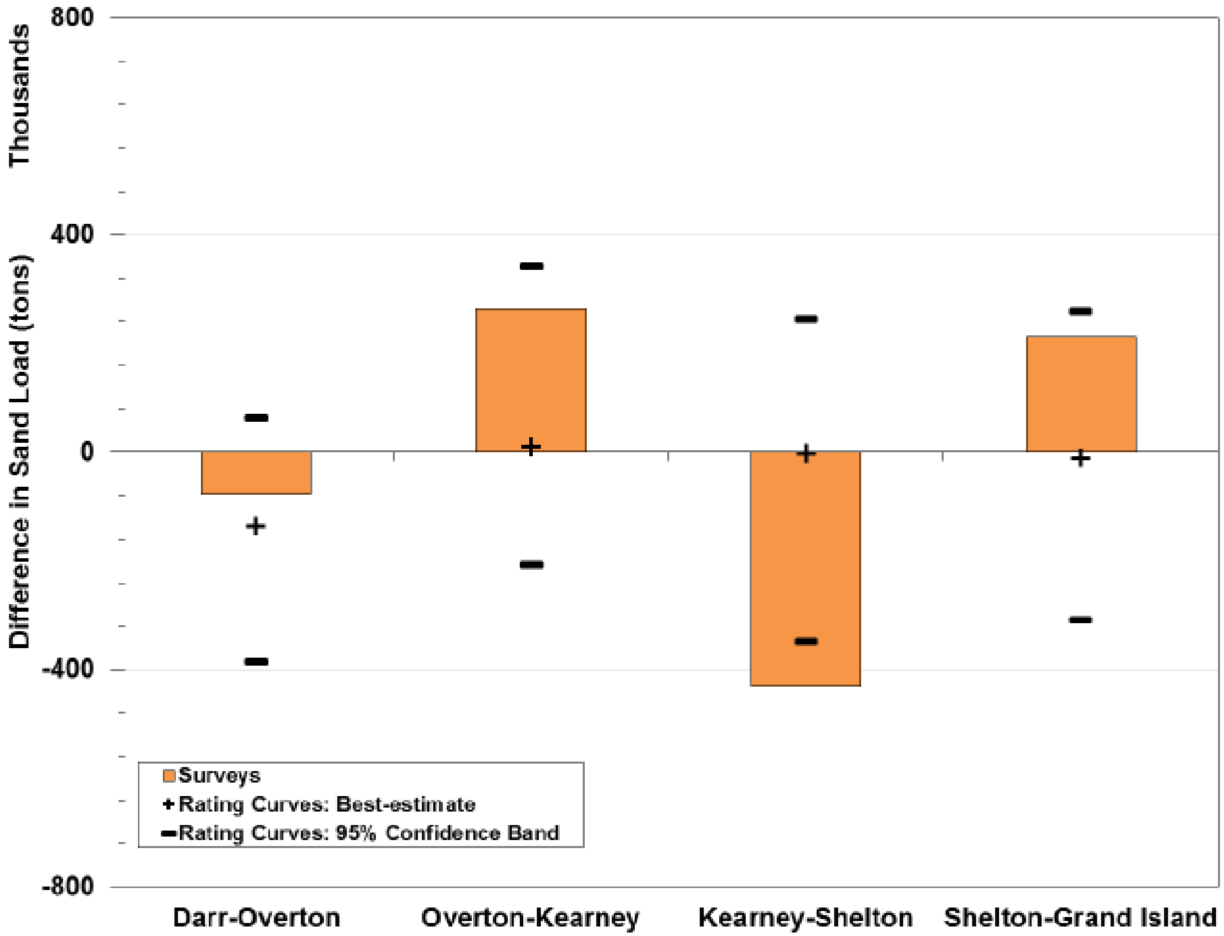

Figure 4.15e. Best-estimate of aggradation/degradation volumes based on the survey data (bars) and mean and upper and lower 95-percent confidence limits on the volumes predicted by the sediment rating curves (symbols) for 2014.

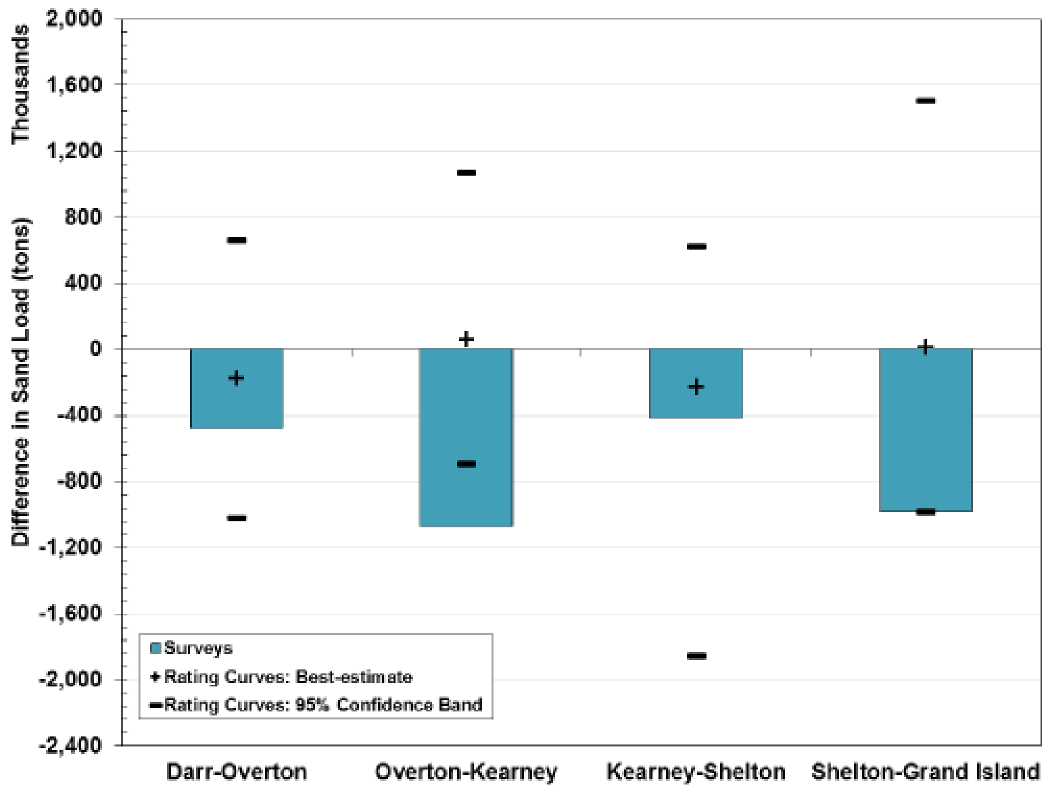

Figure 4.15f. Best-estimate of aggradation/degradation volumes based on the survey data (bars) and mean and upper and lower 95-percent confidence limits on the volumes predicted by the sediment rating curves (symbols) for 2015.

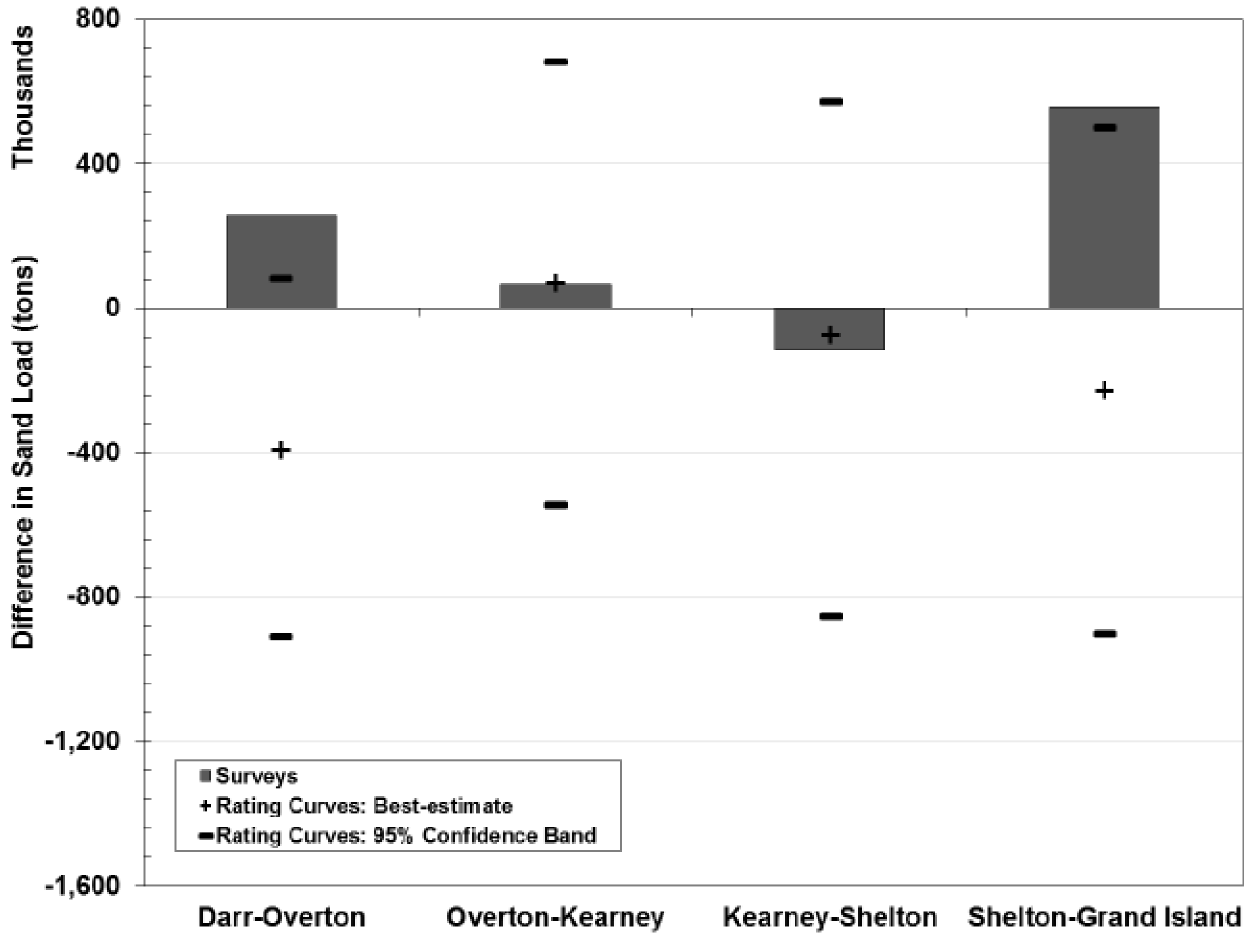

Figure 4.15g. Best-estimate of aggradation/degradation volumes based on the survey data (bars) and mean and upper and lower 95-percent confidence limits on the volumes predicted by the sediment rating curves (symbols) for 2016.

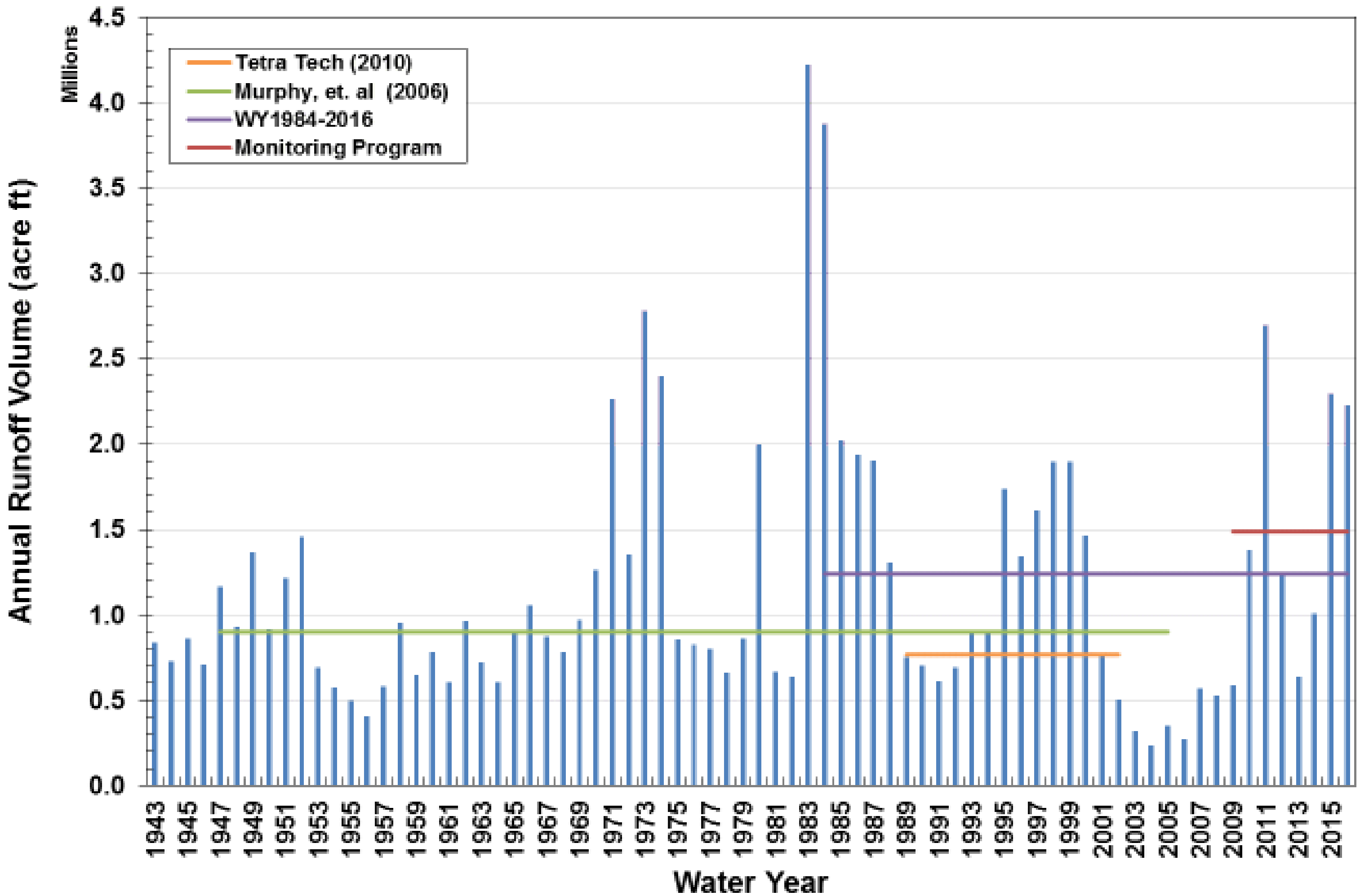

Figure 4.16. Annual total runoff volume at the USGS Overton gage between WY1943 and WY2016. Also shown are the mean flows for the 48-year record used for the DOI et al. (2006) model, the Tetra Tech (2010) model and the 6-year monitoring period.

The rating curves for Overton, Kearney and Grand Island were integrated over the published mean daily flows from the USGS records for the longest available overlapping record (WY1984 through WY2016) to provide longer-term estimates of the annual sediment loads and sediment balance[18]. The best-estimate annual sand load at Overton averaged about 730,000 tons over the 33-year period, and ranged from about 84,000 tons (WY2004) to 2.91M tons (WY1984) (**Figures 4.17** and **4.18**). The sand loads at Kearney during this period averaged about 740,000 tons, and ranged from 75,000 to 2.9M tons, and the loads at Grand Island averaged 900,000 tons, and ranged from 81,000 to 3.4M tons.

Based on the above loads, the best-estimate of the sediment deficit between Overton and Kearney averaged about 8,000 tons over the period and deficit between Kearney and Grand Island averaged 156,000 tons (**Figures 4.19a** and **4.20**, respectively). Based on Monte Carlo simulations similar to those described above, the 95-percent (two-tailed) confidence bands on these estimates are, however, quite large, in every case crossing zero (**Figure 4.19b**). This indicates that, even though the majority of the annual estimates indicate degradation in both reaches, the values are not statistically significant.

To help put the confidence bands on these estimates into perspective, the mean value of the sediment balance from the Monte Carlo simulations for the Overton to Kearney reach was negative (i.e., degradational) in 19 of the 33 years, and the distributions for the individual years suggest an approximately 53-percent chance, on average, that the reach was, in fact, degradational. Similarly, the mean value of the sediment balance for the Kearney to Grand Island Reach was negative in 32 of the 33 years, with an average 71-percent chance that the reach was actually degradational. The mean values from this analysis also indicate that the Kearney to Grand Island reach is more strongly degradational during high-flow years than during low-flow years; whereas, there is essentially no correlation in the Overton to Kearney reach between the sediment balance and the annual runoff (**Figure 4.21a**). Increasing flow volume, however, tends to increase uncertainty in the sediment balance, as clearly seen by the divergence of the confidence bands on the sediment rating curves at flows above about 6,000 cfs (Figures 3.44-3.48, 3.54-3.58). Although the magnitude of bed response is greater in high-flow years due to the increased energy available to transport sediment, there is little statistical evidence to suggest that degradation is more likely in high-flow years than in low-flow years (**Figure 4.21b, c**).

The combination of the above evidence points to a general degradational tendency upstream from Shelton, while the balance between Shelton and Grand Island unclear. The best-estimate of the sediment balance between Darr and Overton is about 210,000 tons of degradation from the rating curves but only about 53,000 tons from the surveys. Inclusion of the rotating panel point data appears to have little effect on the survey-based results. Averaging the results from the two methods indicates a net average-annual deficit in the Darr to Overton reach of about 130,000 tons.

In the Overton to Kearney reach, the rating curve-based estimates indicate an approximate sediment balance (~8,000 ton annual deficit based on the 8-year monitoring period; ~14,000 ton excess based on 33-year record), while the survey based estimate indicates a net annual deficit of about 149,000 tons. Inclusion of the rotating AP data appears to have a greater effect in this part of the monitoring reach, reducing the magnitude of imbalance (whether aggradational or degradational); thus, the 149,000 tons per year (tpy) survey-based estimate is probably an upper-limit value. Based on the combined data, the annual sediment deficit in the Overton to Kearney reach is most likely in the range of 50,000 tons to 75,000 tons.

[18] Longer-term records are not available for the Lexington or the Shelton gages.

Both methods indicate degradation in the Kearney to Shelton reach (~41,000 tpy deficit from the surveys; ~69,000 tpy deficit based on the best-estimate from the rating curves), and inclusion of the rotating APs in the survey-based estimates appears to have very little effect on the survey-based estimates. Based on these results the net annual deficit in the Kearney to Shelton reach is likely in the range of 50,000 tons. The survey data indicate a substantial sediment excess in the Shelton to Grand Island reach of about 194,000 tpy, on average, while the rating curves indicate an approximately 103,000 tpy deficit. As a result, these data do not provide a basis for concluding that a sediment imbalance exists in the Shelton to Grand Island reach. Inclusion of the rotating AP data in the survey-based estimates for this part of the reach also appear to have limited effect on the results. The longer-term estimates for the Shelton to Grand Island reach from the rating curves is consistent with the shorter –term (i.e., 8-year monitoring period) estimates (annual deficits of 156,0000 ton versus 172,000 ton, respectively), while the survey-based estimates indicate a net 151,000 tpy excess.

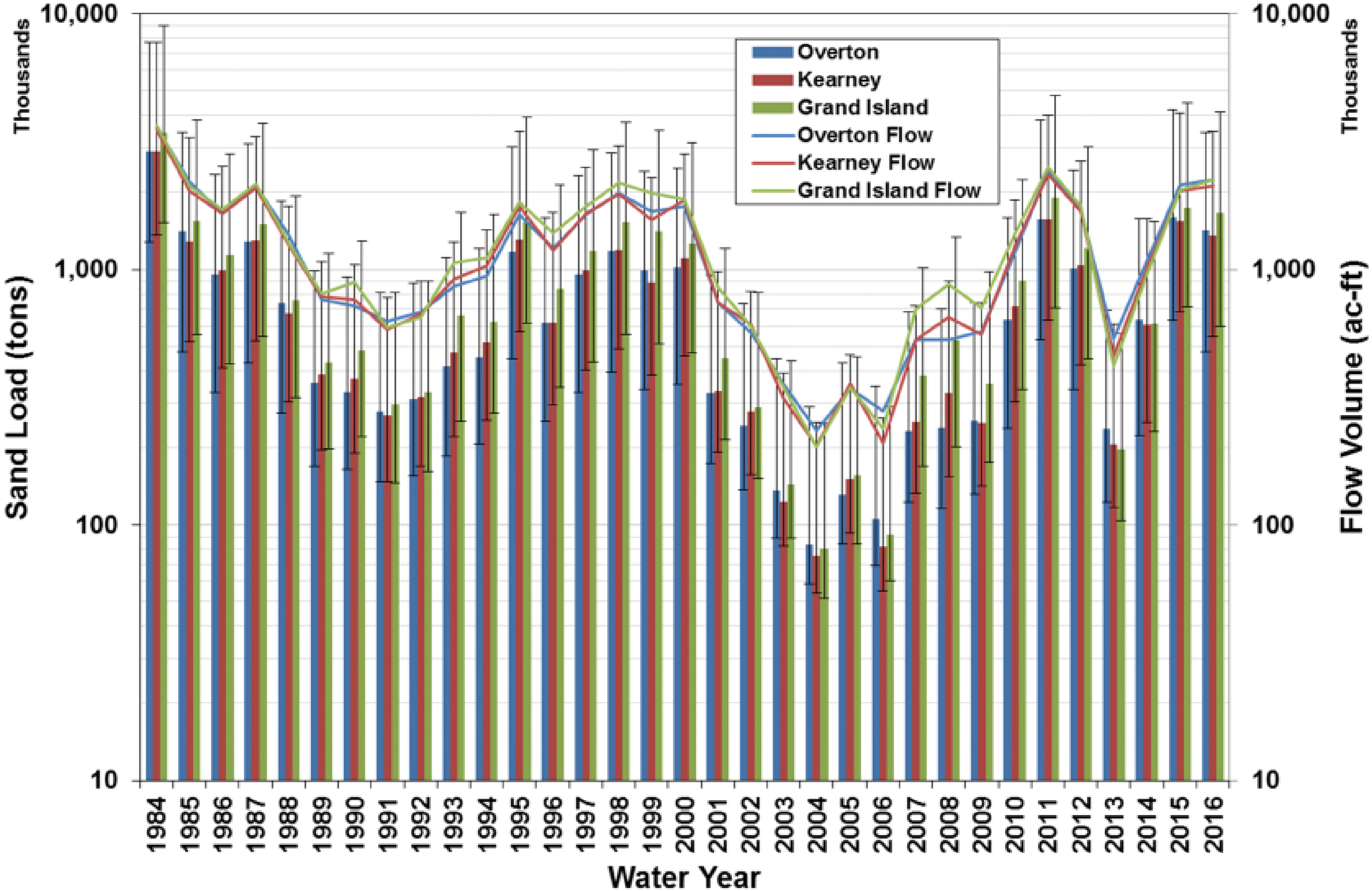

Figure 4.17. Estimated average annual total sand load passing the Overton, Kearney, and Grand Island gages during individual years from WY1984 through WY2016, based on integration of the respective rating curves over the USGS published mean daily flows. Also shown are the upper and lower 95-percent confidence limits from the Monte Carlo simulations.

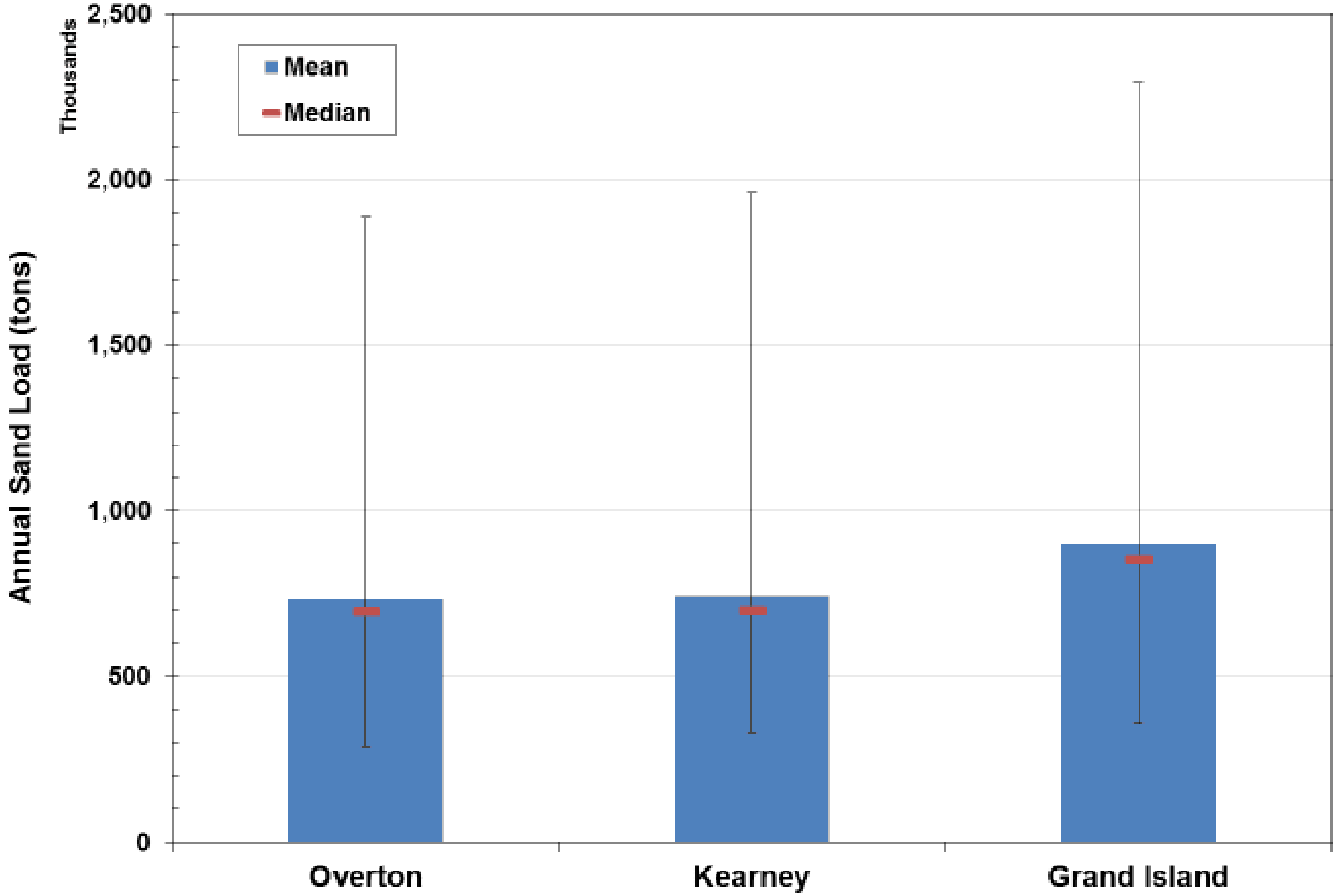

Figure 4.18. Average annual total sand load passing the Overton, Kearney, and Grand Island gages based on integration of the respective rating curves over the USGS published mean daily flows for the period from WY1984 through WY2016. Also shown are the median values and 5th and 95th percentiles from the Monte Carlo simulations.

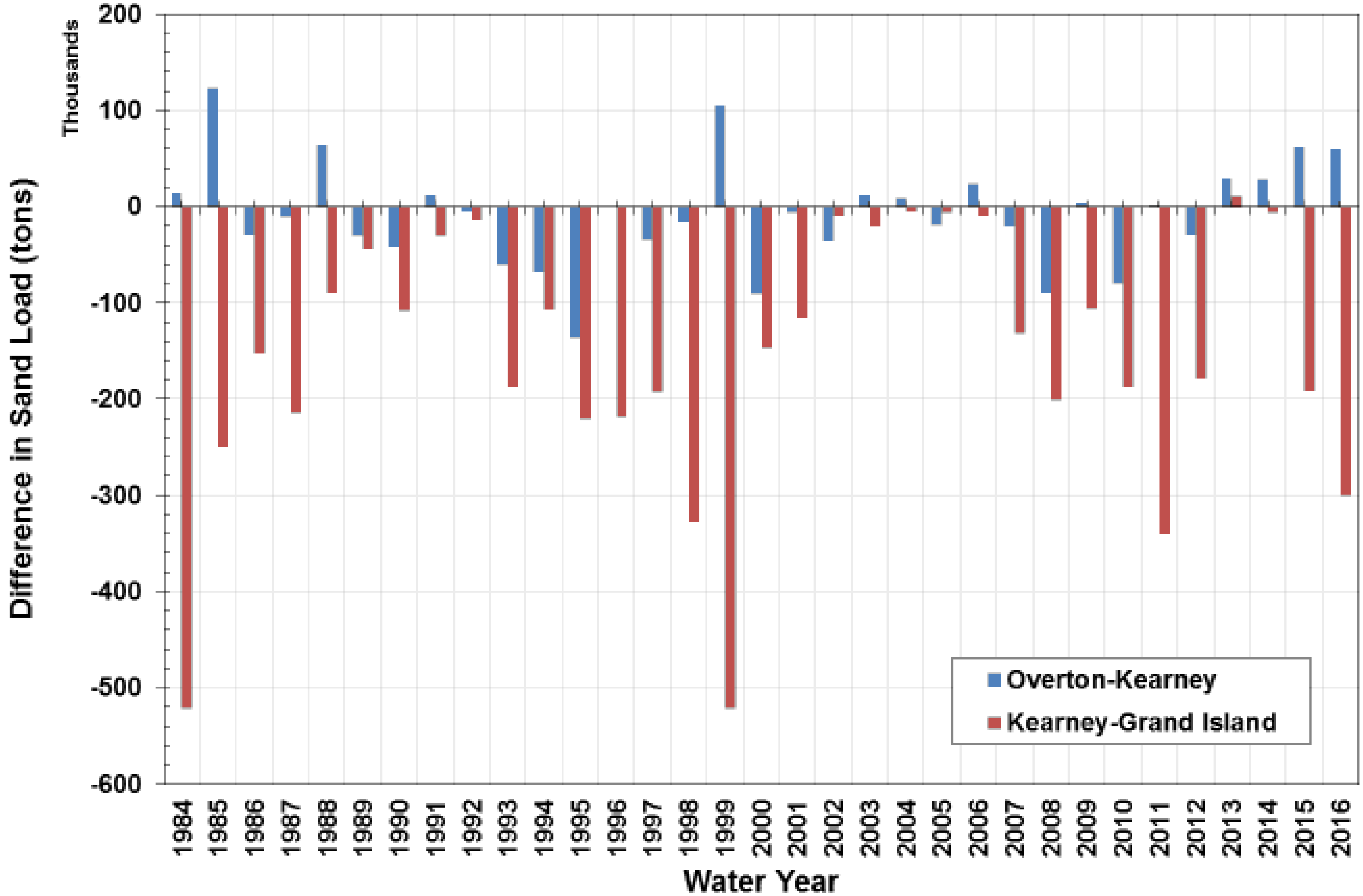

Figure 4.19a Estimated annual sand transport balance between Overton, Kearney and Grand Island from WY1984 through WY2016, based on integration of rating curves produced by the Monte Carlo simulation.

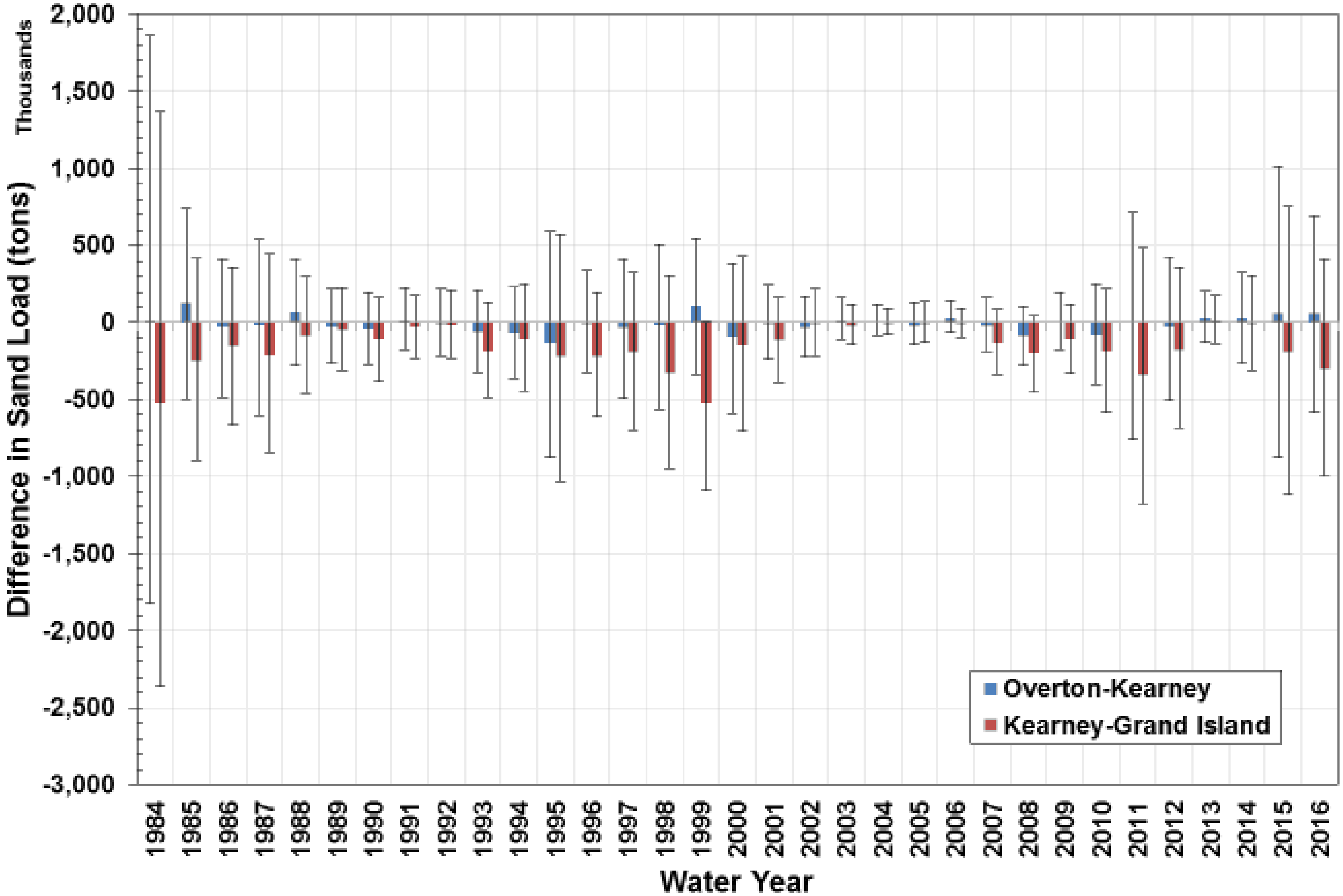

Figure 4.19b. Estimated annual sand transport balance between Overton, Kearney and Grand Island from WY1984 through WY2016. Same as Figure 4.16 with 95% confidence limits from Monte Carlo simulations.

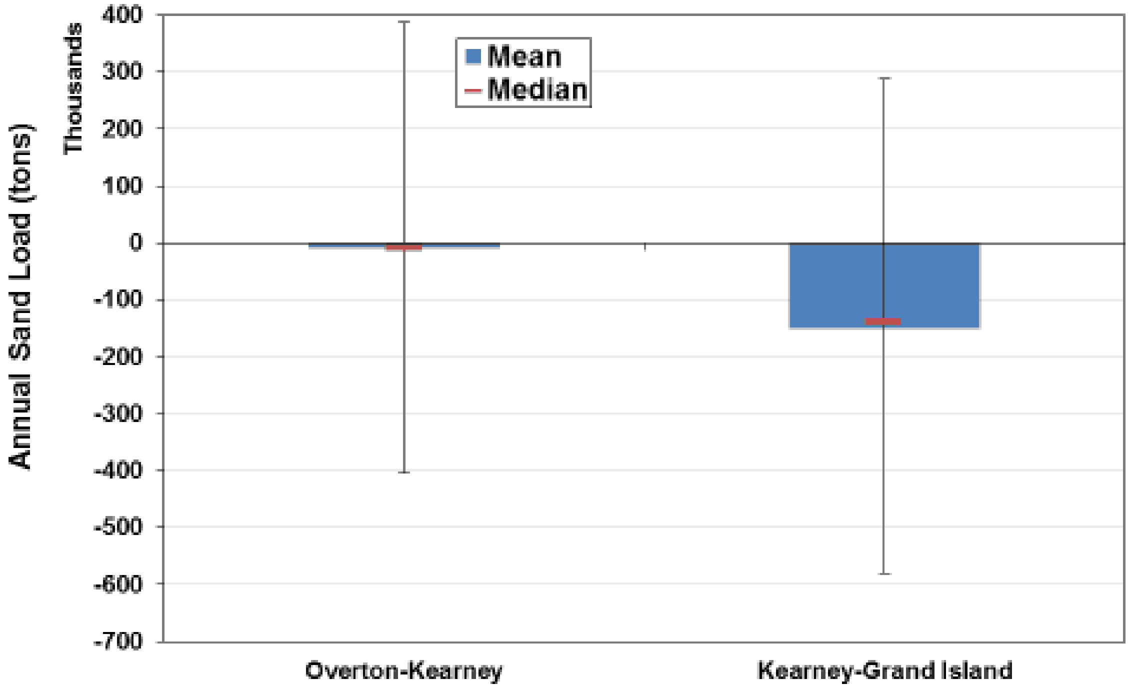

Figure 4.20. Mean and median annual sand transport balance between Overton, Kearney and Grand Island from WY1984 through WY2016. Also shown are the 5th and 95th percentile results from the Monte Carlo simulations.

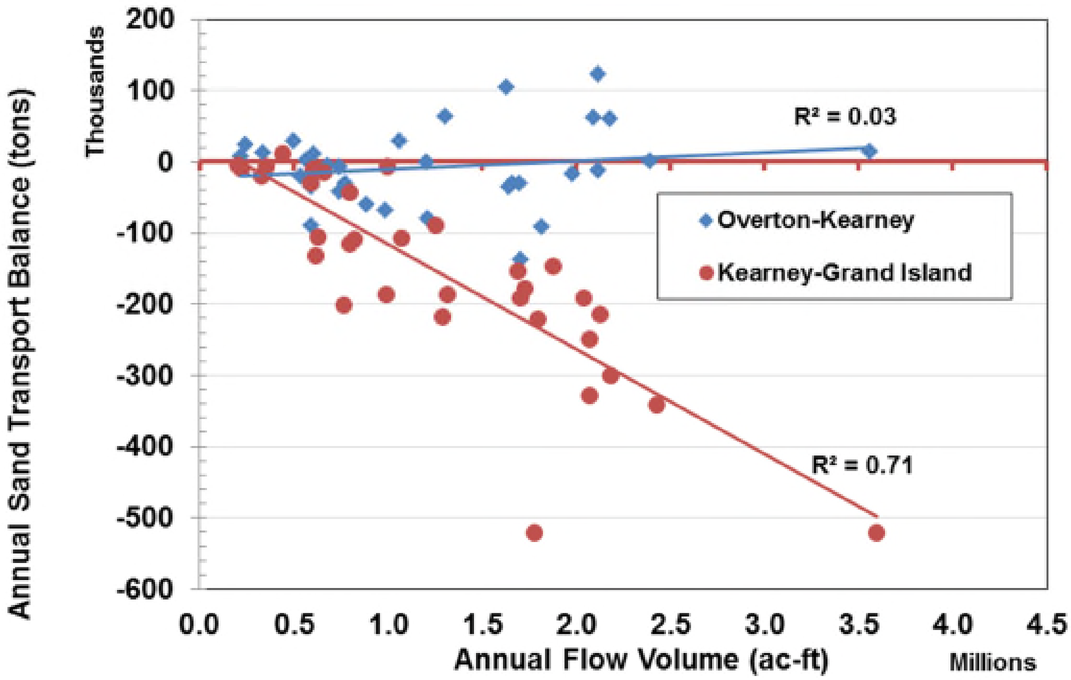

Figure 4.21a. Relationship between estimated mean sand balance and total flow volume in the Overton to Kearney and Kearney to Grand Island reaches.

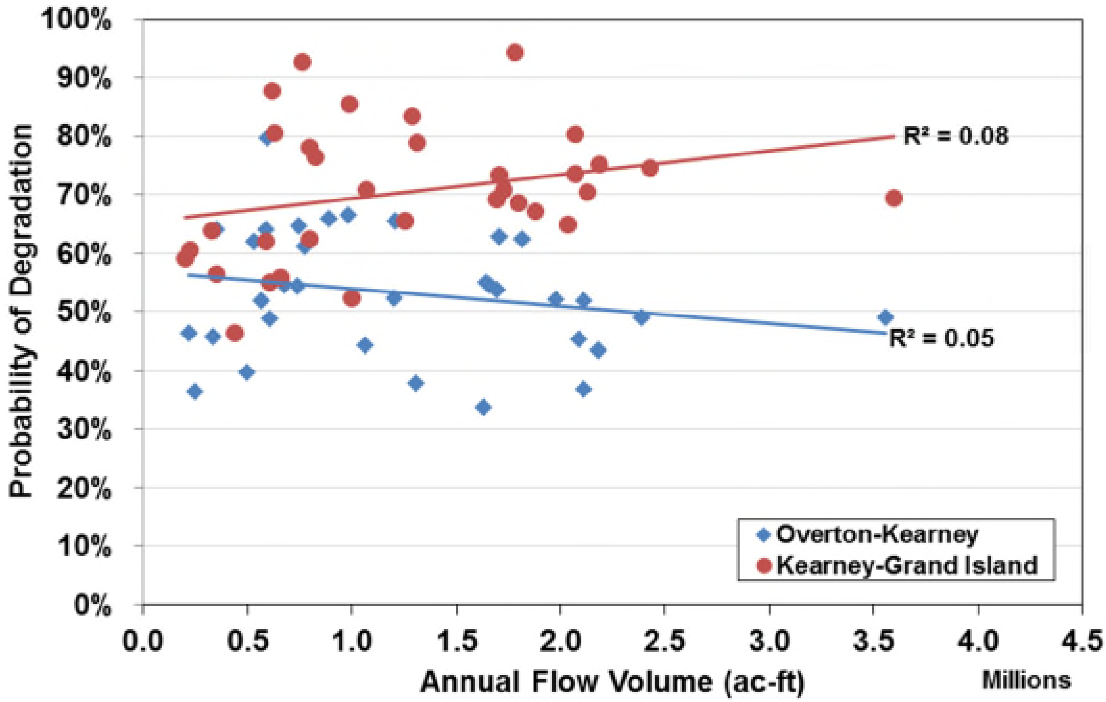

Figure 4.21b. Relationship between annual total flow volume and probability of degradation in the Overton to Kearney and Kearney to Grand Island reaches.

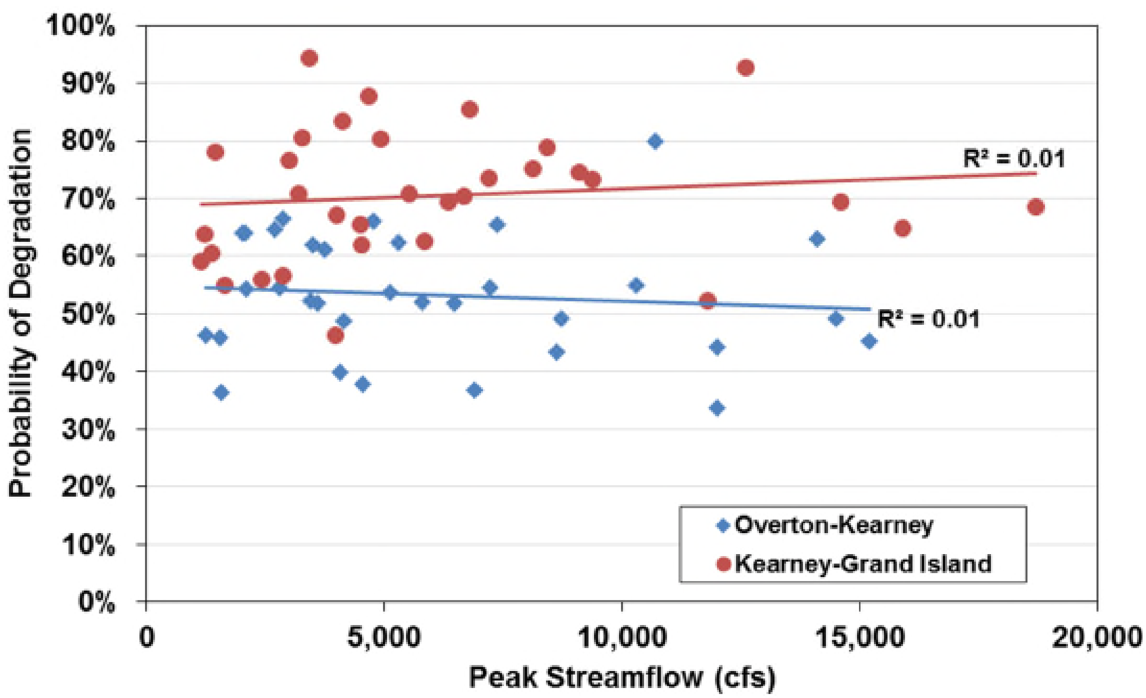

Figure 4.21c. Relationship between annual peak streamflow and probability of degradation in the Overton to Kearney and Kearney to Grand Island reaches.

4.2 Flow #3

> *Increasing $Q_{1.5}$ with Program flows will increase local boundary shear stress and frequency of inundation at the existing green line (elevation at which riparian vegetation can establish.) These changes will increase riparian plant mortality along margins of the channel, raising the elevation of the green line, providing more exposed sandbar area and a wider, unvegetated main channel.*

The extent to which the Greenline Elevation (GLE) and resulting unvegetated widths measured at the pure panel APs are responsive to flow was assessed by correlating these metrics with various discharge metrics. As specified in the DAP, the edges of unvegetated segments along each transect are identified by the GLE points. To remove the effects of river slope in the correlations, the GLE values were also normalized to the 1,200 cfs water surface (i.e., the difference between the GLE and the local 1,200 cfs water surface was used rather than the actual elevation). In addition, the differences in the modeled water-surface elevations (subsequently referred to as stage for brevity) for the applicable discharge metrics were used in the analysis, rather than the actual discharge. The following specific correlations were evaluated:

1. GLE versus stage at annual peak discharge (Q_p, Monitoring Plan Section 5.1.1), defined as the maximum mean daily discharge between January 1 and the date of the survey in each year.
2. GLE versus stage at germination season discharge (Q_{Ger}, Monitoring Plan Section 5.1.2), defined as the either the mean or median mean daily discharge between June 1 and July 15, the primary season for establishment of cottonwood seedlings. For this analysis, the correlations were performed using both the mean and median discharges.
3. Total unvegetated width (W_{unveg}) versus stage at annual peak discharge (Q_P).
4. Total unvegetated width (W_{unveg}) versus stage at germination season discharge (Q_{Ger}).
5. Total unvegetated width (W_{unveg}) versus GLE.

4.2.1. Height of Green Line above 1,200 cfs Water Surface

One of the benchmarks established by the Program is to maintain GLEs at least 1.5 ft above the 1,200 cfs water surface. As noted in Section 3.4.1, the GLE (i.e., *the edge of vegetation on a sand bar or adjacent to a wetted channel, defined by at least 25 percent cover of vegetation*) tends to be responsive to the magnitude of flows. During 2011, when long-duration, high flows persisted throughout the reach, the average GLE at the primary geomorphic transects reached the 1.5 ft benchmark, with the average at or above the benchmark at 16 of the 20 pure panel APs (**Figures 4.22** and **4.23**). The reach-wide average GLE was below the benchmark during all other years, and the benchmark was reached at 3 individual APs in each of 2015 and 2016 when relatively high flows also persisted in the reach. The GLE was below the benchmark at all other APs and all other years during the 8-year monitoring period. This result is not surprising since the vegetation that comprises the green line typically consists of annual species that germinate during the early part of the growing season when flows tend to be elevated.

4.2.2. Green Line Elevation versus Stage at Annual Peak Discharge

The year-to-year difference in GLE is well-correlated to the difference in stage associated with the annual maximum discharges (**Figure 4.24**). Correlation using the Kendall test on the complete data set results in a Kendall's τ of 0.45, and p-value of less than 0.0001 (α=0.05), indicating that the correlation is statistically significant.[19]

[19] It should be noted that the difference between the GLE analysis presented here is based on year-to-year change selected metrics, rather than change vs. 2009, as was the case in Section 3.4.1.

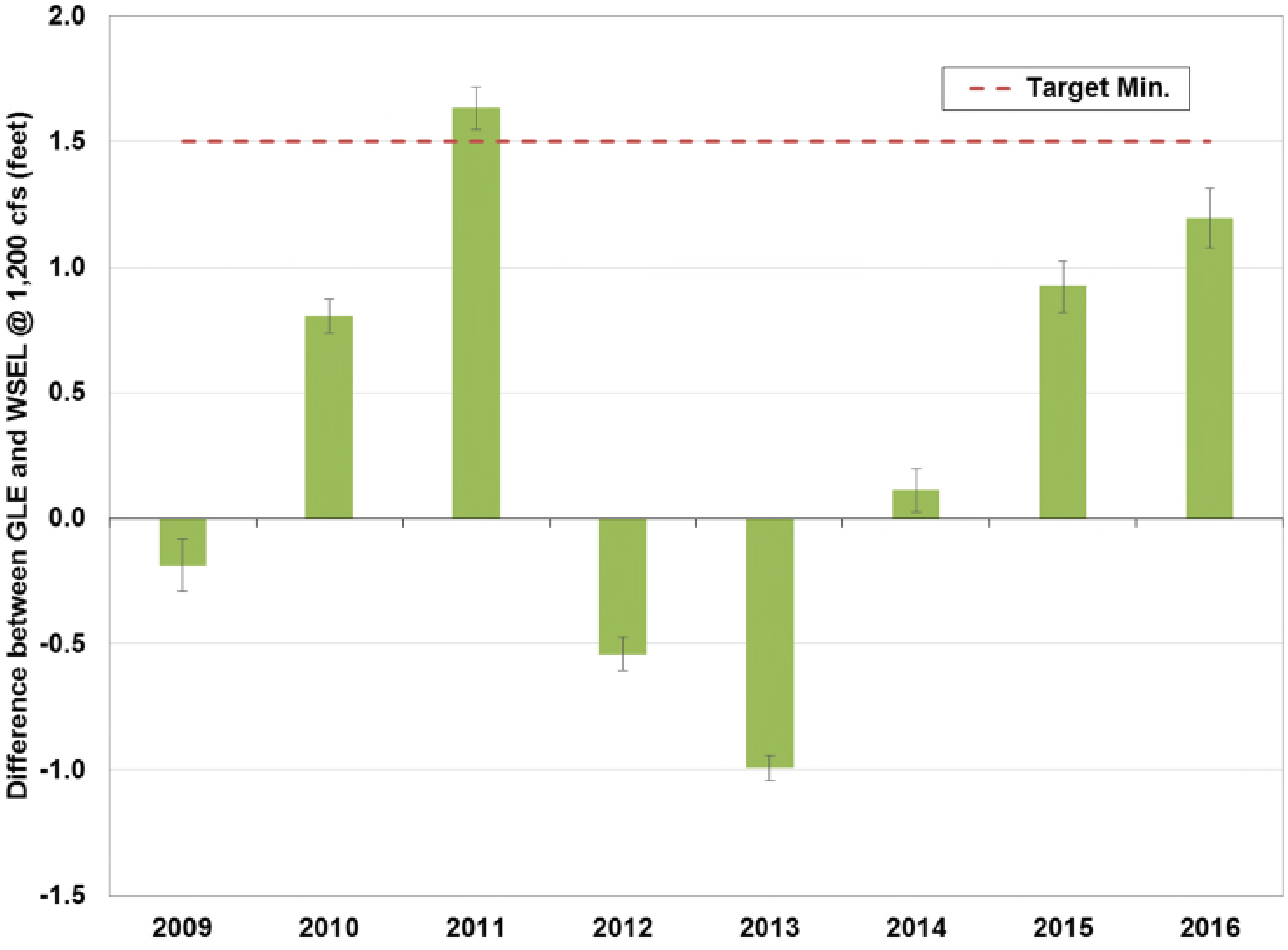

Figure 4.22. Relationship between annual peak streamflow and probability of degradation in the Overton to Kearney and Kearney to Grand Island reaches. Reach-wide average height of the GLE points above the 1,200 cfs water surface at the pure panel APs.

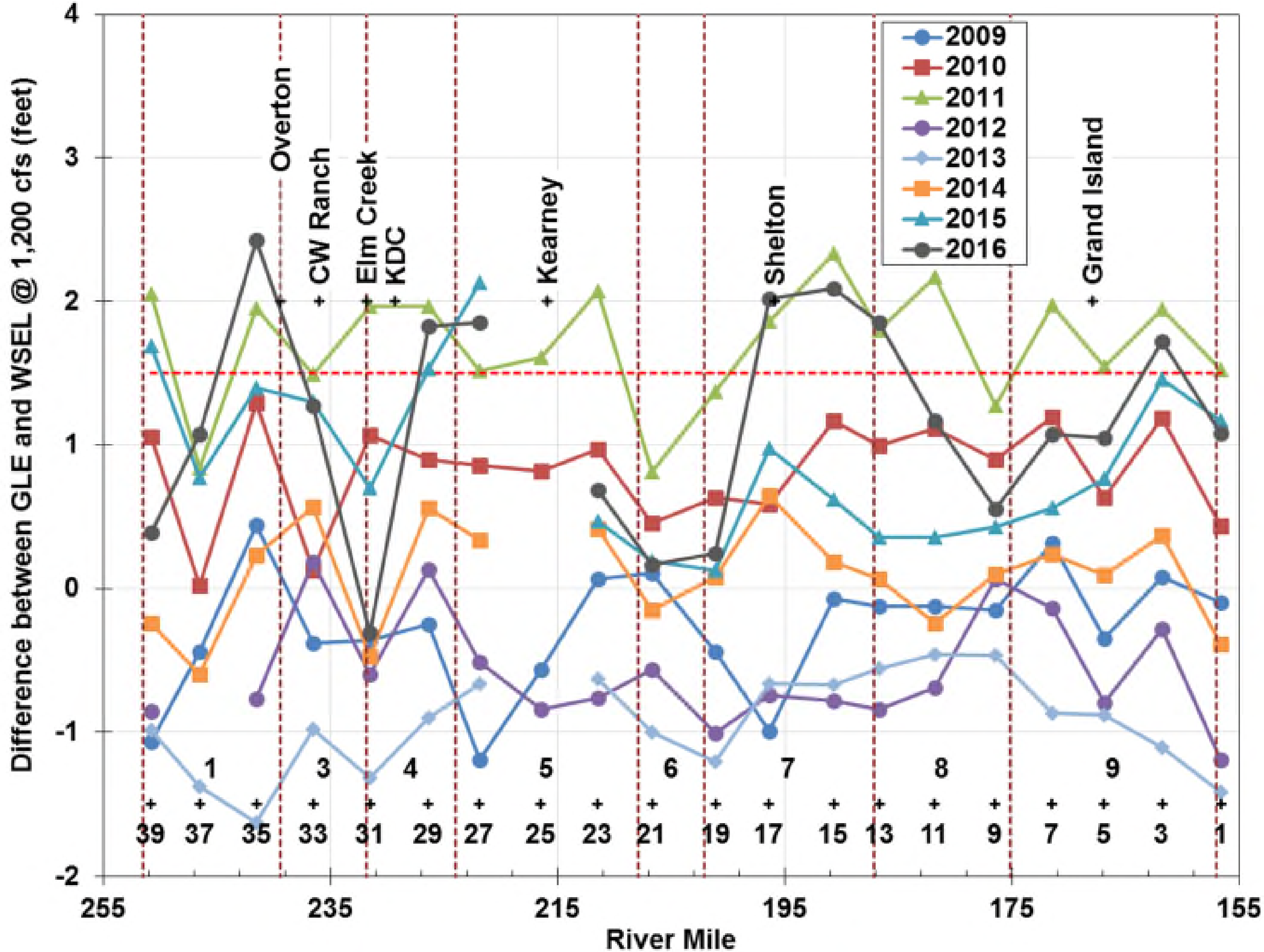

Figure 4.23. Average height of the GLE above the 1,200 cfs water surface at the pure panel APs. Also shown is the 1.5 ft performance benchmark.

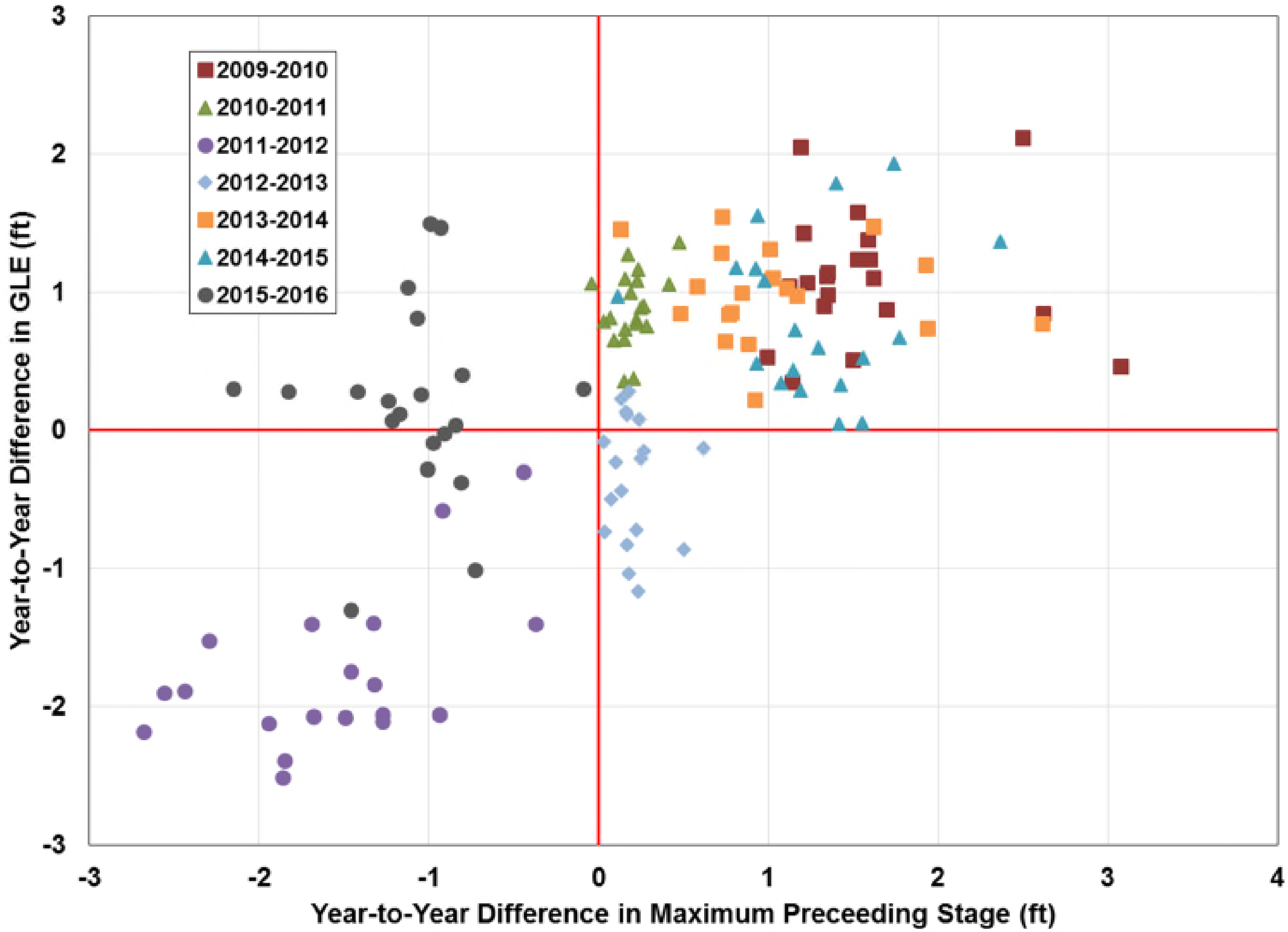

Figure 4.24. Yearly change in GLE versus year-to-year difference in stage at maximum mean daily flow preceding each survey at the pure panel APs (Kendall's $\tau = 0.45$, $p=<0.0001$).

4.2.3. Green Line Elevation versus Stage at Germination Season Discharge

The year-to-year change in GLE is even more highly correlated with the stage at the mean discharge during the germination season than with the annual maximum preceding discharge (**Figure 4.25**; Kendall's τ = 0.69, p<0.0001). The germination season discharges were quite low and very similar in magnitude in 2012 and 2013, and the GLE had generally receded well into the low flow channel, eliminating the potential for contrast between the two data sets. As a result, the data points for the year-to-year changes from SY2012 to SY2013 cluster around the line of zero change in stage. An independent test of the median discharge during the germination season rather than the mean resulted in essentially the same correlation results. The correlation between the year-to-year change in GLE and the stage associated with the maximum discharge **during the germination season** is also statistically significant (Kendall's t = 0.74, p<0.0001), slightly stronger than the mean germination season discharge (**Figure 4.26**).

4.2.4. Total Unvegetated Channel Width

The Program has established a benchmark to maintain a target unvegetated channel width of 1,125 ft, with minimum width of at least 750 ft. As discussed in Section 3.4.2, the reach-wide average unvegetated channel width was less than the minimum value in 5 of the 8 years of the monitoring program, and it was well below the target 1,125-ft width in all years (Figure 3.16b). In 2011, when sustained high flows occurred, the reach-wide average was about 725 ft, and this increased to 835 ft during the wet year in 2015 and increased even farther in 2016 to 850 ft, despite the fact that the germination season flows were much lower than either 2011 or 2015 (Figure 3.3). The relatively large unvegetated width in 2016 is likely due to carry-over conditions from the 2015 high-flow year, coupled with moderately high flows during the 2016 germination season. The year with the largest unvegetated width (average~630 ft) (Figure 3.16b). Individual geomorphic reaches in which the average unvegetated width exceeded the minimum include Reach 4 (2011, 2015 and 2016), Reach 5 (2015), Reach 6 (2010, 2011 and 2014-2016), and Reaches 7 and 9 (2011, 2015 and 2016) (Figure 3.17c). Reach 6 was the only geomorphic reach in which the average width exceeded the target value at any time during the 8-year monitoring period (2015 and 2016).

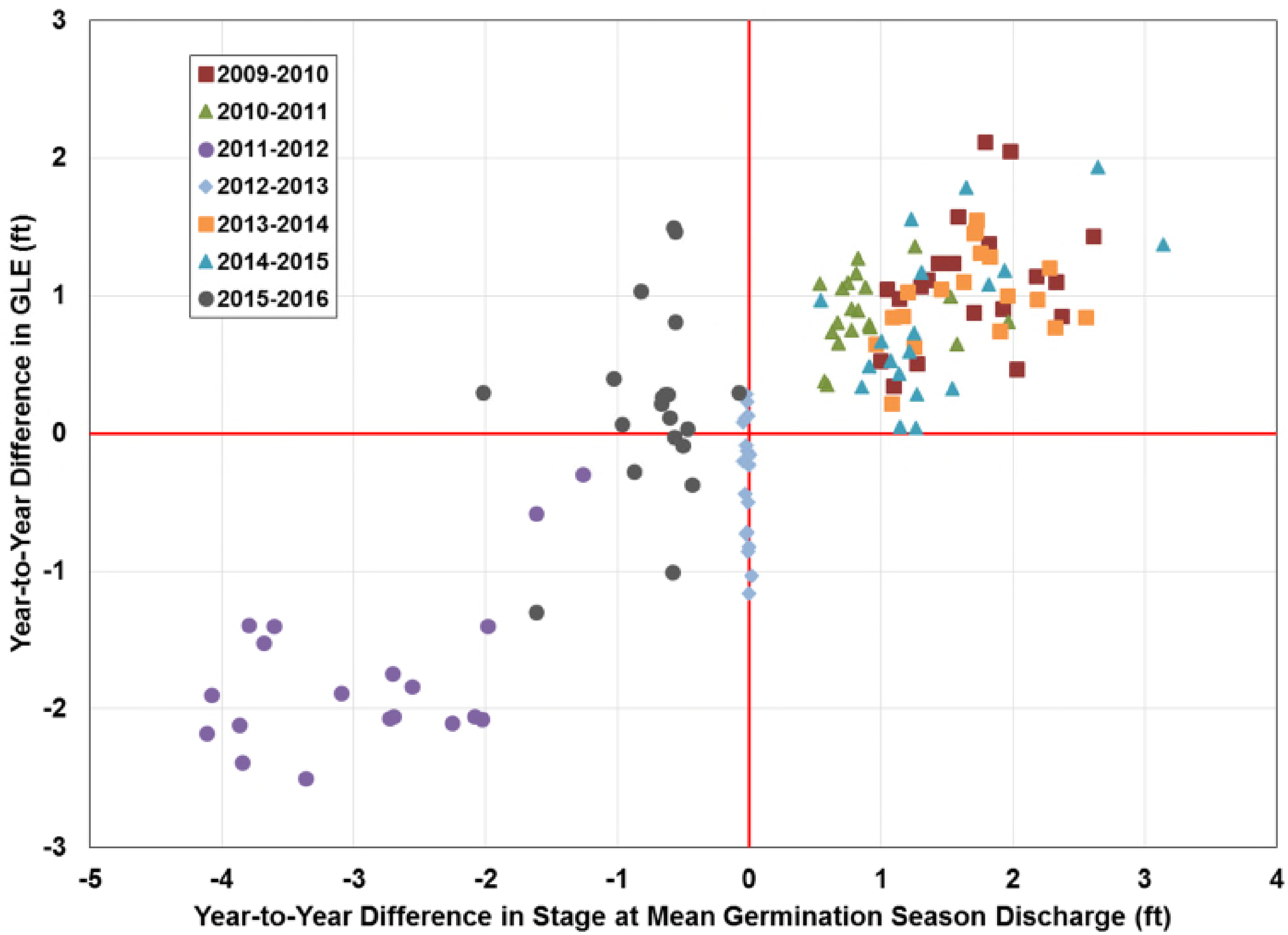

Figure 4.25. Yearly change in GLE versus year-to-year difference in stage at mean germination season discharge preceding each survey at the pure panel APs (Kendall's τ = 0.61, p=<0.0001).

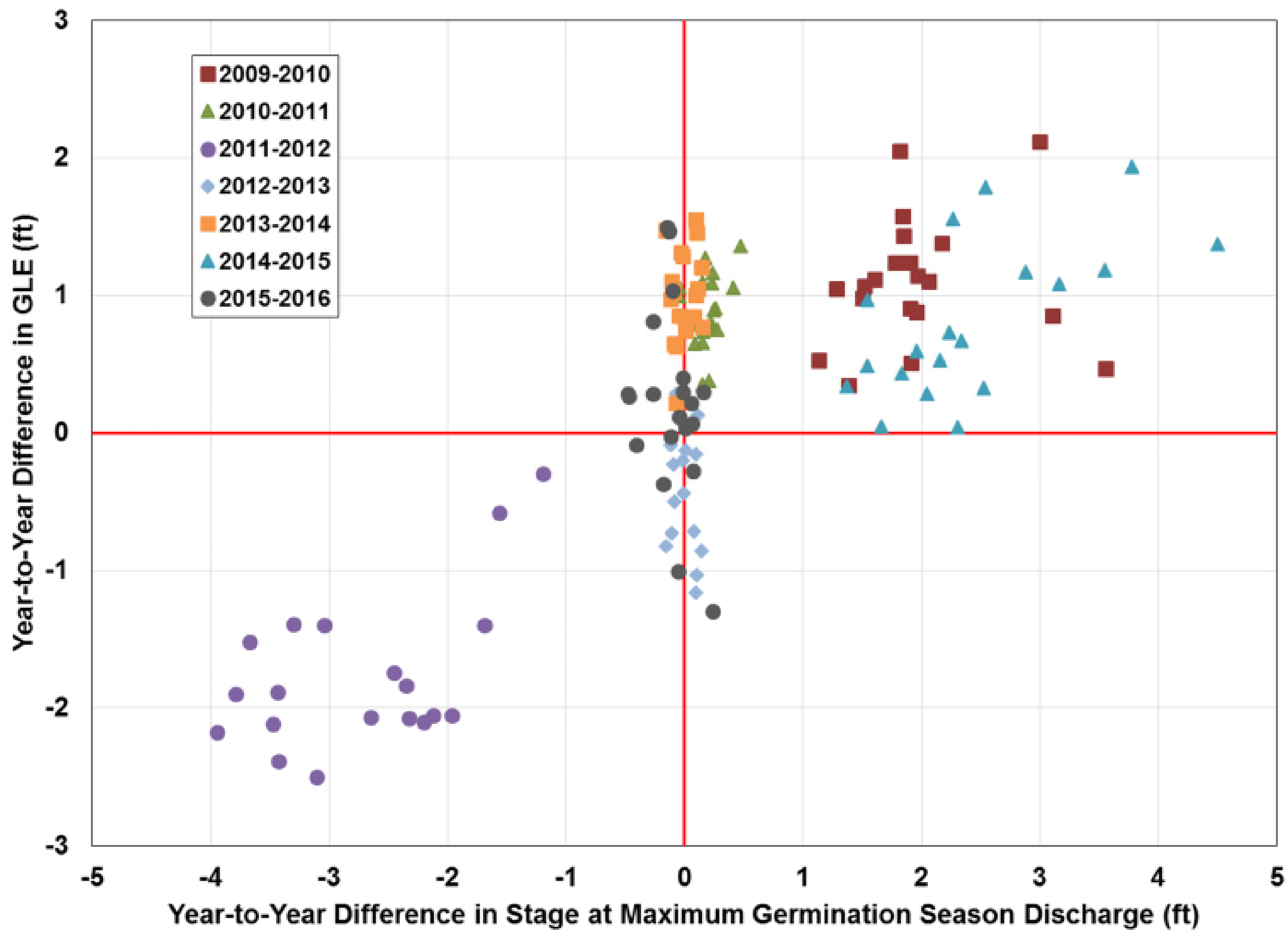

Figure 4.26. Yearly change in GLE versus year-to-year difference in stage at maximum germination season discharge preceding each survey at the pure panel APs (Kendall's τ = 0.53, p=<0.0001).

4.2.5. Total Unvegetated Channel Width versus Stage at Annual Peak Discharge

Correlation between the year-to-year change in total unvegetated channel width and the difference in stage associated with the annual maximum discharge is statistically significant (**Figure 4.27**; Kendall's $\tau = 0.35$, $p<0.0001$).

4.2.6. Total Unvegetated Channel Width versus Stage at Mean Germination Season Discharge

Correlation between the year-to-year change in total unvegetated channel width and the difference in stage associated with the mean germination season discharge is also statistically significant (**Figure 4.28**; Kendall's $\tau = 0.40$, $p<0.0001$).

4.2.7. Total Unvegetated Channel Width versus Green Line Elevation

Similar to the previous two comparisons, the correlation between the year-to-year change in total unvegetated channel width and the corresponding change in GLE is statistically significant (**Figure 4.29**; Kendall's $\tau = 0.43$, $p<0.0001$).

Collectively, all of the results in this section show that both the GLE and unvegetated channel width are responsive to the magnitude of the preceding flows, with the similarly strong correlation between the GLE and the stage associated with both the mean and maximum germination season discharge. This result suggests that inundation that prevents new vegetation and annual species from growing on the sand bars and low elevation areas along the margins of the channel is the key factor in maintaining the unvegetated channel width, as it is defined in the current version of the monitoring plan.

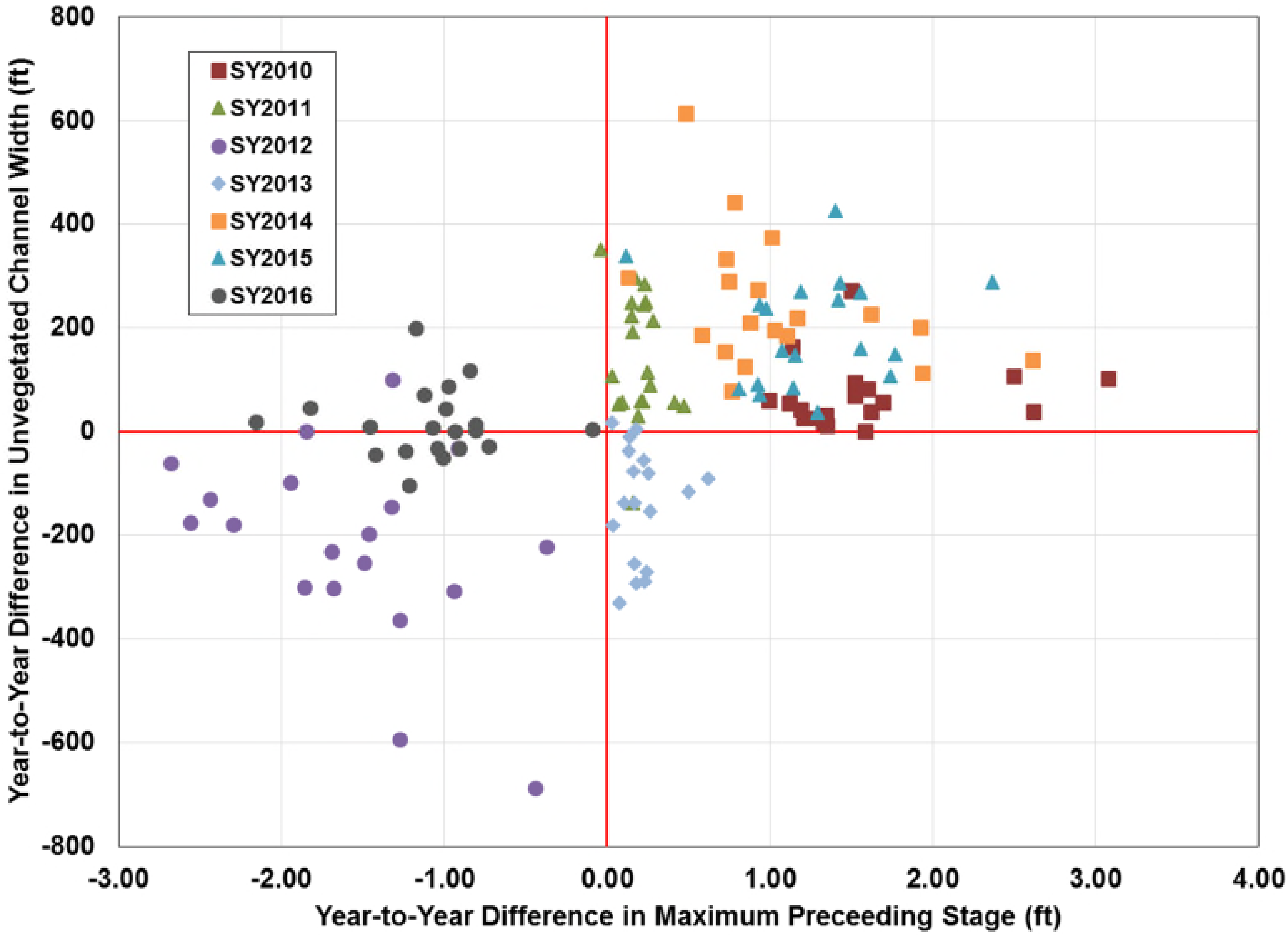

Figure 4.27. Yearly difference in total unvegetated channel width versus year-to-year difference in stage at maximum mean daily flow preceding each survey at the pure panel APs (Kendall's τ = 0.33, p=<0.0001).

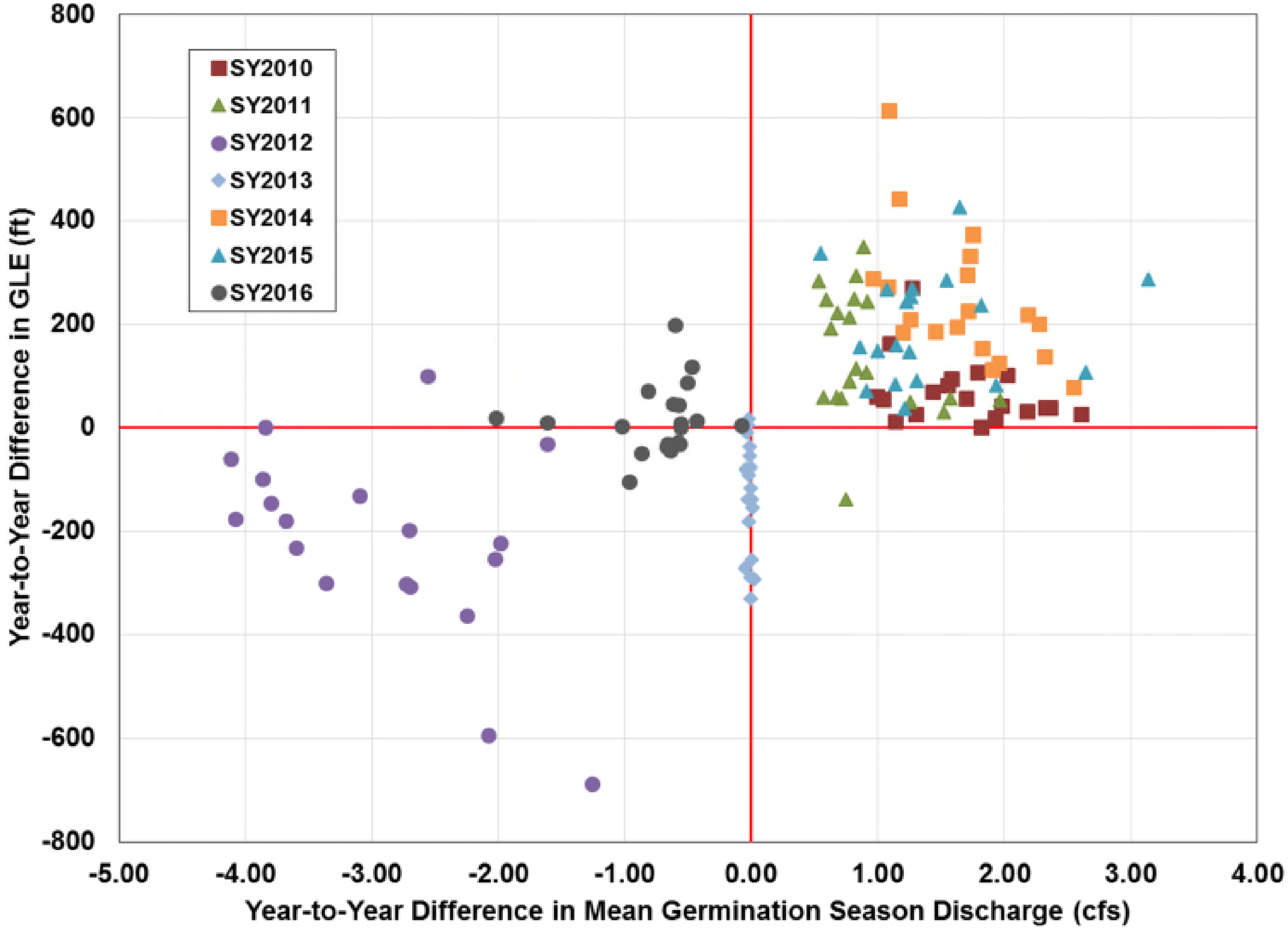

Figure 4.28. Yearly change in total unvegetated channel width versus year-to-year difference in stage at mean discharge during the germination season at the pure panel APs (Kendall's $\tau = 0.37$, p=<0.0001).

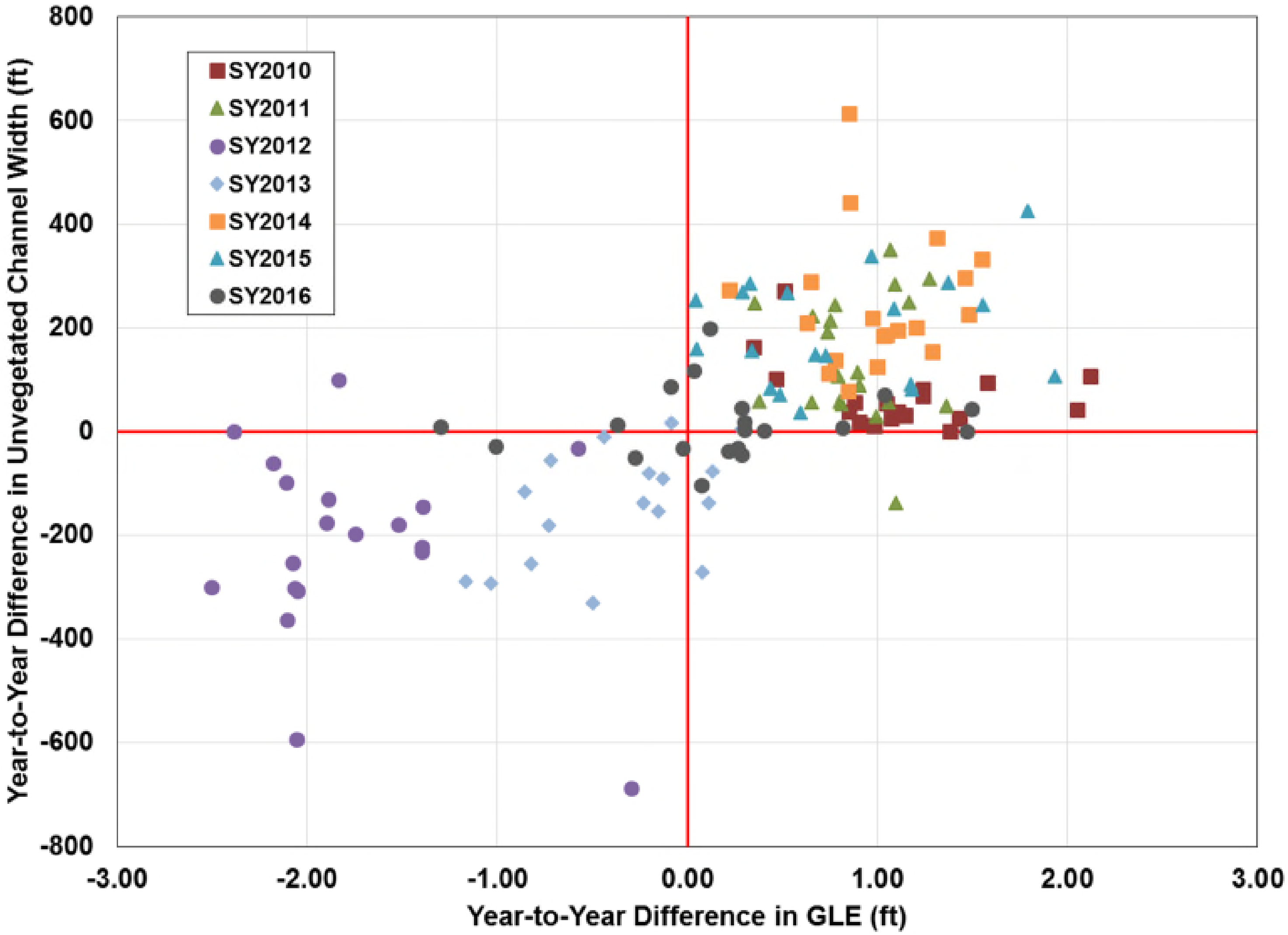

Figure 4.29. Yearly change in total unvegetated channel width versus year-to-year difference in GLE at the primary geomorphic transects of pure panel APs (Kendall's τ = 0.43, p=<0.0001).

4.3 Flow #5

> Increasing the magnitude and duration of the $Q_{1.5}$ will increase riparian plant mortality along the margins of the river. There will be different relations for different species.

Priority Hypothesis Flow #5 postulates that increasing the magnitude and duration of the annual peak discharge will increase riparian plant mortality along the margins of the river, with potentially different relationships for different species. The following section specifically focuses on the relative influence of spraying versus peak flows on the distribution and frequency of common reed (*Phragmites australis*). The analysis was performed using the data from the pure panel APs. Common reed was one of the most prevalent species in the reach during the initial (2009) monitoring survey, in terms of both frequency of occurrence (fourth highest frequency of the sampled species behind ragweed, cocklebur and purple loosestrife) and percent cover (highest of sampled species) (Figures 3.17 and 3.24). The amount of common reed in the overall reach declined substantially between 2009 and 2012 (Cover: 9.1 to 2.7 percent, Frequency: 4.1 to 0.6 percent), and then increased progressively, but at a much slower rate between 2012 and 2015 (Cover: 0.6 to 2.0 percent; Frequency: 2.7 to 4.5 percent) (**Figure 4.30**). The frequency of common reed decreased by a small amount to about 4.1 percent in 2016, but the percent cover actually increased by a small amount to about 2.2 percent.

The variability in the averages among the individual APs was, however, quite high. Based on the percent cover data, common reed was most prevalent in three specific portions of the overall study reach in 2009: AP23 through AP29 near and upstream from Kearney, AP17 and AP19 just upstream from Shelton, and AP1 and AP2 at the downstream end of the reach (**Figure 4.31**). A substantial amount of common reed was also present at AP3 near Grand Island, AP35 in the North Channel at Jeffreys Island and at AP39 just downstream from the Lexington Bridge. With the exception of AP15, AP17, AP25 and AP39, the amount of common reed decreased at all of these anchor points in 2010. At AP17, common reed increased from about 8-percent cover in 2009 to over 16 percent in 2010. The increase at the other three APs was relatively modest. The amount of common reed continued to decline at most of the anchor points from 2010 to 2011, however substantial increases occurred at AP19 and AP27. Generally low levels of common reed persisted through 2013 and 2014, with the most significant increases during this period occurring at AP3, AP23, and AP27. Relatively low level of common reed were present throughout the reach in 2015; however, the levels were somewhat higher than in 2014. The largest increase during the 2014 to 2015 period occurred at AP15 (1% in 2014 to 4.3% in 2015). The amount of common reed in 2016 was similar to 2015, but notable increases occurred at AP1 (1.4% to 8.2%), AP23 (2.3% to 3.9%) and AP31 (1.7% to 4.7%).

A wide range of flows, weather conditions, and Program activities occurred during the eight-year monitoring period that could potentially affect the quantity and distribution of common reed along the reach. Flow conditions could impact growth of common reed and other in-channel vegetation in at least three ways: (1) during low to moderate flows, the river provides an irrigation source, increasing growth potential, (2) high flows during the germination season can inundate the surfaces on which the plants grow, limiting germination potential and plant growth, and (3) during extremely high flows, plants can be removed due to scour around the base of the plants and uprooting due to direct shear or through lateral erosion and undercutting of the plant roots. Weather could also be a factor because growth of most species tends to be stronger during warm, wet periods than either cool, dry or hot, dry conditions. Program activities that affect common reed include disking, mowing and shredding, and herbicide spraying.

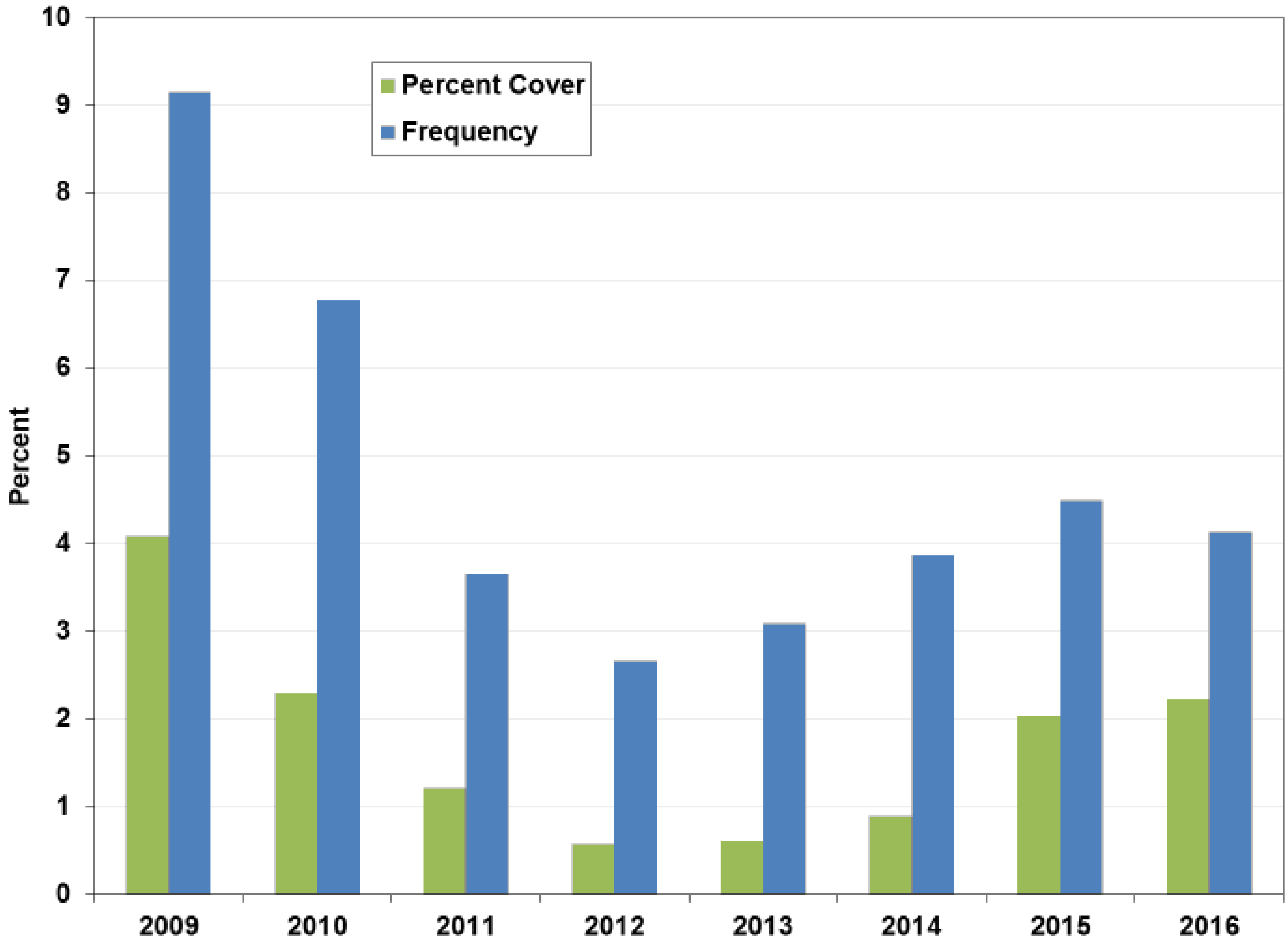

Figure 4.30. Average frequency of occurrence and percent cover for common reed (*Phragmites australis*) on a reach averaged basis observed during each of the six monitoring surveys.

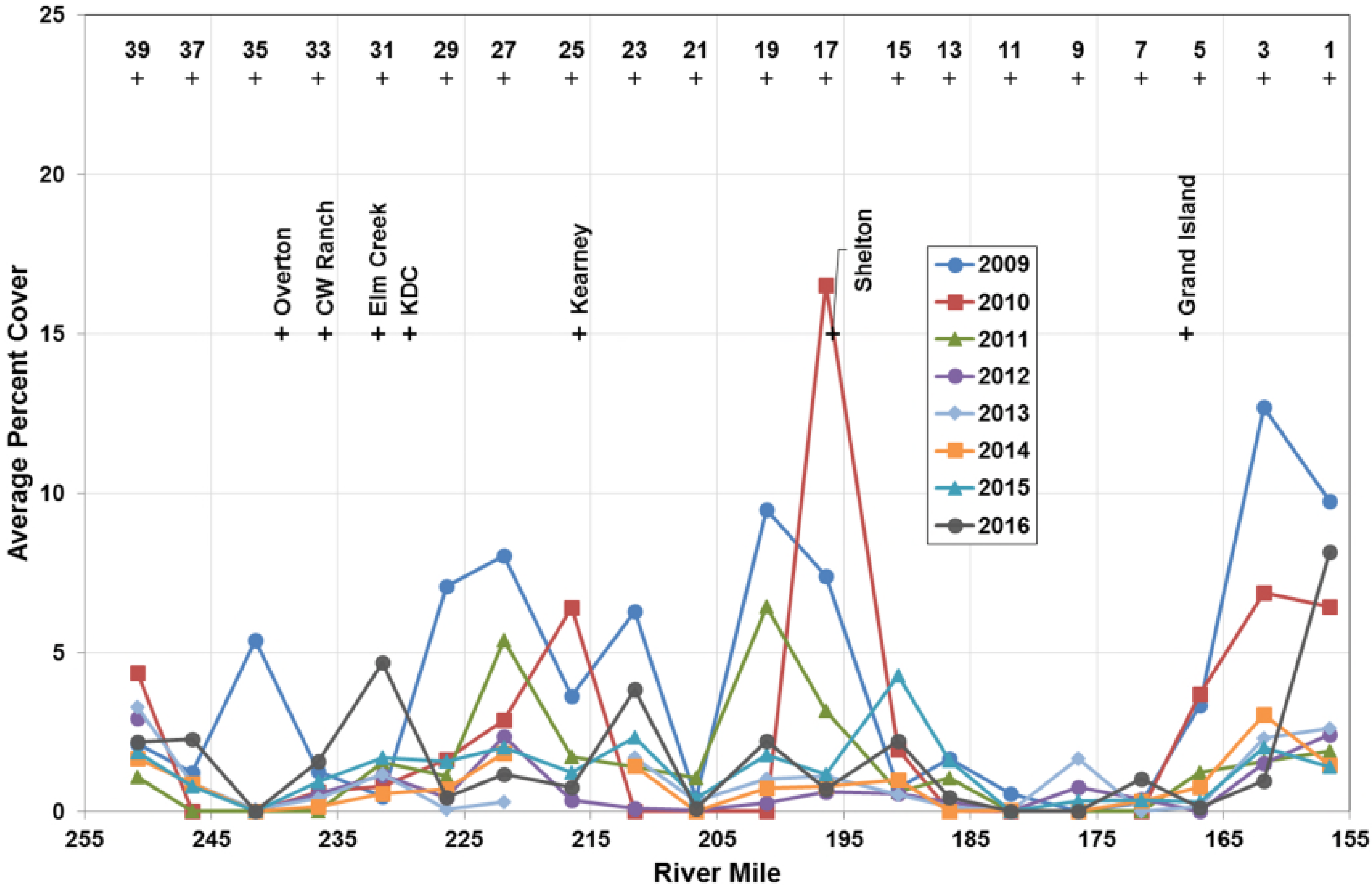

Figure 4.31. Average percent cover of common reed (*Phragmites australis*) at the pure panel anchor points during the six monitoring periods.

Total runoff volume during WY2009 at Overton was only about 52 percent of the long-term average, and this increased to about 120 percent of average in 2010 and nearly 240 percent of average in 2011 (**Figure 4.32**). WY2012 was slightly above normal in terms of total runoff (~110 percent of average); however, the bulk of that runoff occurred during fall 2011. The runoff during the portion of the 2012 growing season preceding the monitoring surveys (April through July) was only about 55 percent of the long-term average. WY2013 was also a very dry year, with the total runoff only about 52 percent of average (including the late-September 2013 flood), but only about 41 percent of average during the portion of the 2013 growing season from April through August. Compared to the long-term average, WY2014 was normal to slightly dry, with total runoff at about 87 percent of the long-term average. WY2015 was the second wettest year since 1990, with total runoff about double the long term average. The period of WY2015 between April 1 and September 1 was the wettest since 1984, with total runoff about 320 percent of the long-term average. Total runoff in 2016 was similar to 2015, the 3rd wettest since 1990, and the runoff between April 1st and September 1st was exceeded only in 1995, 2011 and 2015 during that period.

Three specific variables were considered in evaluating the potential effects of flow on the prevalence of common reed:

1. Inundation depth at the maximum discharge (D_{max}),
2. Duration of inundation (Dur), and
3. Persistence of low flows during the growing season, quantified as the low flow that was equaled or exceeded 90 percent of the time (Q_{low}).

The inundation depth at the maximum discharge (D_{max}) was selected as a surrogate for the effects of high flows, since the maximum velocities and shear stresses at the individual points are not available. A two-dimensional model was developed by Tetra Tech (2012) for the Elm Creek Complex, however, that can provide an indication of the range of anticipated velocities for different flow depths. While the hydraulic characteristics of the APs will vary to some degree from those at the Elm Creek Complex, the range of variability in the relationship between depths and velocities is probably similar. Based on a comparison of the maximum water-surface elevation from the existing 1-dimensional HEC-RAS model with the elevations of the individual quadrats that contained common reed, about 45 percent of the quadrats were not inundated during the growing season in 2009, and this decreased to only 3 percent in 2010 and 5.5 percent in 2011 (**Figure 4.33**). In both 2012 and 2013, more than 90 percent of quadrats with common reed were not inundated due to the persistent low flows. In 2014 and 2015, spring flows were much higher, and only about 13 and 4 percent of quadrats with common reed were not inundated, respectively. About 84 percent of the quadrats were inundated to at least a minimal during the growing season in 2016. The percentage of quadrats inundated to a depth of at least one ft during each growing season ranged from a low of 2 percent to 3 percent in 2012 and 2013 to a maximum of nearly 75 percent to 80 percent in 2012 and 2015.

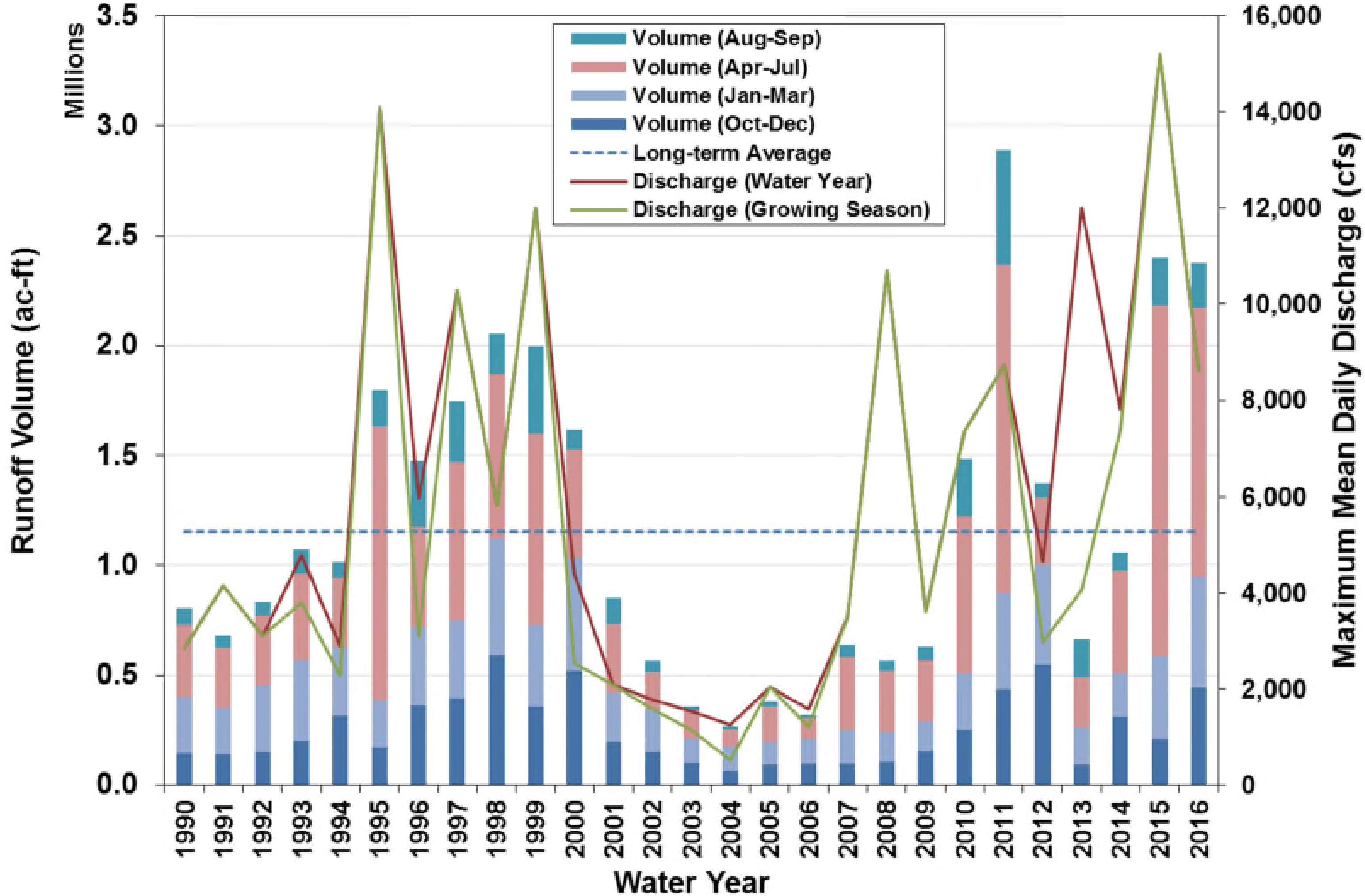

Figure 4.32. Total runoff volume at Overton during four periods of the water year and the maximum mean daily discharge during the entire water year and between April 1 and August 1 (~time of monitoring surveys) from WY1990 through WY2016. Long-term average volume based on gage data from WY1941 through WY2016.

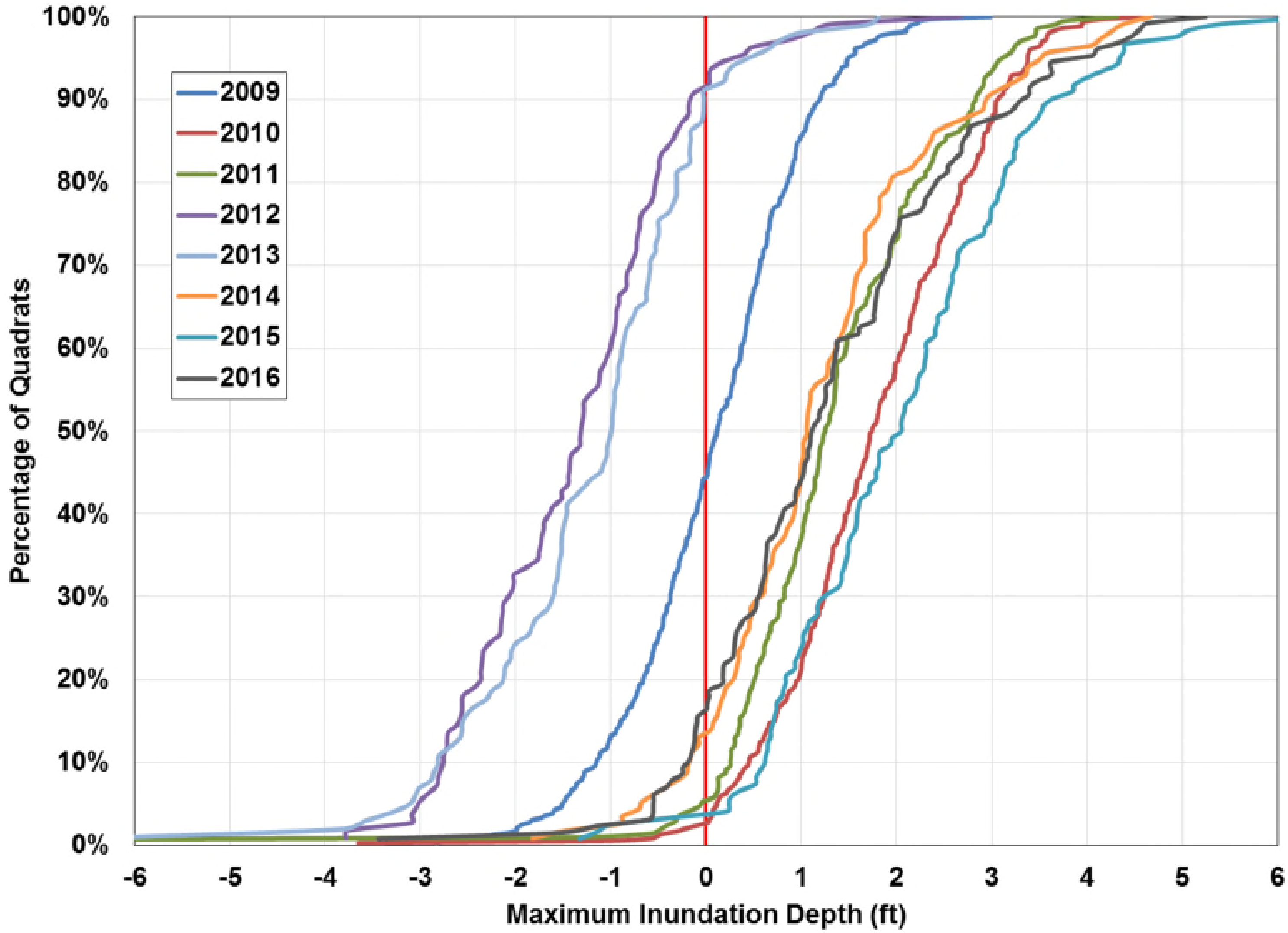

Figure 4.33. Cumulative distribution of inundation depths at the maximum discharge during the growing season for quadrats containing common reed during each of the five monitoring surveys.

Based on results from the Elm Creek 2-D model, maximum velocities at locations with depths in the 1 to 3 ft range are about 6 fps, and most areas have velocities between 1.5 and 4 fps (**Figure 4.34**). Pollen-Bankhead et al. (2011) found that very high velocities, well above those that occur in the Platte River, are required to uproot established common reed plants (**Figure 4.35**); thus, it is unlikely that this process is responsible for the reduction in common reed during the monitoring period. If common reed is removed by the direct action of the water, this most likely occurs through lateral erosion and undercutting of the sandbars and banklines on which the plants are growing (**Figure .36**). While this does occur in the study reach, field observations indicate that it occurs only in limited areas, primarily on the heads, and to a lesser extent, along the margins, of the sand bars. The thick, rhizomatous root structure appears to be very effective in binding the soil and limiting the rate and magnitude of lateral erosion and undercutting in areas where common reed is abundant.

Weather conditions during the monitoring period varied in a manner that is generally similar to the runoff. In 2009, the total precipitation during the portion of the growing season prior to the monitoring surveys (April 1 through July 31, for purposes of this analysis) varied from about 10 inches to 11 inches upstream from Elm Creek to 15.6 inches at the downstream end of the reach (**Figure 4.37**). Precipitation during this period in 2010 ranged from about 12.8 inches at Cozad to more than 19 inches near Grand Island. A similar amount of precipitation was observed in 2011, with the highest measurements occurring near Kearney (~20 inches). Precipitation during 2012 was very low, with total rainfall between April 1 and July 1 of 9.2 inches to 9.4 inches at Kearney and Wood River, 6.7 inches to 7.1 inches at Cozad and Elm Creek, and only about 5.1 inches at Grand Island. Precipitation in 2013 and 2014 were similar to 2009, with approximately 10 inches of rain falling at Cozad, increasing downstream to 13.6 inches (2013) and 15.5 inches (2014) at Grand Island. In 2015, precipitation was somewhat higher than in 2014, ranging from 12.4 inches at Cozad to 16.3 inches at Wood River. More precipitation was observed at Cozad in 2016 (16.0 inches) than in any of the other years, while less precipitation was observed at Wood River than other year (8.6 inches). Overall, 2012 was the driest year, averaging about 7.5 inches at the five gages, and 2010 was the wettest, averaging about 17 inches.

Based on data from the weather station at Grand Island Regional Airport [the only station in the Global Historical Climatology Network (GHCN) in close proximity to the study reach for which long-term temperature records are maintained], the mean daily temperature during April through July is 64.9°F (**Figure 4.38**). In 2009, this period was cooler than average, with mean temperature of 63.4°F. It was slightly warmer than normal in 2010 and 2011 (65.6°F and 65.2°F, respectively), very warm in 2012 (70.3°F), and then slightly cooler than normal (64.2°F) in 2013. In 2014 and 2015, the average growing season temperature was very close to the long term (1938-2015) average, with temperatures of 65.2°F and 64.7°F, respectively. The 2016 growing season temperature of 66.3°F was slightly above average.

A metric that quantifies the overall temperature regime during the growing season that affects plant growth is growing degree days (GDD). GDD is computed based on the deviation of the minimum and maximum temperatures from a reference temperature chosen based on plant or animal species and life stage of interest. GDD values are cumulative measures of heat, as plants will mature in a stepwise manner based on the ambient air temperature in the absence of atypical environmental stressors such as drought or disease. As a result, higher values of GDD indicate greater growth potential. Using a base temperature of 50°F[20], the long-term average GDD (1938 to 2016) at the

[20] The value of GDD is very sensitive to the chosen base temperature. In this case, 50°F was chosen based on the analysis of Gilmore et al. (2010), which correlates GDD and reflectance ratio for remote sensing of Phragmites sp. in coastal environments. The adequacy of 50°F is supported by Galinato (1986), considering the common temperatures required for germination of Phragmites australis seeds.

Grand Island Station was 1,948 (Figure 4.38). In both 2009 and 2015, GDD was below the long-term average (1,769 and 1,851, respectively), 2010, 2011, 2013, and 2014 were about average (1,955, 1,969, 1,981, and 1,987, respectively), and 2016 was slightly above average. The growing season in 2012 had the highest GDD value of the 8 monitoring years (2,487).

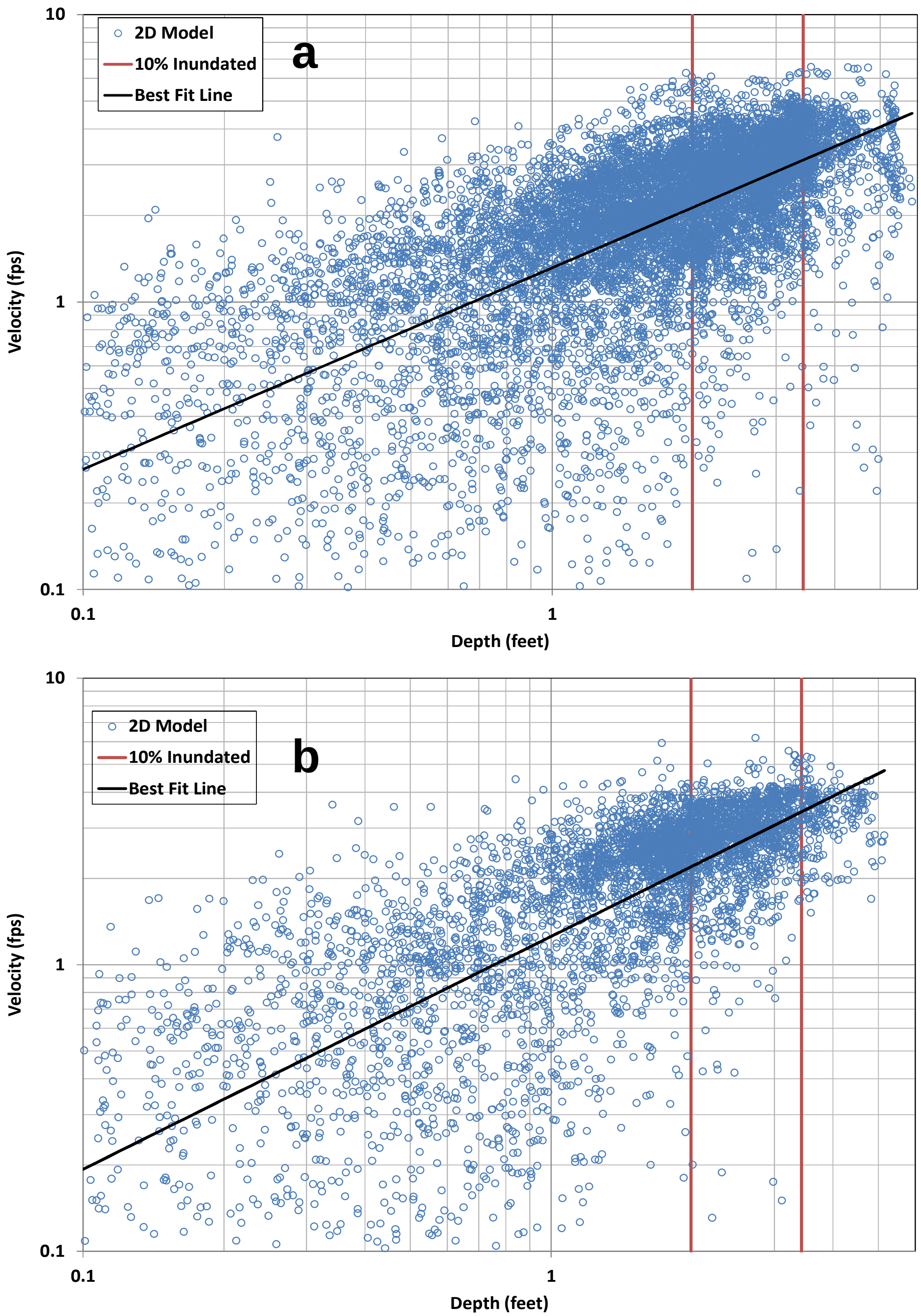

Figure 4.34. Depths and velocities from the Elm Creek 2-D model at a discharge of approximately 3.200 cfs: (a) Elm Creek Bridge to Kearney Diversion Structure, (b) downstream from Kearney Diversion Structure.

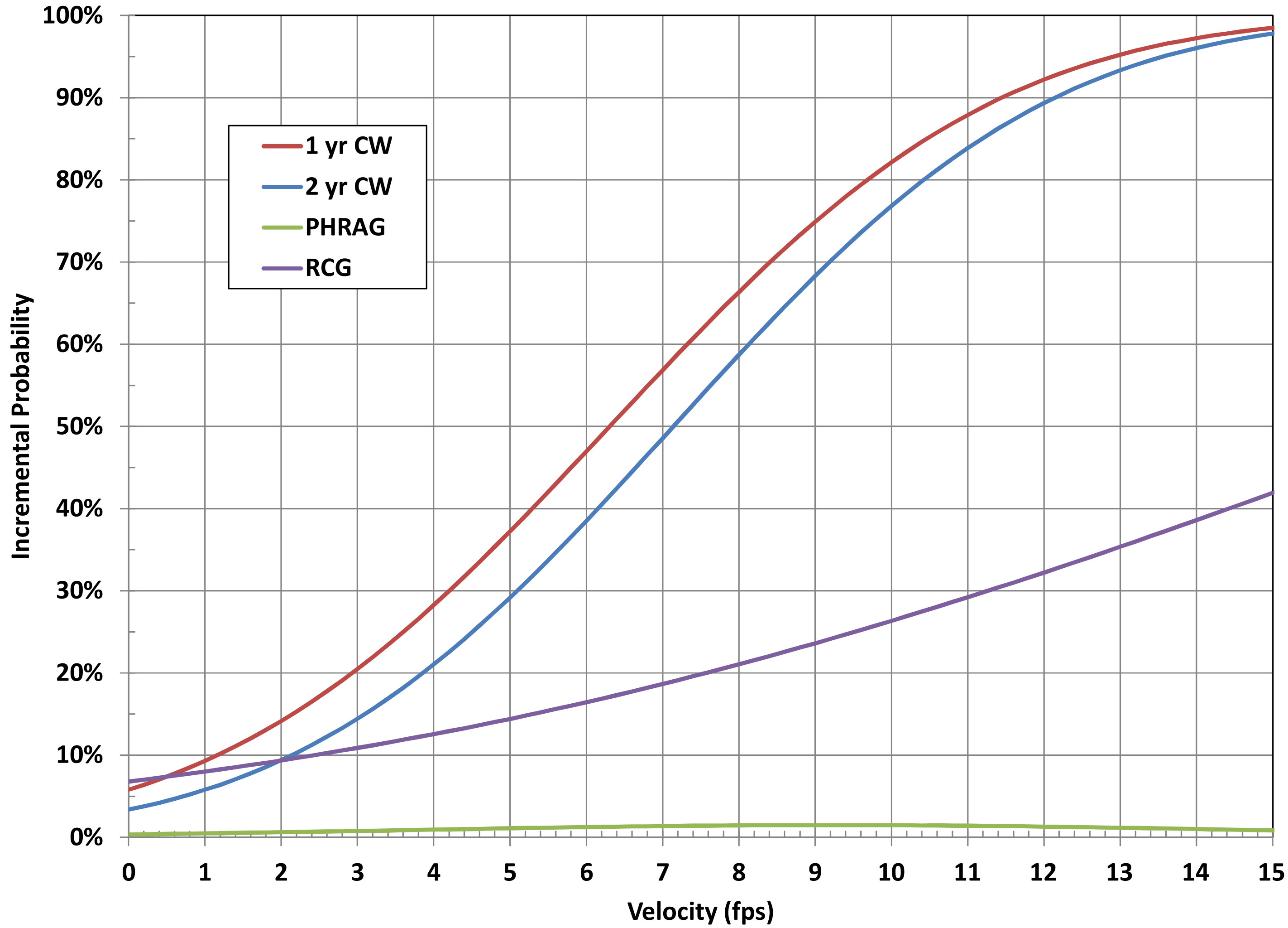

Figure 4.35. Incremental probability of plant removal for 1- and 2-year-old Cottonwood (1- and 2-year CW), common reed (PHRAG) and reed canary grass (RCG) based on results from Pollen-Bankhead et al. (2011).

Figure 4.36. Typical lateral erosion and undercutting of the edge of a sand bar with common reed in the Elm Creek Complex.

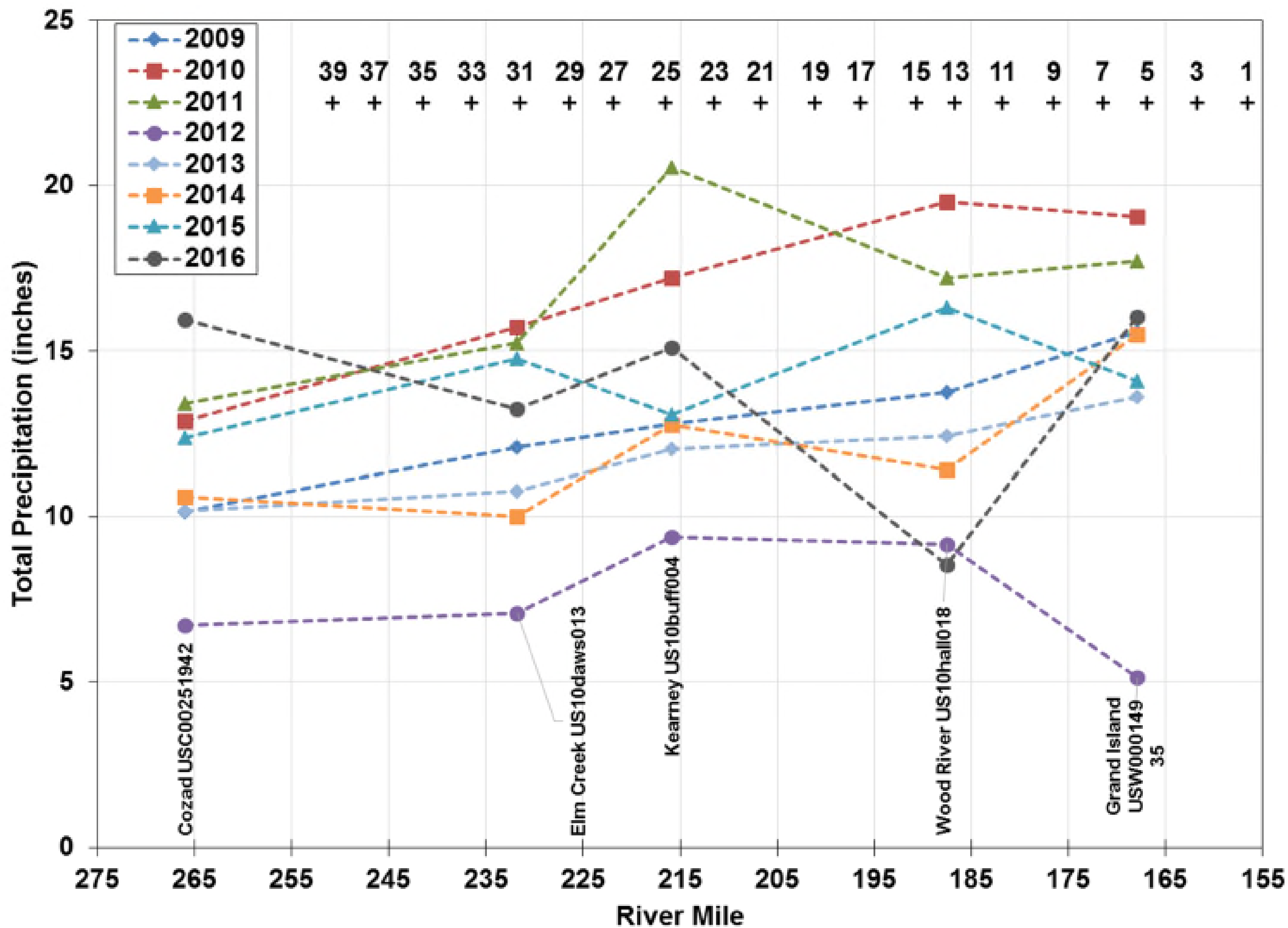

Figure 4.37. Total precipitation during the period from April through July in each of the seven monitoring years at five weather stations along the project reach. [Global Historical Climatology Network (GHCN) station numbers used as the data source follow the names].

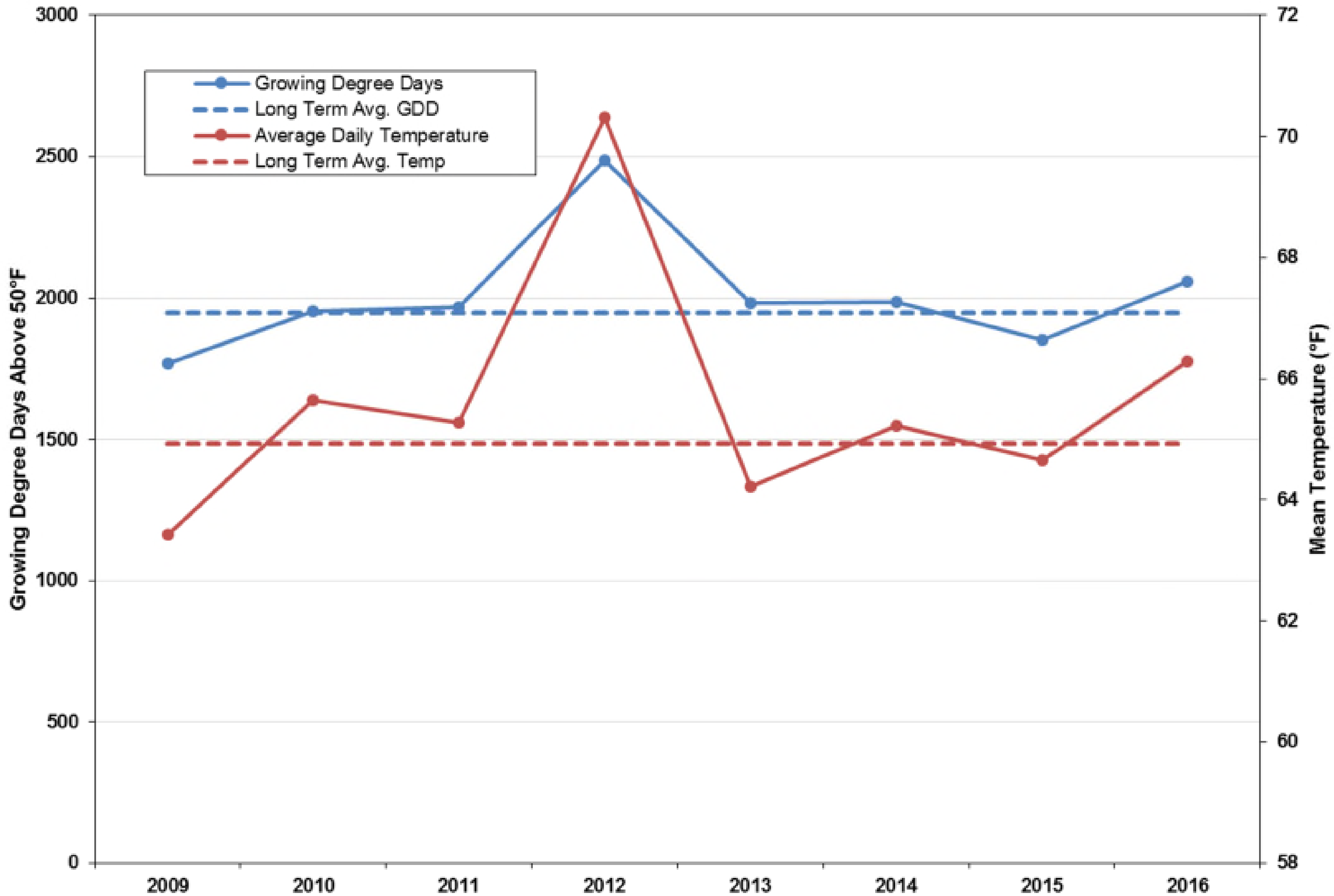

Figure 4.38. Growing degree days (GDD) above a baseline temperature of 50 °F and average temperature at the GHCN Grand Island Station (GCHND Sta USW00014935) during the period from April through July during the monitoring period.

Mechanical actions performed by the Program that can affect the presence and persistence of common reed include herbicide spraying, disking, mowing and shredding on the surface of the sand bars, and in some cases, direct grading to construct new islands. The Program maintains a GIS database documenting these actions that includes the specific limits of spraying. This database was used to identify the anchor points at which spraying occurred (**Table 4.4**). The database was also used to quantify the spraying intensity at each of the pure panel APs by identifying the individual quadrats that fall within the spraying limits, and calculating the percentage of the quadrats that were sprayed prior to each sampling period (**Figure 4.39**). Spraying typically occurs in September and October of each year, with the intensity varying along the reach, based at least in part, on the amount of common reed that is present. Spraying occurred at 7 of the 20 pure panel APs in Fall 2008 (i.e., prior to Survey Year 2009), with about 9 percent of the approximately 4,300 vegetation quadrats that were sampled in 2009 being sprayed (**Figure 4.40**). The spraying intensity was significantly higher in Fall 2009 than all of the other monitoring years, with at least some spraying at 13 of the 20 pure panel APs, and about 28 percent of the approximately 5,900 quadrats being sprayed. After Fall 2009, the spraying intensity ranged from about 4 percent in Fall 2013 and 2014 to 10 percent in Fall 2011.

The database was also used to identify other mechanical actions at the anchor points that could potentially affect the amount of phragmites (**Table 4.5**). Disking was conducted at four of the pure panel APs (AP9, AP11, AP15 and AP19) in 2008, no disking occurred between 2009 and 2012, and only AP11 was disked in 2013. The amount of common reed that was present at AP9 and AP11 in 2009 when the monitoring program began was relatively low; however, AP19 had a relatively large amount, in spite of the disking. None of these APs was sprayed in 2008. Shredding and mowing was conducted at AP7 and AP29 in 2008. About 75 percent of the vegetation quadrats at AP7 were sprayed and no spraying occurred at AP29 in 2008. The monitoring data indicate that little or no common reed was present at AP7, and AP29 had among the largest amounts of common reed in 2009. Shredding and mowing occurred at four of the APs (AP9, AP13, AP37 and AP39), and large, mid-channel islands were mechanically removed at AP33 in Fall 2009. The amount of common reed at these APs was relatively low in 2010. Aside from spraying, the only mechanical actions documented in the Program database for Fall 2010 was shredding and mowing at AP29. With the exception of AP19, AP27 and AP39, the amount of common reed present at the pure panel APs was relatively low in 2011. Spraying was the only documented Program action at the pure panel APs potentially affecting the amount of common reed in Fall 2011, and documented actions other than spraying in Fall 2012 consisted of clearing and grubbing at AP23 and shredding and mowing at AP31. Very little common reed was present at these APs in 2012. From 2013 to 2015, disking and spraying were the only documented program maintenance actions.

Table 4.4. Anchor points at which at least some aerial spraying occurred during the indicated year.

AP	Maintenance Year							
	2008	2009	2010	2011	2012	2013	2014	2015
40	■			■	■	■	■	■
39					■	■	■	■
38	■			■	■	■	■	■
37B	■			■	■	■	■	■
37A	■			■	■	■	■	■
36B	■			■	■	■	■	■
36A	■			■	■	■	■	■
35B	■			■				■
35A	■			■		■	■	■
34	■			■	■	■	■	■
33N	■			■	■	■	■	
33	■			■				■
33S					■			■
32N	■			■		■	■	■
32	■			■		■	■	■
32S								
31	■			■	■	■	■	■
30	■	■	■	■	■		■	
29		■	■	■	■	■	■	
28		■	■	■	■		■	
27		■		■	■		■	
26		■		■	■	■	■	
25		■		■	■	■	■	
24		■		■	■	■	■	
23B		■	■	■	■	■	■	
23A		■	■	■	■	■	■	■
22B		■	■	■	■	■	■	
22A		■	■	■	■	■	■	■
21B		■		■	■	■	■	
21A		■		■	■	■	■	■
20B		■		■	■	■	■	
20A		■		■	■	■	■	■
19B		■	■	■	■	■	■	■
19A		■	■	■	■	■	■	■

AP	Maintenance Year							
	2008	2009	2010	2011	2012	2013	2014	2015
18		■	■	■	■	■	■	
17			■	■	■	■	■	
16			■	■	■	■	■	
15			■	■	■	■	■	■
14		■	■	■	■	■	■	■
13B			■		■	■	■	■
13A		■		■	■	■		■
12B			■		■	■	■	■
12A		■		■	■	■		
11B		■		■	■	■	■	■
11A		■		■	■			■
10C		■		■				■
10B								
10A			■	■	■	■	■	■
10		■		■	■	■	■	
9C		■	■	■		■	■	■
9B		■		■	■	■		■
9A		■		■	■		■	
8D				■	■	■		■
8C		■					■	
8B		■		■				
8A		■		■	■	■	■	
7C				■		■	■	■
7B		■					■	■
7A		■	■	■	■	■	■	
6B				■			■	■
6A		■	■	■	■		■	
5		■	■	■	■	■	■	
4		■	■	■	■	■	■	
3		■	■	■	■	■	■	
2		■	■	■	■	■	■	
1		■	■	■	■	■	■	

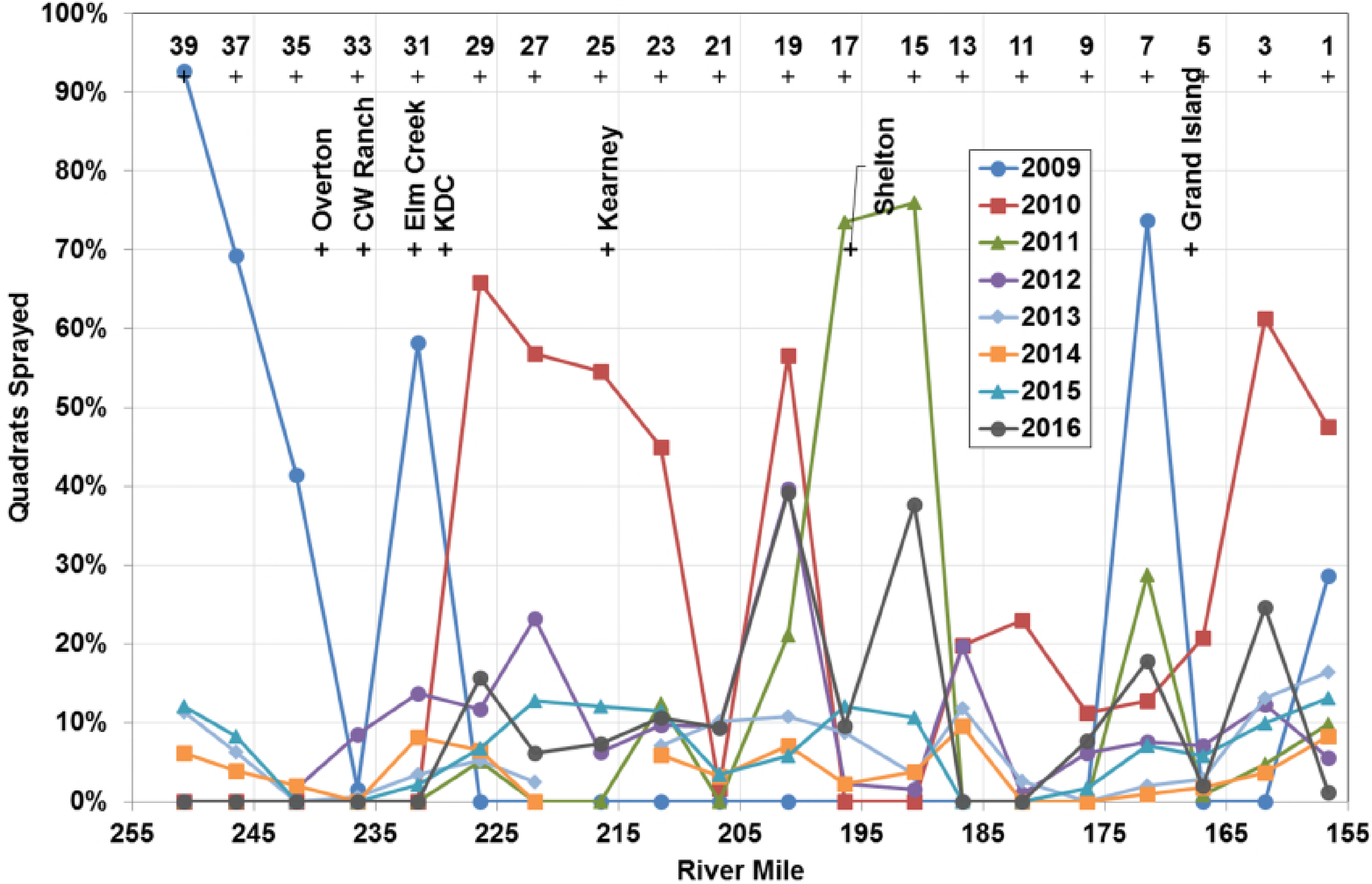

Figure 4.39. Percentage of individual vegetation sampling quadrats sprayed at each of the pure panel APs prior to each sampling period. Spraying typically occurs in early-fall; thus, the spraying indicated for each year occurred during fall of the previous year.

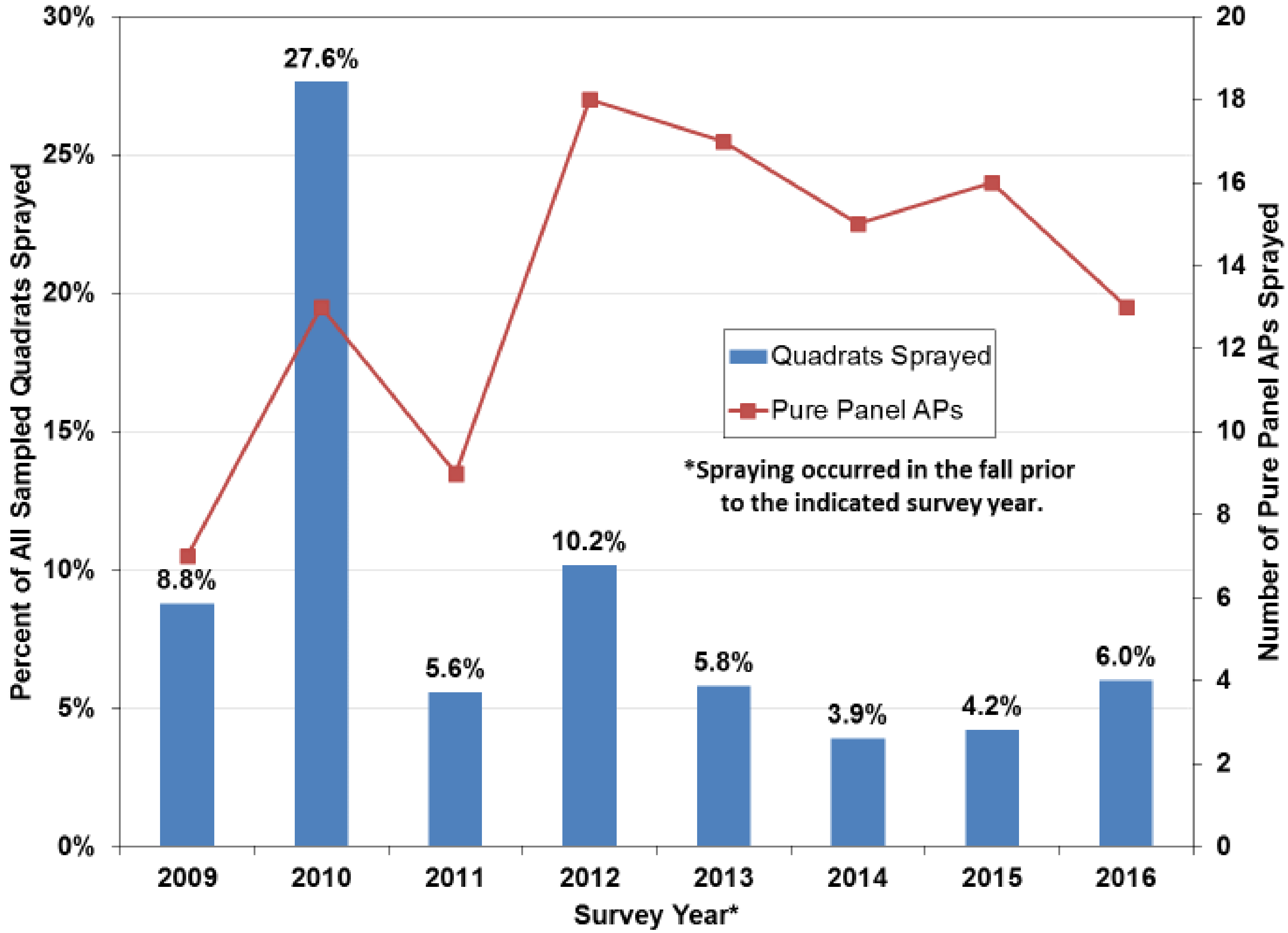

Figure 4.40. Percentage of all sampled quadrats sprayed at pure panel anchor points and number of pure panel APs receiving at least some spraying during the preceding fall of the indicated year. First number in each label is number of quadrats sprayed; second number is total number of sampled quadrats.

Table 4.5. Summary of PRRIP mechanical and other direct treatments at the APs for 2008 through 2015 other than aerial spraying.

Anchor Point	2008	2009	2010	2011	2012	2013	2014	2015
40	Shredding/Mowing	Shredding/Mowing, Chemical						
39	Chemical	Shredding/Mowing, Chemical						No documented actions
38	Tree Clearing, Chemical	Shredding/Mowing						
37A	Tree Clearing	Shredding/Mowing						
35B							Disking	
34		Shredding/Mowing	Shredding/Mowing					
33		Island Construction, Tree Clearing/Removal	Off Channel Habitat	Pre-emergent, Chemical	Prescribed Fire, Noxious Weed Control, Tree Clearing		Disking	
32			Shredding/Mowing, Chemical, Tree Clearing	Herbicide	Prescribed Fire, Noxious Weed Control, Shredding/Mowing		Disking	
31					Shredding/Mowing			
30	Disking	Disking, Chemical	Clear and Smooth, Tree clearing, disking	Grass Seeding, Herbicide, disking	Prescribed fire, tree clearing, Island Construction, disking, Pre-emergent, Noxious Weed Control		Disking	
29	Shredding/Mowing	Shredding/Mowing	Shredding/Mowing					
28	Shredding/Mowing	Shredding/Mowing						
24				Herbicide				
23	Spraying			Herbicide	Clear and Grub			
22	Spraying			Noxious Weed Control, Seedbed Prep, Grass Seeding, Herbicide		Disking	Disking	
21	Spraying,							
20	Spraying							
19	Disking							
18	Disking	Chemical						
16		Chemical	Shredding/Mowing					
15	Spraying							
14	Disking					Disking	Disking	
13B		Shredding/Mowing			Tree Clearing, Seedbed Prep.			
13A				Herbicide				
12				Prescribed Fire, Herbicide, Tree/brush mulching	Disking, Pre-emergent, Shredding/Mowing	Disking	Disking	
11B				Herbicide		Disking		
11A	Disking			Herbicide		Disking		
10A	Disking	Shredding/Mowing, Chemical						
9C		Shredding/Mowing, Chemical						
9A	Disking							
8D	Shredding/Mowing	Shredding/Mowing, Chemical						
8A	Shredding/Mowing	Shredding/Mowing, Chemical						
7C		Shredding/Mowing, Chemical						
7A	Shredding/Mowing	Chemical						
6B	Shredding/Mowing	Shredding/Mowing, Chemical						
6A	Chemical	Chemical						
1	Chemical	Chemical						

Based on the available information related to the above factors, a multiple correlation analysis was conducted using the Spearman correlation coefficient (ρ) to assess whether there is a statistically-significant relationship between average percent cover and year-to-year change in percent cover of common reed at the pure panel APs and the following six variables:

1. Percent of quadrats at the AP sprayed (Percent Sprayed),
2. Maximum depth of inundation averaged over all quadrats (D_{avg}),
3. Average duration of inundation for all quadrats (Dur),
4. Discharge equaled or exceeded 90 percent of the time (Q_{low}),
5. Number of growing degree days during the growing season preceding the monitoring surveys (April through July) (GDD),
6. Total precipitation during the growing season preceding the monitoring surveys (April through July) (Precip).

The Spearman coefficient is based on the ranks of the observations and not their values; thus, it does not rely on assumptions of normality and linearity. The analysis was performed only on the pure panel APs that had more than 3.5-percent average cover during the initial monitoring survey (2009)[21], since changes at those with lower amounts provide little contrast to assess the effects of the various parameters. As illustrated in Figure 4.31, the amount of common reed changed very little at the APs that were not included in the analysis. The analysis for total percent cover of common reed indicates statistically-significant negative correlation only with growing degree days (ρ=-0.43, p<0.0001) and positive correlation with total precipitation (ρ=0.27, p=0.024) (**Table 4.6**).

The positive correlation with spraying is a misleading result, because the spraying was focused on areas with significant amounts of common reed. To overcome this issue, the correlation was also performed on the year-to-year change in percent cover versus the listed variables (**Table 4.7**). Because data on the amount of common reed prior to the 2009 surveys are not available, the data were reduced to only the last 7 years of the surveys. Results of the analysis indicate that the only one of the above variables with which year-to-year change in percent cover of common reed has statistically-significant correlation is percent of quadrats sprayed (ρ=-0.28, p=0.032) (**Figure 4.41**). The lack of correlation with the number of growing degree days, maximum inundation depth, duration of inundation, persistence of low flows during the growing season, and precipitation can be clearly seen in the data plots (**Figures 4.42a-e**). The lack of correlation with maximum inundation depths and duration of inundation, in particular, indicates that high flows are not effective in removing common reed. It is also interesting to note that other mechanical activities (i.e., discing, mowing, shredding) does not appear to have had a substantial influence on the change in percent cover at the three locations where it occurred in conjunction with spraying (see brown dots in Figure 4.41).

[21] This includes APs 1, 3, 5, 17, 19, 23, 25, 27, 29, 35A, and 39.

Table 4.6. Correlation (Spearman) and p-values for percent cover of common reed versus possible influencing variables.

Correlation matrix (Spearman):								
Variables	**Percent of Quadrats Sprayed at Anchor Point**	**Maximum Inundation Depth (ft)**	**Duration of Inundation (days)**	**90% Exceedance Discharge (cfs)**	**Growing Degree Days (GDD)**	**Total Precipitation (in)**	**Percent Cover Total**	**Percent Cover Common Reed**
Percent of Quadrats Sprayed at Anchor Point	**1**	0.117	0.212	0.165	0.056	0.177	0.152	0.048
Maximum Inundation Depth (ft)	0.117	**1**	**0.704**	**0.498**	**-0.329**	**0.605**	0.052	0.052
Duration of Inundation (days)	0.212	**0.704**	**1**	**0.663**	**-0.275**	**0.707**	-0.139	0.174
90% Exceedance Discharge (cfs)	0.165	**0.498**	**0.663**	**1**	**-0.470**	**0.784**	-0.139	0.152
Growing Degree Days (GDD)	0.056	**-0.329**	**-0.275**	**-0.470**	**1**	**-0.406**	-0.149	**-0.430**
Total Precipitation (in)	0.177	**0.605**	**0.707**	**0.784**	**-0.406**	**1**	0.082	**0.270**
Percent Cover Total	0.152	0.052	-0.139	-0.139	-0.149	0.082	**1**	**0.443**
Percent Cover Common Reed	0.048	0.052	0.174	0.152	**-0.430**	**0.270**	**0.443**	**1**
p-values:								
Percent of Quadrats Sprayed at Anchor Point	**0**	0.334	0.078	0.172	0.646	0.144	0.210	0.692
Maximum Inundation Depth (ft)	0.334	**0**	**0.000**	**0.000**	**0.006**	**0.000**	0.670	0.667
Duration of Inundation (days)	0.078	**0.000**	**0**	**0.000**	**0.021**	**0.000**	0.249	0.149
90% Exceedance Discharge (cfs)	0.172	**0.000**	**0.000**	**0**	**0.000**	**0.000**	0.249	0.209
Growing Degree Days (GDD)	0.646	**0.006**	**0.021**	**0.000**	**0**	**0.000**	0.218	**0.000**

Correlation matrix (Spearman):								
Variables	**Percent of Quadrats Sprayed at Anchor Point**	**Maximum Inundation Depth (ft)**	**Duration of Inundation (days)**	**90% Exceedance Discharge (cfs)**	**Growing Degree Days (GDD)**	**Total Precipitati on (in)**	**Percent Cover Total**	**Percent Cover Common Reed**
Total Precipitation (in)	0.144	**0.000**	**0.000**	**0.000**	**0.000**	**0**	0.501	**0.024**
Percent Cover Total	0.210	0.670	0.249	0.249	0.218	0.501	**0**	**0.000**
Percent Cover Common Reed	0.692	0.667	0.149	0.209	**0.000**	**0.024**	**0.000**	**0**

Values in bold are different from 0 at a significance level (α)=0.05

Table 4.7. Correlation (Spearman) and p-values for year-to-year change in percent cover of common reed versus possible influencing variables.

Correlation matrix (Spearman):								
Variables	**Percent of Quadrats Sprayed at Anchor Point**	**Maximum Inundation Depth (ft)**	**Duration of Inundation (days)**	**90% Exceedance Discharge (cfs)**	**Growing Degree Days (GDD)**	**Total Precipitation (in)**	**Change in Percent Cover Total**	**Change in Percent Cover of Common Reed**
Percent of Quadrats Sprayed at Anchor Point	**1**	0.117	0.212	0.165	0.056	0.177	-0.046	**-0.276**
Maximum Inundation Depth (ft)	0.117	**1**	**0.704**	**0.498**	**-0.329**	**0.605**	-0.133	-0.003
Duration of Inundation (days)	0.212	**0.704**	**1**	**0.663**	**-0.275**	**0.707**	**-0.350**	-0.049
90% Exceedance Discharge (cfs)	0.165	**0.498**	**0.663**	**1**	**-0.470**	**0.784**	**-0.510**	-0.033
Growing Degree Days (GDD)	0.056	**-0.329**	**-0.275**	**-0.470**	**1**	**-0.406**	0.127	-0.134
Total Precipitation (in)	0.177	**0.605**	**0.707**	**0.784**	**-0.406**	**1**	**-0.348**	-0.074
Change in Percent Cover Total	-0.046	-0.133	**-0.350**	**-0.510**	0.127	**-0.348**	**1**	**0.334**
Change in Percent Cover of Common Reed	**-0.276**	-0.003	-0.049	-0.033	-0.134	-0.074	**0.334**	**1**
p-values:								
Percent of Quadrats Sprayed at Anchor Point	**0**	0.334	0.078	0.172	0.646	0.144	0.723	**0.032**
Maximum Inundation Depth (ft)	0.334	**0**	**0.000**	**0.000**	**0.006**	**0.000**	0.305	0.980
Duration of Inundation (days)	0.078	**0.000**	**0**	**0.000**	**0.021**	**0.000**	**0.006**	0.708

Correlation matrix (Spearman):								
Variables	**Percent of Quadrats Sprayed at Anchor Point**	**Maximum Inundation Depth (ft)**	**Duration of Inundation (days)**	**90% Exceedance Discharge (cfs)**	**Growing Degree Days (GDD)**	**Total Precipitation (in)**	**Change in Percent Cover Total**	**Change in Percent Cover of Common Reed**
90% Exceedance Discharge (cfs)	0.172	**0.000**	**0.000**	**0**	**0.000**	**0.000**	**0.000**	0.799
Growing Degree Days (GDD)	0.646	**0.006**	**0.021**	**0.000**	**0**	**0.000**	0.329	0.301
Total Precipitation (in)	0.144	**0.000**	**0.000**	**0.000**	**0.000**	**0**	**0.006**	0.568
Change in Percent Cover Total	0.723	0.305	**0.006**	**0.000**	0.329	**0.006**	**0**	**0.009**
Change in Percent Cover of Common Reed	**0.032**	0.980	0.708	0.799	0.301	0.568	**0.009**	**0**

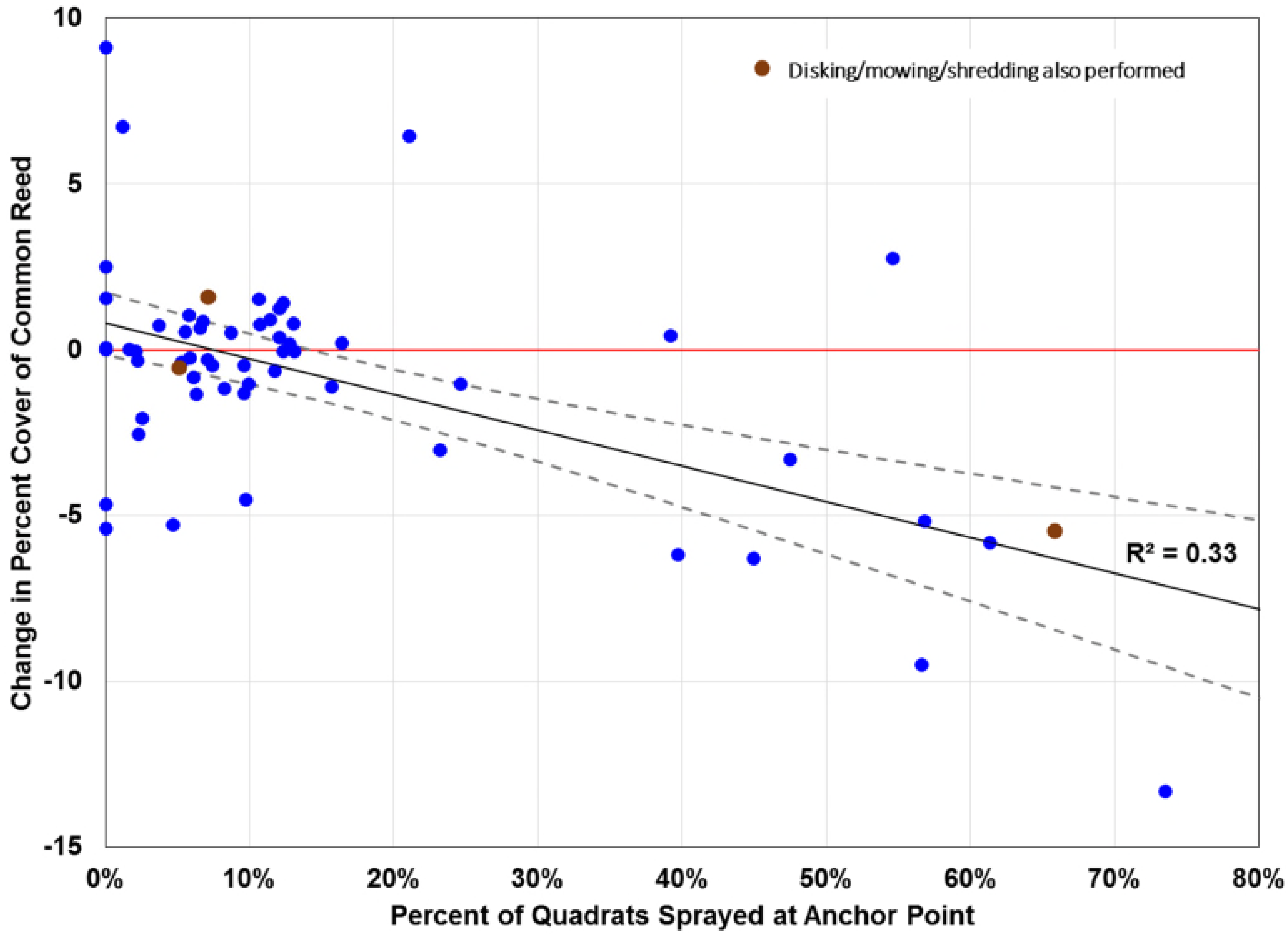

Figure 4.41. Change in percent cover of common reed versus percent of quadrats sprayed at pure panel APs with more than 3.5 percent average cover of common reed during the 2009 survey.

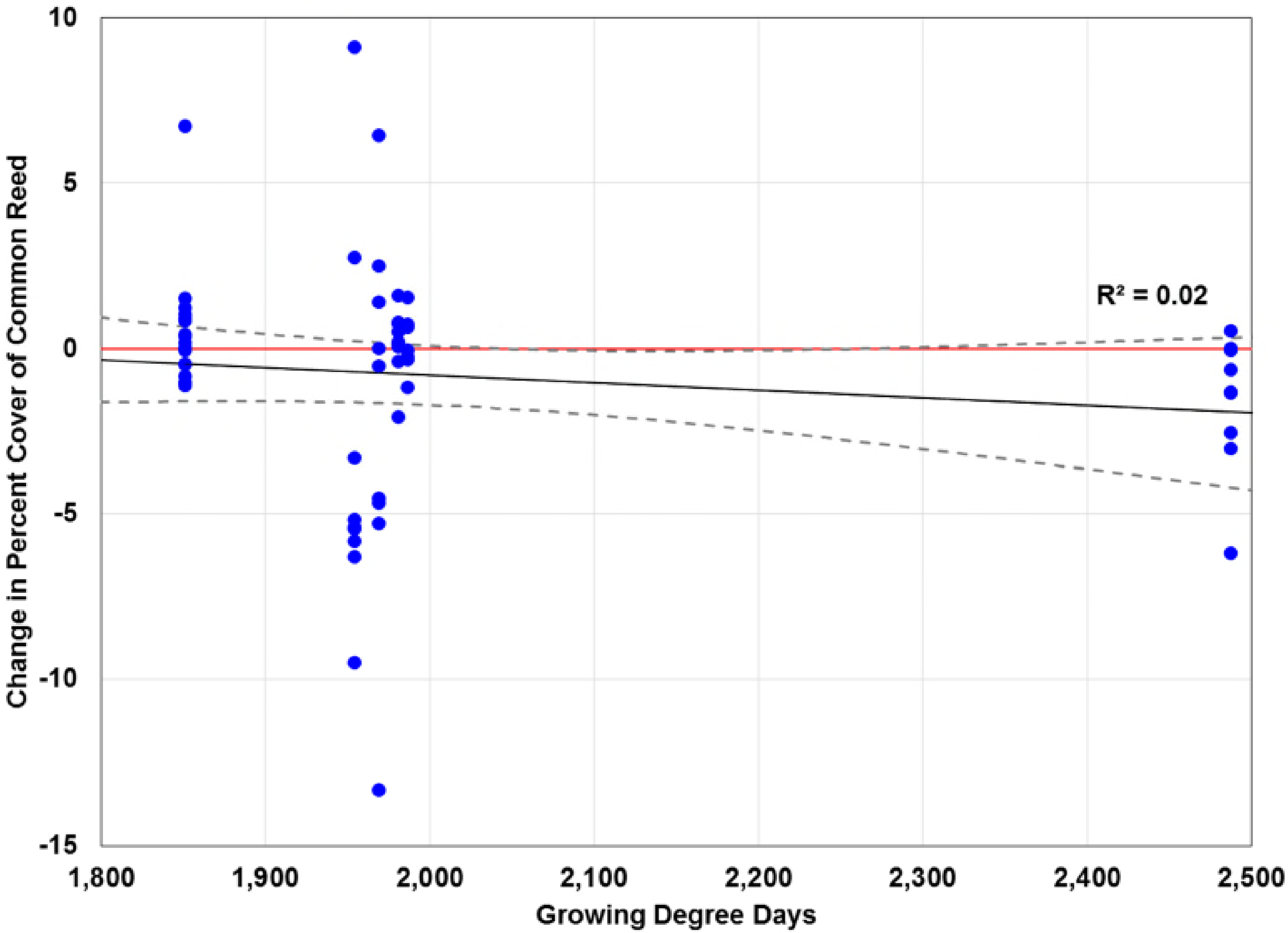

Figure 4.42a. Change in percent cover of common reed versus growing degree days at pure panel APs with more than 3.5 percent average cover of common reed during the 2009 survey.

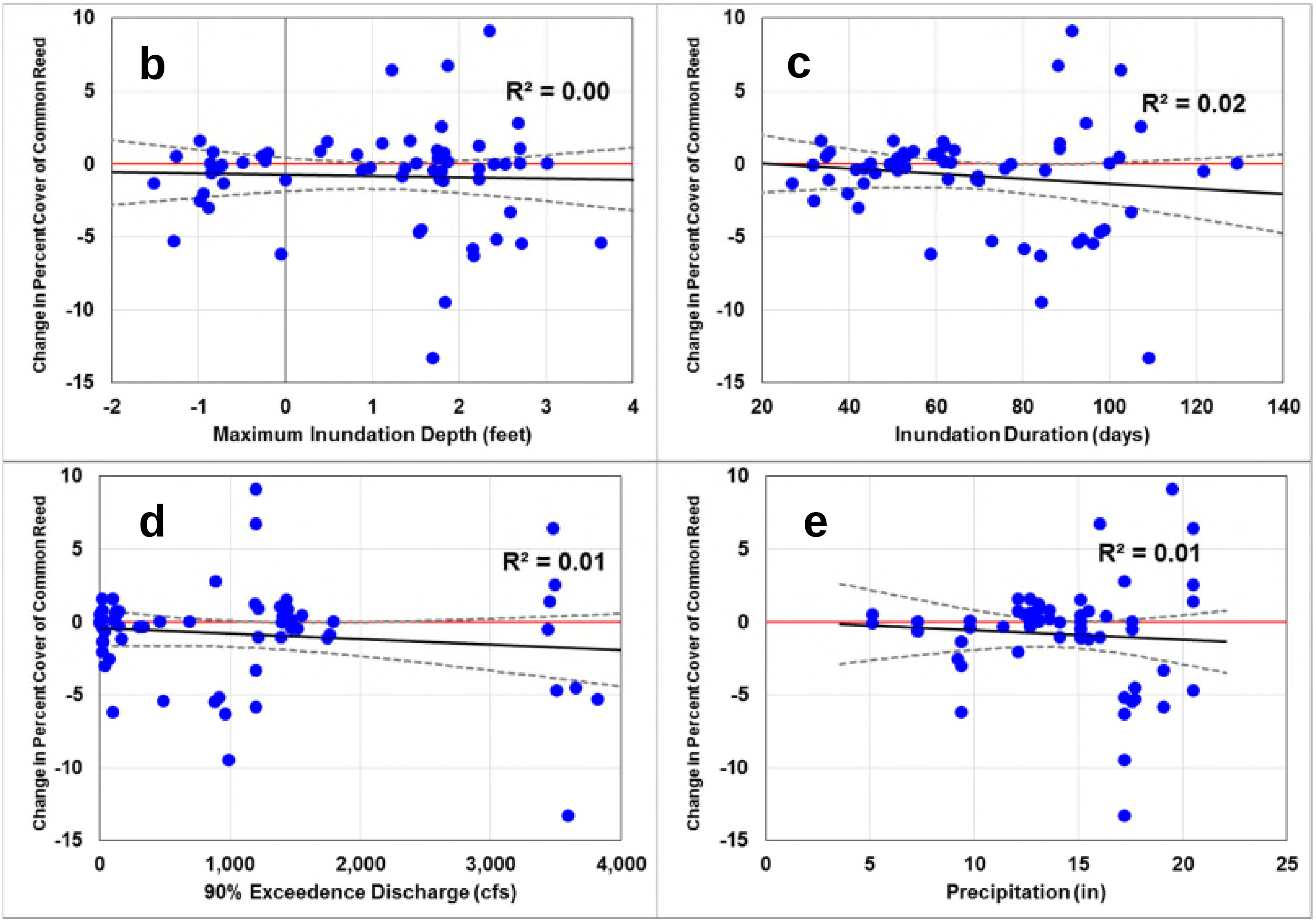

Figure 4.42b-e. Clockwise from top left, change in percent cover of common reed versus average inundation depth, duration of inundation, total precipitation during the growing season measured at Grand Island, and the 90 percent exceedance discharge during the growing season.

4.4 Mechanical #2

Increasing the Q1.5 in the main channel by consolidating 85 percent of the flow, and aided by Program flow and a sediment balance, flows will exceed stream power thresholds that will convert main channel from meander morphology in anastomosed reaches to braided morphology with an average braiding index greater than 3.

The correlation between total unvegetated width (W_{unveg}), braiding index (BI) and percent consolidation at 8,000 cfs was determined to assess the extent to which the above hypothesis is true. Based on the earlier HEC-RAS model that was developed from the 2009 topography and bathymetry, the amount of flow consolidation at the APs ranged from about 40 percent in the main branch at AP7 and AP23 to 100 percent at several locations that are spread throughout the reach (**Figure 4.43**). The length-weighted, average percent consolidation in the areas where all of the flow is not in the primary flow path was about 63 percent based on the 2009 model and about 68 percent based on the 2012 model.

The correlation between these three metrics is relatively weak, but statistically significant at the 95-percent level (**Figures 4.44** through **4.46**; **Table 4.8**). As discussed in Section 3.4.2, the unvegetated widths were greatest during 2011, 2015 and 2016, when long-duration, high flows occurred in the reach prior to the monitoring surveys (Figure 3.17b). The average braiding index changed very little over the 8-year period encompassed by the surveys, although substantive changes did occur at some APs (Figure 3.6b-c). Based on a two-sample t-test, the difference between the total unvegetated width at locations with less than 85-percent flow consolidation and locations with greater than 85 percent flow consolidation is not significantly (α=0.05, t=1.77, p=0.08) (**Figure 4.47a**). The difference in the mean braiding index between these two data sets is, however, statistically significant (α=0.05, t=3.55, p=0.001) (**Figure 4.48a**).

Management actions at AP 9 (Shoemaker Island), AP21 (Rowe Sanctuary) and AP33 (Cottonwood Ranch) have likely altered (or at minimum, masked) the relationships between flow, braiding index and channel width. To assess whether the correlation is different at the sites that have not been affected by the management actions, the data for these three APs were removed, and the statistical tests repeated for the censored data sets. The results indicate that braiding index and unvegetated width are both significantly correlated with flow consolidation (α=0.05, braiding index: t=4.51, p<0.001; unvegetated width: t=4.05, p<0.001), and the strength of the relationship for braiding index increases when AP9, AP21, and AP33 are excluded from the data set (**Figures 4.47b and 4.48b,** Table 4.8).

Table 4.8. Correlation matrix for percent flow consolidation, average braiding index and average unvegetated channel width at all of the pure panel APs, and all pure panel APs, except AP9, AP21 and AP33.

Variables	All Data			Excluding AP 9, 21 and 33*		
	Flow Consolidation at 8,000 cfs	Braiding Index	Unvegetated Width (ft)	Flow Consolidation at 8,000 cfs	Braiding Index	Unvegetated Width (ft)
Correlation matrix (Kendall):						
Flow Consolidation at 8,000 cfs	1	**0.226**	**0.255**	1	**0.238**	**0.307**
Braiding Index	**0.226**	1	**0.217**	**0.238**	1	**0.214**
Unvegetated Width (ft)	**0.255**	**0.217**	1	**0.307**	**0.214**	1
p-values:						
Flow Consolidation at 8,000 cfs	0	**<0.001**	**<0.001**	0	**<0.001**	**<0.001**
Braiding Index	**<0.001**	0	**<0.001**	**<0.001**	0	**<0.001**
Unvegetated Width (ft)	**<0.001**	**<0.001**	0	**<0.001**	**<0.001**	0

Values in bold are different from 0 with a significance level alpha=0.05

*Management activities at AP9, 21 and 33 may have affected the relationship.

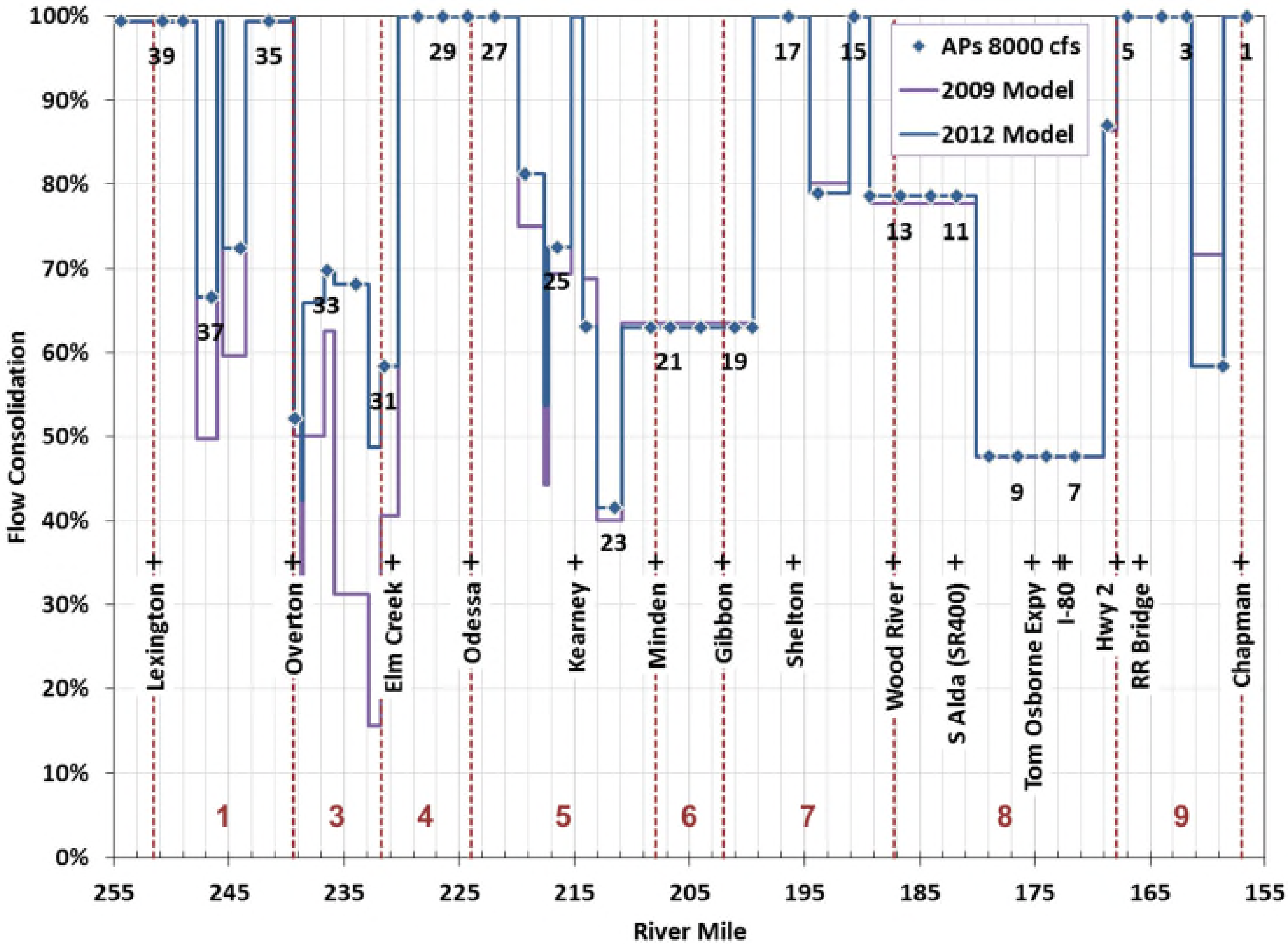

Figure 4.43. Clockwise from top left, change in percent cover of common reed versus average inundation depth, duration of inundation, total precipitation during the growing season measured at Grand Island, and the 90 percent exceedance discharge during the growing season. Percent flow consolidation (i.e., percent of flow in the main flow path) at 8,000 cfs.

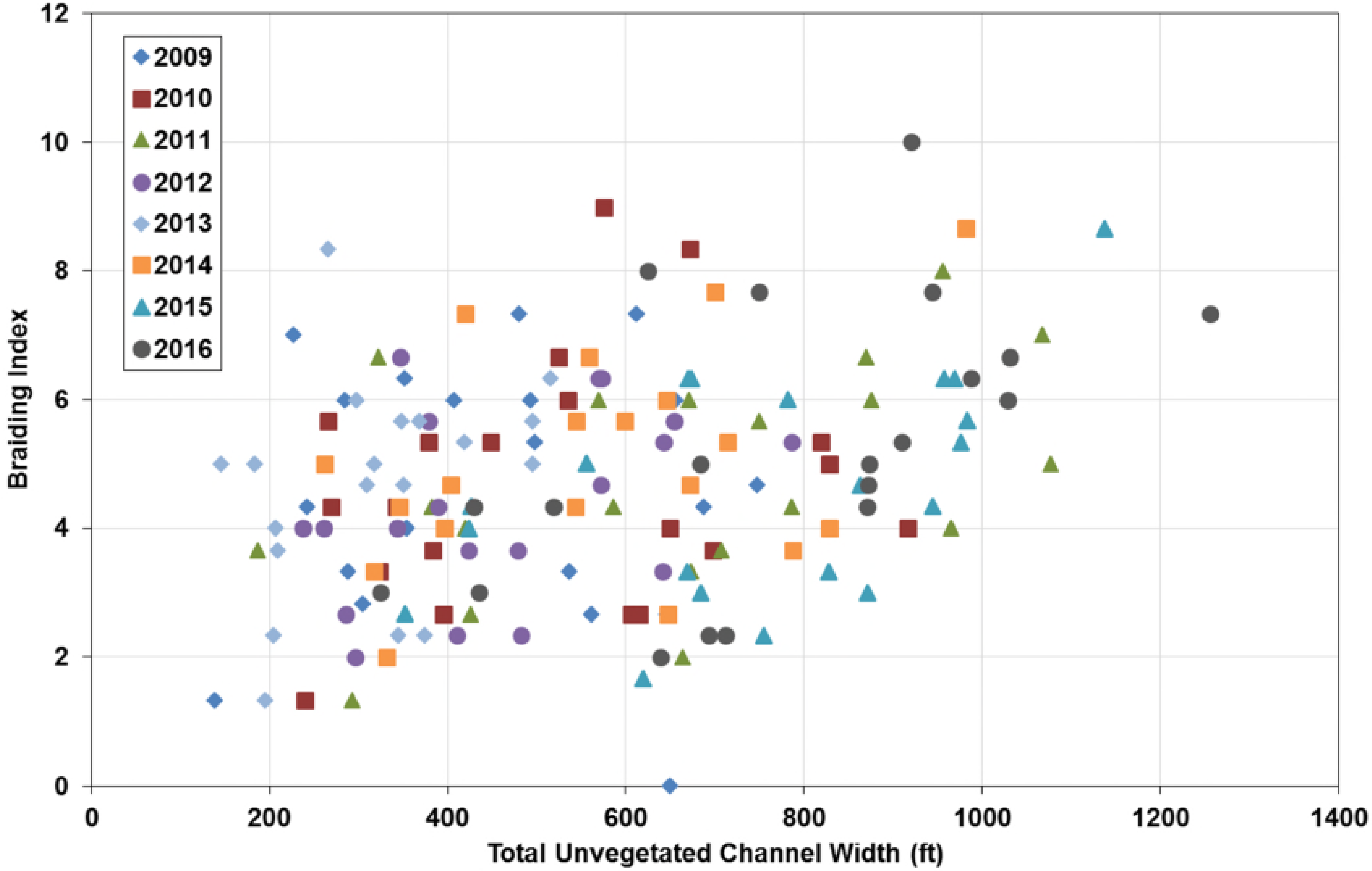

Figure 4.44. Total unvegetated channel width versus braiding index (Kendall's t = 0.22, p<0.001).

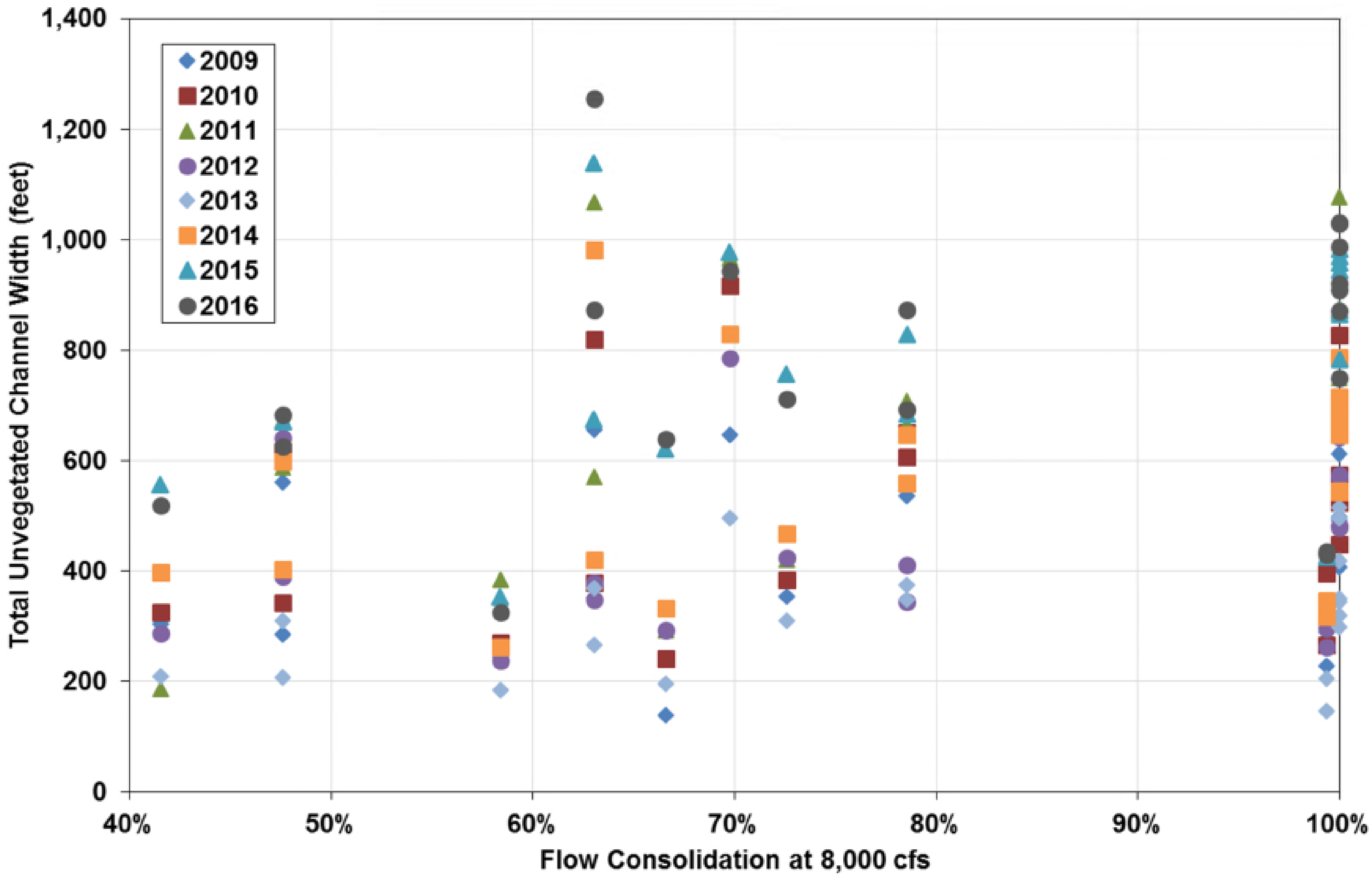

Figure 4.45. Total unvegetated channel width versus percent flow consolidation at 8,000 cfs (Kendall's t = 0.26, p<0.001).

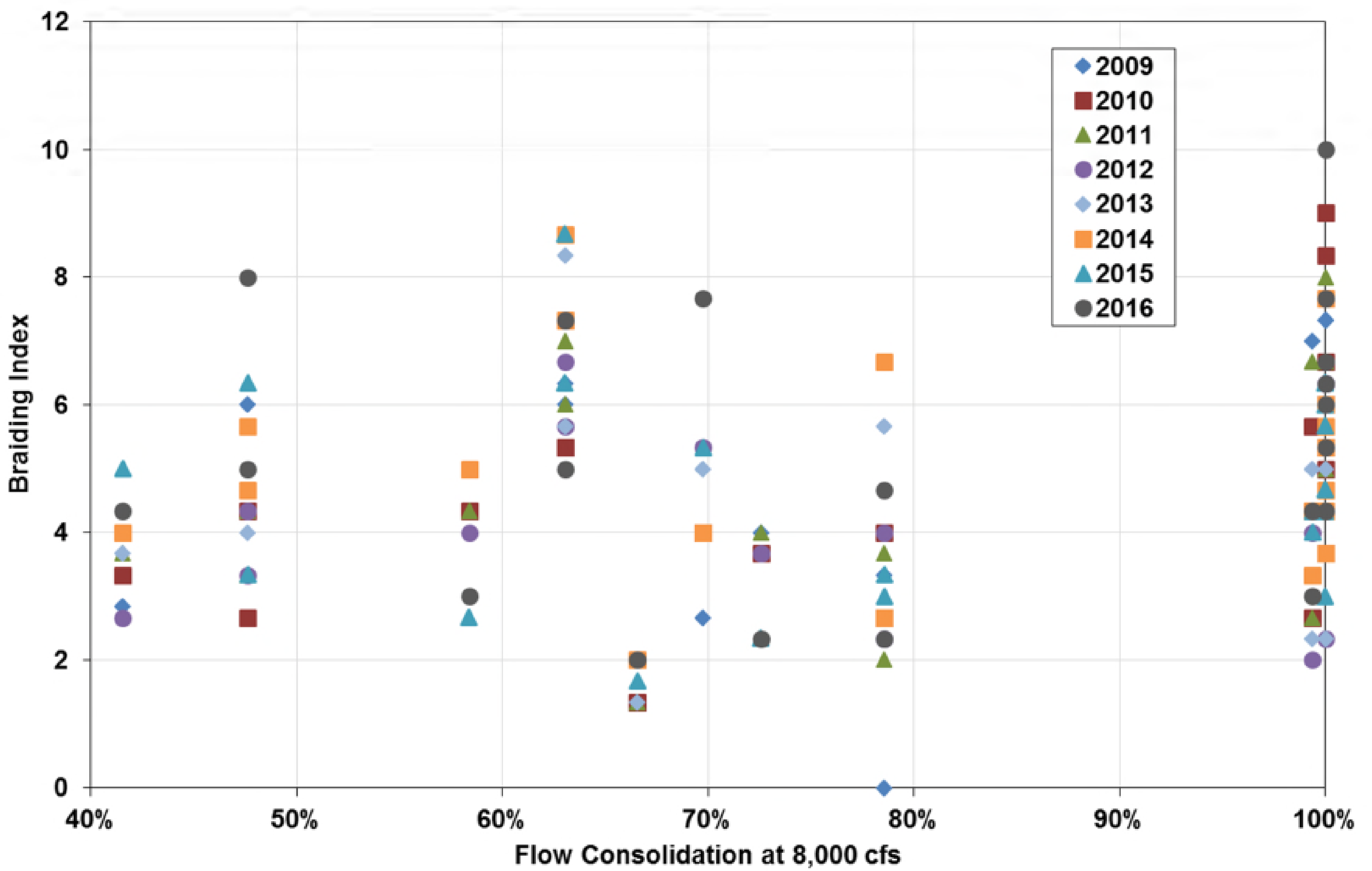

Figure 4.46. Braiding index versus percent flow consolidation at 8,000 cfs (Kendall's t = 0.23, p<0.001).

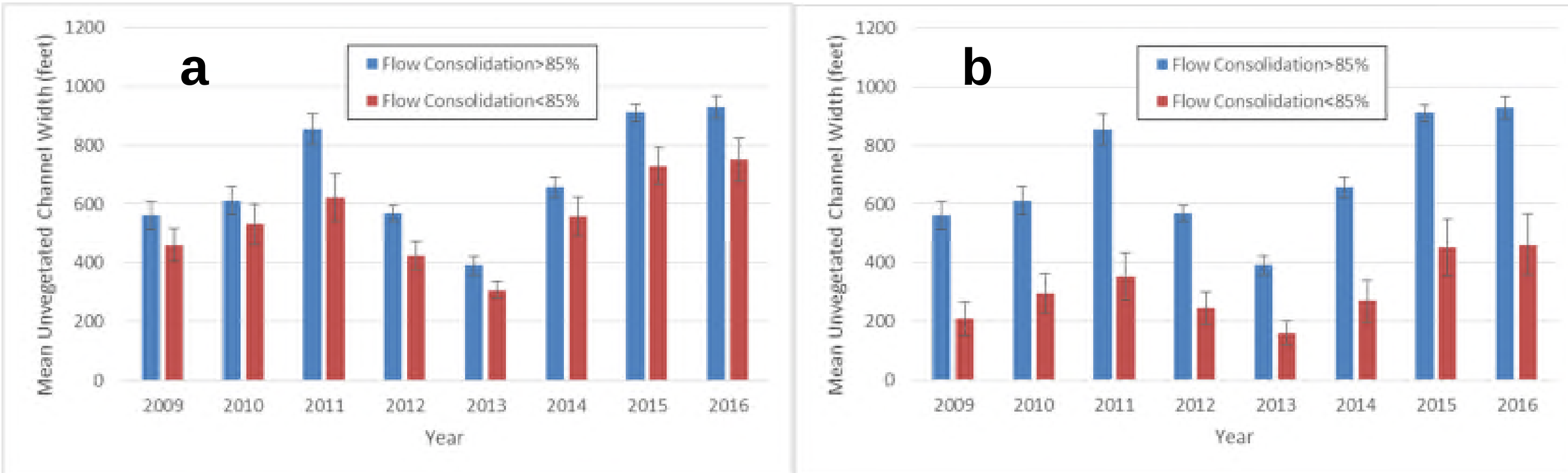

Figure 4.47. Mean unvegetated channel width at sites with greater than and less than 85-percent flow consolidation: (a) All APs, (b) Excluding AP9, AP21, and AP33.

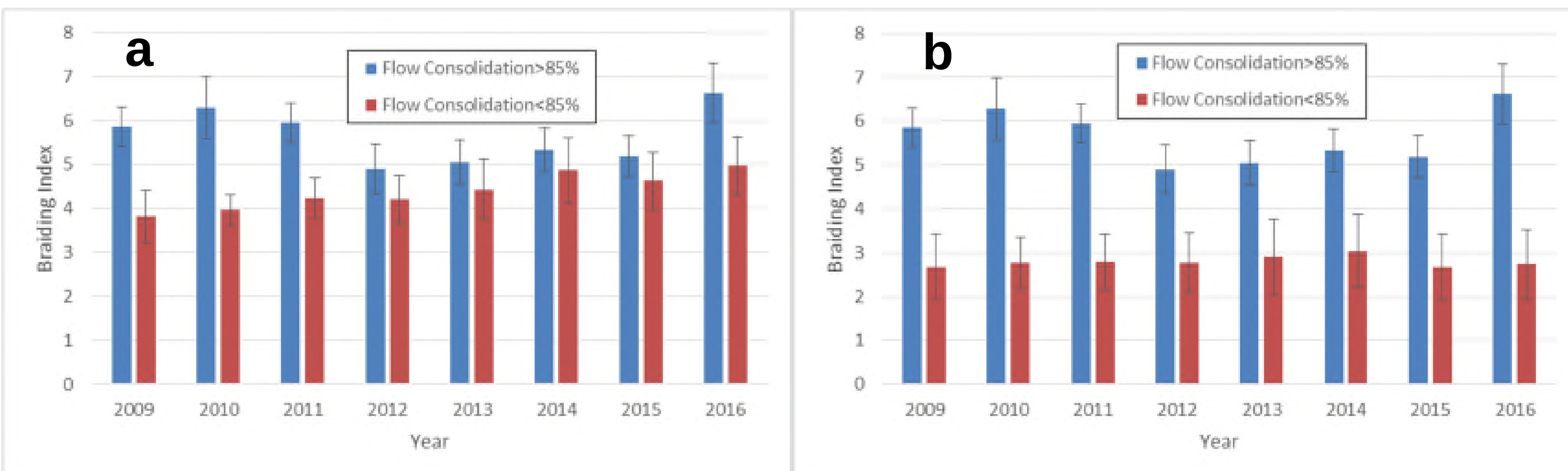

Figure 4.48. Mean braiding index at sites with greater than and less than 85-percent flow consolidation: (a) All APs, (b) Excluding AP9, AP21, and AP33.

Page intentionally left blank

5 SUMMARY AND CONCLUSIONS

With the 2016 field season, the Platte River Geomorphic and Vegetation Monitoring Program completed eight years of detailed field monitoring, and the data have been used to quantify at least 35 individual performance metrics that fall into one of the following six general categories:

1. Hydrologic,
2. Hydraulic,
3. Geomorphic,
4. Vegetation,
5. Sediment, and
6. Whooping Crane (Table 2.3).

This report presents a summary of all eight years of data, including spatial and temporal trends in each of the metrics. To provide a focused and in-depth analysis of key issues of concern to the Program, this report also includes detailed analysis of specific aspects of the following four hypotheses:

1. Flow #1,
2. Flow #3,
3. Flow #5, and
4. Mechanical #2.

Hydrologic conditions during the monitoring period varied considerably, from relatively dry years in WY2009 and WY2013 to three of the wettest years on record (WY2011, 2015 and 2016) (Figure 4.17), providing good contrast to assess the response of the monitoring reach to flow conditions. Although WY2012 ranked as a relatively wet year based on the flows for the entire year, most of the flow volume occurred during Fall 2011; flows during the growing season between April 1st and the monitoring surveys that were conducted in July and August were very low. In fact, the April through July runoff volumes in both 2012 and 2013 were in the lower 25th percentile of years since the early-1940s. The peak discharge in 2015 was relatively high (recurrence intervals of ~17 years, 12 years and 20 years at Overton, Kearney and Grand Island, respectively), and the relatively short-duration, fall peak discharge in 2013 was also relatively high (recurrence intervals of ~12 years at Overton and 6 years at Kearney and Grand Island) (**Figure 5.1 and 5.2**). Peak discharges during the other years were relatively modest.

In addition to the wide range of flow conditions, flow-sediment-mechanical (FSM) actions were conducted during the monitoring period at specific locations along the reach that could potentially affect the channel characteristics at the APs where the monitoring data are being collected. These actions included the Elm Creek and Shoemaker Island Adaptive Management Experiments, the Pilot Sediment Augmentation Project at the Dyer and Cottonwood Ranch sites, additional overbank clearing and grading of sand into the channel at Cottonwood Ranch, and spraying to control common reed (*Phragmites australis*) and other introduced species in several locations along the reach. Additional, related actions were also conducted at the Rowe Sanctuary that likely affect the characteristics of at least AP21.

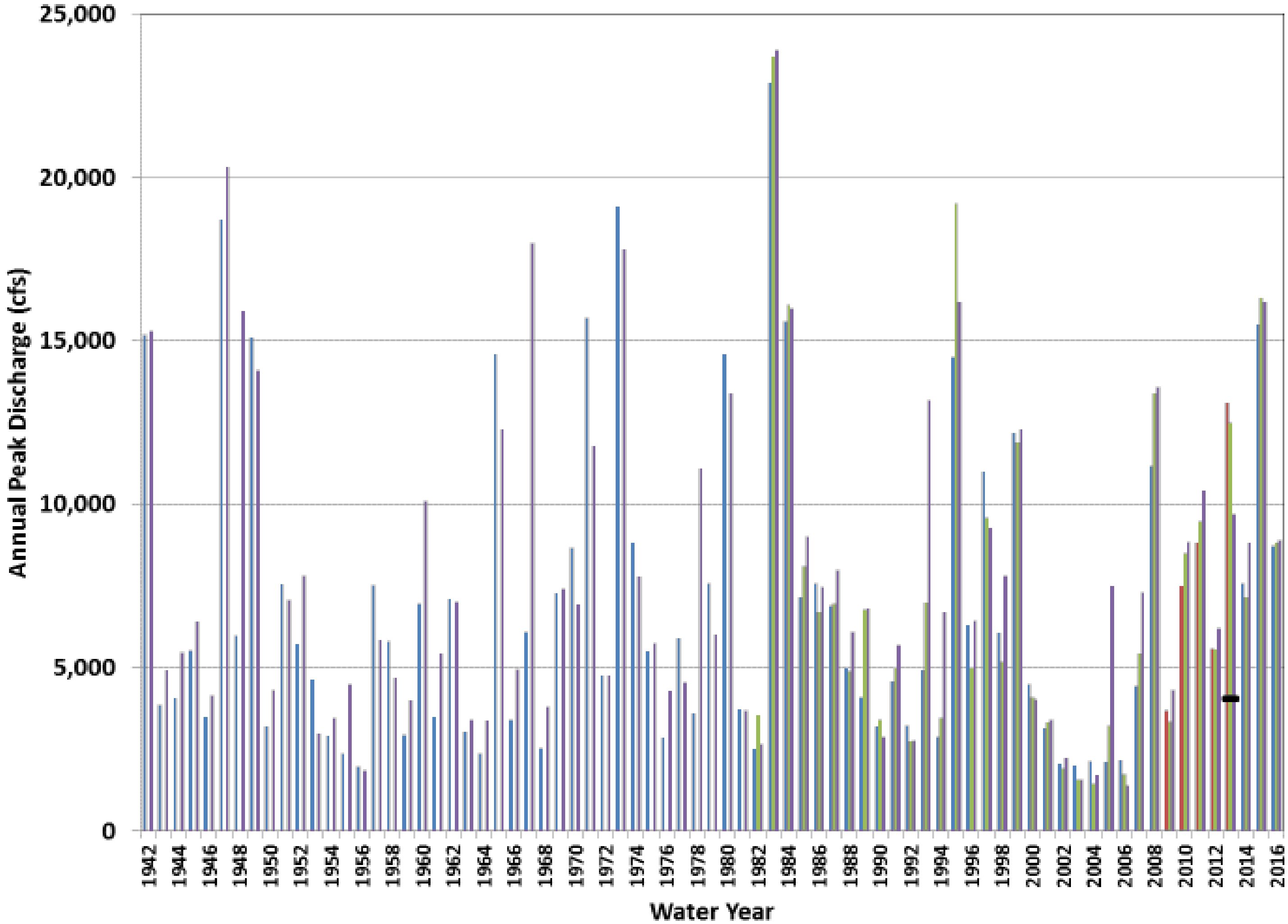

Figure 5.1. Annual peak discharges at the USGS Overton, Kearney, and Grand Island gages (note that Kearney record started in 1982). Also shown by the black mark is the approximate WY2013 peak discharges prior to the September flood at the three locations.

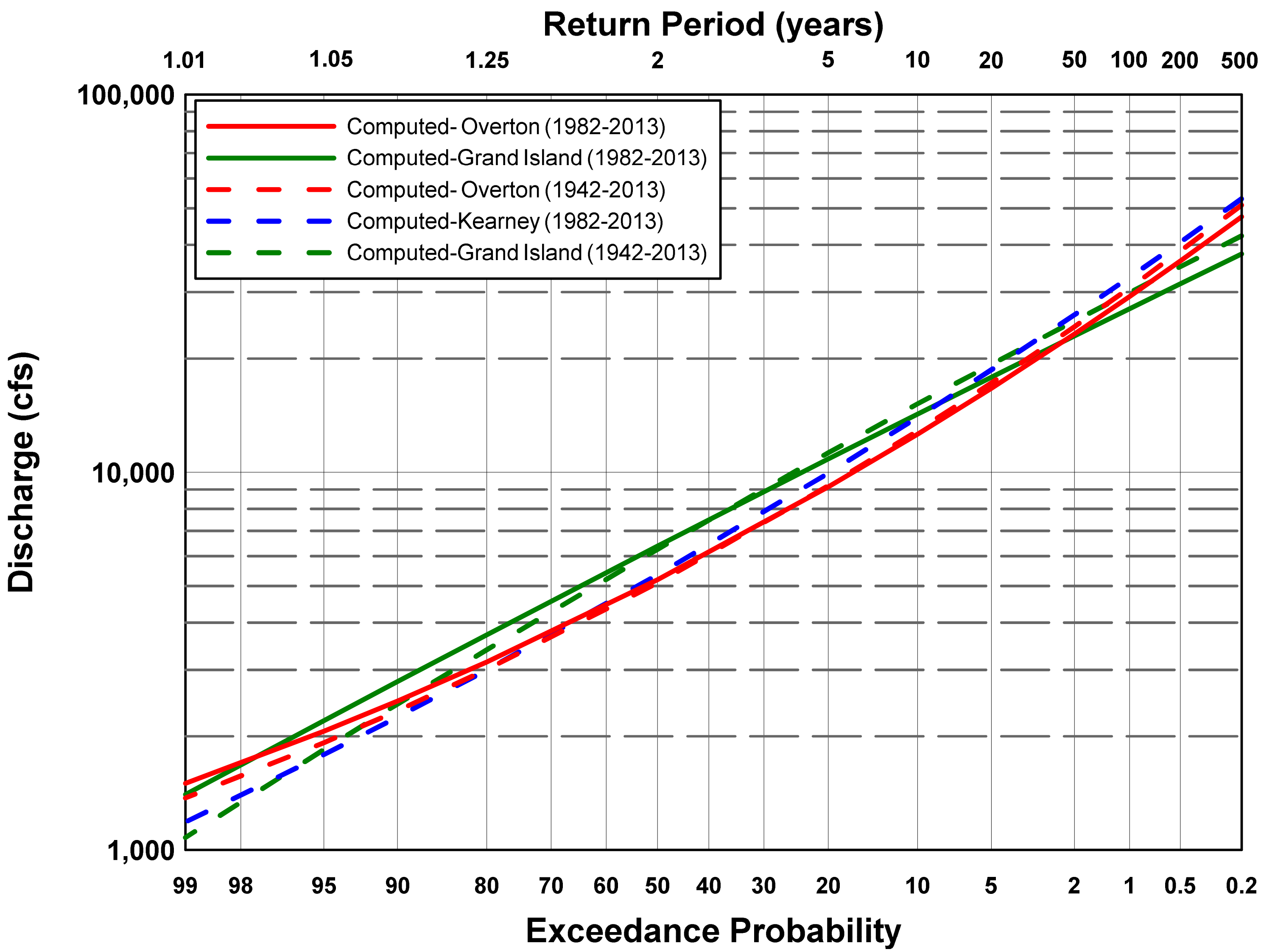

Figure 5.2. Flood-frequency curves for the annual peak flows from WY1942 through WY2013 at the USGS Overton, Kearney (WY1982-WY2013, only), and Grand Island gages.

Key observations from the spatial and temporal trend analysis of the geomorphic and vegetation data include the following:

1. The basic geomorphic and vegetation data provide a basis for evaluating a wide range of trends in the physical response of the reach to flows, Program actions and other factors.

    1.1. The reach-wide average braiding index changed very little during the period, although the index for 2012 was somewhat lower than the other years (Figure 3.6). Geomorphic Reaches 4 (Elm Creek to Odessa; Table 2.1) and 6 (Minden to Gibbon) typically had the highest braiding indices and Reaches 1 (Lexington to Overton), 2 (south channel at Jeffreys Island) and 8 (Wood River to Grand Island) typically had the lowest indices. The braiding indices in 2014 and 2015 in Reach 6 were substantially higher than in previous years. The reason for the large increase in Reach 6 is not apparent, but it could be related to activities at the Row Sanctuary.

    1.2. The reach-wide average total channel width showed a modest (but not statistically significant) increasing trend from 2009 through 2012, and a modest (but not statistically significant) decreasing trend from 2012 to 2015 and then increased by a small amount in 2016 (Figure 3.7). In general, the year-to-year changes in average width were very small. Geomorphic Reaches 4, 6, 7 (Gibbon to Wood River) and 9 (Grand Island to Chapman) have the largest total channel width (all exceeding 1,000-ft in all years), while Reaches 1 and 2 have the narrowest (typically in the range of 500-ft to 550-ft).

    1.3. The reach-wide average wetted channel width at 1,200 cfs was ranged from 450 ft to 480 ft in 2009, 2010 and 2011, increased to about 520 ft in 2012, decreased to about 450 ft by 2014, and then increased to about 540 ft by 2016 (Figure 3.8). The smallest average wetted widths during the 8-year monitoring period occurred in 2009 and 2014. Reaches with the largest wetted channel width generally correspond to the reaches with the largest braiding index and total channel width (i.e., Reaches 4 and 6).

    1.4. The reach-wide average width-to-mean depth ratio at 1,200 cfs varied substantially during the 8-year monitoring period, decline from about 170-ft in 2009 to about 130-ft in 2011, increasing to about 260-ft in 2012, and then declining back to about 160-ft by 2014 (Figure 3.11b). Between 2014 and 2016, the average width-mean depth ratio increased by to about 210-ft. The large decrease in 2014 appears to result from deepening of the channel thalweg (as indicated by the maximum channel depths) during the September 2013 flood and the high flows in June 2014, and this appears to have persisted through the 2015 high flows.

    1.5. Based on the transect surveys at the pure panel APs, the overall monitoring reach from Lexington to Chapman degraded by about 3.2M tons between 2009 and 2011, aggraded by about 5.6M tons during 2012, and then continued to aggrade by about 1.9M tons in 2013 (Figure 3.12b). The reach was slightly degradational (~0.6M tons) in 2014, strongly degradational (~4.3M tons) in 2015, and roughly in-balance in 2016. The overall reach was modestly degradational over the 8-year monitoring period (net loss of about 720,000 tons or about 91,000 tons per year). The bulk of the degradation during the first two years occurred in the portion of the reach upstream from Minden, with Reach 5 showing the most degradation (Figure 3.12c). Between the 2009 and 2010 surveys, Reach 1 through 6 (Lexington to Gibbon) were all degradational, losing a combined 2.6M tons of sediment, while Reach 7 through 9 aggraded by a combined 640,000 tons. Reaches 2, 3, 5 and 7-9 were all degradational between 2010 and 2012, losing a combined 1.8M tons of material, while the remaining reaches aggraded by about 640,000 tons. All of the reaches, except Reach 2 (South change at Jeffreys Island) were aggradation between 2011 and

2012, and most of the reach was aggradational between 2012 and 2013, except Reaches 3, 7 and 7 which lost about 520,000 tons of sediment. The aggrading reaches accumulated a combined total of about 2.4M tons of sediment during the latter period, about 1.3M tons of which occurred in Reach 8. Reaches 1, 4, 5, 7 and 9 were strongly degradational between the 2013 and 2014 surveys, losing a combined total of about 1.4M tons of material. About 800,000 tons of material accumulated in the three aggrading reaches (Reaches 2, 6 and 8) during this period. All of the reaches except Reach 9 were degradation between the 2014 and 2015 surveys, losing a combined total of about 4.6M tons. Reach 9 gained about 160,000 tons of material. During the final year of monitoring, five of the reaches were degradational (Reaches 1, 4, 5, 7 and 9), losing a combined 700,000 tons, while the aggrading reaches gained about 820,000 tons. Over the entire period, Reaches 1 through 5 (Lexington to Mindon) degraded by a combined total of about 3.2M tons (~450,000 tpy, on average), and Reaches 6, 7, 8 and 9 (Mindon to Chapman) aggraded by about 2.5M tons (~350,000 tpy) (**Figure 5.3**).

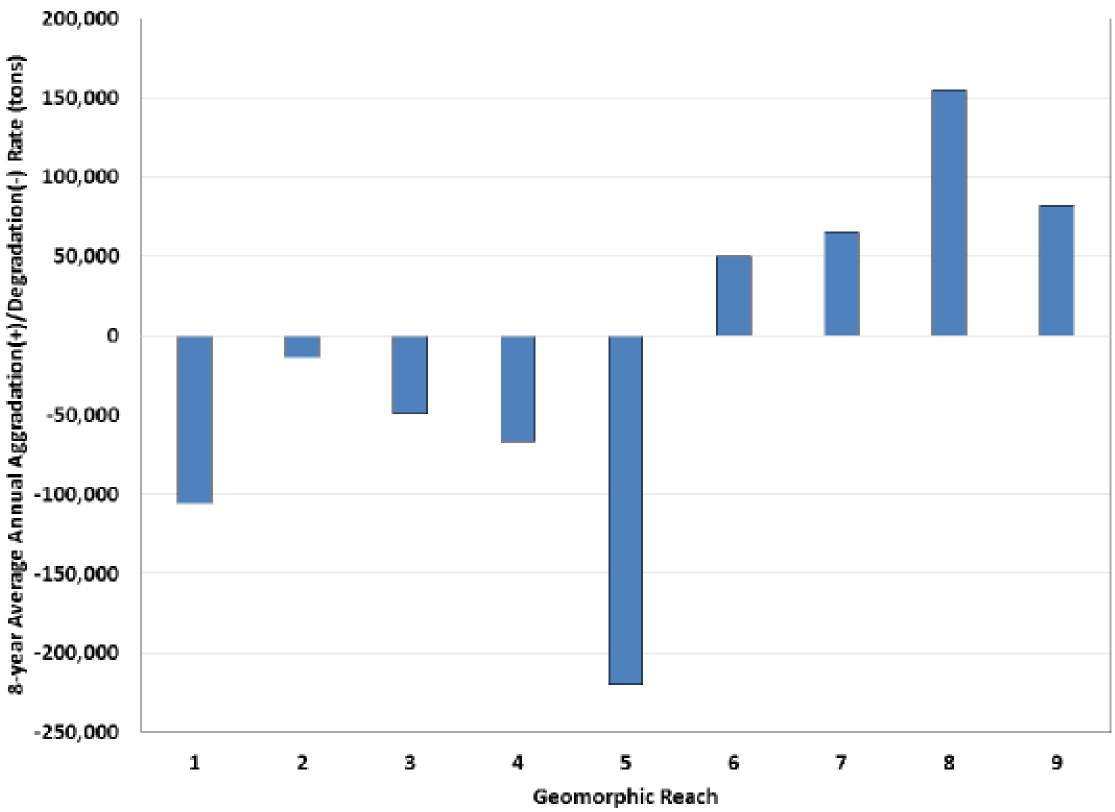

Figure 5.3. Annual aggradation/degradation rate by geomorphic reach over the 8-year monitoring period, based on the cross section surveys at the pure panel APs.

1.6. The green line elevation (GLE), as defined in the monitoring protocol, is very responsive to flow; however, this appears to be primarily related to inundation levels that prevent annual vegetation from establishing rather than scour of the perennial species. The reach-wide average GLE was about one ft higher in 2010 than during the initial survey in 2009, and this increased even further to about 1.9 ft by the 2011 surveys (Figure 3.14b). The low flows in 2012 and 2013 allowed the vegetation to encroach back into the channel to levels that were similar to those in 2009. The average GLE was about 0.9 ft above the

2009 level in 2014, when germination season flows were in the range of 2,500 cfs to 3,000 cfs throughout most of the reach (Figure 3.3), and it increased even further, when germination season flow were unusually high, to about 1.8 ft above the 2009 level. With the moderately high germination season flows, the average GLE stayed about the same in 2016 as in 2015. The only year in which the reach-wide average GLE exceeded the benchmark of 1.5 ft above the 1,200 cfs water surface was 2011 (Figure 4.23).

1.7. The reach-wide average total unvegetated channel width increased substantially from about 500 ft in 2009 to 725 ft in 2011and then declined back to only about 340 ft by 2013 (Figure 3.17). Consistent with the changes in GLE, the unvegetated width increased to about 835 ft by 2015, and it remained about the same (~850 ft) in 2016, the highest level during the monitoring period. Average unvegetated channel width exceeded the benchmark minimum value of 750 ft in both 2015 and 2016.

1.8. Of the four species of primary interest, the frequency of purple loosestrife, common reed and willow declined substantially between 2009 and 2012, and then remained relatively consistent through the remainder of the 8-year monitoring period (Figure 3.18). In contrast, eastern cottonwood occurred relatively infrequently during the first three years, increased substantially during 2012, and then declined back to about midway between the 2011 and 2012 frequencies during the last three years of the monitoring program.

1.9. Purple loosestrife is most common in the portion of the reach downstream from Minden, while common reed is most prevalent in the reaches between Elm Creek and Minden (Reaches 4 and 5), Gibbon and Wood River (Reach 7) and Grand Island and Chapman (Reach 9) (Figures 3.21 and 3.22). Eastern cottonwood is more or less evenly distributed throughout the monitoring reach, although it occurred infrequently in Reaches 2, 6 and 7 during the early years of the monitoring program (Figure 3.23). It remains relatively infrequent in Reach 2, but increased back to level consistent with the adjacent reaches in Reach 6 in 2015 and 2016. Willow was most common in Reaches 4 and 5 (Elm Creek to Minden) in 2009, but declined substantially in those reaches in later years, and it occurred relatively infrequently in the remainder of the reach during the later portion of the monitoring period (Figure 3.24).

1.10. Consistent with the trends in the GLE, the mean height of the four species of primary interest above the 1,200 cfs water surface was generally greatest during the high-flow years in 2010, 2011, 2015 and 2016 (in the range of 1 to 1.8 ft), and lowest during the low-flow years (Figure 3.44c).

1.11. The bed and bar material tends to fine in the downstream direction, with median (D_{50}) sizes of 1 to 2 mm in the upstream part of the reach to less than 1 mm in the downstream part of the reach, although this trend is much stronger for the bed material than the bar material (Figures 3.59 and 3.61). The reach-wide average D_{50} of the bed material became finer during the first four monitoring years (~1.2 mm to about 0.7 mm), but has increased back to about 1 mm in during the last three years (Figure 3.60). Considering the variability of the underlying data, these trends may not be statistically significant. It is also interesting to note that the average D_{50} of the samples collected by the Reclamation in 1989 were about the same as the minimum during the current monitoring period of about 0.7 mm, and this sampling was done after an extended wet period (Figure 4.16).

1.12. Unobstructed channel widths (a key whooping crane metric) were generally greatest during the first four years (reach-wide average of 650 to 720 ft), and then declined substantially to only about 520 ft in 2013 (Figure 3.62). The unobstructed width then increased back to about 620 by 2015, followed by a small decline in 2016 to about 580 ft.

The procedures used to estimate unobstructed channel width evolved over the monitoring period. Prior to the 2013 field season, unobstructed widths were estimated based on vegetation height data collected in the quadrats in relatively coarse height bins, and this lead to considerable uncertainty in computing the value of this metric. Starting in 2013, the widths were directly measured with a laser rangefinder to eliminate as much of the uncertainty as possible. A substantial part of the abrupt change in unobstructed width from 2012 to 2013 is probably due to the change in measurement method. Because they were directly measured, the 2013 through 2016 data should provide more accurate representation of the widths than the earlier data.

2. An understanding of the relative sediment transport balance along the reach is a key factor in evaluating **Hypothesis Flow #1**. The following conclusions can be drawn from the analysis presented in this report.

   2.1. Integration of the best-fit bed and suspended **sand-load rating curves** over the applicable flow records and comparison of the resulting annual loads passing each of the bridges where the measurements were taken indicates that the segment between Darr and Overton was degradational during all years of the monitoring program, with total loss of about 1.5M tons (or about 210,000 tpy) over the 7-year period bracketed by the 2009 and 2016 monitoring efforts (Figure 4.7). The analysis also indicates that the Overton to Kearney reach was in approximate sediment balance over the period, with mild degradation occurring in 2010 and 2012 and mild aggradation during the other years. Total sediment accumulation during the monitoring period was about 96,000 tons, or about 14,000 tpy, on average. The reach between Kearney and Shelton was degradational in all years, with total loss of about 483,000 tons, or about 69,000 tpy. Shelton to Grand Island was also degradational during all years except 2013 and 2015, with net loss of about 725,000 tons or about 104,000 tpy (Figure 4.7).

   2.2. Based on Monte Carlo simulations of the annual sediment loads that take into account the variability in the measured data, there are only two cases (of the 28 combinations of gage-to-gage reaches and years) for which 90 percent confidence bands are on the same side of the boundary between aggradation and degradation (Darr to Overton in SY2012 and SY2013) (Table 4.2). In all other cases, the probability that the best-estimate annual sediment balance is at least in the correct direction is less than 90 percent.

   2.3. Extrapolation of the **aggradation/degradation volumes from the cross-section surveys** at the pure panel APs to the overall length of the segments between the bridges at which the sediment transport measurements were made results in estimates of the sand balance that, in many cases, are quite different from the rating curve-based estimates. In general, the rating curve-based estimates indicate consistent aggradation/degradation trends from year to year, with the magnitude varying with the flow regime, while the trends from the cross-section surveys tend to be very different from year to year in terms of both the direction and magnitude of the change (compare Figure 4.7 with Figure 4.8). For example, the rating curves indicate degradation for all years in the Darr to Overton reach, while the while the direction of change was evenly split between aggradation and degradation on a yearly basis. In fact, the direction of change from the surveys was the opposite of that predicted by the rating curves in 13 of the 28 combinations of years and gage-to-gage reaches (**Table 5.1**). Additionally, the survey-based estimate is within the confidence bands on the rating-curve-based estimates in only 13 of the 28 cases (Table 4.3).

Table 5.1. Comparison of predicted direction aggradation/ degradation trends between rating curves and AP surveys.

Survey Year	Darr-Overton	Overton-Kearney	Kearney-Shelton	Shelton-Grand Island
2010	Same	Same	Same	Opposite
2011	Same	Opposite	Same	Same
2012	Opposite	Opposite	Opposite	Opposite
2013	Opposite	Opposite	Same	Same
2014	Same	Same	Same	Opposite
2015	Same	Opposite	Same	Opposite
2016	Opposite	Same	Same	Opposite
2010-2016	**Same**	**Opposite**	**Same**	**Opposite**

2.4. Unfortunately, data are not available to directly assess the uncertainty in the survey-based estimates. Uncertainty in these estimates stems from at least three factors: (1) uncertainty in the horizontal position and elevation of the individual survey points, (2) uncertainty in how well the three surveyed transects represent the aggradation response of the channel within the individual AP, and (3) uncertainty in how well the response at the AP represents the overall response of the river in the approximately 5-mile segment of the river represented by the AP. Tests of the data using the reported accuracy of the individual points from the RTK-GPS datalogger indicate that the first of these sources of uncertainty is very small compared to the other two sources. Based on the available information about the river from the transects, it is likely that the uncertainty associated with other two factors is relatively large. Comparison of the changes over the 4-year periods using all of the survey data, including the rotating APs with those using only the pure panel AP data indicates that inclusion of more cross sections in the surveys would dampen the magnitude of the year-to-year changes indicated by the data, but would probably not change the direction, especially during years when substantial changes occur (see discussion in Section 4.1.3.

3. The greenline elevation (GLE) and unvegetated channel width data provide a means of assessing the extent to which the unvegetated channel width responds to flow, as postulated by **Hypothesis Flow #3**:

3.1. Based on the reach-wide average, the Program's GLE benchmark of 1.5 ft above the 1,200 cfs water surface was met only in SY2011, when long-duration, high flows persisted in the reach (Figure 4.22).

3.2. GLE is well-correlated to the year-to-year change in stage associated with the annual peak discharge (Figure 4.24), but is even more highly correlated with the discharge during germination season (Figures 4.25 and 4.26). Correlation with the average germination season discharge is actually slightly higher than with the maximum germination season discharge.

3.3. The total unvegetated width is also positively correlated with both the annual peak discharge and the average germination season discharge (Figures 4.27 and 4.28).

3.4. As expected from the above results, total unvegetated width is positively correlated with GLE (Figure 4.29).

4. In relation to **Hypothesis Flow #5**, common reed has been identified as a potentially important factor in preventing the river from sustaining the wide, braided character that is important to good quality habitat for the target species. Both the frequency of occurrence and percent cover of common reed declined during the monitoring period. Several factors that could have contributed to the decline, including Program activities, were identified, quantified to the extent possible, and evaluated using multiple correlation analysis.

    4.1. Analysis of the year-to-year changes in percent cover of common reed versus a range of potential factors shows statistically significant, negative correlation with spraying at a significance-level (α) of 0.05 (Table 4.7; Figure 4.41).

    4.2. Correlation of year-to-year changes in percent cover of common reed was not statistically significant for any of the other factors that were considered, including maximum inundation depth, duration of inundation, 90th percentile (low) flow during growing season, growing degree days, and precipitation) (Table 4.7; Figures 4.41 and 4.42).

5. Flow consolidation is also postulated to be an important factor in maintaining the wide, braided character that is important to good quality habitat (**Hypothesis Mechanical #2**).

    5.1. Both the mean unvegetated channel width and mean braiding index at APs with more than 85-percent flow consolidation are larger than at the sites with less than 85- percent flow consolidation (Figure 4.47 and 4.48). When all sites, including those where management activities that have substantially altered the channel, are considered, the difference in mean braiding index is statistically significant, but the difference in unvegetated channel width is not. When the three APs where the management actions have occurred (AP9, AP21 and AP33) are excluded from the data sets, the differences in both variables is statistically significant.

    5.2. These results suggest that flow consolidation may have a positive influence on both unvegetated channel width and the amount of braiding.

Page intentionally left blank

6 REFERENCES

Auble, G.T., and Scott, M.L., 1998. Fluvial Disturbance Patches and Cottonwood Recruitment along the Upper Missouri River. Montana: Wetlands, Vol. 18, pp. 546–556.

Ayres Associates and Olsson Associates, 2010. Platte River Recovery Implementation Program, Year 1, 2009. Report, Channel Geomorphology and In-Channel Vegetation of the Central Platte River. Prepared for PRRIP, February, 52 p.

Ayres Associates and Olsson Associates, 2011. Platte River Recovery Implementation Program, Year 2 (2010) Report, Channel Geomorphology and In-Channel Vegetation of the Central Platte River. Prepared for PRRIP, March, 45 p.

Ayres Associates and Olsson Associates, 2012. Platte River Recovery Implementation Program, Year 2 (2010) Report, Channel Geomorphology and In-Channel Vegetation of the Central Platte River. Prepared for PRRIP, April, 46 p.

Cohn, T.A., and Gilroy, E.J., 1991. Estimating Loads from Periodic Records. U.S. Geological Survey Branch of Systems Analysis Technical Report 91.01. 81 p.

Daubenmire, R., 1959. A Canopy-Coverage Method of Vegetational Analysis. Northwest.

Duan, N., 1983. Smearing Estimate: A Nonparametric Retransformation Method. Jour. Amer. Stat. Assoc., Vol. 87, pp. 605-610.

Ferguson, R.I. 1986. River Loads Underestimated by Rating Curves. *Water Resources Research*, Vol. 22(1), pp. 74–76.

Fotherby, L.M., 2008. Valley Confinement as a Factor of Braided River Pattern for the Platte River. Geomorphology. Vol. 103, Issue 4, pp. 562–576.

Friesen, B., Von Loh, J., Schrott, J., Butler, J., Crawford, D., and Pucherelli, M., 2000. Central Platte River 1998 Land Cover/Use Mapping Project, Nebraska. Technical Memorandum 8260-00-08, Bureau of Reclamation, U.S. Fish and Wildlife Service, Denver, Colorado.

HDR and Tetra Tech, 2011. 1-D Hydraulic and Sediment Transport Model. Prepared for the Platte River Recovery Implementation Program, January 28, 151 p.

Hirsch, R.M., Helsel, D.R., Coh, T.A., Gilroy, E.J., 1993. Statistical Analysis of Hydrologic Data. In Maidment, D.R. (ed), *Handbook of Hydrology*. McGraw Hill, Inc., pp. 17.1–17.55.

Kaul, B., Sutherland, D., and Rolfsmeier, S., 2011. The Flora of Nebraska; Second Edition. The School of Natural Resources, University of Nebraska–Lincoln, Lincoln Nebraska.

Lichvar, R. and Kartesz, J., 2012. North American Digital Flora: National Wetland Plant List, version 3.0. Accessed: 9 January, 2013. Available: http://wetland_plants.usace.army.mil.

Lichvar, R.W., M. Butterwick, N.C Melvin, and W.N. Kirchner. 2014. 2014 National Wetland Plant List. Engineer Research and Development Center, United States Army Corps of Engineers.

Murphy, P.J., Fotherby, L.M., Randle, T.J., and Simons, R., 2006. Platte River Sediment Transport and Riparian Vegetation Model. Prepared for the Bureau of Reclamation, March, 151 p.

Platte River Recovery Implementation Program, 2006. Attachment 3, Adaptive Management Plan, 254 p.

Platte River Recovery Implementation Program, 2010. PRRIP Channel Geomorphology and In-Channel Vegetation Monitoring, 24 p.

Platte River Recovery Implementation Program, 2012a. Draft Channel Geomorphology and In-Channel Vegetation Data Analysis Plan, 45 p.

Platte River Recovery Implementation Program, 2012b. Adaptive Management on the Platte River, Adaptive Management Plan, 2012 “State of the Platte” Report – Executive Summary, 68 p.

Pollen-Bankhead, Thomas, N.R., and Simon, A., 2011. Draft Platte River Recovery Implementation Program, Directed Vegetation Research Study, Can Short Duration High Flows be used to Remove Vegetation from Bars in the Central Platte River? 102 p.

Rolfsmeier, S. and Steinauer, G., 2010. Terrestrial Ecological Systems and Natural Communities of Nebraska (Version IV – March 9, 2010). Nebraska Natural Heritage Program, Nebraska Game and Parks Commission. Lincoln, Nebraska. Available: http://outdoornebraska.ne.gov/wildlife/programs/legacy/pdfs/Terrestrial%20Ecological%20Systems.pdf. Science 33:43-64. Department of Botany, State College of Washington, Pullman, Washington.

Runkel, R.L., Crawford, C.G., and Cohn, T.A., 2004. Load Estimator (LOADEST): A Fortran Program for Estimating Constituent Loads in Streams and Rivers. Techniques and Methods Book 4, Chapter A5, U.S. Geological Survey, Reston, Virginia.

Scott, M. L., Auble, G.T. and Friedman, J.M., 1997. Flood dependency of cottonwood establishment along the Missouri River, Montana, USA. Ecological Applications, 7(2), 997, pp. 677–690.

Shafroth, P.B.; Auble, G.T., Scott, M.L., 1995. Germination and Establishment of the Native Plains Cottonwood (Populus deltoides Marshall subsp. monilifera) and the Exotic Russian-olive (Elaeagnus angustifolia L.). Conservation Biology. Vol. 9, Issue 5, pp. 1169–1175.

Shaw, R.B. 2008. Grasses of Colorado. University Press of Colorado, Boulder.

Shen, H.W. and Julien, P.Y., 1993. Erosion and Sediment Transport. In Maidment, D.R. (ed), *Handbook of Hydrology*. McGraw Hill, Inc., pp. 12.1–12.6.

Stubbendieck, J., Coffin, M.J., and Landholt, L.M., 2003. Weeds of the Great Plains. Nebraska Department of Agriculture, Bureau of Plant Industry, Lincoln, NE.

Tetra Tech, 2010. Hydraulic and Sediment-transport Modeling for the Platte River Sediment Augmentation Feasibility Study, Nebraska. Appendix B, Modeling Evaluation, Final Platte River from Lexington to Odessa Bridges, Sediment Augmentation Experiment Alternatives Screening Study Summary Report, prepared for Platte River Recovery Implementation Program, September 7, 92 p.

Tetra Tech, 2012. Elm Creek Two-dimensional Hydraulic and Sediment-transport Modeling Report, submitted to Platte River Recover Implementation Program, October 26, 104 p.

Tetra Tech, 2013. Elm Creek FSM Annual Monitoring Report. Prepared for the Platte River Recovery Implementation Program, March, 73 p.

Tetra Tech, 2014. 2013 Elm Creek FSM Annual Monitoring Report. Prepared for the Platte River Recovery Implementation Program, April, 212 p.

Tetra Tech, 2013. 2012 Platte River Data Analysis Report, Channel Geomorphology and In-Channel Vegetation. Prepared for Platte River Recovery Implementation Program, December, 342 p.

Tetra Tech, 2014. 2013 Platte River Data Analysis Report, Channel Geomorphology and In-Channel Vegetation. Prepared for Platte River Recovery Implementation Program, October, 267 p.

Tetra Tech, 2015. 2014 Platte River Data Analysis Report, Channel Geomorphology and In-Channel Vegetation. Prepared for Platte River Recovery Implementation Program, October, 236 p.

Tetra Tech, 2016, 2015 Platte River Data Analysis Report, Channel Geomorphology and In-Channel Vegetation Report. Prepared for Platte River Recovery Implementation Program, October, 280 p.

The Flatwater Group, in association with Tetra Tech and HDR, 2014. Sediment Augmentation Final Pilot Study Report, prepared for the Platte River Recovery Implementation Program, April, 123 p.

Thomas, R.B. 1985. Estimating Total Suspended Sediment Yield with Probability Sampling. Water Resources Research. Vol. 21(9): p. 1381–1388.

U.S. Department of Agriculture-Natural Resources Conservation Service (USDA-NRCS), 2014. The PLANTS Database. National Plant Data Team, Greensboro, NC 27401-4901 USA. Accessed: 9 January. Available: http://plants.usda.gov.

U.S. Department of Interior, Bureau of Reclamation and U.S. Fish and Wildlife Service, 2006. Platte River Recovery Implementation Program, Final Environmental Impact Statement, River Geomorphology, pp. 5–57.

U.S. Geological Survey. 1992. Recommendations for Use of Retransformation Methods in Regression Models Used to Estimate Sediment Loads ["The Bias Correction Problem"]. *Office of Surface Water Technical Memorandum* No. 93.08. December 31.

Walling, D.E. 1977. Limitations of the Rating Curve technique for Estimating Suspended Sediment Loads, with Particular Reference to British Rivers. *In*: Erosion and Solid Matter Transport in Inland Waters, *Proceedings of Paris Symposium*. July. IAHS Publication No. 122, pp. 34–48.

Page intentionally left blank

APPENDIX A.1

Mean Daily Flow-duration Curves for Germination Season

Page intentionally left blank

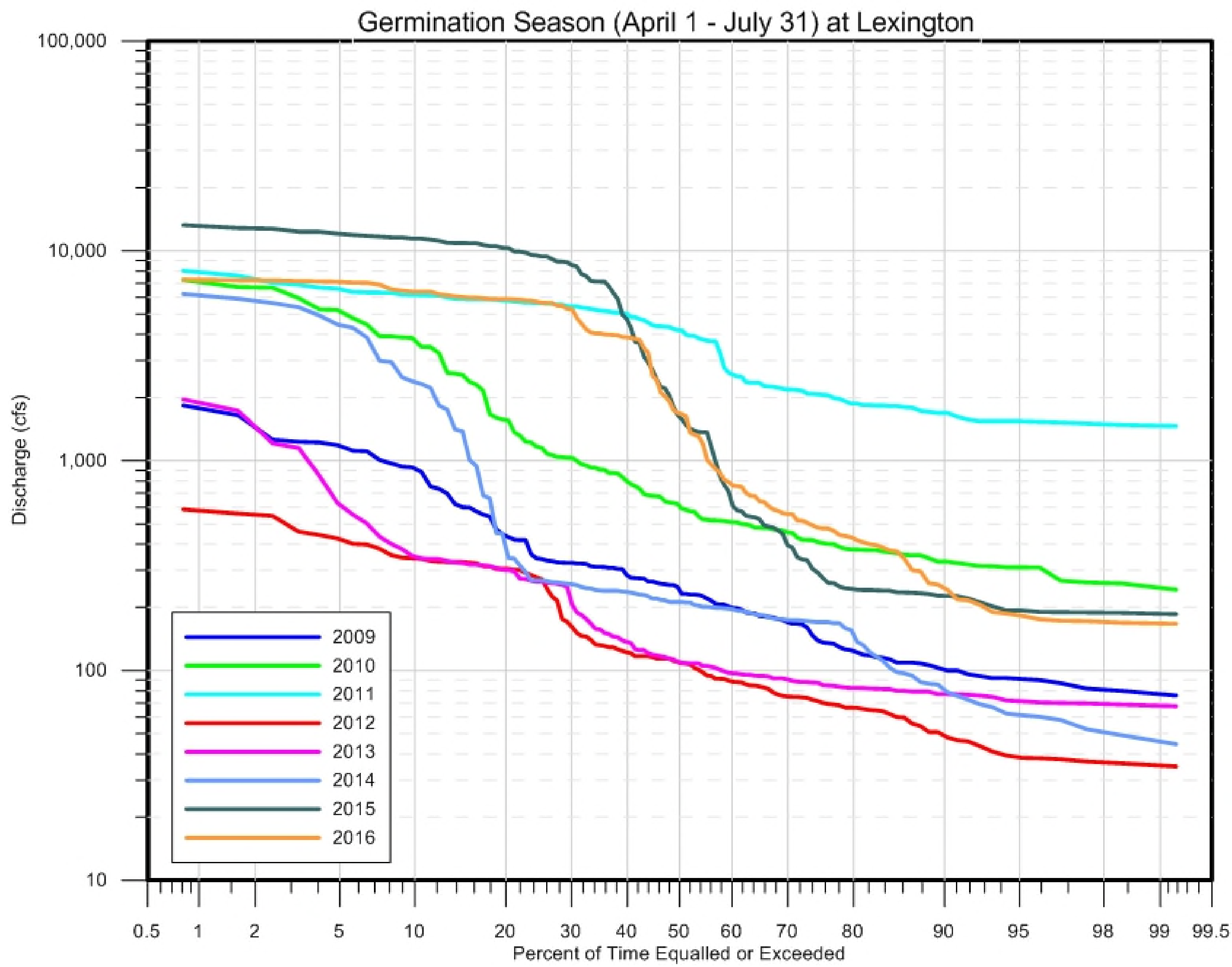

Germination Season (April 1 - July 31) at Lexington
100,000
10,000
1,000
100
10
Discharge (cfs)
0.5
1
2
5
10
20
30
40
50
60
70
80
90
95
98
99
99.5
Percent of Time Equalled or Exceeded
2009
2010
2011
2012
2013
2014
2015
2016

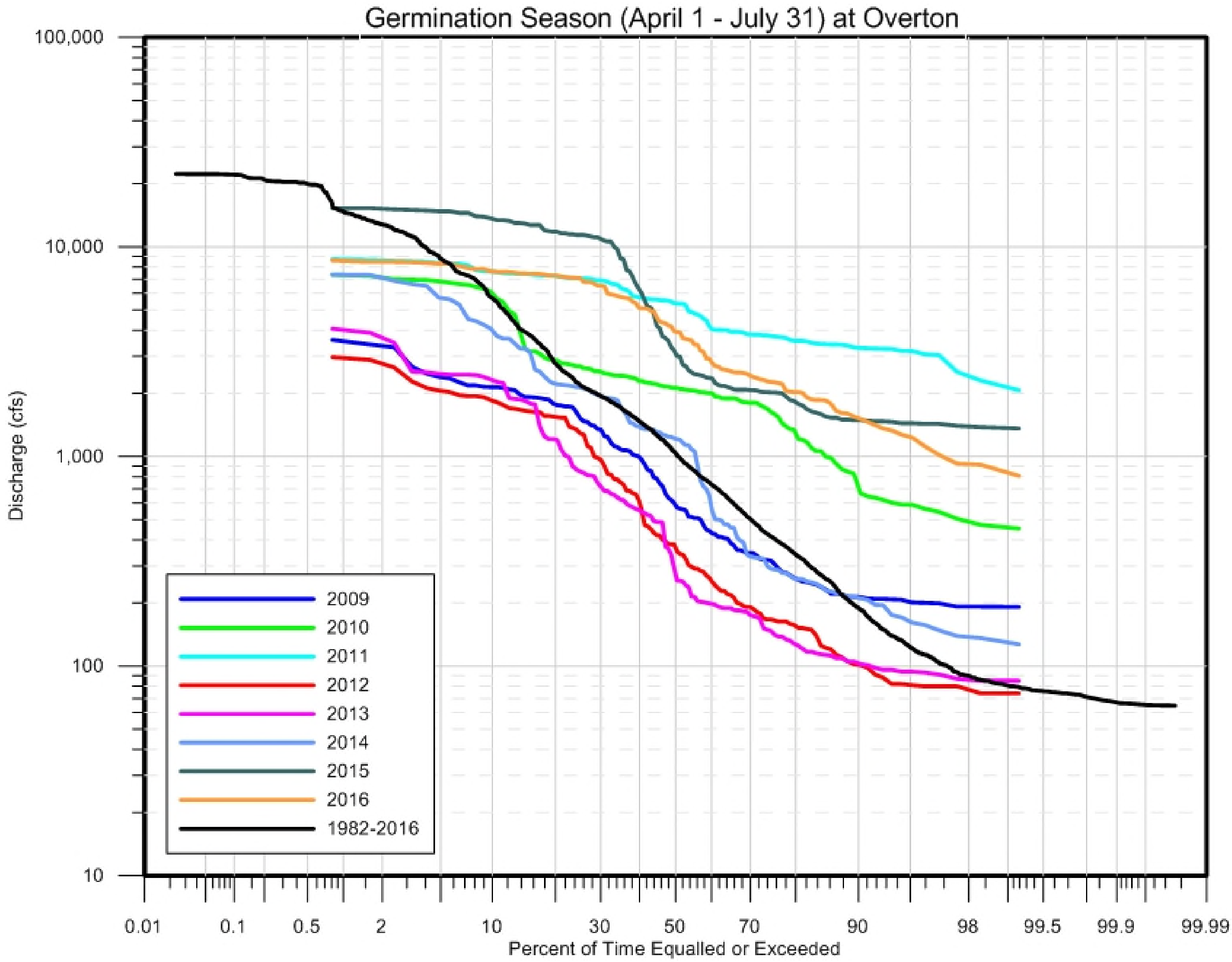
Germination Season (April 1 - July 31) at Overton
100,000
10,000
1,000
100
10
Discharge (cfs)
2009
2010
2011
2012
2013
2014
2015
2016
1982-2016
0.01
0.1
0.5
2
10
30
50
70
90
98
99.5
99.9
99.99
Percent of Time Equalled or Exceeded

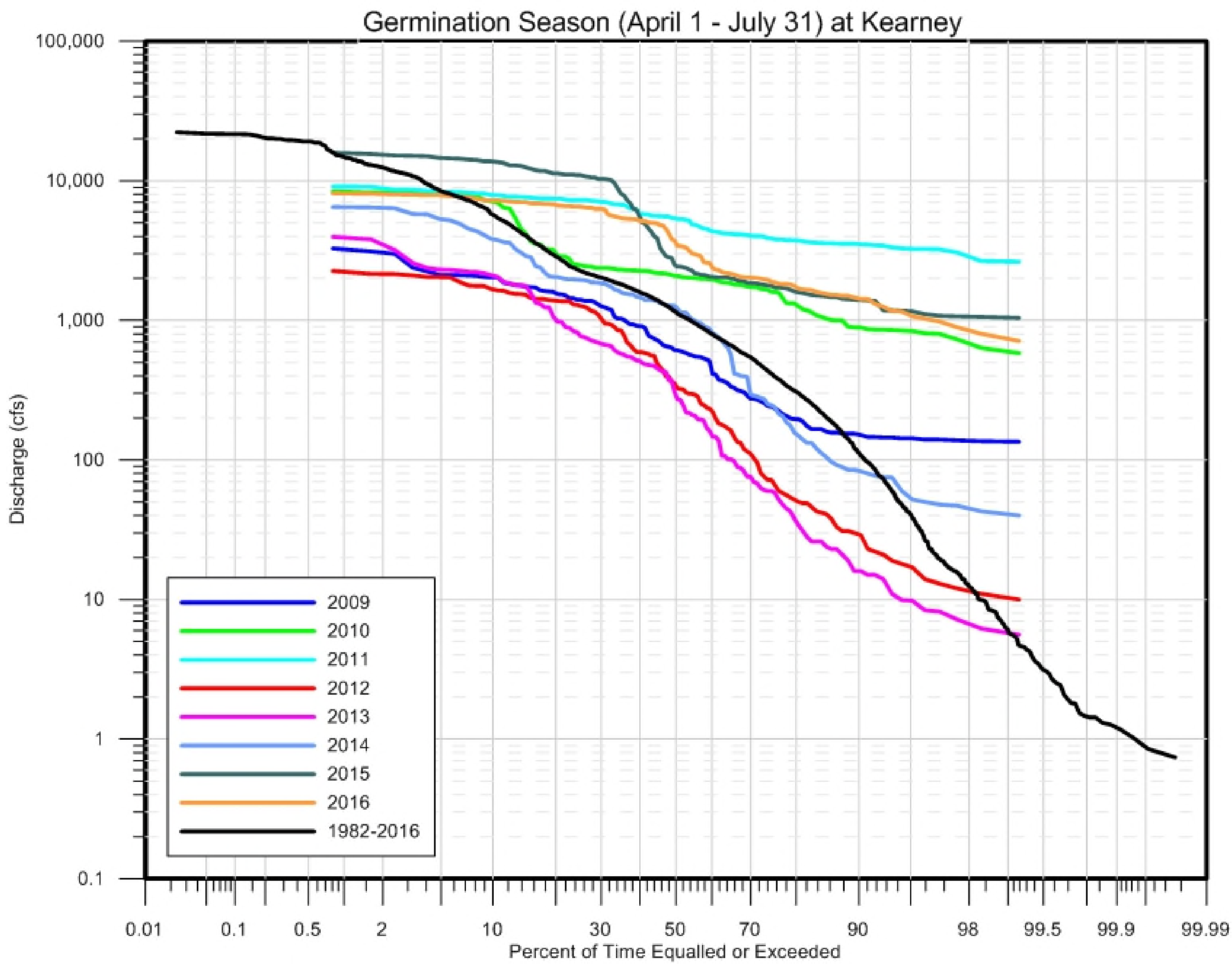

Germination Season (April 1 - July 31) at Kearney
100,000
10,000
1,000
100
10
1
0.1
Discharge (cfs)
2009
2010
2011
2012
2013
2014
2015
2016
1982-2016
0.01
0.1
0.5
2
10
30
50
70
90
98
99.5
99.9
99.99
Percent of Time Equalled or Exceeded

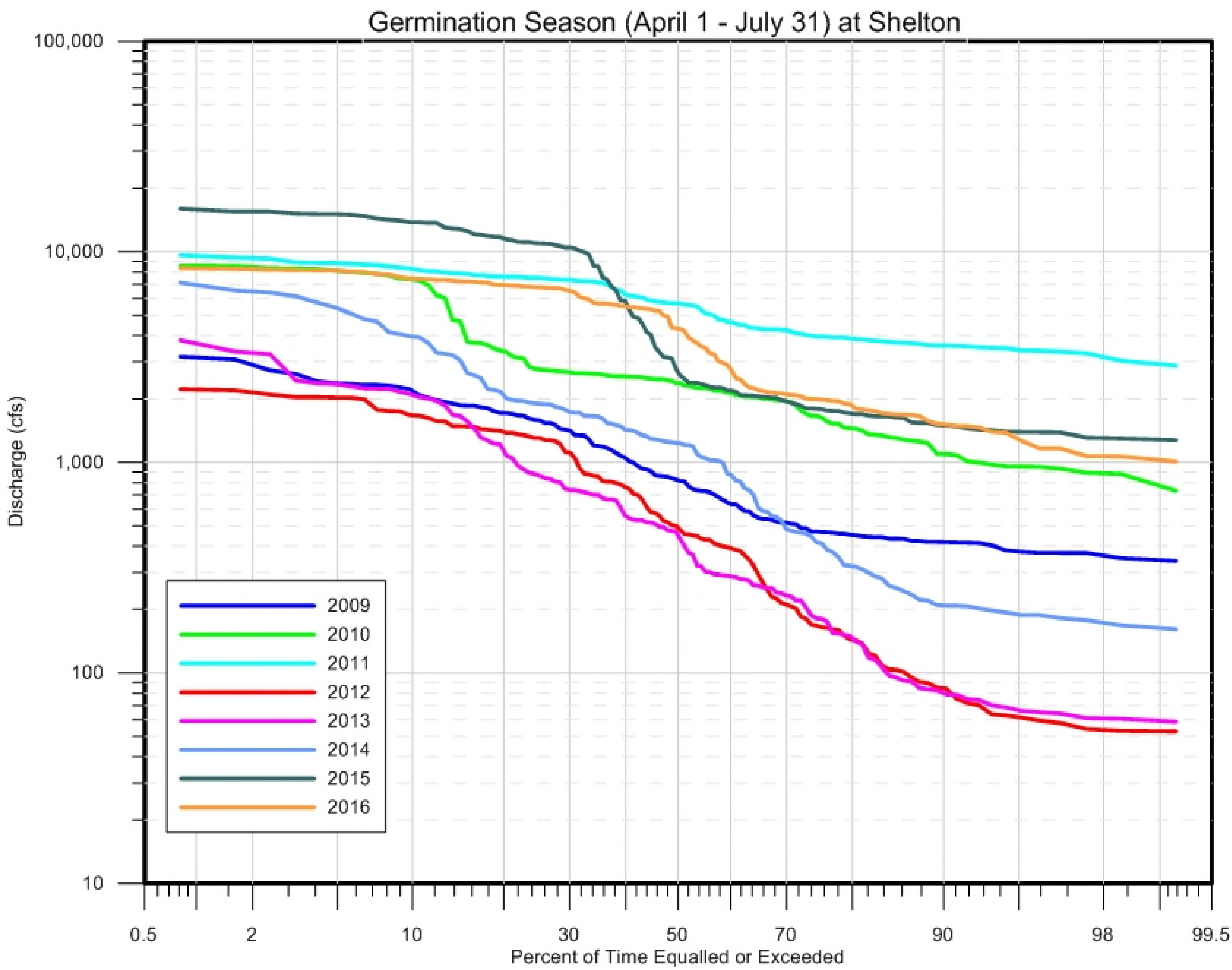
Germination Season (April 1 - July 31) at Shelton
100,000
10,000
1,000
100
10
Discharge (cfs)
2009
2010
2011
2012
2013
2014
2015
2016
0.5
2
10
30
50
70
90
98
99.5
Percent of Time Equalled or Exceeded

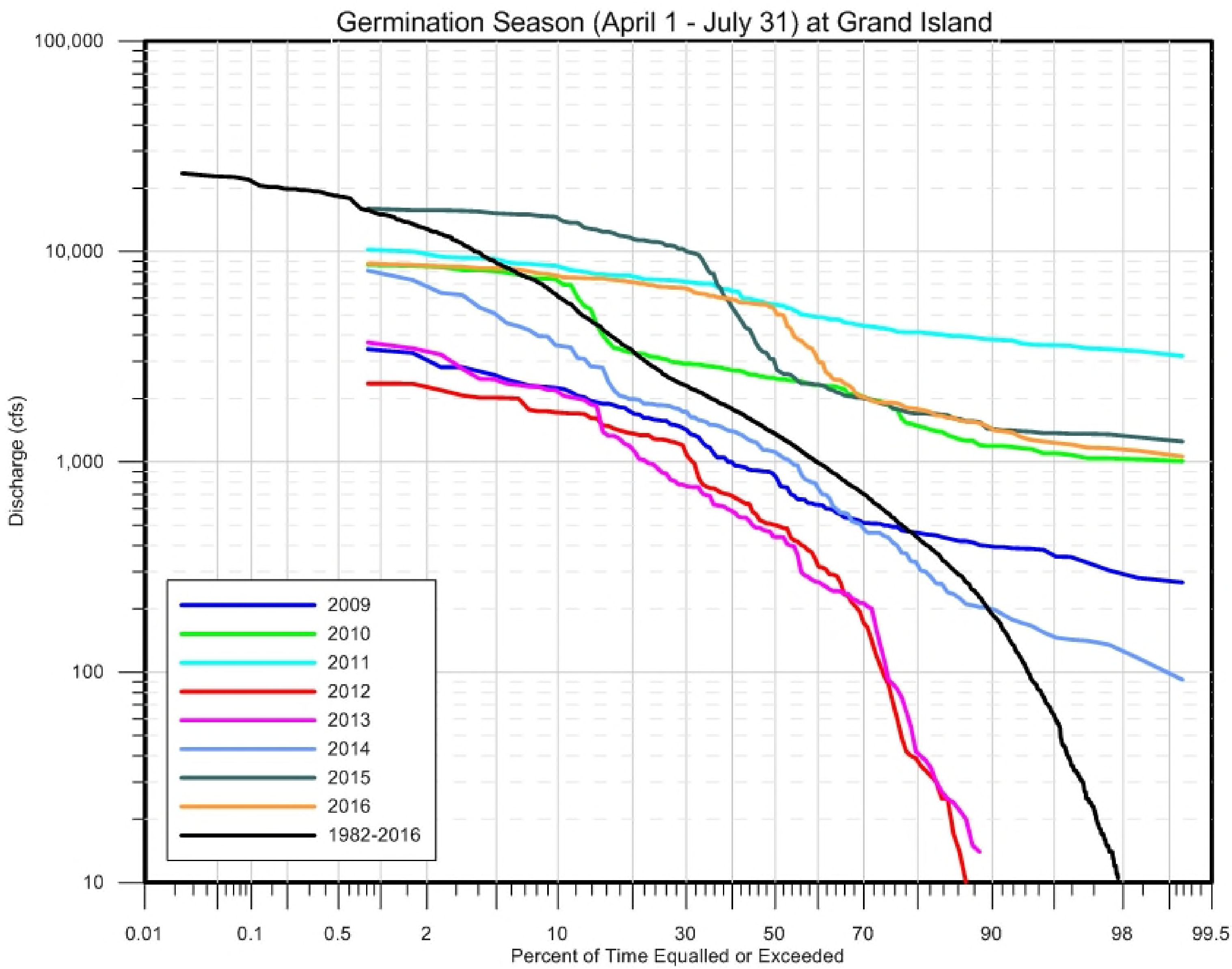
Germination Season (April 1 - July 31) at Grand Island
100,000
10,000
1,000
100
10
Discharge (cfs)
2009
2010
2011
2012
2013
2014
2015
2016
1982-2016
0.01
0.1
0.5
2
10
30
50
70
90
98
99.5
Percent of Time Equalled or Exceeded

APPENDIX A.2

Mean Daily Flow-duration Curves for Spring Whooping Crane

Page intentionally left blank

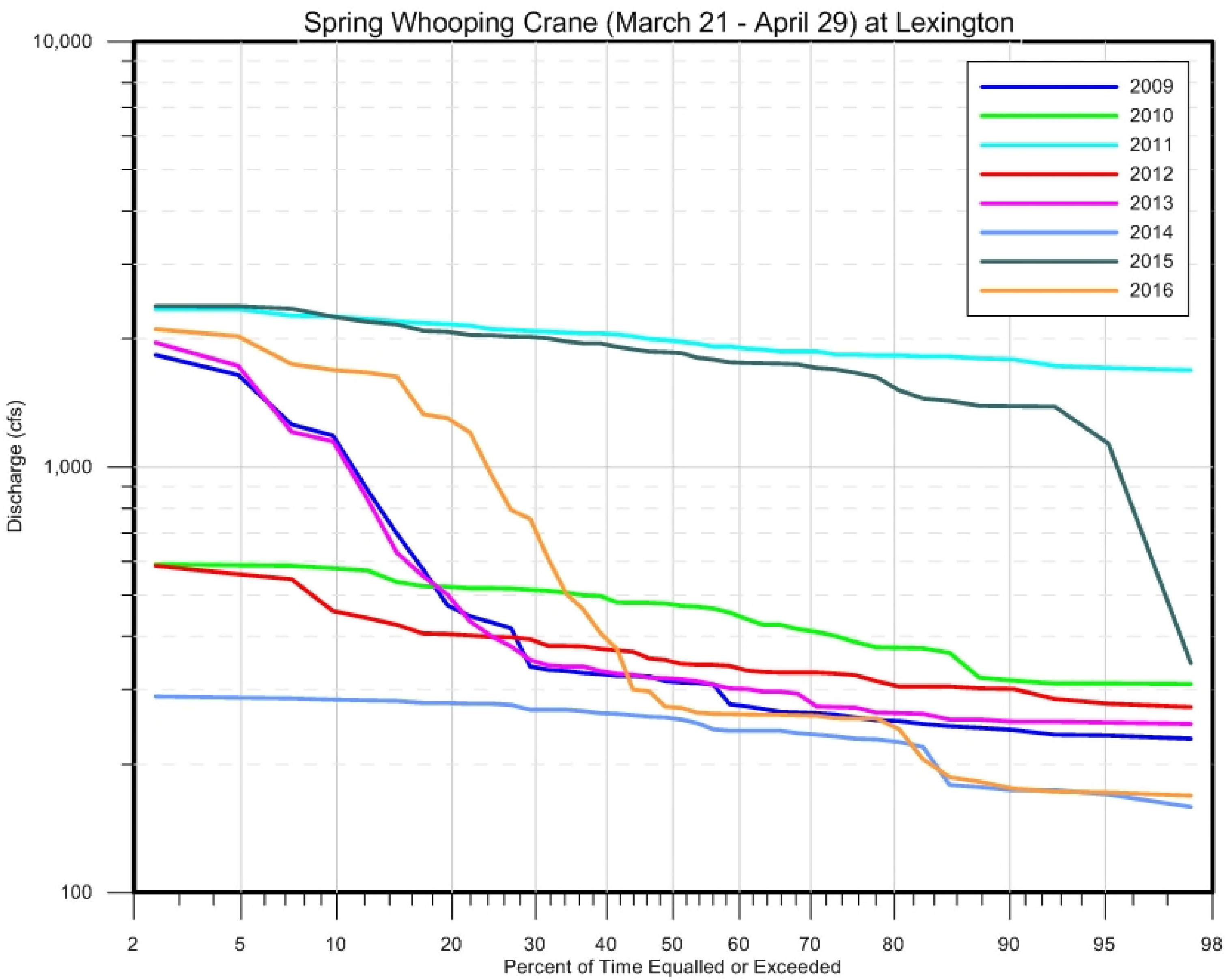
Spring Whooping Crane (March 21 - April 29) at Lexington
Discharge (cfs)
10,000
1,000
100
2
5
10
20
30
40
50
60
70
80
90
95
98
Percent of Time Equalled or Exceeded
2009
2010
2011
2012
2013
2014
2015
2016

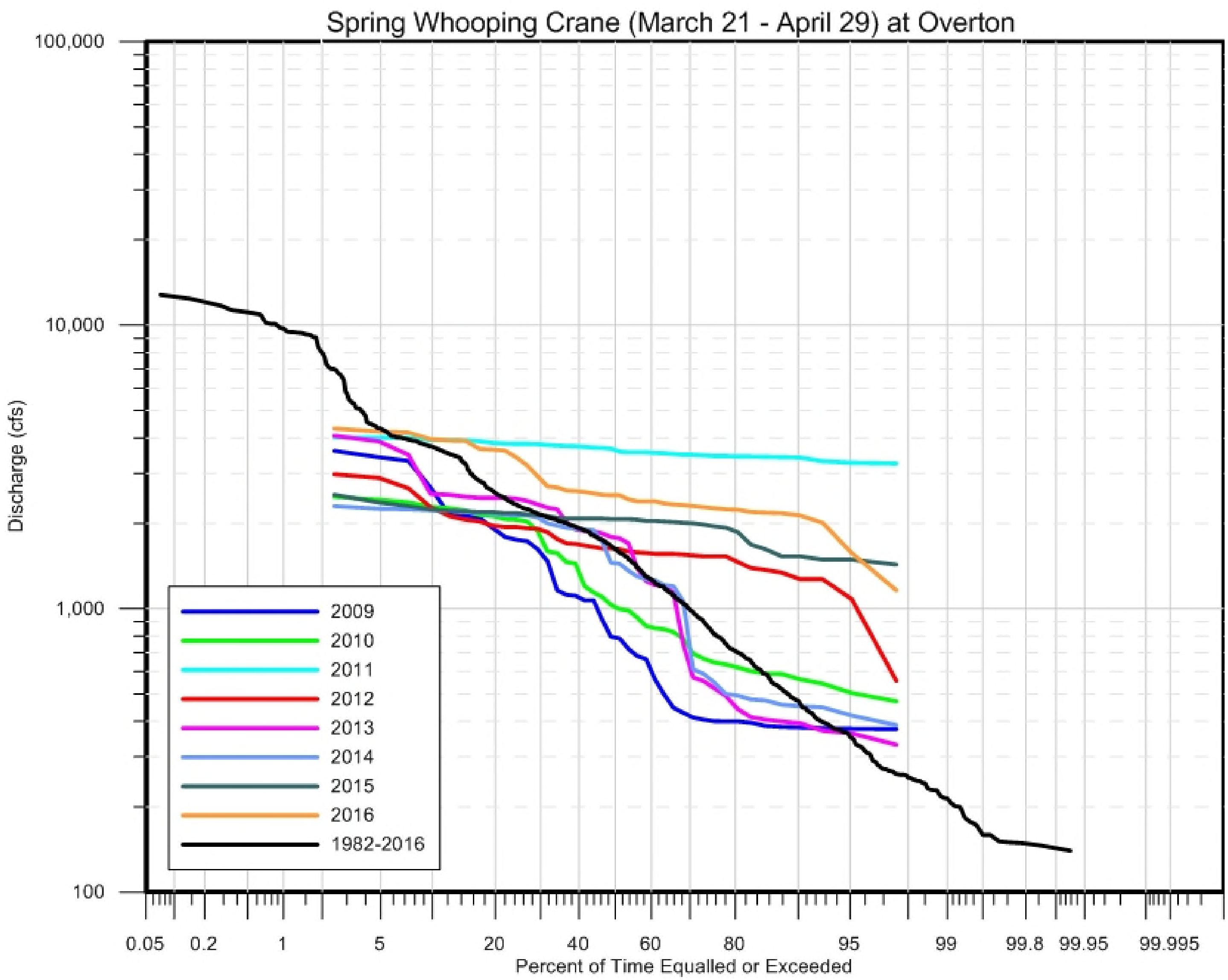
Spring Whooping Crane (March 21 - April 29) at Overton
Discharge (cfs)
100,000
10,000
1,000
100
2009
2010
2011
2012
2013
2014
2015
2016
1982-2016
0.05
0.2
1
5
20
40
60
80
95
99
99.8
99.95
99.995
Percent of Time Equalled or Exceeded

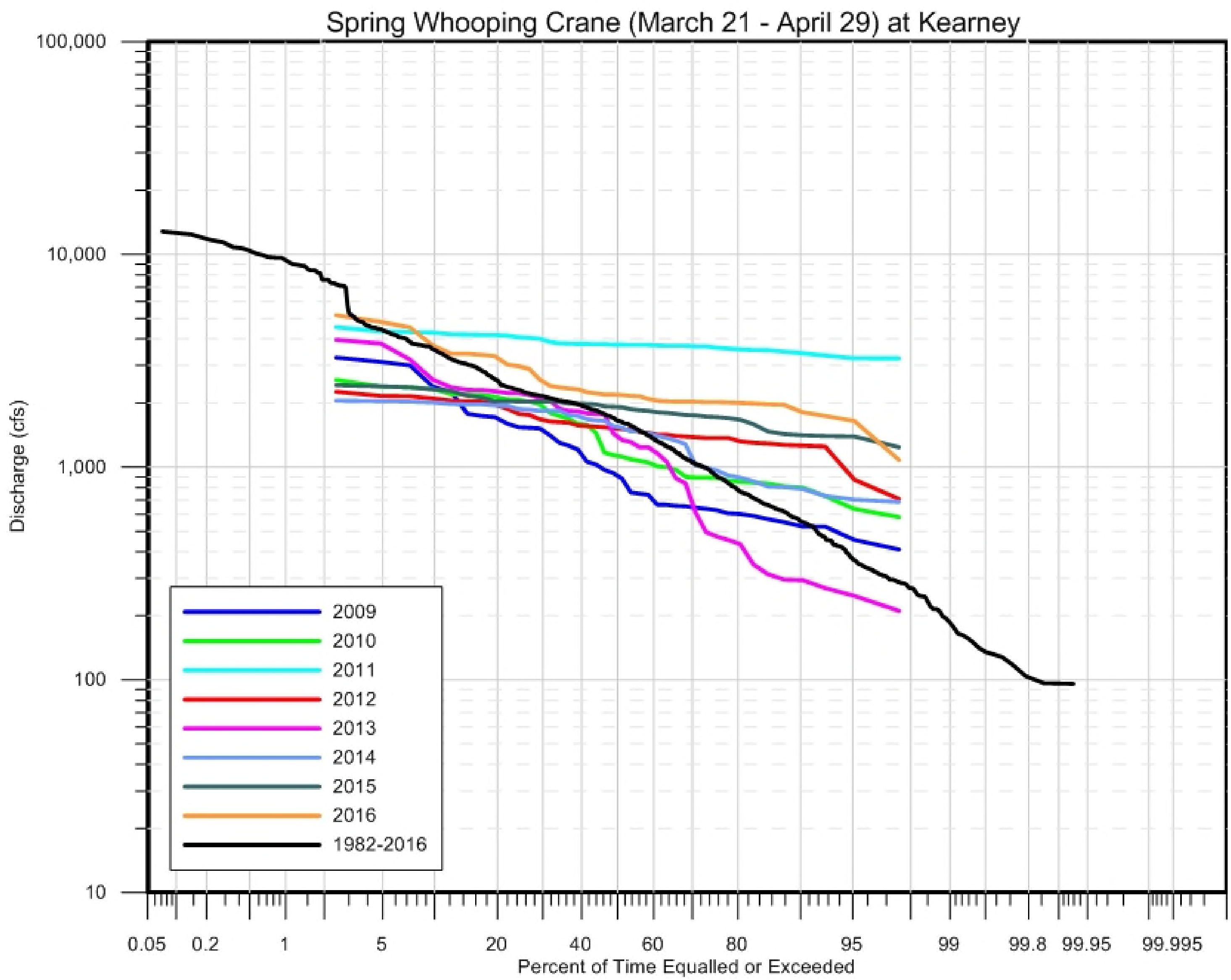

Spring Whooping Crane (March 21 - April 29) at Kearney
Discharge (cfs)
100,000
10,000
1,000
100
10
0.05
0.2
1
5
20
40
60
80
95
99
99.8
99.95
99.995
Percent of Time Equalled or Exceeded
2009
2010
2011
2012
2013
2014
2015
2016
1982-2016

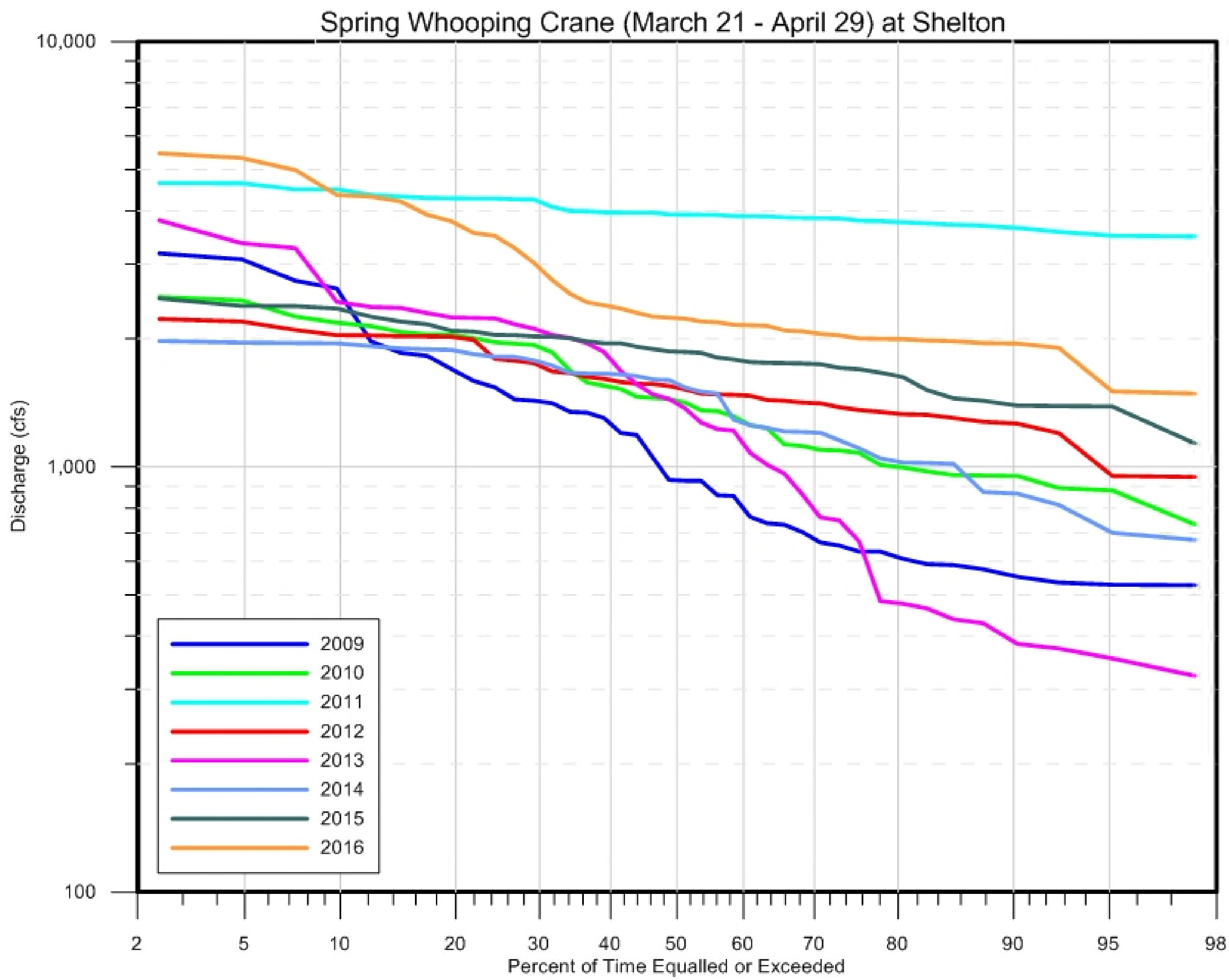

Spring Whooping Crane (March 21 - April 29) at Shelton
10,000
1,000
100
Discharge (cfs)
2
5
10
20
30
40
50
60
70
80
90
95
98
Percent of Time Equalled or Exceeded
2009
2010
2011
2012
2013
2014
2015
2016

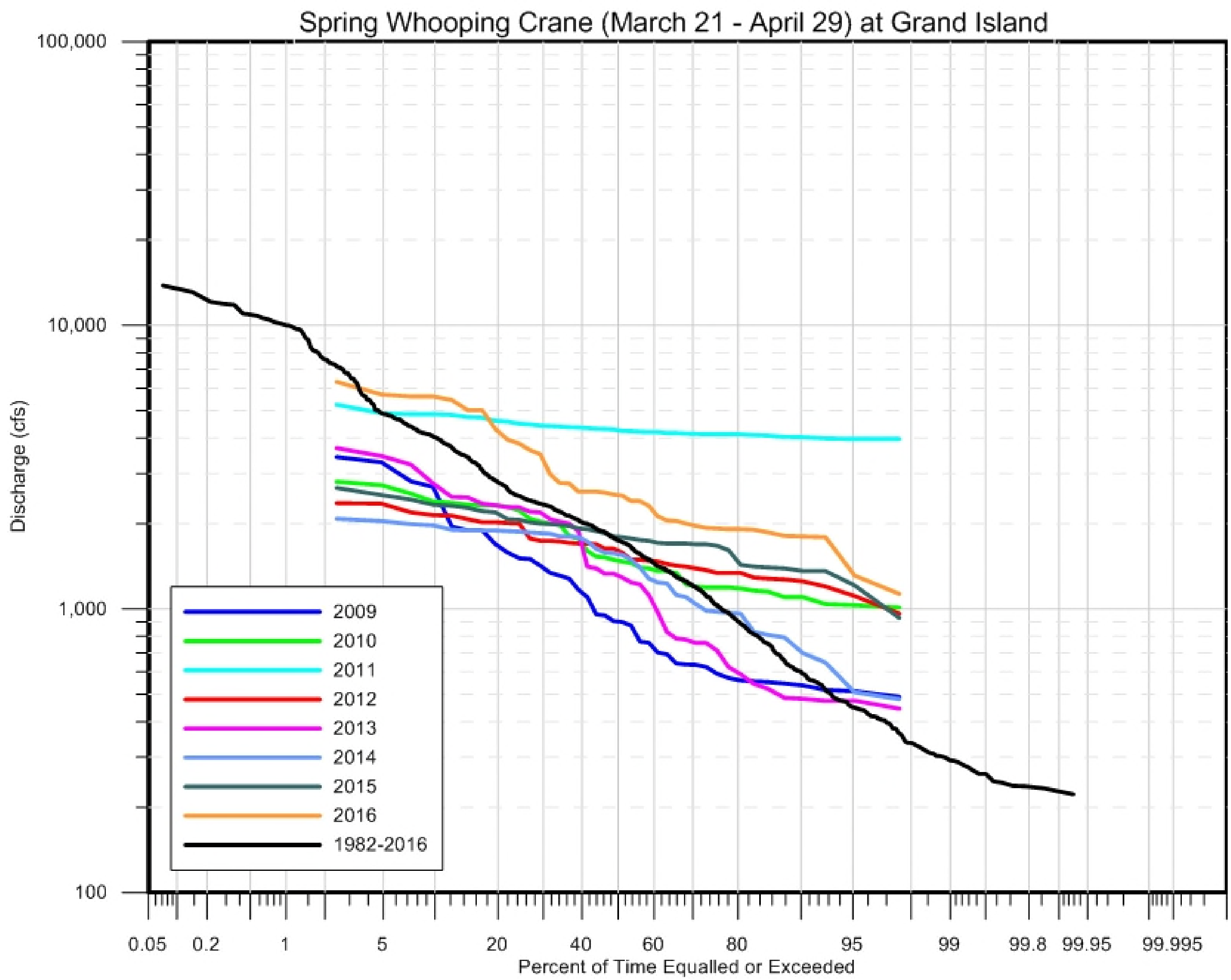

Spring Whooping Crane (March 21 - April 29) at Grand Island
100,000
10,000
1,000
100
Discharge (cfs)
2009
2010
2011
2012
2013
2014
2015
2016
1982-2016
0.05
0.2
1
5
20
40
60
80
95
99
99.8
99.95
99.995
Percent of Time Equalled or Exceeded

APPENDIX A.3
Mean Daily Flow-duration Curves for Fall Whooping Crane

Page intentionally left blank

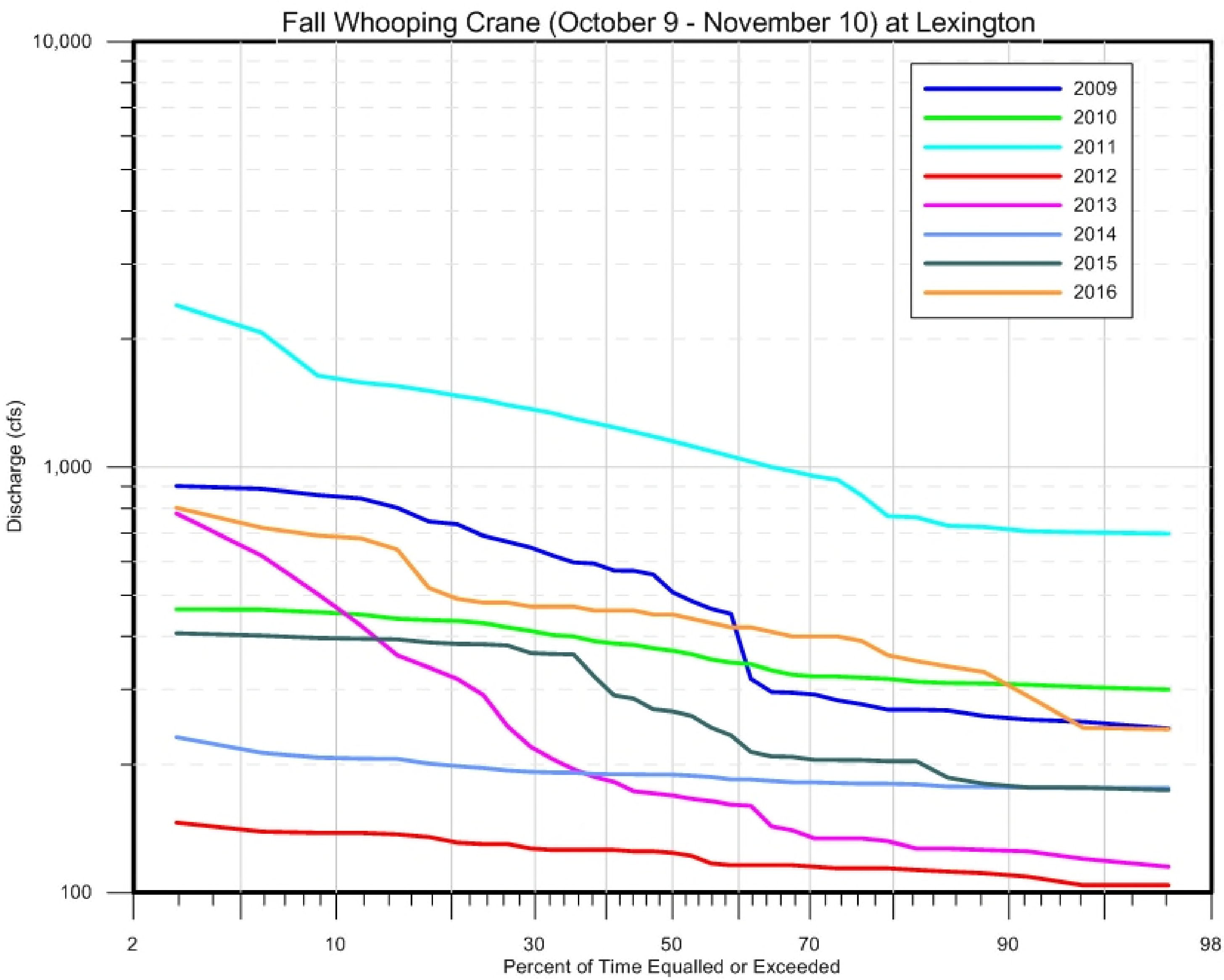
Fall Whooping Crane (October 9 - November 10) at Lexington
10,000
1,000
100
Discharge (cfs)
2
10
30
50
70
90
98
Percent of Time Equalled or Exceeded
2009
2010
2011
2012
2013
2014
2015
2016

A.3.3

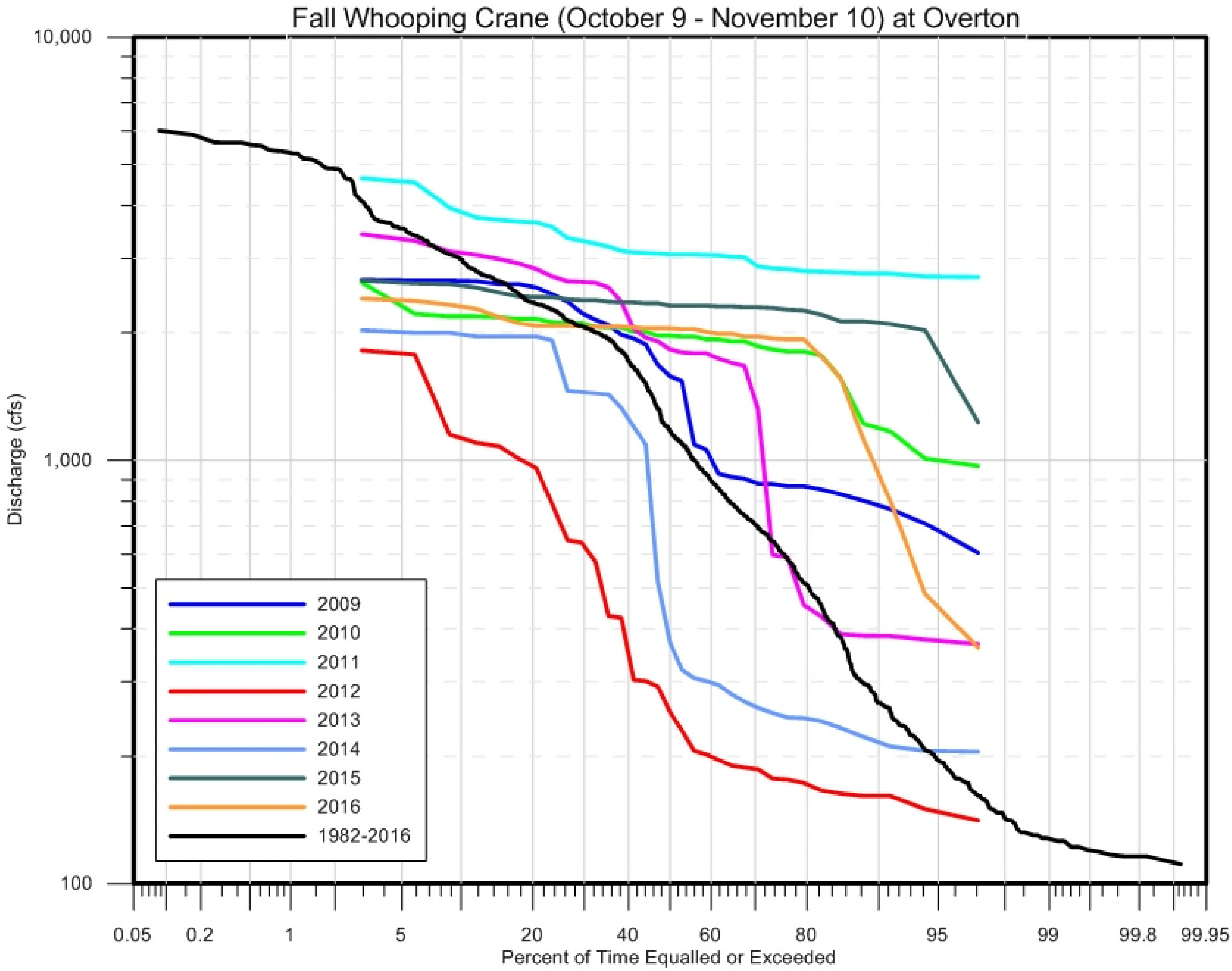
Fall Whooping Crane (October 9 - November 10) at Overton
10,000
1,000
100
Discharge (cfs)
2009
2010
2011
2012
2013
2014
2015
2016
1982-2016
0.05
0.2
1
5
20
40
60
80
95
99
99.8
99.95
Percent of Time Equalled or Exceeded

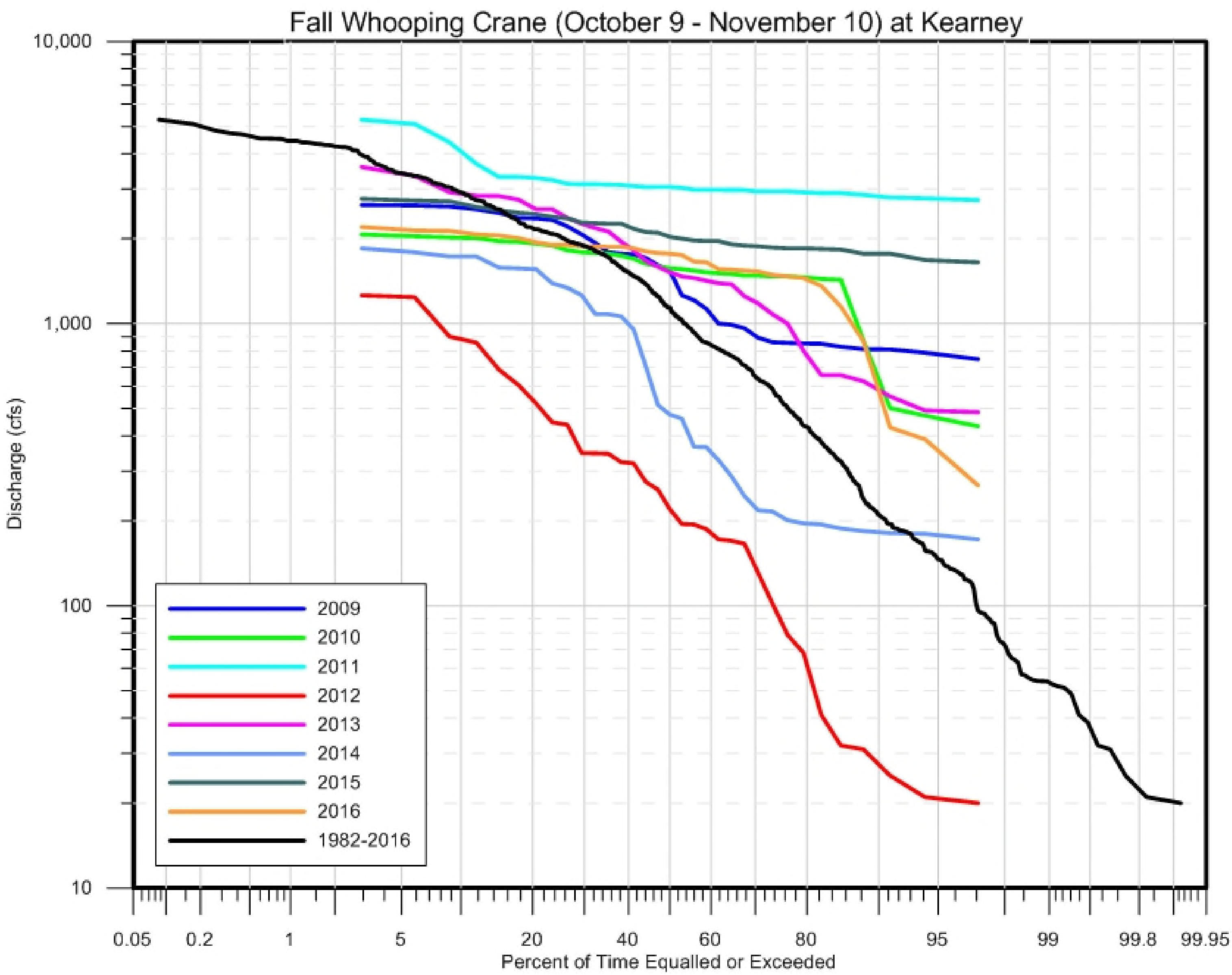

Fall Whooping Crane (October 9 - November 10) at Kearney
10,000
1,000
100
10
Discharge (cfs)
0.05
0.2
1
5
20
40
60
80
95
99
99.8
99.95
Percent of Time Equalled or Exceeded
2009
2010
2011
2012
2013
2014
2015
2016
1982-2016

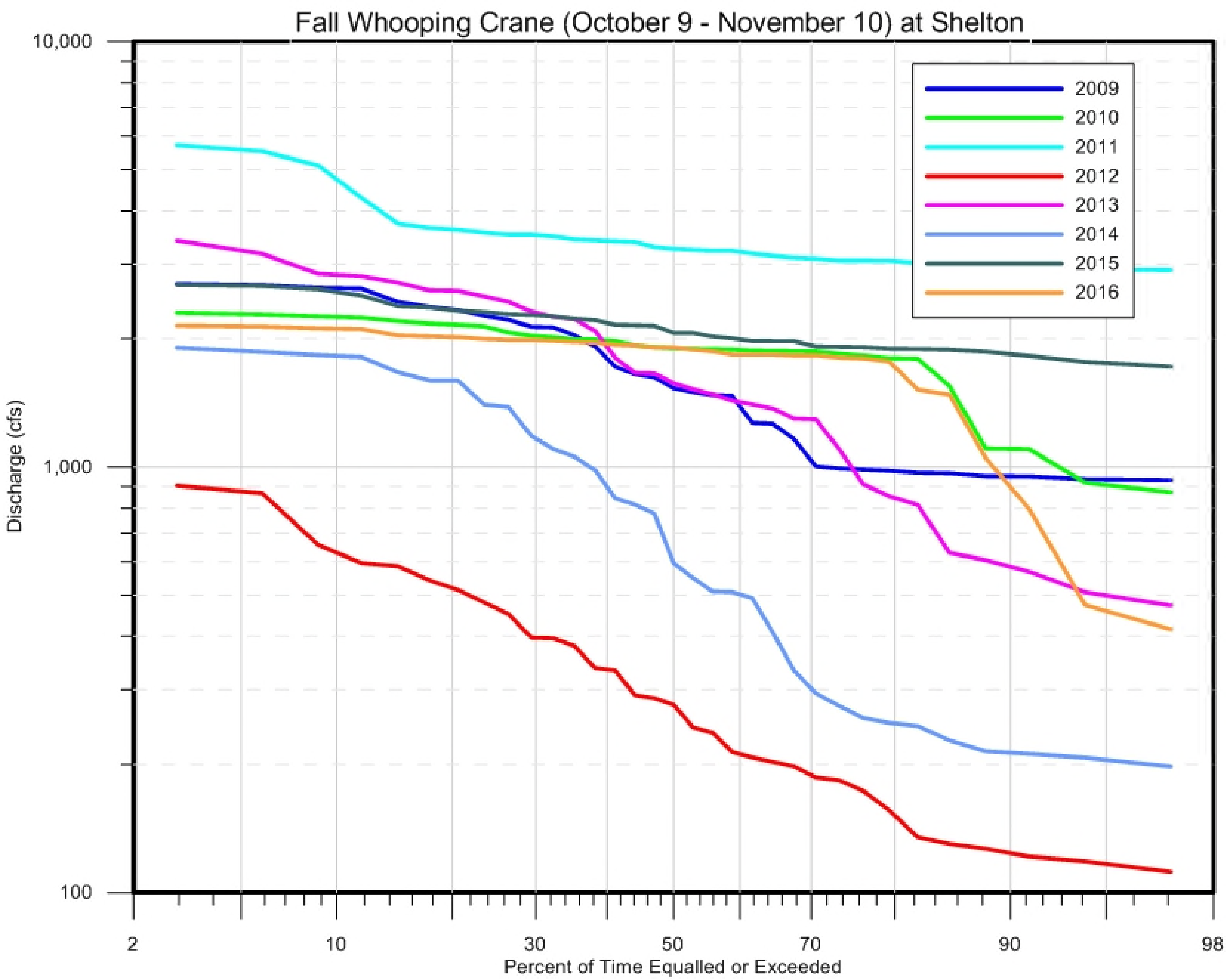

Fall Whooping Crane (October 9 - November 10) at Shelton
10,000
1,000
100
Discharge (cfs)
2
10
30
50
70
90
98
Percent of Time Equalled or Exceeded
2009
2010
2011
2012
2013
2014
2015
2016

A.3.6

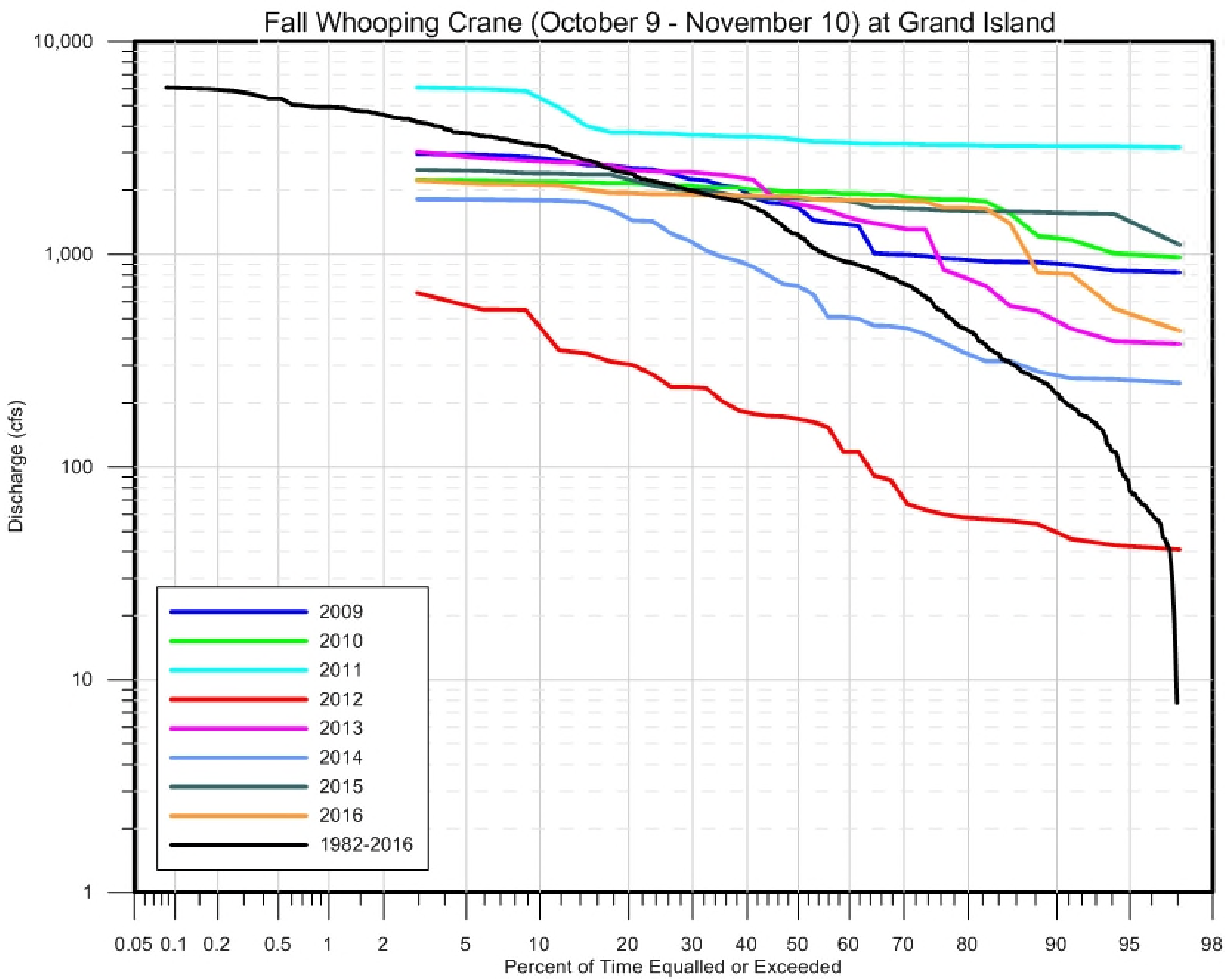
Fall Whooping Crane (October 9 - November 10) at Grand Island
10,000
1,000
100
10
1
Discharge (cfs)
2009
2010
2011
2012
2013
2014
2015
2016
1982-2016
0.05 0.1 0.2 0.5 1 2 5 10 20 30 40 50 60 70 80 90 95 98
Percent of Time Equalled or Exceeded

APPENDICES B.1 through B.8

Appendix B.1: Summary of Geomorphic and Selected Vegetation Metrics – 2009
Appendix B.2: Summary of Geomorphic and Selected Vegetation Metrics – 2010
Appendix B.3: Summary of Geomorphic and Selected Vegetation Metrics – 2011
Appendix B.4: Summary of Geomorphic and Selected Vegetation Metrics – 2012
Appendix B.5: Summary of Geomorphic and Selected Vegetation Metrics – 2013
Appendix B.6: Summary of Geomorphic and Selected Vegetation Metrics – 2014
Appendix B.7: Summary of Geomorphic and Selected Vegetation Metrics – 2015
Appendix B.8: Summary of Geomorphic and Selected Vegetation Metrics – 2016

Page intentionally left blank

APPENDIX C
Vegetation Data

Page intentionally left blank